OAK RIDGE NATIONAL LABORATORY LIBRARIES
3 4456 0599530 1

ORNL/HUD/MIUS-28
nd Volume of ORNL/HUD/MIUS-27)

Cy129

USE OF COAL AND COAL-DERIVED FUELS IN TOTAL ENERGY SYSTEMS FOR MIUS APPLICATIONS

VOLUME II

hudmius

MODULAR INTEGRATED UTILITY SYSTEMS

improving community utility services/ supplying electricity, heating, cooling, and water/ processing liquid and solid wastes/ conserving energy and natural resources/ minimizing environmental impact

ERDA - FOSSIL ENERGY

DIVISION OF COAL CONVERSION AND UTILIZATION

OAK RIDGE NATIONAL LABORATORY
CENTRAL RESEARCH LIBRARY
DOCUMENT COLLECTION
LIBRARY LOAN COPY
DO NOT TRANSFER TO ANOTHER PERSON
If you wish someone else to see this document, send in name with document and the library will arrange a loan.
UCN-7969
(3 3-67)

OAK RIDGE NATIONAL LABORATORY

OPERATED BY UNION CARBIDE CORPORATION FOR THE ENERGY RESEARCH AND DEVELOPMENT ADMINISTRATION

Printed in the United States of America. Available from
National Technical Information Service
U.S. Department of Commerce
5285 Port Royal Road, Springfield, Virginia 22161
Price: Printed Copy $10.50; Microfiche $2.25

This report was prepared as an account of work sponsored by the United States Government. Neither the United States nor the Energy Research and Development Administration, nor any of their employees, nor any of their contractors, subcontractors, or their employees, makes any warranty, express or implied, or assumes any legal liability or responsibility for the accuracy, completeness or usefulness of any information, apparatus, product or process disclosed, or represents that its use would not infringe privately owned rights.

ORNL/HUD/MIUS-28
(Second Volume of ORNL/HUD/MIUS-27)
UC-90e

Contract No. W-7405-eng-26

USE OF COAL AND COAL-DERIVED FUELS IN TOTAL ENERGY SYSTEMS FOR MIUS APPLICATIONS

Volume II

A. P. Fraas

T. D. Anderson
W. J. Boegly, Jr.
J. H. DeVan
R. S. Holcomb
H. Inouye
M. E. Lackey
S. A. Reed
P. L. Rittenhouse
G. Samuels
C. L. Segaser
J. J. Tudor

Research sponsored jointly by:

Division of Energy, Building Technology and Standards
Office of Policy Development and Research
U.S. Department of Housing and Urban Development
under
HUD Interagency Agreement No. IAA-H-40-72 ERDA 40-333-72

and

Division of Coal Conversion and Utilization
Office of Fossil Energy
Energy Research and Development Administration
under
ERDA Contract No. E(49-18)-1742

APRIL 1976

OAK RIDGE NATIONAL LABORATORY
Oak Ridge, Tennessee 37830
operated by
UNION CARBIDE CORPORATION
for the
ENERGY RESEARCH AND DEVELOPMENT ADMINISTRATION

CONTENTS

		Page
1.	INTRODUCTION	1.1
	References	1.5
2.	AVAILABILITY AND COSTS OF COAL AND COAL-DERIVED FUELS	2.1
	Coal	2.1
	The Resource Base	2.1
	Recoverable Resources	2.1
	Availability	2.6
	Coal Costs	2.8
	Coal Values at Mine	2.8
	Transportation Cost	2.11
	Rail	2.11
	Barge	2.13
	Pipeline	2.13
	Trucking	2.13
	Coal-Derived Fuels	2.13
	Coal Gasification	2.13
	Coal Liquids	2.16
	Solvent-Refined Coal	2.16
	Methanol	2.17
	Cost of Coal-Derived Fuels	2.17
	Coal and Limestone Preparation for Fluidized Bed System	2.20
	Use of Coal in Municipal Waste Treatment	2.25
	Coal Preparation for Filtering Sewage	2.25
	Preparation of Coal-Sludge Mixtures for Combustion	2.26
	Incineration Tests	2.26
	Coal Feed Rates to the Sewage Plant	2.27
	Summary of System Design Considerations	2.27
	Organic Wastes as a Fuel Source	2.29
	References	2.33
3.	COMPARISON OF TYPES OF COMBUSTION SYSTEM	3.1
	Basic Combustion Considerations	3.1

Combustion Efficiency 3.1
Effects of Excess Air on Stack Losses 3.1
NO_x Emissions 3.2
Stack Gas Temperature Limitations 3.2
Types of Burner 3.4
Stationary Grates 3.4
Traveling Grates 3.4
Open Flame Burners 3.6
Fluidized Bed Combustion of Coal 3.6
Summary 3.7
Development Status of Fluidized Bed Combustion Systems 3.9
Coal Combustion System Development Efforts 3.9
Sulfur Removal 3.12
Regeneration of the Lime 3.12
NO_x Formation 3.14
Control of Fluidized Bed Combustion Systems 3.14
Effects of Bed Operating Pressure 3.16
Combustion Gas-Side Corrosion 3.17
Development Problems 3.17
Sulfur Removal 3.18
Conventional Furnaces 3.19
Throwaway Scrubbing 3.21
Regenerable Scrubbing 3.24
Environmental Impact 3.26
Economic Analysis 3.28
Fluidized-Bed Furnaces 3.30
Ca/S Ratio 3.32
Type of Coal 3.34
Type of Additive 3.37
Combustion Temperature 3.39
Fluidizing Velocity 3.39
Additive Particle Size 3.43
Fines Recycle 3.43
Bed Height 3.47

Operating Pressure 3.48
Other Operating Variables 3.48
Estimated Sulfur Retention in Fluidized Bed for Gas Turbine Plant 3.49
Particulate Emission Control 3.49
Particulate Emission Regulations 3.49
Particulate Control Methods 3.50
Dry Inertial Collectors 3.55
Wet Scrubbers 3.57
Fabric Filters 3.57
Electrostatic Precipitators 3.62
Summary 3.65
Particulate Removal From Flue-Gas of a Typical Fluidized Bed Combustion System 3.70
References 3.77
4. COMPARISON OF THE PERFORMANCE AND COST OF TYPICAL POWER UNITS WITH DIFFERENT FUELS 4.1
MIUS Requirements 4.1
Unit Size 4.1
Average Load Factor 4.3
Maintenance 4.3
Comparison of the Performance and Cost of Typical Systems . . . 4.3
Estimation of Electrical and Heat Loads 4.6
Estimation of Efficiencies and Costs 4.8
Discussion of Results 4.9
Advanced Concepts 4.10
Fuel Cells 4.11
Solar Energy 4.13
Magnetohydrodynamic Generators 4.14
Helium Gas Turbine 4.15
Potassium Vapor Cycle 4.15
Dissociating Gas Cycles 4.15
Supercritical CO_2 Cycle 4.16
Summary 4.16
System Reliability 4.17
Closed Cycle Gas Turbine 4.17

Conventional Open Cycle Gas Turbines 4.19
Fluidized Bed Waste Incinerators 4.19
Coal Stokers 4.19
Reliability of Multiengine Power Plants 4.21
Quantitative Analysis of Reliability 4.23
References 4.27
5. CYCLE ANALYSIS FOR FLUIDIZED BED COMBUSTION GAS TURBINE SYSTEMS 5.1
Description of Cycles Considered 5.1
Open Cycles 5.1
Closed Cycles 5.7
Induced Draft Fan 5.9
System Performance Analysis 5.13
Choice of Turbine Characteristics 5.13
Rotary Regenerators vs. Fixed Matrix Recuperators 5.15
Choice of Temperatures 5.16
System Pressure Loss Components 5.16
Waste Heat Recovery 5.17
Effects of Recuperators, Regenerators, Intercooling and Reheat 5.17
Closed vs. Open Cycles 5.19
Effects of Pressure Ratio of Net Work Output 5.19
Effects of Recuperator Effectiveness and System Pressure Losses 5.24
Effects of Design Parameters on Costs 5.24
General Effects 5.37
Relations Between Heat Exchanger Cost and Cycle Efficiency . . . 5.37
Effects of Recuperator Effectiveness 5.37
Effects of Turbine Inlet Temperature 5.40
Effects of Pressure Ratio 5.40
Effects of Compressor Inlet Temperature 5.40
Effects of Intercooling and Reheat 5.40
Effects of Fuel Costs on Power Costs 5.48
Effects of Part-Load Operation 5.48
Costs of Open and Closed Cycles 5.56
References 5.58

6. CONCEPTUAL DESIGNS FOR FLUIDIZED BED GAS TURBINE SYSTEMS 6.1
Fluid Bed and Furnace Layouts 6.1
Plenum Chamber Walls 6.5
Bed Depth 6.5
Economizer 6.6
Bed Floatation Limitation 6.8
Bed Support Plate 6.10
Typical Layouts 6.12
Heat Exchanger Design Charts for a Coal-Fired Gas Turbine System 6.20
Basic Relations 6.25
Calculational Procedure and Design Charts for Heat Exchanger Effectiveness 6.26
Tube Matrix Proportions 6.26
Heat Transfer Coefficient 6.30
Fluid Bed 6.30
Recuperator 6.33
Economizer 6.34
Waste Heat Boiler 6.38
Cooler 6.41
Calculational Procedure for the Construction of Charts for Pressure Drop 6.43
Heat Exchanger Selection 6.45
Fuel and Limestone Feed System Concepts 6.46
Solids Feed into the Retention Components 6.49
Concepts of Retention Components 6.52
Transport System 6.55
Blending 6.60
Adaptation of Commercially Available Systems 6.66
Systems Preferred for Development 6.67
Plant Layouts 6.67
Particulate Removal Equipment 6.68
Fuel and Limestone Feed Systems 6.68
Capital Cost 6.74
References 6.78

7. HOT CORROSION AND STRENGTH OF SUPERALLOYS 7.1
Effect of Alloy Composition 7.1
Effect of Environment 7.1
Corrosion Mechanism 7.3
Gas-Metal Reactions in Helium 7.3
Corrosion in Fluidized Beds 7.4
High Temperature Strength Considerations 7.5
Effects of a Hot Gas Environment on Mechanical Properties 7.5
Candidate Alloys 7.7
Carbon and Low-Alloy Steels 7.8
High-Alloy Ferritic Steels 7.8
Ferritic Stainless Steels 7.8
Austenitic Stainless Steels 7.8
Fe-Ni-Base Alloys 7.8
Ni-Base Alloys 7.9
Co-Base Alloys 7.9
Conclusions 7.9
References 7.10
8. INSTRUMENTATION AND CONTROL 8.1
MIUS Requirements 8.1
Diurnal Variations in Load 8.2
Seasonal Variations in Building Heating Loads 8.2
Control of Conventional Boiler Furnaces with Coal Stokers . . . 8.3
Control of Fuel-Air Ratio 8.3
Control of Fluidized Bed Coal Combustion Systems Coupled to Steam Boilers 8.4
Basic Concept Envisioned for the Fluidized Bed Coal Burning Gas Turbine 8.5
Control System Design Precepts 8.5
References 8.10
9. MAJOR PROBLEM AREAS 9.1
Minimal Program to Design, Construct, and Test a Demonstration Unit 9.1
Analytical Design and Layout Studies 9.3
Bench Tests 9.3

Detail Design and Construction 9.5
System Tests 9.5
Basic Technology 9.7
Materials Compatibility Studies 9.7
Characterization of Furnace Environment 9.7
Corrosion of Bed and Duct Materials 9.8
Turbine Bucket Erosion, Corrosion, and Deposits 9.9
APPENDIX A A.1
APPENDIX B B.1
APPENDIX C C.1

CHAPTER 1

INTRODUCTION

A program for developing a coal-fueled Modular Integrated Utility System (MIUS) is being jointly sponsored by the Department of Housing and Urban Development (HUD), Office of Policy Development and Research; and the Energy Research and Development Administration (ERDA), Fossil Energy (formerly Office of Coal Research of the Interior Department); at the Oak Ridge National Laboratory (ORNL). This program had its inception some years ago when HUD foresaw the impending energy shortage and initiated work on small total energy systems for use with new housing complexes. In these systems the waste heat from the thermodynamic cycle used to generate electricity is used to heat both domestic hot water and buildings in the winter and for absorption air conditioning systems in the summer. ORNL has been assisting HUD in this work, first by looking at the problems of supplying heat to building complexes from district heating systems tied to central stations,[1] and subsequently by examining various small total energy systems. Hundreds of such systems are in use currently in the U.S. making use of diesel or gas engines or small gas turbines.

A good notion of the Modular Integrated Utility System (MIUS) envisioned by HUD is given by the artist's concept in Fig. 1.1 which shows a small power plant adjacent to a new housing development. The solid waste from the building complex would be transported pneumatically to the power plant where it would be burned and thus provide 5 to 10% of the fuel. The sewage treatment plant adjacent to the power plant could make use of waste heat to accelerate digestion of the sewage as well as supply methane to the power plant for use as fuel. The air and gas discharges vented from components of the sewage plant could be used as part of the combustion air for the power plant, thus avoiding emission of odors. The treated water discharged from the sewage plant would be held up in a small pond or lake which would be part of the landscaping, and would also serve as a supply of cooling water for the power plant and air conditioning equipment.

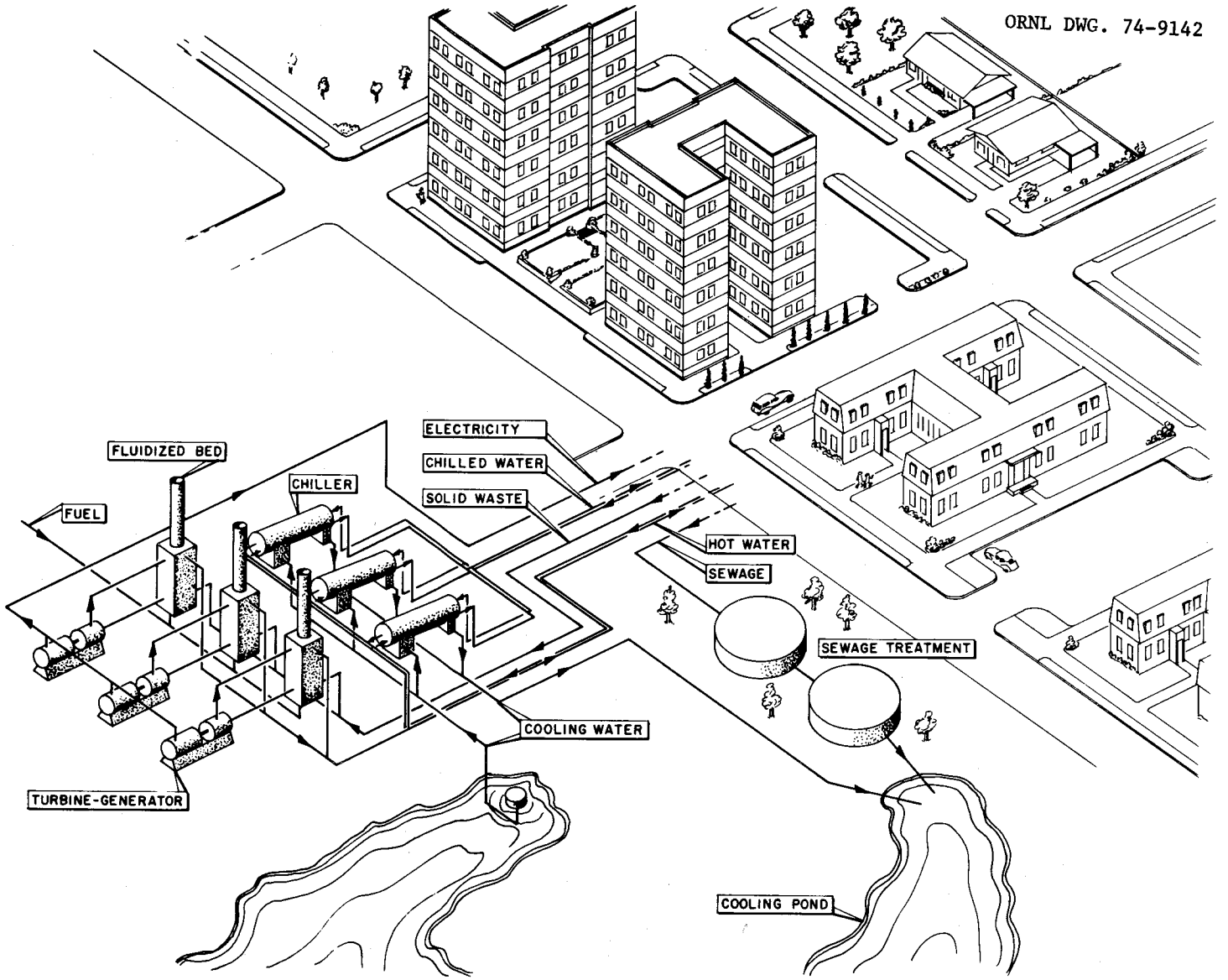

Fig. 1.1. Artist's concept of a modular integrated utility system.

The majority of the housing complexes sponsored by HUD have involved 500 to 1000 residential units for which the electrical power requirements have run 1 to 2 MW(e). Extensive experience with power plants for installations of this sort indicates that to obtain good reliability from diesel or gas engines or conventional gas turbines it is essential to employ four or more units. Because of seasonal and diurnal variations in the load, the load factor is normally only 60 to 70%. Thus, for an installation designed for a full load of 1.5 MW(e), the usual practice is to employ four engine-generator units of about 600 kW(e) of which two would normally be in operation, one would be on standby for load peaks in unfavorable weather, and the fourth could be down for maintenance. Thus, the design power output range of interest for MIUS applications is 500 kW(e) to 1000 kW(e) per unit. This is an important factor in choosing a power conversion system because some systems (e.g., steam turbines) do not perform well in small sizes.

The critical shortages of gas and fuel oil that began to develop early in 1973 coupled with the lack of near-term supplies of fuel from coal gasification and liquefaction led to an examination of the possibilities of employing coal on-site as the fuel, particularly moderately high sulfur coal because of its ready availability. A review of the problems of sulfur removal led to the conclusion that it would be well to consider a fluidized bed coal combustion system. This combustion system makes it possible to remove about 90% of the sulfur in the coal by combining it with crushed limestone in the bed to give calcium sulfate. To do this a tube bank in the bed must be employed to keep the bed temperature to the range of 1500 to 1700°F, the region required for good conversion of the sulfur to calcium sulfate. Operation of the bed at this temperature also serves to avoid NO_x formation from nitrogen in the combustion air and fusion of the ash.

In selecting a power conversion system, the poor efficiency of steam turbines in small sizes makes a gas turbine a logical candidate for the thermodynamic cycle. Inasmuch as the air fed to the turbine will be heated by the tube bank in the bed and will not contain fly ash from the coal, turbine bucket erosion will not be a problem. Good heat transfer coefficients will prevail both in the high pressure air inside the tubes in

the fluidized bed and between the fluidized bed and the tube walls. The fluidized bed combustion system will operate well with liquid or gaseous fuel, char, a low sulfur coal, or solid organic waste, hence it could also be used as an incinerator.

A preliminary study indicated that with this system around 80% of the energy in the fuel would be available for use, about one-third as electricity and the balance as heat in the form of 250°F hot water obtained from a waste heat recovery heat exchanger.

This appeared sufficiently attractive that ORNL proposed to HUD that a thorough study of the concept be initiated,[2] and, if this proved favorable, that a program be launched to design, develop, and construct a demonstration unit. HUD then approached OCR, and this led to an agreement between them to sponsor such a program.[3] Arrangements were then made with the USAEC for ORNL to undertake this work. The objectives of Phase I of the program, "Concept Preliminary Evaluation," were stated in the Memorandum of Understanding[3] to be the investigation and evaluation of various ways in which coal and coal-derived fuels might be employed in MIUS systems. The fuels to be considered include high and low sulfur bituminous coals, lignite, anthracite, the products of various coal gasification, liquefaction, and solvent refining processes, coal loaded with sewage sludge after being used as a filtering medium, and coal mixed with residential and industrial solid wastes. The potential performance of all types of power conversion system that might be used with these fuels should be evaluated together with the problems foreseen in the development effort for each system. The following report has been prepared to summarize the results of this Phase I study.

References

1. A. J. Miller et al., Use of Steam-Electric Power Plants to Provide Thermal Energy to Urban Areas, ORNL-HUD-14 (January 1971).

2. Letter to G. S. Leighton, Department of Housing and Urban Development from A. J. Miller, Oak Ridge National Laboratory, July 6, 1973.

3. Memorandum of Understanding Between the Department of Interior and the Department of Housing and Urban Development on a Cooperative Program Entitled Modular Integrated Utility System (April 1974).

CHAPTER 2

AVAILABILITY AND COSTS OF COAL AND COAL-DERIVED FUELS

Coal

The Resource Base. Coal deposits are widely distributed throughout the United States as shown in Fig. 2.1. The coal resource base is estimated to be 3.21 trillion tons,[1] equivalent in energy content to over 1000 years at the total energy consumption rate of the U.S. in 1970. Approximately one-half or 1.56 trillion tons, lies in beds more than 14 in. thick at depths of 3000 ft or less in mapped and explored areas. The distribution of the 1.56 trillion tons by rank (type of coal) and by state is shown in Fig. 2.2 and Table 2.1. Of the total bituminous resource, two-thirds is located east of the Mississippi with Illinois containing the largest quantity of any state. Sub-bituminous coal is predominantly contained in the Rocky Mountain States of Montana, Wyoming, and Colorado and in Alaska. New Mexico also has substantial reserves. About 98% of the nation's lignite is located in North Dakota and Montana.

Recoverable Resources. The coal resource base described above does not constitute a usable resource because of both technical and economic constraints. Coal considered to be available at present prices with present technology are the measured and indicated reserves with 1000 ft or less of overburden, and in beds of thicknesses (1) 28 in. or more for bituminous and anthracite, and (2) 5 ft or more for sub-bituminous and lignite. On this basis, available reserves total 394.1 billion tons[1] (about one-eighth of the total resource base) distributed by rank as follows: (1) bituminous - 66%, (2) sub-bituminous - 18%, (3) lignite - 13%, and (4) anthracite - 3%. A breakdown of available reserves by rank and state is given in Table 2.2.

Of the 394.1 billion tons considered to be available, 45 billion tons are strippable and most of this would be recoverable, since the recovery factor for strip-mined coal exceeds 90%. For deep-mined coal, however, the recovery factor with present mining practices is about 50% so that of the 349.1 billion tons of deep-minable reserves, only about 175 billion tons are recoverable. The recoverable underground and strippable reserves are summarized as follows:

ORNL–DWG 74–12791

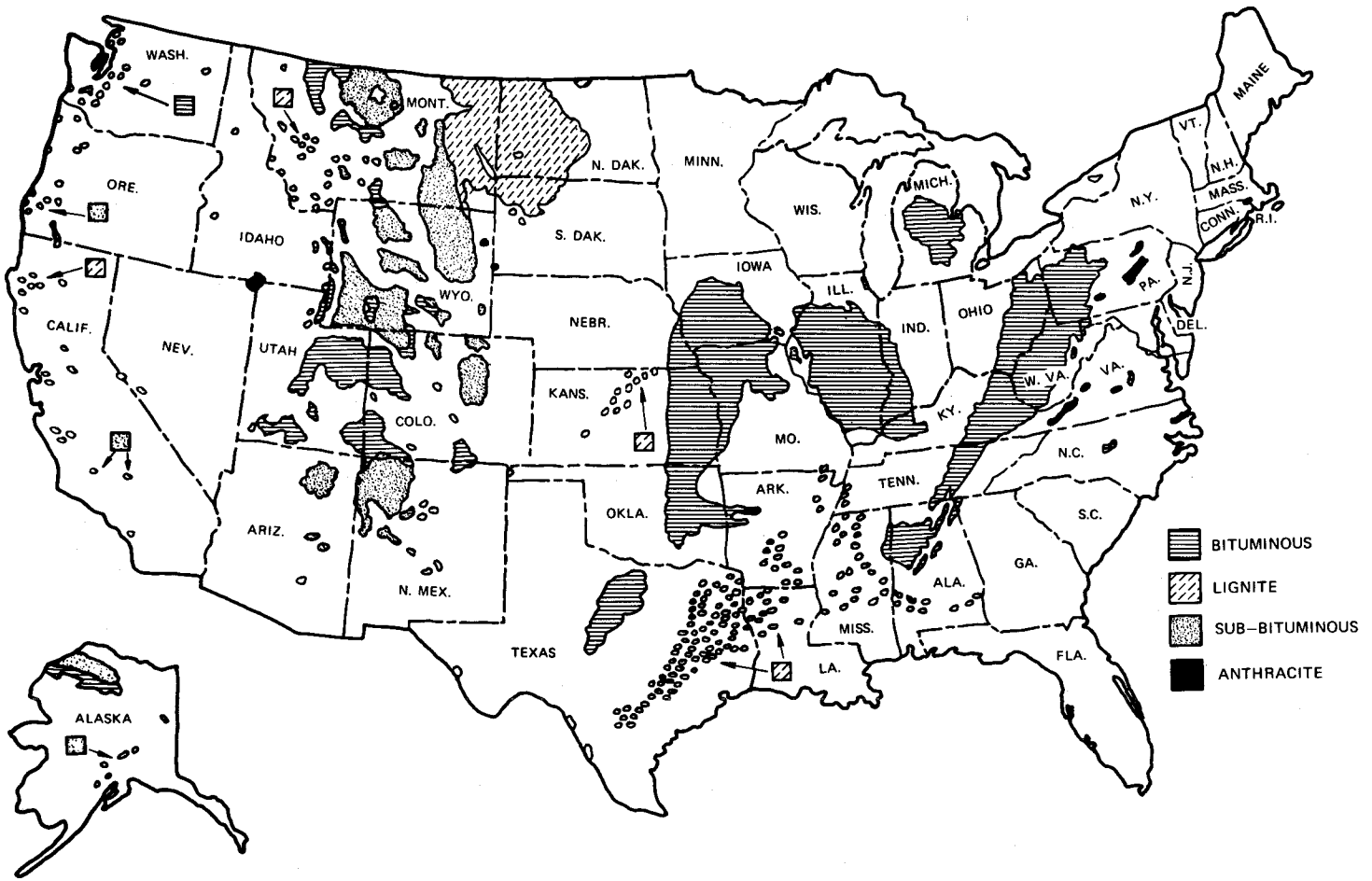

Fig. 2.1. Coal fields of the conterminous United States.

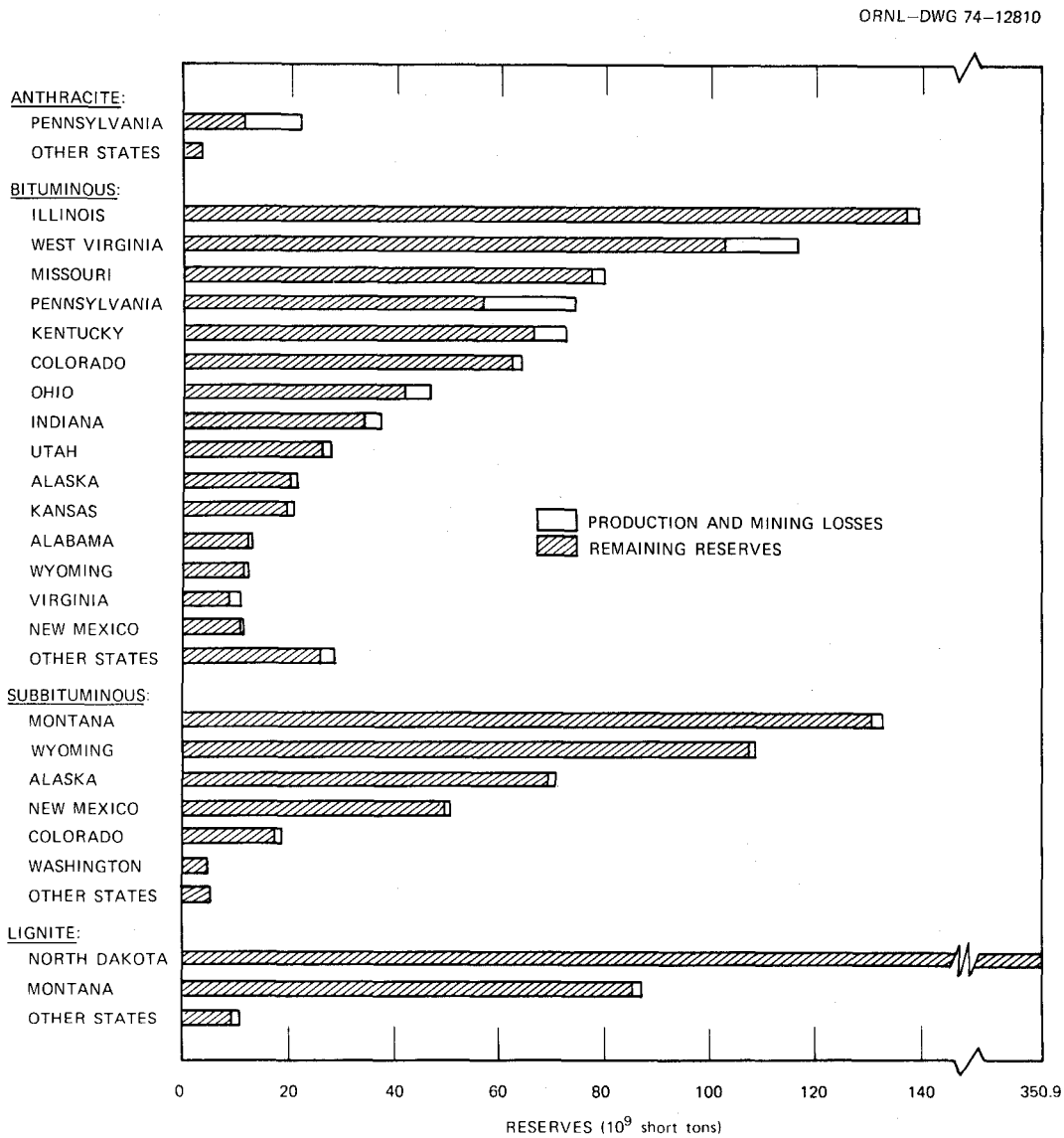

Fig. 2.2. Estimated original and remaining coal reserves, by rank, in the United States, January 1, 1965.

Table 2.1. Estimated Remaining Coal Reserves of the United States, by Rank, Sulfur Content, and State, on January 1, 1965

Coal Rank and State	Sulfur content, percent									Total
	0.7 or less	0.8-1.0	1.1-1.5	1.6-2.0	2.1-2.5	2.6-3.0	3.1-3.5	3.6-4.0	Over 4.0	
Bituminous coal:										
Alabama	889.2	1,189.3	5,421.7	5,182.8	458.8	417.4	-	-	18.6	13,577.8
Alaska	20,287.4	1,100.0	-	-	-	-	-	-	-	21,387.4
Arkansas	-	-	1,128.4	293.1	154.0	-	40.3	-	-	1,615.8
Colorado	25,178.3	37,237.2	-	-	-	-	-	-	-	62,415.5
Georgia	-	76.0	-	-	-	-	-	-	-	76.0
Illinois	-	573.7	4,942.4	2,615.1	809.6	16,583.8	33,650.4	57,652.2	19,062.0	135,889.2
Indiana	197.5	173.0	3,645.2	4,248.8	3,543.4	4,110.5	10,872.8	5,105.9	2,944.0	34,841.1
Iowa	-	-	-	-	-	-	117.1	-	6,405.4	6,522.5
Kansas	-	-	519.9	519.7	1,038.7	2,070.6	4,148.0	8,287.3	4,153.8	20,738.0
Kentucky:										
West	-	-	1,119.6	162.0	336.3	3,793.6	12,759.3	13,643.3	5,081.3	36,895.4
East	13,639.9	8,491.9	2,286.8	1,658.8	1,158.3	2,154.4	24.7	-	-	29,414.8
Maryland	-	-	-	124.6	191.8	208.2	378.6	56.4	220.4	1,180.0
Michigan	-	-	-	-	-	-	-	205.0	-	205.0
Missouri	-	-	-	-	-	-	6,456.7	20,669.2	21,634.1	78,760.0
Montana	51.2	218.2	205.0	397.2	400.0	175.0	40.0	27.0	591.0	2,104.6
New Mexico	5,212.0	5,474.0	-	-	-	-	-	-	-	10,686.0
North Carolina	-	-	-	-	-	110.0	-	-	-	110.0
Ohio	-	611.0	369.0	2,110.2	2,750.4	7,810.5	9,785.3	10,148.2	8,439.4	41,024.0
Oklahoma	250.6	772.2	825.0	368.1	-	-	577.2	19.1	490.6	3,302.8
Oregon	-	14.0	-	-	-	-	-	-	-	14.0
Pennsylvania	44.0	1,154.4	7,624.4	12,424.9	19,689.5	9,995.6	5,287.6	1,150.5	580.6	57,951.5
Tennessee	3.3	160.9	715.9	258.7	178.2	190.5	219.7	43.8	68.5	1,839.5
Texas	-	-	-	-	7,978.0	-	-	-	-	7,978.0
Utah	8,551.4	13,584.0	-	1,524.9	-	-	-	-	3,997.7	27,658.0
Virginia	1,981.5	6,077.5	1,637.1	-	123.9	-	-	-	-	9,820.0
Washington	898.9	672.1	-	-	-	-	-	-	-	1,571.0
West Virginia	20,761.0	26,710.6	21,819.7	13,290.6	8,496.1	2,491.8	3,147.4	5,949.2	-	102,666.4
Wyoming	6,222.2	6,596.6	-	-	-	-	-	-	1.1	12,819.9
Other States[1]	-	616.0	-	-	-	-	-	-	-	616.0
Total	104,168.4	111,502.6	52,260.1	45,179.5	47,307.0	50,111.9	87,505.1	122,957.1	103,688.5	724,680.2
Percent of total	14.4	15.4	7.2	6.2	6.5	6.9	12.1	17.0	14.3	100.0
Subbituminous coal:										
Alaska	71,115.6	-	-	-	-	-	-	-	-	71,115.6
Colorado	13,320.8	4,908.7	-	-	-	-	-	-	-	18,229.5
Montana	94,084.4	36,728.0	0.5	1,303.7	-	-	-	-	-	132,116.6
New Mexico	38,735.0	12,000.0	-	-	-	-	-	-	-	50,735.0
Oregon	87.0	87.0	-	-	-	-	-	-	-	174.0
Utah	-	-	150.0	-	-	-	-	-	-	150.0
Washington	3,693.8	500.0	-	-	-	-	-	-	-	4,193.8
Wyoming	35,579.7	72,315.6	-	-	-	-	-	-	8.6	107,903.9
Other States[2]	-	4,047.0	-	-	-	-	-	-	-	4,047.0
Total	256,616.3	130,586.3	150.5	1,303.7	-	-	-	-	8.6	388,665.4
Percent of total	66.0	33.6	0.1	0.3	-	-	-	-	(3)	100.0
Lignite:										
Alabama	-	-	20.0	-	-	-	-	-	-	20.0
Arkansas	280.0	70.0	-	-	-	-	-	-	-	350.0
Montana	60,214.5	24,141.6	2,660.9	-	-	464.7	-	-	-	87,481.7
North Dakota	284,129.1	34,987.3	31,581.6	-	-	-	-	-	-	350,698.0
South Dakota	-	2,031.0	-	-	-	-	-	-	-	2,031.0
Texas	-	-	6,902.0	-	-	-	-	-	-	6,902.0
Washington	-	116.6	-	-	-	-	-	-	-	116.6
Other States[4]	-	42.0	-	-	-	-	-	-	-	42.0
Total	344,623.6	61,388.5	41,164.5	-	-	464.7	-	-	-	447,641.3
Percent of total	77.0	13.7	9.2	-	-	0.1	-	-	-	100.0
Anthracite:										
Alaska	2,101.0	-	-	-	-	-	-	-	-	2,101.2
Arkansas	-	-	-	145.5	286.3	-	-	-	-	431.8
Colorado	-	90.0	-	-	-	-	-	-	-	90.0
New Mexico	-	6.0	-	-	-	-	-	-	-	6.0
Pennsylvania	12,211.0	-	-	-	-	-	-	-	-	12,211.0
Virginia	335.0	-	-	-	-	-	-	-	-	335.0
Washington	5.0	-	-	-	-	-	-	-	-	5.0
Total	14,652.0	96.0	-	145.5	286.3	-	-	-	-	15,179.8
Percent of total	96.5	0.6	-	0.9	2.0	-	-	-	-	100.0
Grand total	720,060.3	303,573.4	93,575.1	46,628.7	47,593.3	50,576.6	87,505.1	122,957.1	103,697.1	1,576,166.7
Percent of total	45.7	19.3	5.9	3.0	3.0	3.2	5.5	7.8	6.6	100.0

[1]Arizona, California, Idaho, Nebraska, Nevada

[2]Arizona, California, Idaho

[3]Less than 0.1 percent

[4]California, Idaho, Louisiana, Nevada

NOTE: Air quality standards for new plants without sulfur dioxide removal equipment require bituminous coal of no more than 0.7% sulfur. However, Western coals, because of lower heat content, are limited by these standards to less than 0.5% sulfur.

SOURCE: U.S. Bureau of Mines.

Table 2.2. Total Estimated Remaining Measured and Indicated Coal Reserves of the United States as of January 1, 1970* (In Beds 28 in. and More Thick, for Bituminous, Anthracite and Semi-Anthracite, and 5 ft or More Thick for Subbituminous and Lignite Beds - Million Tons)

State	Remaining Measured and Indicated Reserves				
	Bituminous	Subbituminous	Lignite	Anthracite Semi-Anthracite	Total
Alabama	1,731	0	†	0	1,731
Alaska	667	5,345	‡	§	6,012
Arkansas	313	0	†	67	380
Colorado	8,811	4,453	0	16	13,280
Georgia	18	0	0	0	18
Illinois	60,007	0	0	0	60,007
Indiana	11,177	0	0	0	11,177
Iowa	2,159	0	0	0	2,159
Kansas	328	0	0	0	328
Kentucky West	20,876	0	0	0	20,876
Kentucky East	11,049	0	0	0	11,049
Maryland	557	0	0	0	557
Michigan	125	0	0	0	125
Missouri	12,623	0	0	0	12,623
Montana	862	31,228	6,878	0	38,968
New Mexico	1,339	779	0	2	2,120
North Carolina	Ψ	0	0	0	†
North Dakota	0	0	36,230	0	36,230
Ohio	17,242	0	0	0	17,242
Oklahoma	1,583	0	0	0	1,583
Oregon	**	**	0	0	**
Pennsylvania	24,078	0	0	12,525	36,603
South Dakota	0	0	757	0	757
Tennessee	939	0	0	0	939
Texas	**	0	6,870	0	6,870
Utah	9,155	150	0	0	9,305
Virginia	3,561	0	0	125	3,686
Washington	312	1,188	0	0	1,500
West Virginia	68,023	0	0	0	68,023
Wyoming	3,957	25,937	‡	0	29,912
Other States	**	**	46	0	46
Total	261,510	69,080	50,781	12,735	394,106

*Figures are reserves in ground, about half of which may be considered recoverable. Includes all beds under less than 1,000 ft of overburden and over 28 in. in bed thickness for bituminous and anthracite and 5 ft or more for subbituminous and lignite.

†Small reserves of lignite in beds less than 5 ft thick.

‡Small reserves of lignite included with subbituminous reserved.

§Small reserves of anthracite in the Bering River Field believed to be too badly crushed and folded to be economically recoverable.

ΨNegligible reserves with overburden less than 1,000 ft.

**Data not available to make estimate.

	Recoverable Reserves (billions of tons)
Deep Minable	175
Strippable	45
Total	220

The recoverable reserves are equivalent to about 65 years at a rate of consumption equivalent to the total national energy use in 1970.

Most of the low sulfur coal is located in the western United States in the form of strippable sub-bituminous coal and lignite. As shown in Fig. 2.3 of the 45 billion tons of strippable reserves, about 25 billion tons are low sulfur located in the Rocky Mountain States.[2]

Availability. It is evident that the coal reserves are adequate to meet almost any demand in the foreseeable future. The limiting factors on the use of coal are (1) environmental constraints on mining and combustion, (2) coal industry development, and (3) transportation.

Most of the present concern is related to the effects of strip mining on land and water. It should be noted, however, that underground mining is not without adverse impacts, including death and injury rates approximately five times higher than for strip mining.[3] The Coal Mine Health and Safety Act of 1969 set tighter standards to reduce the hazards of underground mining. A side effect of the Act was to decrease productivity and increase capital investments required for deep mining. As a consequence, strip mining accelerated because of the improvement in the relative competitive position of this form of mining. Strip mining now accounts for approximately one-half of the total coal production. Because of the trend to more stripping and the vast devastation of land and water resources that has been experienced in some areas, many proposals, ranging from improved reclamation practices to outright bans, have been made to reduce the adverse effects of strip mining. Reclamation of strip-mined areas involves backfilling, compacting, soil conditioning, regrading, and revegetation to achieve a natural appearance. Current estimates[3-5] for reclamation range from $2000 to $6000 per acre, the latter figure corresponding to 20¢ to 30¢ per ton of coal (for coal yields of 20,000 to 30,000 tons/acre). For

ORNL -DWG 74 12793

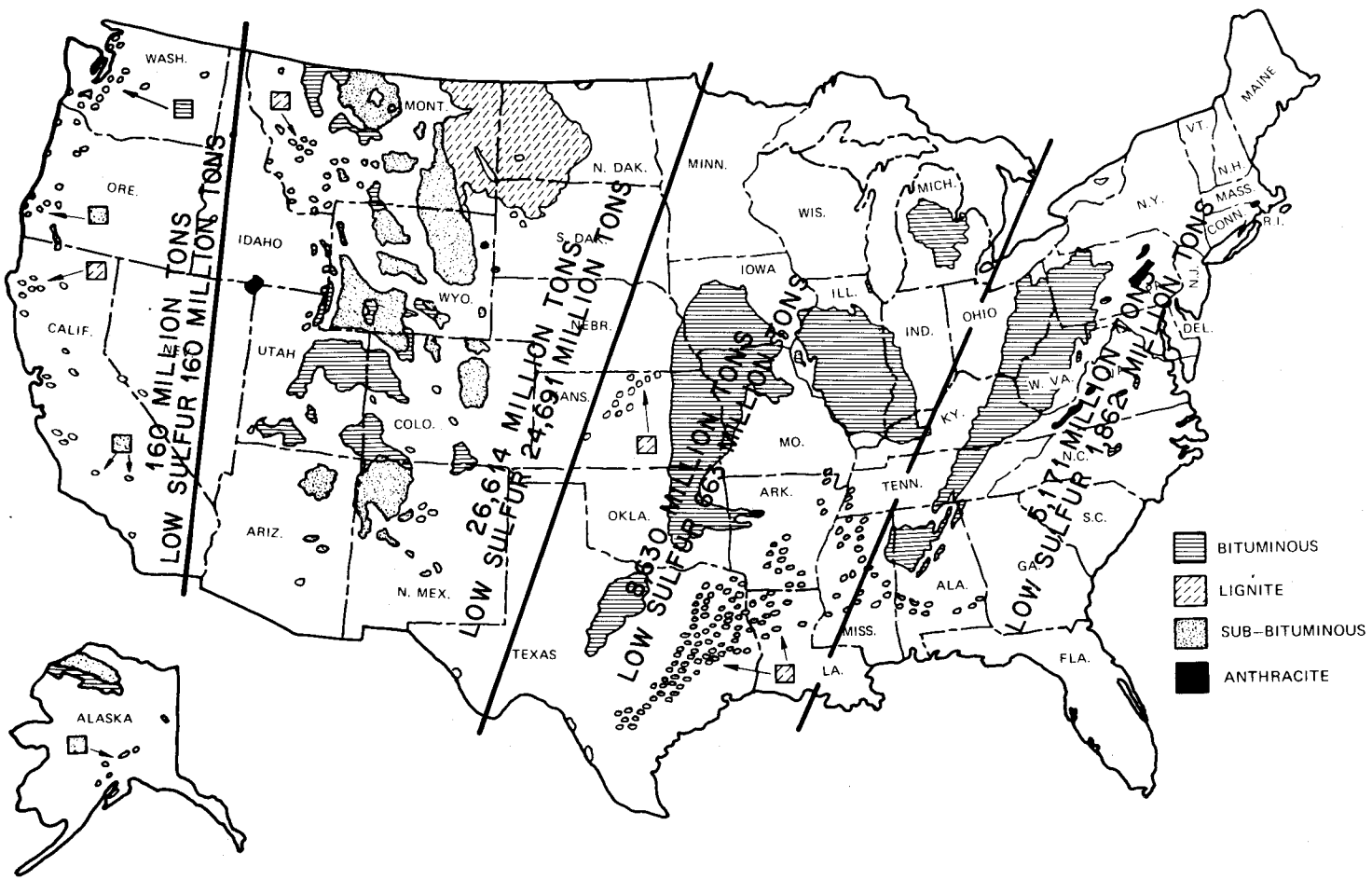

Fig. 2.3. Strippable reserves of the conterminous United States, by region.

western coal from thick beds, the surcharge for reclamation might be only 3¢ to 4¢ per ton. It would appear, if these figures are correct, that the issue in strip mining is not reclamation costs since the contribution to the cost of coal would be minor. Rather, the issue seems to concern the question of what constitutes acceptable reclamation. There is no reasonable way to restore stripped land to its original condition — only to a condition that some would consider acceptable. Ultimately, society must make the judgment concerning benefits and costs of surface mining. If, as some have suggested, surface mining were banned, the ability of coal to satisfy a larger portion of our nation's energy needs would be seriously impaired. The National Petroleum Council (NPC)[6] estimates that the coal production would decline by over 40% at least until 1985 if stripping were banned.

Coal production and coal processing in some western states pose additional environmental and societal problems. Water use associated with strip reclamation, slurry pipelines, and, in particular, coal gasification plants, could be significant. Such use would be in direct competition with established agricultural and industrial activities. The water question will be an important issue in the expansion of the coal industry in the West.[7]

Coal Costs

Coal Values at Mine. After a long period of stability, the price of coal started rising significantly after 1969. From 1965 through 1969, the U.S. average price (f.o.b. mine) of coal sold on the open market was about 25¢/10^6 Btu (constant 1974 dollar basis).[8,9] By 1972 the average price had risen to about 35¢/10^6 Btu. Figure 2.4 shows the price trends through 1972 — the last year on which complete data are available. U.S. average prices tend to reflect the value of coal mined east of the Mississippi. Also shown in Fig. 2.4 are prices for sub-bituminous coal and lignite produced in selected western states; generally, prices for western coal have tended to decline with time — at least through 1972.

The data of Fig. 2.4 are based on reports by the U.S. Bureau of Mines[8,10] and the National Coal Association.[9,11] Modifications to the original data were made to convert from cost per unit weight to cost per unit energy and to convert to a constant 1974 dollar basis. Although the heating value of

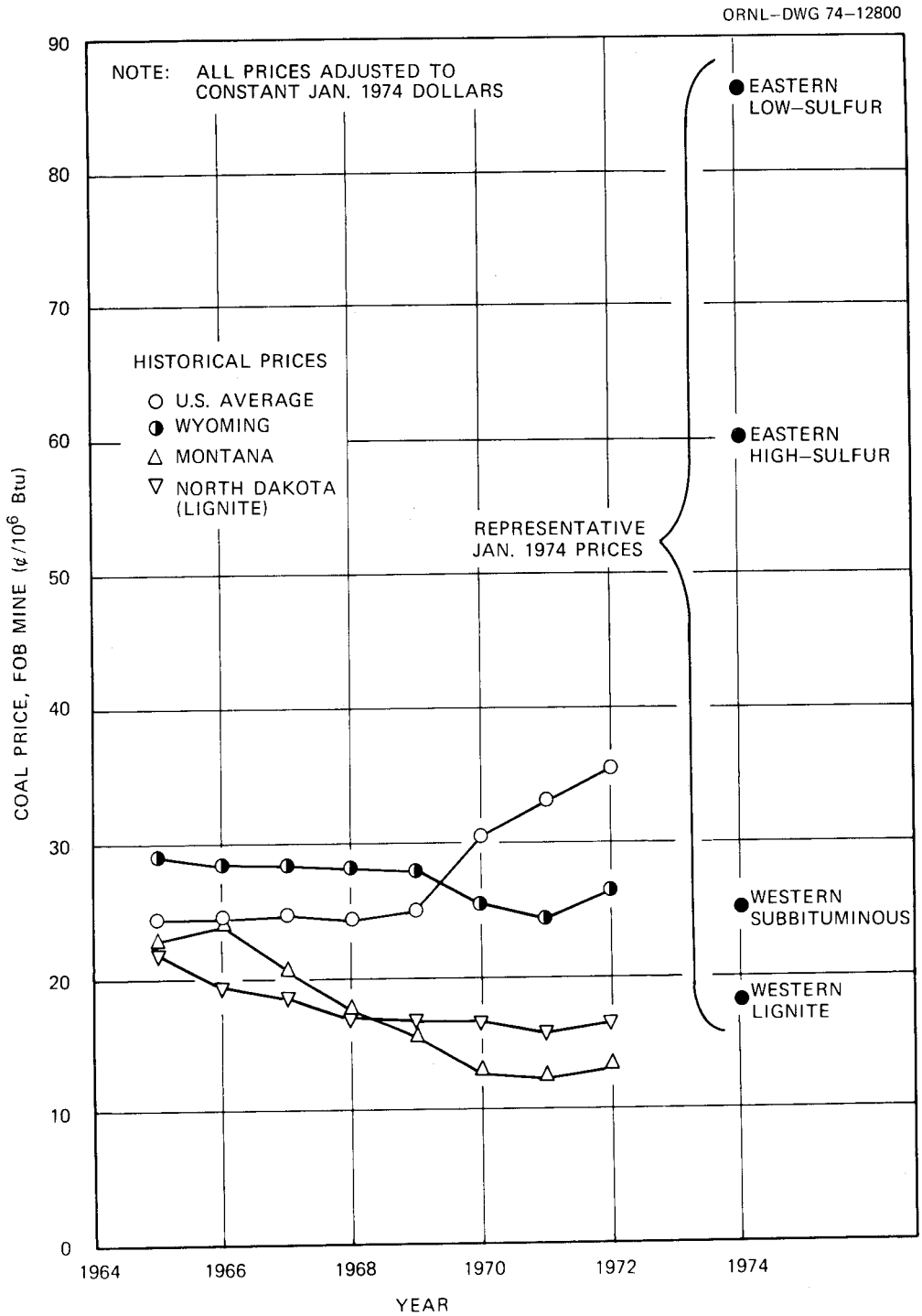

Fig. 2.4. Trends in coal prices.

coal varies substantially even within a given rank, the following values, used by the NPC,[6] were adopted for this study:

Rank	Heating Value (million Btu/ton)
Bituminous	23
Sub-Bituminous	17
Lignite	13.5
Anthracite	25.4

Price adjustments to January 1974 were made using the wholesale price index for industrial commodities.

Although there are no compilations of current coal prices, it is evident from various reports that coal prices, along with those of other fuels, rose dramatically in late 1973 and early 1974.

The Tennessee Valley Authority (TVA)[12] reports that prices range from \$8 to \$30/ton (f.o.b. mine) depending on the type of contract, quality of coal, and location. A reasonable range for high sulfur (3 to 4%) strip-mined coal from western Kentucky and southern Illinois is \$12 to \$18/ton (f.o.b. mine) or 50 to 75¢/10^6 Btu. Coal purchases for AEC plants in Kentucky and Tennessee made in the fall of 1973 were at a price of \$9.75/ton.[13] Recent (January 1974) prices were about \$15/ton (3.4% sulfur, 12,500 Btu/lb) or 60¢/10^6 Btu. The South Carolina Public Service Authority reported[14] a coal price jump of 39% in the last five months of 1973. As of January 1, 1974, the delivered price was \$17.25/ton. After allowing for transportation, the mine price is inferred to be \$12 to \$14/ton. Public Service Electric and Gas Company (New Jersey) (PSE&G) paid an average of \$25.36/ton for low sulfur coal delivered to their plants during January 1974.[15] This represented a 44% increase from the average price in October 1973. The range on January 1974 delivered prices paid by PSE&G was from \$22.90/ton for coal under contract to \$29.51/ton for spot purchases. These figures suggest a mine price of 18 — \$25/ton for eastern low sulfur coal.

Recent data available on western coal prices are sketchy. Nebraska Public Power District purchased Colorado and Wyoming low sulfur coal for

55 to 62.7¢/10^6 Btu (delivered) during October and November 1973.[16,17] Allowing $5.00/ton for delivery to plants at Lincoln and Bellvue, the derived mine cost would be 30 to 43¢/10^6 Btu.

November 1973 purchases by Black Hills Power and Lighting[17] of subbituminous low sulfur coal from Wyoming for plants at Osage, Wyoming, and Lead, South Dakota, ranged in delivered prices from 20.3 to 32.8¢/10^6 Btu. Since the power plants are relatively near coal fields, the transportation cost would presumably be on the order of 5¢/10^6 Btu. Recent delivered prices of lignite at plants in North Dakota and Montana ranged from 11.6 to 28.7¢/10^6 Btu.[17] Since these power plants are near the lignite deposits, the transportation component of the delivered price should be small. The general impression is that western coal prices have not increased as substantially as those for eastern coal.

Representative prices as derived from the sources described above are shown in Table 2.3 and range from 18¢/10^6 Btu for western lignite to 128¢/10^6 Btu for Pennsylvania anthracite coal. Average coal prices for February 1974 by sulfur content are given for each state in Appendix B. In determining the future applicability of coal to uses ordinarily satisfied by other fuels, it is necessary to judge whether the recent large price increases for eastern coal represent a response to a short-term supply-demand situation or whether they are permanent.

Transportation Cost. Long distance movement of coal is by rail, barge, and in one case, pipeline. Rail is by far the most important form of transportation but barge movement on inland waterways is significant. Coal slurry pipelines are expected by some to become an important mode of transportation especially for moving western coals to regions of high energy use.

Rail. The average rail cost for coal shipment is about 10 mills/ton-mile.[6] Rates are influenced by a number of factors but the most important are (1) distance, (2) volume, and (3) whether shipment is by individual cars or by unit train. TVA data[18] for one particular power plant, located approximately 100 miles from the mine, indicate rates of about 14 mills/ton-mile for individual cars and 13 mills/ton-mile for unit train. In a study of coal pipelines, Wash and Thompson[18] suggest a rate of 5 to 6 mills/ton-mile for long haul unit trains. The NPC[6] indicates a rate of 5 mills for some unit train hauls. The 1970 National Power Survey[19] presented a range

Table 2.3. Representative Prices (f.o.b. Mine) for Coal as of First Quarter 1974

	Heating Value (Btu/lb)	Cost/ton ($)		Cost/10^6 Btu(¢)	
		Rep. Value	Range	Rep. Value	Range
Bituminous (Eastern)					
High Sulfur (>3%)	11,500	14	10-18	60	43-78
Low Sulfur (<1%)	11,500	20	16-25	86	69-108
Sub-Bituminous (Western)					
Low Sulfur (∿0.5%)	8,500	4.25	3.40-6.80	25	20-40
Lignite (Western)					
Low Sulfur (∿0.5%)	6,750	2.50	1.60-3.25	18	12-24
Anthracite	12,700	32.50	20-45	128	79-177

Table 2.4. Coal Transportation Costs for Various Modes of Long-Haul Movement

	Cost per 100 Miles (¢/10^6 Btu)					
	Unit Train		Barge		Pipeline	
	Base	Range	Base	Range	Base	Range
Bituminous	2.4	2.0-2.8	1.3	1.1-1.5	1.7	1.3-2.8
Sub-Bituminous	3.2	2.6-3.8	1.8	1.5-2.1	2.4	1.8-3.8
Lignite	4.1	3.3-4.8	2.2	1.9-2.6	3.0	2.2-4.8

of 3.5 to 8 mills per ton-mile for unit train and 1.5 to 4 mills for integral coal trains. Burlington Northern's estimate, as reported by Oak Ridge National Laboratory (ORNL),[20] for unit train transport of western coal from Gillette, Wyoming, to St. Louis, Missouri, (1,074 miles) is $5.94/ton or 5.5 mills/ton-mile.

For evaluation purposes, it is assumed that short haul (approximately 100 miles) rail transport would cost 13 mills/ton-mile with a range of 10 to 15 mills/ton-mile. Long haul (500 miles) rates were assumed to be 5.5 mills/ton-mile with a range of 4.5 to 6.5.

Barge. U.S average barge rates are reported[6] to be 3 mills/ton-mile and with large volume contracts as low as 2.5 mills. An ORNL study[20] indicated a rate of 3.5 mills/ton-mile for barge shipment of coal from St. Louis to Madison, Indiana. In the present study a base rate of 3 mills/ton-mile, with a range of 2.5 to 3.5, is assumed.

Pipeline. Wash and Thompson[18] derived slurry pipeline costs for various transport distances and capacities. For a 1000-mile pipeline, estimated costs ranged from 3 mills/ton-mile for a capacity of 18 million tons/yr to 6.5 mills per ton-mile for a capacity of 6 million tons per year. A representative value of 4 mills, with a range of 3 to 6.5, was selected for the present study.

Basic unit transportation cost data for long hauls assumed for the present study are summarized in Table 2.4. The cost per million Btu for 100 miles of movement for three ranks of coal were derived using assumed heating values discussed previously.

Trucking. Coal transport by truck seldom exceeds a distance of 60 miles. The cost of coal delivery by truck varies with distance, terrain and local labor rates. Typical rates in the Tennessee Valley are $18/hr for a tandem or semitrailer truck carrying 24 tons of coal. Thus over a distance range of 10 to 50 miles the cost varies between $1.50 to $2.50/T of coal.

Coal-Derived Fuels

Coal Gasification. One of the possible ways to use coal and meet emission standards is through a two-stage combustion process in which coal is partially oxidized in a gasifier, the particulates and sulfur compounds

are scrubbed from the gas stream and the gas is then burned in a boiler or furnace. Depending upon the process employed the product gas may range in higher heating value from 130 to 1000 Btu/scf. When air and steam are used, a low Btu gas is produced which has a heating value of 130 to 300 Btu/scf. If the air is enriched in oxygen or if oxygen is substituted for air, an intermediate Btu gas having a heating value of 300 to 500 Btu/scf can be produced. Alternately pipeline quality gas (∿1000 Btu/scf) may be produced by employing an additional catalytic methanation step after the gas has been purified. The principal coal gasification processes which are available commercially are:

1. The Lurgi process offered by American Lurgi Company, New York, N. Y.
2. The Koppers-Totzek process offered by Koppers Company, Pittsburgh, Pennsylvania.
3. The Wellman-Galusha process supplied by the McDowell Wellman Company, Cleveland, Ohio.
4. The Winkler process offered by Davy Powergas, Inc., Lakeland, Florida.

A summary of the characteristics and status of the processes is presented in Table 2.5. As noted in Table 2.5, some processes are not capable of utilizing all ranks of coal. Consequently it is necessary to match the equipment with the particular coal feed.

A number of other coal gasification processes are currently under active development in the U.S. These are concerned largely with the coal gasification and coal hydrogenation reactions and with the method of heat supply. A development program between the Office of Coal Research (OCR) and the American Gas Association (AGA) is now underway and funded at the level of $30 million per year. The major emphasis of this program is on three processes: Hygas, CO_2 Acceptor, and Bigas.[21] Independently, the Bureau of Mines is actively involved in work on two processes. The most advanced of these, with respect to stage of development, is the Synthane process.

Other processes which are being investigated include Atgas, Molten Carbonate, and Hydrane.[21] It should also be noted that some development

Table 2.5. Characteristics of Commercial Processes for the Production of Low and Intermediate Btu Gas from Coal

Process	Gasifier Type	Gasifier Pressure (psig)	Oxidizing Medium	Comments
Lurgi	Downward moving stirred bed, nonslagging	300-450	Air or oxygen	Process is in commercial operation on sized, noncaking coal. Plans are under way to test operation on caking bituminous coal.
Koppers-Totzek	Concurrent solid-gas combustion, slagging	1-5	Oxygen or oxygen-enriched air	Process is in commercial operation using oxygen. Offered in sizes to 35 tons of coal per hr. Tests are planned using enriched air. Can handle any type of coal.
Wellman-Galusha	Downward moving stirred bed, nonslagging	1-300	Air or oxygen	Process is in commercial operation using coke or noncaking coals, mostly in the steel and ceramics industries. Is commercially offered in sizes to 7000 lb per hour of bituminous coal. Bureau of Mines has a pilot plant operating on caking coal at pressures up to 125 psig, capacity about 20 tons/day. Tests are planned at 300 psig to increase throughput.
Winkler	Fluidized bed	15	Air or oxygen	Sixteen installations were built outside the U.S. from 1926-1960 with generator capacities of 100-300 x 10^6 Btu/hr. Three installations are presently in operation. Process description states it will operate on all coals. Tests are planned at 15 atm.

work is needed for the catalytic methanation of intermediate Btu gas to produce pipeline quality gas. This work is under way and it is not anticipated that the methanation step will delay the commercial development of pipeline quality gas via coal gasification.

Coal Liquids. Heavy fuel oils can also be produced from coal. Since a great deal of the sulfur in coal is tied up as inorganic constituents of the ash, it is possible, by liquefaction and removal of the ash, to produce a heavy fuel oil (or deashed coal) from which a portion of the sulfur has been removed. This material has a high melting point above 93°C (200°F). The sulfur content of the deashed coal depends on the coal feed. The usual type of processing consists of contacting coal (in a slurry oil vehicle) with hydrogen at 1000 to 5000 psia and 399 to 454°C (750 to 850°F). Under these conditions, the coal depolymerizes sufficiently so that the total mixture can be filtered to recover the heavy oil product and a solid residue.

Coal liquefaction is not as close to commercialization as coal gasification. However, there are some definite advantages to liquefaction as compared to high-Btu gasification which merit consideration. Less hydrogen is required to convert coal ($CH_{0.7-0.9}$) to a liquid fuel (about $CH_{1.1}$) than is needed for production of pipeline gas (CH_4), and synthetic fuel oil is easy to store. Transportation of oil costs only about half as much as pipeline gas transmission. The energy conversion efficiency of coal liquefaction is considerably better than that for high-Btu gas production with present technology.

Four major processes offer merit in coal liquefaction and are being funded by the OCR (over $20 million each). These processes are H-Coal,[28,29] Consol,[22] COED,[23,24] and Solvent Refined Coal.[25-27]

Solvent-Refined Coal. If the only objective of coal treating is the production of a clean fuel, then hydrogenation to produce solution can be minimized and be followed by ash separation and conversion of sulfur to a removable form. Solvent refining was initiated with the limited objective of producing a low-cost antipollution alternative to residual oil and natural gas for use under boilers.

At present none of these processes is commercial but each has reached a pilot plant stage. Commercial production is projected to be about 1983.

Methanol. The technology for making methanol or "methyl fuel" via coal gasification is available. Several types of suitable coal gasifiers are available and at least two methanol synthesis processes are in commercial use. However, no integration of this technology has been attempted on a currently commercial scale of production. Because of its high cost, methanol holds no promise as a base fuel for large boilers. However, since it can readily be transported and stored in conventional equipment it might be of interest as a standby fuel for a MIUS. It is a clean, nonpolluting fuel and it has been demonstrated to be suitable for firing boilers.[30]

Cost of Coal-Derived Fuels. Production of high Btu gas, liquid fuels and solvent refined coal will undoubtly be carried out at or near the mine mouth to obviate the cost of coal transport. Because of the lower heating values of low or intermediate Btu gas, it is not economical to transport them except for short distances. Consequently, they must be produced at or near the point of use.

Cost projection for the various fuels were prepared using plant equipment and operating costs which have been published or cost data which was provided by equipment vendors. The reference case assumed a mine mouth coal cost of 50¢/10^6 Btu based on eastern coal. For low and intermediate Btu gas it was assumed that coal would be shipped by train for a distance of 100 miles with a subsequent haul by truck of 25 to 50 miles. This transport cost would add an additional 25¢/10^6 Btu to the cost of delivered coal (75¢/10^6 Btu total). All calculations were based on a 22.2% fixed charge rate on capital. The projected costs (in 1974 dollars) based on these ground rules are presented in Table 2.6 along with the projected year of proven demonstration. Commercial plants would be expected to be in operation about two years after successful completion of the demonstration plant program.

The projected cost of high Btu gas is based on economic data for El Paso Gas Company's proposed Burnham Coal Gasification Project which recently received tentative approval from the Federal Power Commission. Essentially all coal gasification projects to produce pipeline quality gas have been proposed by gas transmission companies. This synthesis gas will be mixed with natural gas from various sources for delivery throughout the

Table 2.6. Status and Projected Cost of Coal-Derived Fuels

Technology	Status	Projected Price, $\$/10^6$ Btu	Projected Year of Proven Demonstration Operation
Low or Intermediate Gas from Coal	Pilot Plant	1.86 - 2.37	1978
High Btu Coal Gasification	Pilot Plant	2.39*	1981
Coal Liquefaction	Small Pilot Plant	1.58 - 1.92*	1982
Solvent Refined Coal	Pilot Plant	1.07 - 1.30*	1981
Methanol from Coal	Demo	2.91*	1981

*Cost at mine mouth exclusive of transportation costs.

pipeline network. Consequently the selling price of the gas will be the prevailing rate at the point of use.

A major consideration in assessing the economics of an on-site coal gasification or liquefaction plant for a MIUS installation is the effect of the size of coal gasification or liquefaction plants on both the capital cost and the size of the crew required for their operation. The latter is important because it represents a major factor in the operating costs of the system. Fortunately, data are available in an OCR publication[21] for the OCR projected capital cost of such plants as a function of the coal feed rate in tons per day. A long dashed line for this projection is presented in Fig. 2.5. Data given in the same report for the construction cost and operating crew size are also plotted in Fig. 2.5, and a line has been drawn through the lower portion of the scatter band of points for the operating crew size. These data will be used in the next section for appraising the relative merits of on-site coal gasification and liquefaction plants with respect to fluidized bed coal combustion systems. It should

ORNL DWG. 75-16530

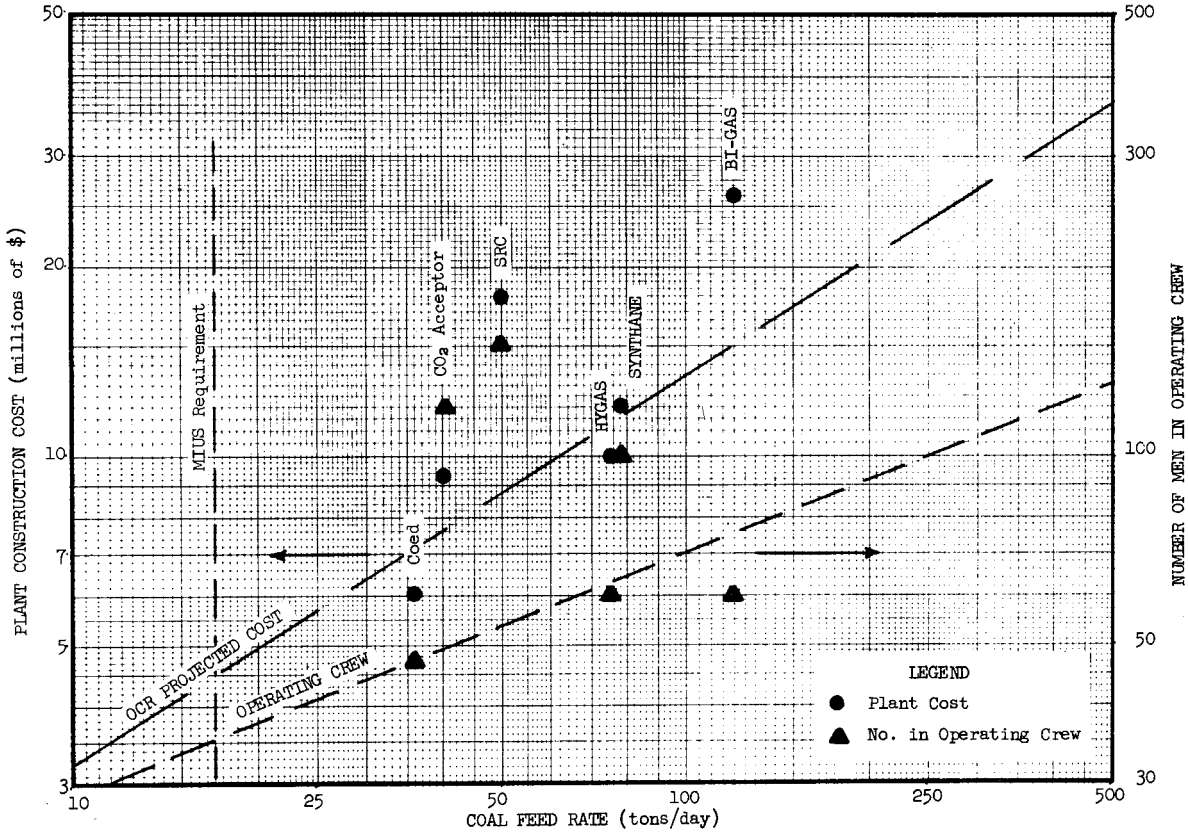

Fig. 2.5. Effects of plant capacity on plant construction cost and operating crew size for coal gasification and liquefaction. (Data from "Clean Energy from Coal," OCR, 1973).

be mentioned that an independent comprehensive study at ORNL has yielded substantially the same values as OCR projections in Fig. 2.5.[31]

Coal and Limestone Preparation for Fluidized Bed System

In an effort to assess the cost of coal for a fluidized bed system as a function of the particle size a reference design for a coal and limestone preparation plant was prepared. This plant would process run-of-the-mine coal and limestone to the desired particle size and serve as a distributor to supply a complex of MIUS systems. The handling and preparation process illustrated in Fig. 2.6 includes receiving, storage, crushing, and conveying of the coal and limestone to carriers for distribution to various systems located remotely from the preparation site.

Coal or limestone arrives at the plant by unit train or truck, is discharged into the receiving hoppers, and is transferred over magnetic head pulleys (to remove tramp iron) to an open pit dead storage system. The dead storage system includes sufficient capacity to accommodate interruptions in the limestone or coal delivery of up to four weeks duration.

The coal or limestone is conveyed from the stockpile to the transfer house and from there to the hammer mills where it is ground to minus 1/8 + 0 in size. The product from the hammer mills is classified to insure that particles larger than 1/8 in. are separated from the finished product and are recycled to the hammer mills for further processing. The finished product is conveyed to covered storage bins to await distribution to ultimate consumers.

Shown in Table 2.7 are costs and power requirements as derived from a study of a coal preparation system proposed by the U. S. Bureau of Mines for a coal gasification plant.[32] The items listed are only those required for coal and limestone crushing and do not include any of the pulverizing equipment required for a coal gasification plant. The costs listed were escalated 20% to allow for price changes from 1970 to 1974.

The limestone preparation was assumed to be a joint operation with the coal facility. The cost of the limestone portion of the preparation plant was assumed to be 25% of the cost for the coal, bringing the total cost to $4,430,000 and the electric power requirements to 1.8 kWhr per ton of coal processed.

ORNL DWG. 75-14461

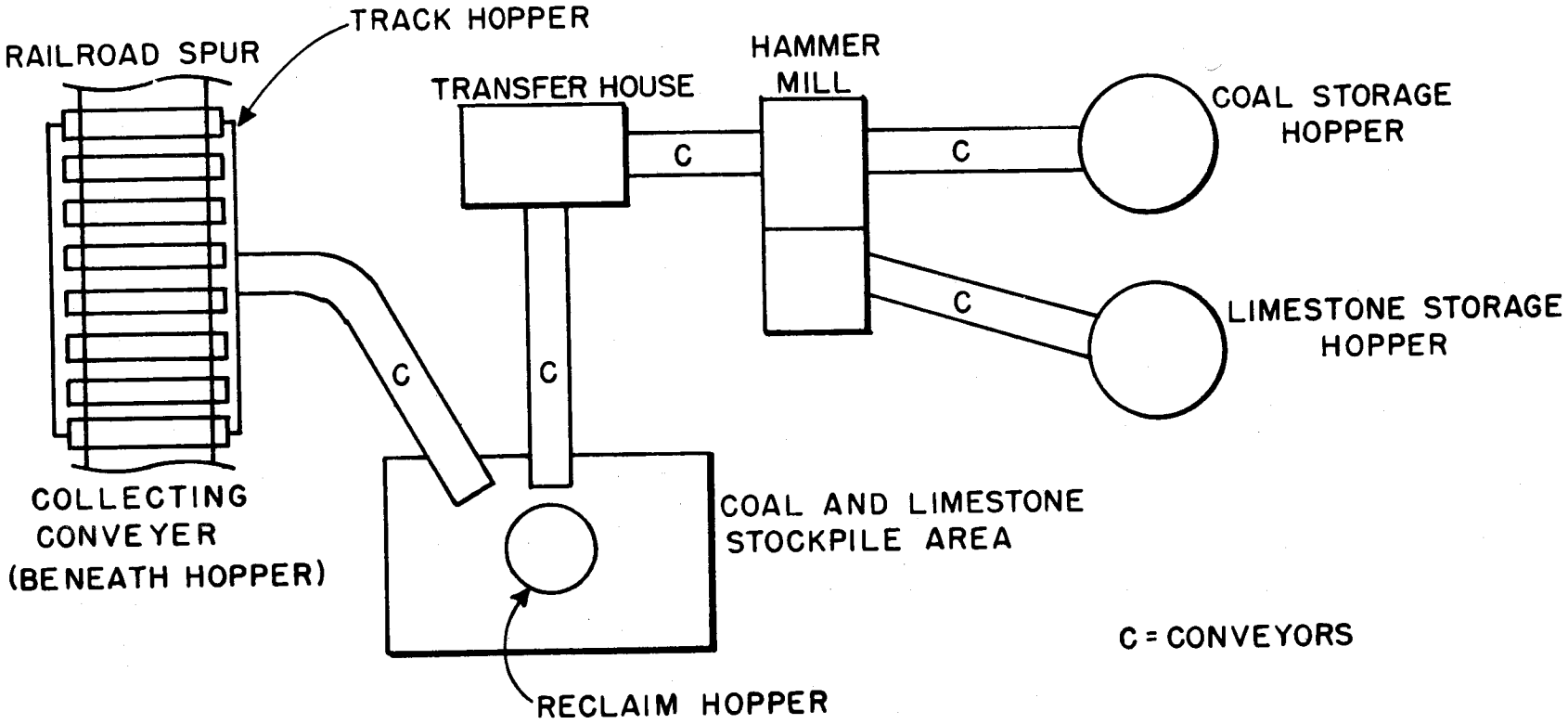

Fig. 2.6. Coal and limestone preparation plant.

Table 2.7. Costs and Power Requirement for A Coal Preparation Facility to Supply 4.7 x 10^6 Tons of Minus 1/8 + 0-Inch Coal Annually

	Cost ($)	Power Requirement (hp)
Track hopper and collecting conveyor	310,000	18
Stockpile feed and reclaim conveyors	87,000	80
Reclaim hopper	11,000	-
Transfer house	8,000	-
Hammer mill feed and product conveyors	138,000	80
Hammer mills	117,000	720
Reclaiming cyclones and dust control	194,000	150
Product storage hopper	117,000	-
Installation and construction	1,380,000	-
Engineering, administrative, and contingency	1,182,000	-
Total	3,544,000	1,048

The following process assumptions were made in order to obtain the unit cost of the coal and limestone preparation as a function of production:

1. One operator required per 100 tons of coal and associated limestone processed per hour.
2. The operator labor charges would be $5/hr.
3. The maintenance charge would be 1/5 of the operator labor charge.
4. Overhead and administration charge would be 100% of the operator and maintenance labor charges.
5. The productivity factor would be 0.9.
6. The electric power cost would be 30 mils.
7. The cost of the coal and limestone facility will vary as the 0.6 power of the processing rate.

Using these assumptions the unit cost of the coal and associated limestone production facility for yearly production rates from 1000 to 1,000,000 tons were obtained. The values are given in Fig. 2.7 as functions of the capitalization charge and the number of 8 hr shifts per week that the plant would be operated.

The total coal requirements for a 2000 kW(e) total energy installation is estimated to be approximately 6000 ton/yr. Table 2.8 shows the delivered unit cost of coal and limestone for various numbers of 2000 kW(e) installations using a 15% capitalization charge and the lower one of the two curves for 5 and 21 shift/week. A delivery charge of $1 per tons was made independent of the number of facilities served.

Table 2.8. Unit Cost of Coal and Associated Limestone Delivered to a 2000 kW(e) Total Energy Installation

Number of Installations	Delivered Unit Cost ($/ton)
1	10.25
15	3.00
150	1.47

For comparison, the coal and associated limestone preparation charge at 15% capitalization and 21 shifts per week operation for a production rate of 10^6 ton/yr is 47¢/ton as compared to 81¢/ton for the pulverized coal prepared for the gasification plant described in Ref. 32. The balance of the charges of Table 2.8 are middleman's charges for coal handling and delivery.

On-site preparation of the fuel and limestone for the total energy system was considered. The problems associated with unloading, storing, and control of dusting of the run-of-mine coal and limestone at the energy installation site would probably increase the remote single installation preparation cost by $2 to $3/ton over the cost of prepared coal from a distributor with a capacity for 20 MIUS installations.

ORNL DWG. 75-14490

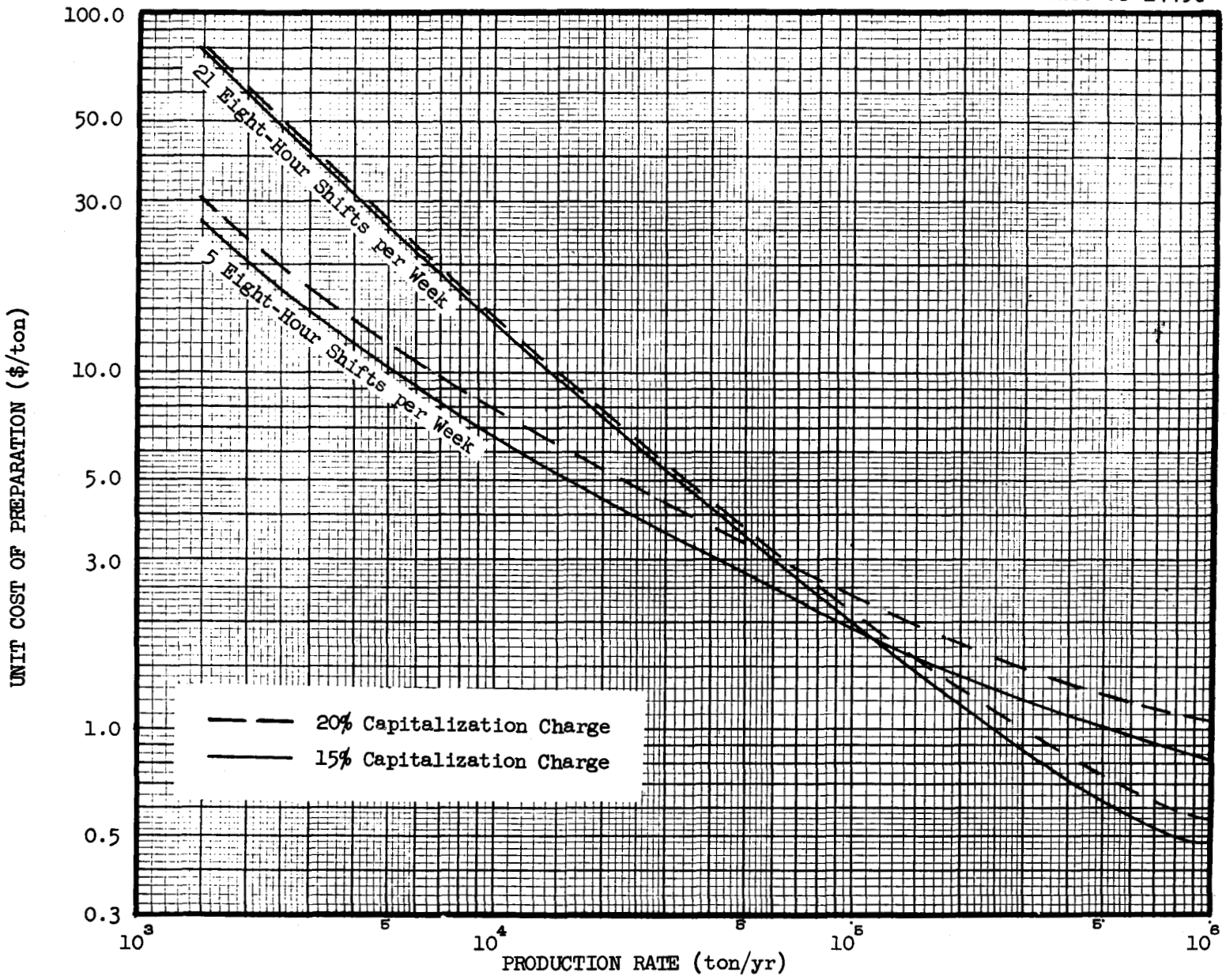

Fig. 2.7. The unit cost of the preparation of coal and associated limestone to minus 1/8 + 0 inch size.

Use of Coal in Municipal Waste Treatment

Considerable interest has developed in the use of coal as a filter medium for sewage treatment. It is of special interest in the MIUS system where the spent coal sewage sludge mixture could be used as fuel in the fluidized bed furnace.

The Rand Development Corporation (RDC) has investigated the feasibility of a coal-based sewage treatment process under a contract with the Office of Coal Research.[33] Basically, finely ground coal was used as a filter media for raw sewage and secondary effluent (tertiary treatment). Good suspended solids removal was observed; however, only partial removal of dissolved organics was achieved. The detailed report by RDC covers coal preparation and operation in considerable detail, and estimates costs for IMGD and larger plants. Also discussed is what to do with the coal used.

Coal Preparation for Filtering Sewage

Coal preparation seems to be a critical step in this process. The mesh size proposed is 18 x 120, with the following allowable offsize limits.

1. Oversize - 1 to 2% within one screen size larger.
2. Undersize - 5 to 15% on two screen sizes smaller.
3. Dust - 1.5% smaller than 270 mesh.

The study indicates that a three-step process (grinding, sizing, and dust removal) is necessary to meet these limits. Conventional coal processing technology has developed in two areas: breaking coal into large pieces for shipment from the mines, and crushing coal into dust to fuel power-generating boilers. The 18 x 120 mesh size required for filtration falls between the above sizes, and engineering technology for its production is limited.

Following the coal preparation step, the coal is slurried and placed in the filter. The filter operates downflow and at periodic intervals a scraper removes a thin layer of coal and suspended solids from the top of the filter and transfers it to waste tanks. This represents the material available for burning or incineration.

Preparation of Coal-Sludge Mixtures for Combustion

Limited batch studies on dewatering and incineration were conducted. It was found that the sludge settles to fifty percent solids in one hour. Centrifugation and pressure filtration produce a somewhat higher concentration. The solids content was increased to 67% when coal sewage sludge was dewatered and "blown" with compressed air in a filter press.

Incineration Tests

Incineration tests were conducted by the Detroit Stoker Company in their steam boiler and by Pope, Evans, and Robbins in a laboratory-scale fluidized bed combustor. The Detroit Stoker test was not successful because the stoker system was not designed to handle sludge with a 48% moisture content. Sludge with a 34% moisture content was burned with 83% efficiency in the Pope, Evans, and Robbins test. This test shows that coal sludge can be used as a fuel, although at only 90% of the efficiency of lower moisture-content coal normally used in power plants. This means that heat recovery for steam or power production is feasible, but the means of achieving this are not yet sufficiently developed.

Coal with 50% or higher moisture content can be burned continuously with usable heat recovery; special equipment for handling wet coal will be required, however. Where the sludge will be used for power production, the simplest method might be to mix the sludge with sufficient dry coal to reduce the moisture to a level acceptable for standard equipment. Special design appears necessary if higher moisture contents are to be used and further experimental work may be required.

Air pollution control requirements must be considered in any incinerator design. Depending on the type of incineration equipment and coal used, some amount of particulate matter will have to be removed from the stack gases prior to discharge. It is expected that this can be accomplished using existing particulate removal technology. A more serious problem, at the present time, is the regulations governing the sulfur content of coal and allowable sulfur dioxide emissions. An efficient and economical sulfur removal system has yet to be developed although a number of systems are under study. In lieu of emission control, many regulatory agencies have

limited the allowable concentration of sulfur in the fuel coal. The maximum allowable concentration varies throughout the country up to 2.0%. The sulfur concentrations of both the coal and the filtered solids must be considered with respect to air pollution requirements.

Coal Feed Rates to the Sewage Plant

Some idea of treatment efficiencies can be obtained from Table 2.9. It can be seen that suspended solids removal is about the same for raw or settled sewage; however, more coal is required for raw sewage. In the case of secondary effluent, 92% of the solids were already removed and the filter "polished" the effluent to 98% removal. Whether this step is justifiable will depend on local circumstances.

Comparing the removal efficiencies in Table 2.9 with EPA standards as defined under the Water Pollution Control Act of 1971,[34] it can be seen that only the filtered or unfiltered secondary effluent will meet currently defined standards (85% removal of solids and BOD). Thus, although the coal filter is rather effective in itself, pretreatment by biological or chemical process, or post-treatment by chemical means will be required.

Coal consumption (amount purchased) is 11.8 tons/million gallons for raw sewage, and 1.7 tons/million gallons of secondary effluent treated. For 1000 residential units, the daily volume of waste produced is about 270,000 gal (1000 units x 3.4 people/unit x 80 gas/capita/day). This would require a coal consumption of 3.19 tons/day for raw sewage and 0.46 tons/day for treating secondary effluent.

Summary of System Design Considerations

In a report analyzing the RDC study, the following conclusions were reported:[35]

1. Coal filtration provides excellent suspended solids removal, but dissolved organics are only partially reduced.
2. Coal filtration by itself will not provide sufficient treatment of domestic sewage to meet present water quality criteria. The process may be applicable for one-step industrial waste treatment where only suspended organics need be removed.

Table 2.9. Treatment Efficiencies - Coal Filtration Process

	Percent Removals		
	Suspended Solids	BOD	COD
Raw Sewage	92	55	66
Settled Sewage[a]	92	74	80
Secondary Effluent[b]	98	96	89

[a]This is the total removal for both settling and filtration. Primary settling alone removed 50% of the suspended solids, 50% of the BOD, and 51% of the COD.

[b]This is the total removal for secondary treatment and filtration. The secondary treatment reduced suspended solids by 92%, BOD by 88%, and COD by 84%.

3. The most promising application of coal filtration is a pre- or post-treatment step for suspended solids removal in series with a treatment for removing dissolved organics. Applications may include tertiary domestic sewage treatment of filtration of industrial wastes high in organic suspended solids.
4. The coal filtration process will be economically competitive only when heat is recovered from all of the coal used. This can be most practically accomplished by borrowing coal from a pulverized coal user.
5. The concept of deep-bed precoal filtration is applicable to wastewater treatment. One-step treatment may be possible if an organic adsorptive medium such as coal char or activated carbon is used.

Organic Wastes as a Fuel Source

The quantity of raw organic wastes produced each year in the United States is well in excess of 2 billion tons. In many cases these waste materials pose serious problems in proper disposal. Turning the wastes to usable energy could, in principle, alleviate the disposal problem as well as reduce the demand for depletable energy resources. There are two general methods for converting organic wastes to useful energy: (1) direct burning with the production of steam for space conditioning, industrial uses, or power generation and (2) chemical processing to convert wastes to higher value liquid, gaseous, or solid fuels.

The production of steam and electric power by direct burning of urban solid wastes has been practiced to a limited extent in the United States but the major experience is in Europe, especially in Germany.[36] The lack of application in the U.S. has been influenced by the low cost of fossil fuels and low population density relative to Europe. Continued urbanization with attendant waste disposal problems and the impending shortage of some fossil fuels have served to stimulate interest in the potential for energy recovery from waste products. Recently a number of demonstration projects involving heat recovery from urban waste incineration have been undertaken. For example, in Nashville, Tennessee, a waste incinerator-boiler providing energy for heating and cooling of mid-city buildings will go into operation in 1974.[37] The city of St. Louis, in a cooperative venture with the Union Electric Company, is providing municipal solid waste for use in power plant boilers.[38,39]

Chemical processing of solid wastes into high quality fuels, although technically feasible, is not practiced on a commercial scale since processes have not been fully developed. Research and development is currently being conducted on several processes.[36,40]

The quantities of wastes from various sources, as estimated by Anderson,[40] are shown in Table 2.10. The listed data are for dry, ash-free, organic matter. The first column of Table 2.10 gives the quantity generated and the second column shows the quantity that might be available for energy production. Wastes in the second category are those that are presently concentrated by feedlot operation, municipal collection, etc., to such an

Table 2.10. Dry, Ash-Free, Organic Wastes Generated and Potentially Collectable for 1971

Source	Quantity (million tons/year)	
	Total Generated	Total Available
Animal Wastes	200	26.0
Urban Refuse	129	71.0
Logging and Other Wood Refuse	55	5.0
Agricultural and Food Wastes	390	22.6
Industrial Wastes	44	5.2
Sewage Solids	12	1.5
Miscellaneous	50	5.0
Total	880	136.3

(Source: Larry L. Anderson, Energy Potential from Organic Wastes: A Review of the Quantities and Sources, Bureau of Mines Information Circular IC-8549, 1972.)

Table 2.11. Potential Electricity and Oil Production from Collectable Organic Wastes for 1971

Source	Annual Potential Power Production[a]		Annual Potential Oil Production[b]	
	Billion kWhr	% of Demand	Million Barrels	% of Demand
Animal Wastes	39.0	2.4	32.5	0.6
Urban Refuse	107.0	6.6	88.8	1.5
Logging and Wood Wastes	7.5	0.5	6.3	0.1
Agricultural and Food Wastes	33.9	2.1	28.3	0.5
Industrial Wastes	7.8	0.5	6.5	0.1
Sewage Solids	2.3	0.1	1.9	nil
Miscellaneous	7.5	0.5	6.3	0.1
Total	205.0	12.7	170.6	2.9

[a]Based on 8000 Btu/lb of dry, ash-free wastes and conversion to electricity at 32% efficiency.

[b]Based on net production of 1.25 barrels per ton of waste.

extent that recovery may be feasible. As will be noted, animal and farm wastes constitute a major portion of organic materials generated but recovery of these wastes is difficult. Urban refuse represents the most abundant recoverable source of organic wastes. Since all raw wastes are rather low in energy content per unit weight and volume, their conversion to either electricity or other forms of energy would need to be accomplished locally; otherwise transportation costs would be prohibitive.

The energy production potential of organic wastes, reasonably collectable in 1971, is illustrated in Table 2.11. If all collectable wastes were converted to electricity at the national average conversion efficiency of 32%, the power production for 1971 would have been 205 billion kWhr or nearly 13% of the national demand. If all collectable wastes were converted to oil at a net production of 1.25 barrels per ton of waste,[40] the oil production for 1971 would have been about 171 million barrels or 2.9% of the national consumption for that year.

The best candidates for electricity production are the wastes generated in urban areas since there exists a system for collection, and waste generation corresponds geographically to the need for electricity. The urban related wastes (urban refuse, industrial wastes, and sewage solids) would have accounted for about 7% of the national electricity demand for 1971. Looking to the future, the usable urban wastes will increase but not at the rate of electricity demand. For example, EPA estimates[38] indicate that urban waste collection will increase by about 3.4% per year to 1980 whereas electricity demand will increase at a rate roughly twice this amount. Thus, it appears that the potential electricity production from wastes will decline in relation to the total electrical demand.

As indicated earlier, heat recovery and power generation from wastes have not been practiced extensively in the United States primarily because fossil fuel costs have been sufficiently low to make energy recovery from wastes uneconomical. However, with fossil fuel prices increasing very rapidly, it seems reasonable to assume that energy recovery from wastes will become competitive. In addition to providing an important supplement to energy supplies for urban areas, the use of organic wastes for energy could help resolve the disposal problem. Nevertheless, energy from organic wastes will never have a large impact simply because the quantity of energy contained in collectable wastes is small in relation to the energy demand.

For MIUS systems probably the most sensible approach would be to burn the solid wastes from the building complex. These could be reduced to the required particle size, mixed with the coal, and fed with the coal to the fluidized bed combustion chamber. This would not only serve to dispose of the solid wastes, but it would also provide from 5 to 8% of the fuel requirements. Experience with solid waste incinerator systems has shown problems with clogging of the fuel feed system with unusual forms of scrap material. These problems would probably make it necessary to have an operator in attendance during periods when solid waste was in use as a fuel. The burning of the solid waste could be taken care of in a few hours during the day shift to minimize personnel costs.

References

1. Paul Averitt, Coal Resources of the United States, USGS Bulletin 1275, January 1, 1967.

2. Strippable Reserves of Bituminous Coal and Lignite in the United States, Bureau of Mines Information Circular 8531, 1971.

3. Council on Environmental Quality, "Energy and the Environment: Electric Power," August 1973.

4. Federal Council for Science and Technology, Committee on Energy R&D Goals, Panel Report on Extraction of Energy Fuels, June 1972.

5. C. L. Wilson, A Plan for Energy Independence, Foreign Affairs, pp. 657-675, July 1973.

6. U.S. Energy Outlook, Coal Availability, National Petroleum Council 1973.

7. Business Week, February 9, 1974, p. 14a, Letter from Powder River.

8. U.S. Bureau of Mines, Mineral Yearbook 1971 Volume I: Metals, Minerals, and Fuels.

9. National Coal Association, Bituminous Coal Data-1970 Edition, March 1971.

10. U.S. Bureau of Mines, Mineral Industry Surveys, Coal-Bituminous and Lignite in 1972, November 15, 1973.

11. National Coal Association, Bituminous Coal Facts, 1972.

12. Personal Communications, Frank Alford, TVA Chattanooga, February 15, 1974.

13. Personal Communications, Marvin Schwenn - Union Carbide Nuclear Division, Oak Ridge, Tennessee, February 15, 1974.

14. Public Power Weekly Newsletter, Published by American Public Power Association, No. 74-04, p. 4, January 25, 1974.

15. The Wall Street Journal, Soft Coal Prices Soared 118.5% in 3 Months; Marginally Efficient Mines are Reopening, February 8, 1974.

16. Weekly Energy Report, Vol. 2, No. 3, January 21, 1974

17. Electrical Week, February 11, 1974.

18. E. J. Wash and T. L. Thompson, Slurry Pipelines--Energy Movers of the Future, The Oil and Gas Journal, pp. 45-50, Vol. 71, No. 52, December 24, 1973.

19. The 1970 National Power Survey - Part III, Federal Power Commission, p. III-3-118, 1970.

20. C. L. Bazelmans et al., Study of Options for Control of Emissions from an Existing Coal-Fired Electric Power Station, ORNL-TM-4298, September 14, 1973.

21. Clean Energy from Coal Technology, U.S. Department of the Interior, Office of Coal Research, 1973.

22. Engineering Evaluation and Review of Consol Synthetic Fuel Process, Foster Wheeler Corp., February 1972.

23. Sherman K. Reed, Project COED (Char, Oil, Energy, Development), FMC Corporation, September, 1966.

24. Howard A. Shearer, Economic Evaluation of COED Process Plus Char Gasification, American Oil Company, September 1972.

25. B. K. Schmid and W. C. Bull, Production of Ashless, Low-Sulfur Boiler Fuels from Coal, Pittsburgh and Midway Coal Mining Company, September 1971.

26. Economic Evaluation of a Process to Produce Ashless, Low-Sulfur Fuel from Coal, Pittsburgh and Midway Coal Mining Company, OCR R&D Report No. 53, November 1959.

27. Everett Huffman, Southern Services, Inc., Personal communication to J. E. Jones, Jr., ORNL, February 1974 and June 1974.

28. Clarence A. Johnson et al., Scaleup Factors in the H Coal Process, Hydrocarbon Research, Inc., Presented at the 65th Annual AIChE Meeting, November 1972.

29. Commercial Process Evaluation of the H Coal Hydrogeneration Process, Hydrocarbon Research, Inc., PB-174 696, 1965.

30. D. Garret and T. O. Wentworth, Methyl-Fuel, A New Clean Source of Energy Paper No. 9 presented at the American Chemical Society 1973 Annual Meeting, Division of Fuel Chemistry, August 27, 1973.

31. A Cooperative Study of Industrial Energy Alternatives, USAEC Report prepared by ORNL and a group of Industrial Participants, to be published.

32. An Economic Evaluation of Synthane Gasification of Pittsburgh Seam Coal at 1000 psia followed by Shift Conversion, Purification, and Single-Stage Tube Wall Methanation, Process Evaluation Group, MRED, U.S. Department of the Interior, Bureau of Mines Report 72-9A, October 1971.

33. Development of a Coal-Based Sewage-Treatment Process, Final Report on Contract No. 14-01-0001-483, Office of Coal Research Report No. 55, Washington, D. C. 20240.

34. Water Pollution Control Act of 1972, P.L. 92-300, 1972, See also, Environmental Protection Agency Regulations on Secondary Treatment Information, 40 CFR 133; 38 FR 22298, August 17, 1973.

35. Evaluation of a Coal-Sewage Treatment Pilot Plant, Office of Coal Research R&D Report No. 63 (Contract No. 14-32-0001-1205), Washington, D. C. 20240.

36. N. L. Drobny et al., Recovery and Utilization of Municipal Solid Waste - A Summary of Available Cost and Performance Characteristics of Unit Processes and Systems, Report SW-10c, Prepared by Battelle Memorial Institute for the U.S. Environmental Protection Agency, 1971.

37. Waste Powers the Environment, Building Systems Design, p. 15-17, September 1972.

38. Energy Recovery from Waste, Report SW-36 d.i., Prepared by Horner and Shifrin, Inc., for the U.S. Environmental Protection Agency, 1972.

39. F. E. Wisely et al., Use of Refuse as Fuel in an Existing Utility Boiler, Published in Proceedings of 1972 National Incinerator Conference sponsored by the ASME, New York, N. Y., June 4-7, 1972.

40. L. L. Anderson, Energy Potential of Organic Wastes: A Review of the Quantities and Sources, Bureau of Mines Information Circular IC-8549, 1972.

CHAPTER 3

COMPARISON OF TYPES OF COMBUSTION SYSTEM

Many types of combustion system have been evolved. Usually each type has been developed because it showed special advantage for burning a particular type of fuel, or because it was found to be particularly suited to a particular type of power conversion system. This chapter summarizes the characteristics of those systems developed primarily to burn coal or coal derived fuels with special attention to the features, problems, and merits peculiar to the fluidized bed coal combustion system. These include the efficiency of combustion heat release rates obtainable, stack gas emissions, heat transfer surface design, and the problems peculiar to particular types of power conversion system.

Basic Combustion Considerations

Combustion Efficiency

An important consideration in evaluating the performance of a combustion system is the combustion efficiency, i.e., the fraction of the chemical energy available in the fuel that is actually released in the combustion process. The combustion efficiency may be reduced, for example, by incomplete combustion as evidenced by the presence of substantial amounts of CO in the stack gas. There may be other losses in the form of partially oxidized hydrocarbons or particles of unburned carbon leaving with the stack gas. To reduce these losses to a minimum the usual practice is to operate with a small amount of excess air and provide sufficient time in the combustion zone to give ample opportunity for all of the fuel present to react with the oxygen.

Effects of Excess Air on Stack Losses

A number of practical considerations to be discussed later make it essential to reject the products of combustion to the stack at a temperature in the range of 200 to 300°F. The heat required to raise these gases from ambient air temperature to the stack gas temperature commonly represents 10 to 20% of the heat available from the fuel. As the amount of excess air is increased beyond the ideal stoichiometric amount required

for reaction of the fuel, the amount of heat lost in the stack gases is increased. That is, going from 0% to 100% excess air will double the stack losses. Thus, there is a strong incentive to make use of a combustion system that will give complete combustion with a minimum amount of excess air, hopefully no more than 10%.

NO_x Emissions

An important consideration in choosing a combustion system is the amount of NO_x to be expected in the stack gases. Power plants are generally having difficulty meeting the new air quality standards. Some insight into the problem is given by Fig. 3.1 which shows the equilibrium NO_x concentration as a function of flame temperature for a range of excess air flow rates.[1] In point of fact, the NO_x content of the combustion gases often will be less than indicated by Fig. 3.1 because it was calculated for equilibrium conditions. Depending on the flame temperature, the time required for the formation of NO_x is ordinarily of roughly the same order as the transit time for the gases through the hot portion of a short flame, hence equilibrium conditions are not reached. As indicated in Fig. 3.1 the NO_x concentration in the stack gas can be reduced by reducing the flame temperature, or reducing the amount of excess air. The latter approach has been found effective for certain special types of burner fueled with natural gas, but for the fuels of prime interest in this study the most effective approach is to reduce both the excess air and the flame temperature. For open flame burners the latter can be accomplished by recirculating some cooled exhaust gas, and this approach is being used in some steam power plants.[2] Under any circumstances it is important to minimize the excess air.

Stack Gas Temperature Limitations

A major factor in limiting the amount of heat that can be removed from the stack gases before rejecting them from a practical system is the tendency of SO_2 to react with the H_2O from combustion to form sulfurous acid whose dew point is much higher than that of water vapor so that it will condense on the walls of the stack where it will attack either metal or ceramic surfaces. As a consequence, one of the key considerations in

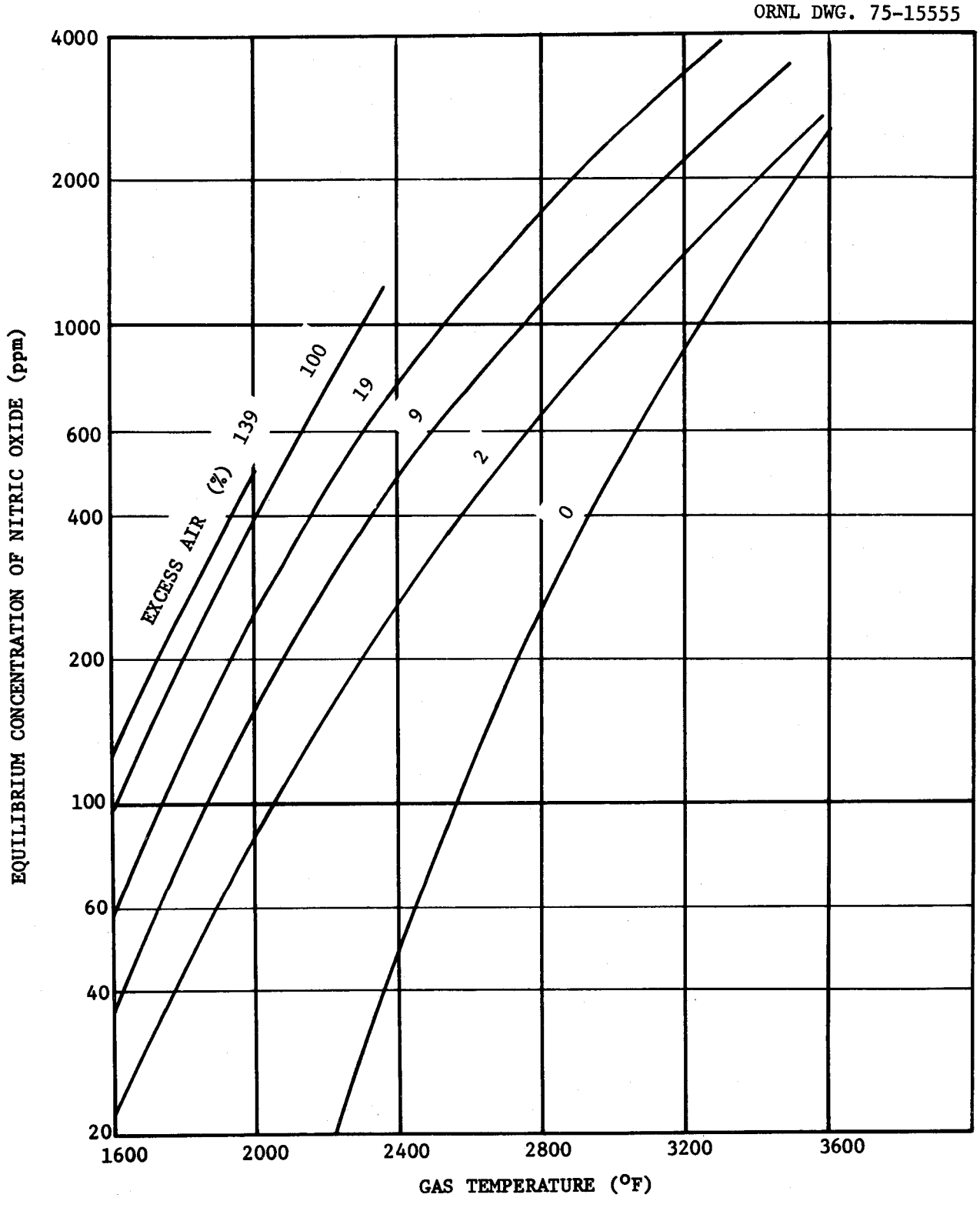

Fig. 3.1. Effects of gas temperature and the amount of excess air on the calculated equilibrium nitric oxide concentration in the combustion products.

the design of a system is the expected maximum SO_2 content of the stack gas and hence the lower stack gas temperature limit that can be employed in the design. It is interesting to note that if a fluidized bed coal combustion system is employed to remove the bulk of the sulfur in a fluidized bed so that the SO_2 content of the stack gases is markedly reduced, this will permit a lower stack gas temperature and hence a higher plant thermal efficiency. Figure 3.2 shows this effect.[3]

Types of Burner

Stationary Grates

The earliest steam power plants made use of a stationary grate over which coal was spread, air was admitted from below through openings in the grate, and the coal was burned in large open flat beds. This system functions best if coal is added to the bed in the form of lumps of an appropriate size — usually 1 to 3 in. — because fines are inclined to fuse into a tarry cake to give a non-uniform air flow distribution through the bed and uneven combustion. The system is commonly hand-fired to maintain a uniform bed thickness and ashes are periodically scraped off to the side. Automatic firing systems have been devised; they usually involve pushing fresh coal out onto the stationary grate. The stationary grate systems do not lend themselves well to close control of the fuel-air ratio (an important factor to be discussed later) and work well only with selected grades of lump coal. The excess air is commonly 60% or more, and the combustion efficiency is often only about 80% because many of the fines in the coal fall out with the ash and some of the volatiles escape up the stack unburned.

Traveling Grates

Efforts to automate coal firing of boilers and permit the use of a wider range of grades of coal led to the development of traveling grate stokers. In these a bed of coal 6 to 12 in. thick is fed with an automatic stoker from one end of the traveling grate and ashes are dumped off the other end. Movement of the grate agitates the bed a bit, tending to break up regions in which caking occurs. The system is currently used

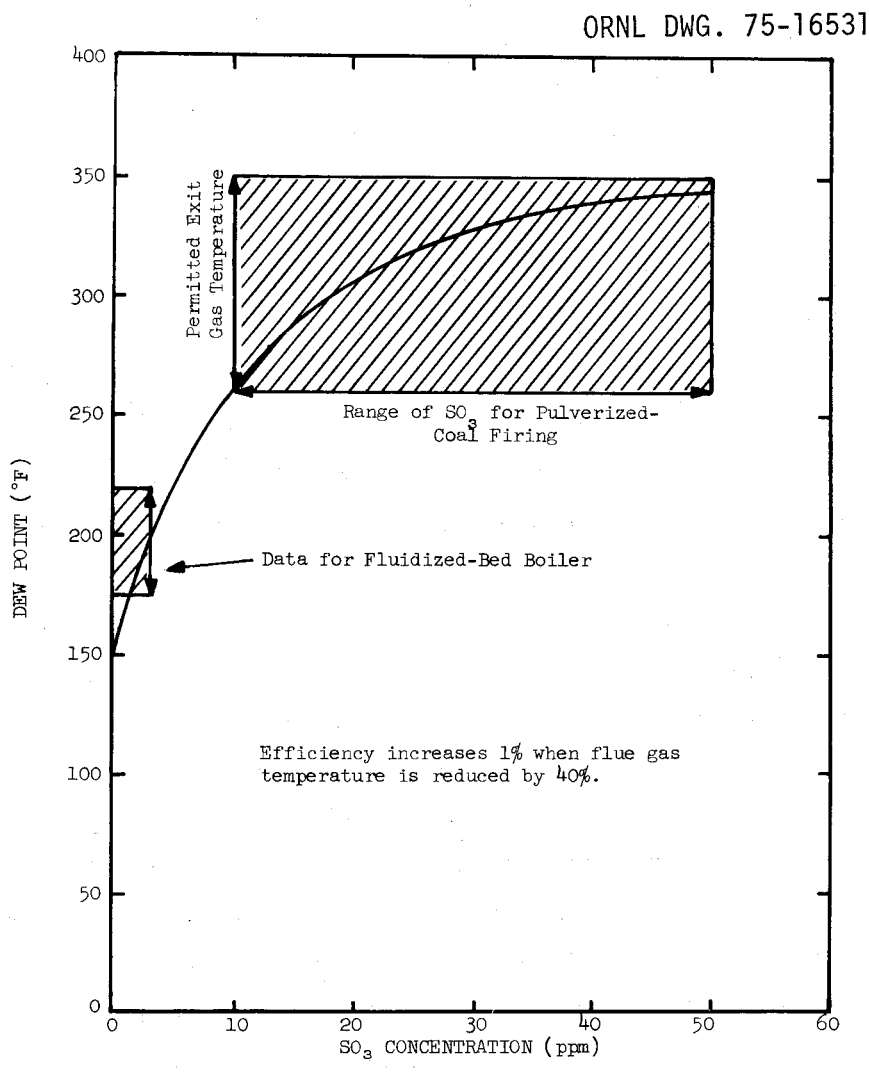

Fig. 3.2. Effects of sulfur concentration on the dew point of stack gases. (Ref. 3).

not only for burning coal but also for burning mixtures of coal and solid waste. A disadvantage is that the high operating temperature of the traveling grate leads to a substantial amount of maintenance. Control of the fuel-air ratio is better than for a stationary grate system but it still leaves much to be desired because of variations in the air flow resistance of the bed from one local region to another. The excess air usually runs 40% or more.[4]

Open Flame Burners

Relatively simple and compact burner geometries can be used to mix liquid or gaseous fuels with air to give large open flames. Similarly, finely powdered coal can be blown through an open flame burner to give an essentially similar flame. This makes it possible to design and build a large steam boiler so that it can operate with whatever fuel is most economical or available at any particular time simply by changing out the burners and the fuel-air ratio can be controlled closely to give ∿99% combustion efficiency with only 10% to 20% excess air. The plant efficiency can be improved further by using a regenerator to preheat the combustion air. Thus, a large fraction of modern steam plants, particularly on the east coast, have been designed and built so that they can burn either residual fuel oil or powdered coal almost equally well, and can be converted to use natural gas with only a small loss in performance. The loss in performance stems from the fact that in these furnaces much of the heat is transmitted from the hot gases to the furnace walls by thermal radiation from hot glowing carbon particles if residual fuel oil or powdered coal are employed. However, if natural gas is used, it burns with a pale blue flame from which relatively little energy is emitted by thermal radiation. In furnaces designed primarily for operation on coal or residual fuel oil with the water-cooled walls of the furnace serving at the boiler portion of the steam generator, the capacity of the unit is reduced when gas is employed as the fuel.

Fluidized Bed Combustion of Coal

The development of fluidized bed catalytic cracking and reforming processes based on fluidized beds made up of particles of clay catalyst

began in the 1930's and has led to the extensive development of fluidized beds for processes requiring the reaction of solids and gases.[5] The system depends on the fact that when air is blown up through a bed of small particles at an appropriate velocity, the particles begin to float and the bed behaves as if it were a turbulent liquid. The bed ordinarily does not have a sharply defined free upper surface, but, as the solid fraction decreases in the upper regions of the bed, the air velocity also decreases and the air dynamic forces tending to lift the particles are reduced. Gas circulation upward through the bed is not perfectly uniform but tends to be somewhat irregular with large bubbles forming here and there. These tend to move upward at a higher than average velocity and blow some particles out of the bed at sufficient velocity so that they tend to arc through trajectories well above the nominal upper surface of the bed. The large surface area and continuous agitation of the bed gives a high reaction rate and a uniform distribution of both the reaction rate and the temperature throughout the bed. This work on fluidized beds for chemical process system led to the discovery that the heat transfer coefficient in fluidized beds is high — of the order of 50 to 100 $Btu/hr \cdot ft^2 \cdot °F$. This in turn suggested the possibility of designing a fluidized bed coal combustion system for a steam boiler, the idea being that the boiler size and cost could be much reduced by taking advantage of the high heat transfer coefficient characteristic of fluidized beds. When public pressure to reduce sulfur emissions became a major consideration, the notion of employing a fluidized bed of limestone to remove the sulfur as calcium sulfate was investigated with highly encouraging results. Concurrently with this fluidized beds were developed for burning both industrial and residential solid wastes.[6,7] Other work demonstrated that the fluidized bed combustion system could be used to burn char, high sulfur residual fuel oil, or any of a number of gaseous fuels with a combustion efficiency of over 99% with the excess air running less than 10%.

Summary

The major consideration in the choice of a burner or combustion system for any application is its suitability for use with a wide range of fuels to give a high combustion efficiency with relatively little excess air.

Further, for MIUS applications, it is important to employ a combustion system that will burn high sulfur coal and yet reduce the sulfur emissions in the stack gases to a level consistent with both present and probably future EPA standards. As will be discussed later in this chapter, there is no process currently available that would be effective in removing sulfur from stack gases following combustion of high sulfur coal and yet would be economically acceptable for MIUS applications, particularly when operational and maintenance requirements are considered.

In attempting to give perspective to the many problems associated with a choice of combustion system for MIUS applications, Table 3.1 was prepared to indicate the suitability of the typical combustion systems described

Table 3.1. Suitability of Typical Combustion Systems for Use with Different Types of Fuel for Installations Designed to Meet EPA Standards Without Equipment for Removing Sulfur from the Stack Gases

Type of Fuel	Stationary Grate	Moving Grate	Open Burner	Fluidized Bed
High sulfur bituminous coal				x
Low sulfur bituminous coal	x	x	x	x
Lignite	x	x	x	x
Anthracite	x	x	x	x
Char (from coal conversion plants)			?	x
Natural and high Btu gas			x	x
Medium Btu gas			x	x
Low Btu gas			x	x
No. 2 fuel oil			x	x
Residual fuel oil-low sulfur			x	?
Residual fuel oil-high sulfur				?
Liquid fuel from coal			x	?
Domestic solid waste + coal		x		x
Sewage sludge + coal		x		x
Wood waste + coal				x

above for use with the different types of fuel that might be used in a MIUS application. Note that only the fluidized bed combustion system appears to show promise for handling the full range of fuel types specified for this

study, i.e., high and low sulfur bituminous coal, lignite, anthracite, gaseous and liquid fuel derived from coal, mixtures of residential or industrial waste with coal, or mixtures of sewage sludge and coal derived from filter beds in small sewage plants.

Question marks have been placed in the column for the fluidized bed combustion system for residual fuel oil and liquid fuel from coal. This has been done because there has been some difficulty with coking of the fuel nozzles in the course of efforts to burn high sulfur fuel oil in a fluidized bed coal combustion system. There is insufficient experience in this area to draw a firm conclusion with respect to feasibility.

Developmental Status of Fluidized Bed Combustion Systems

Inasmuch as this report is especially concerned with fluidized bed coal combustion systems, it seems in order at this point to include a special section to review the developmental background of the system.

Coal Combustion System Development Efforts

Work on fluidized bed combustion of coal began in the 1950's. In some instances the objective was to burn fuels such as anthracite fines, lignite, and washery tailings that did not burn well in other types of combustion systems. The bulk of the work was directed at trying to get lower cost steam boilers by taking advantage of the high heat transfer coefficient in a fluidized bed. The most significant effort was started about 10 years ago in the U.K. by the Central Electricity Generating Board,[8] and has been continued at the British Coal Utilization Research Association Laboratory.[5,9] Most of the work at BCURA has been with beds having a cross-sectional area of about 8 ft^2. Some of the British effort was supported by EPA, and BCURA's program is continuing under a recent OCR contract. In the U.S. Pope, Evans, and Robbins in Alexandria, Virginia, under both OCR and EPA funding, has operated several beds at atmospheric pressure, including a bed having a cross-sectional area of 10 ft^2 and fitted with a carbon-burnup cell.[10,11] The objective in work on the latter has been to develop a small fluidized bed combustion chamber and boiler of about 100 MW(t) output that would lend itself to shop fabrication and shipment by rail. The work has

emphasized the solution of practical design and operating problems. Basic heat transfer, flow, and performance data accumulated by the British have more recently been supplemented with EPA funding by small-scale studies (using beds 6 in. to 12 in. in diameter) at the Argonne National Laboratory[12] and Esso Research[13] on the basic problems of fluidized beds with the prime emphasis on optimizing the pollution control capabilities and developing a method for reconstituting the lime so that one would not be confronted with a waste disposal problem for the large amounts of calcium sulfate that will be produced. Pope, Evans, and Robbins has also worked on the lime regeneration problem.[10] Both Westinghouse and Foster Wheeler have carried out plant design studies, and at the time of writing Foster Wheeler is working with Pope, Evans, and Robbins on the fluidized bed steam generator mentioned above.[11,14]

Fluidized beds have been used extensively for roasting sulfide ores.[15] Over 200 units are currently in operation, sometimes primarily to make sulfuric acid or sodium sulfite (for paper mills) and sometimes primarily to obtain metal oxides for reduction to the metal, but usually for both purposes. The heat released in the roasting operation often requires heat removal from the bed; this is accomplished with boiler tubes in the bed.

Work on fluidized bed combustion in the U.S. has also included the incineration of solid wastes, both industrial and domestic. Copeland Systems Incorporated has about 30 units in service for disposal of industrial wastes including not only obvious fuel materials such as sawdust but also slurries such as paper pulp mill waste liquor with as little as 35% solids.[7] The latter are sprayed downward into a fluidized bed of red hot sand, and the heat of combustion of the solids is sufficient to sustain the reaction. Dorr-Oliver has about 80 incinerator units in service, burning mostly industrial and domestic sewage sludge in aqueous suspension.[16] Concentration of the material to give about 35% organic content is achieved by settling. A fluidized bed for burning municipal solid waste has been under development at Combustion Power Inc., under EPA contracts for about 8 years.[17] In this system the compressor of a gas turbine feeds air to a fluidized bed of sand into which shredded solid waste (mostly paper) is injected. The hot gases leaving the bed drive the turbine to produce a net electrical power output. The system has also been operated with coal as the fuel under a contract with OCR.[17]

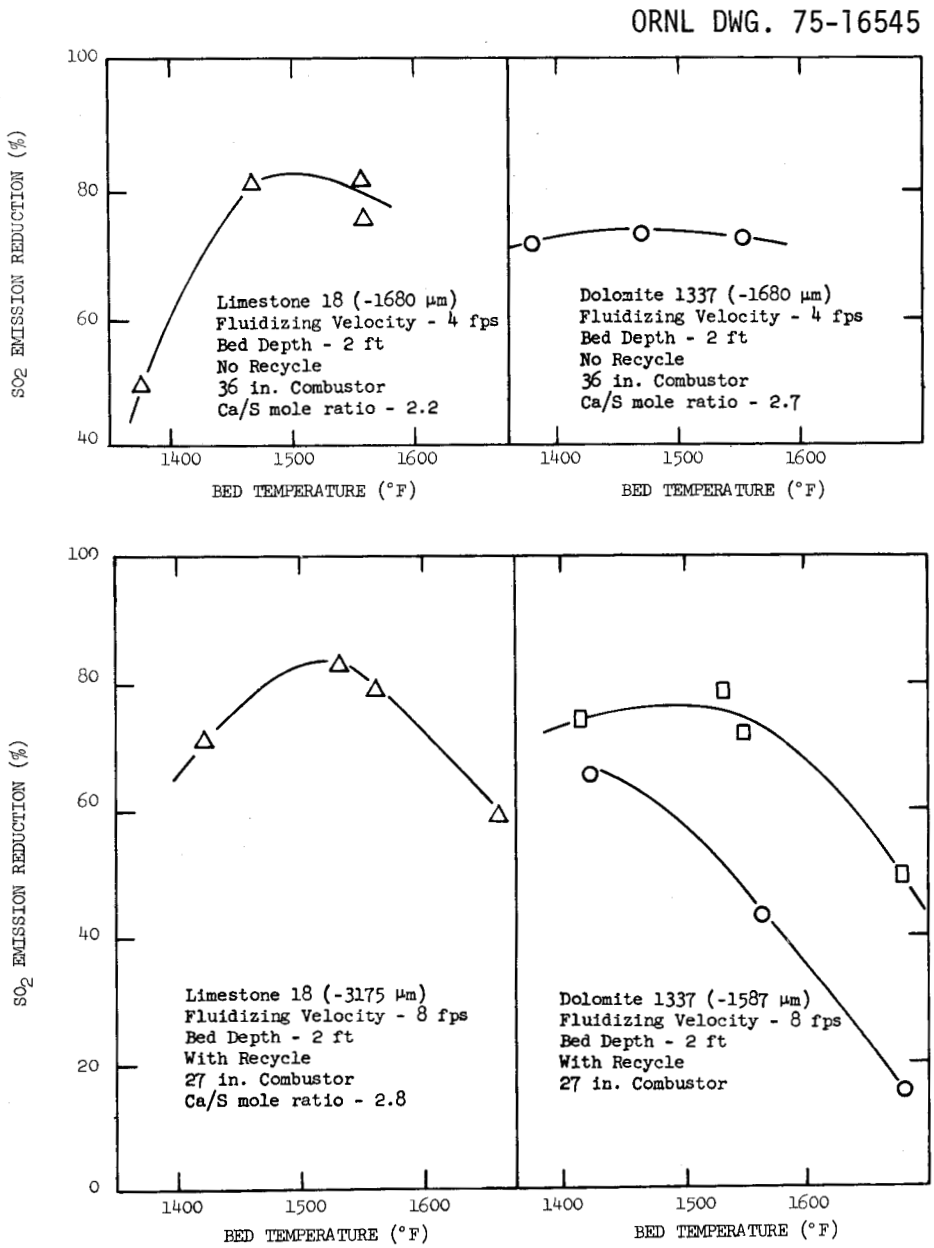

Fig. 3.3. Effect of bed temperature of SO_2 reduction for Pittsburgh coal. (Ref. 18).

Some notion of the amount of operating experience that has been gained with fluidized bed coal combustion systems is given by Table 3.2.

Table 3.2. Summary of Operating Experience with Fluidized Bed Combustion Systems

Organization Responsible for Design and Construction	Fuel	Objective	Sum Total Operating Time-hour
Copeland Systems, Inc.	Wood waste, pulp mill waste, misc. organic wastes	Incineration, in some cases heat recovery	$\sim 10^6$
Dorr-Oliver, Inc.	Sewage sludge	Incineration	$\sim 10^6$
	Pyrites	Roasting to yield SO_2 for acid or sulfite and/or metal oxide for reduction	$\sim 3 \times 10^6$
BCURA	Coal	R&D on fluidized bed combustion of coal and high sulfur residual fuel oil	$\sim 10^4$
Pope, Evans, and Robbins, Inc.	Coal	R&D on fluidized bed combustion of coal	~9000
Argonne National Laboratory	Coal	R&D on fluidized bed combustion of coal and lime regeneration	700
Combustion Power, Inc.	Municipal solid waste, wood waste and coal	Incineration with electrical energy as a by-product	471 (total on bed) 271 (with turbine)
Esso Research	Coal	R&D on coal combustion and lime regeneration	~100

Sulfur Removal

The effectiveness with which SO_2 emissions can be reduced by removing sulfur as $CaSO_4$ in a fluidized bed combustion system depends on many factors. The two most important are the calcium-sulfur feed ratio and the fluid bed operating temperature. The effects of these two parameters on SO_2 emissions are shown in Figs. 3.3 and 3.4. The matter is complicated by the fact that limestone from different strata vary substantially in their characteristics including their effectiveness in removing sulfur.[18]

Regeneration of the Lime

It would be advantageous to regenerate the lime in the bed and thus reduce both the consumption of limestone and the quantity of ash that must

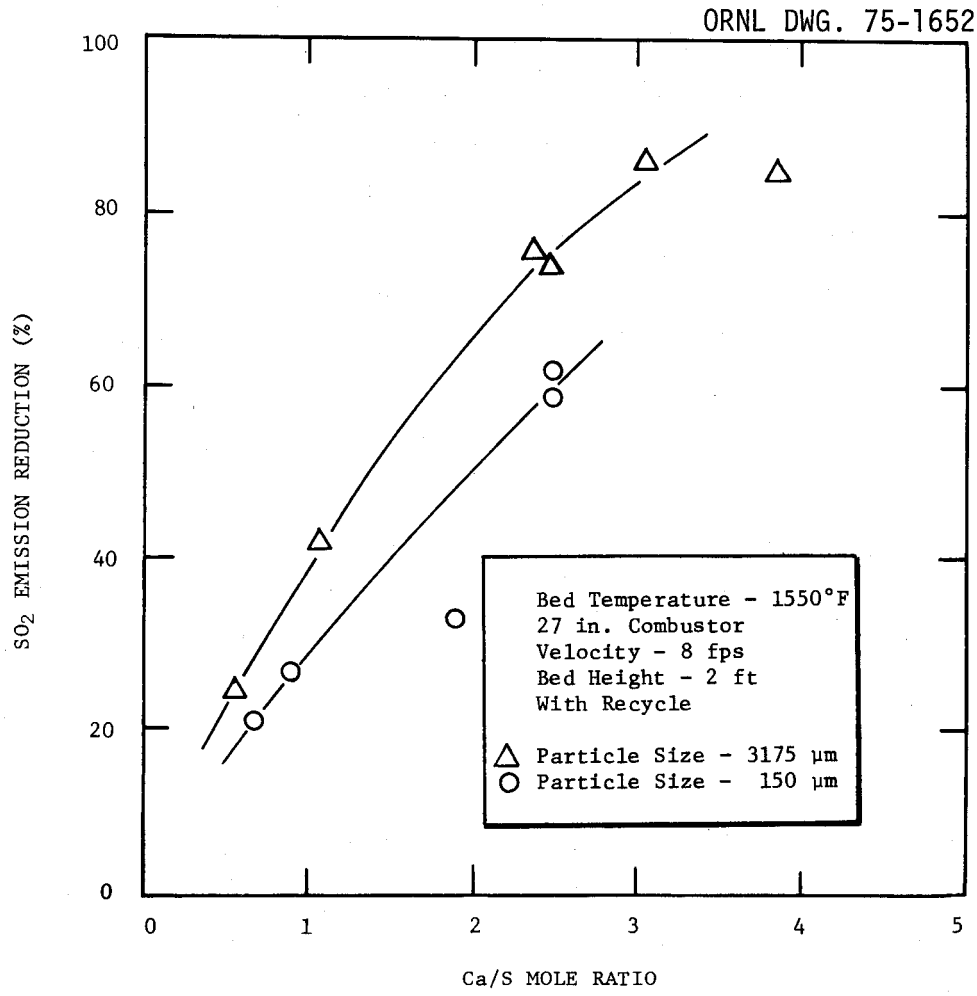

Fig. 3.4. Effect of Ca/S ratio and additive particle size on SO_2 reduction (high fluidizing velocity) for Pittsburgh coal and Limestone 18. (Ref. 18).

be hauled away. Processes have been investigated that would yield element sulfur, a saleable product. While somewhat different processes have been contemplated in the lime regeneration work carried out by ANL, Esso, and Pope, Evans, and Robbins as mentioned above, they all depend on roasting calcium sulfate under mildly reducing conditions to evolve a gas rich in sulfur dioxide. Because of the high temperature necessary for the roast, about 1950°F, the regenerated lime has sharply less reactivity than fresh lime. Fresh stone must be supplied at a rate amounting to an appreciable fraction of the sulfur to be captured, on a stoichiometric basis, and a comparable amount of lime must be withdrawn for sale or disposal. To avoid this disadvantage, workers at The City College of New York have proposed a regeneration scheme which would depend on reduction of the calcium sulfate by a gas containing hydrogen or carbon monoxide to yield calcium sulfide, and on subsequent reaction of the calcium sulfide with steam and CO_2 to produce $CaCO_3$ and H_2S, from which sulfur may be produced in elemental form more readily than from SO_2.[19] Westinghouse has carried out plant design studies that have included a favorable economic assessment of The City College scheme.[14]

NO_x Formation

The low combustion temperature characteristic of fluidized bed combustion tends to keep the formation of NO_x to a low level, but the gas transit time through the high temperature region is sufficiently long that the equilibrium concentration of NO_x can be reached. As shown in Fig. 3.5 this makes the NO_x concentration in the stack gas quite sensitive to the amount of excess air,[9] and this in turn places a premium on the use of a control scheme that will hold the amount of excess air to a low level.

Control of Fluidized Bed Combustion Systems

Fluidized bed combustion systems can be operated over a wide range of bed temperatures and amounts of excess air, but Figs. 3.3, 3.4, and 3.5 indicate that there is a strong incentive to keep the excess air to less than 10% and the bed temperature to around 1600°F. These conditions pose control problems if steam boiler tubes are used to remove heat from the bed because the heat transfer coefficient between the bed and the tubes

ORNL DWG. 75-16534

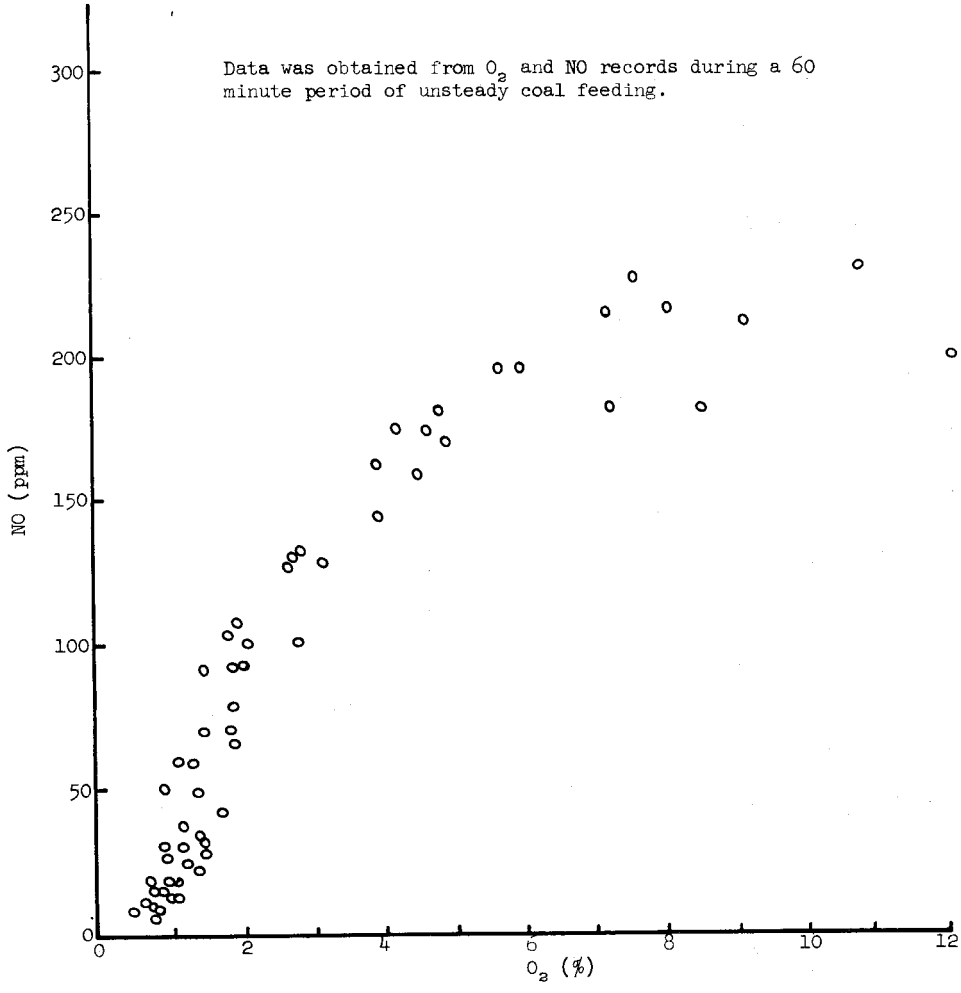

Fig. 3.5. Correlation of O_2 and NO concentrations in the exhaust gas. (Ref. 9.)

is high and is essentially independent of the combustion air flow rate, while at the same time the heat transfer coefficient for water boiling in tubes is very high and essentially independent of the water flow rate. As a consequence, the output will not be reduced from the full power design condition by reducing either the combustion air flow rate or the feed water flow rate. The temperature difference between the bed and the boiler could be reduced by reducing the bed temperature, but this would have an adverse effect on sulfur removal. (See Fig. 3.3.) The only courses that can be followed are to reduce the output by reducing the coal feed rate and providing a large amount of excess air (thus reducing the boiler thermal efficiency) or by the more awkward step of reducing the amount of bed material by removing some to an auxiliary storage hopper. This may be accomplished by changing the bed depth or by compartmentalizing the bed. Either approach reduces the effective heat transfer surface area in the bed, and thus reduces the heat removal rate. However, either approach poses serious problems in controlling the water flow distribution through the boiler tubes.

The control problem is vastly eased if a fluidized bed coal combustion chamber is cooled with a tube bank that serves as the heater in a gas turbine system. The heat transfer coefficient for the gas inside the tubes is roughly proportional to the gas mass flow rate, hence the power output of the system can be varied continuously over a wide range. This is particularly important under startup, idle, and shutdown conditions where quenching of combustion presents a problem if there are boiler tubes present in the bed that will tend to reduce the bed temperature below the ignition point. These are such vital problems that the control concept envisioned for the gas turbine system is discussed later in a separate chapter.

Effects of Bed Operating Pressure

Most of the work on fluidized bed combustion has been carried out at atmospheric pressure. However, work at BCURA has shown that higher heat release rates can be obtained if the bed is pressurized. Further, the

depth of the bed can be increased essentially in direct proportion to the bed operating pressure while holding the pumping power losses constant. This type of system is particularly advantageous if the bed is used in a combined gas turbine-steam cycle with heat removed from the bed for the steam system and the hot gases from the bed allowed to expand through a gas turbine. The principal question associated with this approach is the extent to which corrosion and erosion of the turbine buckets may prove to be a problem.

Combustion Gas-Side Corrosion

The rate of corrosive attack on the combustion gas side of iron-chrome-nickel alloy tubes in a fluidized bed coal combustion chamber has received little attention. Viewed from the standpoint of basic considerations the situation looks very promising because the bulk of the corrosion in steam generators, gas turbines, and petroleum refinery equipment stems from the vaporization of sulfates and vanadates in high temperature flames (2500 to 3000°F) and their subsequent deposition as liquids on heat exchanger surfaces that operate in the temperature range from 1200 to 1500°F. At the relatively low operating temperature of the fluidized bed (∿1600°F) the vapor pressure of sulfates and vanadates is so low that this mode of attack should not occur.

There are some experimental data from British tests carried out at 1550°F with a variety of iron-chrome-nickel alloys. These tests showed that the 300 series stainless steels gave a weight loss in a 500 hr test equivalent to 1 mil/year. This is surprisingly low because one would expect that agitation of the bed would act to abrade the protective oxide film from the stainless steel. The British also found evidence of sulfur penetration in some of the stainless steel specimens but the data are insufficient for evaluation.

Development Problems

The major problems that have been experienced in the development work outlined above have been with the feed of the coal and limestone into the bed, blowthrough of fines and separation of these fines from the gases leaving the bed, and either the regeneration of the calcium sulfate to

calcium oxide or finding some commercial use for the calcium sulfate-ash mixture produced from the process. Relatively little difficulty has been experienced in getting good combustion in the bed, the principal problem being the avoidance of excessive burning rates and hot spots at the points where the coal is introduced into the bed. Note that the bulk of the work carried out to date has been with beds having areas of 1 to 10 ft^2 where agitation of the bed is reasonably effective in distributing the coal. However, the beds envisioned in this study will have areas of 30 to 50 ft^2, hence scale-up uncertainties include problems associated with devising provisions for a large number of coal feed points across the bed, the distribution of coal and limestone across the bed, the upper limits of gas velocity and bed depth, the size and spacing of heat transfer tubes, the control of power level, and the decrepitation rates and reactivities of various limestones and dolomites after recycling.

Sulfur Removal

The Clean Air Act, as amended in 1970, provides that the Environmental Protection Agency (EPA) shall establish, for new stationary sources, national performance standards that reflect the best system of emission reduction that has been adequately demonstrated. These standards[20] have been issued for the emission of sulfur dioxide for fossil-fired steam plants that have a rating of 250,000,000 Btu/hr or greater. The emission standard for coal-fired plants of this size was set at 1.2 lb/million Btu of heat input. Further, under the provisions of the 1970 amendments to the Clean Air Act, each state is required to develop and submit an implementation plan for approval by the EPA. The implementation plan must include emission control regulations designed to achieve and maintain national ambient air quality standards. To meet this requirement, many states have adopted standards covering the emission of sulfur dioxide from fossil-fuel burning plants. A review[21] of the regulation in 25 states reveals that most of the states have set standards for the emission of sulfur dioxide from coal-fired plants at about the EPA standard, 1.2 lb/million Btu. A few states allow a higher level of emission. Only six states have set lower limits for such emission, and in three of these states the lower limits apply only

in very large cities. One of the strictest standards has been adopted in New Jersey, that has a statewide limit of 0.2% sulfur in the coal burned, which is equivalent to a sulfur dioxide emission rate of about 0.3 lb/mil Btu.

The resulting situation is that in most states only coal with a sulfur content of from 0.2 to 1%, or 2% in a few states, may be burned for fuel without removal of some part of the sulfur either from the coal or as sulfur dioxide from the flue gases. The required retention of the sulfur dioxide to meet emission limits of 0.3 and 1.2 lb/million Btu as a function of the weight percent of sulfur in the coal is shown for coal with a heating value of 12,500 Btu/lb in Fig. 3.6. For example, the higher limit requires a 75% retention of SO_2 and the lower limit requires a 94% retention for 3% sulfur in the coal.

Conventional Furnaces

Several methods for removal of sulfur or sulfur dioxide from coal and oil burned in conventional furnaces have been investigated. The major part of this work has been devoted to two processes: limestone injection into the furnace followed by wet scrubbing of the flue gases, and wet-limestone scrubbing of the flue gases.[21]

In the first process, ground limestone is mixed with the coal and injected along with the coal into the burning zone of the furnace. Part of the sulfur in the coal is absorbed by calcium in the limestone in the same manner as is done in the fluidized bed furnace. There is one very important difference in the process in the conventional furnace and the fluidized bed, and that is the temperature of the coal-limestone mixture in the combustion zone. The temperature is in excess of 2000°F in the conventional furnace. Experience with the fluidized bed has shown that for the most effective sulfur removal, the bed must be maintained at between 1400 and 1700°F.[18] This is accomplished by placing the boiler or heat transfer tubes in the bed where combustion occurs. Results[21,22] of pilot-plant tests of limestone injection in conventional furnaces have shown that only about 40 to 50% sulfur removal can be achieved. The remaining sulfur must be removed as SO_2 by wet scrubbing of the flue gases. Also, problems with ash buildup on boiler surfaces were encountered. These

ORNL DWG. 75-16542

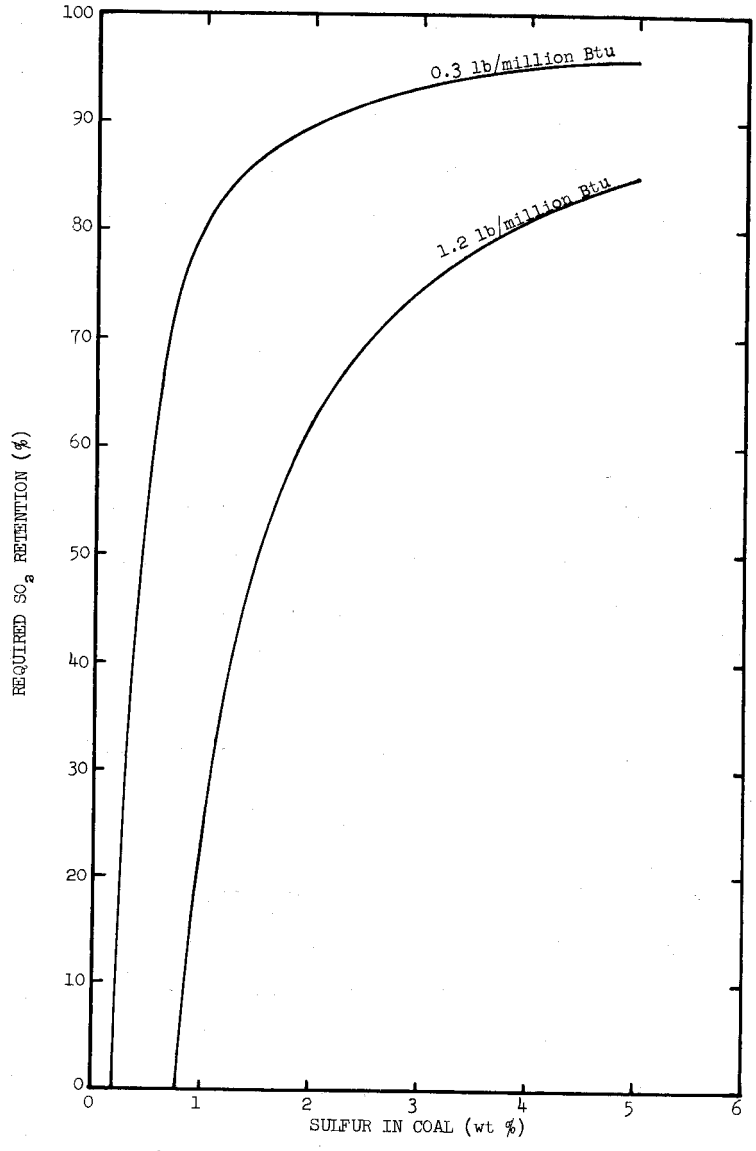

Fig. 3.6. Required SO_2 retention to limit emission to 0.3 or 1.2 lb/million Btu for 12,500 Btu/lb coal.

results have led to a reduced interest in limestone injection and to a greater emphasis on wet-limestone scrubbing of the flue gases as the method of SO_2 removal in conventional furnaces.

The wet-limestone scrubbing process[22] employs a slurry of ground limestone to react with the SO_2 in the flue gases. The slurry and flue gas are usually first contacted in a venturi scrubber for fly ash removal and then in two or more stages of packed contacters. The gas from the final scrubber passes through a demister, a reheater and induced-draft booster fans. The used limestone is removed as sludge and the water is recycled to eliminate any liquid discharge. A flow diagram is shown in Fig. 3.7.

Almost all of the scrubbing processes remove SO_2 (an acidic gas) with an aqueous solution or slurry of alkaline material. These processes require a scrubber with liquid recirculation and mist elimination, gas fans, duct-work and dampers, and gas reheat to restore plume buoyancy. If fly ash particulate are not removed by an electrostatic precipitator, the scrubber system generally must be expanded to allow for particulate as well as SO_2 removal, especially with regenerable scrubbing, because particulates are usually unacceptable in the regeneration system.

The scrubbing processes all require alkali handling systems to provide for alkali makeup and for product recovery or disposal. The throwaway processes generally dispose of removed sulfur as a waste sludge of calcium salts and require greater than stoichiometric input of alkali. The regenerable processes convert product solutions or solids to sulfur or sulfuric acid and recycle alkali, so very little alkali makeup is required.

Throwaway Scrubbing

The lime and limestone slurry scrubbings processes have the greatest commercial appeal to the U.S. utilities. The flue gas is scrubbed with a 5-15% slurry of calcium sulfite/sulfate containing small amounts of continuously added lime (CaO) or limestone ($CaCO_3$). The solids are continuously separated from the slurry and usually disposed of in a settling pond. The processes are complicated by simultaneous dissolution and crystallization of the solids in the scrubber. Calcium scaling and plugging can occur in the scrubber and demister, and sufficient residence

ORNL DWG 73-5891RI

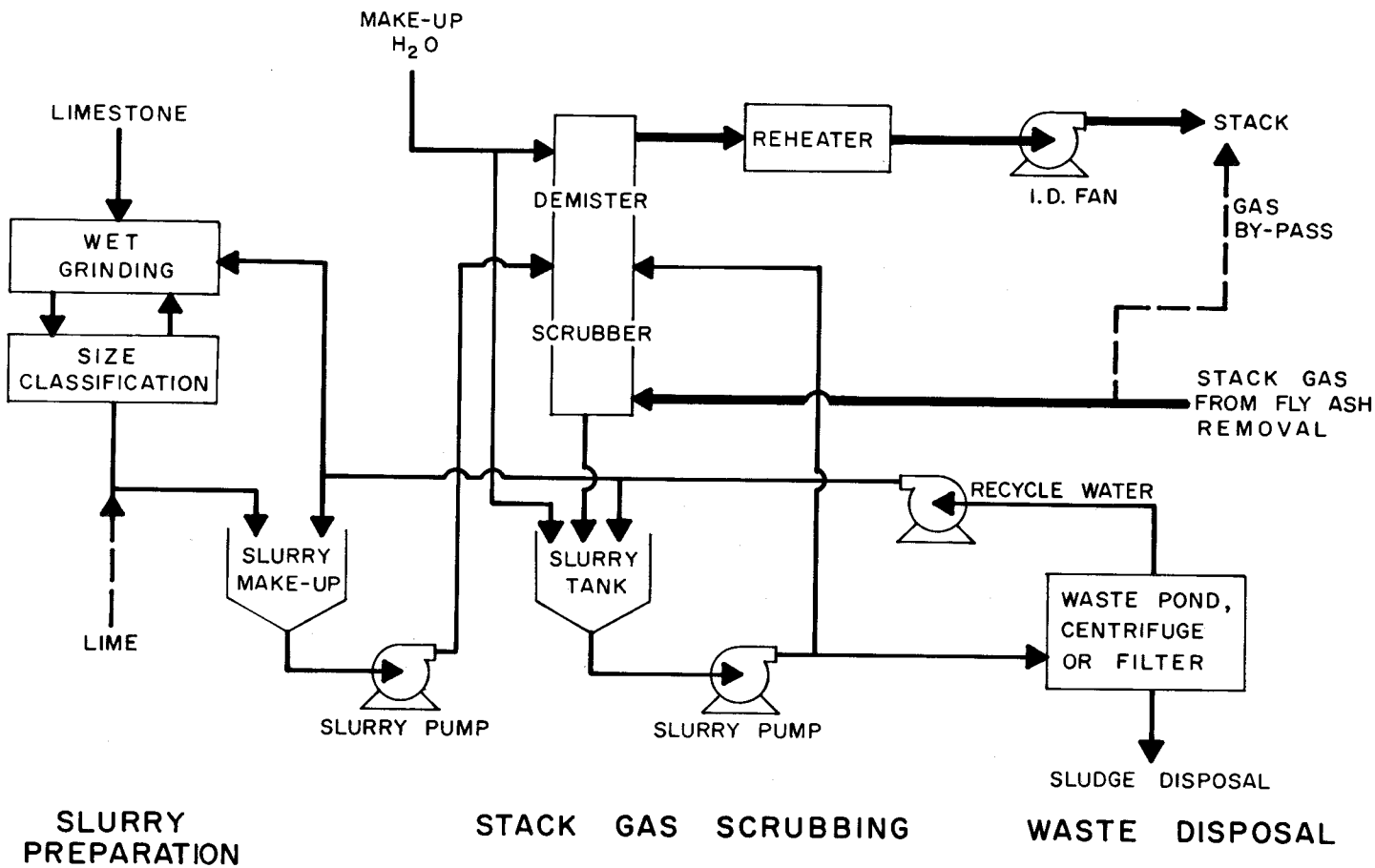

Fig. 3.7. Wet lime/limestone scrubbing process.

time and liquid recirculation must be provided for reaction of the solids with SO_2. In addition the high solids concentration tends to cause equipment erosion and corrosion. Not the least of the problems is disposal of the "solid" waste, usually a sludge "mud" composed of tiny crystals and containing about 50% water with dissolved calcium and trace metals from the fly ash.

The lime/limestone scrubbing processes are being offered by a number of developers, and systems are being planned and constructed for over 20 plants.

A number of developers are working on double alkali systems that regenerate the scrubbing solution by reacting it with lime or limestone to form waste calcium sulfite/sulfate sludge and recycle alkaline solution. The waste solids should be washed to remove dissolved sodium salts but otherwise present the same waste disposal problem as slurry scrubbing. The highly efficient sodium alkali solution permits use of very simple scrubbers such as single-stage venturii to remove both SO_2 and particulates. General Motors Corporation and Caterpillar Tractor Company are designing and constructing industrial boiler applications of double alkali systems using lime regeneration. Major development of limestone regeneration has been carried on by Showa Denko and Kureha in Japan. A 200-MW Japanese application was scheduled to start up in 1973. EPA is supporting pilot plant work by A. D. Little to generate design date on alternate double alkali processing schemes.

Chiyoda of Japan has developed a throwaway scrubbing process with a different mode of SO_2 removal. The SO_2 is absorbed in dilute sulfuric acid containing ferric ion which complexes with it. In a separate vessel the retained SO_2 is air-oxidized to sulfuric acid. The product stream of dilute acid is neutralized with lime or limestone to form a high quality, large crystal size gypsum product that is easily disposed of and may even be marketable. The system has been tested on an oil-fired boiler and with simulated coal fly ash impurities. One commercial system is operating in Japan and several more are under construction.

Regenerable Scrubbing

There are three basic techniques for regeneration of a spent alkali scrubbing solution or slurry.

1. Direct thermal treatment to produce SO_2.
2. Acid decomposition of the alkali to SO_2 and sulfates followed by secondary conversion of the sulfates to acid and alkali.
3. Direct reaction of the scrubbing solution with hydrogen sulfide (H_2S) or CO to produce sulfur or H_2S.

Thermal treatment is the most direct approach and is also better developed. Reaction with H_2S or CO will probably be the most cost effective approach since it can directly produce sulfur rather than SO_2.

Many of the regenerable processes produce concentrated gaseous SO_2 as an intermediate product. Conversion of the SO_2 to sulfuric acid is straightforward via reaction with air in a contact acid process. Conversion to sulfur is more difficult. Allied Chemical Company has successfully operated a very large plant (500 LT/day) producing sulfur by reaction of methane with a smelter gas containing 15% SO_2 at temperatures greater than 816°C (1500°F). The primary reactor is followed by a secondary clean-up Claus system reacting residual H_2S and SO_2 to sulfur. The process should work equally well on gases containing 95% SO_2. Another approach to sulfur involves reacting SO_2 with H_2 at 371°C (700°F) to form H_2S, followed by reaction of the remaining SO_2 with H_2S in a Claus system. Sulfur can also be produced by reaction with CO at 371°C (700°F). Regenerable processes that produce H_2S can use the conventional Claus technology to make sulfur.

The Wellman-Lord process uses direct thermal regeneration of sodium sulfite/bisulfite scrubbing solution. The solution is completely evaporated to crystallize sodium sulfite for alkali makeup and generate water vapor containing the removed SO_2. The SO_2 is concentrated to 95% by condensation of the water. Heat at 121°C (250°F) for the evaporator can be supplied by low pressure turbine steam or a heat pump. Residual sulfate formed by SO_3 pickup or oxidation in the scrubber cannot be regenerated and is usually purged as sodium sulfate solids containing 5-10% of the sulfur removed from the stack gas.

Wellman-Lord systems have been treating stack gas from a sulfuric acid plant since 1970 and a Claus plant (sulfur recovery) and oil-fired boiler since 1971 (in Japan). Two new units treating sulfuric acid and Claus tail gas are being started up in the U.S. EPA is co-funding a 100-MW utility demonstration with Northern Indiana Public Service that is due to start up in late 1974. The demonstration will incorporate production of sulfur by the Allied Chemical process.

The magnesium oxide (MgO) scrubbing process, developed in the U.S. by the Chemico Corporation differs from the lime scrubbing system in that a MgO slurry is used as the absorbent. The spent slurry is treated to recover the MgO for reuse, and by-product sulfuric acid is produced. As described by Chemico, the spent slurry from a number of plants would be processed at a central location, and the regenerated MgO would be returned to the user. They believe that the sale of sulfuric acid would pay for the reduction step and still give a satisfactory return on investment to the user.

With EPA co-funding, Chemico has constructed a MgO scrubbing system for a 150-MW oil-fired boiler at Boston Edison Company. The calciner and acid plant are located at Runford, R.I. A similar system has been constructed for Potomac Electric Company for a coal-fired boiler. It too will use the calcining facilities at Rumford. Operation of the system at Boston has demonstrated utilization of the recycled MgO and better than 90% SO_2 removal, although numerous minor problems have been encountered with handling of solids.

The Stone & Webster/Ionics and the NH_3-bisulfate processes use acid decomposition. The spent alkaline solution (mostly bisulfite salts) is reacted with strong bisulfate acid to produce concentrated SO_2 gas and sulfate salts. The Stone & Webster/Ionics process uses electrolysis to convert sodium sulfate solution to sodium hydroxide and sulfuric acid (or sodium bisulfate). The NH_3-bisulfate process uses thermal decomposition of molten ammonium sulfate to ammonium bisulfate and NH_3. Sulfates produced in the scrubbers cannot be regenerated by acid decomposition, but can be removed by neutralizing a portion of the bisulfate acid with limestone to produce gypsum waste. If sulfuric acid is produced from the SO_2, the Stone & Webster/Ionics process can purge sulfates as dilute sulfuric acid for acid plant water makeup. EPA and Wisconsin Electric Company are currently

co-funding a pilot plant demonstration of the Stone & Webster/Ionics process. Tennessee Valley Authority (TVA) has piloted ammonia scrubbing and acid decomposition. NH_3 scrubbing has a problem with the formation of an ammonium salt particulate fume that escapes from the scrubber. Table 3.3 summarizes the various processes and their state of commercial development.

Table 3.3. Comparative Levels of Development-Commercial Systems

Process	Representative Commercial Applications	Technology Gaps
Lime Scrubbing	25 MW Oil - 1970 150 MW Coal - 1972 430 MW Coal - 1971[a]	Scaling and plugging Erosion Waste disposal
MgO Scrubbing	150 MW Oil - 1972[a] 125 MW Coal - 1973	Demo sulfur production Solids handling
Wellman-Lord	Acid and sulfur plants 70 MW Oil - 1971 100 MW Coal - 1973	Na_2SO_4 purge reduction Demo sulfur production
Double Alkali	BaSO Kiln - 1971 40 MW Coal - 1973 200 MW Oil - 1973	Waste disposal Solids handling

[a]These systems have not yet successfully started up.

Environmental Impact

Generally, all of the systems can achieve 90-95% SO_2 control, so this is not a valid consideration for ranking. Table 3.4 ranks the systems primarily on the basis of the form of the sulfur product. In order of increasing environmental insult the products are elemental sulfur, sulfuric acid, gypsum ($CaSO_4$), and calcium sulfite/sulfate sludge. Sulfuric acid is less desirable than sulfur because it is more difficult to ship and market and is not a disposable waste. Calcium sulfite/sulfate sludge is least desirable because of its chemical oxygen demand and large volume per ton of sulfur. Other considerations of environmental impact include the quantity and quality of waste materials from sorbent degradation.

MgO is the cleanest process; no waste products are expected from its operation. Limestone scrubbing would have the largest quantity of waste

material with 8-13 tons of wet sludge per ton of sulfur. The fluidized bed would be much superior in that it would not only give a much reduced tonnage but also it would give dry calcium sulfate rather than gelatinous calcium sulfite.

Table 3.4. Comparative Environmental Impact

Process	Products and Waste Per Ton Sulfur Abated
1. MgO	3 tons H_2SO_4 (100%) or 1 ton sulfur
2. Regenerable sodium alkali scrubbing	0.95 tons sulfur 0.25 tons Na_2SO_4 or $CaSO_4$
3. Regenerable ammonia scrubbing	0.95-1.0 tons sulfur 0.0-0.15 tons $(NH_4)_2\ SO_4$
4. Acid neutralization (Chiyoda or Hitachi carbon)	5.5 tons dry $CaSO_4$
5. Lime throwaway scrubbing (Slurry or double alkali)	6-9 tons $CaSO_3/SO_4$ wet sludge
6. Limestone throwaway scrubbing	8-13 tons $CaSO_3/SO_4$ wet sludge

The quality and quantity of calcium sludge product vary with the type of throwaway process. The Chiyoda and Hitachi processes directly produce a high quality marketable gypsum by neutralization of dilute sulfuric acid. Throwaway processes using lime make less sludge than one using limestone because of greater utilization (lower stoichiometry) of the calcium value. Improvements are under development in the sludge volume and quality from lime/limestone scrubbing systems. In disposal ponds, settled sludge from limestone scrubbing is 40-50% water and occupies 300 ft^3 per ton of contained sulfur.

The regenerable scrubbing processes using sodium or ammonium alkali produce some sulfate that cannot be regenerated. Sodium sulfate can be marketed as such or converted to calcium sulfate for solid waste disposal. Ammonium sulfate can be marketed or decomposed to N_2 and SO_2.

Ammonia scrubbing processes may suffer from sulfite/sulfate fume formation. There appear to be solutions to this problem but their costs are not included in current cost estimates and their feasibility has not been tested. In addition, ammonia scrubbing will emit 25-100 ppm of gaseous NH_3.

Almost all of the systems have potential for particulate emissions as entrained solids, slurry, or solution, but such entrainment is easily eliminated with solution scrubbing and can be eliminated for slurry scrubbing and solids contacting by the proper design of mist eliminators and cyclones.

Most of the commercial applications of stack gas cleaning are being designed for 80-90% SO_2 removal, but potentially most processes could achieve up to 90% removal. The Stone & Webster/Ionics and Sulfoxel processes are immediately capable of 99% SO_2 removal. If a stage of sodium hydroxide scrubbing were added, Wellman-Lord and double alkali could achieve up to 99% removal. Such effective SO_2 removal may be necessary for future abatement of sulfur pollutants.

Economic Analysis

The cost of stack gas cleaning is an important criterion in process evaluation because it will ultimately determine the process to be used if other considerations are equal. At the same time, process economics is the most difficult criterion to generalize on a comparative basis. On the basis of cost information from contractors and other sources, the Control Systems Laboratory, EPA, prepared and presented information representing the costs of the major wet scrubbing processes.[23] This information base has been expanded to include the double alkali and citrate processes.[24]

Essentially all economic comparisons published to date have been aimed at utility systems based on 500 MW generating capacity (or larger), 3.5% S coal, a retrofit system and 60% load factor. On this basis EPA[6] estimates installed capital costs of $24-36/kW for throwaway systems and $39-55 per kW for recovery systems. These costs include particulate waste removal at $1/ton, no credit for sulfur product and no costs for waste disposal facilities which are usually $5-10/kW. These published costs are considerably lower than recent estimates prepared by the TVA for throwaway lime or limestone slurry systems.[25] The TVA estimates are shown in Table 3.5.

Table 3.5. TVA Cost Estimates of Lime/Limestone Stack Gas Cleaning Systems*

Size, Type	Installed Cost $/kW
500 MW - Retrofit	60
500 MW - New Installation	50
100 MW - Retrofit	70-90

*1975 dollars, assumes developed technology. TVA estimates total operating cost for a 500-MW retrofit system, at 14.9% fixed charge rate, to be 2.7 mils/kWhr, about half of which is operating cost.

The variation of costs with source parameters (size, sulfur content, load factor, etc.) is much greater than the variation of costs between processes. Depending on source conditions, the annualized cost of limestone scrubbing may conceivably vary from 40-99¢/10^6 Btu. The annualized costs include operating costs and 22.2% capital charges for depreciation and return on investment.

Throwaway processes are favored by simultaneous particulate scrubbing and SO_2 removal, low costs of waste disposal, and lack of a sulfur product market; regenerable processes are favored by high waste disposal costs, and a major impact on costs. The throwaway processes cost about the same as the regenerable processes because the added complexities of calcium slurry scrubbing balance the requirement for sorbent regeneration and product recovery.

As viewed by EPA, the least costly processes are those newer systems under development represented by the double alkali process. However these new systems are only expected to reduce annualized costs 15-20%.

The annualized costs are primarily composed of capital charges for depreciation, return on investment, and maintenance, but utilities and materials costs are significant. The energy requirements of the processes are represented in Table 3.6. The throwaway processes have the lowest energy requirements but the greatest material requirements. The lime scrubbing process would require a total increase in fuel consumption at the power plant of about 3.5%; Stone & Webster/Ionics, 10.7%.

Table 3.6. Process Energy Requirements[a]

Representative Process	Energy as % of Power Plant Output	
	Power	Fuel
Throwaway Scrubbing		
Limestone Scrubbing	2.2	1.6
Lime Scrubbing	1.9	1.6
Chiyoda	2.2	1.6
Regenerable Scrubbing (to S)		
Wellman-Lord	4.5[b]	3.1
MgO	2.2	5.6
Stone & Webster/Ionics	7.6	3.1
NH_3-Bisulfate	1.9	5.1
Citrate, Sulfoxel	2.0	3.1

[a]Based on coal with 3.5% sulfur.

[b]Includes 2.5% derating of power output for steam consumption (5% at 15 psig).

Thus it may be concluded that for industrial boilers:

1. Reasonably waste-free flue gas cleaning processes are or will soon be available at annualized costs of $\leq$ 50¢/10^6 Btu.

2. Lime scrubbing and the Wellman-Lord system are in commercial practice. Other processes have specific development problems.

3. Cost differences between processes are rarely greater than 15%. Throwaway processes are significantly less costly only where waste disposal is cheap.

4. Regenerable processes offer less potential for environmental degradation by waste products, although sale of the by-product could be a problem.

Fluidized-Bed Furnaces

The motion of the particles in a fluidized bed provides an ideal environment for contacting limestone with sulfur oxides in the bed. The movement of the particles provides uniform contact with the sulfur oxides

Table 3.7. Estimated Annual Operating Cost of a Limestone Slurry System for Sulfur Dioxide Removal

Basis: 830,000 lb steam/hr, 49 tons/hr coal (23.8 x 10^6 Btu/ton), 3.5% sulfur, 80% plant factor (292 days/yr) 75% scrubbing efficiency, equipment capital cost $6,210,000. 49 x 24 x 292 x 0.035 x 0.75 = 9014 tons/yr of sulfur removed.

Capital charges @ 22.2% fixed charge rate	$1,378,620
Limestone (5 T/T sulfur) @ $8/T	360,560
Grinding and slurry preparation (100 kWhr/T limestone) @ 15 mils/kWhr	1,352
Water (3000 Gal/T sulfur removed) @ 15¢/1000 gal	4,056
Repairs and maintenance materials (3% of capital)	186,300
Disposal (15 T of 50% solids per T of sulfur) @ $4/T	540,840
Labor ($14,520/yr per man) 2.5 men/shift	108,900
Fringes @ 40% of labor	43,560
Total annual operating cost	$2,624,188

Cost per T of sulfur removed - $291

Cost per million Btu - 32¢

and creates erosion of the sulfated shell and exposes unreacted surfaces. The bed operating temperature range is favorable for this chemical reaction.

A considerable amount of experimental work has been done with fluidized beds during the past few years and this has shown that this system has very good potential as a method of sulfur removal from fossil fuels. Results obtained by Pope, Evans and Robbins,[11] Argonne National Laboratory,[26] and the National Coal Board[18] of England demonstrate that up to 97% of the sulfur content of the coal burned in a fluidized bed can be reacted with limestone and thus be removed as an air pollutant in the form of SO_2. Each of these investigators has found that the degree of sulfur removal varies quite widely depending upon a rather large number of variables. There appears to be good agreement as to which are the more important variables and most of the results agree on the effect of a particular factor. A comprehensive analysis of these variables and their effects is given in Ref. 18.

The effects of nine of the more important variables are considered in the following discussion in order to point up their importance in arriving at a system that can achieve the desired rate of sulfur removal. These variables include:

1. Ca/S ratio
2. Coal type
3. Additive type
4. Combustion temperature
5. Fluidizing velocity
6. Additive particle size
7. Fines recycle
8. Bed height
9. Operating pressure

Ca/S Ratio

The Ca/S mole ratio is the most significant variable determining the reduction in SO_2 emission. The SO_2 emission is reduced and approaches zero as the ratio of calcium to sulfur is increased. The sulfur retention is almost independent of the sulfur content of the coal at a given value of the Ca/S mole ratio. The % sulfur retention as a function of Ca/S ratio is illustrated in Fig. 3.8. The percent sulfur retention is defined as:

$$\frac{\text{Sulfur in coal} - \text{Sulfur in gas}}{\text{Sulfur in coal}} \times 100$$

This includes the benefit of the natural tendency of the coal to retain some of its sulfur even without any limestone addition, which may often amount to about 10%. The sulfur retention increases from 61 to 93% as the Ca/S ratio is increased from 1.3 to 3.3. These data are from Ref. 18 for Pittsburgh coal and Limestone 18 with a particle size of 1680 μm or less at a bed temperature of 1560°F, a fluidizing velocity of 4 fps, a bed height of 2.2 ft. and without fines recycle.

The sulfur retention at a given Ca/S mole ratio is dependent upon the other variables. For a given coal and type of calcium-bearing additive, the sulfur retention is improved with lower fluidizing velocities, a bed temperature of around 1500°F, smaller additive particle size, increased bed height and with recycle of the fines larger than about 10 μm.

ORNL DWG. 75-16532

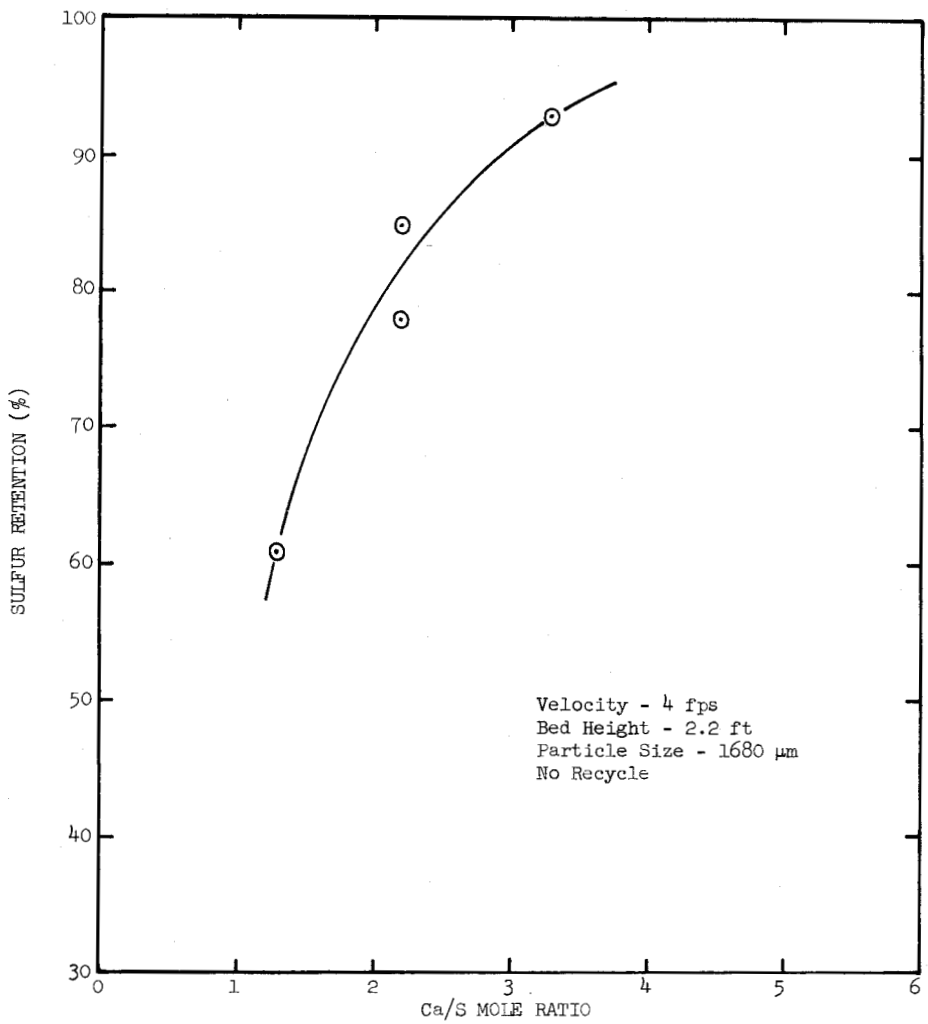

Fig. 3.8. Sulfur retention vs. Ca/S mole ratio for Pittsburgh coal and Limestone 18 at 1560°F. (Ref. 3).

Type of Coal

The most important coal property is the sulfur content, since the quantity of additive required for a given percentage of sulfur retention is approximately proportional to this and the percentage SO_2 reduction that must be achieved in order to obtain a particular SO_2 emission is lower with a low-sulfur coal. A direct comparison of coals with different sulfur content may be made by plotting the percentage SO_2 reduction against the Ca/S mole ratio. All the coal types should fall on the same curve if the SO_2 removal is a function of the Ca/S ratio only and independent of the sulfur content itself. Data from the National Coal Board[18] for four types of coal are shown in Fig. 3.9. The results for three of the coals fall together generally but the results for the Welbeck coal are up to 15% higher. The other three coals had sulfur contents ranging from 2 to 4.4%, but the Welbeck coal had only 1.3% S. The investigators state that the probable explanation of the higher SO_2 reduction with Welbeck coal is its low sulfur content, which had the consequence that there was a low additive feed rate. The low feed rate led to a longer residence time and could have resulted in a higher degree of sulfation, particularly if particle attrition was an important effect.

Another possible explanation for variation in SO_2 reduction among different types of coal has been proposed by workers at Westinghouse.[14] They analyzed data from the National Coal Board tests and felt that the results showed a trend with the swelling index of the coal rather than the sulfur content. Their smoothed curves of % S retention against Ca/S ratio are shown in Fig. 3.10. They show a distinct curve for each of four types of coal with the sulfur retention increasing with a decrease in the swelling index. The Welbeck coal gave the best results of the four types, but the results of the other three did not correlate with sulfur content. The effect of swelling index is explained by the faster release of volatiles from the coals with low swelling indices. Both the National Coal Board and Westinghouse indicate the sulfur removal may be influenced by the ratio of inorganic to organic sulfur in the coal.

Another coal property that is thought to probably be of importance is the composition of the ash material in the coal. Westinghouse[14] workers make reference to results obtained by the Bureau of Mines where they found

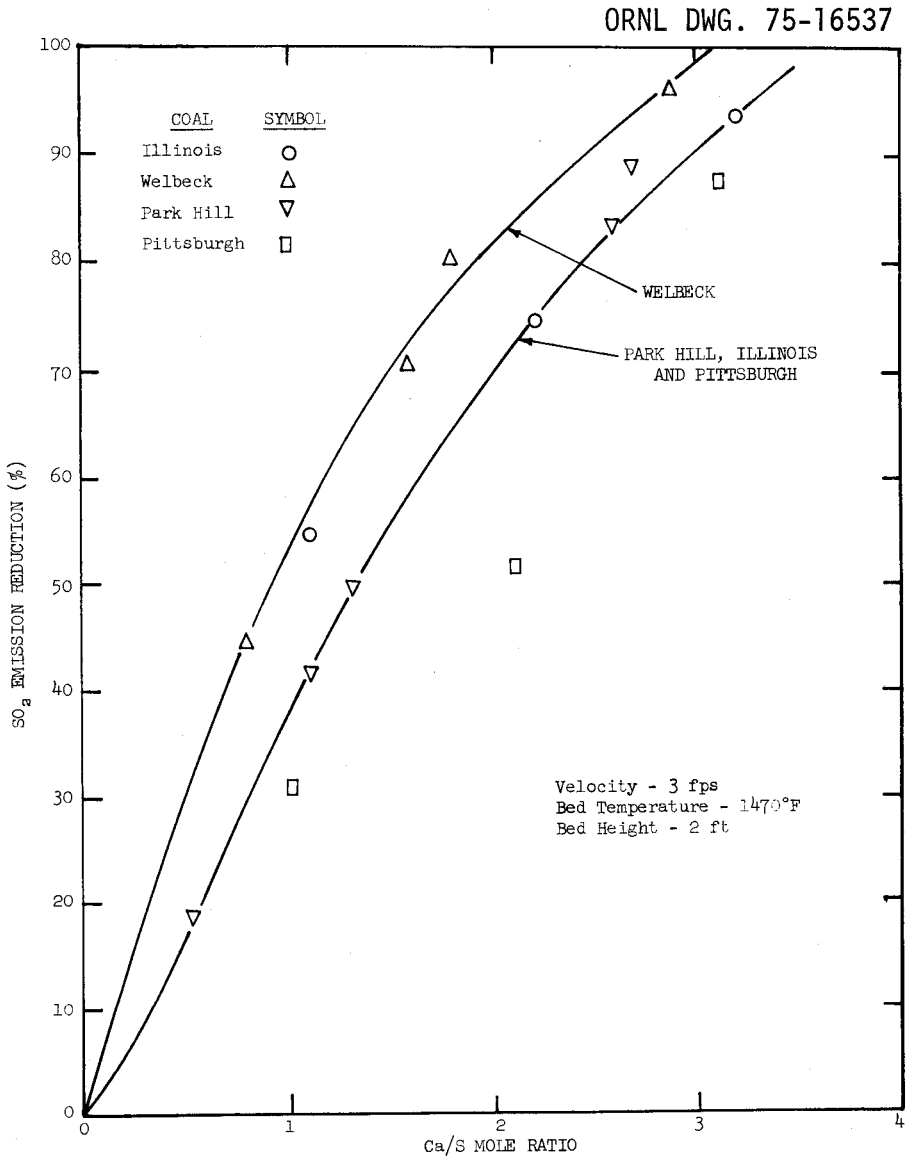

Fig. 3.9. Comparison of SO_2 reduction for different coals with U.K. limestone. (Ref. 18).

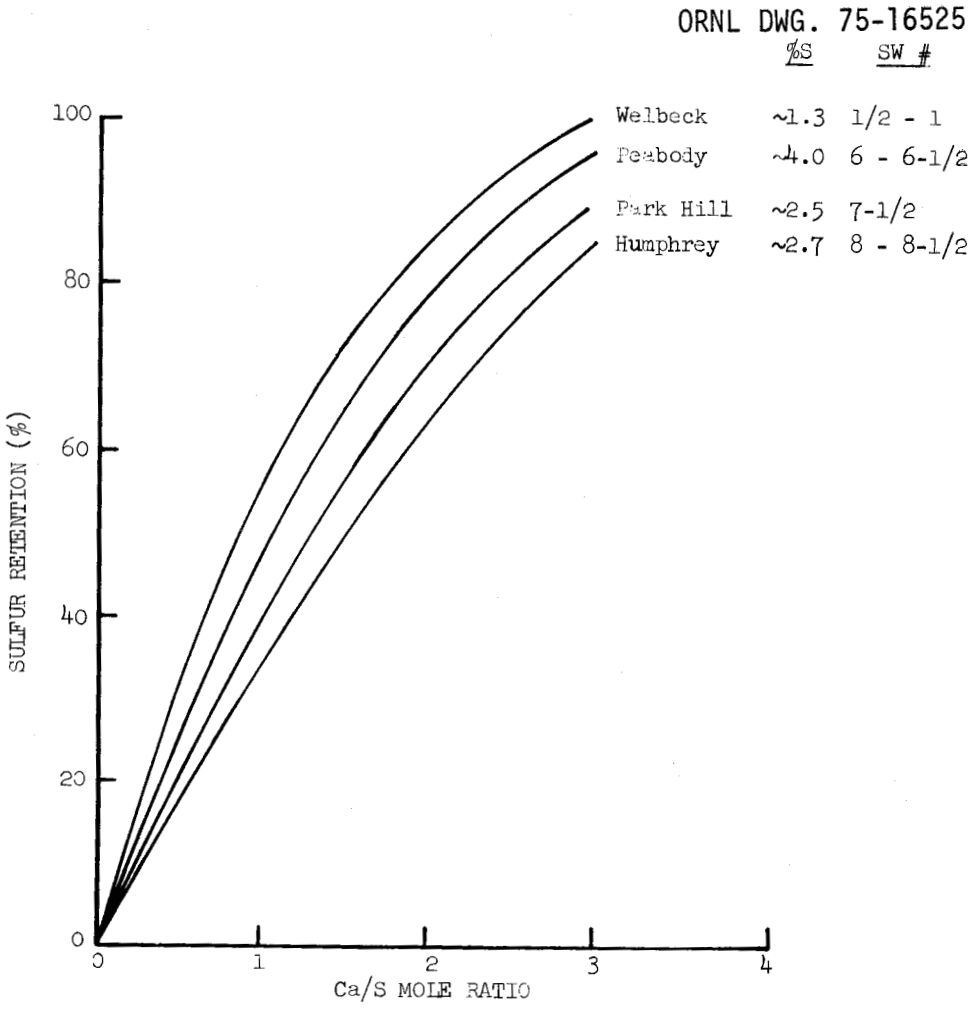

Fig. 3.10. Effect of Ca/S on sulfur retention for various coals. (Ref. 14).

that with a high-ash coal containing silicate materials the formation of a glassy coating from the reaction of the lime and silicates occurred. This glassy coating reduced the sulfur removal to about 15%. When the same coal was washed, reducing the amount of ash material, sulfur removals of 89 to 94% were obtained.

Type of Additive

Limestones and dolomites from several sources have been used as additives to provide the calcium for tests in coal-burning fluidized beds. The National Coal Board[18] ran tests with Dolomite 1337 (28.9% CaO), Limestone 18 (45.7% CaO), Limestone 1359 (55.7% CaO) and U.K. Limestone (55.4% CaO). It was found that on a molar basis the four additives can be placed in descending order of effectiveness as follows:

Limestone 18
U.K. Limestone and Dolomite 1337
Limestone 1359

A plot of percent sulfur retention against Ca/S ratio is given in Fig. 3.11 for Limestone 18 and Dolomite 1337 with Pittsburgh coal at a temperature of 1470°F and a velocity of 4 fps. Since the calcium content of dolomites is lower than that of limestones the effectiveness of dolomite on a weight basis is lower than limestone of the same effectiveness on a molar basis. Thus, on a weight basis, the above order of effectiveness is changed to:

Limestone 18
U.K. Limestone
Limestone 1359
Dolomite 1337

Pope, Evans, and Robbins[11] ran a number of experiments with Dolomite 1337 and Limestone 1359 in a fluidized bed burning Ohio No. 8 seam Pittsburgh coal. They found that the dolomite was more effective on a molar basis, but the limestone was more effective on a weight basis, which agrees with the National Coal Board's results.

ORNL DWG. 75-16526

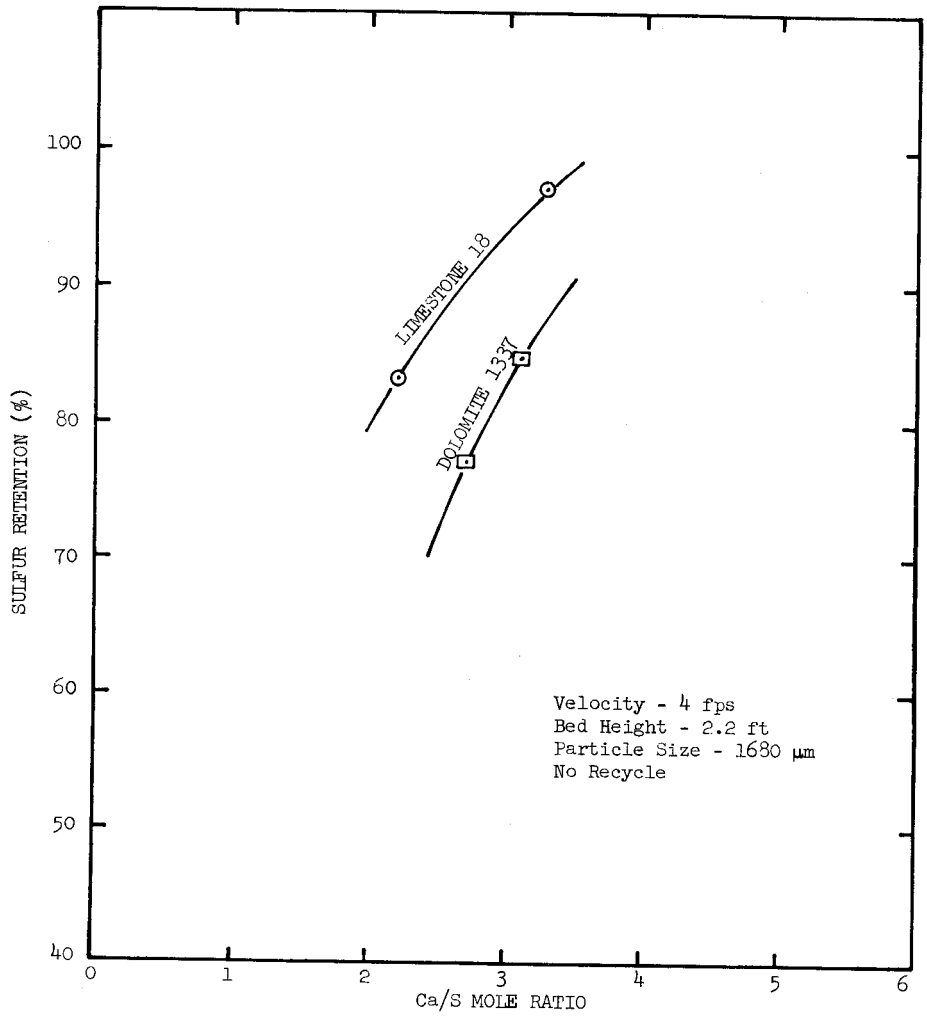

Fig. 3.11. Sulfur retention vs. Ca/S mole ratio for Limestone 18 and Dolomite 1337 with Pittsburgh coal at 1470°F. (Ref. 18).

Combustion Temperature

Studies of the effect of the combustion temperature of the fluidized bed on sulfur retention by the National Coal Board[18] indicate that for most operating conditions there is an optimum temperature between 1400°F and 1600°F at which the percent sulfur retention is a maximum, decreasing from that value at both lower and higher temperatures. The influence of bed temperature appears to be related to findings from laboratory studies of Limestone 18 that the reaction rate constant varies with temperature in a manner that depends on the fraction of the lime utilized. With less than 20% of the lime converted, the reaction rate constant continues to rise with temperature up to at least 1650°F, but as the fraction of lime reacted increases, a peak develops in the curve, and becomes more pronounced as the percent lime utilized is increased as shown in Fig. 3.12. The percent sulfur retention vs temperature is shown for Limestone 18 and Dolomite 1337 for a fluidizing velocity of 4 fps in Fig. 3.13. It may be observed that the curve peaks much more sharply for limestone than for dolomite.

It was found that the decrease in sulfur retention above the optimum temperature is somewhat less for lower fluidizing velocities and for higher values of Ca/S ratio. The latter effect is probably due to the decrease in lime utilization with higher values of Ca/S ratio.

Fluidizing Velocity

The sulfur retention was found to decrease as the fluidizing velocity was increased in the experiments performed by the National Coal Board.[18] Some of the data that show this trend are presented in Fig. 3.14 for Pittsburgh Coal and Limestone 18 for three combinations of additive particle size and Ca/S ratio. While the velocity was not varied over the full range of 2-11 fps for a constant set of conditions, the results indicate that the sulfur retention would decrease continuously as the velocity is increased over that range with all the other variables being held constant.

The effect of the fluidizing velocity is attributed to the decrease in gas residence time and a reduction in solids residence time due to higher bed voidage with increased gas velocity.

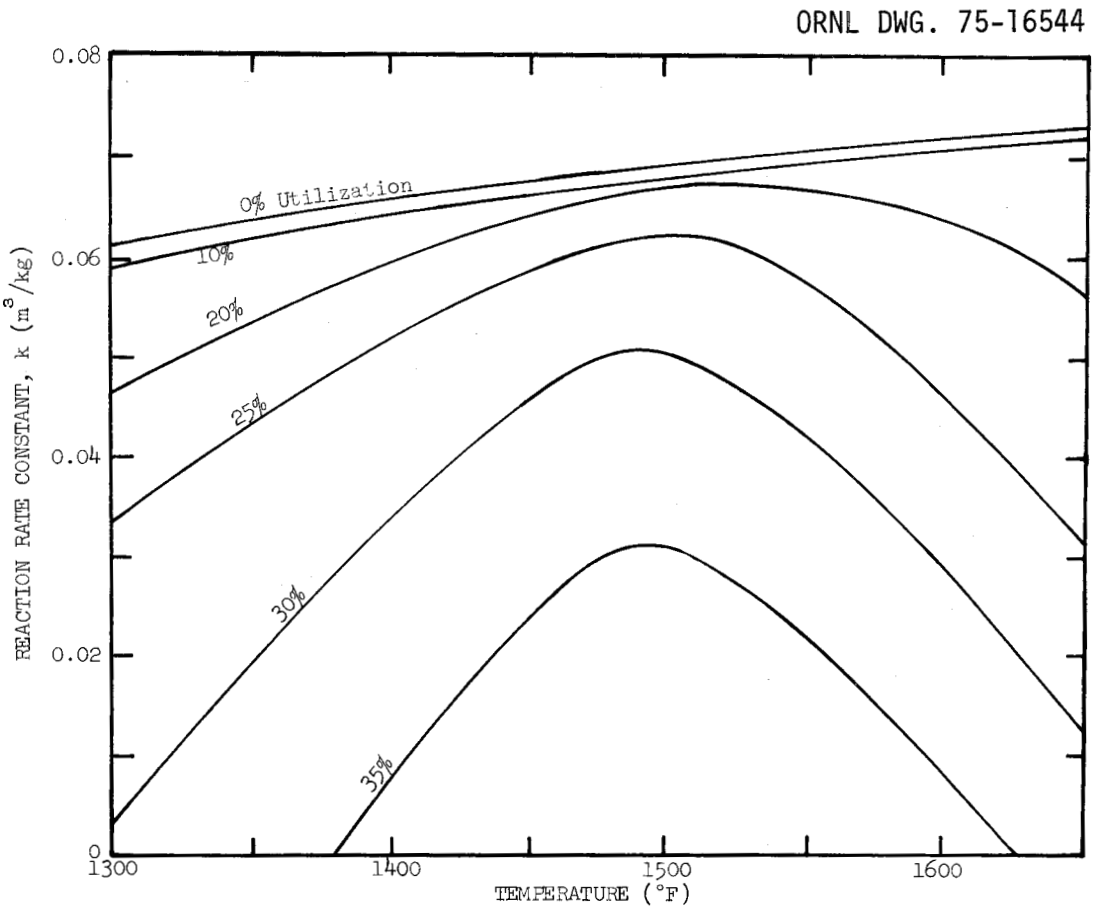

Fig. 3.12. Variation of reaction rate constant with temperature and percent utilization of Limestone 18 for a particle size of 1000 - 2060 μm.

ORNL DWG. 75-16528

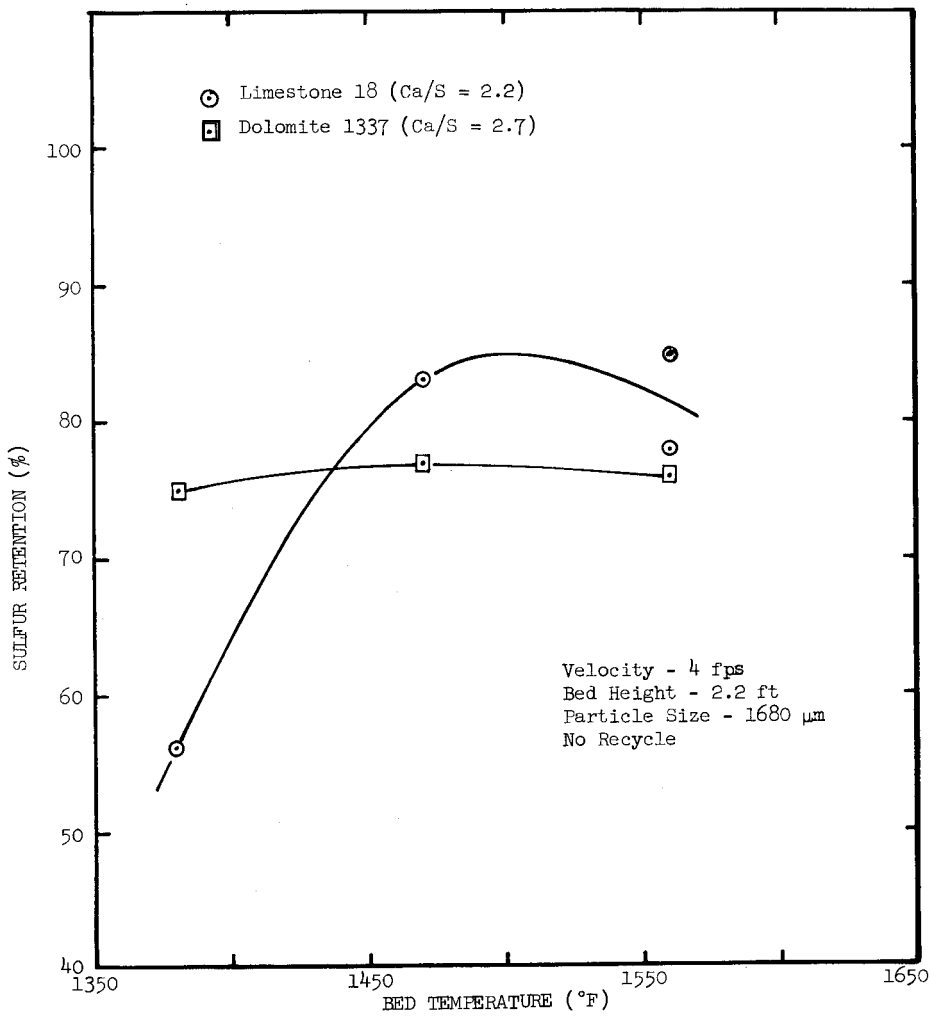

Fig. 3.13. Sulfur retention vs. bed temperature for Limestone 18 and Dolomite 1337 with Pittsburgh coal. (Ref. 18).

ORNL DWG. 75-16541

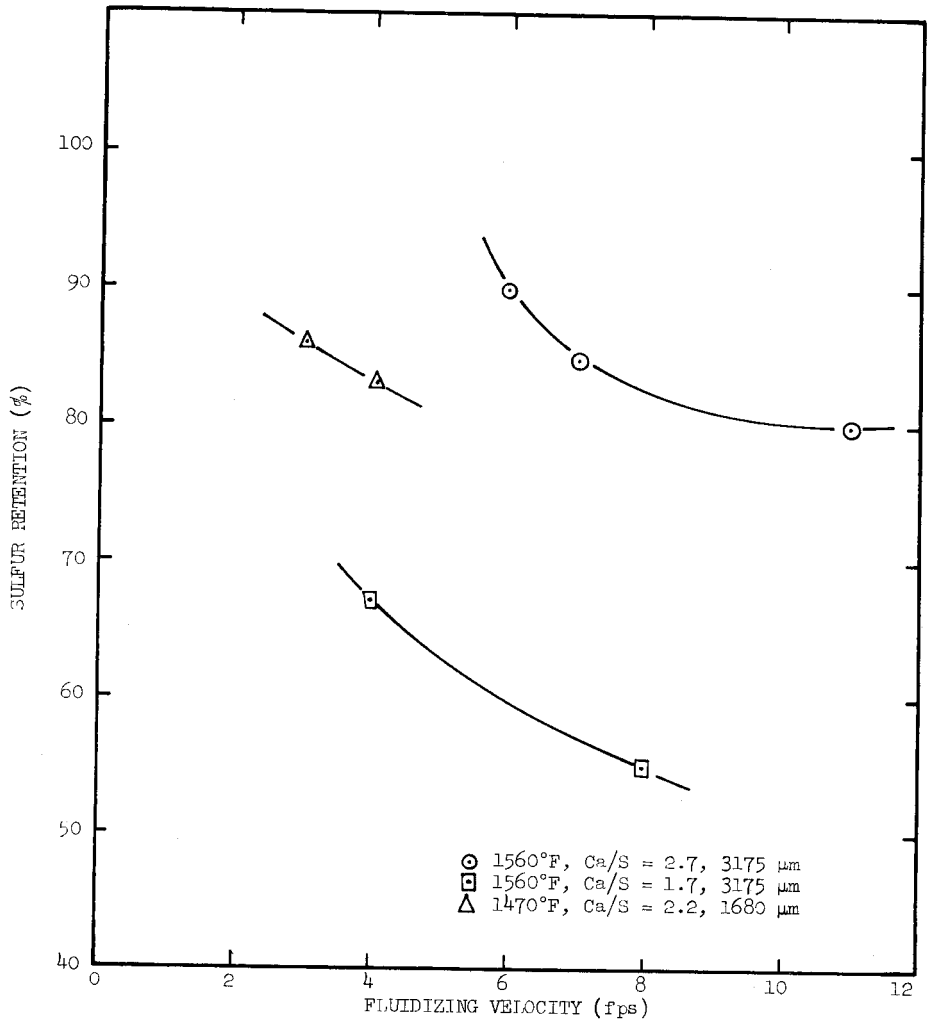

Fig. 3.14. Sulfur retention vs. fluidizing velocity for Pittsburgh coal and Limestone 18. (Ref. 18).

Additive Particle Size

Reduction in additive particle size could be expected to improve sulfur retention in fluidized beds from the increase in surface area. However, smaller particle size may result in increased carryover from the bed and hence reduce the additive residence time, leading to reduced SO_2 removal. Further reduction in particle size below that where rapid carryover occurs will not greatly affect the residence time in the bed and would be expected to increase sulfur retention. Thus, there may be a critical particle size for a given velocity where the sulfur retention reaches a minimum value, and then increases for finer particle sizes.

The results found in tests by the National Coal Board[18] indicate that such a minimum value may exist. The reduction in SO_2 emission is shown for Limestone 18 with particle sizes of 150 and 3175 μm at a gas velocity of 8 fps in Fig. 3.15. In this case the smaller particle size led to a reduction in sulfur retention. In Fig. 3.16 the results for Limestone 1359 with particle sizes of 125 and 1680 μm at a gas velocity of 3 fps are shown. At this velocity the reduced particle size led to an improvement in sulfur retention. The results for Limestone 18 for particle sizes of 1680 and 3175 μm and 8 fps are shown in Fig. 3.17. The smaller particles gave improved performance, indicating a benefit from increased surface area, with no loss due to more carryover for this size change. No effect from particle size was found for Dolomite 1337.

Pope, Evans and Robbins[11] found an increase in sulfur retention when the particle size of Limestone 1359 was reduced from 74 μm to 44 μm at a velocity of 12 fps. This further indicates the possibility of a particle size giving minimum sulfur retention.

It appears from the data available thus far that one could expect to find the highest values of sulfur retention by using limestone particles ground at least as fine as 44 μm in size.

Fines Recycle

Fine particles that are carried over from the coal-burning fluidized bed contain unburned carbon resulting in a loss in combustion efficiency. This loss of carbon can be reduced by passing the discharge stream through a mechanical separator and recycling the particles back to the bed. The

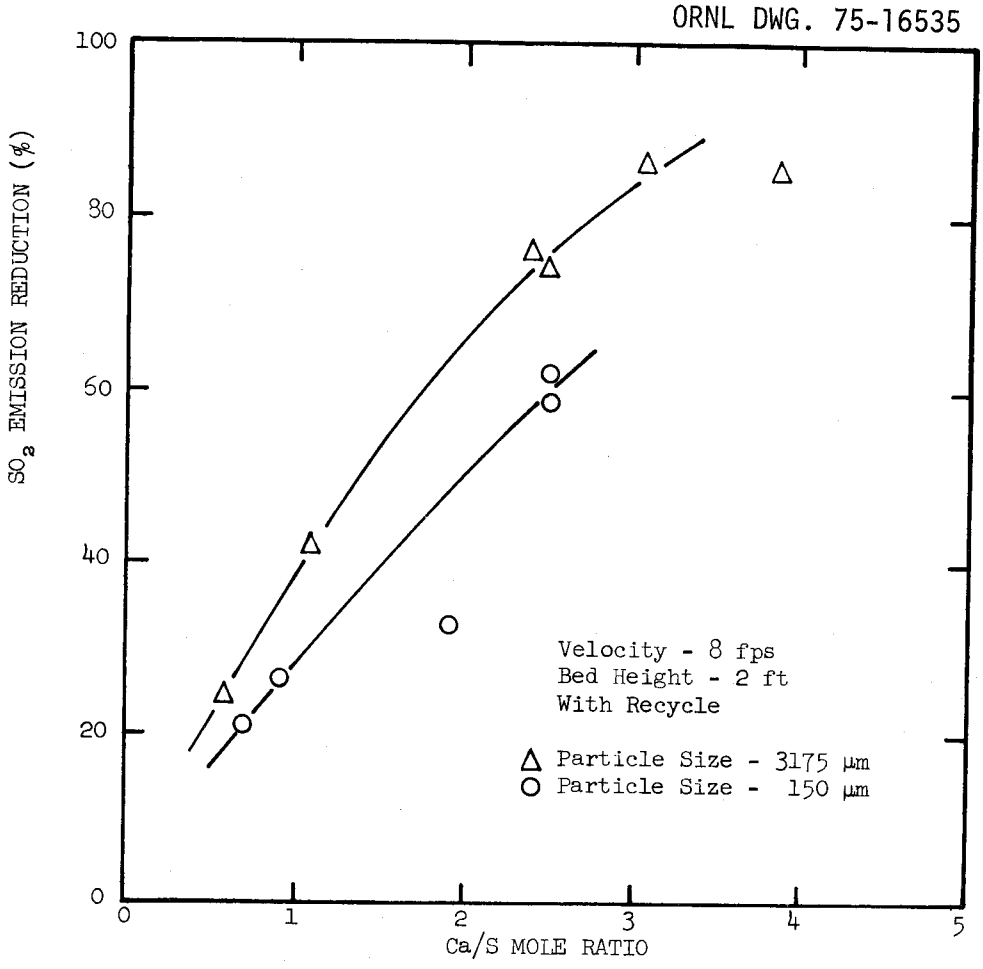

Fig. 3.15. Effect of additive particle size on SO_2 reduction for Pittsburgh coal and Limestone 18 at 1550°F. (Ref. 18).

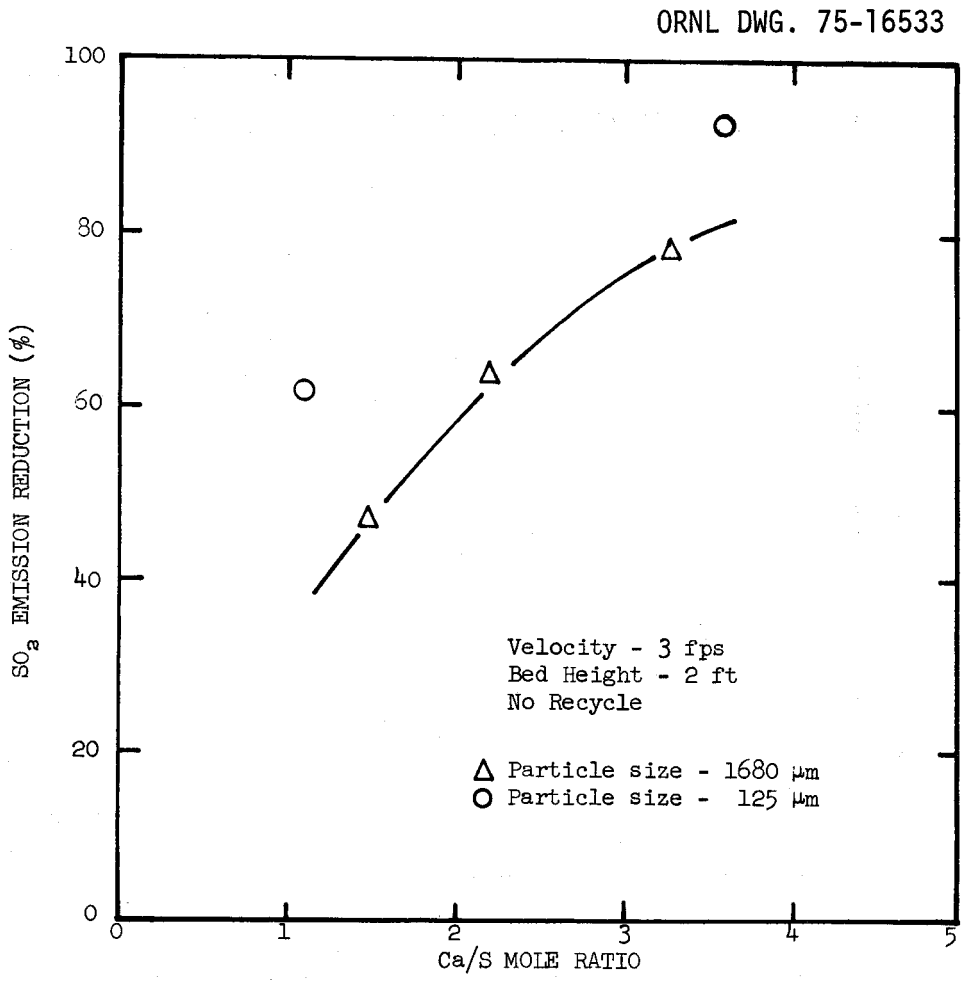

Fig. 3.16. Effect of additive particle size on SO_2 reduction for Illinois coal and Limestone 1359 at 1470°F. (Ref. 18).

ORNL DWG. 75-16529

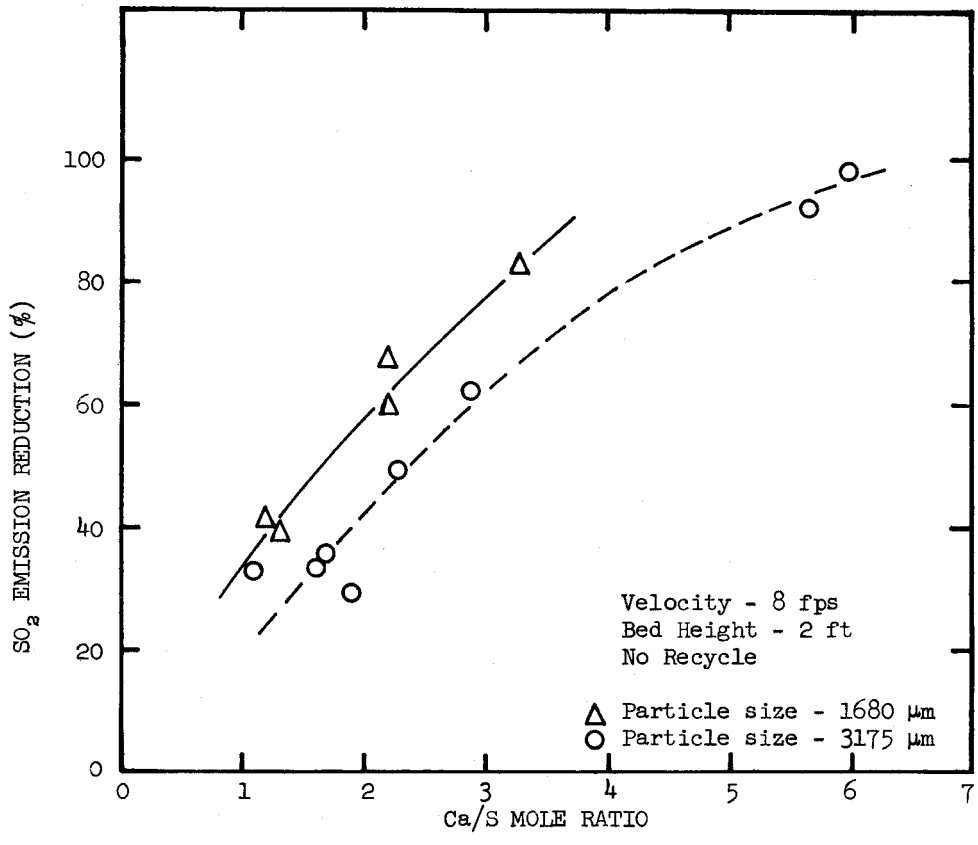

Fig. 3.17. Effect of additive particle size on SO_2 reduction for Limestone 18 at 1560°F. (Ref. 18).

fines carried out of the bed also contain incompletely utilized lime so that it might be expected that fines recycling will improve the sulfur retention for a given value of Ca/S ratio of the fresh feed material. An improvement in sulfur retention with fines recycle was found by the National Coal Board.[18] For Pittsburgh coal and Dolomite 1337 with a bed height of 3.8 ft, velocity of 2 fps, Ca/S ratio of 1.6 and bed temperature of 1470°F the percent sulfur retention was increased from 76 to 99% when the discharge particles above 10 μm were recycled. For Pittsburgh coal and Limestone 18 with a bed height of 2 ft, velocity of 8 fps, Ca/S ratio of 2.45 and bed temperature of 1560°F of fines is probably less effective at higher temperatures, since the reaction rate constant decreases for temperatures above 1500°F as the percent of lime utilized is increased.

Bed Height

Increase in the height of the fluidized bed increases the residence time of both gas and solids and would be expected to improve the sulfur retention. The National Coal Board[18] investigated the effects of bed height in a few tests and found a small increase in sulfur retention as the bed height is increased. With Pittsburgh coal and Dolomite 1337 at a velocity of 8 fps, Ca/S ratio of 5.4 and a bed temperature of 1560°F the sulfur retention increased from 88 to 90% when the bed height was increased from 2.7 to 4 ft. With Illinois coal and Limestone 1359 at a velocity of 3 fps, Ca/S ratio of 2.2 and a bed temperature of 1470°F a change in bed height from 2 to 3 ft resulted in an increase in the sulfur retention from 64 to 73%.

Bed heights of about 2 ft are recommended at atmospheric pressure to insure good mixing of the coal and a low fluidizing velocity of about 2 fps will give good sulfur retention at reasonable values of Ca/S ratio. If it is desired to increase the power density by increasing the velocity, the bed height should be increased in proportion to the velocity to avoid the requirement of high values of Ca/S ratio. However, the pressure drop may become excessive at atmospheric pressure if the bed height is increased greatly. If the system pressure is increased in proportion to the bed height, the pressure drop may be kept at an acceptable fraction of the inlet pressure.

Operating Pressure

Increase in operating pressure at the same gas velocity and bed height reduces the solids residence time in the bed in proportion to the increase in pressure. This might be expected to reduce sulfur retention below that for atmospheric pressure.

Increase in pressure can also be expected to inhibit calcination. This is because at atmospheric pressure the partial pressure of CO_2 is below the equilibrium value with $CaCO_3$ at temperatures above about 1380°F. At pressures greater than 2 atm, the partial pressure of CO_2 is above equilibrium at 1470°F and calcination cannot occur. This would prevent pore formation in limestone and reduce sulfur retention. The equilibrium partial pressure of CO_2 with $MgCO_3$ is very high, so that the $MgCO_3$ in dolomite can be expected to calcine at increased pressure giving access to internal surfaces and give better sulfur retention for dolomite than for limestone.

Results from tests reported by the National Coal Board[18] on the effects of pressure showed a reduction in sulfur retention for Pittsburgh coal with Limestone 18 from 77 to 66% when the pressure was increased from 1 to 5 atm. For the same increase in pressure, the sulfur retention increased from 80 to 98% with Dolomite 1337 without recycle of carryover fines. With recycle, the sulfur retention was reduced from 99 to 94% with Dolomite 1337 going from 1 to 5 atm pressure. Dolomite 1337 was more effective on both a molar and total weight basis than Limestone 18 when operating at 5 atm pressure.

Other Operating Variables

In addition to the nine variables above there are other factors that may affect the sulfur retention of a fluidized-bed furnace. These include the spacing of the coal feed points, the diameter and spacing of the heat transfer tubes, and the height of the freeboard above the tube-filled bed.

If the coal feed points are spaced much more widely apart than those used in the tests, a variation in local temperature might lead to a radial variation of sulfur retention resulting in an overall higher SO_2 emission for a given Ca/S ratio of the feed material.

The diameter and spacing of the heat transfer tubes in the bed may affect both the degree of mixing in the bed and the size of gas bubbles that form in the bed. The size of the gas bubbles in turn affect the contact between gas and solids.

The height of the freeboard above the bed proper may affect the sulfur retention since partially reacted calcium can continue to absorb SO_2 in the freeboard and contribute to the effective residence time of the particles.

Estimated Sulfur Retention in Fluidized Bed for Gas Turbine Plant

In order to achieve good thermal efficiency, the plant must operate with a fairly high air temperature at the gas turbine inlet. A temperature of 1500°F was selected as a good compromise between considerations of efficiency and reliability. This in turn requires that in order to heat the air in the tubes the fluidized bed must operate at about 1650°F. The bed will operate at atmospheric pressure and a bed height of about 1 1/2 ft and fluidizing velocity of 2 fps were selected. Using Limestone 18 ground to a size of 44 μm or less with the carryover particles recycled back to the bed will probably give the best sulfur retention. Based on the experimental results previously discussed, it is estimated that for this system a 75% sulfur retention can be achieved at a Ca/S ratio of 2, and about 90% at a Ca/S ratio of 3. Further increase in the Ca/S ratio should yield sulfur retention approaching 100%.

Particulate Emission Control

Particulate Emission Regulations

The Environmental Protection Agency (EPA) on December 23, 1971, published Standards of Performance for New Stationary Sources.[20] These regulations imposed certain restrictions on emissions from fossil-fired steam generators scheduled to be constructed or modified after August 17, 1971. In addition, the individual states are to enact legislation spelling out rules and regulations that would implement the national program of achieving the air quality standards established by EPA.

Each state may adopt the new EPA emission standards as written or impose higher standards of control. For presently operating sources of emission, the individual states may apply more relaxed standards. Eventually the standards for all sources will probably have to be brought up to the new EPA level.

The EPA standard for the discharge of particulate matter into the atmosphere was set at a maximum of 0.1 lb per million Btu heat input per hr and the emissions are not to exceed 20% capacity. However, these standards apply only to fossil-fuel fired steam generating units of >250 million Btu/hr heat input.

Table 3.8 summarizes data for individual states on particulate emission. Note that the average value for the permissible emission of solids from smaller power plants (<10 million Btu/hr) is approximately 0.6 lb/Btu input.

Continued research[27] on the effect of particles under 2 μm has shown that these particles are the most damaging to human health. The trend is toward more stringent regulations regarding the removal of fine particles from stack emissions. Heretofore most emission control has restricted the total mass of particulate discharge with no regard to the fine particles.

The State of New Mexico's Environmental Improvement Agency has issued new regulations governing the emissions on new coal-fired furnaces placed in service after December 31, 1974. They are limiting total emission to 0.05 lb/10^6 Btu heat input and further limiting the emission of particles under 2 μm in size to no more than 0.02 lb/10^6 Btu.[26]

Particulate Control Methods

The separation of the particulates from the flue gas is made possible by certain differences in properties: 1) the large size of the fly ash particles (1 micron to over 100 microns) as compared to the flue-gas molecules, 2) the density of the fly ash (0.03 lb/ft^3), 3) the electrical properties permitting separation by ionization and migration to charged plates.

The techniques used in the separation of particulates from flue-gas rely upon these differences. The collection equipment can be grouped into the following general categories:

1. Dry inertial collectors.
2. Wet scrubbers.
3. Fabric filters
4. Electrostatic precipitators.

Table 3.9 lists the characteristics of various types of collectors.

Table 3.8. Regulations in Selected States for Maximum Allowed Solids Emission from Fuel Burning in Indirect Heat Exchangers

	Heat Input Million Btu/hr	Solids Emission lb/Million Btu Input
Georgia	<10	0.7
	>2,000	0.24
Florida	<250	Latest technology
	>250	0.1
Alabama	<10	0.5, 0.8
	>250	0.12
Chicago	All	0.1
Illinois	<10	1.0
	>250	0.1
Connecticut	All	0.2
Idaho	<10	0.6
	>10,000	0.12
Iowa	Below Max allowable	APS-1 (ASME)
	Max. urban	0.6
	Max suburban	0.8
Kentucky	<10	0.56, 0.75, 0.80
	>10,000	0.11, 0.15, 0.18
Louisiana	All	0.6
Maine	<10	0.6
	>150	0.3
Michigan	<100,000*	0.3 lbs/1000 lbs gas
	>100,000*	to 0.19 lbs/1000 lbs gas
Minnesota	Urban	0.4
	Suburban	0.6
Mississippi	<10 (old)	0.8
	<10 (new)	0.6
	>10,000 (old)	0.24
	>10,000 (new)	0.19
Missouri	<10	0.6
	>10,000 (old)	0.18
	>2,000 (new)	0.10
Montana	<10	0.6
	>10,000 (old)	0.19
	>10,000 (new)	0.12
Nevada	<10	0.6
	>10,000	0.09
	>100,000	0.024
North Dakota	<10 (new)	0.6
	>10,000 (new)	0.24
	>100,000 (new)	0.18
New Jersey	<10	0.6
	>1,000	0.1
New Mexico	<30	0.70
	>30	0.50
New York	<10	0.60
	>10	$1.02\ R^{0.781}$ lbs/hr
North Carolina	<10	0.6
	>10,000	0.1
Ohio	<10 (1)	0.4
	(11)	0.6
	>1,000 (1)	0.1
	(11)	0.15
Oklahoma	<10	0.6
	>10,000	0.1
Oregon	All (old)	0.2 gr/scf
	(new)	0.1 gr/scf
Pennsylvania	<50	0.4
	>600	0.1
Tennessee	>10	0.6
	>10,000	0.1
Vermont	<10	0.5
	>300	0.1
	>1,000 (new)	0.02
Virginia	<25	0.6
	>10,000	0.15
Wyoming	<10	0.6
	>10,000 (old)	0.19
	(new)	0.10

*lbs steam/hr.

Source: Journal of the Air Pollution Control Association, May, 1973.

Table 3.9. Dust Collective Equipment

Types of Dust Collecting Equipment	Particle Size Microns	Loading Grains/ Cu. Ft.	Collection Efficiency Weight %	Pressure Loss Gas, In. W.G.	Pressure Loss Liquid Psi.	Utilities Per 1,000 Cfm.	Gas Velocity, Fpm.	Size Range Limits, 1,000 Cfm.	Space Required, (Relative)
Dry inertial collectors									
Settling chamber	>50	>5	<50	<0.2	-	-	300-600	None	Large
Baffle chamber	>50	>5	<50	0.1-0.5	-	-	1,000-2,000	None	Medium
Skimming chamber	>20	>1	<70	<1	-	-	2,000-4,000	50	Small
Louver	>20	>1	<80	0.5-2	-	-	2,000-4,000	30	Medium
Cyclone	>10	>1	<85	0.5-3	-	-	2,000-4,000	50	Medium
Multiple cyclone	>5	>1	<95	2-6	-	-	2,000-4,000	200	Small
Impingement	>10	>1	<90	1-2	-	-	3,000-6,000	None	Small
Dynamic	>10	>1	<90	Provides head	-	-	-	50	
Wet scrubbers									
Gravity spray	>10	>1	<70	<1	20-100	0.5-2 gpm.	100-200	100	Medium
Centrifugal	>5	>1	<90	2-6	20-100	1-10 gpm.	2,000-4,000	100	Medium
Impingement	>5	>1	<95	2-8	20-100	1-5 gpm.	3,000-6,000	100	Medium
Packed bed	>5	>0.1	<90	1-10	5-30	5-15 gpm.	100-300	50	Medium
Dynamic	>1	>1	<95	Provides head	5-30	1-5 gpm., 3-20 hp.	3,000-4,000	50	Small
Submerged nozzle	>2	>0.1	<90	2-6	None	No pumping	3,000	50	Medium
Jet	0.5-5	>0.1	<90	Provides head	50-100	50-100 gpm.	2,000-20,000	100	Small
Venturi	>0.5	>0.1	<99	10-30	5-30	3-10 gpm.	12,000-42,000	100	Small
Fabric filters	>0.2	>0.1	<99	2-6	-	-	1-20	200	Large
Electrostatic precipitators	<2	>0.1	<99	0.2-1	-	0.1-0.6 kw.	100-600	10-2,000	Large

Note: The terms expressing concentration, or loading, can be defined as light = ½ - 2, moderate = 2 - 5, and heavy = 5+ grains/cu. ft.
Particle size: fine, 50% in ½ - 7 micron size range; medium, 50% in 7 - 15 micron size range; coarse, 50% over 15 microns.

Source: January 27, 1969/ Chemical Engineering

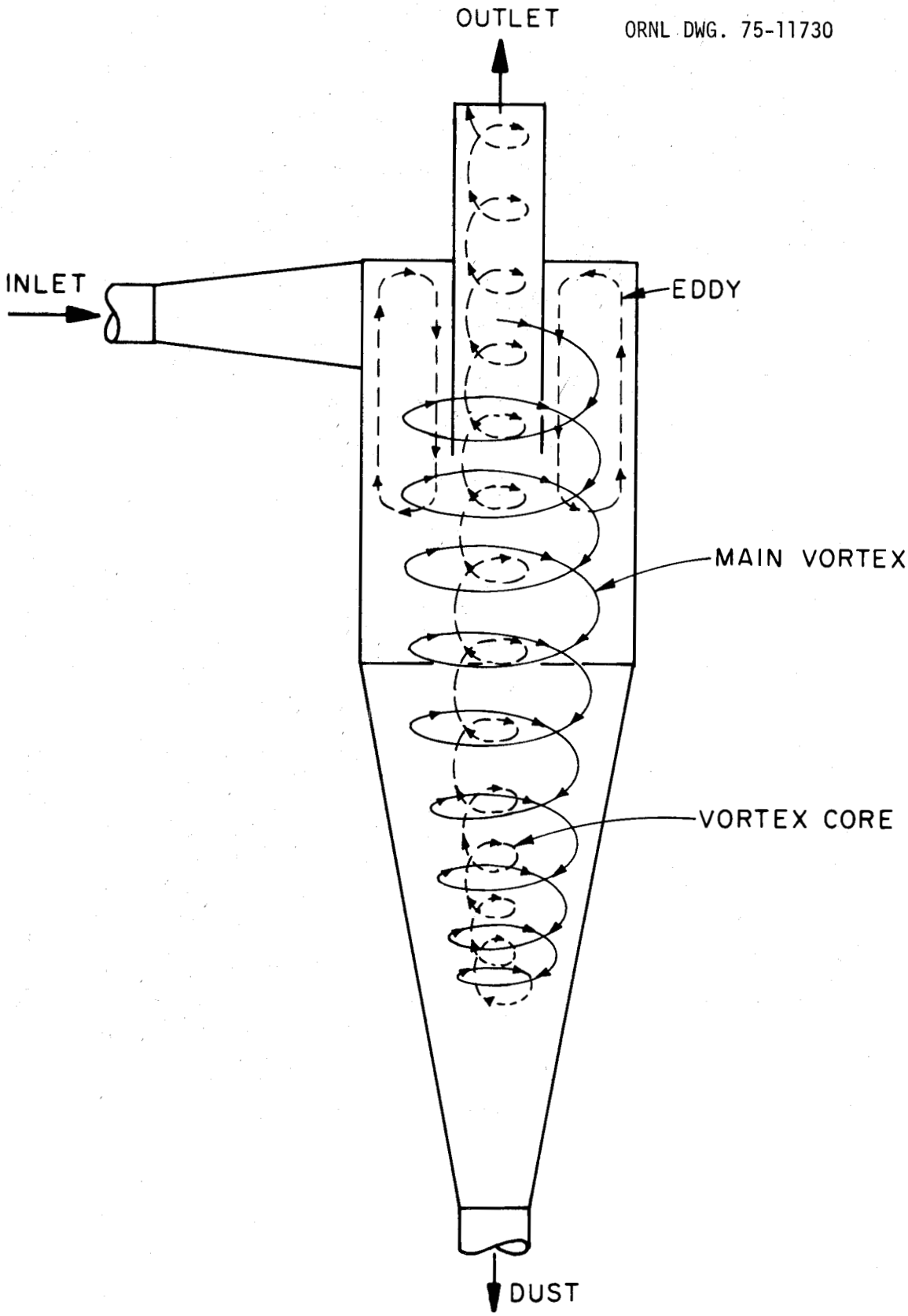

Fig. 3.18. Typical cyclone collector.

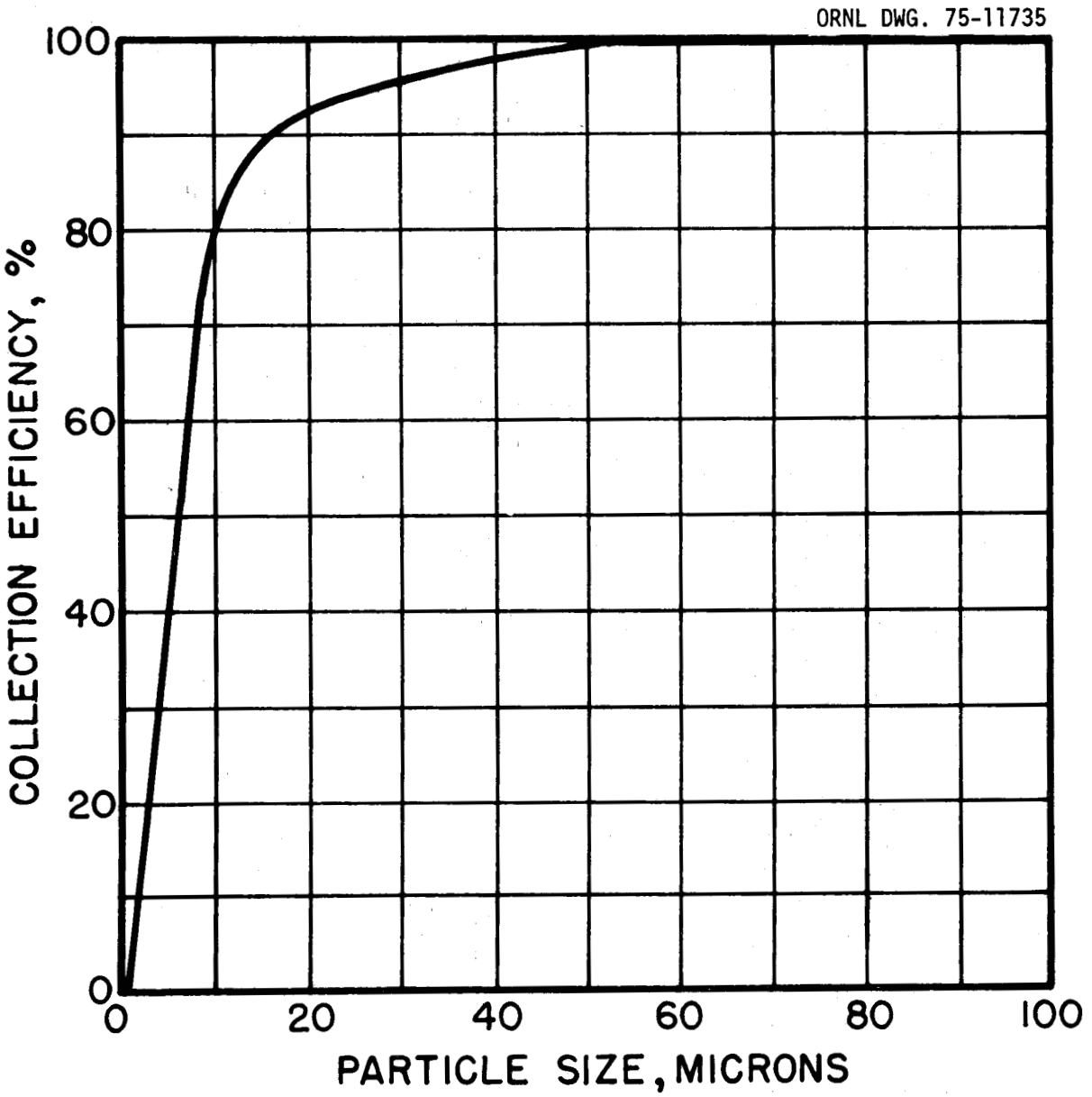

Fig. 3.19. Fractional efficiency curve for a cyclone collector.

Dry Inertial Collectors

Dry inertial collectors are obtainable in many forms; gravity settling chambers, baffle chambers, skimming chambers, impingement separators, cyclone collectors, etc. Because of their simplicity of design, low cost and reliability the cyclone collector (Fig. 3.18) is frequently used as a first stage collector for coal-burning furnaces. In this role it can be classified as a low cost, low efficiency design capable of eliminating the larger (>10 micron) particles as a first-cut in the separation process.

The physical arrangement of the cyclone collector forces the inlet gas into a vortex in which the inertial force (radial component) separates the dense particles from the flue-gas. In the collector shown, the inlet gas forms a spiral vortex downward. As it progresses down the narrowing core, it reverses its downward path and forms a narrow ascending core towards the exit in the top of the collector.

Cyclone collectors operate in the 80 to 90% overall efficiency range. The efficiency of separation is generally depicted on a fractional efficiency curve as indicated in Fig. 3.19. In actual practice the curve is determined by actual performance testing on a known particulate suspension. Favorable increases in efficiency may be obtained by an increase in particle size and density, an increase in the tangential velocity, or by a decrease in gas viscosity or cyclone diameter. By decreasing the collector diameter the tangential velocity increases (assuming a constant volume through-put) and the combination of effects produces an increase in collection efficiency. This process, of course, is limited by the increase in pressure drop that is acceptable. It should be noted that the efficiency drops off rapidly for the removal of particles below 10 microns in size.

For a reasonable increase in cost, increased efficiency in separation and a decrease in space and head room needed can be achieved by the use of a multi-cyclone as pictured in Fig. 3.20. Banks of small diameter cyclones are mounted in parallel and are provided with a common inlet plenum. Units of this type are able to collect particles down to 5 microns with good efficiency and if fabricated of high alloy steels, they may be operated up to 1200°F.

ORNL DWG. 75-11738

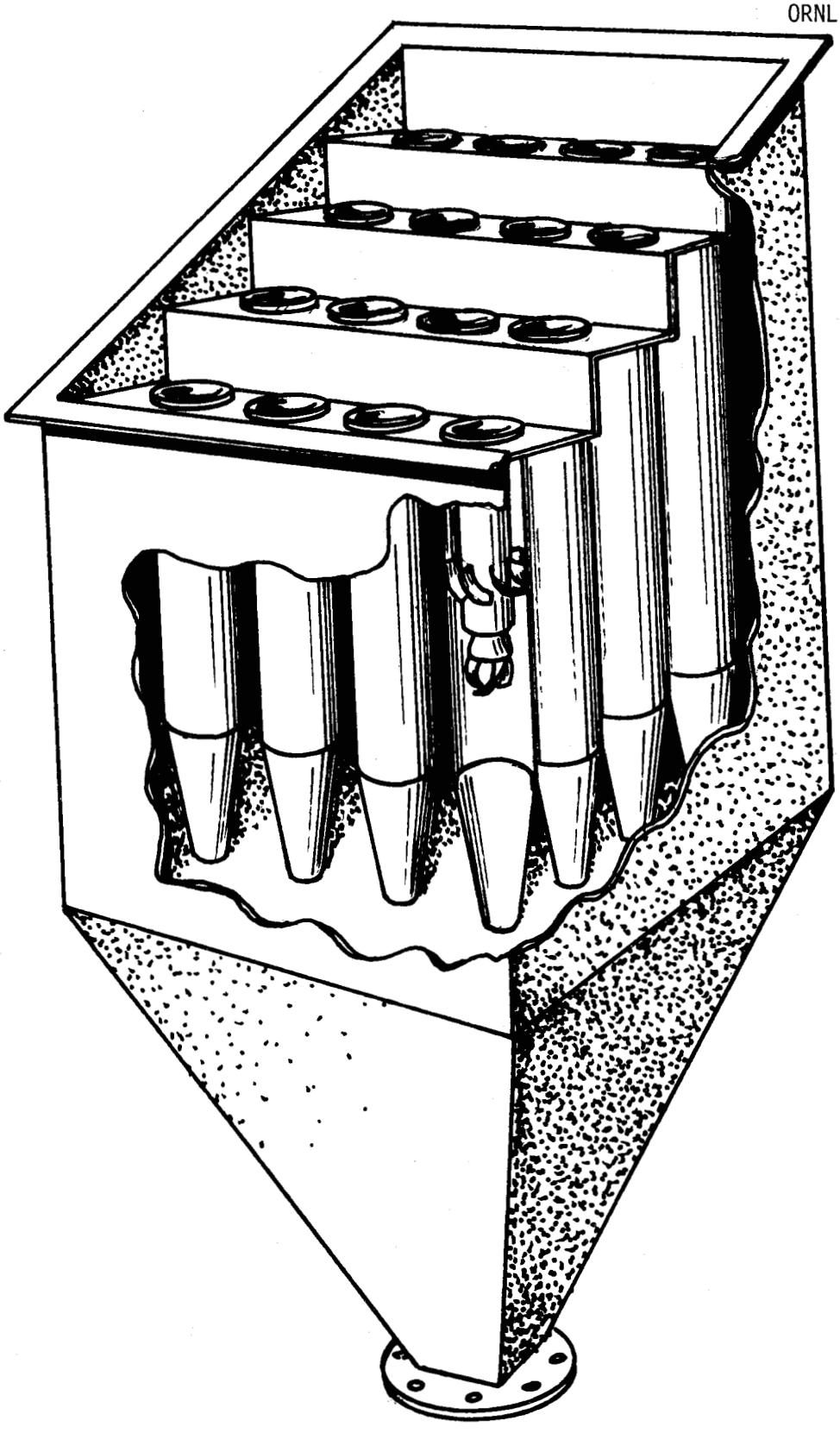

Fig. 3.20. Multi-cyclone collector.

Wet Scrubbers

Wet collectors rely on two mechanisms for removing particulate matter.

1. Providing a liquid droplet for wetting of the particle which increases their effective size, enabling easier separation.
2. Impingement of these particles on collecting surfaces where they can be flushed off.

Types of wet collectors commonly used are spray chambers, impingement plate scrubbers, venturi scrubbers, cyclone-type scrubbers, orifice-type scrubbers, and packed bed scrubbers.

Wet collectors maintain a constant ΔP (at constant air volume). However, in order to obtain the high degree of efficiency in the separation of fines (< 2 microns), a high-pressure drop is required (40 in. to 100 in. H_2O) which is prohibitive in pumping power required. They are able to handle corrosive gases or aerosols and space requirements are small. They have no secondary dust disposal problems but the sludge disposal problem is formidable. A typical wet-venturi scrubber and associated curve showing efficiency vs particle removal size in terms of pressure drop required is shown in Fig. 3. 21.[29] The cost of wet scrubbers is in the medium range. They are seldom used in fly-ash separation from flue-gas because of the high cost of operation and the problems of sludge disposal. They are most useful in applications where the sludge can be returned to the primary process and partially recovered.

Fabric Filters

The simplest collector in principle and maintenance and the oldest in concept is the fabric filter. This filter is also inherently efficient, removing particles over 1 micron in size with efficiencies of 99% or higher. Filters are also able to separate out particles as small as 0.1 micron in size. They are the easiest of all collectors to operate and maintain and require moderate power to operate. The capital costs are in the medium price range.

The major disadvantage is the temperature limitation (500° maximum for currently available fabrics), and the increased cost per yard for high temperature-rated fabric. A high dew point in the carrier gas also is disadvantageous in the "caking" of the particulate matter tends to clog the filter bag.

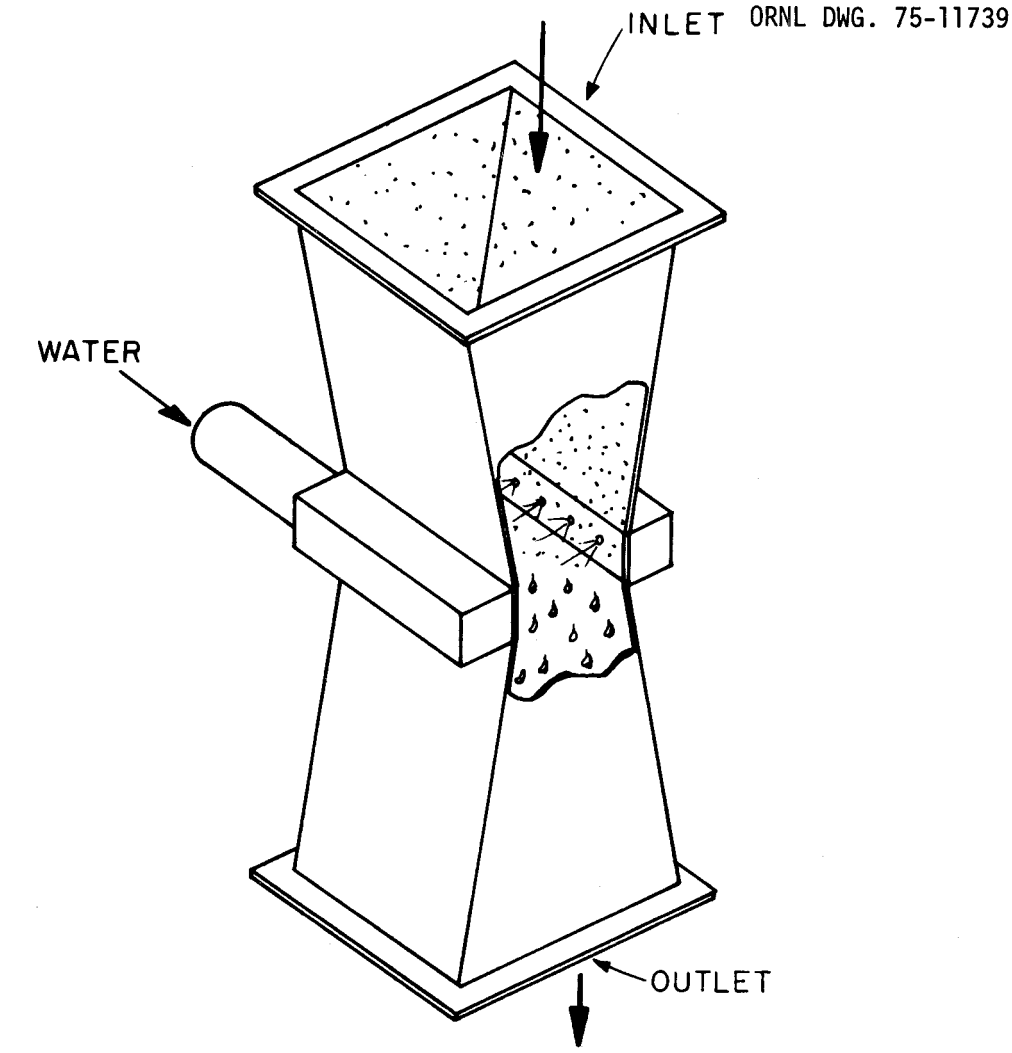

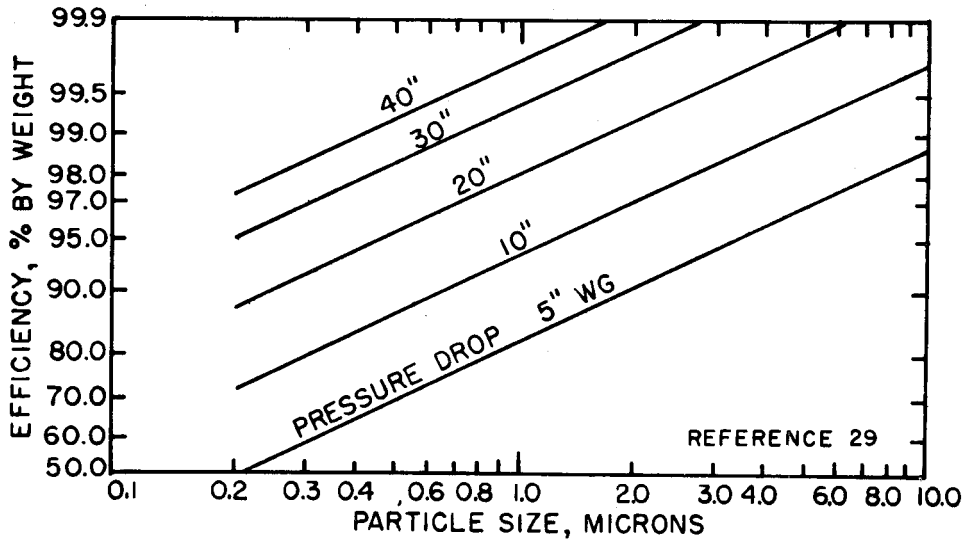

Fig. 3.21. Venturi type wet scrubber with typical efficiency curve.

Filter bags are normally tubular or envelope shaped and are hung in rows in what is known as a baghouse. The number of bags varies according to the baghouse arrangement and/or the capacity required. The baghouse itself may be a single compartment or sectionalized so that one compartment may be cleaned while the others are still in service. Figure 3.22 illustrates a typical baghouse.

The mechanism for separation is the capture and retention of the particulate matter by the fibers of the fabric filter. The actual mechanism of separation may be interception, diffusion, inertial impaction, electrostatic attraction or settling by gravity. As caking of the dust continues, collection is also helped by the sieving action of the mat or cake. This caking, of course, leads to the necessity for periodic cleaning of the bags. This periodic cycle of cleaning results in a variation in pressure drop (at a constant flow rate) that is linear with time. This pressure drop is a function of filter resistance, dust concentration, velocity of flow, and the gas mass density. The effect on the pressure drop by varying the dust loading and/or the flow rate in a compartmentalized baghouse is illustrated in Fig. 3.23.[30]

Cleaning of the dust-laden bags may be accomplished by manual shaking, mechanical shaking, or by bag flexing. Manual or mechanical shakes break the dust loose by vibration. Flexing of the bags is generally accomplished by reverse air flow. These systems all require shutdown of the compartment or compartments being cleaned to eliminate re-entrainment of the dust particles. This cyclic rotation of compartment cleaning permits continuous operation.

An alternative scheme consists of an automatic isolation and diversion system that permits cleaning of the bags in sequence without interruption of the operation of the entire unit.

The selection of the filter cloth is largely dependent on the process effluents effect on the cloth. The most important factors to consider are temperature, chemical attack, and humidity. Also to consider are the two types of cleaning — periodic and continuous. The periodic cleaning systems employ a woven fabric with filter velocities of 1.5 fpm to 3.0 fpm, and the continuously cleaned filters use a felted filter and operate in the 3 fpm to 25 fpm filter velocity range.

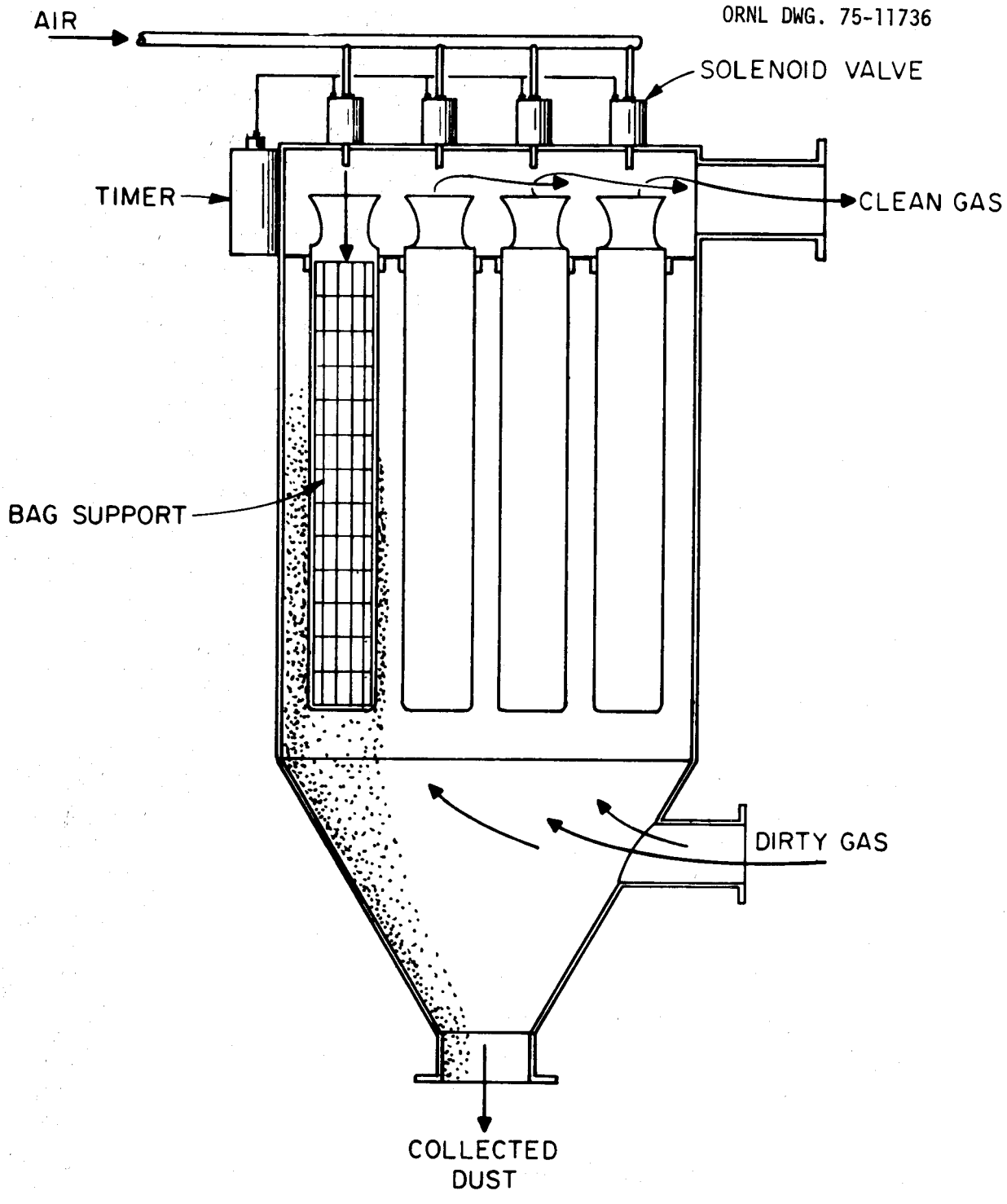

Fig. 3.22. Continuously cleaned fabric filter and Baghouse using Timed jets of air to remove accumulated dust.

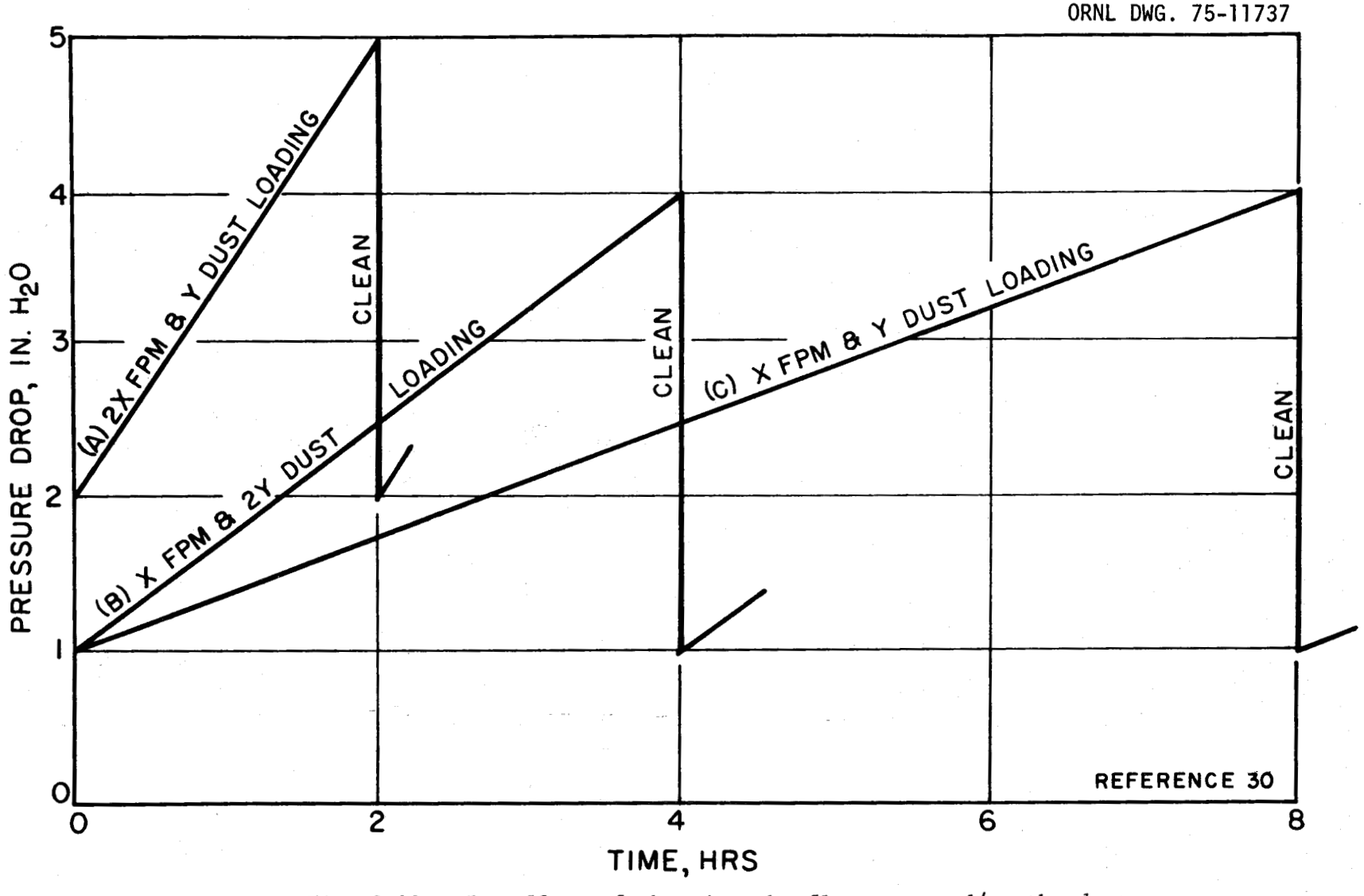

Fig. 3.23. The effect of changing the flow rate and/or the dust loading on the cleaning cycle and pressure drop of a bay filter.

For the higher temperatures newer type filter bags of glass fibers and the aromatic polyamides are used. When there is high relative humidity of the carrier-gas, seal welded baghouses are used with fans located on the clean gas side.

The cost of installed cloth-filters is in the medium price range, the controlling factor being the material. Filter fabric characteristics are tabulated in Table 3.10.

Electrostatic Precipitators

The high-voltage electrostatic precipitator is a highly favored type of collector because of its high overall efficiency and its ability to collect particles of less than 1 micron in size. Efficiencies exceeding 99% are attainable. It is a proven, reliable collector for coal-fired boilers. Because of the higher initial and operating cost most electrical precipitators are generally employed in larger installations, i.e., 50,000 to 2,000,000 cfm gas volume. Operating pressures range from below atmospheric to 150 lb in.^{2} guage, and are capable of operating at temperatures to 750°F. The pressure drop is low, seldom exceeding 0.5 in. of water.

The principle of operation involves the placing of an electron charge on the particulate suspended in the flue gas. This is accomplished by applying high voltage to an electrode suspended in the gas stream. The intense corona produced between this electrode and the grounded collector plate furnishes the negative ions that bombard the suspended particles. The migration of the particles then proceeds to the collector plates where they are collected and then dislodged by vibration or flushing by liquid to a receiving hopper. Figure 3.24 shows schematically the principle of operation.

The high initial cost requires an investment considerably higher than for other types of collectors; however, they are reliable and require little maintenance over long periods of time. Space requirements are comparable to that required for a baghouse.

The major disadvantage of the electric precipitator is its inability to separate particulate matter of high resistivity. The relatively narrow range of resistivity for the efficient separation of fly ash is about 10^8 to 10^{10} ohm-cm. In the "cold" precipitator (one that operates at

Table 3.10. Filter Fabric Characteristics

Fiber	Operating Exposure °F Long	Operating Exposure °F Short	Supports Combustion	Air permeability[a] cfm/ft^2	Composition	Abrasion	Resistance[b] Mineral Acids	Resistance[b] Organic Acids	Resistance[b] Alkali	Cost[c] Rank
Cotton	180	225	yes	10-20	Cellulose	G	P	G	G	1
Wool	200	250	no	20-60	Protein	G	G	F	P	7
Nylon[d]	200	250	yes	15-30	Polyamide	E	P	F	G	2
Orlon[d]	240	275	yes	20-45	Polyacrylonitrile	G	G	G	F	3
Nomex[d]	425	500	no	25-54	Polyamide	E	F	E	G	8
Fiberglass	550	600	yes	10-70	Glass	P-F	E	E	P	5
Teflon[d]	450	500	no	15-65	Polyfluoroethylene	F	E	E	E	9

[a] cfm/ft^2 at 0.5 in. W.G.

[b] P = Poor, F = Fair, G = Good, E = Excellent

[c] Cost rank, 1 = lowest, 9 = highest cost

[d] Dupont registered trademark

Source: Air Pollution Control, Guidebook to U.S. Regulations, Hertzendorf, Martin S.

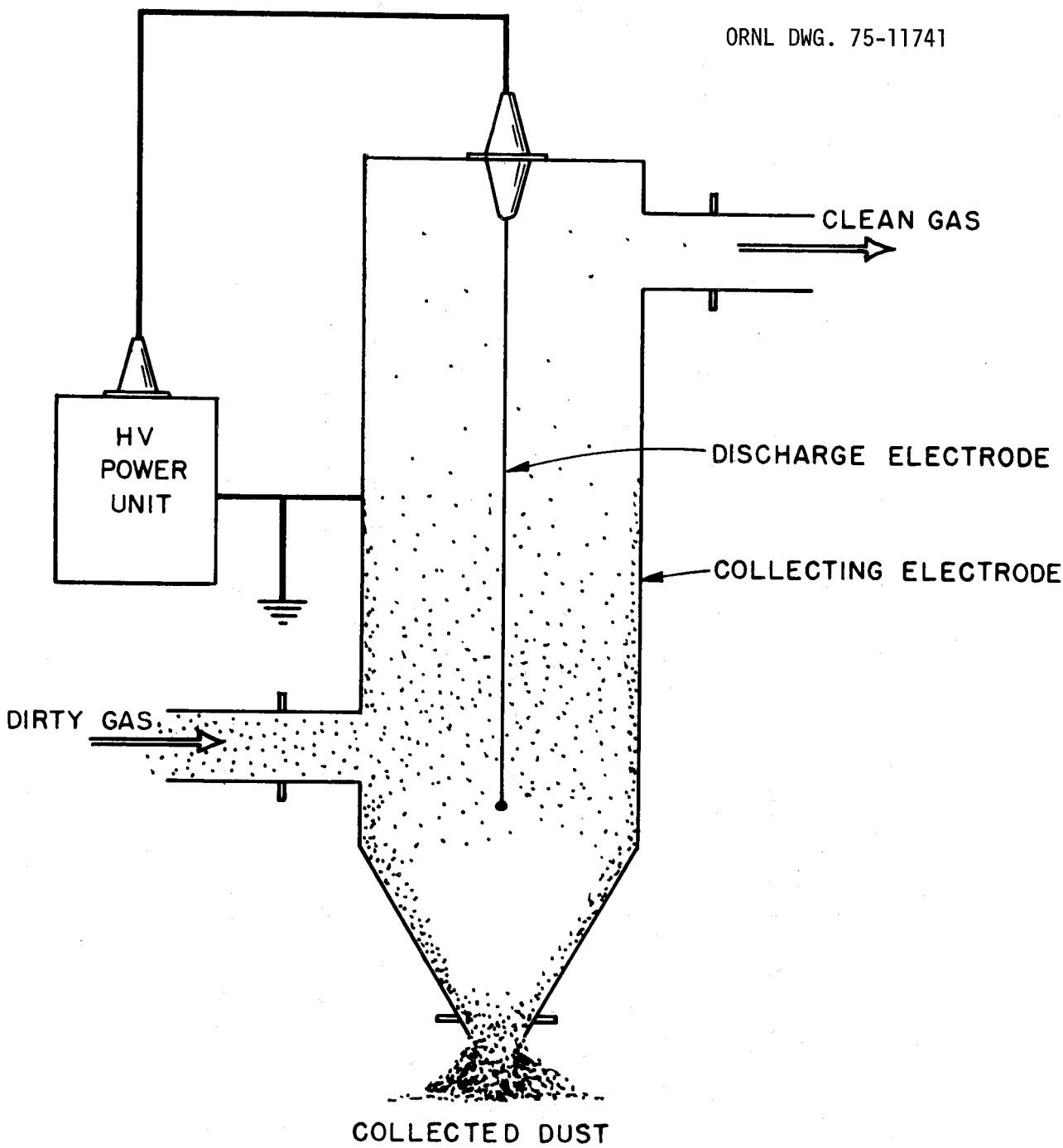

Fig. 3.24. Schematic of a high-voltage electric precipitator.

approximately 250 to 300°F) coal must have 2 to 3% sulfur content to insure that the resistivity is low enough for efficient separation.

By operating at 400°F or above the conductivity is no longer dependent on surface conditions (see Fig. 3.25) but on the volume conduction inherent in the fly ash itself.[31] This enables one to burn low sulfur content coal and still maintain efficient separation. If desired the electric precipitator may precede the regenerator (Fig. 3.26).

Summary

Table 3.11 is a compilation of the major advantages and disadvantages of commonly used collection devices. The first step in the selection of a collector system for the separation of particulate matter requires a careful compilation of information and data on the carrier gas and the suspended particulate matter. Most important is the correct determination of the dust concentration in grains/ft^3 and the dust particle size in microns as well as the distribution of each size in percentage by weight.

Knowing what goes into the collector system and what emissions are permissible from the stack, one can then take an educated look at collectors and/or collection systems. Taking into account all of the variables involved (initial cost, operating and maintenance cost, collection efficiency, pressure loss, etc.) one can then select the optimum system for the particular application. Due to the recent environmental impact upon industry, many dust removal systems have been too quickly installed without proper attention to tailoring the design to the conditions.

Another important consideration is the selection of equipment that will adequately do the job at minimum cost. Figure 3.27 shows comparative installed cost of major types of collectors.[32] In comparing costs one must also take into account the annual operating and maintenance costs as well as the life expectancy.

A look at the total annual cost in percent of installed cost is as follows:

Dry Inertial Collectors (Cyclones)	∿19%
Wet Scrubbers	∿25%
Fabric Filters	∿22%
Electrostatic Precipitators	∿11%

Table 3.11. Advantages and Disadvantages of Collection Devices

Collector	Advantages	Disadvantages
Gravitational	Low pressure loss, simplicity of design and maintenance.	Much space required. Low collection efficiency.
Cyclone	Simplicity of design and maintenance. Little floor space required. Dry continuous disposal of collected dusts. Low to moderate pressure loss. Handles large particles. Handles high dust loadings. Temperature independent.	Much head room required. Low collection efficiency of small particles. Sensitive to variable dust loadings and flow rates.
Wet Collectors	Simultaneous gas absorption and particle removal. Ability to cool and clean high-temperature, moisture-laden gases. Corrosive gases and mists can be recovered and neutralized. Reduced dust explosion risk. Efficiency can be varied.	Corrosion, erosion problems. Added cost of wastewater treatment and reclamation. Low efficiency on submicron particles. Contamination of effluent stream by liquid entrainment. Freezing problems in cold weather. Reduction in buoyancy and plume rise. Water vapor contributes to visible plume under some atmospheric conditions.
Electrostatic Precipitator	99+ percent efficiency obtainable. Very small particles may be collected. Particles may be collected wet or dry. Pressure drops and power requirements are small compared to other high-efficiency collectors.	Relatively high initial cost. Precipitators are sensitive to variable dust loadings or flow rates. Resistivity causes some material to be economically uncollectable. Precautions are required to safeguard personnel from high voltage.
Electrostatic Precipitator	Maintenance is nominal unless corrosive or adhesive materials are handled. Few moving parts. Can be operated at high temperatures (550° to 850°F).	Collection efficiencies can deteriorate gradually and impreceptibly.
Fabric Filtration	Dry collection possible. Decrease of performance is noticeable. Collection of small particles possible. High efficiencies possible.	Sensitivity to filtering velocity. High temperature gases must be coolec to 200 to 550°F. Affected by relative humidity (condensation). Susceptibility of fabric to chemical attack.

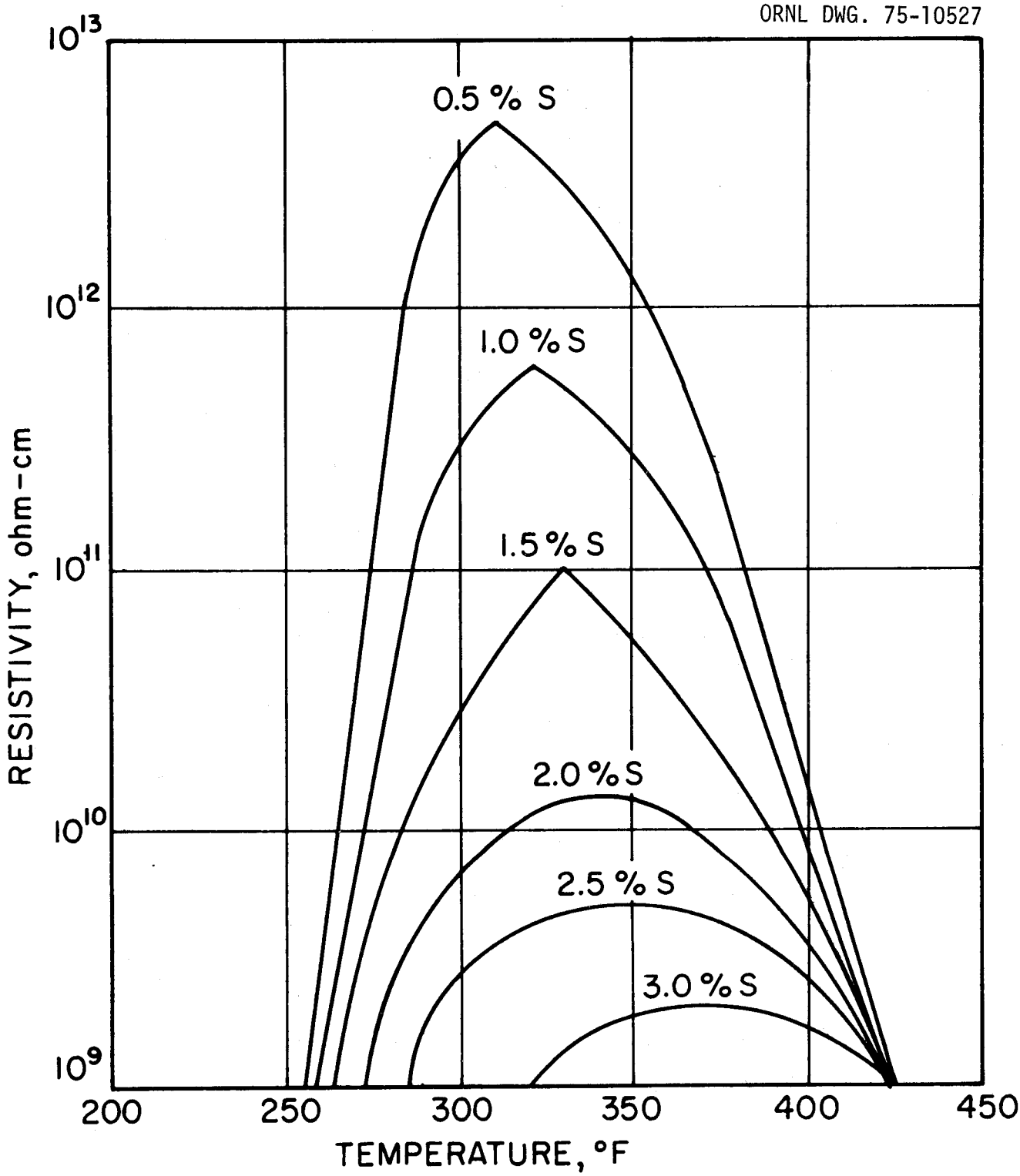

Fig. 3.25. Resistivity vs. temperature of fly-ash.

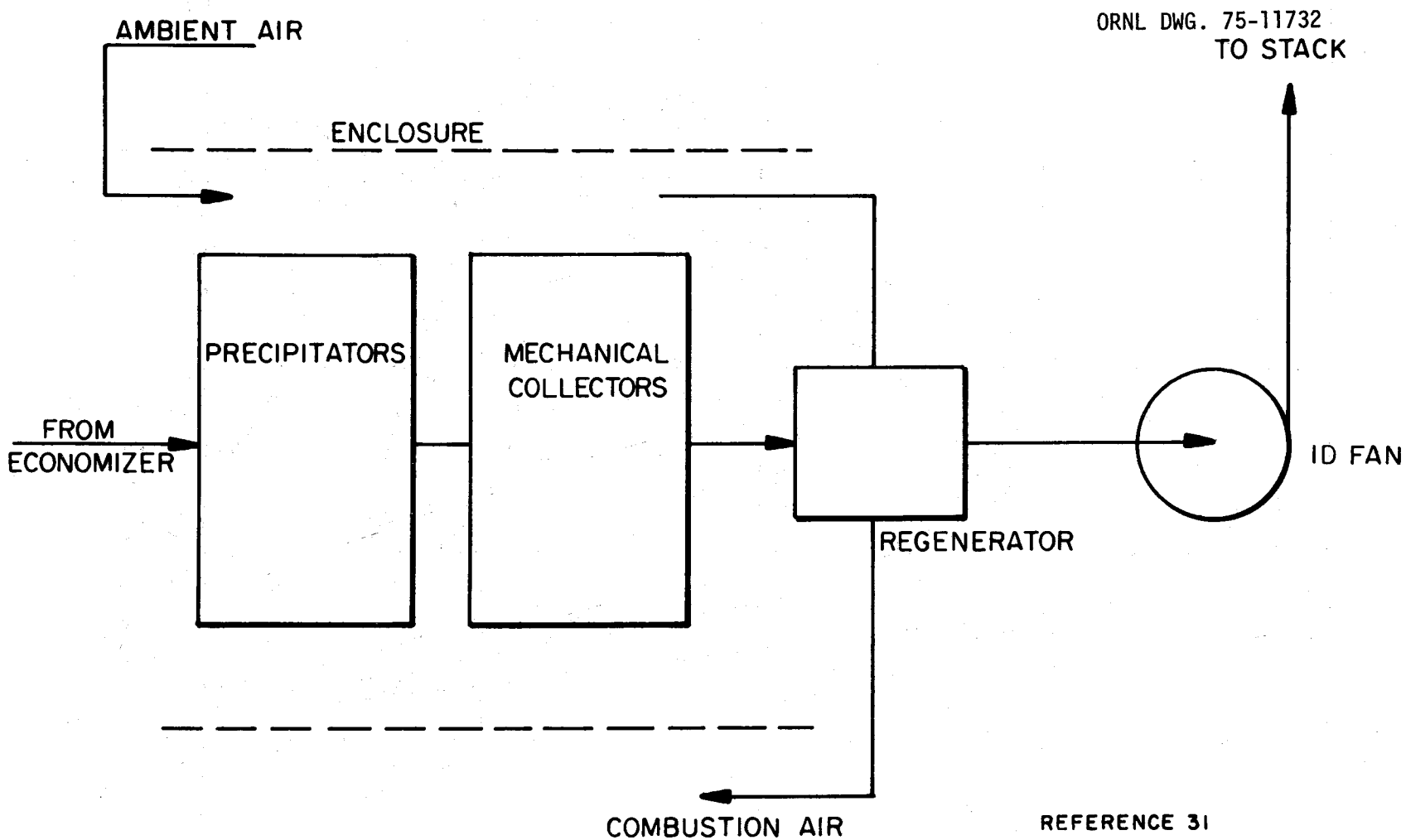

Fig. 3.26. Hot inlet temperature obtained for "hot" electrostatic precipitators by locating them ahead of the regenerator.

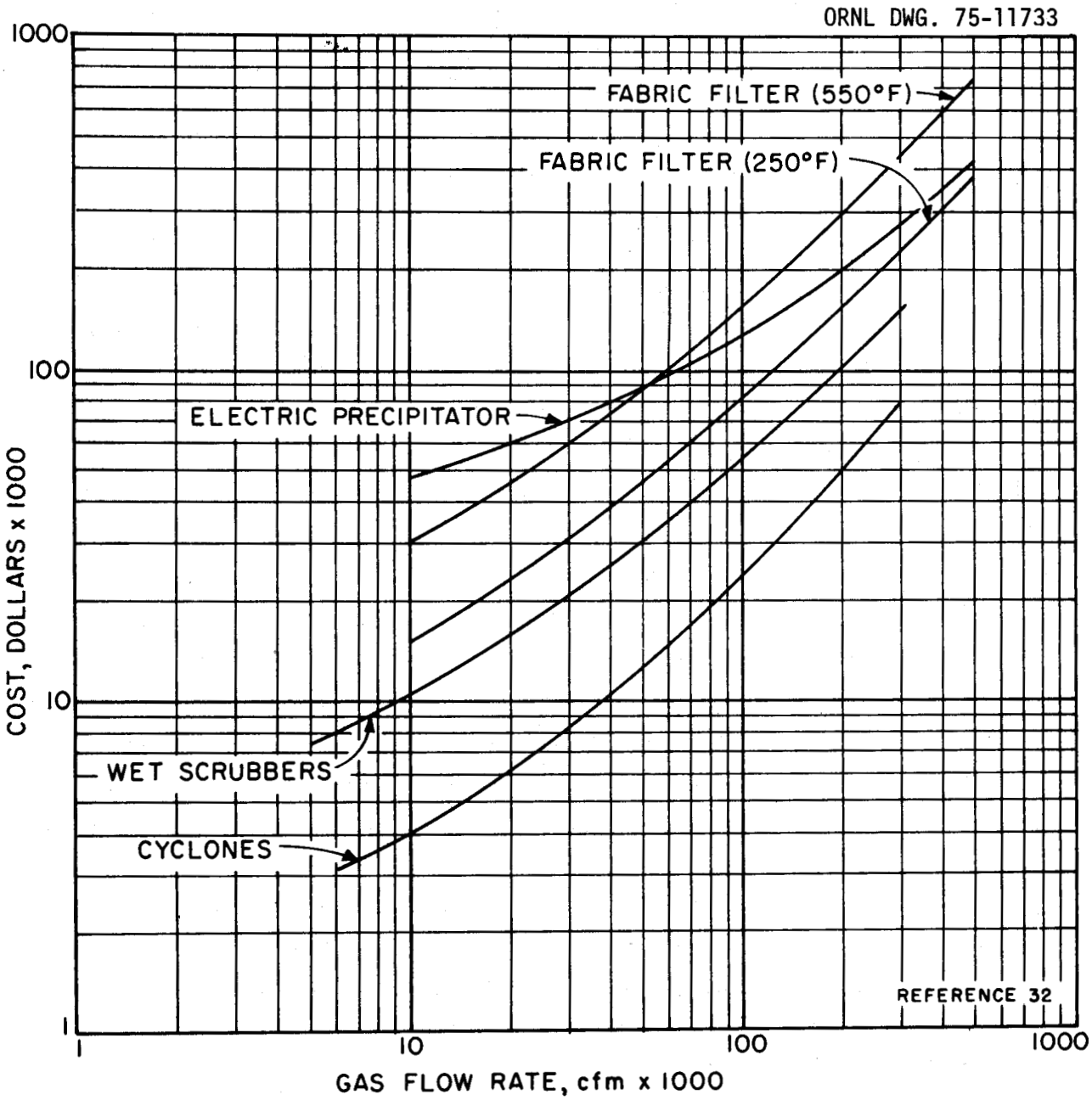

Fig. 3.27. Installed costs of collectors.

It is evident that the selection of the optimum dust collection system should be based on a careful study and evaluation of all the variables involved as well as giving possible consideration to changing the overall system configuration.

Particulate Removal from Flue-Gas of a Typical Fluidized Bed Combustion System

A realistic goal for particulate removal would be the 0.6 lb/million Btu heat input per hour maximum emission now standard in most states. In addition the concern over the atmospheric and health effects of the smaller (< 2 microns) particles is pertinent and should be considered.[27] This will influence the design of all particulate removal equipment incorporated in future total energy systems. Another important controlling factor in the selection of collectors is the cost and space requirements. Figure 3.28 is a flow study of a typical particulate collection system suitable for use in a fossil fuel-fired fluidized bed combustion plant. The flow chart shows four fluidized bed combustion modules integrated into a single power plant. Each module would have its own first stage cyclone separator and regenerator. The flue-gas from the bed would first pass through a cyclone seperator in which ∿89% of the particulate matter would be collected. A portion of the collected dust would be reinjected into the bed and the remainder removed. The emission of flue-gas from the cyclone separator then would pass through a regenerator, heating the ambient air feed to the bed, thence to a compartmentalized baghouse serving all four modules.

Table 3.12 is a calculation[33] of collector efficiency for a high-efficiency cyclone followed by a fabric filter. The assumed dust loading from the fluidized bed of 10.8 grains/ft^3, the fractional efficiencies from Figs. 3.29[14] and 3.30[34], and the size distribution of particles[14] from Fig. 3.31 are the basis for calculating the amount of stack emissions.

These data are fairly representative of data surveyed from several sources.

If one were to assume a power plant of 2.4 megawatt output and a gas flow rate of 16,000 cfm, the maximum particulate emission allowed can be calculated as follows:

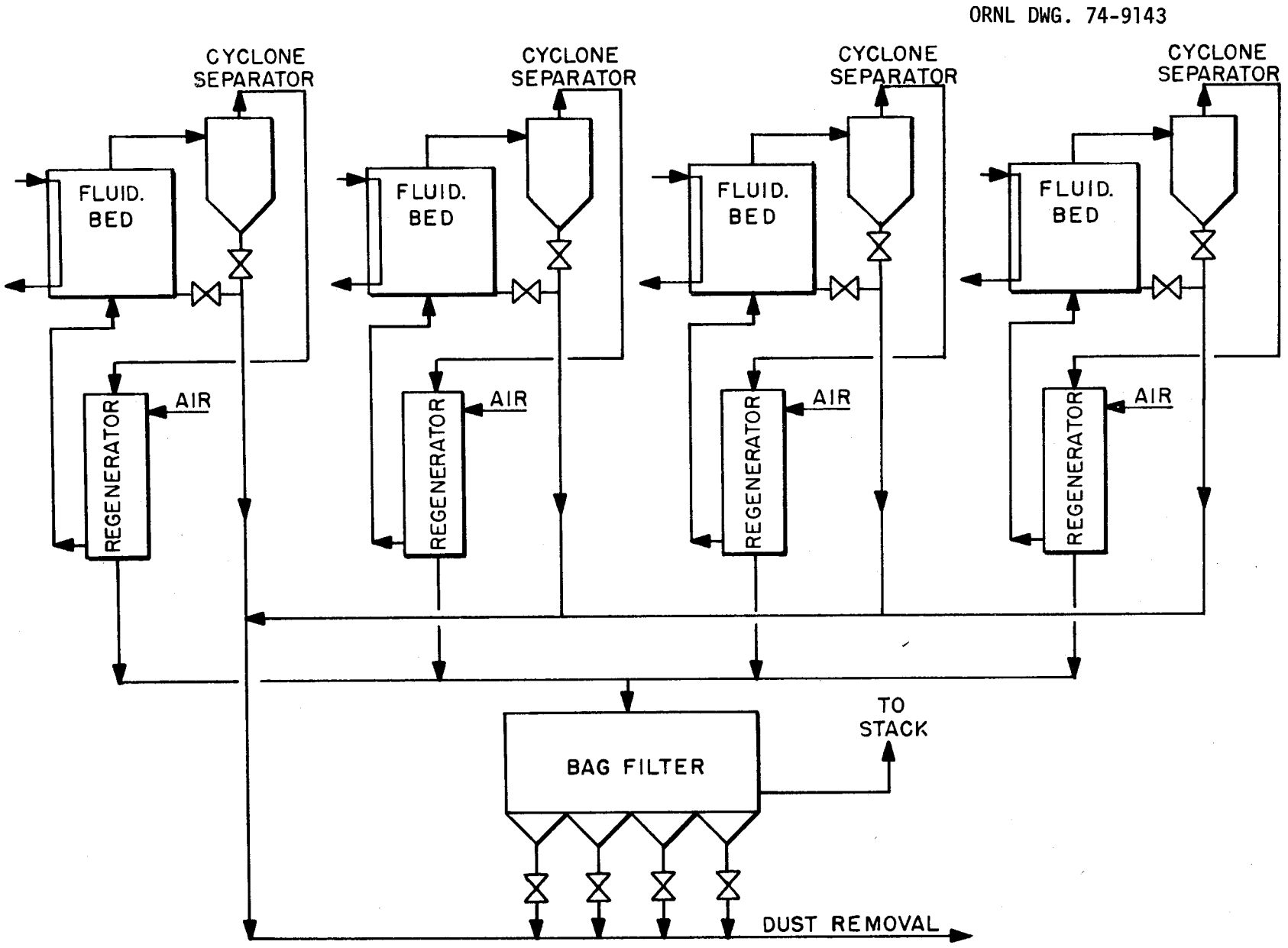

Fig. 3.28. Flow diagram of a typical dust collection system for the removal of particulates from fluidized bed flue-gas.

Table 3.12. Summary of Calculations for Collector Efficiency

Particle Size Distribution Microns	Particle Size Midpoint Microns	Fraction of Total Dust in Range* %	Cyclone Efficiency at Midpoint** %	Cyclone Dust Collected %	Cyclone Dust Emitted %	Fabric Filter Efficiency at Midpoint* %	Fabric Filter Dust Collected %
<2	1	6	0	0	53.6	99.5	53.3
2-5	$2\frac{1}{2}$	3	0	0	26.8	100	26.8
5-10	$7\frac{1}{2}$	3	65	2.0	8.9		8.9
10-20	15	5	88	4.4	5.3		5.3
20-30	25	5	93.5	4.7	2.7		2.7
30-40	35	4	96.1	3.8	1.8		1.8
40-60	50	6	98.4	5.9	.9		.9
60-80	70	6	99.6	6.0	--		--
80-100	90	5	99.85	5.0	--		--
100-200	150	18	100	18.0	--		--
200-300	250	10		10.0	--		--
300-400	350	7		7.0	--		--
400-500	450	8		8.0	--		--
500-1000	750	13		13.0	--		--
1000+	--	1		1.0	--		--

*Data from Fig. 2.13,

**Data from Fig. 2.12.

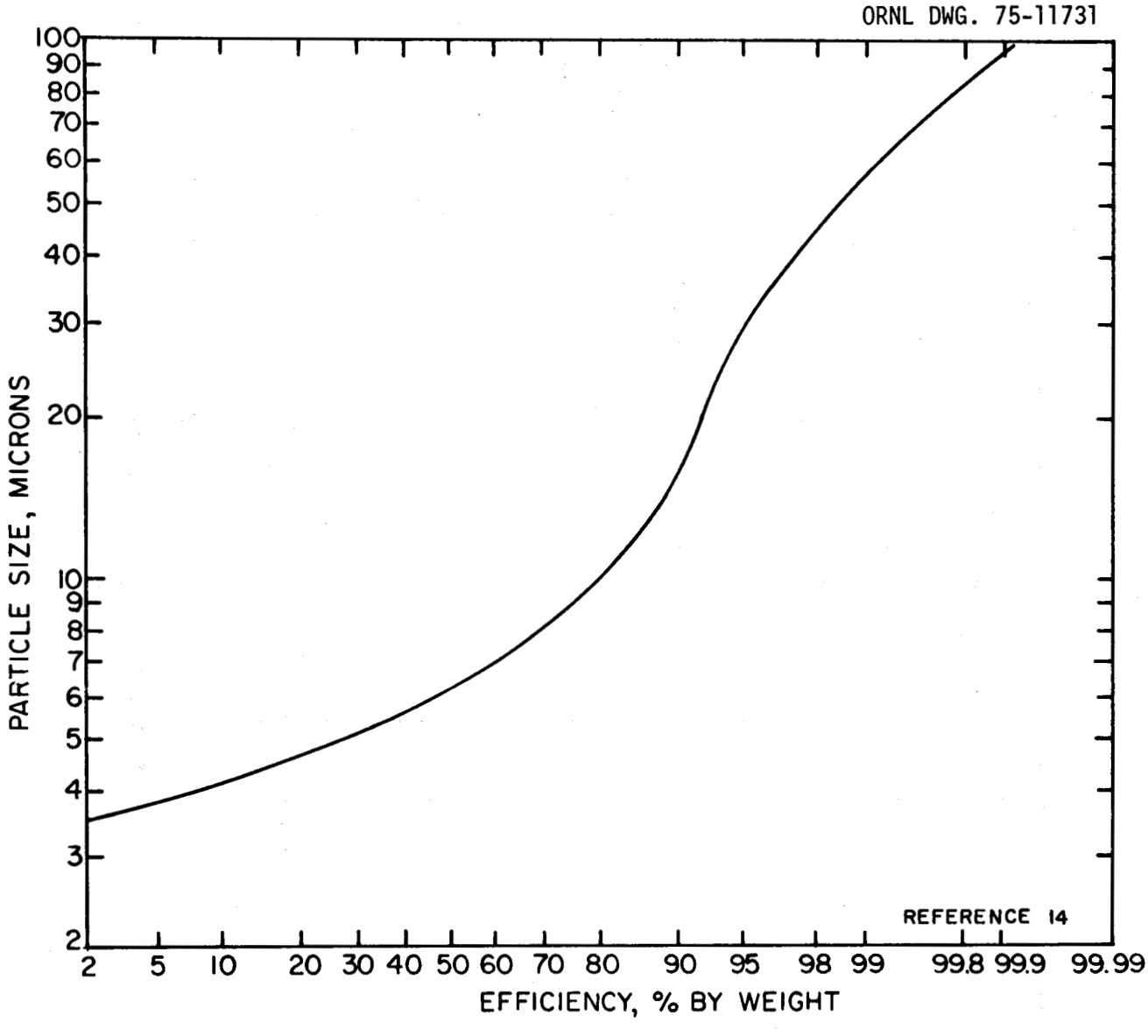

Fig. 3.29. Typical fractional efficiency curve for a cyclone separator.

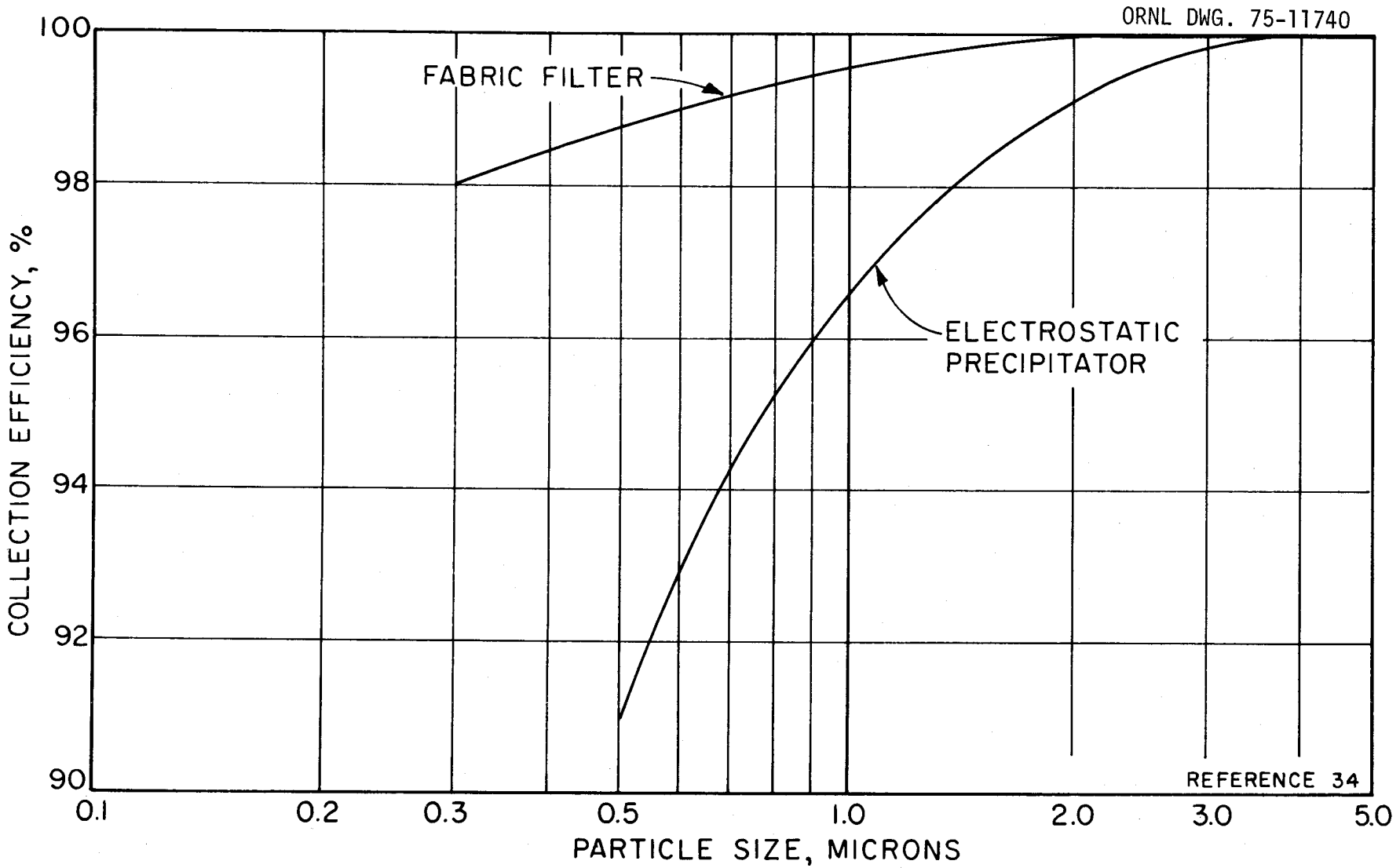

Fig. 3.30. Fractional efficiency curves for typical fabric filters and electrostatic precipitators.

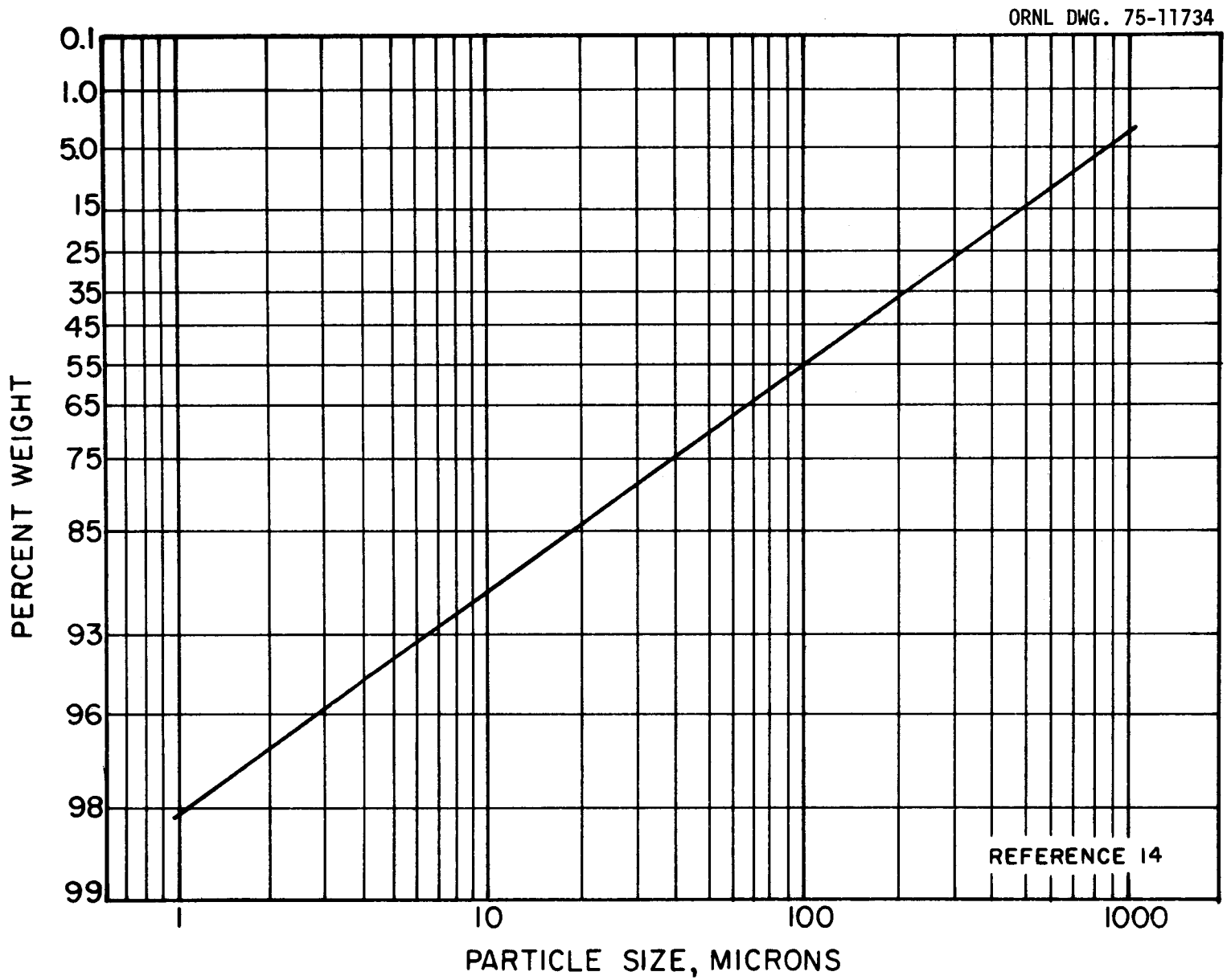

Fig. 3.31. Estimated size distribution of particulates in flue-gas emitted from a fossil-fuel fired fluidized bed.

$$8.2 \times 10^6 \text{ Btu} \times 0.6^* \frac{\text{lb}}{\text{hr}} \times 7000 \frac{\text{grains}}{\text{lb}} \times \frac{1}{16{,}000} \frac{\text{min}}{\text{ft}^3} \times$$

$$\frac{1}{60} \frac{\text{hr}}{\text{min}} = 0.03 \text{ grains/ft}^3$$

Assuming a dust loading into the collection system of 10.8 grains/ft^3, (Ref. 14) and a calculated overall efficiency of 99.97% (Table 3.12), the emission to the stack would be approximately 0.003 grains/ft^3.

The choice of a cyclone separator for the first stage is based on the ability of the cyclone to remove the medium and course particles with good efficiency at low cost. It is also capable of operation at the high temperature coming from the bed (∿1200°F). For the final separation additional cyclones are unsuitable for the collection of fine particles. Electrostatic precipitators are a possibility but their efficiency is not so good at the lower gas flow rate and their cost is high, especially below 50,000 cfm. The electrical resistivity of the dust is also high. Wet scrubbers are a possibility and are moderate in installed cost but operating expense is high and the wet dust disposal is a problem.

It appears then that a fabric filter is a good choice for the following reasons:

1. Its installed cost is lower than the electrostatic precipitator at the gas flow rate and temperature being considered.
2. It has the ability to remove fine (1/2 - 7 micron) particles very efficiently (>99%).
3. Operating cost is reasonable and competitive with the electrostatic precipitator.
4. The dust collected is dry and therefore easier to dispose of.
5. Drop in effectiveness is easily detectable.
6. It is easy to maintain because of its simplicity.

Meeting the new emission standards will require a much closer scrutiny of all the factors involved and would naturally entail a more detailed study than the above preliminary comparisons.

---

*Average value obtained from Table 3.8.

References

1. H. H. Sonderling, W. W. Pepper, B. P. Breen, and A. W. Bell, Operation of Scattergood Steam Plant Unit 3 Under Los Angeles County Air Pollution Control District Rule 67 for Nitrogen Oxides Emissions, pp. 1236-1239, Conference Proceedings of the 1971 Intersociety Energy Conversion Engineering Conference, Boston, Massachusetts, August 3-5, 1971.

2. Lubomyr Kurylko, Control of Nitric Oxide Emissions from Furnaces by External Recirculation of Combustion Products, paper presented at the ASME Winter Annual Meeting, Washington, D.C., November 28-December 2, 1971.

3. Clean Energy from Coal--A National Priority, 1973 Annual Report for Calendar Year 1972, Office of Coal Research, Supt. of Documents Stock No. 2414,00056.

4. W. N. Barnard, F. O. Ellenwood, and C. F. Hirshfeld, Heat--Power Engineering, John Wiley & Sons, Inc., New York, New York, 1935.

5. A. M. Squires, Species of Fluidization, Chemical Engineering Progress, Vol. 58, p. 66, April 1962.

6. H. R. Hoy and J. E. Stanton, Fluidized Combustion Under Pressure, paper presented at the Joint Meeting of the Chemical Institute of Canada and the AIChE, Toronto, May 24, 1970.

7. J. Kleinau, Pulp and Paper Mill Sludge Incineration, Paper presented at the 1st Secondary Fibre Pulping Conference, October 22-25, 1968.

8. J. S. M. Botterill and D. E. Elliott, Fluidized Beds: Answer to Peak Power? Engineering, p. 146, July 21, 1964.

9. Pressurized Fluidized Bed Combustion Progress Report No. 10, prepared for the Office of Coal Research, Department of the Interior, by the National Research Development Corporation, London SWL 651, August 1973.

10. E. B. Robinson et al., Study of Characterization and Control of Air Pollutants from a Fluidized-Bed Combustion Unit: The Carbon-Burnup Cell, report from Pope, Evans, and Robbins to the Environmental Protection Agency, February 1972.

11. Development of Coal-Fired Fluidized Bed Boilers, Pope, Evans, and Robbins Final Report Vol. 1, OCR R&D Report No. 36, Contract No. 14-01-0001-478, February 1970.

12. A. A. Jonke et al., Pollution Control Capabilities of Fluidized-Bed Combustion, paper submitted for publication in AIChE Symposium Series "Air 1971," April 1972.

13. A. Skopp et al., Studies of the Fluidized Lime-Bed Coal Combustion Desulfurization System, Esso Research and Engineering Company, Government Research Division, Linden, New Jersey, 1971.

14. Evaluation of the Fluidized Bed Combustion Process, Vol. I Summary Report, Westinghouse Research Laboratories, Pittsburgh, Pennsylvania, 1972.

15. J. L. Stollery, Fundamentals of Fluid Bed Roasting of Sulfides, Engineering and Mining Journal, October 1964.

16. R. S. Millward, Refinery Waste Treatment and Fluosolids Sludge Combustion, Paper presented at the Antipollution Fair, Milan, Italy, November 1972.

17. D. A. Furlong and G. L. Wade, Use of Low Grade Solid Fuels in Gas Turbines, paper prepared for presentation at the ASME Winter Annual Meeting, New York, New York, November 17-21, 1974.

18. Final Report on Reduction of Atmospheric Pollution, Fluidized Combustion Control Group, National Coal Board, London, England, prepared for the Environmental Protection Agency, September 1971.

19. A. M. Squires and R. A. Graff, Panel Bed Filters for Simultaneous Removal of Fly Ash and Sulfur Dioxide. III. Reaction of Sulfur Dioxide with Half-Calcined Dolomite, Journal of Air Pollution Control Association, Vol. 21, pp. 272-276, 1971.

20. Standards of Performance for New Stationary Sources, EPA, Federal Register, 36, No. 247, Part II, December 23, 1971.

21. R. B. Engdahl, A Critical Review of Regulations for the Control of Sulfur Oxide Emissions, Journal of the Air Pollution Control Association, Vol. 23, No. 5, pp. 364-375, May 1973.

22. C. L. Bazelmans, F. T. Binford, et al., Study of Options for Control of Emissions from an Existing Coal-Fired Electric Power Station, USAEC Report ORNL-TM-4298, Oak Ridge National Laboratory, September 1973.

23. J. K. Burchard, G. T. Rochelle et al., Some General Economic Considerations of Flue Gas Scrubbing for Utilities, Proceedings of Conference on Sulfur in Utility Fuels: The Growing Dilemma, Drake Hotel, Chicago, October 25-26, 1972 (Electrical World).

24. G. T. Rochelle, A Critical Evaluation of Processes for the Removal of SO_2 from Power Plant Stack Gas, Presented at the 66th Annual Meeting of the Air Pollution Control Association, June 24-28, 1973.

25. Tennessee Valley Authority Status Report - Control of Sulfur Oxides, Presented at the Environmental Protection Agency Hearings, October 1973, Washington, D.C.

26. G. J. Vogel, E. L. Carlis, et al., Reduction of Atmospheric Pollution by the Application of Fluidized-Bed Combustion and Regeneration of Sulfur-Containing Additives, Annual Report July 1971-June 1972, Report No. ANL/ES-CEN-1005, Argonne National Laboratory.

27. N. R. Iammartino, Fine Particles Start Coming Under Scrutiny, Chemical Engineering, July 10, 1972.

28. Particulate Emissions from Coal-Burning Equipment, Air Quality Control Regulation 504, New Mexico Environmental Improvement Board, March 25, 1972.

29. Air Pollution Manual, Part II, Control Equipment, American Industrial Hygiene Association.

30. J. M. Kane, Operation, Application, and Effectiveness of Dust Collection Equipment, Heating and Ventilatings Reference Section, August 1952.

31. W. G. Henke, The New "Hot" Electrostatic Precipitation, Combustion, October 1970.

32. M. S. Hertzendorf, Air Pollution Control, Guidebook to U.S. Regulations.

33. G. D. Sargent, Dust Collection Equipment, Chemical Engineering, January 27, 1969.

34. N. R. Iammartino, Technology Gears Up to Control Fine Particles, Chemical Engineering, August 21, 1972.

CHAPTER 4

COMPARISON OF THE PERFORMANCE AND COST OF TYPICAL POWER UNITS WITH DIFFERENT FUELS

The evaluation of various power plant systems for MIUS applications presented in this chapter took as its point of departure the extensive work at ORNL carried out for HUD in recent years. This work has included the use of central stations coupled to district heating systems,[1] operation of absorption air conditioning systems coupled to district heating systems,[2] solid waste collection and disposal problems,[3] and a critical examination and evaluation of a wide variety of components and systems for MIUS installations.[4-11] In addition, the background gained at ORNL in work on small portable nuclear power plants for military applications together with an examination of a wide range of advanced concepts for use with both fossil and nuclear fuels as well as solar power plants has provided a wealth of material and local expertise directly applicable to the problem at hand.[12-14]

MIUS Requirements

Unit Size

The building complex size that appears to have been of greatest interest to HUD has been in the range of 500 to 1000 residential units. (The largest complex built to date under HUD auspices has not exceeded 1000 residential units.) However, the range of interest in studies for HUD has extended to complexes of 2000 to 3000 units. Much of the study work has centered on a reference design system of 720 units, commonly referred to as the Model A System.[5] The peak summer and winter demands for energy for various purposes in the Model A reference design complex together with the annual usage in each case are summarized in Table 4.1. Inasmuch as this system has been used so extensively in previous studies carried out for HUD, it has been chosen as the reference design building complex for a comparison of the various systems considered in this chapter. Note that the electrical demand for this model peaks in the summer because over 500 kW(e)

Table 4.1. Summary of Model A Demands and Usage
(Table from Ref. 5)

	Summer Demand	Winter Demand	Annual Usage
Apartments (Normal)[1]			
Electrical, kW, kWhr	756	756	4.91×10^6
Cooling, ton, ton-hr	907		1.41×10^6
Heating, Btu/hr, Btu		18.9×10^6	29.1×10^9
Domestic hot water, Btu			15.5×10^9
Apartments (Auxiliary)[1]			
Fan-coils, kW, kWhr	113	113	$.99 \times 10^6$
Apartment Building Equipment Room[1]			
Hot water pumps, kW, kWhr	12	12	$.11 \times 10^6$
Chilled water pumps, kW, kWhr	12		$.04 \times 10^6$
Central Equipment Building			
Hot water pumps, kW, kWhr	17	34	$.18 \times 10^6$
Chilled water pumps, kW, kWhr	50		$.10 \times 10^6$
Cooling tower fans and pumps, kW, kW/hr	90		$.20 \times 10^6$
Centrifugal chillers, kW, kWhr	438		$.56 \times 10^6$
Miscellaneous equipment, kW, kWhr	20	15	
Total Electrical Demand, kW	1508	930	
Total Electrical Usage, kWhr			7.09×10^6

[1]Demands and usages in the apartments or apartment building include a 5% distribution loss.

are required for the air conditioning system. Over half of this load might be carried by an absorption air conditioning system.

As indicated in Chapter 1, extensive experience has indicated that, to obtain good reliability, it is necessary to make use of a number of power plant units operating in parallel to provide redundancy. The usual procedure is to have two units on-stream most of the time with a third unit on standby to carry peak loads while the fourth unit could be out of service for maintenance. On this basis the size of the individual power plant unit for the Model A building complex would be about 500 kW(e). Thus, for the purposes of this study the design power output range per turbine-generator unit in the power plant has been taken as 500 to 1000 kW(e).

Average Load Factor

Both analyses and reviews of operating experience indicate that the load on individual power plant units will usually run from 50% to 90% of full load, and will average close to 70%. This will lead to a loss in thermal efficiency by an amount that will depend on the type of power plant. Figure 4.1 shows this effect for some typical cases.

Maintenance

Previous studies have shown that operating costs will be excessive unless the power plant units can be operated in a semi-unattended mode with relatively little difficulty with outages or requirements for maintenance. Unfortunately, it is extremely difficult to assess the degree to which a new system will prove capable of meeting this essential requirement.

Comparison of the Performance and Cost of Typical Systems

A variety of typical small power plants adapted to MIUS applications have been evaluated and compared in Table 4.2 with conventional systems that depend on central stations for their supply of electricity. For reference purposes five systems based on central stations are given at the top of Table 4.2. The first of these would be coupled to a housing complex using a gas-fired steam boiler for providing domestic hot water and building heating. Air conditioning would be provided by individual room

ORNL DWG. 76-4472

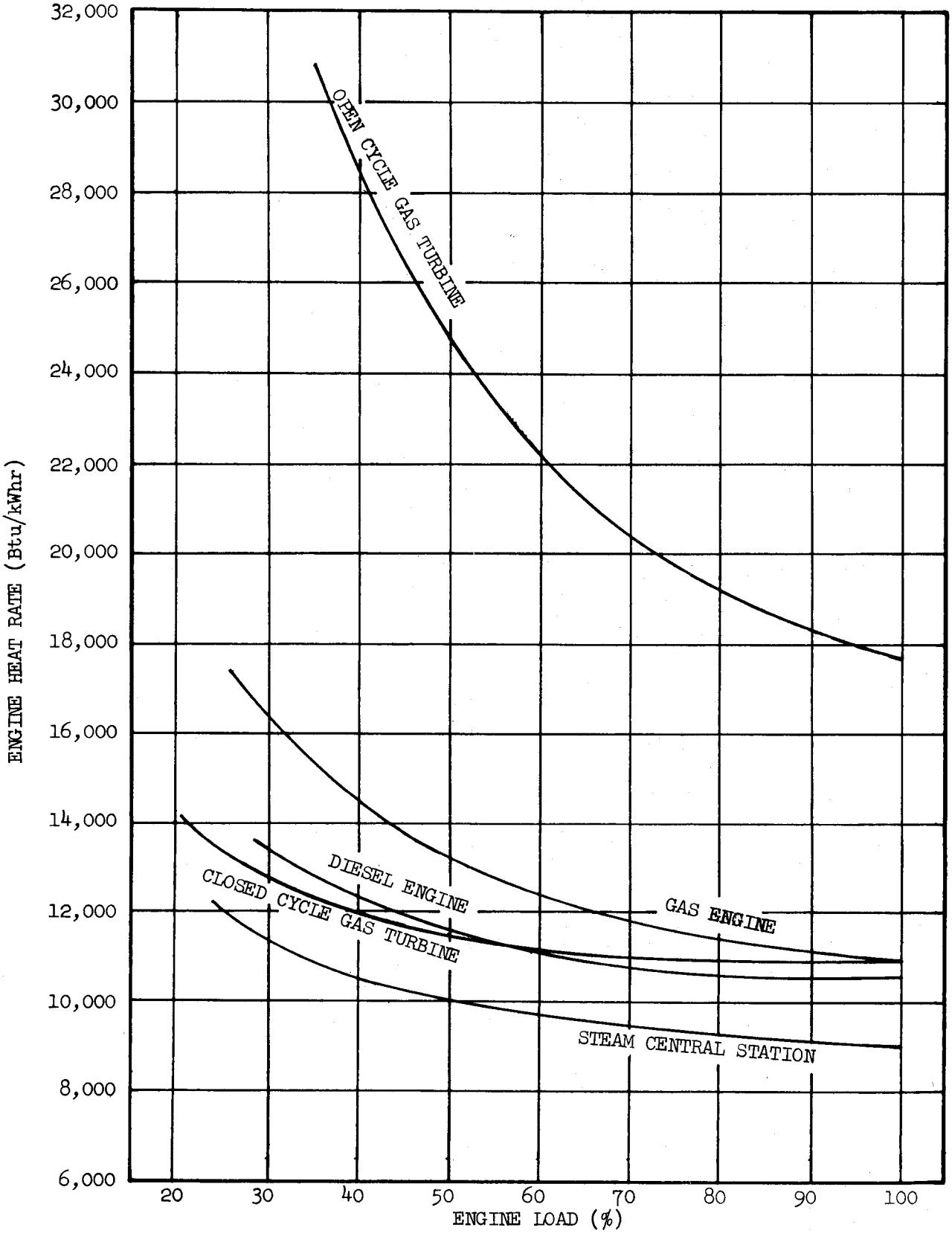

Fig. 4.1. Effects of load on the heat rate for typical diesel and gas engines, open and closed cycle gas turbines, and a large steam central station.

Table 4.2 Summary of Major Considerations in Choosing a Power Conversion System for Building Complexes

Major conditions: Philadelphia area $400/kW(e) = capital cost of fossil fuel central station and electrical transmission system. Domestic hot water consumption = 600 Btu/yr residential unit at 150°F.

System	Average Load Conversion Efficiency from Fuel to Electricity ~%	Estimated Fuel Consumption per year per Residential Unit ~10^6 Btu	Estimated Capital Cost $/Residential Unit	Estimated Unit Cost for Operating Personnel mils/kWhr	Range of Fuels Useable*	Principal Developmental Problems
Central station, gas-fired steam boiler	32	185	3,000	7	C,G,O,W	S removal
Central station, electrical resistance heat	32	228	4,700	4	C_s,C,G,O,W	S removal
Central station, electric motor driven heat pump	32	170	4,250	6	C_s,C,G,O,W	S removal
Central station, district heating system	32	149	3,785		C_s,C,G,O,W	Installation of huge district heating system
LWR central station, district heating system	28	164	4,100		U	Installation of huge district heating system
Gas engine-natural gas	29	148	3,260	10	G	None
Gas engine-on-site coal gasification	20	211	16,760	160	C_s,C,G	Reliability, corrosion, S removal
Diesel engine-fuel oil	32	134	3,260	10	O	None
Diesel engine-on-site coal liquefaction	23	192	16,760	148	C_s,C,O	Reliability, corrosion, S removal
Conventional gas turbine-natural gas or oil	23	176	3,260	10	G,O	None
Conventional gas turbine-on-site coal gasification	16	252	16,760	160	C_s,C,G,O	Reliability, corrosion, S removal
Open cycle gas turbine with fluid bed	23	176	4,100	15	C_s,C,G,O,W	Reliability, hot corrosion in bed
Closed cycle gas turbine with fluid bed	29	140	4,000	15	C_s,C,G,O,W	Reliability, hot corrosion in bed
Steam turbine-conventional furnace	16	254		15	C,O,G	New turbine-generator required reliability
Steam turbine-fluidized bed	16	254		15	C_s,C,O,G,W	Reliability, control, hot corrosion
Steam engine-conventional furnace	16	254		15	C,G,O	None
Steam engine-fluidized bed	16	254		15	C_s,C,G,O,W	Reliability, corrosion, S removal

*Legend for Fuel Type - C_s High sulfur coal
C Low sulfur coal
G Gas
O No. 2 fuel oil
W Solid wastes
U Uranium

air conditioning units. The second system considered would be the same except that electrical resistance heat would be employed for both building heating and domestic hot water. The third system considered would make use of heat pumps with electric motor-driven Freon compressors for both building heating and air conditioning. The fourth system would make use of a central station to provide not only electricity but also hot water via a district heating system. The first four central stations were assumed to be coal-fired; the fifth is based on a light water fission reactor (LWR).

The first of the small power plants, or MIUS systems, employs gas engine-generator sets with waste heat recovery from the engine cooling jackets and exhaust systems. Two versions of such an installation were included, the first making use of natural gas and the second making use of gas from an onsite coal gasification plant. The next two systems considered were similar but would use diesel rather than gas engines. The next system is a conventional open cycle gas turbine fueled with gas or oil. Over 100 such systems are in operation in building complexes in the U.S. As with the gas and diesel engines, a variation on this system making use of gas from an on-site coal gasification plant was also included. In addition to these, a small steam turbine-generator unit coupled first to a conventional furnace and then to a fluidized bed coal combustion system was considered, and, similarly, a reciprocating steam engine coupled to a generator, again with first a conventional furnace and then with a fluidized bed coal combustor. Finally, both an open cycle gas turbine and a closed cycle gas turbine-generator unit coupled to a fluidized bed coal combustor were considered and compared with the other systems. Table 4.2 summarizes the major considerations of interest in choosing a power conversion system for a building complex.

Estimation of Electrical and Heat Loads

The electrical and heat loads on a building complex vary with the time of day, the season of the year, from weekdays to Saturdays or Sundays, with the outside air temperature, the humidity, and with the location in the country. Further, in attempting to carry out any set of calculations that compare the characteristics of different MIUS systems, one needs to make many arbitrary assumptions. For example, the energy required for heating

domestic hot water is commonly taken as from 4000 to 6000 kWhr/yr. It is usually assumed that the water would be heated to 150°F. This is hotter than is necessary for almost all applications, and one obvious way to save energy is to reduce the temperature of the domestic hot water supply to 120°F; this should cut the heat losses substantially. Similarly, in carrying out calculations it is often assumed that the temperature in the residential units would be held at a constant level of 75°F. A substantial savings in energy can be realized if a deadband of 5 to 10°F is provided, e.g., if the air conditioning system is not turned on until the air temperature drops below 70°F. Even greater savings could be effected if a still lower room temperature were accepted for the winter months. Further, in view of the rapidly rising cost of energy, it seems likely that much better thermal insulation will be provided for buildings, and this in turn will lead to substantial energy savings for both heating and cooling. Still another factor for MIUS applications has to do with the use of hot water storage to permit saving heat from those periods during the day in winter when the requirements for electricity yield more waste heat than can be used immediately for building heating, and then the stored heat can be used at night when the requirements for heat will be greater than the amount of heat available from the generation of electricity. With the rising cost of energy, hot water storage during the daytime will make possible a marked savings in overall energy utilization. Some indication as to the magnitude of this energy savings is given by the study presented in Appendix I of this report. The possible annual energy savings that might be effected in this way appears to be around 10%. It should be mentioned that extensive use of thermal energy storage in the form of superheated water is employed in the total energy system of the city of Munich, where it has been found to be very attractive economically.

A major factor influencing the electrical heat load on the prime mover is whether or not the air conditioning system makes use of absorption type air conditioning equipment. However, even if full use of the waste heat from the prime mover is employed for absorption air conditioning, for most cities the peak air conditioning loads make it necessary to employ some electric motor-driven Freon compressors. The degree to which the absorption air conditioning equipment must be supplemented with electric

motor-driven compressors is very much a function of the location in the United States, but the capacity of the two systems is commonly roughly the same.

Estimation of Efficiencies and Costs

Any effort to compare different MIUS systems from the standpoint of the efficiency with which they make use of the energy in the fuel and the capital and operating costs for the system of necessity require that one make a large number of somewhat arbitrary assumptions. Efforts to carry out such studies not only at ORNL but at the Bureau of Standards and at the NASA Johnson Space Center at Houston have entailed substantially different values for many of the input assumptions. In spite of these differences, the results generally fall within 10% of a mean where the studies are for similar plant locations. In fact, even shifting the plant location from say Philadelphia to Dallas, Texas ordinarily does not lead to a drastic difference in either the efficiency of energy utilization or the capital cost.

The detailed procedure followed in carrying out a set of calculations may differ substantially in the detail in which the input data on outside air temperature, electrical loads, etc., are introduced into the calculations. The study presented in Appendix C indicates that substantial differences in the extent to which a detailed treatment is made really have relatively little effect on the results. In the study of Appendix C, for example, three different approaches yielded differences in fuel consumption of only plus or minus 4%.

For purposes of this report it seemed that a reasonably representative comparison of different systems could be obtained by making use of a set of comparisons of MIUS systems in the Philadelphia area as presented in Ref. 5. Perturbations were applied to the original study to handle the cases of Table 4.2 that were not included in the original study. The principal assumptions made are listed at the top of Table 4.2; for further details the reader is referred to Ref. 5. The principal new element introduced in the present analysis was the consideration of on-site coal gasification or liquefaction plants. For these plants it was assumed that the efficiency of conversion of the coal into gaseous or liquid fuel would run 70%

from the standpoint of the available energy in the fuel. The coal-fired gas turbine plants considered were the representative open cycle and closed cycle plants of Chapter 6.

Discussion of Results

In reviewing the results of the calculations presented in Table 4.2, probably the most important point to note is that on-site coal gasification or liquefaction lead to estimated capital costs per residential unit of the order of 4 times the values for any of the other approaches except that in which electricity from the central station is used to provide electrical resistance heat for the building heating requirements, in which case the factor is about 3. Further, on-site coal gasification or liquefaction leads to a low conversion efficiency from the energy in the fuel to electricity, and as a consequence a high annual fuel consumption expressed as 10^5 Btu/yr per residential unit. The most promising contenders from the standpoints of efficiency of use of the energy in the fuel and capital costs are the central station coupled to a district heating system or to electric motor driven heat pumps on the one hand, and on the other MIUS systems with conventional gas or diesel engines or the proposed closed cycle gas turbine coupled to a fluidized bed coal combustion chamber. The latter has the disadvantage that it will require a substantial amount of money for development to determine feasibility, but it has the major advantage that it could operate on any type of fuel including solid wastes and high sulfur coal. These advantages appear to be so great that the effort required to investigate the feasibility of the system appears to be very much in order.

Although small steam turbine-generator or engine-generator units at first appear to be obvious contenders, they are actually ill-suited to MIUS applications both because of their low efficiency in converting the energy in the fuel into electricity and their high capital costs. The low efficiency of the small steam turbines stems from the fact that in these small sizes it is necessary to make use of partial admission, and this leads to a low turbine efficiency. An alternative would be to go to a very small high speed unit which could employ full admission, but no such units are commercially available, and they would require frequency conversion equipment.

Further, even in these small high speed units the Reynolds number is relatively low, and this leads to a substantially lower turbine efficiency than can be obtained in large central stations. The relatively poor efficiency of reciprocating steam engines stems from the fact that they cannot use high steam pressures and temperatures to good advantage because of difficulties with lubricating the engine cylinder walls.

Another factor having a serious adverse effect on the operating costs of small, on-site coal gasification or liquefaction plants for MIUS systems is the requirement of such plants for operating personnel. As indicated in Chapter 2, Fig. 2.21, the number of men required to operate a coal gasification or liquefaction plant is not very much dependent on plant size because the number of control functions that must be carried out is the same irrespective of the plant output. It is believed that a fluidized bed coal combustion system will entail far less difficult process control and requirements and will be relatively insensitive to deviations from desired values, hence it will not require an operating crew in constant attendance. This, of course, remains to be demonstrated.

Advanced Concepts

The various concepts presented in Table 4.2 and discussed in the previous section all make use of power conversion equipment in commercial use except for the fluidized bed coal combustion system. This clearly requires the development of some advanced technology, and the question arises as to how it compares with other advanced systems in performance potential, degree of difficulty of the developmental problems envisioned, and the time required to carry a developmental program to the point where a commercially viable system could be built. This section includes a discussion of each of the principal candidates for an advanced system. To provide some perspective, the amount of money and time that has already gone into R&D work on each system is also included together with a discussion of the principal problems that have been encountered.

Fuel Cells

The direct production of electricity from the combustion of hydrogen in fuel cells has been the subject of research and development for the past half century. From the latter 1920's to the early 1950's the bulk of the effort was funded in an attempt to obtain propulsion systems for submarines. Secret but intensive efforts making use of some of the world's outstanding physical chemists were carried out in the U.S., the UK, France, and Germany from about 1930 up into the early 1950's. At that time two things became evident; on the one hand the practicality and outstanding performance of the nuclear submarine had been demonstrated so that the need for fuel cells for submarines faded, and on the other hand the failure of about 30 years of intensive high class research and development to yield a practical fuel cell made the probability of a successful unit progressively more remote.

At about this time the space program began to develop rapidly and the need for a relatively short-lived electrical power source for manned space missions became well-defined. A review of the results of the fuel cell developmental effort for submarines led to the conclusion that it should be possible to develop a suitable unit for space applications where the required life would be only three to five weeks. Note that one advantage envisioned for the fuel cells was that the water produced could be used by the crew. An intensive and expensive program was launched to obtain a fuel cell that would satisfy the requirements for manned spacecraft, and this program was successful. Its cost was over $500,000,000.

When the R&D effort on the manned space program began to taper off in the latter 1960's, the organizations with the greatest background of experience with the fuel cells closed out their effort. (These included Union Carbide, Allis Chalmers, etc.). The only major program to continue has been that conducted by Pratt and Whitney Aircraft with funding largely from the gas and electric utility companies. The funding in recent years has been roughly $5,000,000/yr; the funding for the 1973 to 1977 period is projected to run about $40,000,000. Of this about two-thirds would come from utilities and one-third from Pratt and Whitney.

In turning to technical accomplishments, one finds that Pratt and Whitney has built 90 units for NASA that were designed to yield 1.5 kW(e). Some of these have operated for as much as 2,000 hr. Pratt and Whitney

is currently working on a 15 kW(e) module which is to be followed by a 1 MW(e) module that would be assembled into 26 MW(e) units.

The developmental problems have included some extremely difficult instrumentation and control problems, particularly monitoring and maintaining within close limits the concentration and PH of the electrolytes.[15] The instrumentation available for this purpose is subject to drift and requires frequent recalibration. The most serious problem, however, is posed by the requirement for a precious metal catalyst. Silver has been used with some success, but the only really satisfactory performance obtained to date has been from cells using platinum as the catalyst. The lowest platinum inventory obtained to date in Pratt and Whitney cells with a reasonably long life has amounted to 250 mg/W. The current market price of platinum (June 1974) is about $200/troy ounce, or $6.43/g. This amounts to a capital investment of about $1600/kW(e) just for the platinum. Pratt and Whitney hopes to reduce this platinum inventory by a factor of 10; when viewed from the perspective of the last half century of effort, the prospects for accomplishing this do not appear promising. However, if they do succeed in producing such a cell with a long life and a high reliability, they have contracts with a number of utilities to supply 26 MW(e) modules at a price of $185/kW(e). The anticipated life of these modules would be 40,000 hr.

For MIUS applications Pratt and Whitney estimates that the thermal efficiency of their units in producing electrical power will be about 40%. They estimate that about 28% of the energy in the fuel can be removed as heat at a temperature of around 250°F, about 6% can be removed as heat at about 150°F, and about 12% can be removed as heat at 115°F. The balance will be lost to the surrounding atmosphere by thermal radiation and convection. It should be noted that increasing the temperature has an adverse effect on cell life.

In summary, an enormous amount of money has been spent in the past half century on the development of fuel cells. If the Pratt and Whitney targets for cost, performance, life, and reliability can be met, the units would be very attractive for MIUS applications. A large development program is underway; at this stage it appears prudent to wait and see to what degree it may prove successful.

It has been suggested that fuel cells might be made to operate using coal. The sensitivity of the catalyst in the fuel cells to trace amounts of impurities is so great that it appears that the developmental problems will be vastly more serious if the hydrogen for fuel cells is derived from coal rather than from natural gas or light petroleum distillates.

Solar Energy

Efforts to develop solar energy have been underway for about a century. The largest solar power plant built to date was built in Egypt in 1912 and produced 50 hp for pumping irrigation water. Many modest programs on solar energy have been carried out in the U.S. and Europe since 1930, of which perhaps the most successful was a program at M.I.T. aimed primarily at the solar heating of houses.[16] A basic difficulty is that the efficiency with which solar energy can be converted into heat falls off rapidly as the collection temperature is increased. As a consequence, the only efforts that have been commercially successful have been those that produce domestic hot water at 120 to 150°F. A large program on solar energy systems is underway at the time of writing under the direction of the National Science Foundation; there is great hope that this research will yield an economically competitive commercial system suitable for heating and air conditioning homes as well as supplying domestic hot water. The prospects for collecting solar energy at a sufficiently high temperature to yield an attractive thermodynamic cycle appear much less promising, but a substantial effort is also directed toward this end.

In comparing a solar heating system with a fossil fuel MIUS system one finds that there are pronounced differences in the areas of application. The installation with solar heating system still needs power from an electric utility, the building design must be tailored carefully to take maximum advantage of the incident solar energy, and the economics are heavily dependent on the climate at the site. A MIUS system, on the other hand, can be retrofitted to any existing building complex, it is insensitive to the detail design and orientation of the buildings, and derives its attractive features from the fact that in producing the electricity required it has provisions for recovering the waste heat from the

thermodynamic cycle for use in heating and air conditioning the building complex.

Direct conversion of solar energy into electrical energy appears so attractive that it has received a great deal of attention. Under the space program NASA has spent hundreds of millions of dollars on this approach, and the solar cells used in spacecraft have been outstandingly successful. However, the efficiency with which these solar cells convert the incident solar energy into electricity is only about 6%, and their cost is roughly $1,000,000/kW(e). A number of large programs are continuing in this area; if they prove as successful as the enthusiasts hope, the results could yield some commercial units for MIUS applications. However, there seems to be general agreement that such an achievement is decades away.

Magnetohydrodynamic Generators

Substantial programs on the development of magnetohydrodynamic generators have been underway in the U.S., Western Europe, and the U.S.S.R. for the past 20 years. The investment in the U.S. program alone has been over $40,000,000. The longest operating time achieved in the U.S. to date is a few hundred hours with an output of about 150 kW(e). The maximum thermal efficiency obtained has been of the order of 1%. Units normally operate using liquid oxygen with a hydrocarbon fuel, but some have employed powdered coal. A few units have been operated with air rather than liquid oxygen by using a regenerative heat exchanger.

The experimental units to date have not borne a close resemblance to units that could be commercially attractive. For example, for commercial applications liquid oxygen would be prohibitively expensive. Further, to obtain a long life the walls of the generator would have to be cooled; this would result in substantial heat losses, and would degrade the thermal efficiency. If the walls are not cooled, the corrosion problem becomes impossible, but if they are cooled, thermal stress problems become extremely difficult. A large fraction of the technical experts who have reviewed the situation are doubtful that a commercially viable unit can be developed in the next 10 or 20 years. If it should prove possible, the unit would probably be much too large for MIUS applications.

Helium Gas Turbine

The closed cycle gas turbine will yield a slightly higher thermal efficiency if operated on helium rather than air, and the cost of the heat exchanger equipment can be reduced.[17,18] However, the proportions of the compressor and turbine would be very different from those for air, and no helium gas turbine equipment is currently available commercially. In the small size system of interest for MIUS applications, preliminary estimates indicate that the increased cost to assure the high degree of leak tightness required for a helium system would more than offset the savings in the cost of the heat exchangers that would be made possible by going from air to helium as the working fluid. Thus, it seems best at this stage to concentrate the effort available on an air cycle system. If this proves successful, firm cost data for the heat exchangers will be available and a much better evaluation of the relative cost of the helium and air systems can be made than is possible at this date.

Potassium Vapor Cycle

Analyses and experiments indicate that a potassium (or cesium) vapor topping cycle superimposed on a conventional steam cycle should make possible a thermal efficiency in excess of 50% in large power plants.[18] Two studies indicate that such a system looks particularly attractive if a fluidized bed coal combustion chamber is employed to heat the potassium boiler.[19,20] However, in the small sizes required for MIUS applications the low Reynolds number in the turbines would lead to a drastic drop in the efficiency of the turbines. Even more serious, the complexity of the system would lead to excessively high capital charges.

Dissociating Gas Cycles

It is possible to reduce the compressor work in a gas turbine cycle by making use of a dissociating gas such as aluminum chloride or N_2O_4.[21,22] That is, at the relatively low temperatures that prevail in the compressor, aluminum chloride will be present as Al_2Cl_6, but it will dissociate in the heater to $AlCl_3$ and hence the volume of gas passing through the turbine will be doubled by dissociation and the work output of the turbine will be increased relative to the value obtainable if dissociation did not occur in

the heater. The dissociating gas cycles have the further advantage that the dissociation process leads to higher heat transfer coefficients in both the heater and the cooler. However, the dissociating gases that appear attractive as thermodynamic cycle working fluids are not attractive from the standpoint of corrosion and chemical thermodynamics. The NO_2-N_2O_4 cycle, for example, implies handling a gas at red heat with the corrosive characteristics of hot fuming nitric acid. Similarly, free chlorine from the aluminum chloride cycle poses serious corrosion problems. Although protective coatings may at first appear as attractive possibilities, the rate of solid state diffusion through such coatings at high temperature is sufficiently high so that it is doubtful that coatings would prove effective in yielding the life required for a truly practical unit.

Supercritical CO_2 Cycle

One way of improving the efficiency of a thermodynamic cycle by reducing the compressor work is to make use of CO_2 and operate at or near the super-critical pressure and temperature at the inlet to the compressor. Such a cycle has been considered for both nuclear and fossil fuel power plants.[17,23] However, it happens that the efficiency obtainable is little different from that obtainable from a steam cycle, and, as in the steam cycle, the Reynolds number in the turbine and compressor in small power units is low so that it is difficult to obtain a good efficiency from these components. As a consequence, for the power output range of interest for MIUS applications this cycle does not appear to be attractive.

Summary

Table 4.2 summarizes the principal figures of merit that are of interest when appraising the merits of the various advanced power conversion systems discussed above. Note that, except for the gas turbine coupled to a fluidized bed coal combustion system, either the fundamental characteristics of the system make it unsuitable for the small power outputs required for MIUS applications, or the developmental problems appear too formidable for the system to be a good candidate for HUD sponsorship for MIUS applications.

System Reliability

However difficult it may be to estimate the cost of candidate systems for MIUS applications, it is even more difficult to estimate their reliability. It is hard to find good data on the reliability of systems that are in use, but, where a new system such as the proposed closed cycle gas turbine coupled to a fluidized bed combustion chamber is to be employed, one has an even tougher problem and can only attempt to infer the reliability from operating experience with similar components for similar system. Thus the problem becomes one of assembling as much pertinent data as possible, and then attempting to assess it. This procedure has been followed here.

Closed Cycle Gas Turbine

Ten closed cycle gas turbine plants have been built and operated[24,25] The first of these was started up in 1941 near Zurich, Switzerland, and operated for over 20 years with an excellent record for reliability.[24] Data for the next eight that have been built and which are still operating are presented in Table 4.3. Insufficient data have been obtained with the tenth plant to include it in the Table 4.3. Note that three of the eight plants in Table 4.3 operate on coal, two on blast furnace gas, one on mine gas plus coal, and one on lignite. While not explicitedly stated in the table, a major reason for the use of closed cycle systems in these plants was to provide good part-load fuel economy. As indicated earlier in Fig. 4.1, a plant that must operate much of the time at reduced loads will suffer a marked loss in thermal efficiency. Another major reason for the use of a closed cycle in many of these plants was the use of fuels that could not be employed in an open cycle gas turbine, i.e., coal or lignite. An indication of the reliability of these plants is given by the last line in the table which indicates the fraction of the total time the plants have been on-stream. These values may be compared with the average for steam central station units in the U.S. for which the availability also runs about 80%. Thus, it is evident that the reliability of closed cycle gas turbines is comparable to that of central station steam plants.

Table 4.3. Current Closed-Cycle Gas Turbine Plants
(Data from Ref. 26)

Plant	Ravensbury, Germany	Toyotomi, Japan	Oberhausen, Germany	Coburg Germany	Nippon Kokan Japan	Kashira, Russia	Haus Aden, Germany	Gelsenkirchen, Germany
Working medium	Air	Air	Air	Air	Air	Air	Air	Air
Fuel	Coal	Natural gas	Coal	Coal	Blast furnace gas	Lignite	Mine gas plus coal	Blast furnace gas/oil
Compressor inlet temperature, °C	20	20	30	20	25	20	20	20
Compressor inlet pressure, atm	7.2	7.2	8	7.3	6.7	7	9.3	10.2
Turbine inlet temperature, °C	660	660	710	680	680	680	680	711
Turbine inlet pressure, atm	27	27	32	27-1/2	29	29	31	38-1/2
Speed turbo set, rpm	12,750	13,000	6,640	8,820	6,600	6,640	8,220	6,650
Speed alternator, rpm	3,000	3,000	3,000	3,000	3,000	3,000	1,500	3,000
Continuous output, MW	2.3	2	13.75	6.6	12	12	6.4	17.25
Efficiency at terminals, %	25	26	29.5	28	29	28	29.5	30
Heat supply, 10^9 cal/hr	2.1-3.5	--	16-24	7-14	--	8-10	6.7	17-25
Compressor type	Radial	Radial	Axial	Axial/ Radial	Axial	Axial	Axial	Axial
Turbine type	Axial	Axial	Axial	Axial	Axial	Axial	Axial	Axial
Commissioning date	1956	1957	1960	1961	1961	1962	1963	1967
Operating hr as of end 1971	89,300	90,000	72,000	71,700	54,500	54,500	67,500	24,000
Fraction of time on stream, %	73	79	82	82	62	69	96	68

Conventional Open Cycle Gas Turbines

Quite a number of small power plants employing four to eight open cycle gas turbine-generator units of 350 kW(e) to 1000 kW(e) have been operated in the U.S. during the past 15 years. One particularly significant application from the reliability standpoint has been power supplies for major computer centers.[26] For this application the incidence of power failures causing a forced outage of the computer has been found to be lower by a factor of 4 to 20 than had been the experience when power was supplied from a public utility. (Outages in the latter case usually stemmed from lightning or storm damage.) Table 4.4 summarizes the operating experience with four such installations. Note that the total operating time accumulated in other, non-computer applications with the same model gas turbine-generator unit totals over 2×10^6 hr.

Fluidized Bed Waste Incinerators

There has been no effort to operate a fluidized bed coal combustion system in a commercial plant, hence there are no data available from this quarter. However, over 200 fluidized bed combustion systems are in operation in the U.S. for roasting pyrite ores and over 100 are used as incinerators for the disposal of solid wastes and/or slurries with a high organic solids content. Detailed data on the reliability of these systems are not available, but the manufacturers of the systems state that their systems stay on-stream 24 hr/day, seven days a week throughout the year with very few forced outages.

Coal Stokers

Coal stokers employing a feed system similar to that contemplated for the proposed MIUS system have been in operation in the U.S. for the past 50 yr. Hundreds of thousands of these units have been installed in private residences, apartment buildings, and commercial establishments, many in the size range required for the MIUS system. The units of particular interest here have employed a worm feed system that conveys coal from a bin or hopper to an aperture through which the coal falls into a moderately high velocity air stream which carries the coal particles into an open cup burner. Discussions with an engineer who has been intimately involved in

Table 4.4. Summary of Operating Experience with Multiengine Open Cycle Gas Turbine Power Plants Used at Installations Employing Large Computers*

(Numbers given without parentheses are for the total operating time. In most cases the engines have never been overhauled. Where they have been overhauled, the maximum time between overhauls is given in parentheses.)

Organization	Western	Continental	USAF ADWS	United
Turbine No. 1	42,777	41,523 (38,121)	42,480	3,729
Turbine No. 2	42,892	42,022	42,697	15,542
Turbine No. 3		858		14,092
Turbine No. 4				14,885
Total	85,669	84,403	85,177	48,248
As Of	12/1/72	12/9/72	12/2/72	12/4/72

NOTE: Grand total 303,497 hr.
Grand total of all engine model 831 turbogenerator installations is 1,938,095 hr.

*Data Courtesy of Garrett Corporation.

work on these systems for nearly 50 yr indicate that relatively little difficulty has been encountered with these units except when pieces of tramp iron (such as railroad spikes) come in with the coal, get into the worm, and jam it.[27] This experience is consistent with that of the writer (A. P. Fraas) who was closely associated with a number of these systems in apartment houses in the 1930's where the units were normally looked after only twice a day for removal of clinkers from the burner cup; attention other than this was rarely required.

Reliability of Multiengine Power Plants

A good indication of the reliability of both piston engines and gas turbines in multiengine power plants is given by a comprehensive study made for the U.S. Army in connection with deployment of the Nike-X missile system. In this study an overall availability of about 0.96 was reported for both piston engine and gas turbine prime movers.[28] Of the 4% average down time observed, about 1% was attributed to forced outages and 3% to scheduled maintenance actions. The surprising aspect of these data is that for the piston engines, the mean time between failure was only slightly over 500 hr and the mean time to repair about 2.5 hr. Most of the outages were for items such as failures in water hose connections, lube oil, and cooling water piping and ignition systems. The data for turbines ranged from a mean time between failure of 700 hr with a 6.4 hr mean time to repair for 1000-hp units to a mean time between failure of 16,000 hr and a mean time to repair of 25.3 for 6700-hp units.

Another source of information on operating experience with gas, diesel, and dual-fuel engines is a set of ASME reports on diesel and gas engine installations.[29] However, in these reports, the manner in which the data are shown is ambiguous. For example, some installations with a number of units report the total hours that some of the units were out of service and use a dash or leave a blank for the other units, while other installations report "none" for units that were not out of service. It is not clear whether the dash or blank means not available or no trouble. In the following analysis of these installations, the conservative assumption was made that a dash or blank means "not available." The 1971 report lists a total of 40 engines out of service for a total of 10,255 hr for emergency

repairs and 105 engines with no emergency outage. The average time for repairs was 226 hr for those engines requiring repair and the average time out of service for all engines was 71 hr during the year (8760 hr).

Similar data are also reported for time out of service for normal maintenance. In this case, a total of 84 engines were out of service a total of 23,149 hr of which 78 engines were not out of service for normal maintenance. The average time out of service for the engines requiring normal maintenance was 276 hr and the average time for all engines was 143 hr.

The fraction of the time out of service should be based on the total running hours per year (rather than 8760 hr/year), which, for the above plants, averages about 3500 hr. Thus the availability of the units in terms of emergency outages is 0.98 and in terms of normal maintenance is 0.960. The overall availability is 0.94.

These data are for large, low-speed units and may be somewhat pessimistic. In addition to the problems of interpreting the data, 30% of the total outage time was accumulated by only three units, and it is not known whether these prolonged outages were necessary or stemmed from a lack of incentive to place the units back in operation. Reference 30 states that a total availability (including time out for maintenance) of over 96% is commonplace for large marine diesels. Two other reports[31,32] give data concerning mean time between failure without giving the time required to repair the unit. Reference 32 reports a failure rate of 89 per 10^6 hr or 1 per 11,236 hr. Reference 33 reports the results of a survey of small high-speed piston engines used in total energy plants. These data showed that, for one manufacturer, the failure rate was 1 per 9460 hr, and, for a second manufacturer's engines, the failure rate was 1 per 3020 hr. If one assumes an average repair time of 100 hr for these smaller engines, the availability in terms of emergency of unscheduled outage is between 0.99 and 0.967.

Most of the downtime for normal maintenance will be for minor and major overhauls. Generally, an engine will require two minor and one major overhaul every 30,000 to 40,000 running hours, or on the order of 50,000 elapsed hours. The total downtime during this 50,000 hr will be between 1000 and 1500 hr, and the availability will be 0.98 to 0.97. However, there will probably be some overlapping of the above estimates of

downtime; for example, if an engine goes down for emergency repair about the time an overhaul is due, the two would be combined.

Quantitative Analysis of Reliability

The meaning of the expression "the reliability of a system" depends on the function and purpose of the system. If the system is inaccessible for repair or maintenance, the reliability can be expressed as (1) the mean time between failures, which depends on the mean time between failures of the individual components of the system, or (2) the probability of some number of hours of operation before a failure. For systems that can be repaired, reliability is usually expressed as the availability of the system, which depends on both the mean time between failures and the time required to repair the system; that is, availability is the fraction of time (also the probability) that the system is capable of performing its intended function.

A MIUS power-generation system will consist of several parallel generator units, and the overall system reliability or availability will depend on the availability of the individual units, the number of units, and the excess capacity installed. For a generation system consisting of N generator units, all with an availability A, and with the availability of the units independent of each other, the probability of x and only x units being out of service is

$$P_x = \frac{N!}{(N - x)!\ x!}\ A^{(N - x)}(1 - Z)^x$$

The dependence of P_x on N, x, and A is illustrated in Fig. 4.2.

Figure 4.2 can be used to determine the probability of having some number of engines (N - x) operation or, as shown in Fig. 4.3, the probability of having x or more engines out of service. It should be noted that the probability of occurrence of the various combinations, assuming the probability to be uniform with time, also represents the fraction of time that this combination occurs. Thus the probability calculations shown in Fig. 4.3 are expressed as hours per year.

In order to illustrate the manner in which the above information can be applied, assume an installation having four 500 kW generators and a

ORNL DWG. 75-14481

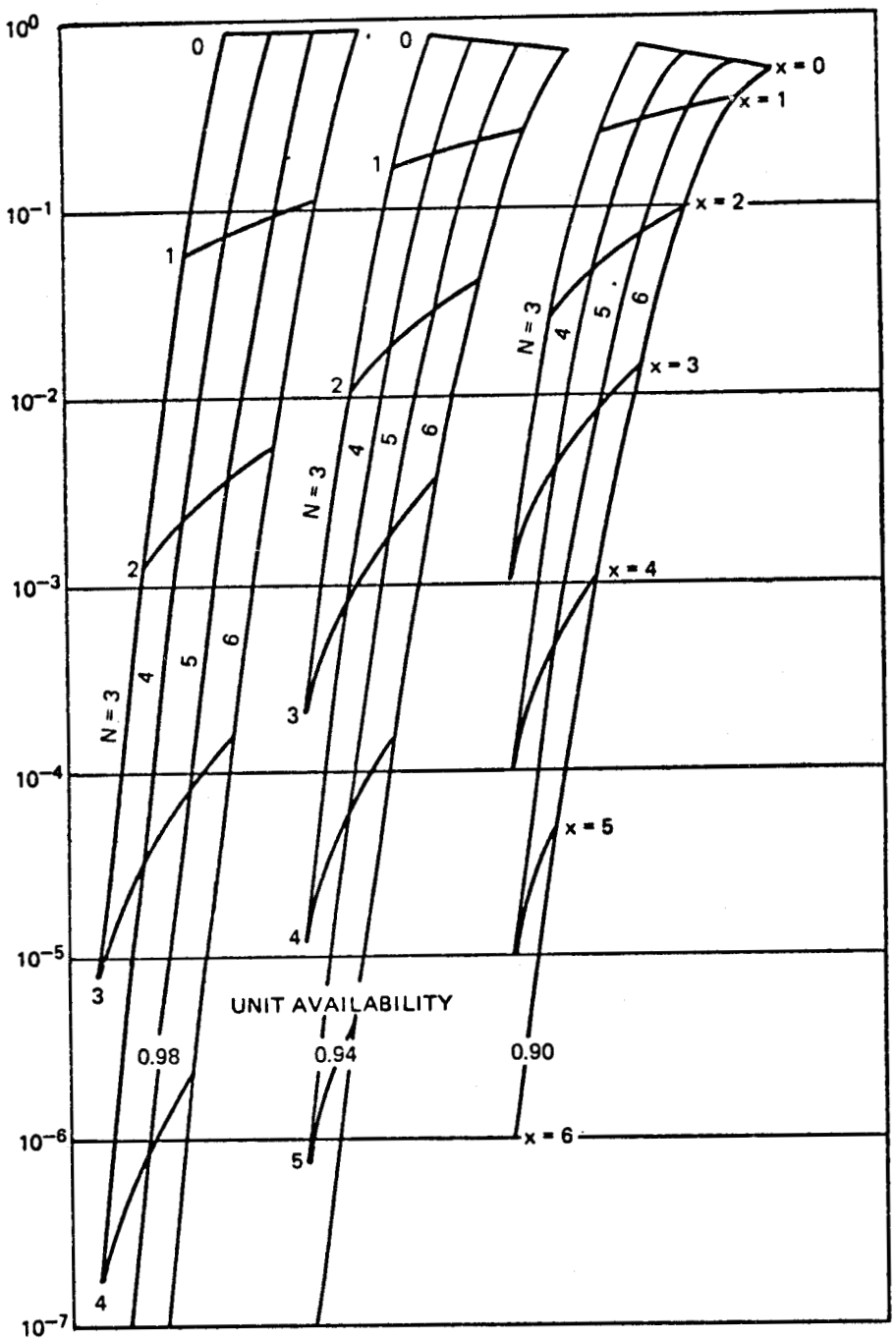

Fig. 4.2. Probability of simultaneous outages as a function of units installed and unit availability. N = number of units; x = number of units out of service.

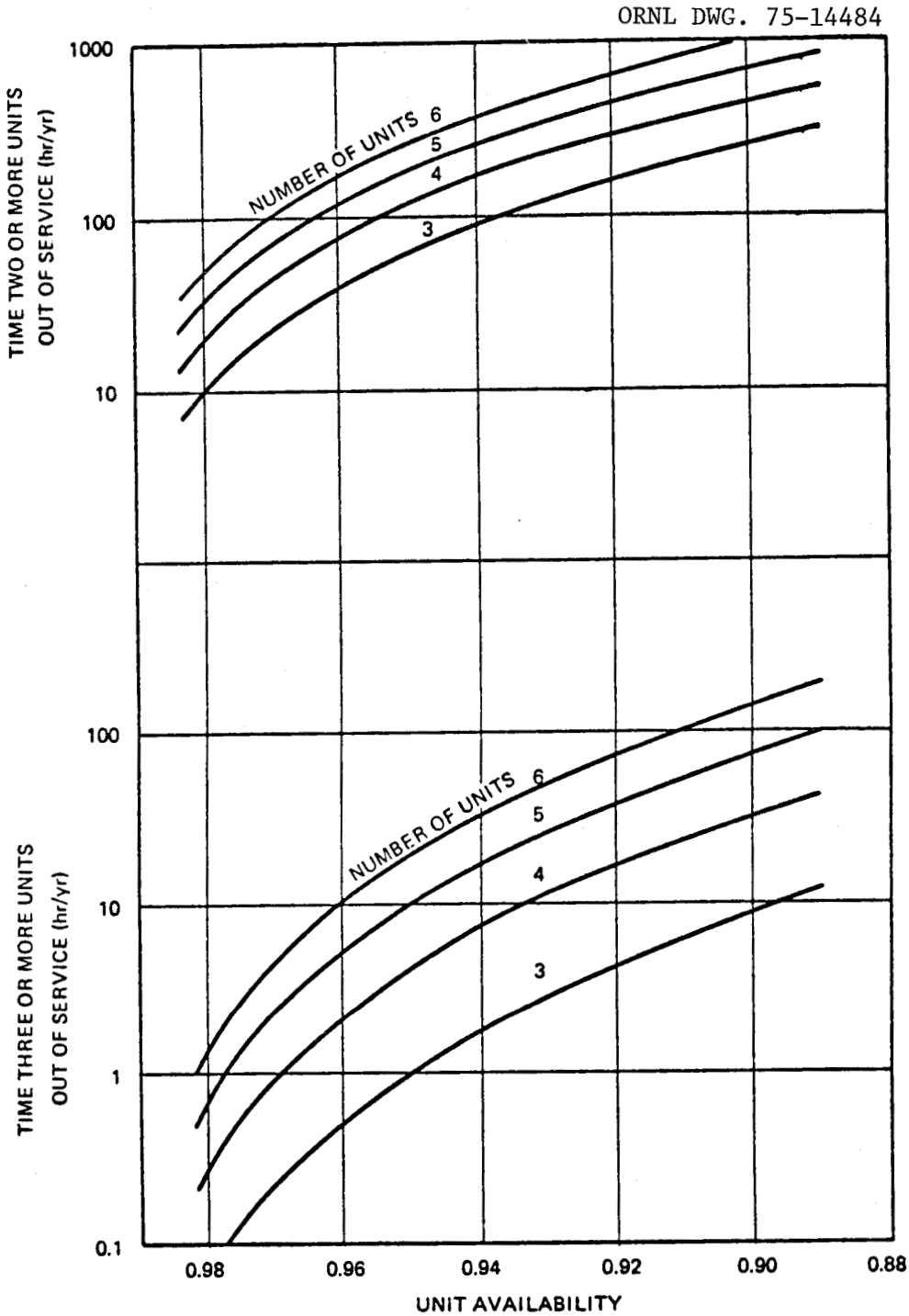

Fig. 4.3. Plant downtime as a function of units installed and unit availability.

critical electrical load of 1000 kW, i.e., the maximum anticipated uninterruptable load. (This assumes that the power required for air conditioning can be interrupted in an emergency with no serious consequences.) The availability of the generators in relation to emergency outages may be taken as 0.98 and, for normal maintenance, as 0.97. With all four generators in service (or on standby) the critical load can be supplied unless three or more units go out. The probability of this happening can be determined by adding the probabilities of four and three engines being out of service. The value is 0.0000315 and is shown in Fig. 4.3 as 0.28 hr/year. This value is too low because it does not consider normal maintenance. Including the time down for normal maintenance, the probability of not being able to meet the critical load is the probability of losing two of the three engines in service, which is 0.00118, times the fraction of time that a generator is out of service for normal maintenance, which is 0.12. Thus the probability is 0.000142 or 1.2 hr/year, which is less than the 5 hr/year experienced by electric utility customers in this country.

Obviously there are a large number of combinations of equipment sizes that may be used in a MIUS plant, and the selection of both the number and the size of the units will depend on the plant load characteristics. The above selection of four 500-kW units to meet a 1000-kW critical load was based on a previous study at ORNL for a 720-apartment complex which indicated that a peak load of 1500 kW occurred in the summer.[5] However, about 500 kW was due to compression air conditioning, and, since the compressors were located in the equipment building and under control of the plant operator, this load could be dropped in the event of a multiple-engine failure and consequently was not considered as part of the critical load.

Although the above discussion is for turbines and piston engines, the procedures can be applied to other equipment items for which availability data can be obtained. However, in other systems, such as heating or air conditioning, one would also be interested in the probability of supplying part of the load. The above type of analysis can also be extended to include the mean time between multiple failures[33] and also the effects of having engines of different sizes[34] rather than a uniform size.

References

1. A. J. Miller, H. R. Payne, M. E. Lackey, G. Samuels, M. T. Heath, E. W. Hagen, and A. W. Savolainen, Use of Steam-Electric Power Plants to Provide Thermal Energy to Urban Areas, Civil Defense Research Project, ORNL-HUD-14, January 1971.

2. H. R. Payne, MIUS Technology Evaluation — Lithium Bromide-Water Absorption Refrigeration, ORNL-HUD-MIUS-7, February 1974.

3. W. J. Boegly, Jr., V. O. Haynes, E. C. Hise, A. L. Compere, and W. L. Griffith, MIUS Technology Evaluation — Solid Waste Collection and Disposal, ORNL-HUD-MIUS-9, September 1973.

4. G. Samuels and J. T. Meador, MIUS Technology Evaluation — Prime Movers, ORNL-HUD-MIUS-11, April 1974.

5. G. Samuels, R. C. Robertson, W. J. Boegly, L. Breitstein, R. E. Gant, W. L. Griffith, J. T. Meador, A. J. Miller, H. R. Payne, and C. L. Segaser, Initial Comparisons of Modular-Sized Integrated Utility Systems and Conventional Systems, ORNL/HUD/MIUS-6 (in publication).

6. I. T. Dudley, Fuel Cell Technology Evaluation for MIUS Program, unpublished memorandum, January 1973.

7. J. T. Meador, MIUS Technology Evaluation — Comparison of Trenching Costs for Separate and Common Trenching, ORNL/HUD/MIUS-15, February 1976.

8. W. J. Boegly, Jr., I. Spiewak, D. G. Thomas, S. A. Reed, W. L. Griffith, A. L. Compere, and H. W. Wright, MIUS-Technology Evaluation — Collection, Treatment, and Disposal of Liquid Wastes, ORNL-HUD-MIUS-16, December 1974.

9. C. L. Segaser, MIUS Technology Evaluation — Thermal Energy Storage of Materials and Devices, ORNL-HUD-MIUS-23, November 1975.

10. C. J. Claffey and C. L. Segaser, MIUS Technology Evaluation — Compression Refrigeration Systems for Air Conditioning, ORNL/HUD/MIUS-19, February 1976.

11. W. R. Mixon, S. B. Ahmed, W. J. Boegly, W. H. Brown, A. L. Compere, R. E. Gant, W. L. Griffith, V. O. Haynes, J. O. Kolb, J. T. Meador, A. J. Miller, K. E. Phillips, G. Samuels, C. L. Segaser, E. D. Sundstrom, and J. V. Wilson, Technology Assessment of Modular Integrated Utility Systems, ORNL/HUD/MIUS-24 (in publication).

12. A. P. Fraas, Design Considerations and Proposed Designs for Steam Turbine-Generator Units for Terrestrial Power Plants of 30 kW(e) to 2 MW(e), USAEC Report ORNL-TM-1837, June 1967.

13. A. P. Fraas, Review of Development Status of Small Turbine-Generator Units Suitable for the Navy Undersea Power Plant, USAEC Report ORNL-TM-3586, September 1972.

14. A. P. Fraas, H. C. McCurdy, A. M. Perry, and G. Samuels, Preliminary Study of Typical Small Portable Reactor Power Plants Potentially Suited to Navy Undersea Installations, USAEC Report ORNL-TM-3580, March 1973.

15. N. A. Cook, Analysis of Fuel Cells for Vehicular Applications, Society of Automotive Engineers, January 8-12, 1968.

16. H. C. Hottel and J. B. Howard, New Energy Technology, M.I.T. Press, Cambridge, Massachusetts, 1971.

17. M. Bender et al., Comparative Features of Gas-Cooled Fast Reactors, Oak Ridge National Laboratory Internal Report.

18. A. P. Fraas, Topping and Bottoming Cycles, Proceedings of the 9th World Energy Conference, Division 4, September 22-27, 1974.

19. A. P. Fraas, A Fluidized Bed Coal Combustion System Coupled to a Potassium Vapor Cycle, 65th Annual Meeting of the AIChE, New York, November 26-30, 1972.

20. R. J. Rossbach, Final Report: Study of Potassium Topping Cycles for Stationary Power, GESP-741, NASA Contract No. NAS3-17354, General Electric Co., Energy Systems Programs, November 13, 1973.

21. A. K. Crasin et al., Physical and Technical Principles of Creating Atomic Power Stations with Fast Neutron Gas Reactors Cooled by Dissociating N_2O_4, A/CONF. 49/P/431, Byelorussia, July 1971.

22. M. Blander, L. G. Epel, A. P. Fraas and R. F. Newton, Aluminum Chloride as a Thermodynamic Working Fluid and Heat Transfer Medium, USAEC Report ORNL-2677, Oak Ridge National Laboratory, September 21, 1959.

23. E. G. Feher et al., Investigation of Supercritical (Feher) Cycle, Report No. AFAPL-TR-68-100, Air Force Aero Propulsion Laboratory, October 1968.

24. C. Keller, The Escher Wyss-AK Closed Cycle Turbine, Its Actual Development and Future Prospects, Trans. ASME, Vol. 67, p. 791, 1946.

25. State-of-the-Art of HTGR Gas Turbine Technology, USAEC Gulf GA-A12098, Gulf General Atomic Company, June 1, 1973.

26. R. MacKay, The Gas Turbine as a Source of Continuous Precise Power, ASME Paper No. 69-GT-20, presented March 13, 1969 at the 14th Annual Gas Turbine Conference.

27. Personal communication from S. H. Beach, Space Comfort, Inc., to A. P. Fraas, June 20, 1974.

28. 1971 Report on Diesel and Gas Engines Power Cost, ASME, New York, January 1971.

29. R. W. Parisian, How Reliable are Today's Prime Movers?, Power, Vol. 114, No. 1, p. 45-47, January 1970.

30. F. M. Swengel, Big Diesels for Power Plants, Power Eng., Vol. 72, No. 3, p. 38-40, March 1968.

31. A. P. Fraas, Estimating the Reliability of Systems, USAEC Report ORNL-TM-2200, May 1968.

32. M. G. Gamze, A Critical Look at Total Energy Systems and Equipment, Proceedings of the 7th Intersociety Energy Conversion Engineering Conference, San Diego, California, September 25-29, 1972.

33. H. Halperin and H. A. Adler, Determinations of Reserve Generating Capability, AIEE Trans., Vol. 72, p. 530-539, August 1958.

34. H. A. Adler and K. W. Miller, A New Approach to Probability Problems in Electrical Engineering, AIEE Trans., Vol. 65, p. 630-632, October 1946.

CHAPTER 5

CYCLE ANALYSIS FOR FLUIDIZED BED COMBUSTION GAS TURBINE SYSTEMS

It was thought initially that the system could be simplified by employing an open cycle gas turbine. Four cycles of this type were examined,[1] and one was found to yield good performance at full load. However, part-load performance was poor, and this led to examination of the performance characteristics of closed cycles. These were found to give attractive performance both at full load and part load. This chapter presents a brief description of the principal cycles considered together with a discussion of the major problems and design compromises that became apparent as design studies were made in each case.

Description of Cycles Considered

Open Cycles

The first cycle considered was chosen to provide a base case for reference purposes. This cycle, shown in Fig. 5.1, directs the entire output of the compressor into a conventional coal-fired furnace from which the hot gases pass to the turbine. For this approach, the amount of fuel added would be limited to that required to raise the mean gas temperature to the desired turbine inlet temperature, i.e., the system would operate with ∿400% excess air. The average combustion gas temperature at full power would thus be limited to about 900°C (1700°F), the temperature limit imposed by the turbine buckets. A waste heat recovery boiler would remove heat from the stack gases so that they would leave the system at 300°F.

The second cycle considered is similar to that commonly used for closed cycle gas turbines in that the air from the compressor is heated in a tube matrix before entering the turbine. This cycle, shown in Fig. 5.2, directs about 20% of the output of the gas turbine into a conventional coal-fired furnace from which the hot gases pass over the tube matrix used

ORNL DWG. 74-4769

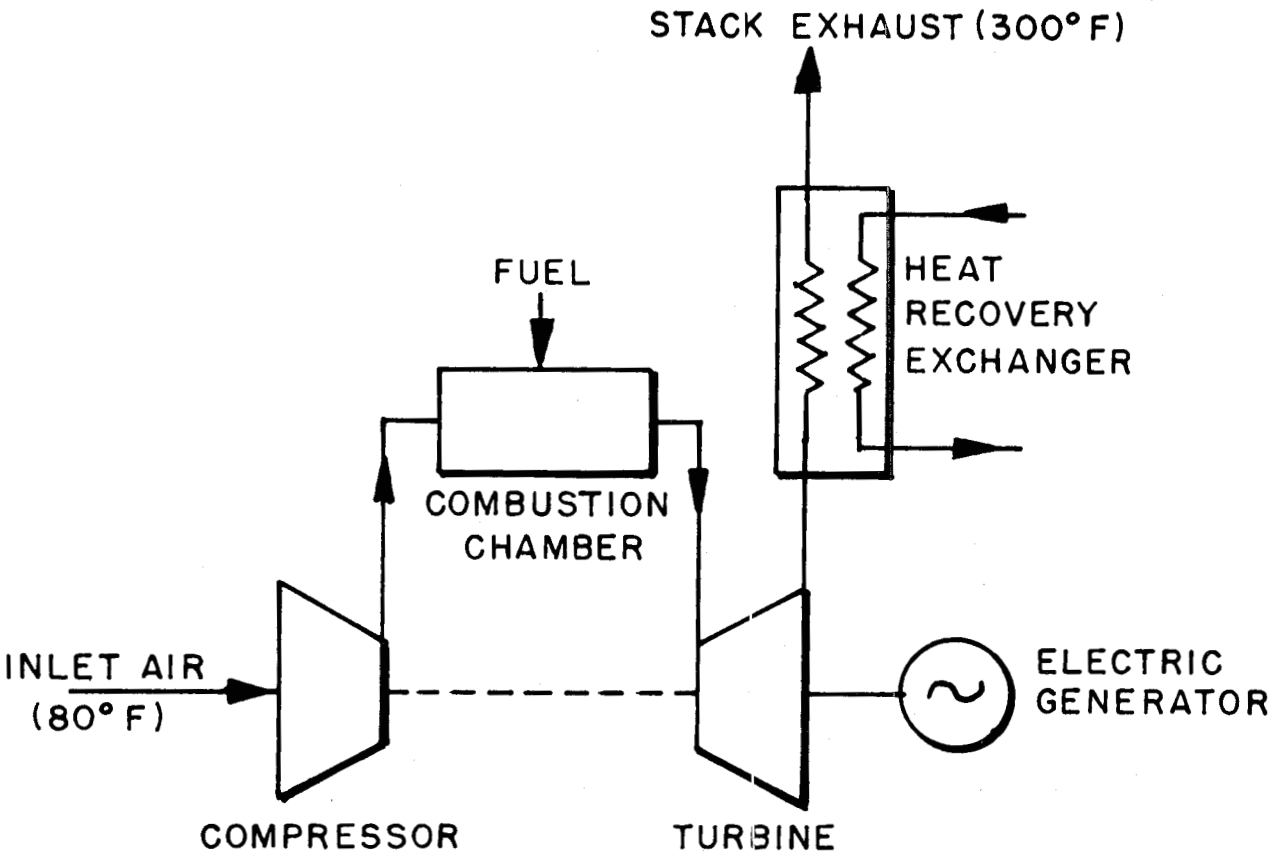

Fig. 5.1. Flow sheet for a simple open cycle gas turbine with a conventional oil-fired burner and fitted with a waste heat recovery unit.

ORNL DWG. 75-16536

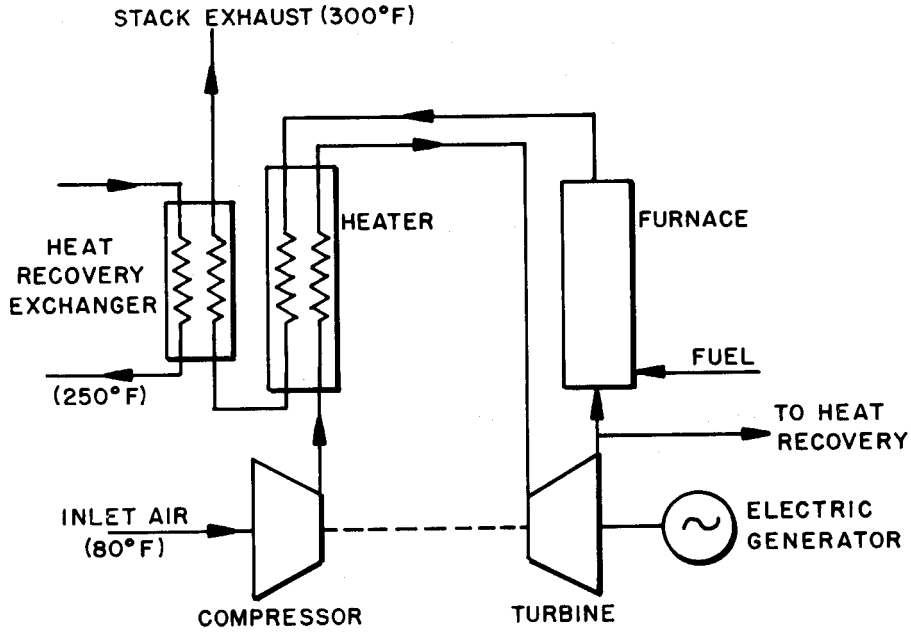

EXTERNAL COMBUSTION GAS TURBINE OPEN CYCLE
WITH A CONVENTIONAL FURNACE

Fig. 5.2. Flow sheet for a simple open cycle gas turbine heated with a conventional coal-fired furnace and fitted with a waste heat recovery unit.

to heat the turbine air. The balance of the hot air leaving the turbine goes to a heat recovery unit. For this approach, the amount of fuel added could be close to the stoichiometric amount. Note that care must be taken in the design of the heater tube matrix to avoid endangering the tubes in the air heater as a consequence of local velocity and temperature effects that might cause hot spots. The heat transfer matrix for this heater would serve the dual function of absorbing the heat from combustion and also as a recuperator to recover a fraction of the heat in the hot air leaving the gas turbine. It was assumed that this heat exchanger would be designed so that the hot combustion gases would leave it at a temperature of 235°F above the compressor outlet temperature. A waste heat recovery boiler would then remove additional heat from the stack gases so that they would leave the system at 300°F.

The third system considered, that shown in Fig. 5.3 is similar to that described above except that it employs a fluidized bed combustion chamber instead of a conventional furnace and thus reduces the size and cost of the furnace and heater. Note that an economizer region is employed above the fluidized bed to transfer as much heat as possible from the combustion gas to the cycle and thus improve the cycle efficiency. With this arrangement, about 25% of the air leaving the turbine would be fed to the fluidized bed, and the balance would go directly to a waste heat boiler. This system has the advantage that it provides for the removal of about 90% of the sulfur in the coal burned and also gives a high heat transfer coefficient in the air heater without danger of hot spots. It has the disadvantage that some of the heat in the air leaving the turbine and fed directly to the waste heat boiler could have been used to obtain a higher fraction of the energy in the fuel as electricity by employing it to preheat the air from the compressor before feeding it to the heater-furnace unit. This shortcoming could be corrected by employing the system shown in Fig. 5.4 in which the portion of the turbine discharge air not fed to the fluidized bed combustion chamber would pass first through a recuperator before flowing to the waste heat boiler. With this system an even higher overall thermal efficiency can be obtained than for the system of Fig. 5.3. However, it has the disadvantage of somewhat greater complexity and a somewhat higher capital cost

ORNL DWG. 74-4763

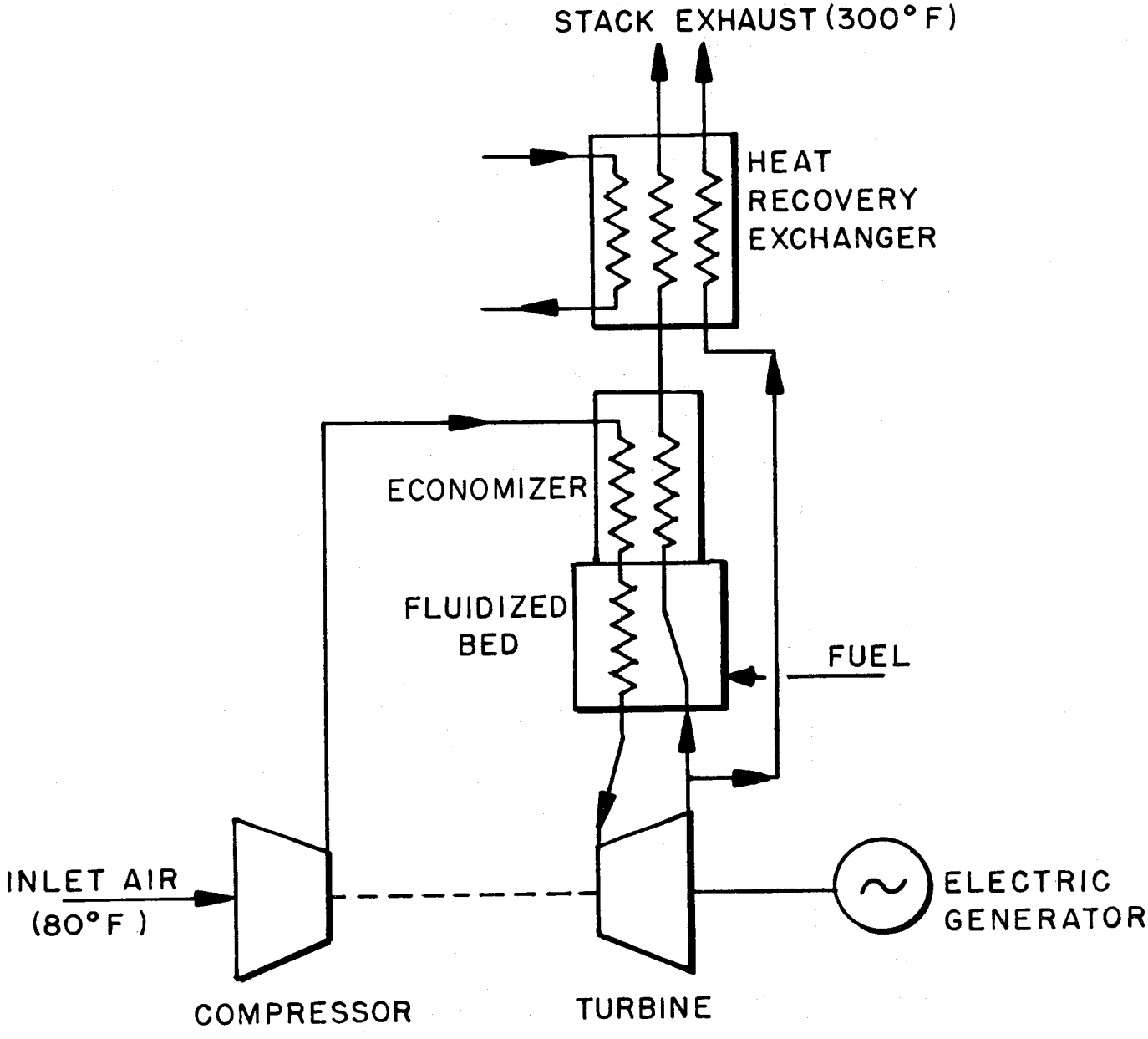

Fig. 5.3. Flow sheet for a simple open cycle gas turbine heated with a fluidized bed coal combustion chamber and fitted with a waste heat recovery unit.

ORNL DWG. 74-4770

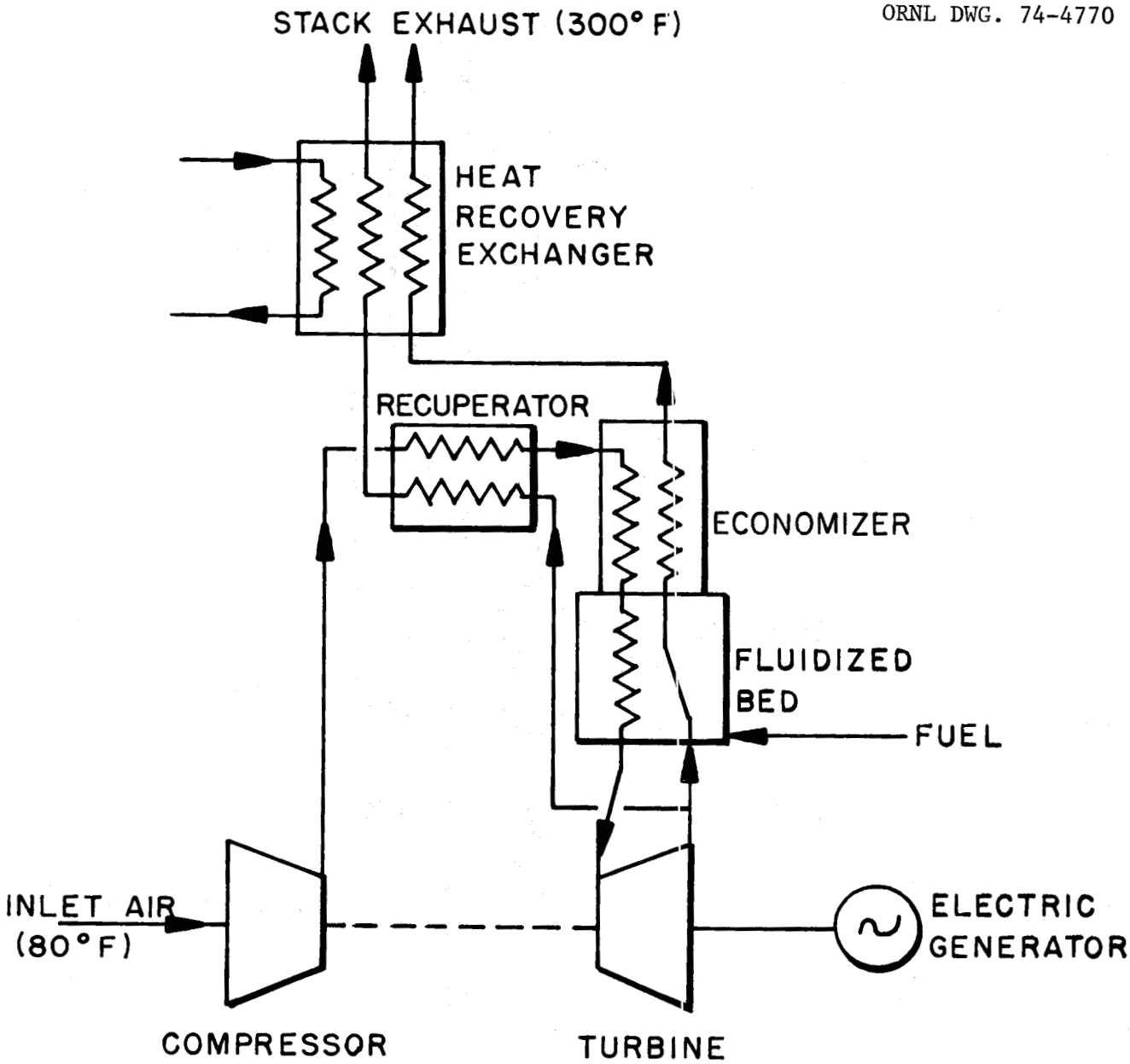

Fig. 5.4. Flow sheet for an open cycle gas turbine heated with a fluidized bed coal combustion chamber and fitted with both a recuperator and a waste heat recovery unit.

than the system of Fig. 5.4, but it probably would give a lower capital cost than the system of Fig. 5.2.

Closed Cycles

For MIUS applications much of the operating time must be at part load with a substantial amount of reserve capacity immediately available. In an open cycle the only way to reduce the power output is to reduce the turbine inlet temperature, and this reduces the cycle efficiency. Further, it reduces the volume flow rate through the turbine. Thus, a gas turbine with fixed rotor and stator blades running at constant speed to maintain a constant generator output frequency will be subject to substantial shifts in the operating points for the gas flow through the compressor and turbine, and this will lead to reductions in efficiency. These losses could be avoided with variable angle stator blades in the compressor and/or turbine, but commercial units with such features are not available. In the closed cycle system, on the other hand, the temperature structure through the entire system can be kept essentially constant and hence the relative velocities in the rotors and stators of the compressor and turbine can be kept fixed so that the efficiency will not change; the power output can be changed simply by varying the basic pressure in the system. This can be accomplished by alternately discharging air from the compressor outlet to reduce the output or from the storage tank back to the system to vary the basic pressure level in the gas turbine system. Thus, both the turbine and compressor operating points can be kept close to their peak values, and a high cycle efficiency can be obtained over a wide range of loads.

The first closed cycle considered was that shown in Fig. 5.5. It is essentially similar to the open cycle of Fig. 5.4 except that all of the turbine output is directed through the recuperator, and a cooler is added downstream of the recuperator so that the air can be recycled through the compressor inlet. This arrangement was found to give performance comparable with that of the cycle of Fig. 5.4, but it was clear that it would be desirable to have a larger fraction of the heat of combustion go into the air heated by the fluidized bed and a smaller fraction go into the waste heat boiler. This can be accomplished by applying a regenerator in the combustion gas stream so that the air admitted to the fluidized bed could be

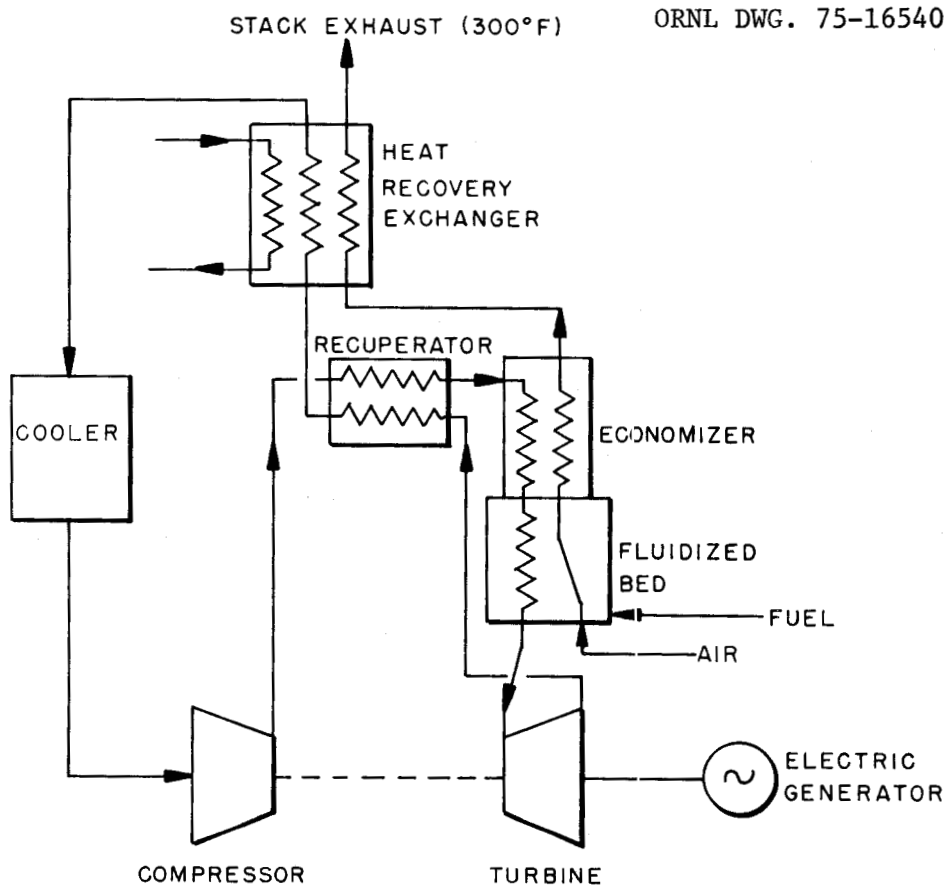

Fig. 5.5. Flow sheet for a closed cycle gas turbine heated with a fluidized bed coal combustion chamber and fitted with a recuperator, a heat recovery unit, and a cooler.

preheated. This would have the additional advantages of giving improved combustion conditions in the fluidized bed. A system of this type is shown in Fig. 5.6. Note that it has the further advantage that there is only a single waste heat boiler, thus simplifying both the fabrication and the control problems. Preheating the air admitted to the fluidized bed combustor has the additional advantage of giving improved combustion conditions in the fluidized bed, at least up to a point. The principal limitations on the use of a regenerator is the extent to which the combustion air can be heated prior to admission to the bed. BCURA experience indicates that temperatures up to about 600°F yield good conditions, but it may be that a temperature as high as 1000°F might give troubles such as coking in the fuel lines going into the bed. For purposes of this analysis it was assumed that this would not constitute a limitation.

The seventh cycle considered is similar to that above except that two stages of compression with an intercooler were employed to reduce the compression work. This cycle is shown in Fig. 5.7. The intercooler between the two stages of compression reduces the compressor work and thereby increases the fraction of fuel energy that is converted to electrical power. The intercooler provides a possible additional control parameter in that a reduction in the amount of intercooling results in a reduction of electrical power production without changing other operating variables.

The eighth cycle considered is similar to that above except that two turbine stages with reheat were employed to allow a higher unit energy input to the air stream without increasing the maximum air temperature. This cycle is shown in Fig. 5.8. The reheat allows a higher energy input per pound of working air stream for a given compressor work input, thus a greater fraction of fuel energy goes into the production of electric power.

Induced Draft Fan

In the systems of Figs. 5.5 to 5.8 it may be noted that an induced draft fan is required. In other cases studied, induced draft fans were added to the systems of Figs. 5.3 and 5.4 to reduce the back pressure on the turbine and thus increase the thermal efficiency. The reason for this is that only about 1/5 of the air flow from the turbine will pass through the fluidized bed coal combustion system with its high back pressure. Thus,

ORNL DWG. 74-9138

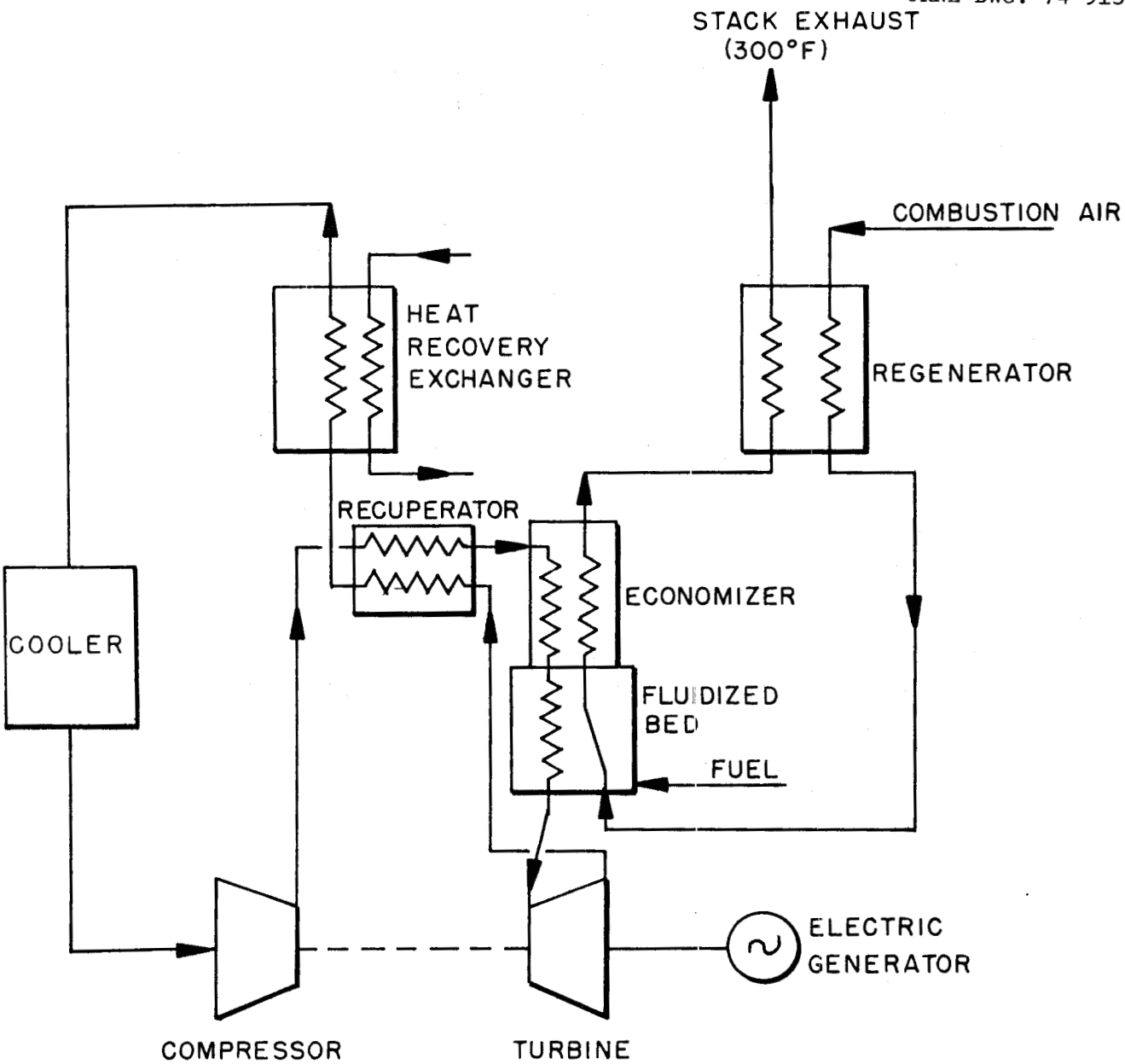

Fig. 5.6. Flow sheet for a gas closed cycle turbine with a fluidized bed coal combustion chamber supplied with combustion air preheated with a regenerator, and fitted with a recuperator, a waste heat recovery unit, and a cooler.

ORNL DWG. 75-16538

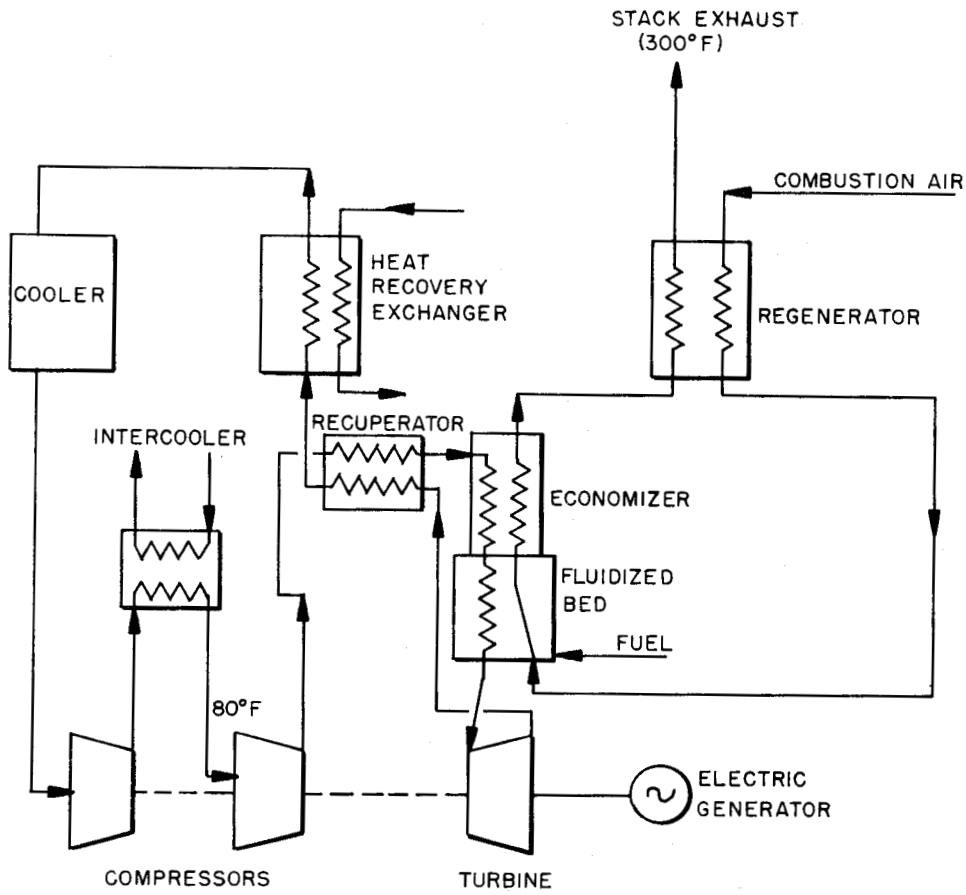

Fig. 5.7. Flow sheet for an intercooled closed cycle gas turbine with a fluidized bed coal combustion chamber supplied with combustion air preheated with a regenerator, and fitted with a recuperator, a waste heat recovery unit, and a cooler.

ORNL DWG. 75-16539

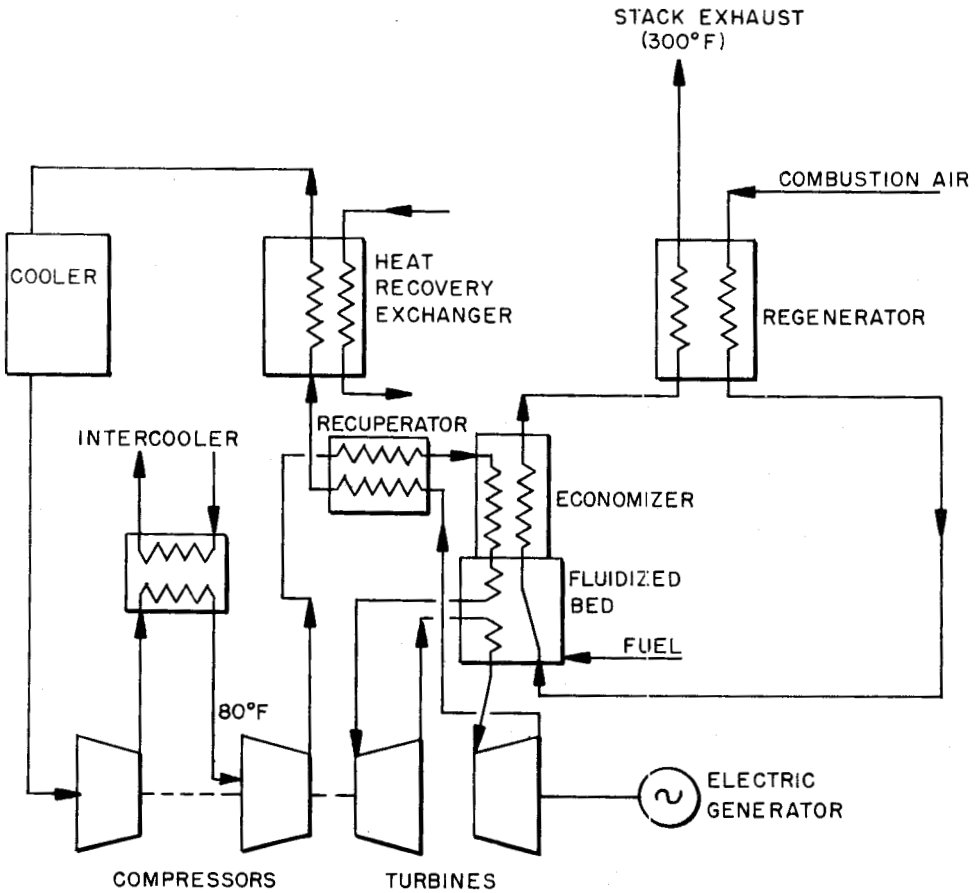

Fig. 5.8. Flow sheet for an intercooled and reheated closed cycle gas turbine with a fluidized bed coal combustion chamber supplied with a combustion air preheated with a regenerator, and fitted with a recuperator, a waste heat recovery unit, and a cooler.

it is better to have a separate fan to overcome this pressure drop because it must work on only one-fifth of the air flow through the turbine. In the systems of Figs. 5.5 and 5.6 it would have been possible to employ a forced draft fan which would have had the advantage of reducing the fan power requirement by about 35%. However, it is desirable to maintain the pressure in the dusty portions of the system below atmospheric so that air leakage will be into the system rather than out of it. This should help greatly to prevent the dispersal of fine coal dust and ash, and hence much of the unpleasantries commonly associated with coal-fired plants.

System Performance Analysis

It was evident from the beginning of the study that a number of objectives must be met in evolving a design. As indicated in the previous chapter if the system is to be competitive with central stations, the thermal efficiency from the electrical power generation standpoint should be over 25% and preferably over 30% for typical part-load operating conditions, and a large fraction of the waste heat from the thermodynamic cycle should be recovered at a temperature of about 250°F. To accomplish this one must clearly use a regenerator or recuperator because the simple open cycle gas turbine could not meet this objective. There is no question that a gas turbine with suitable heat exchangers could be built to give the desired efficiency, but it is also essential that the cost of these heat exchangers not be excessive, and therein lies a very difficult set of design problems. Thus, a major question to be answered in the design analysis was whether it would be possible to satisfy both the thermal efficiency requirements and the cost requirements. In addition, the system must be designed to be simple and reliable so that it can be operated semi-unattended to keep the operating costs to an acceptable level.

Choice of Turbine Characteristics

The performance of a gas turbine cycle is quite sensitive to the choices of pressure ratio, compressor efficiency, and turbine efficiency, while the cost of the heat exchangers in a closed cycle system is very much dependent on the choice of the pressure for peak load operation. Thus, it

was highly important that the choice of these parameters be consistent with the corresponding values that could be obtained in commercially available equipment. The problem was discussed with a number of gas turbine experts and the characteristics of both U.S. and European units currently available were examined. The manufacturers of units that appeared to be most attractive were then contacted for further information. It was particularly important that a unit be chosen that would lend itself to installation in a closed cycle without appreciable modification. This in turn meant that units in which the combustion chamber was mounted externally to the basic cylindrical envelope of the gas turbine were the principal contenders. Only a few such units in the size range desired — 300 to 1000 kW(e) — could be found. Data for representative performance characteristics of these units were then obtained and used for parametric studies. Two sets of such studies were carried out, one for actual units that have been built and a second set for the somewhat higher performance characteristics of units under development but not yet on the market. For the latter, data presented in Ref. 2 on the compressor and turbine efficiencies to be expected were employed.

All of the turbines in the proper size range that are currently available were designed for operation in a simple open cycle and hence make use of a relatively high pressure ratio, i.e., between 6 to 1 and 12 to 1. However, our current parametric studies showed the same results as a host of earlier studies by other groups; namely, that, for a closed cycle with recuperation, the optimum pressure ratio is between 3 and 4 to 1. The pressure ratio obtainable from any given engine, of course, varies with the speed so that a production engine could be operated at a reduced speed to give a lower pressure ratio. This would require a change in the gear box between the turbine and generator, but this is a relatively straightforward step. It has the important implication that, if a 12 to 1 pressure ratio engine is operated with a pressure ratio of 4 to 1 but in a system in which the pressure at the inlet to the compressor is raised to 3 atmospheres, the compressor discharge pressure will be the same as for the standard open cycle with a pressure ratio of 12 to 1. This in turn indicates that the strength of the casings and other elements in the system should be adequate for operation in a pressurized system.

The principal problems envisioned if a gas turbine designed for open cycle operation is employed in a closed cycle system are possible difficulties with thrust bearing loads stemming from axial pressure imbalances and possible difficulties with a gradual buildup of a coke deposit on the heat transfer surfaces in the recuperator caused by trace amounts of oil leakage from the bearings into the compressor inlet air stream. If it should prove difficult to keep this sort of oil leakage to an acceptable level, it may prove possible to burn out the coke deposits by raising the operating temperature of the recuperator from time to time. In this connection it should be noted that coke deposits in some of the "self-cleaning" ovens on domestic electric ranges are cleaned out by an hour or so of operation at 575°F.

Rotary Regenerators vs. Fixed Matrix Recuperators

Central stations commonly employ rotary regenerators for preheating the combustion air. These consist of a rotating heat transfer matrix with the hot stack gas flowing through one portion where the heat is transferred from the gas to the solid matrix. The hot solid is then carried by rotation of the matrix into the cold fluid where it gives up its heat to the air supplied to the furnace. This gives a substantially less expensive heat exchanger than conventional tubular or plate fin heat exchangers in which the two fluid streams are on opposite sides of a common wall. The principal difficulty with the rotating regenerator is leakage from the high pressure stream to the lower pressure stream. This is not serious if the pressure differential is small as is the case for the regenerator in the combustion gas stream of Fig. 5.6. However, the use of such a unit to exchange heat from the turbine exhaust stream to the compressor discharge stream is likely to lead to substantial air leakage losses between the two because it is difficult to maintain a good seal across the faces of the rotating drum, particularly in view of thermal expansion problems. For this reason our studies to date have been predicated on the use of a conventional tubular heat transfer matrix for the recuperator rather than a rotary generator for the heat transfer step between the turbine air discharge and the compressor air discharge. A rotary generator has been used, however, for preheating the combustion air because the pressure differential there is small (see Fig. 5.6).

Choice of Temperatures

As indicated in the section on fluidized bed coal combustion systems, sulfur removal considerations limit one's choice of fluidized bed operating temperature to the range from 810 to 930°C (1500 to 1700°F). Inasmuch as the turbine performance improves with increasing temperature up to the point at which the turbine life is adversely affected by higher temperatures — ∿816°C (1500°F) — it was decided to carry out the design studies on the basis of an 816°C (1500°F) turbine inlet temperature with a fluidized bed operating temperature of 900°C (1650°F). With an air pressure of 12 atm inside the tubes and the good heat transfer coefficient characteristic of the fluidized bed side, this gives an adequate temperature differential between the bed and the heated air stream to keep the surface area requirements of the heat transfer matrix in the fluidized bed to a reasonable level.

Previous studies in the MIUS program indicate that the waste heat recovery unit should be operated at a temperature of about 120°C (250°F). For good cycle efficiency it is desirable to reduce the temperature of the air entering the compressor in the closed cycle to as low a temperature as possible consistent with the cost of the cooler. Scouting calculations indicated that for a standard outside air or cooling water temperature of 15°C (60°F), a 27°C (90°F) compressor inlet temperature represents a good compromise. It should be noted in connection with the design of the cooler that not all of the heat rejected in the cooler would be wasted; a portion of it can be used for heating the domestic hot water which is normally supplied at a temperature of 65°C (150°F). It could also be used as a feed heater for the main waste heat recovery unit. However, for purposes of the initial study credit was taken only for its use for heating domestic hot water.

The temperature of the gas discharged to the stack was taken to be 150°C (300°F) in order to assure that condensation of moisture in the gases coupled with SO_2 (which would dissolve in the condensed moisture) would not lead to serious attack of the material in the stack.

System Pressure Loss Components

A range of pressure losses between the compressor and turbine was considered in the parametric studies. The approach taken was to consider three cases, i.e., turbine pressure ratios equal to 85, 90, 95,

and 100% of the compressor pressure ratio. This gave system pressure losses equivalent to 15, 10, 5, and 0% of the pressure ratio.

Waste Heat Recovery

In that portion of the analyses concerned with waste heat recovery the earlier calculations were carried out assuming the use of boilers that would produce 250°F steam. This is an excellent way to supply heat to an absorption refrigeration system, but for building heating it is generally better to employ a hot water circulation system. Analyses indicated that when all factors are considered it will probably prove best to design the waste heat recovery system to yield 250°F hot water. Inasmuch as this yielded little difference in the cost of the heat recovery units and made possible both a reduction in the cost of the cooler and a more favorable distribution of heat recovery between the domestic hot water system and the building heating and air conditioning, the analyses for the closed cycles were made for waste heat recovery with water heaters rather than water boilers. This eliminates the need for a vapor separator, simplifies the design of the heat exchanger, makes it easy to store thermal energy as superheated water to accommodate diurnal variations in the ratio of heat to electrical loads, and provides greater flexibility in control of the entire system to accommodate seasonal variations in the load distribution.

Effects of Recuperators, Regenerators, Intercooling, and Reheat

The ideal cycle efficiencies for the eight cycles considered have been plotted in Fig. 5.9 as a function of pressure ratio. In all cases, the calculations for Fig. 5.9 were for a single set of design conditions, i.e., a turbine inlet temperature of 1500°F, an 80°F compressor inlet temperature, a 90% recuperator effectiveness, a 10% system pressure loss, and turbine and compressor efficiencies of 87% and 84% respectively. Note that a pronounced improvement in cycle efficiency is obtained when a recuperator is added to the cycle, and that the peak cycle efficiency is obtained with a relatively low pressure ratio for the recuperated as opposed to the non-recuperated cycles. Note, too, that adding a regenerator in going from the cycle of Fig. 5.5 to that of Fig. 5.6 yields a pronounced gain in efficiency.

ORNL DWG. 74-9144

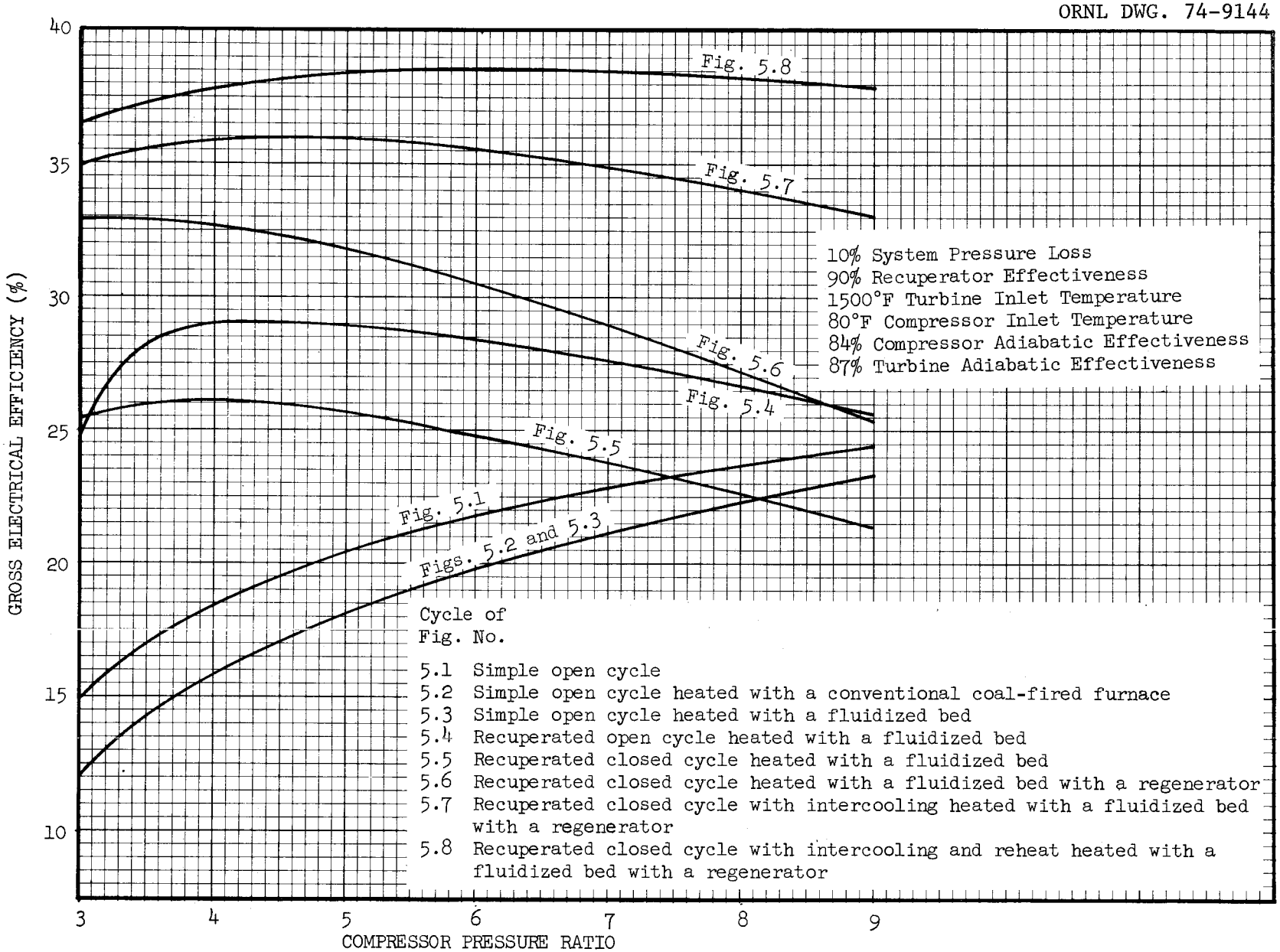

Fig. 5.9. Comparison of the cycle efficiency of representative gas turbine systems.

Addition of intercooling and reheating also improves the thermal efficiency but relatively less than for the other changes, and the extra costs would be substantial. Further, the additional pressure drop penalties associated with intercooling and/or aftercooling were not included; these would reduce the apparent advantage in efficiency. As a consequence, it appears that the cycle of Fig. 5.6 with a recuperator, economizer, and regenerator represents a good compromise between cycle efficiency and capital cost.

Closed vs Open Cycles

There is no difference in efficiency between ideal open and closed cycles that are otherwise similar except that the introduction of a cooler causes both an additional pressure drop in the system and an increase in the compressor inlet temperature. The former loss can be made almost negligible, but the latter is appreciable. Figure 5.10 shows this effect for a cycle with a recuperator and regenerator. Similar curves are given in Figs. 5.11 and 5.12 for cycles with intercooling and reheat.

As indicated above, in actual cycles with commercially available engines there is a pronounced loss in efficiency in going from full load to part-load, primarily because this requires a reduction in the turbine inlet temperature. It was primarily for this reason that the closed cycle was considered for MIUS applications. However, a further major advantage to the closed cycle was found to be the pronounced reduction in the cost of the heat exchangers that becomes possible if the closed cycle system is pressurized.

Effects of Pressure Ratio on Net Work Output

The curves for cycle efficiency in Fig. 5.10 favor a compression ratio between 3 and 4. However, another important factor is the net work output per pound of air; this parameter has been plotted as a function of pressure ratio in Fig. 5.13. These curves indicate that increasing the pressure ratio from 3.5 to 6 would yield an increase in work output of 15% from a given turbine-compressor unit. However, going to a pressurized closed cycle system may increase the output of an existing machine to the limits of the load carrying ability of the shaft, particularly when allowances are made for the effects of derating the speed to reduce the pressure ratio.

ORNL DWG. 74-9145

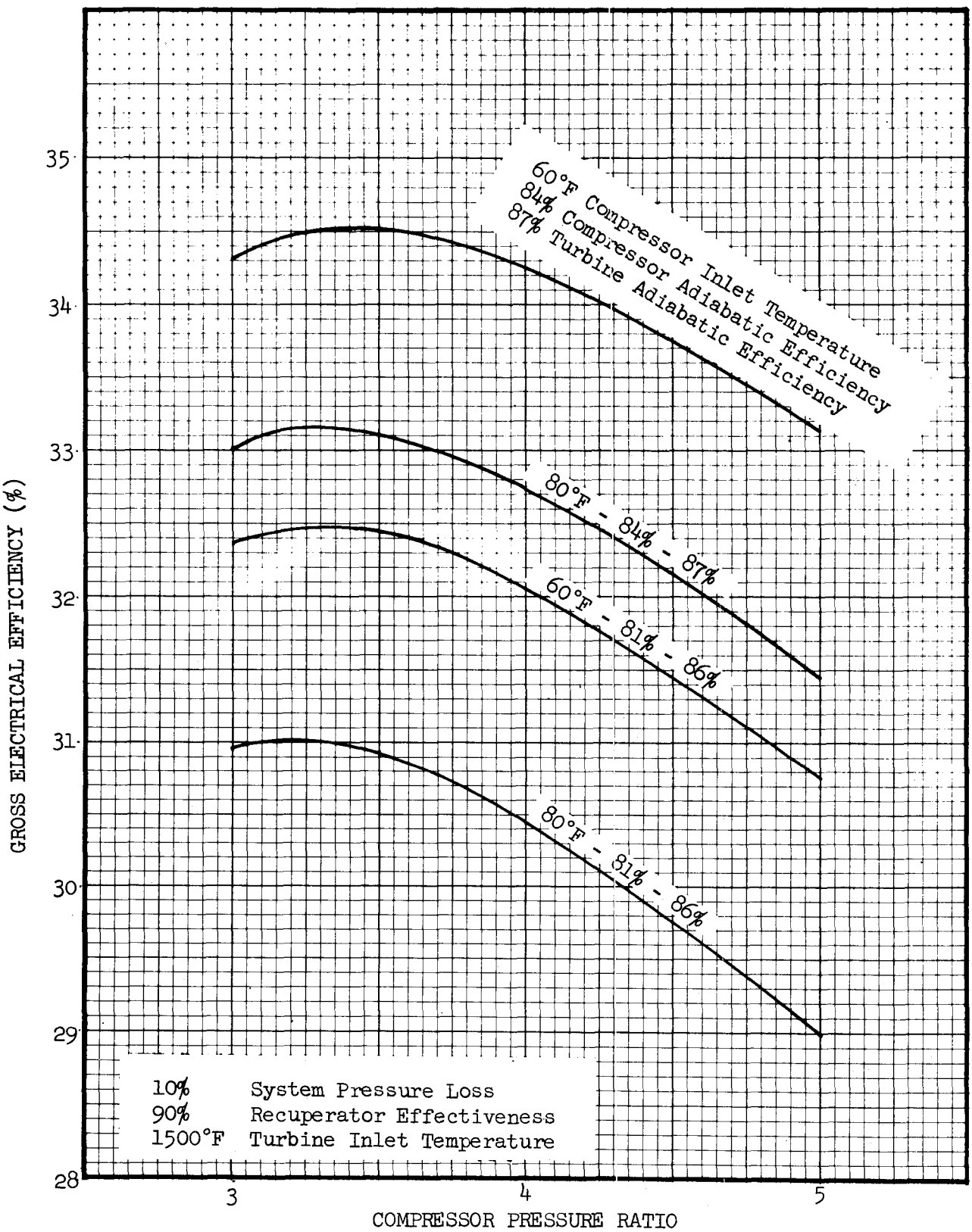

Fig. 5.10. Effects of component efficiency and compressor inlet temperature upon the gross electrical efficiency for a regenerative cycle without intercooling or reheat.

ORNL DWG. 76-2664

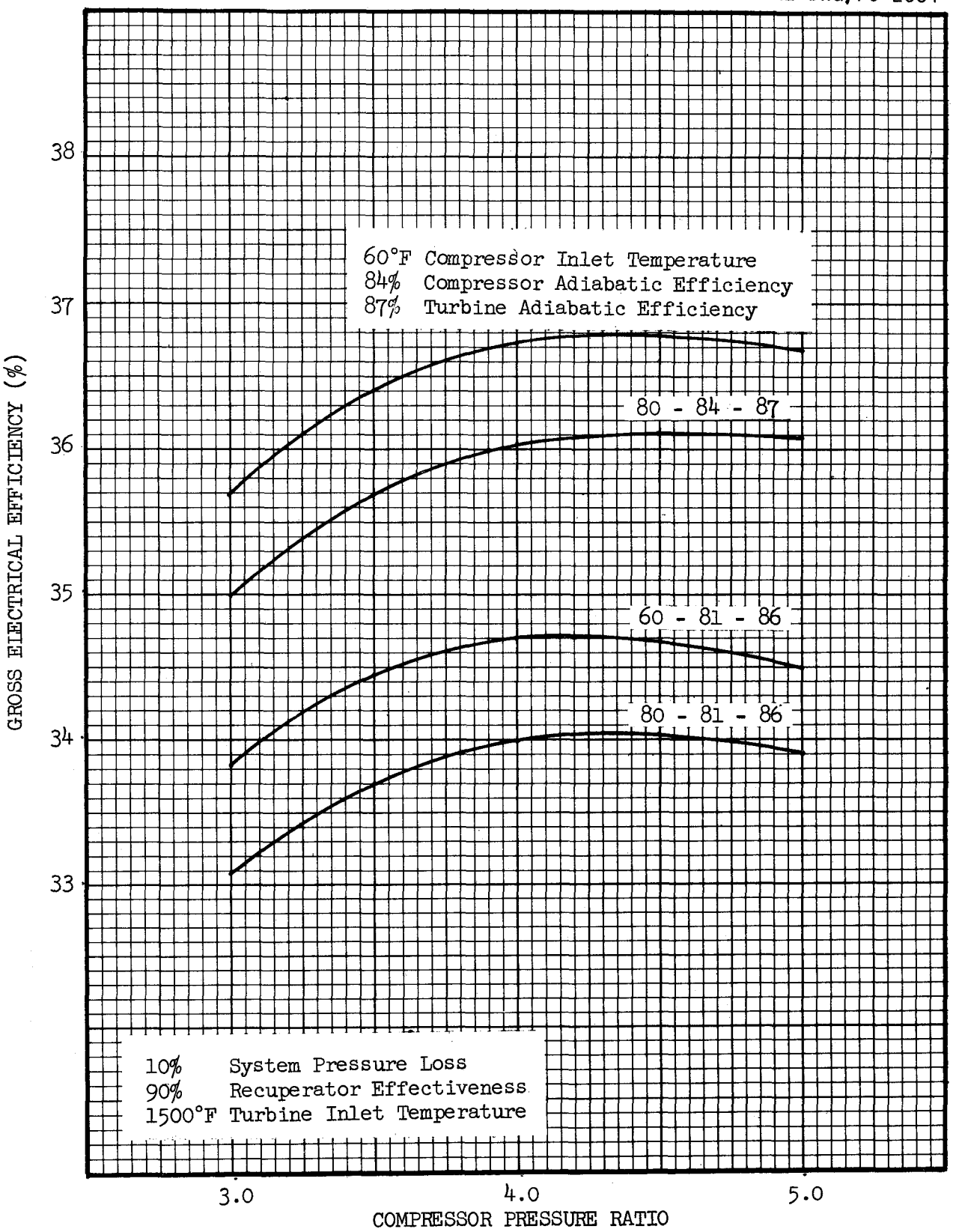

Fig. 5.11. Effect of component efficiency and compressor inlet temperature upon the gross electrical efficiency for a regenerative cycle with intercooling.

ORNL DWG. 76-2665

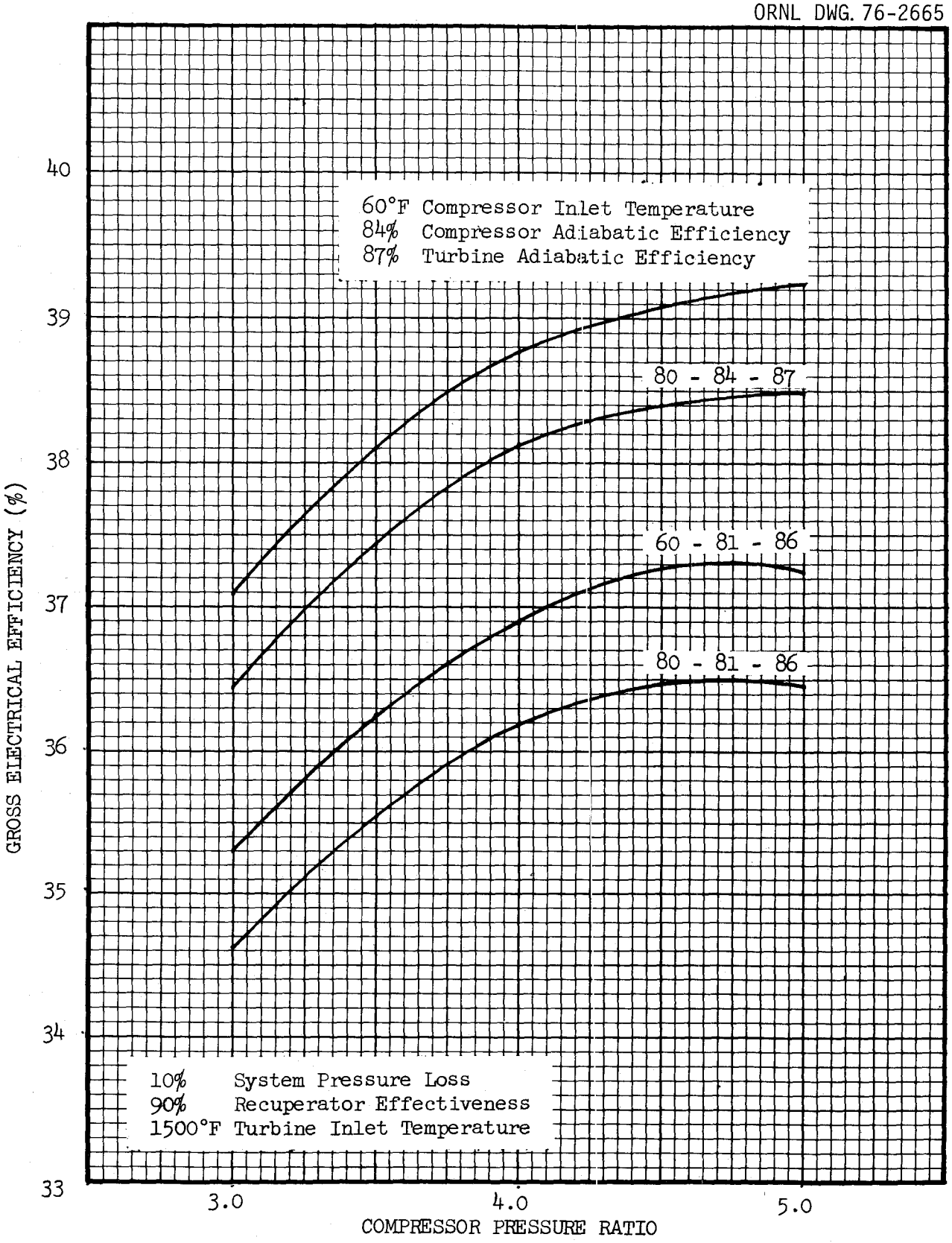

Fig. 5.12. Effect of component efficiency and compressor inlet temperature upon the gross electrical efficiency for a regenerative cycle with both intercooling and reheat.

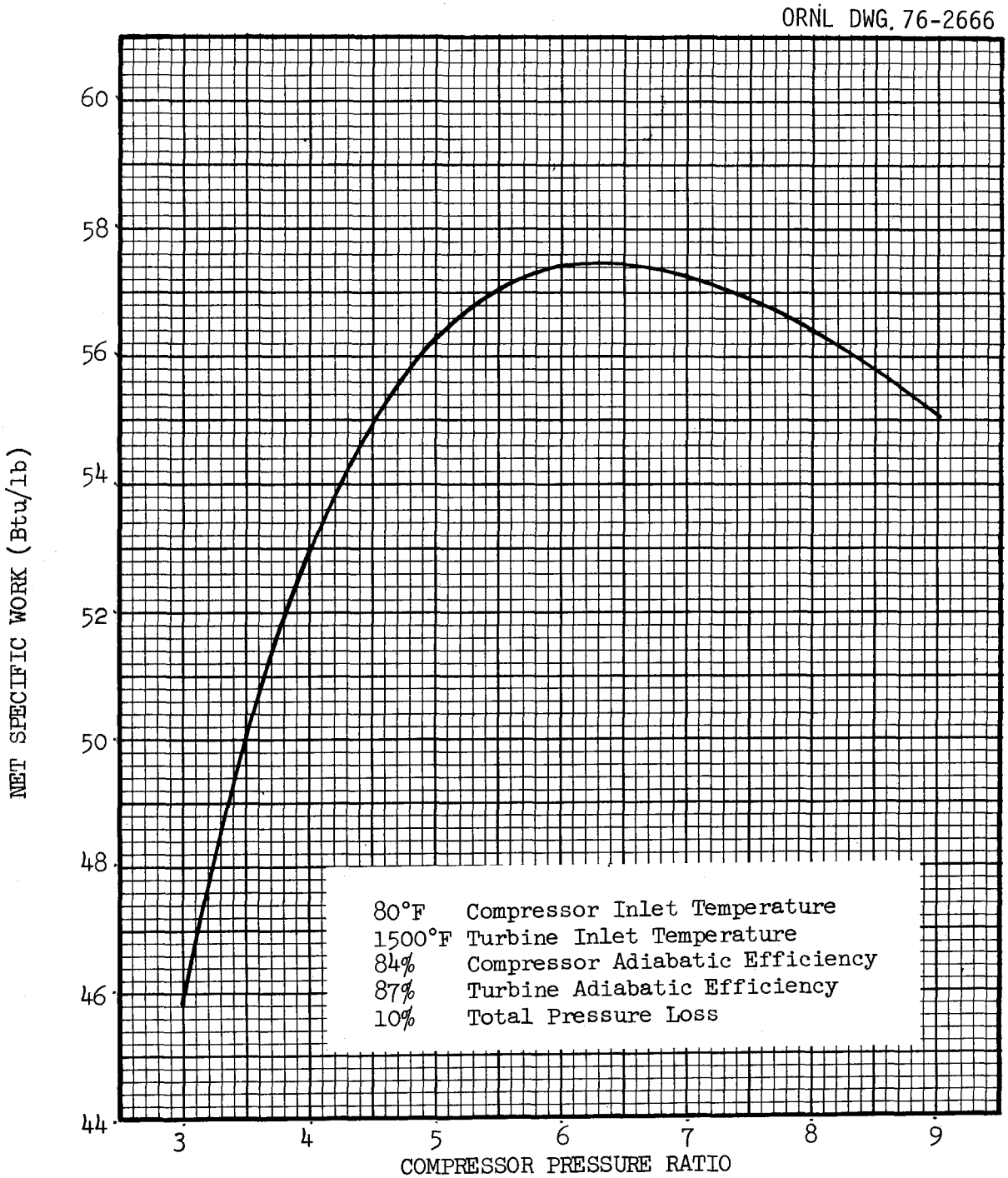

Fig. 5.13. Effects of pressure ratio on the net work output per pound of air from a recuperated cycle with no allowances for auxiliaries.

Effects of Recuperator Effectiveness and System Pressure Losses

Scouting calculations indicated that within the restraints outlined above the most important factors affecting the cycle efficiency are the pressure ratio, the recuperator effectiveness, and the pressure losses in the system components between the compressor and the turbine. The effects of these parameters are shown in Figs. 5.14 to 5.25 for the three cycles of Figs. 5.6, 5.7, and 5.8. Separate curves are given for each combination of cycle, compressor inlet temperature, and set of turbine and compressor efficiencies.

Effects of Design Parameters on Costs

It is clear from the preceding section that a closed cycle with a recuperator and regenerator would give a system that would convert at least 25%, and possibly over 30%, of the energy in the fuel into electricity if the recuperator effectiveness is high and the system pressure drop is low. To achieve these values it is necessary to employ large heat exchangers. Thus, the question becomes one of balancing the increasing capital cost of the large heat exchangers against the increases in thermal efficiency. This involves not only many subtle compromises in heat exchanger design but also problems in cost estimation and questions of overall system design. In carrying out the study the many compromises required were arrived at by a process of iteration with extensive feedback between the performance analysis covered in this chapter and the system design studies covered in the next chapter. In preparing this report the details of design decisions, compromises, and procedures were placed in the next chapter on system design and the design charts evolved were placed in Appendix A. That work was the basis for the analysis of the relations between heat exchanger costs and cycle performance presented in this section. Suffice it to say here that in choosing representative heat transfer matrices for the various heat exchangers in the system, the problems were discussed with a number of vendors. It was then decided that, for reference design purposes, it would be best to make use of simple round tube heat transfer matrices for the recuperator, economizer, and fluidized bed. For the waste heat boiler and cooler it was decided to use 1 in. diameter round tubes with circular fins.

ORNL DWG 76-2667

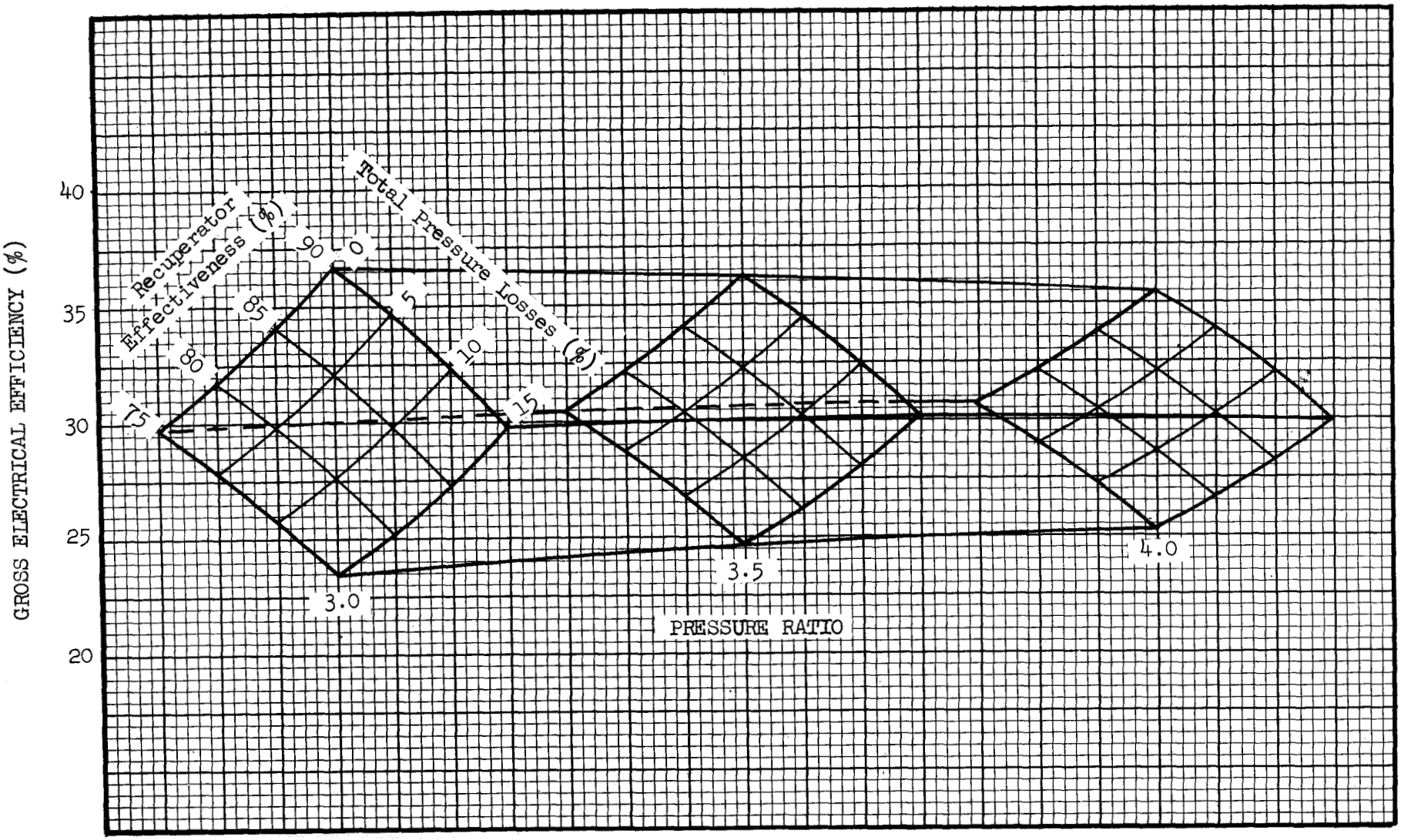

Fig. 5.14. Gross electrical efficiency for a regenerative cycle without intercooling or reheat as a function of the recuperator effectiveness, the system total pressure losses, and the compressor pressure ratio at a compressor inlet temperature of 60°F, a compressor adiabatic efficiency of 81%, a turbine inlet temperature of 1500°F, and a turbine adiabatic efficiency of 86%.

ORNL DWG 76-2668

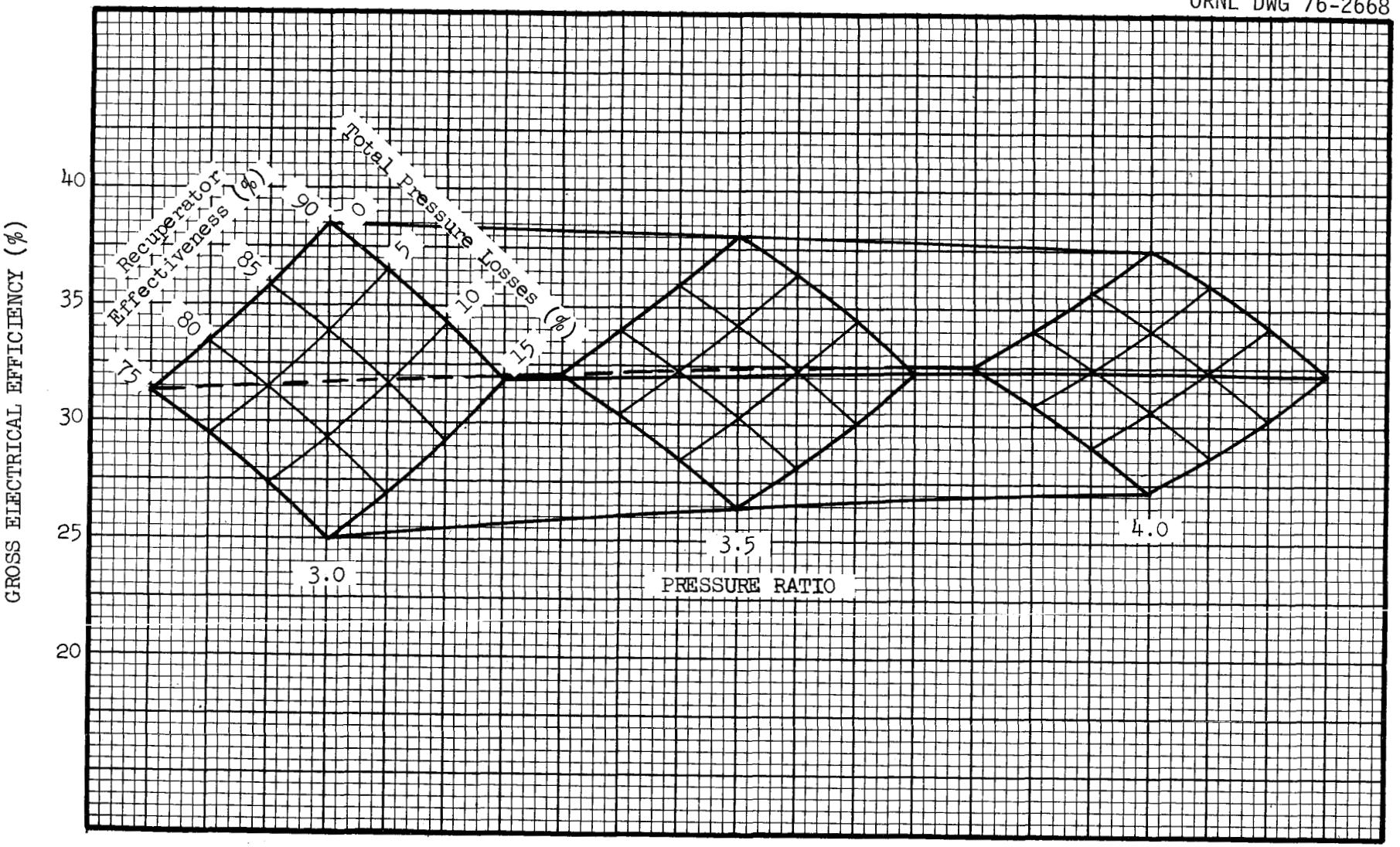

Fig. 5.15. Gross electrical efficiency for a regenerative cycle without intercooling or reheat as a function of the recuperator effectiveness, the system total pressure losses, and the compressor pressure ratio at a compressor inlet temperature of 60°F, a compressor adiabatic efficiency of 84%, a turbine inlet temperature of 1500°F, and a turbine adiabatic efficiency of 87%.

ORNL DWG 76-2669

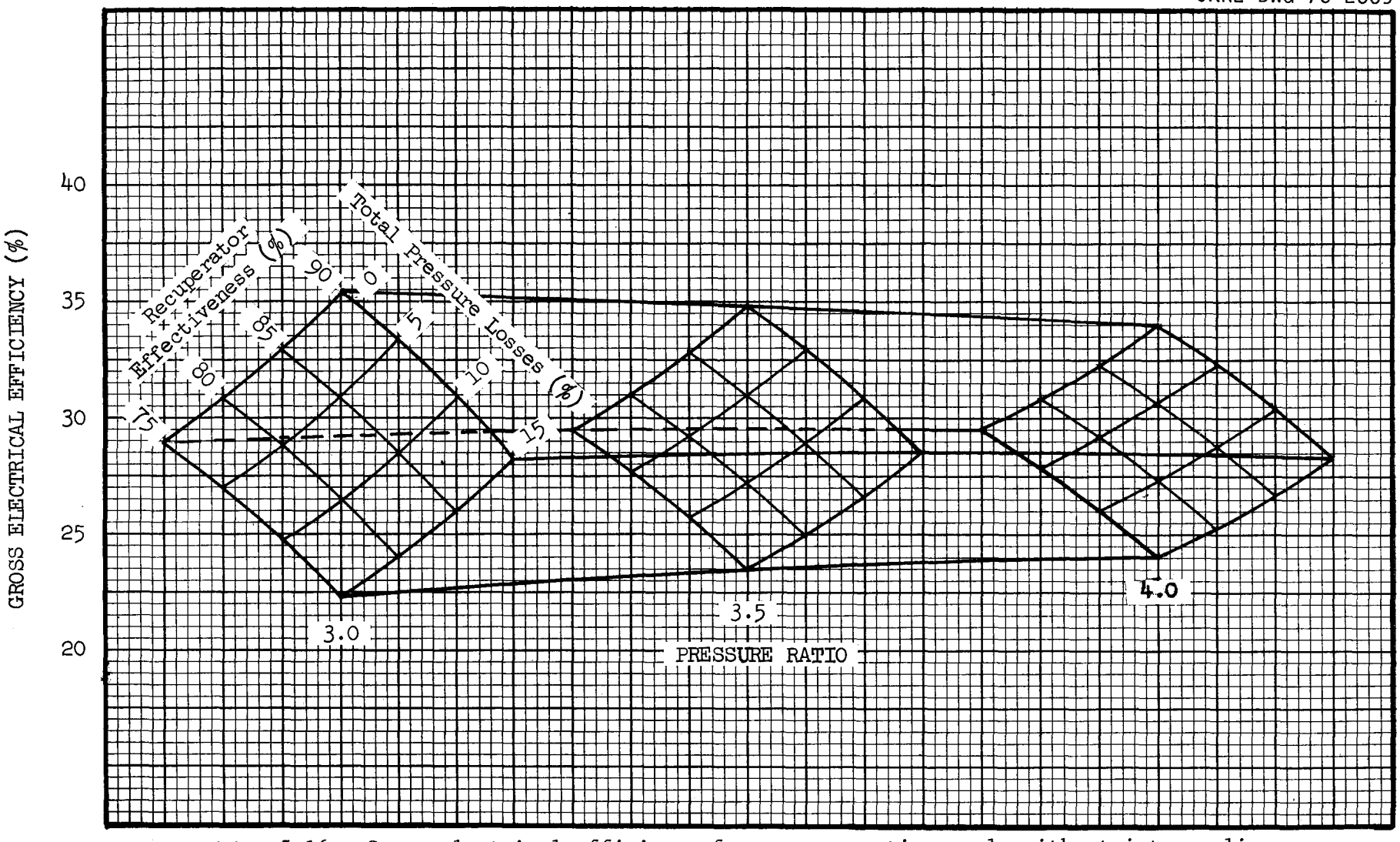

Fig. 5.16. Gross electrical efficiency for a regenerative cycle without intercooling or reheat as a function of the recuperator effectiveness, the system total pressure losses, and the compressor pressure ratio at a compressor inlet temperature of 80°F, a compressor adiabatic efficiency of 81%, a turbine inlet temperature of 1500°F, and a turbine adiabatic efficiency of 86%.

ORNL DWG 76-2670

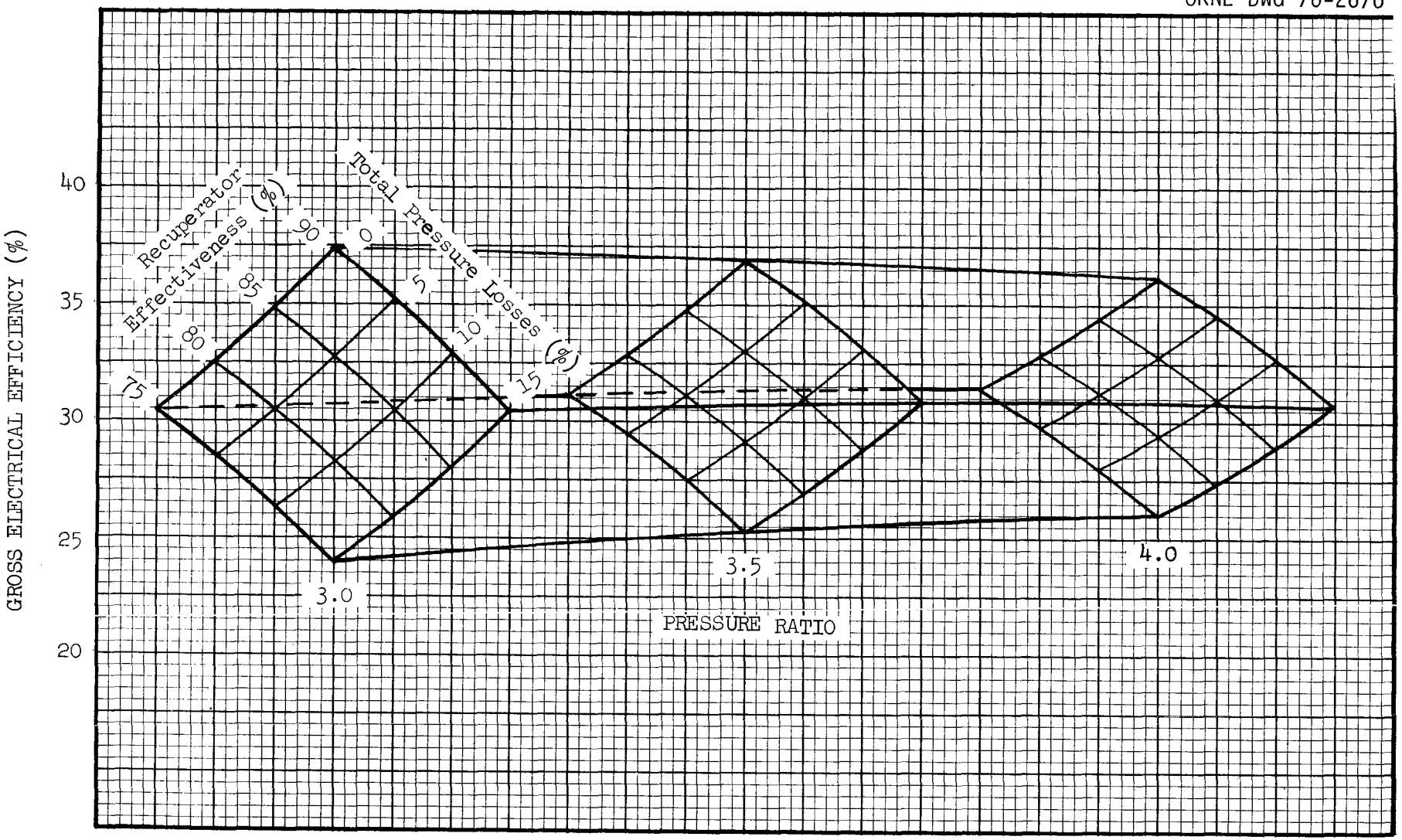

Fig. 5.17. Gross electrical efficiency for a regenerative cycle without intercooling or reheat as a function of the recuperator effectiveness, the system total pressure losses, and the compressor pressure ratio at a compressor inlet temperature of 80°F, a compressor adiabatic efficiency of 84%, a turbine inlet temperature of 1500°F, and a turbine adiabatic efficiency of 87%.

ORNL DWG 76-2671

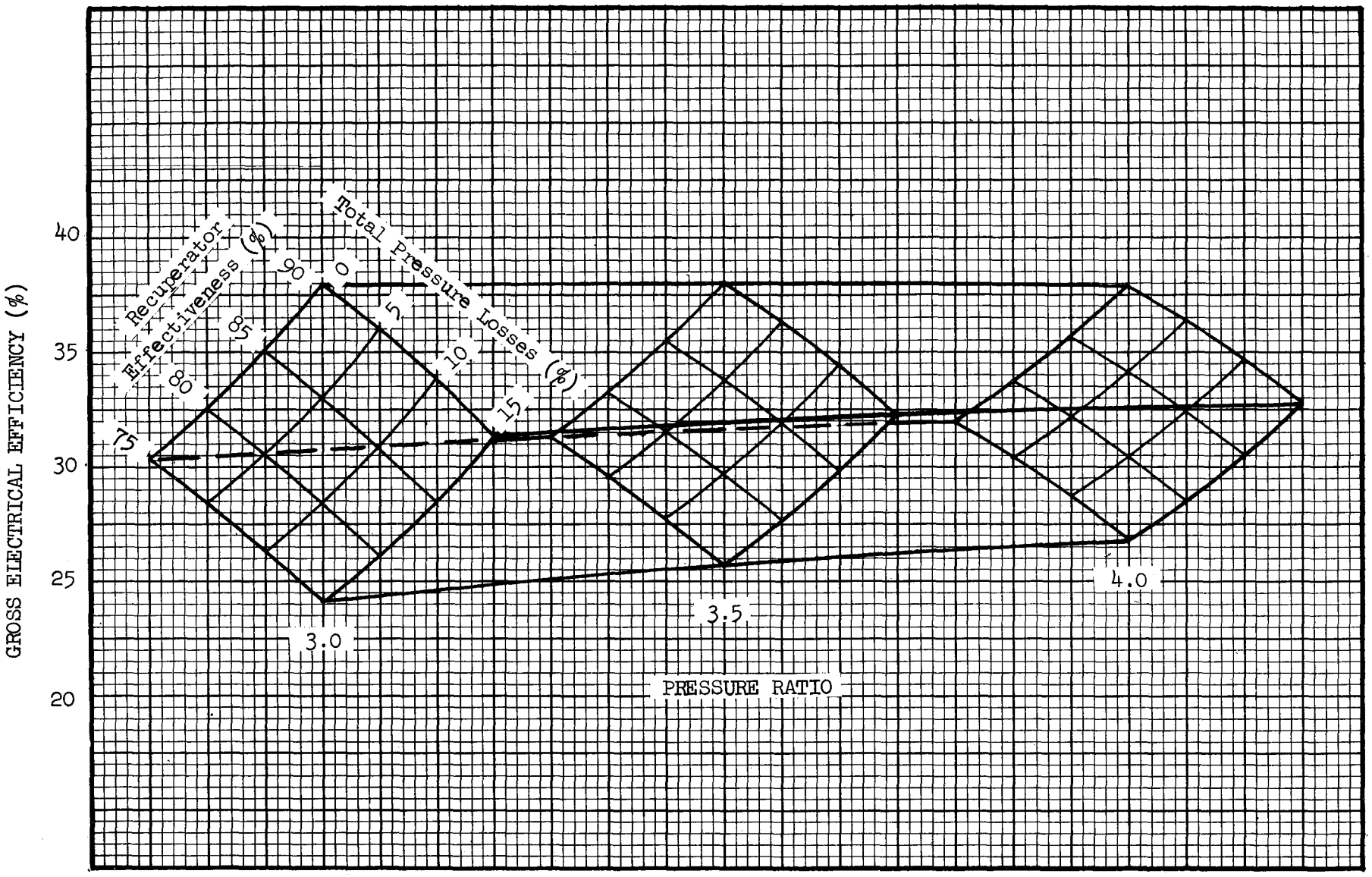

Fig. 5.18. Gross electrical efficiency for intercooled regenerative cycle without reheat as a function of the recuperator effectiveness, the system total pressure losses, and the compressor pressure ratio at a compressor inlet temperature of 60°F, a compressor adiabatic efficiency of 81%, a turbine inlet temperature of 1500°F, and a turbine adiabatic efficiency of 86%.

ORNL DWG 76-2672

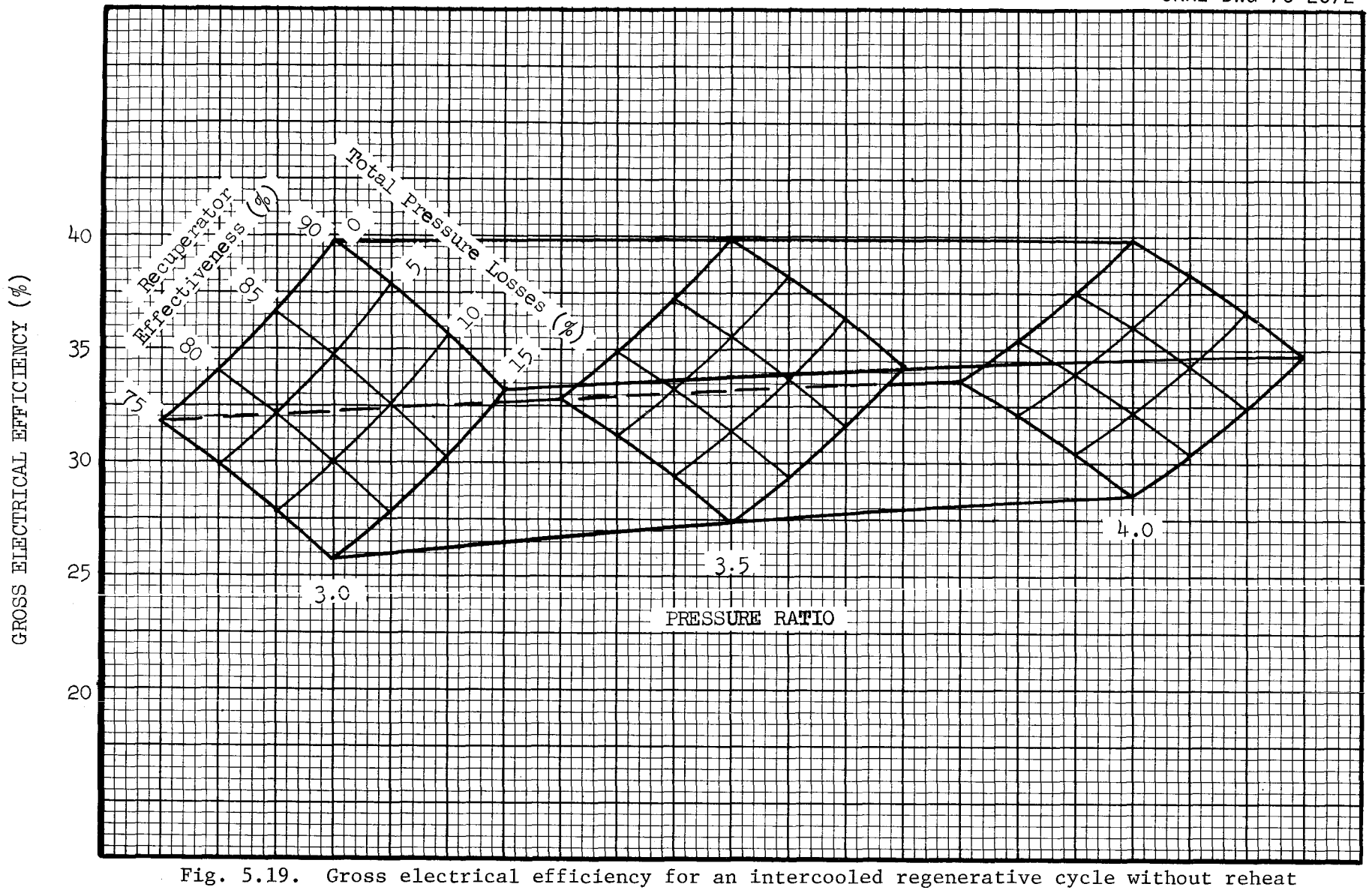

Fig. 5.19. Gross electrical efficiency for an intercooled regenerative cycle without reheat as a function of the recuperator effectiveness, the system total pressure losses, and the compressor pressure ratio at a compressor inlet temperature of 60°F, a compressor adiabatic efficiency of 84%, a turbine inlet temperature of 1500°F, and a turbine adiabatic efficiency of 87%.

ORNL DWG 76-2673

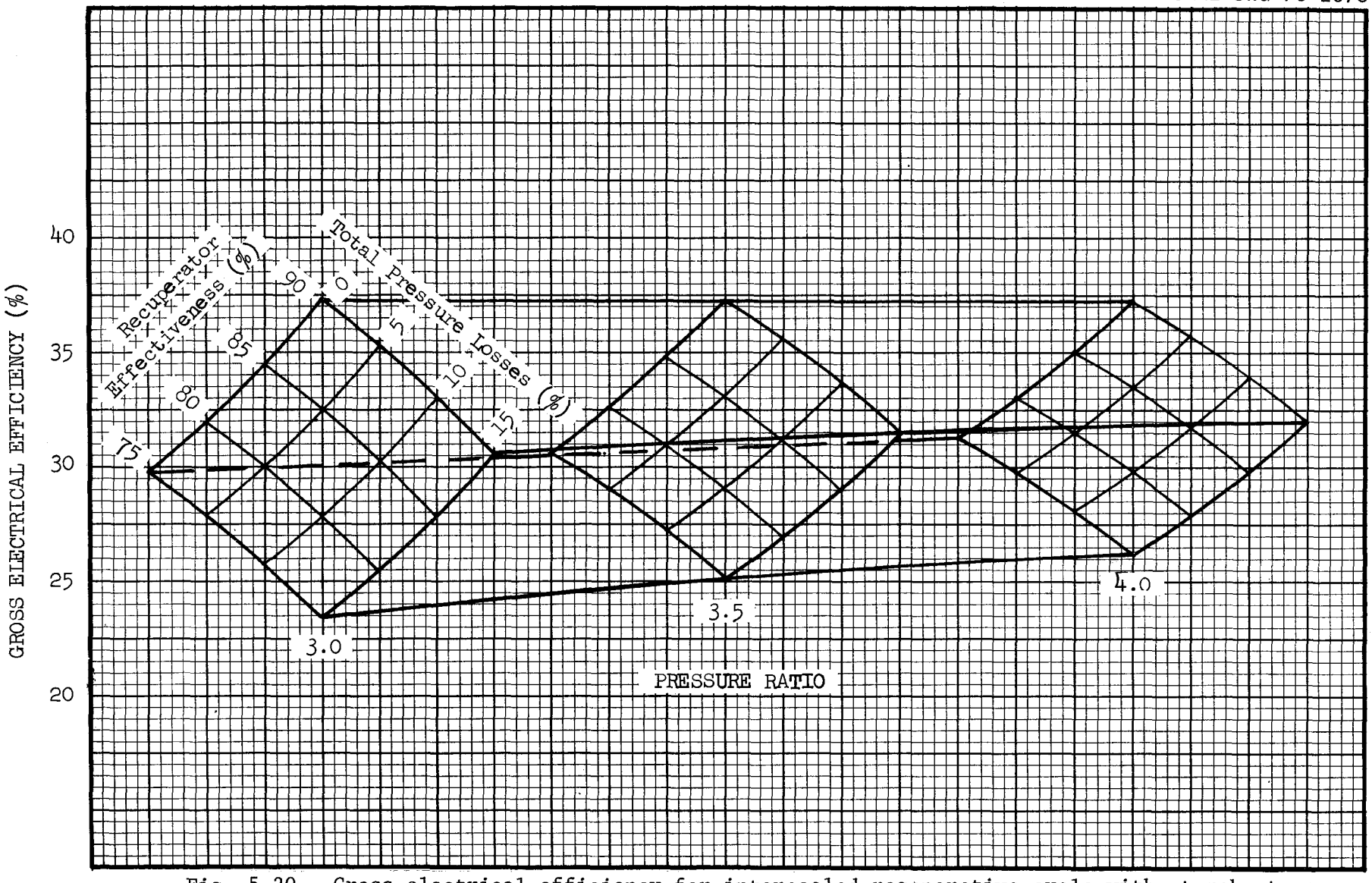

Fig. 5.20. Gross electrical efficiency for intercooled regenerative cycle without reheat as a function of the recuperator effectiveness, the system total pressure losses, and the compressor pressure ratio at a compressor inlet temperature of 80°F, a compressor adiabatic efficiency of 81%, a turbine inlet temperature of 1500°F, and a turbine adiabatic efficiency of 86%.

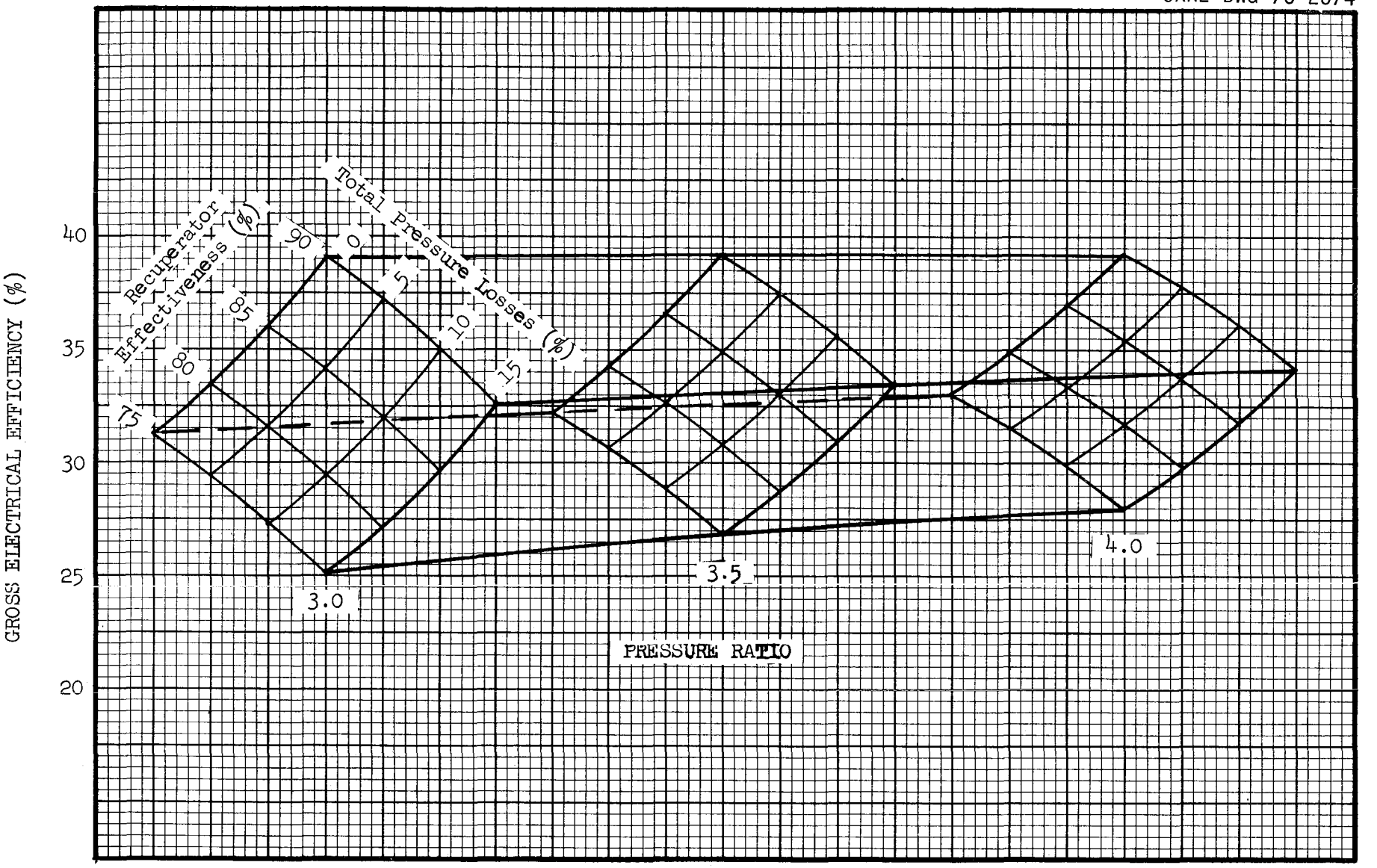

Fig. 5.21. Gross electrical efficiency for an intercooled regenerative cycle without reheat as a function of the recuperator effectiveness, the system total pressure losses, and the compressor pressure ratio at a compressor inlet temperature of 80°F, a compressor adiabatic efficiency of 84%, a turbine inlet temperature of 1500°F, and a turbine adiabatic efficiency of 87%.

ORNL DWG 76-2675

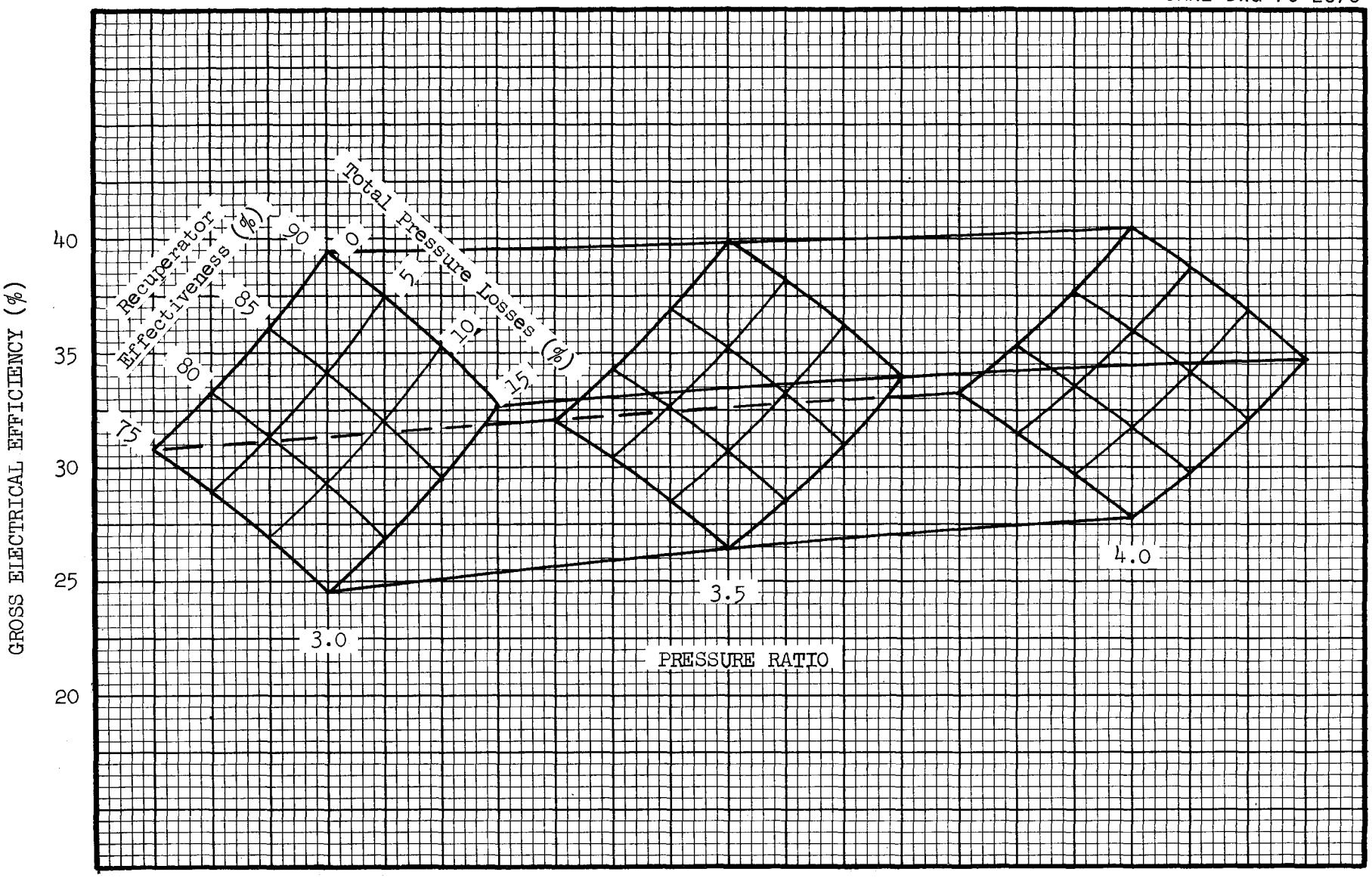

Fig. 5.22. Gross electrical efficiency for an intercooled regenerative cycle with reheat as a function of the recuperator effectiveness, the system total pressure losses, and the compressor pressure ratio at a compressor inlet temperature of 60°F, a compressor adiabatic efficiency of 81%, a turbine inlet temperature of 1500°F, and a turbine adiabatic efficiency of 86%.

ORNL DWG 76-2676

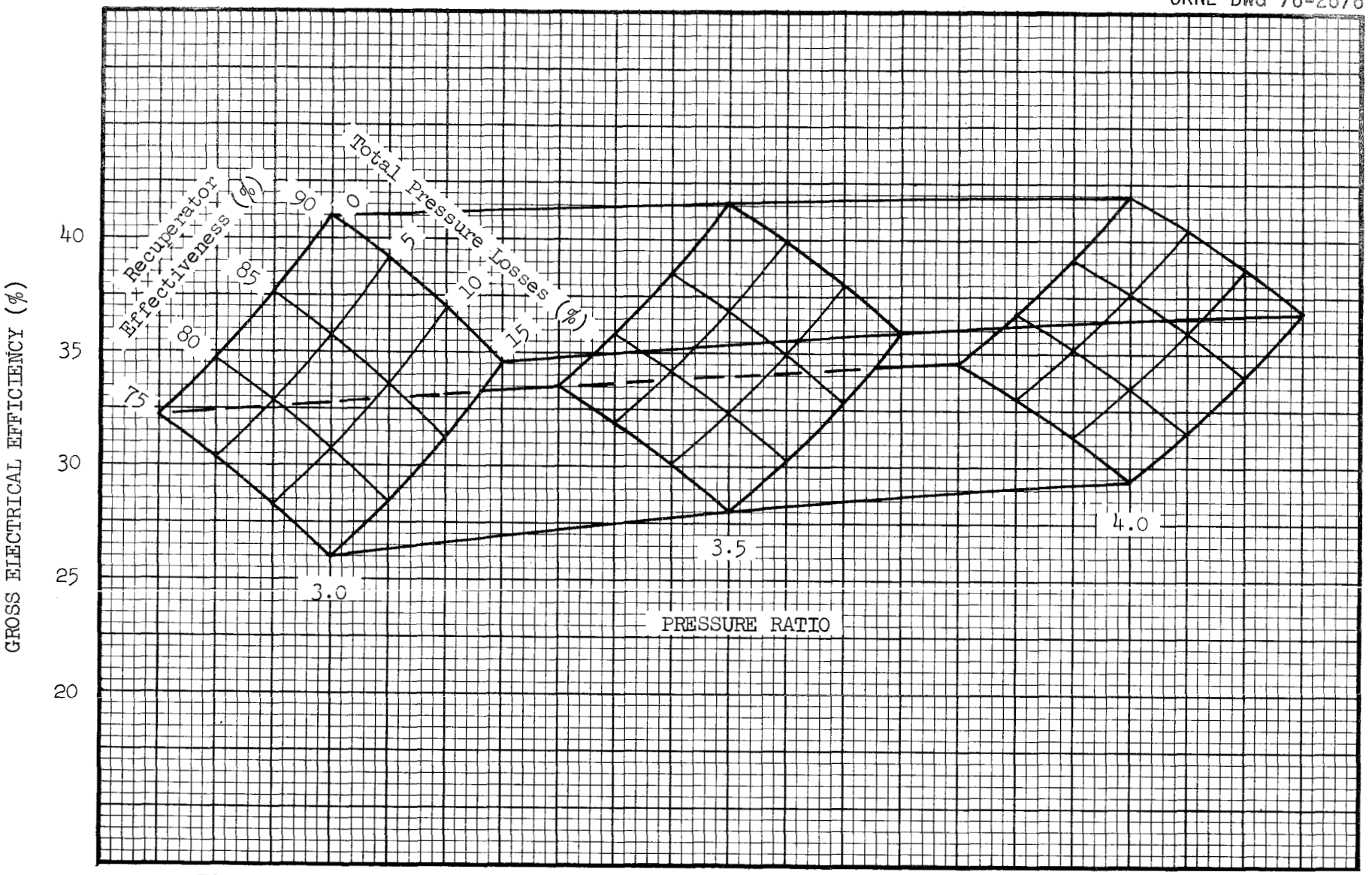

Fig. 5.23. Gross electrical efficiency for an intercooled regenerative cycle with reheat as a function of the recuperator effectiveness, the system total pressure losses, and the compressor pressure ratio at a compressor inlet temperature of 60°F, a compressor adiabatic efficiency of 84%, a turbine inlet temperature of 1500°F, and a turbine adiabatic efficiency of 87%.

ORNL DWG 76-2677

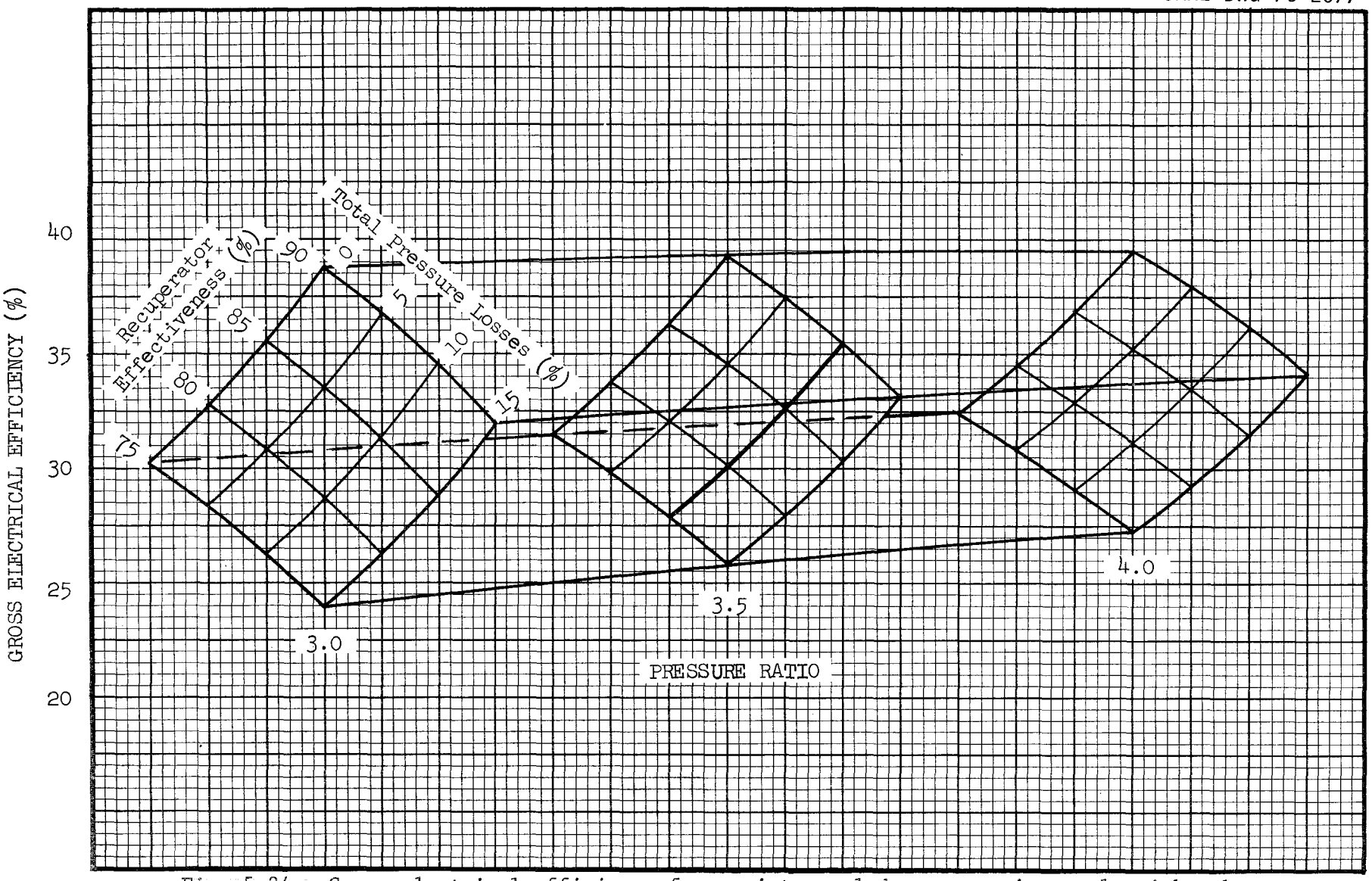

Fig. 5.24. Gross electrical efficiency for an intercooled regenerative cycle with reheat as a function of the recuperator effectiveness, the system total pressure losses, and the compressor pressure ratio at a compressor inlet temperature of 80°F, a compressor adiabatic efficiency of 81%, a turbine inlet temperature of 1500°F, and a turbine adiabatic efficiency of 86%.

ORNL DWG 76-2678

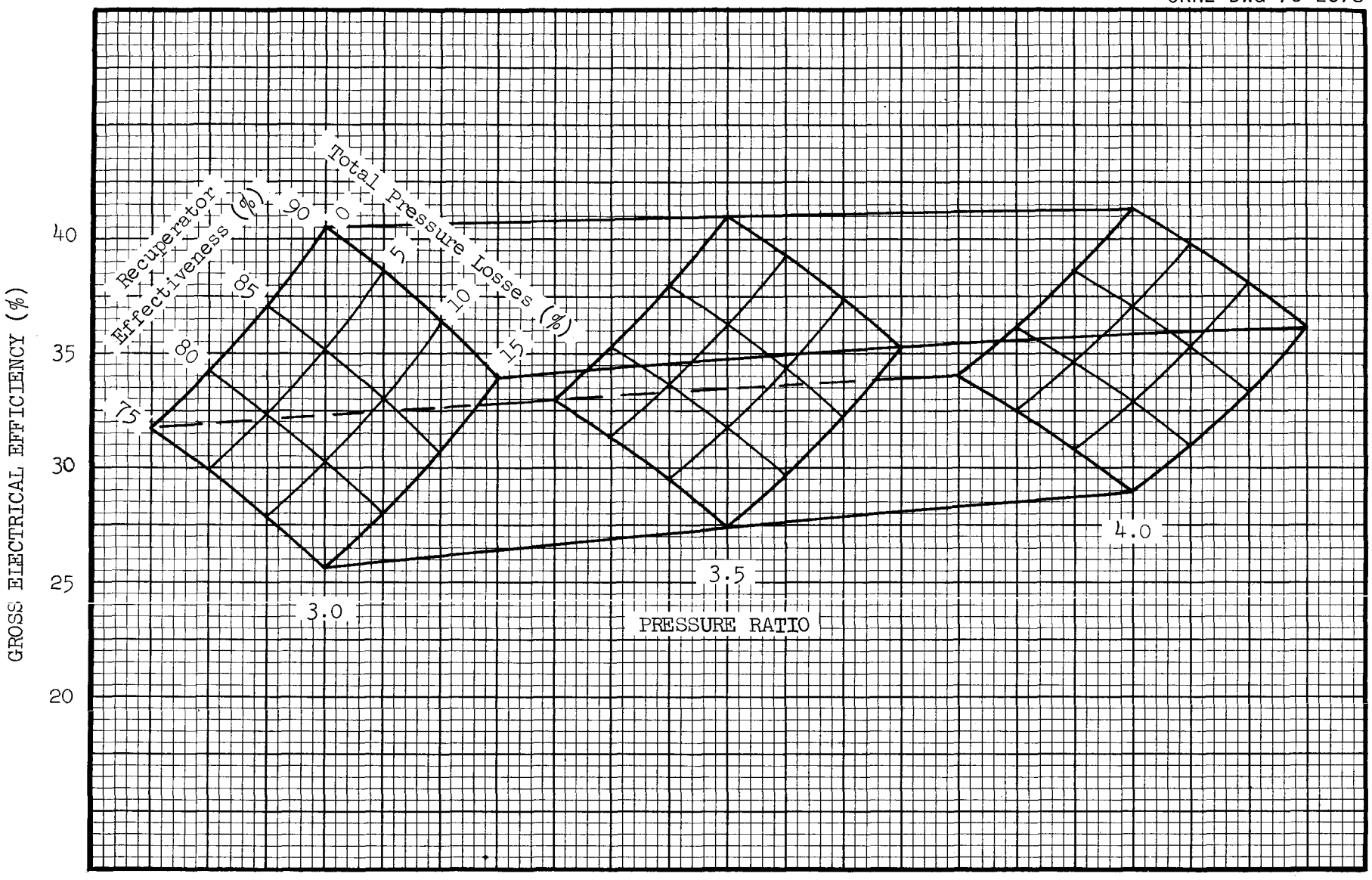

Fig. 5.25. Gross electrical efficiency for an intercooled regenerative cycle with reheat as a function of the recuperator effectiveness, the system total pressure losses, and the compressor pressure ratio at a compressor inlet temperature of 80°F, a compressor adiabatic efficiency of 84%, a turbine inlet temperature of 1500°F, and a turbine adiabatic efficiency of 87%.

Discussions with vendors indicated that the performance of the recuperator might be improved by using a plate fin unit, and that this probably could be obtained at a lower cost than for the tubular reference design. For the initial study, however, the simpler round tube configuration was employed.

General Effects

Good perspective on the overall problem is given by the set of curves in Fig. 5.26 showing the thermal efficiency and heat exchanger costs for a representative system of the type shown in Fig. 5.6 as a function of the design value chosen for the effectiveness of the heat transfer matrix in the recuperator, and the waste heat boiler. Curves are given for three pressure loss ratios, i.e., $\Delta P/P$ = 5, 7.5, and 10%. Note that a good design compromise from the cost and efficiency standpoints is given by designing for heat exchanger effectivenesses of around 85% with a pressure loss ratio of 5 to 7.5%.

Relations Between Heat Exchanger Cost and Cycle Efficiency

In attempting to visualize the effects of design parameters on the two figures of merit of prime interest, i.e., the heat exchanger capital cost and the cycle efficiency it was found helpful to use these quantities as the coordinates for plotting data from the cycle calculations. In these curves the term "Net Electrical Efficiency" was used to mean the efficiency of the idealized cycle with allowances for system pressure losses. No allowances were made for bearing losses, losses in the generator, or power requirements for auxiliaries such as the induced draft fan. These factors would yield an efficiency for an actual plant about three points lower than the net electrical efficiency as defined here.

Effects of Recuperator Effectiveness. The effects of recuperator effectiveness and system pressure losses are shown in Fig. 5.27 for the cycle of Fig. 5.6. These curves show that the cycle efficiency can be increased markedly by reducing the system pressure losses down to the 5% to 7.5% range with little effect on the heat exchanger costs. Further, increasing the recuperator effectiveness up to 90% gives a pronounced

ORNL DWG. 74-4767

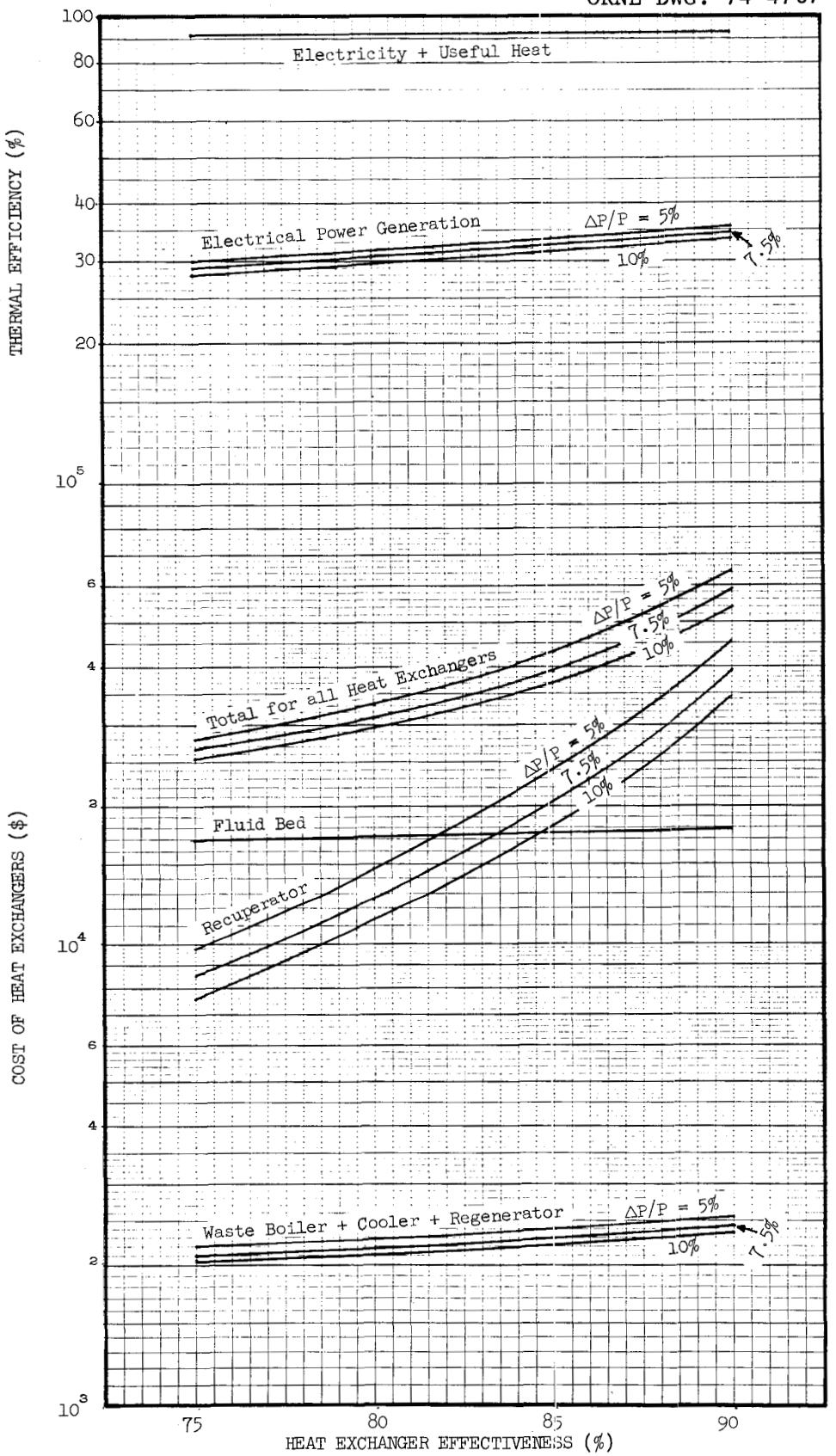

Fig. 5.26. Effects of heat exchanger effectiveness in the bed, economizer, recuperator, and waste heat boiler on the cycle efficiency and heat exchanger costs for the cycle of Fig. 5.6 for a pressure ratio of 4:1, compressor and turbine efficiencies of 84 and 87% respectively, and an electrical power output of 600 kW(e).

ORNL DWG. 74-9147

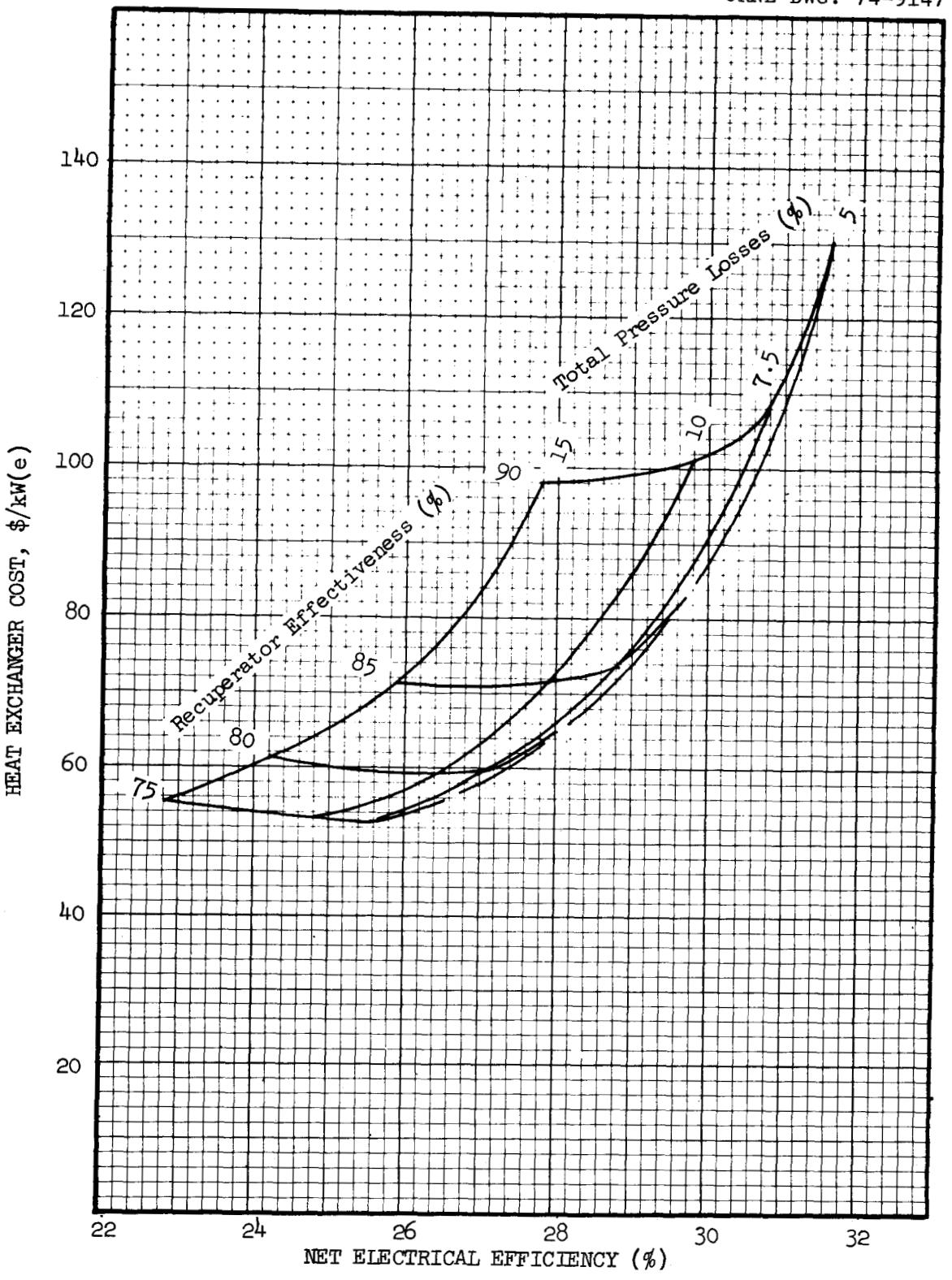

Fig. 5.27. Capital cost of the heat exchangers used in a regenerative cycle without intercooling or reheat as a function of the recuperator effectiveness, the system total pressure losses, and the net electrical efficiency. The system is operated at a compressor pressure ratio of 3.5:1 at an inlet temperature of 80°F, a compressor adiabatic efficiency of 84%, a turbine inlet temperature of 1500°F and a turbine adiabatic efficiency of 87%. Fluidized bed temperature = 1650°F.

improvement in cycle efficiency with only a modest effect on heat exchanger costs. Inspection of the curves favors a recuperator effectiveness of 90% and a system pressure loss of 7.5%.

Effects of Turbine Inlet Temperature. Figure 5.28 indicates that increasing the turbine inlet temperature with a constant fluid bed temperature of 1650°F not only increases the cycle efficiency but also actually reduces the heat exchanger costs. This occurs in spite of the increased heat transfer surface area required in the fluidized bed because the cycle output per pound of air increases, thus reducing the capital charges for the other heat exchangers. This suggested that the effects of turbine inlet temperature should be investigated for a constant temperature difference of 150°F between the turbine air inlet and fluidized bed temperatures. Figure 5.29 shows these effects, and, as expected, indicates a greater cost advantage for the higher turbine inlet temperatures. Figure 5.30 shows the effect of a still different perturbation, i.e., changing the fluidized bed temperature while holding the turbine inlet temperature constant. This has relatively little effect on the costs and none on the cycle efficiency.

Effects of Pressure Ratio. Figure 5.31 shows the effects of compressor pressure ratio on costs and efficiency. This clearly favors the use of a pressure ratio of 3.5:1 for heating effectivenesses ranging from 75% to 90%.

Effects of Compressor Inlet Temperature. Figure 5.32 shows that reducing the compressor inlet temperature from 100°F to 60°F yields an increase in cycle efficiency of about two points and a reduction in heat exchanger costs of about 10%. This emphasizes the advantages of a supply of cold water for the cooler.

Effects of Intercooling and Reheat. Figures 5.27 through 5.32 were prepared for the closed cycle of Fig. 5.6 with a recuperator and a regenerator. The effects of adding intercooling and reheat can be seen by comparing Fig. 5.33 with Fig. 5.27. A further comparison can be made between Figs. 5.30 and 5.34; these indicate that if intercooling and reheat are employed, the pressure ratio should be increased from 3.5:1 to about 5:1.

ORNL DWG 76-2679

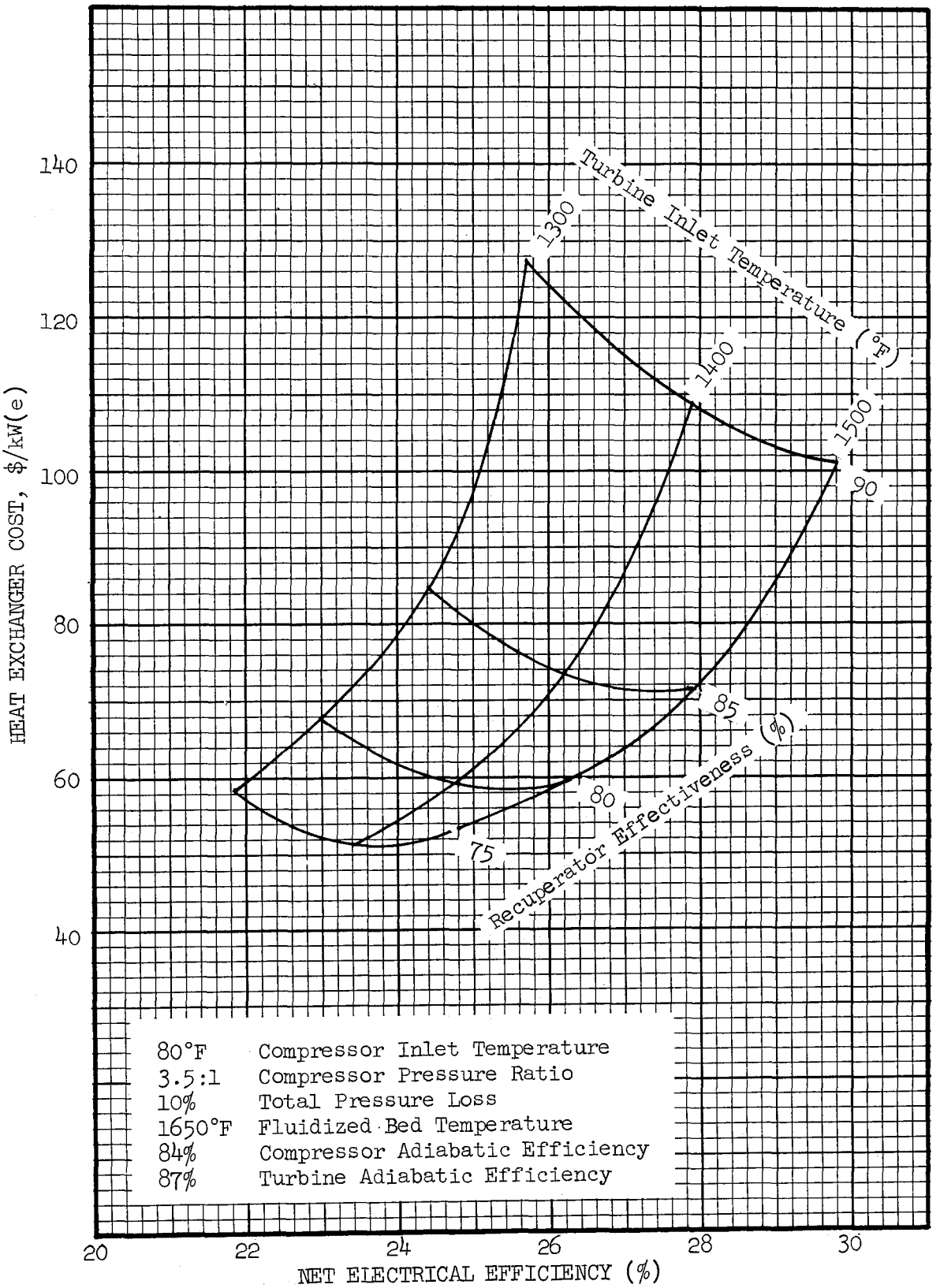

Fig. 5.28. Capital cost of the heat exchangers used in a regenerative cycle without intercooling or reheat as a function of the recuperator effectiveness, the turbine inlet temperature, and the net electrical efficiency.

ORNL DWG 76-2680

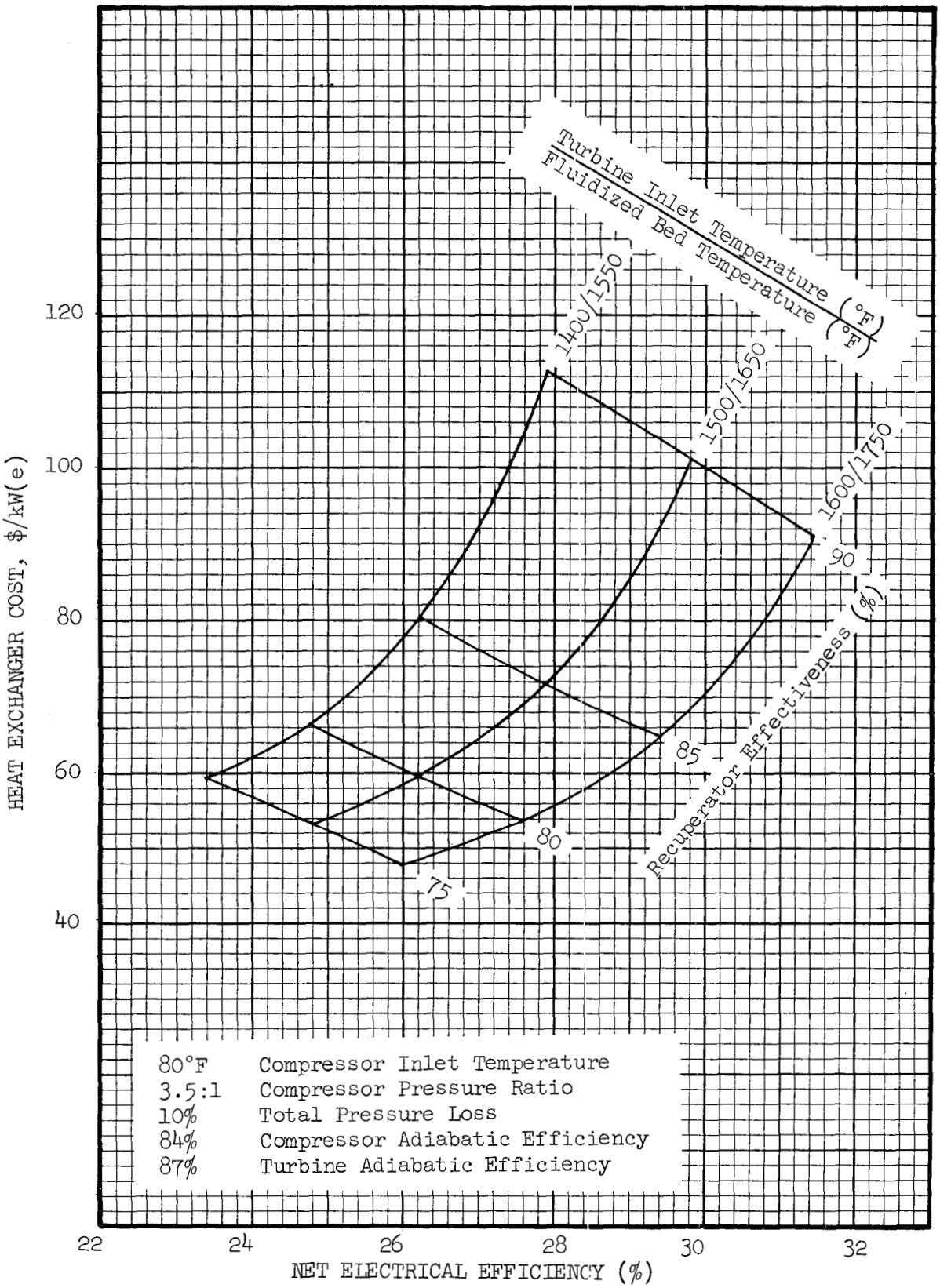

Fig. 5.29. Capital cost of the heat exchangers used in a regenerative cycle without intercooling or reheat as a function of the recuperator effectiveness, the turbine inlet temperature, the fluidized bed temperature, and the net electrical efficiency.

ORNL DWG 76-2681

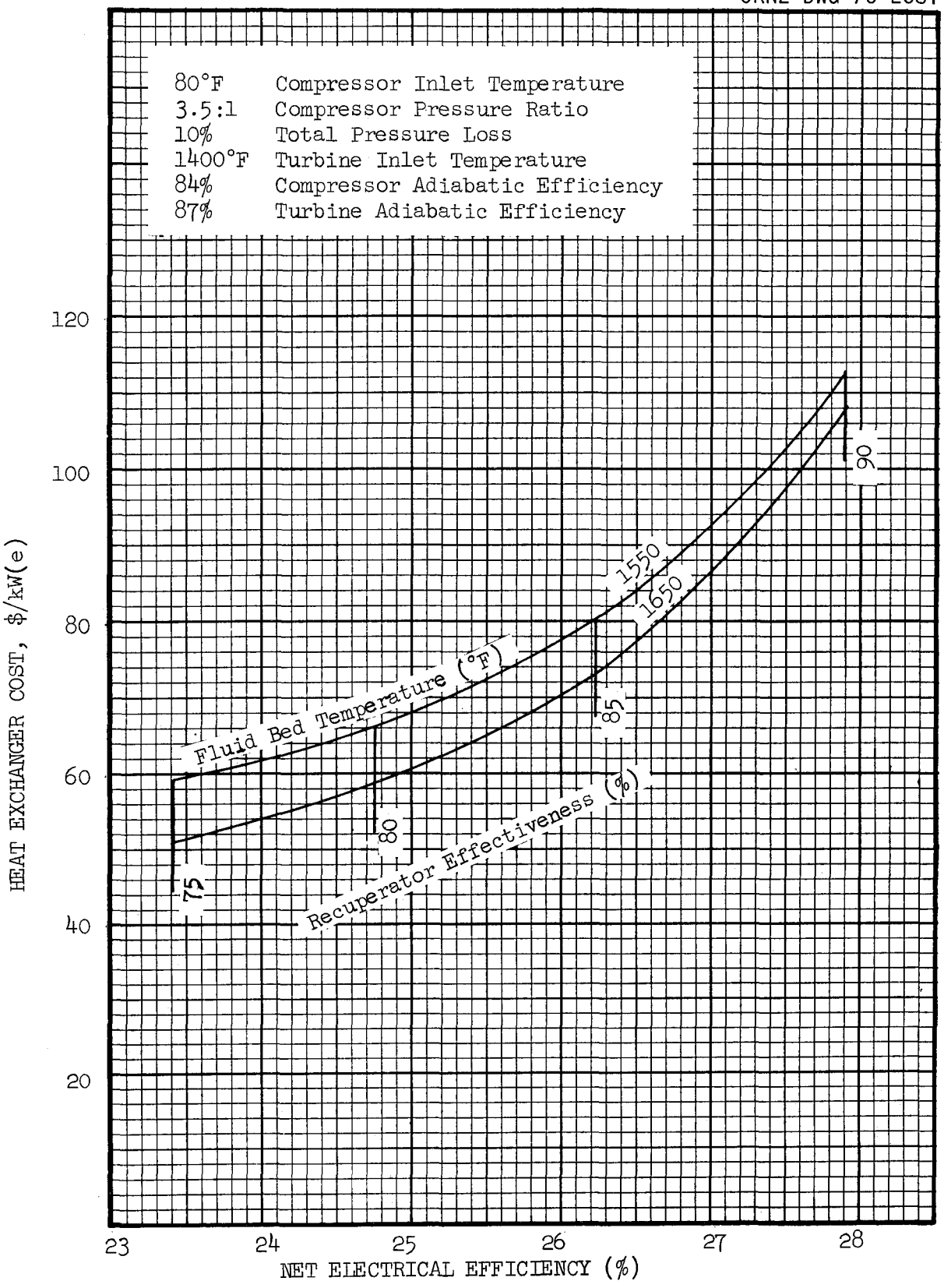

Fig. 5.30. Capital costs of the heat exchangers used in a regenerative cycle without intercooling or reheat as a function of the recuperator effectiveness, the fluidized bed temperature, and the net electrical efficiency.

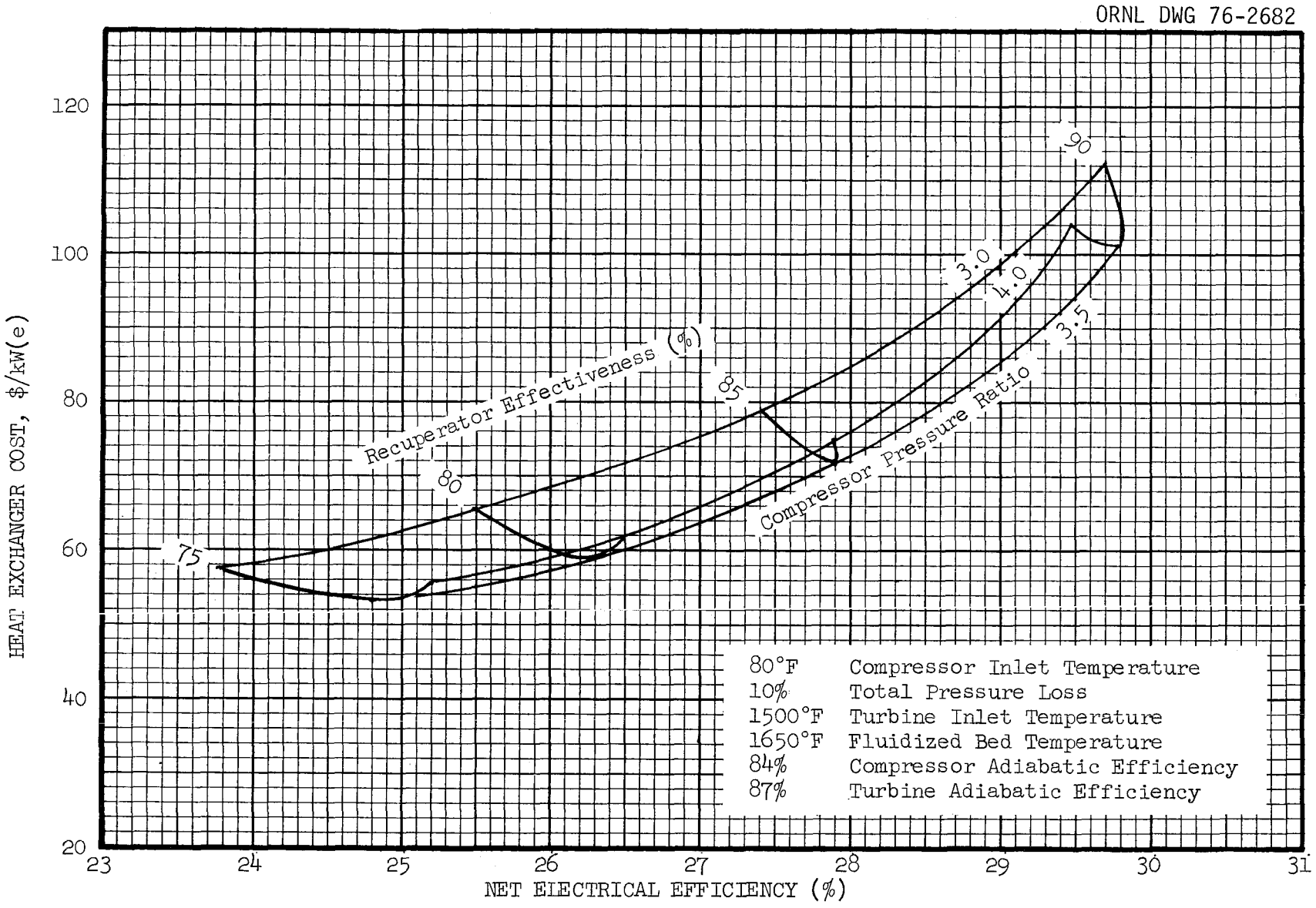

Fig. 5.31. Capital cost of the heat exchangers used in a regenerative cycle without intercooling or reheat as a function of the recuperator effectiveness, the compressor pressure ratio, and the net electrical efficiency.

ORNL DWG 76-2683

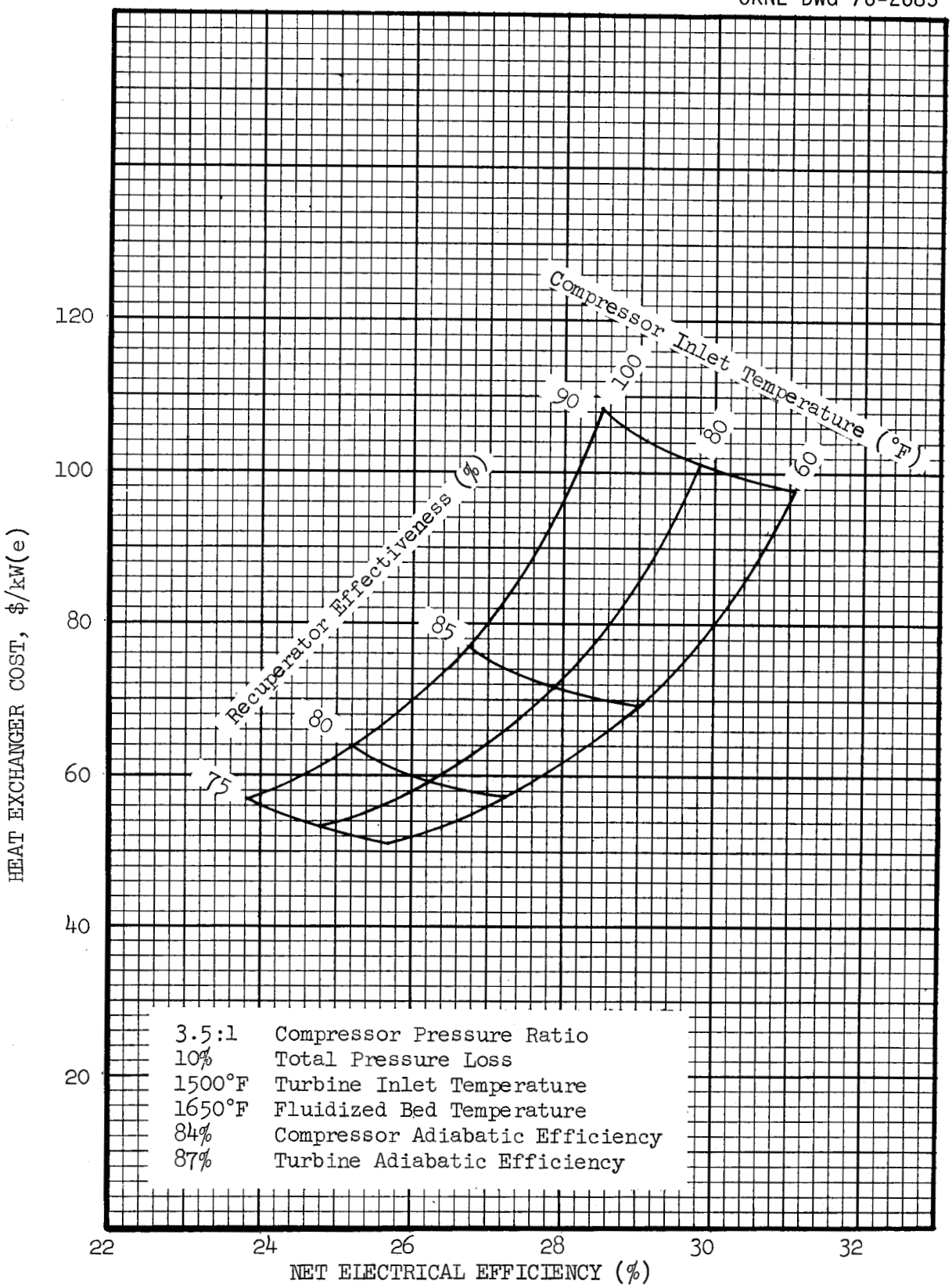

Fig. 5.32. Capital cost of the heat exchangers used in a regenerative cycle without intercooling or reheat as a function of the recuperator effectiveness, the compressor inlet temperature, and the net electrical efficiency.

ORNL DWG 76-2684

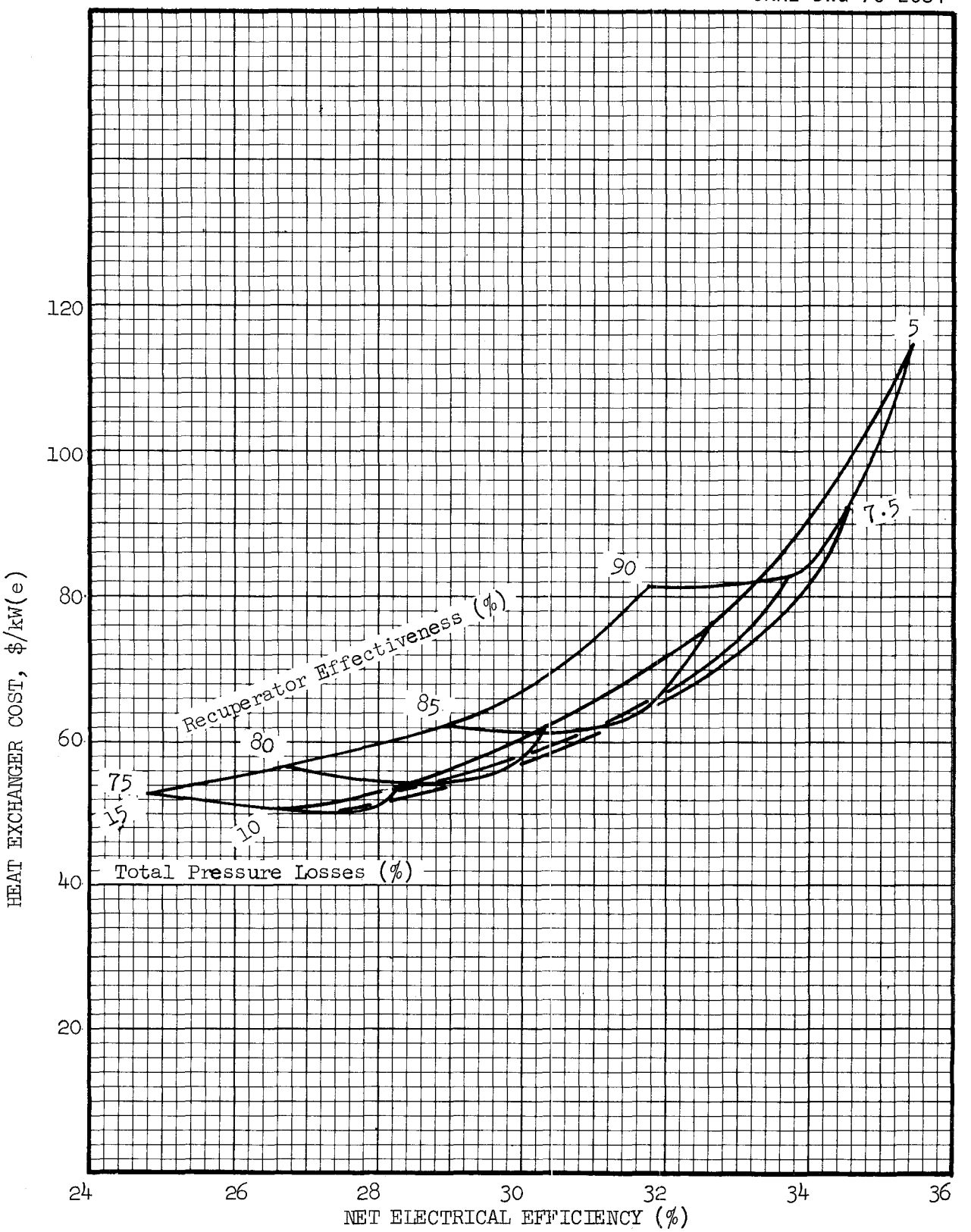

Fig. 5.33. Capital cost of the heat exchangers used in an intercooled regenerative cycle with reheat as a function of the recuperator effectiveness, the system total pressure losses, and the net electrical efficiency. The system is operated at a compressor pressure ratio of 3.5:1 at an inlet temperature of 80°F, a compressor adiabatic efficiency of 84%, a turbine inlet temperature of 1500°F and a turbine adiabatic efficiency of 87%. Fluidized bed temperature = 1650°F.

ORNL DWG 76-2685

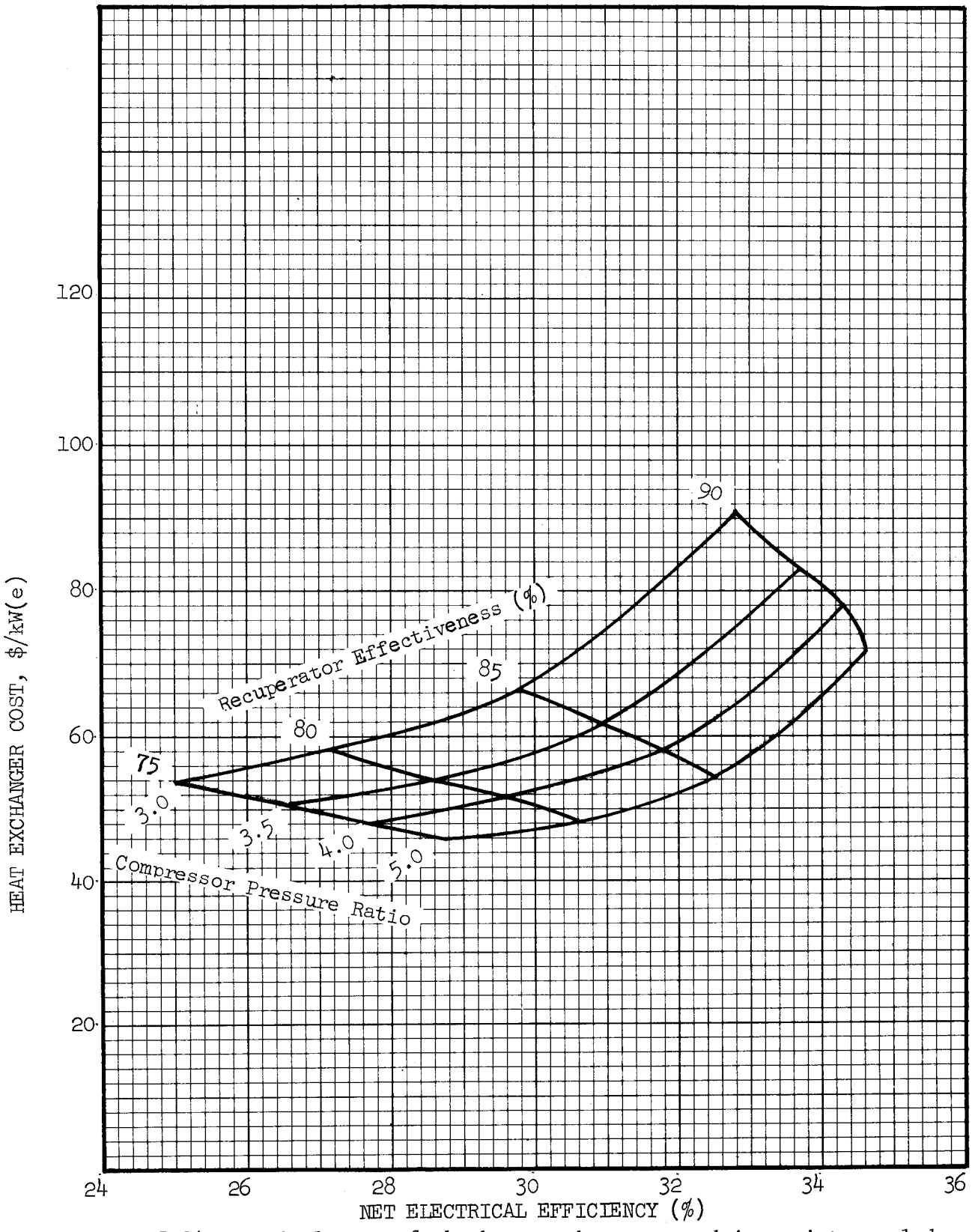

Fig. 5.34. Capital cost of the heat exchangers used in an intercooled regenerative cycle with reheat as a function of the recuperator effectiveness, the compressor pressure ratio, and the net electrical efficiency.

Effects of Fuel Costs on Power Costs

In attempting to evaluate the merits of increasing the capital cost of the heat exchangers to obtain an increase in cycle efficiency, a series of curves was prepared to give the portion of the electric power costs represented by the fuel and the capital cost of the heat exchangers. Other capital and operating charges were considered to be insensitive to the design variables considered in this set of curves.

Figure 5.35 presents the effects of fuel cost, recuperator effectiveness, and system pressure losses for the cycle of Fig. 5.6 assuming capital charges of 15%. Figure 5.36 gives a similar set of curves for capital charges of 20%. Note that the electric power cost is relatively insensitive to the recuperator effectiveness and system pressure loss, but is heavily dependent on fuel cost. As expected, the higher the fuel cost the greater the advantages accruing from increasing the cycle efficiency by increasing the recuperator effectiveness and reducing the system pressure loss. Essentially similar curves are shown in Figs. 5.37 and 5.38 for the cycle of Fig. 5.8 with intercooling and reheat. To facilitate a comparison between the two cycles, representative curves for both cycles are presented on the same coordinates in Fig. 5.39. These show a small advantage for the use of intercooling and reheat if the fuel cost is high, but little advantage for the lower fuel costs. Note that at least part of the cost reduction implied by Fig. 5.39 for intercooling and aftercooling would be offset by increased costs associated with the greater complexity of the system.

Effects of Part-Load Operation

The effects of part-load operation on the overall thermal performance of the two systems of Figs. 5.6 and 5.8 when operating with a system total pressure loss of 5% and a 90% effective recuperator are shown in Figs. 5.40 and 5.41. The basis of these calculations was that the hot water demand was constant at a thermal equivalent of 60% of 70% of the maximum electrical load and that the space heating requirements were a maximum of 175% of 70% of the maximum electrical load. In these calculations, therefore, after the hot water demand was satisfied any useful thermal energy remaining was applied to the 175% requirement. When the 175% requirement was satisfied, the remaining energy was discarded. These calculations were

ORNL DWG. 74-9146

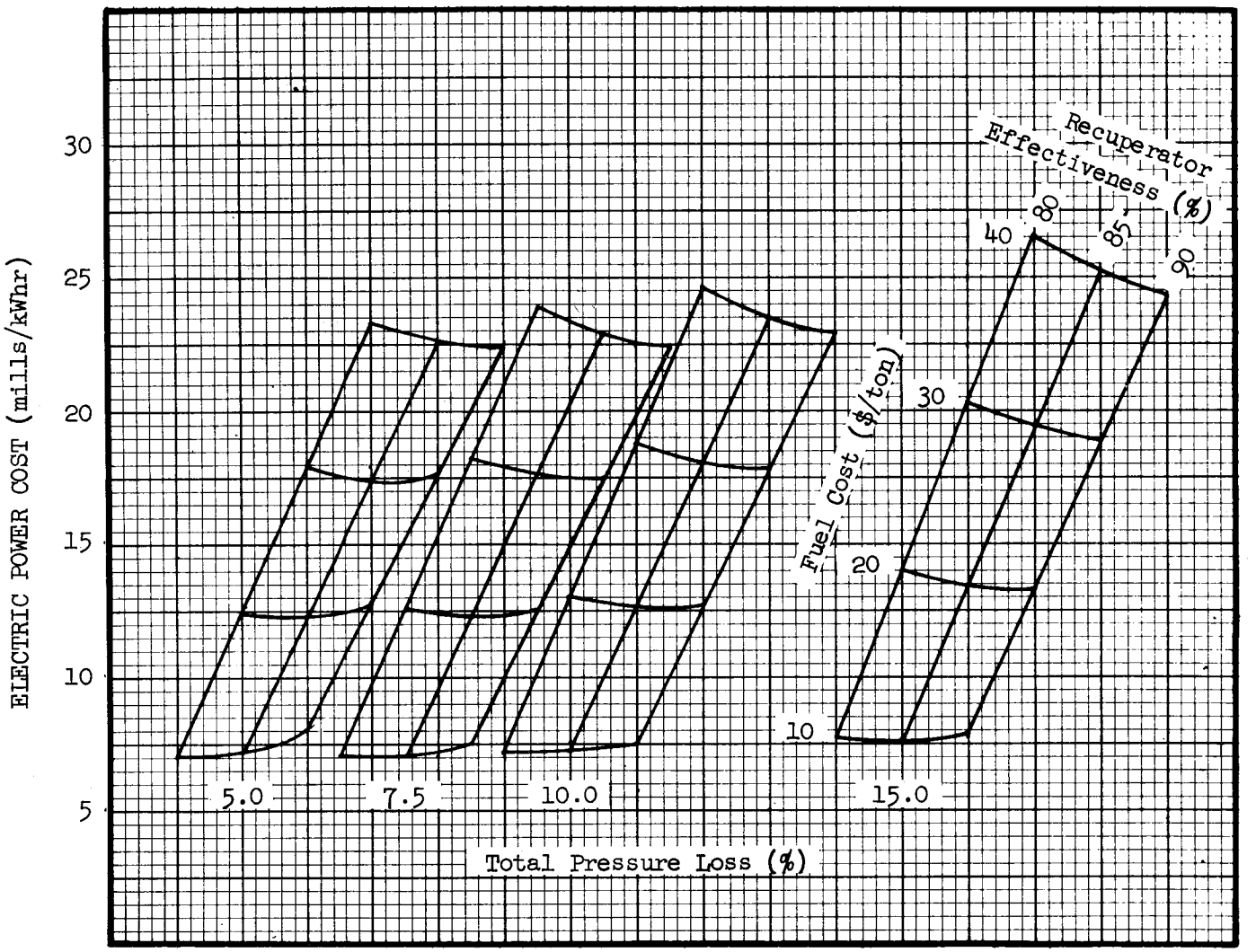

Fig. 5.35. Fractional electrical power cost associated with the fuel and heat exchanger cost for a regenerative cycle without intercooling or reheat at a load factor of 70% and 15% capitalization. The system is operated at a compressor pressure ration of 3.5:1 and an inlet temperature of 80°F, a compressor adiabatic efficiency of 84%, a turbine inlet temperature of 1500°F and a turbine adiabatic efficiency of 87%. Fluidized bed temperature = 1650°F.

ORNL DWG 76-2686

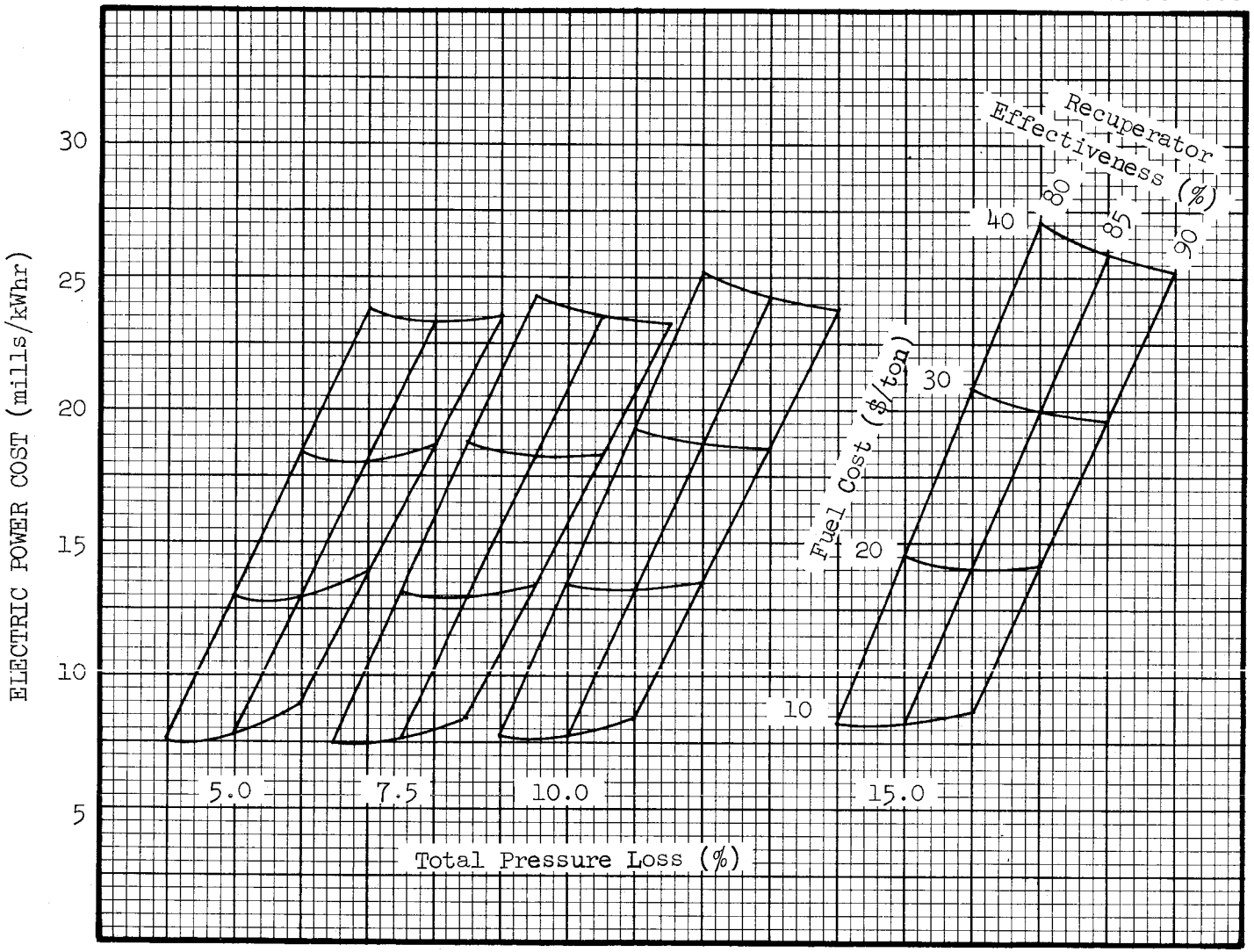

Fig. 5.36. Fractional electrical power cost associated with the fuel and heat exchanger cost for a regenerative cycle without intercooling or reheat at a load factor of 70% and 20% capitalization. The system is operated at a compressor pressure ratio of 3.5:1 and an inlet temperature of 80°F, a compressor adiabatic efficiency of 84%, a turbine inlet temperature of 1500°F and a turbine adiabatic efficiency of 87%. Fluidized bed temperature = 1650°F.

ORNL DWG 76-2687

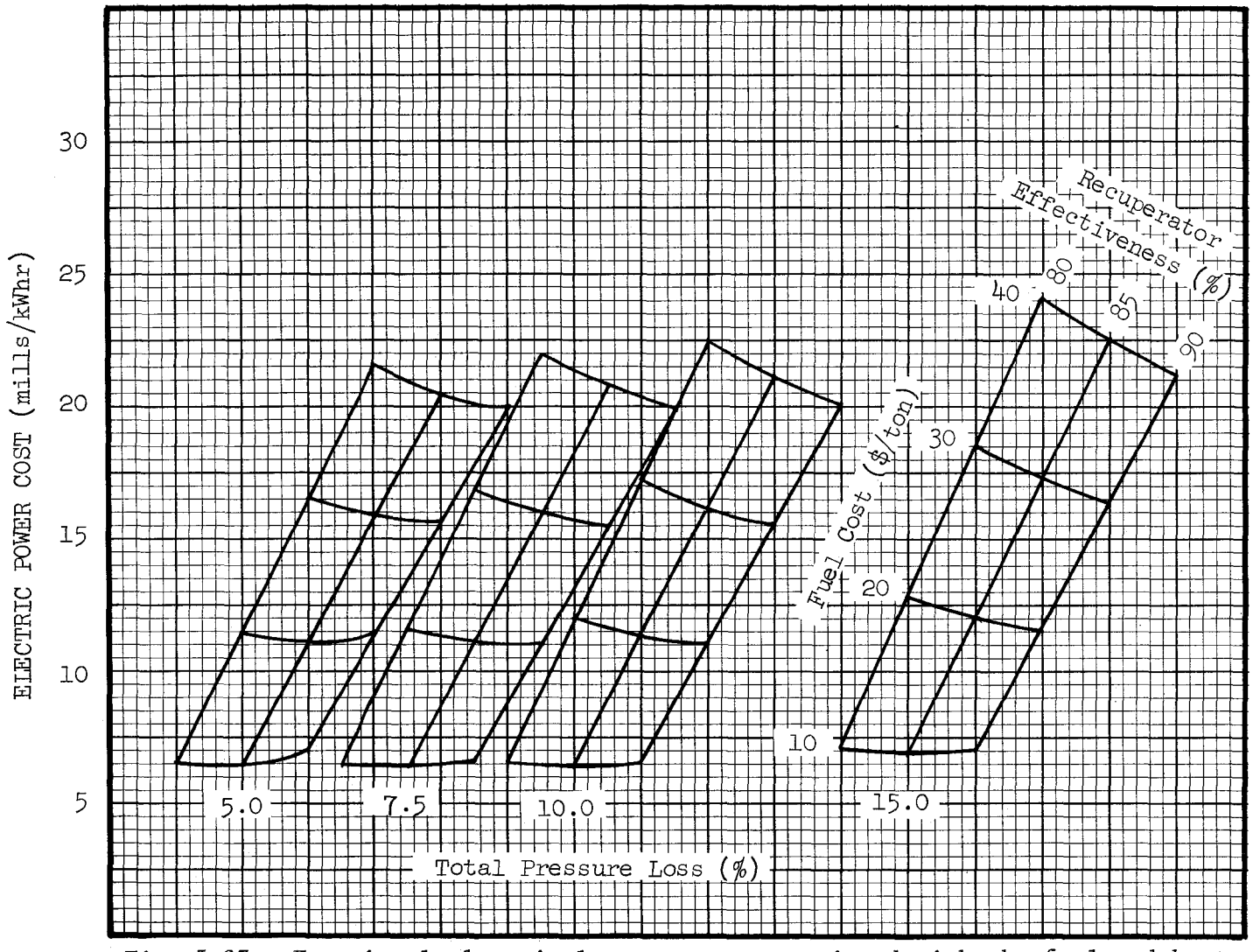

Fig. 5.37. Fractional electrical power cost associated with the fuel and heat exchanger cost for a regenerative cycle with intercooling and reheat at a load factor of 70% and 15% capitalization. The system is operated at a compressor pressure ratio of 3.5:1 and an inlet temperature of 80°F, a compressor adiabatic efficiency of 84%, a turbine inlet temperature of 1500°F and a turbine adiabatic efficiency of 87%. Fluidized bed temperature = 1650°F.

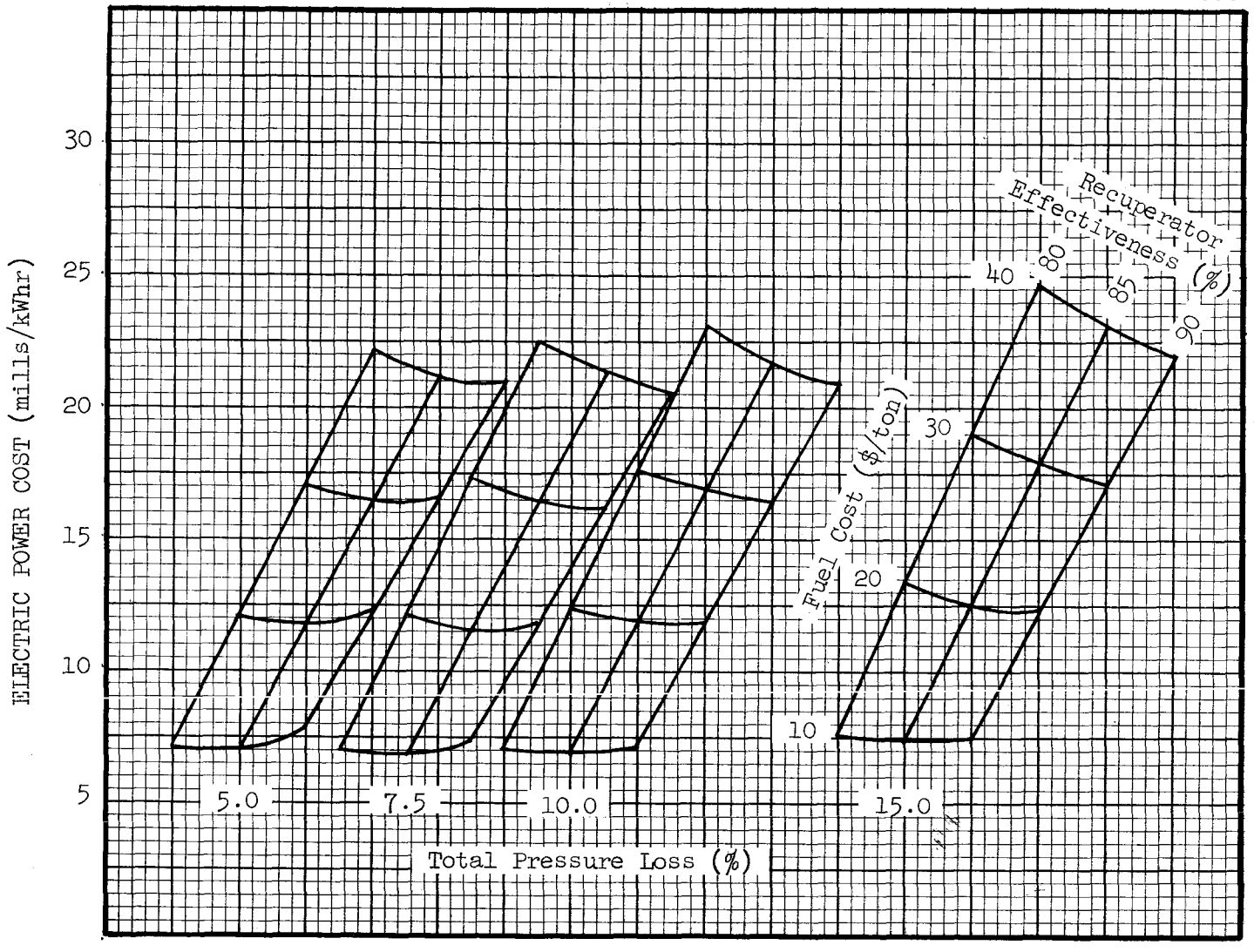

Fig. 5.38. Fractional electrical power cost associated with the fuel and heat exchanger cost for a regenerative cycle with intercooling and reheat at a load factor of 70% and 20% capitalization. The system is operated at a compressor pressure ratio of 3.5:1 and an inlet temperature of 80°F, a compressor adiabatic efficiency of 84%, a turbine inlet temperature of 1500°F and a turbine adiabatic efficiency of 87%. Fluidized bed temperature = 1650°F.

ORNL DWG 76-2689

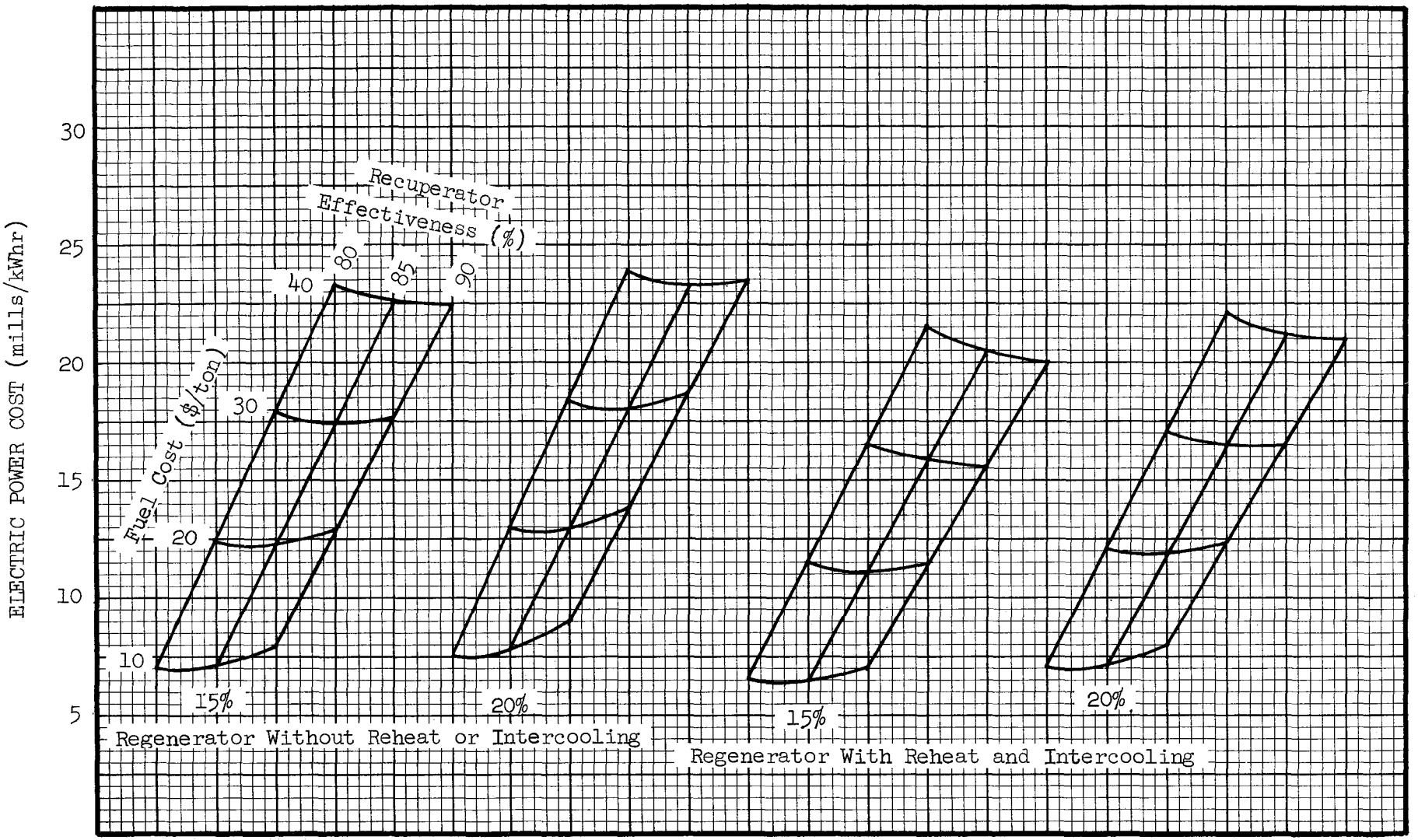

Fig. 5.39. Comparative fractional electrical power costs associated with the fuel and heat exchanger cost for a regenerative cycle with and without intercooling and reheat at a load factor of 70% and 5% total pressure losses. The systems are operated at a compressor pressure ratio of 3.5:1 and an inlet temperature of 80°F, a compressor adiabatic efficiency of 84%, a turbine inlet temperature of 1500°F and a turbine adiabatic efficiency of 87%. Fluidized bed temperature = 1650°F.

ORNL DWG 76-2690

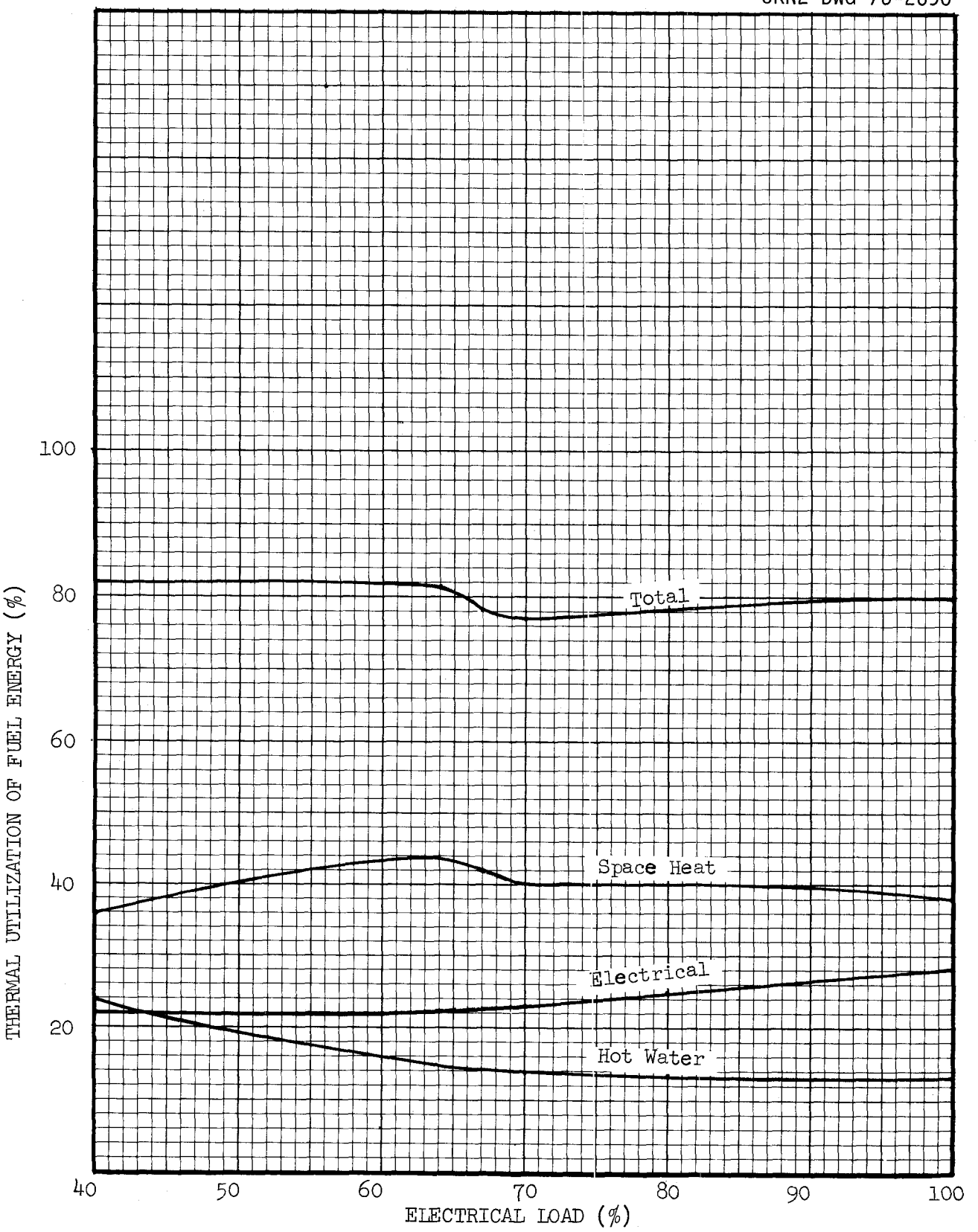

Fig. 5.40. The distribution of the thermal utilization of fuel energy in a regenerative cycle without intercooling ore reheat operating at a compressor ratio of 3.5:1, a recuperator effectiveness of 90% and a system total pressure loss of 5%.

ORNL DWG 76-2691

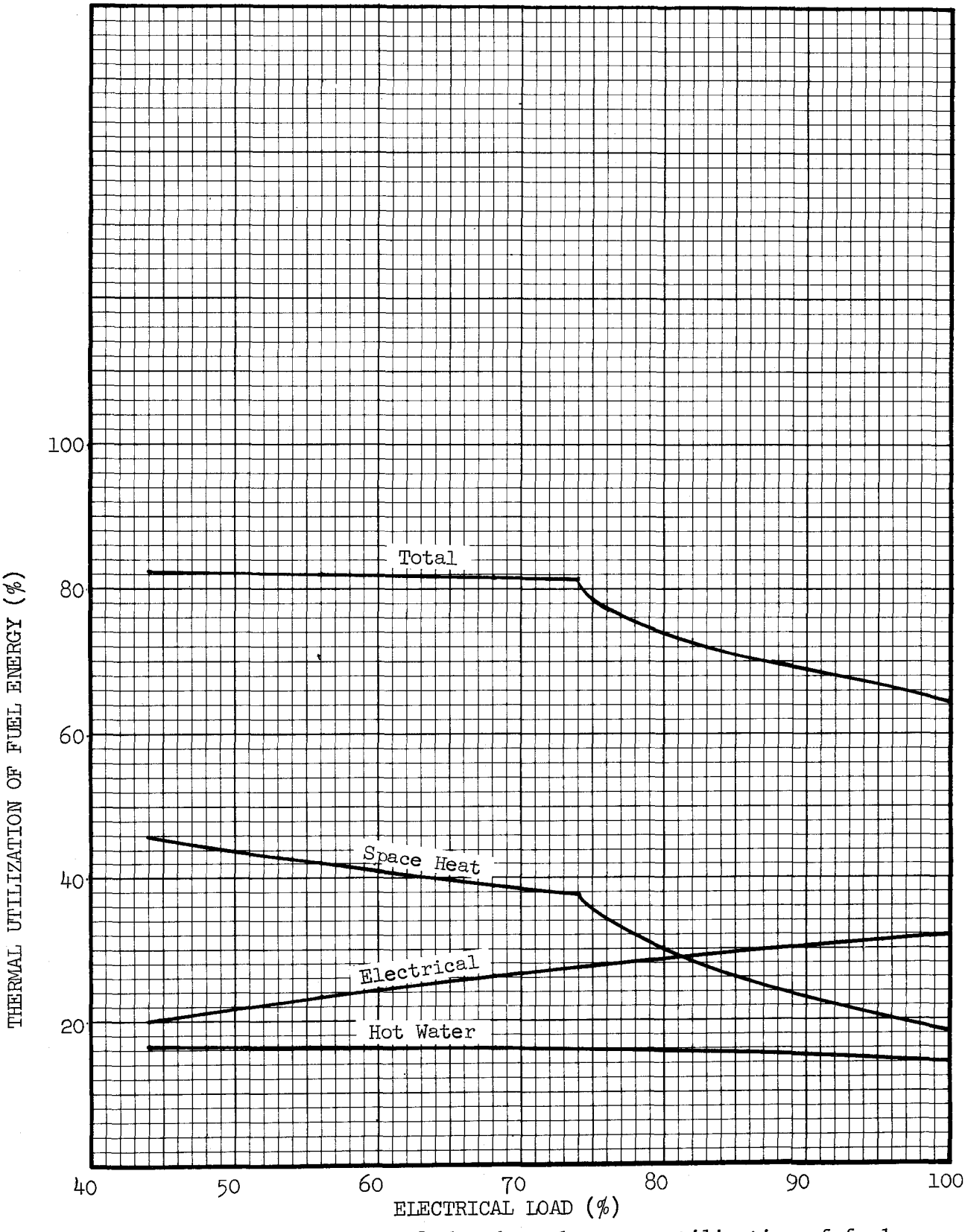

Fig. 5.41. The distribution of the thermal energy utilization of fuel energy in an intercooled regenerative cycle with reheat operating at a compressor pressure ration of 3.5:1, a recuperator effectiveness of 90%, and a system total pressure loss of 5%.

all made for a net electrical efficiency of 90% of the gross electrical efficiency, a system heat loss of 5%, and the higher heating value of the input coal used as fuel. The space heat was supplied to water varying in temperature between 160°F and 200°F and the hot water heat was supplied to water varying in temperature between 60°F and 150°F. The inlet temperature of the compressor was varied between 80°F and 180°F to obtain electrical load variations. At an inlet temperature of 180°F, the cycle pressure was decreased to further decrease the electrical load.

Inspection of Fig. 5.40 which gives the results of the calculation for the regenerative cycle without either intercooling or reheat indicates an integrated total energy utilization of 79.9% with a variation of 76% to 82% over the electrical load range of 40% to 100%. Figure 5.41 which gives the results of the calculation for the intercooled regenerative cycle with reheat indicates an integrated total energy utilization of 77.4% with a variation of 65% to 83% over the electrical load range of 40% to 100%.

Costs of Open and Closed Cycles

There is little difference in efficiency at full load between open and closed cycles, but there are substantial differences in the capital costs for a plant of a given full load capacity. If one employs an existing gas turbine engine, for example, it will have been designed for operation without a recuperator. Thus it will be necessary to operate the engine at a reduced speed and pressure ratio, and this will cut its net output about in half if it is operated in an open cycle. If it is operated in a closed cycle, however, the compressor inlet pressure can be increased by a factor of 3.4 if its original design pressure ratio were 12. Thus the engine output in a closed cycle can be increased by a factor of about 3.4, and this will reduce the capital cost of the turbine and compressor per unit of output by the same factor. The cost of the heater, economizer, recuperator, and waste heat recovery unit are also strongly affected. After allowing for mass flow rate effects, for the same effectiveness and pressure drop ratio the cost of each heat exchanger will be 40% as great for the closed as for the open cycle. Further, a more favorable set of proportions can be obtained in the fluidized bed. On the other hand, the closed cycle requires

not only a cooler but also a supply of cooling water, although about 60% of the heat rejected can be used to advantage for heating domestic hot water if the latter is heated to 150°F. If the hot water supply temperature is reduced to 120°F, nearly all of the heat rejected through the cooler can be used for heating domestic hot water, and very little additional cooling water will be required.

Estimates indicate that after allowing for the above factors the overall cost of the reference design plant (described in the next chapter) would be increased by about one-third in going from a closed cycle to an open cycle. Thus it appears well worth while to employ a closed cycle just from the capital cost standpoint, although the prime reason initially was the much better thermal efficiency at part load.

References

1. A. P. Fraas and G. Samuels, Small Coal-Burning Gas Turbines for Total Energy Systems, ORNL/MIUS report, to be published.

2. Automobile Gas Turbine Optimization Study, Final Report of Study Prepared by AiResearch Manufacturing Company for the Environmental Protection Agency, Office of Air Programs Contract 68-04-0012, Garrett Report AT-6100-R7, July 14, 1972.

CHAPTER 6

CONCEPTUAL DESIGNS FOR FLUIDIZED BED GAS TURBINE SYSTEMS

A series of designs for fluidized bed coal combustion systems coupled to gas turbines has been devised to meet the basic MIUS requirements of 500 to 1000 kW(e) per unit using the results from the cycle analysis work of the previous section as the point of departure. Sulfur removal considerations coupled with allowable stresses in alloys that seem suitable for use in the fluidized bed led to a choice of a bed operating temperature of 1650°F for reference design purposes. The principal considerations that went into the design of the fluidized bed itself are indicated in Chapter 3 on combustion systems. This chapter is concerned primarily with the evolution of typical layouts designed to meet all of the boundary conditions that could be envisioned. These conditions are summarized in Table 6.1.

Fluid Bed and Furnace Layouts

Several basic planforms for the fluidized bed were considered including a circular bed, a rectangular bed, and a square bed. The circular bed would have had the advantage that if the furnace were pressurized the cost of the furnace shell would be kept to a minimum. However, the savings in cost associated with this appear to be largely offset by the extra complexity of the tube bending operations required. For example, to assure a fairly uniform circulation of particles in the fluidized bed, one would like to keep the spacing between tubes constant, and this in turn implies the use of an involute curve such as that indicated in Fig. 6.1. Other factors including assembly and possible disassembly for maintenance combined with cost considerations to favor the use of a square furnace with simple hair pin-shaped loops in the bed as in Fig. 6.1. With this square configuration the tube banks for the furnace can be built in four panels and assembled as indicated in Fig. 6.2. Note that the hair pin loops for the tubes on the east and the west sides of the furnace lie at one level in the bed while those for the north and south faces lie at another level.

Table 6.1. Basic Precepts for the Design of the Fluidized Bed-Heater-Economizer Unit

1. The unit would be employed with a closed cycle gas turbine with an economizer, recuperator, and regenerator.
2. The economizer would be built as an integral part of the heater.
3. The bed operating temperature will be 1650°F, a value that should keep the maximum heater tube wall temperature below 1600°F.
4. The combustion air temperature into the bed will be 1000°F.
5. The compressor outlet pressure will be 12 atm.
6. The turbine air pressure drop will be no more than 18 psi.
7. The combustion air pressure drop through the bed should be kept low to reduce the pumping power. This implies a bed depth of no more than 40 in.
8. The superficial velocity of the combustion gas leaving the bed should be between 2.5 and 10 ft/sec.
9. The maximum particle size should be small enough so that the bed can be fluidized at 25% of the design value for the combustion air flow rate.
10. The heat transfer rate to the turbine air should give a proper heat balance with the heat released by combustion.
11. The heater tube length-diameter ratio should be such that the turbine air will leave the bed at 1500°F with a 1650°F bed temperature.
12. The combustion gas temperature leaving the economizer should approach the temperature of the turbine air entering the economizer within 50°F.
13. The tube centerline spacing in the bed should be three times the tube diameter.
14. The tube bend radius should not be less than 3 tube diameters to permit cold bending of the tubes.
15. The number of heater tubes in the bed and the size of the bed should be such that the walls of the plenum chamber above the bed should be covered with one continuous layer of tubes.
16. The tube wall thickness should be sufficient so that the pressure stress will be below that for a creep-rupture life of 10^5 hr.
17. The bends in the tubes should all be in the same plane wherever possible.
18. There should be no intermediate manifolds or welds in the heater tubes between the economizer inlet and the heater outlet.

ORNL DWG. 75-12316

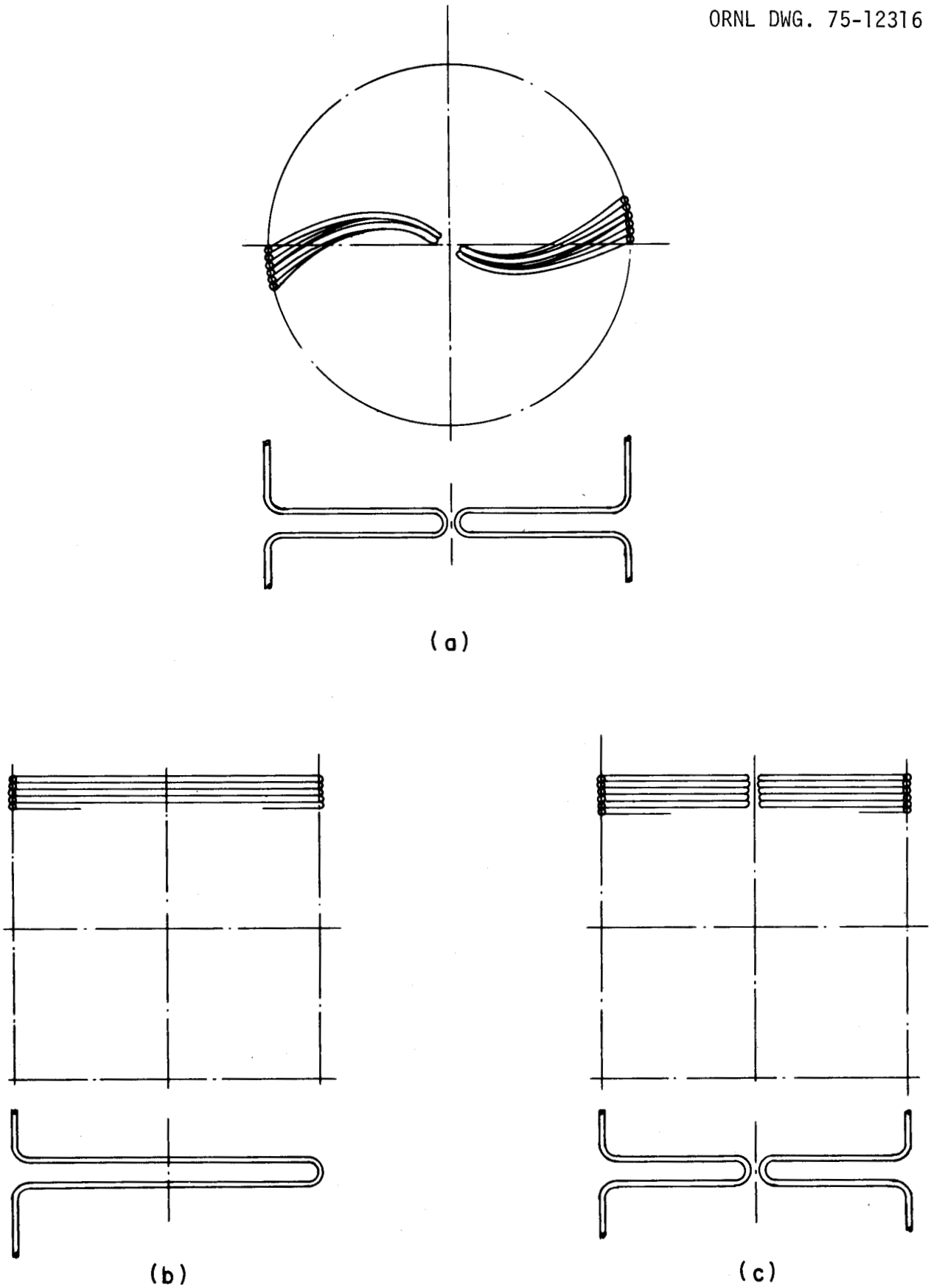

Fig. 6.1. Typical arrangements of tubes in the fluidized bed.

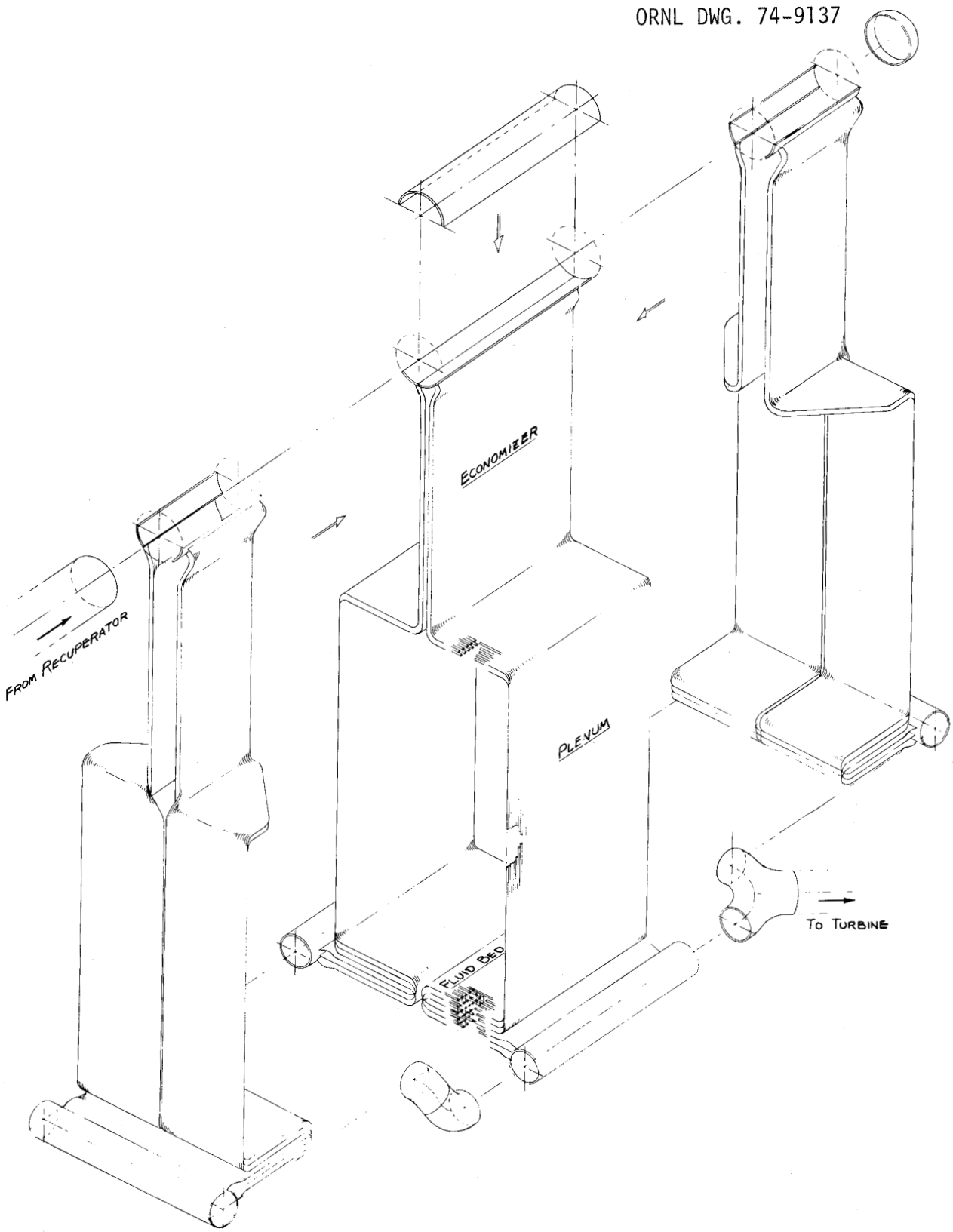

Fig. 6.2. Panel configuration of tube banks designed to facilitate fabrication and assembly of the fluidized bed furnace-heater-economizer unit.

Plenum Chamber Walls

It is desirable to take advantage of the high radiant heat flux from the upper surface of the bed by covering the walls of the plenum chamber above the bed with tubes that are an integral portion of the heater system. Inasmuch as experiments at BCURA indicate that the tube centerline spacing should be at least 3 tube diameters to give good particle circulation in the bed, this means that it is desirable to make use of three levels of tube bank in the bed for each wall of the plenum chamber so that the tubes will be immediately adjacent to each other in the plenum chamber wall. This approach has the advantage that the radius of curvature in the hair pin bend of the bed can be increased to a level such that there should be no difficulty in cold bending the tubes. Of course, it would be possible to have the tubes spaced on centers of $\sim$2 diam in the plenum chamber wall and depend on a refractory lining outside the tubes to absorb the thermal radiation coming through the interstices between the tubes and then re-radiate it back to the back sides of the tubes. This would have the advantage that it would increase the heat input per unit of length of the tubes in the plenum chamber wall and thus tend to give a lower pressure drop in the tubes for a given heat input rate. However, it has the disadvantage that the refractory lining would have to run at a higher temperature than would be the case if the plenum chamber wall were completely covered with tubes, and this would increase both its cost and the heat losses to the surroundings.

Bed Depth

The air velocity through the bed required to fluidize it is independent of the bed depth. As a consequence, the pumping power required to force air through the bed is directly proportional to the bed depth because the bed acts as if it represented a static head of fluid that acts as a back pressure on the air supply ports in the bed support plate. Thus, there is a strong incentive to minimize the bed depth to minimize the pumping power losses for circulating the combustion air through the bed. On the other hand, the amount of unburned carbon in the fines blown through the bed and out into the cyclone separator increases as the bed depth is reduced, hence there is an incentive to use as deep a bed as practicable.

In addition to these considerations, one finds that geometric problems in getting tubes into the bed and integrated into the plenum chamber wall above the bed place limitations on the heat removal obtainable from a bed of a given size. These are closely tied to heat transfer and fluid flow considerations in the turbine air stream as will be discussed later. Efforts to evolve designs that would meet all of the boundary conditions have generally yielded bed depths in the range from 18 to 36 in.

Economizer

To minimize the number of tube-to-header joints and thus reduce costs for fabricating the heater assembly, it is advantageous to incorporate the economizer in the furnace-fluidized bed-tube matrix system. Four configurations for accomplishing this were considered. In the first of these the economizer region was formed by running the tubes inward from the top of the plenum chamber and then upward through a rectangular duct that was not far from being square. See Fig. 6.3a. This required a rather complex set of out-of-plane bends to connect the economizer region to the plenum chamber wall. To avoid this, a second layout was evolved in which the plenum chamber over the bed through a narrow annulus surrounding a hollow square as in Fig. 6.3b. This gave a fairly high velocity of the combustion gases over the outside of the tubes and hence a fairly good heat transfer coefficient. This heat transfer coefficient was augmented by thermal radiation from the walls of the passage which would be heated above the tube temperature by the hot gases. The disadvantage of this approach is that it leads to a rather bulky system with a larger surface area through which heat would be lost to the surroundings and would require a substantially larger amount of relatively expensive ceramic lining material. A third approach considered was to place the economizer tubes in a cruciform matrix as in Fig. 6.3c to give a double layer of tubes instead of the single layer of the annular arrangement shown in Fig. 6.3b. This arrangement requires out-of-plane bends in only a few of the tubes; the bulk of them can be plane bends. The fourth arrangement considered makes use of the square furnace, while the tubes on the north and south sides would require a diagonal out-of-plane section to traverse the top of the furnace and bring them into line with the tubes for the east and west sides. See Fig. 6.3d.

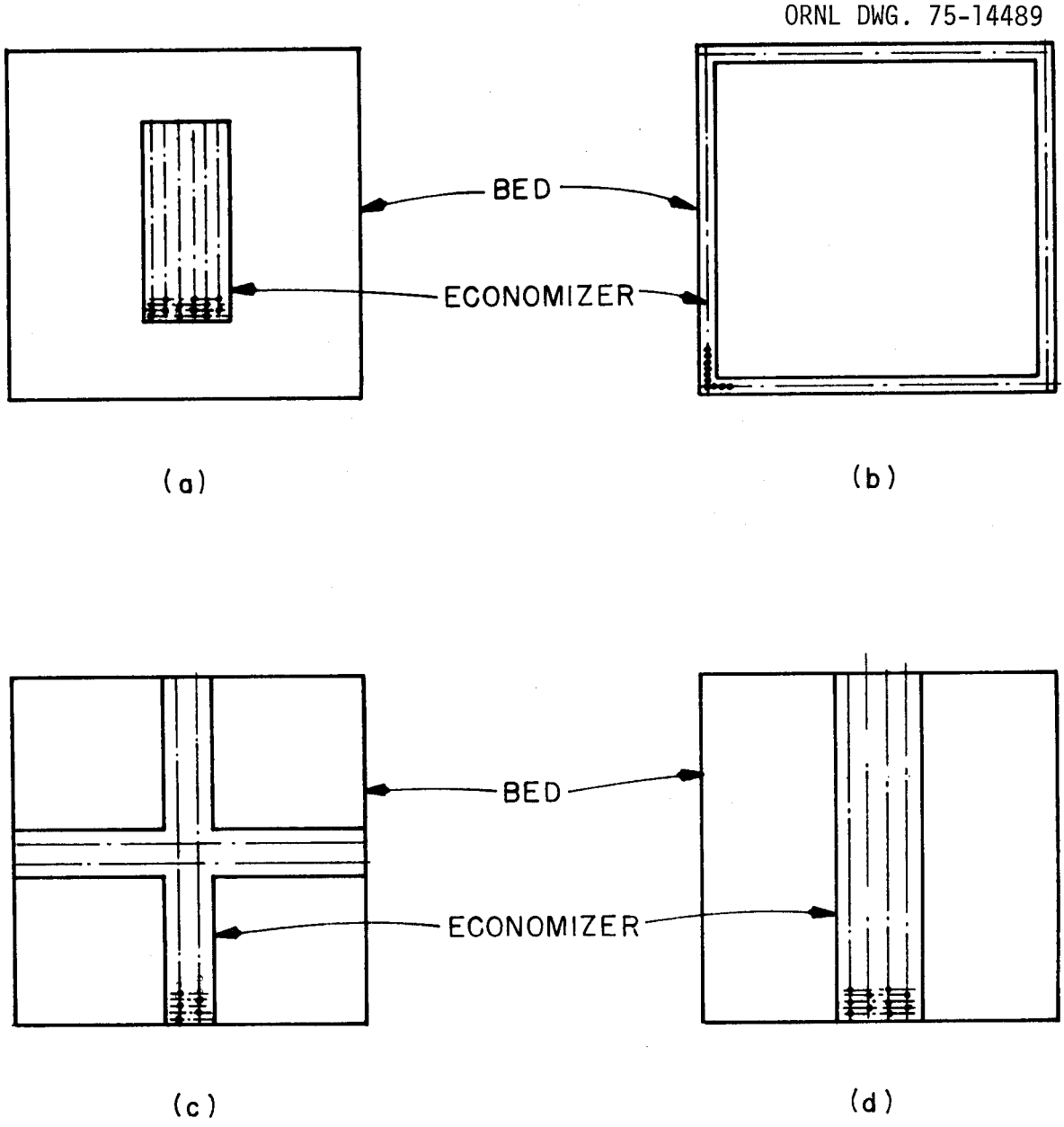

Fig. 6.3. Top views of four different arrangements of the tube matrix for the economizer as positioned relative to the fluidized bed.

This arrangement gives lower heat losses and a simpler and less expensive manifold system than the arrangement of Fig. 6.3c. It also has the advantage that it lends itself to fabrication of separate panels for each side that can be assembled in the manner indicated in Fig. 6.2.

Bed Floatation Limitation

For a fluidized bed to operate properly the air flow through the bed must be high enough to float the particles and produce the agitation and circulation alluded to above.[1] However, the air flow rate ought not be so high as to blow a large fraction of the smaller diameter particles out of the bed so that they are carried off with the stack gas. Some insight into these limitations is given by Fig. 6.4 which shows the relation between particle diameter and the superficial velocity of the gas leaving the bed for these two limits. Curves are given for three different densities of the settled bed, i.e., the bed density prior to fluidization. It should be noted that when the bed is fluidized, experience has shown that its depth tends to increase by roughly 30%. The settled density of the bed depends mainly on the density of the particles, and this varies somewhat with the mineral content of the coal. Inasmuch as the particle size in the bed will vary substantially about a mean value, the range of superficial velocities for satisfactory operation is substantially less than is implied by Fig. 2. For example, if one were to assume a mean particle diameter of 2500 microns (0.1 in.) with a settled bed density of 1.6 g/cm^3, the superficial velocity of the combustion gas leaving the bed could be varied by a factor of about 20 without giving difficulty with particle carryover or settling of the bed. However, if particles about one-third the average size are to be kept from blowing out of the bed, the range of superficial air velocities that would be permissible would be reduced to a factor of 6, while if particles one-fifth the average size are not to be blown out of the bed the superficial velocity could be varied by only a factor of 4 between the minimum for fluidizing the bed and the maximum usable without excessive carryover. Thus, for the range of interest in this case the superficial velocity leaving the bed could be varied from about 1 m/sec to about 4 m/sec. Figure 6.4 indicates that a somewhat wider range of air velocity might be

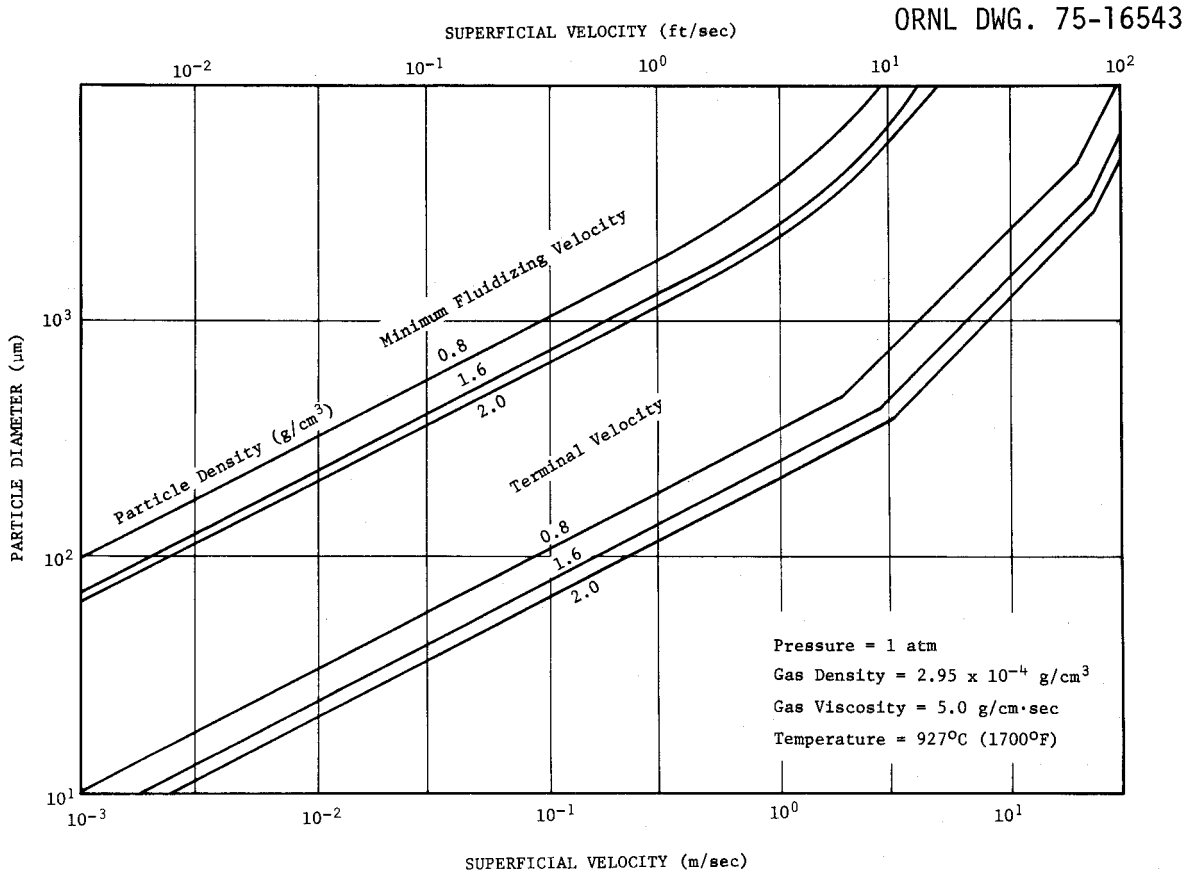

Fig. 6.4. Effects of particle size on both the minimum gas velocity leaving the bed for full fluidization and for the velocity at which the particles will be carried up through and out of the plenum above the bed.

employed if the particle size were cut in half, i.e., the coal and limestone feed crushed to 1/16 mesh instead of 1/8-in. mesh.

Bed Support Plate

The plate or grid upon which the fluidized bed rests must include openings through which air can flow into the fluidized bed. These openings must be sufficiently small so that particles from the bed will not pour downward through the openings when the air flow is stopped, although they need not be so small that they will prevent a few fine particles from sifting through and falling down into the plenum chamber under shutdown conditions. Thus, the openings ought to be smaller than the larger particles in the bed so that these can act to plug the openings and thus act as an effective dam to prevent more than a few of the fines from sifting through. One way of accomplishing this would be to make use of porous plates that might contain either a large number of small holes or they might be formed as has been done by Combustion Power, Inc. by using a stainless steel sheet about 1/16-in. thick that has been slit to form expanded metal grid plates, the openings expanded slightly, and then the plates rolled to reduce the size of the openings. A third approach might be to make ceramic or cast iron tiles perhaps 4-in. square with a close array of round holes similar to those employed in gas burner plates. The tapered holes would facilitate casting the material as they would provide "good draw" in making the molds, and, by mounting them with the small ends of the holes upward, any particles that sifted into the holes would be able to fall freely through them without blocking them. Any of these three types of porous plate could be mounted on a support grid that would be cooled by the air in the plenum chamber so that it would run close to the plenum chamber air temperature rather than close to the bed temperature. A note of caution to be added is that under shutdown conditions circulation of air in the plenum chamber will be almost nil, and hence the grid will approach the temperature of the bed rather closely so that its temperature might become excessive if the shutdown procedure were to allow the bed temperature to continue to be close to the normal operating temperature.

A second approach that might be taken to the design of air ports in the bed plate is that indicated in Fig. 6.5. Any of a variety of canopies

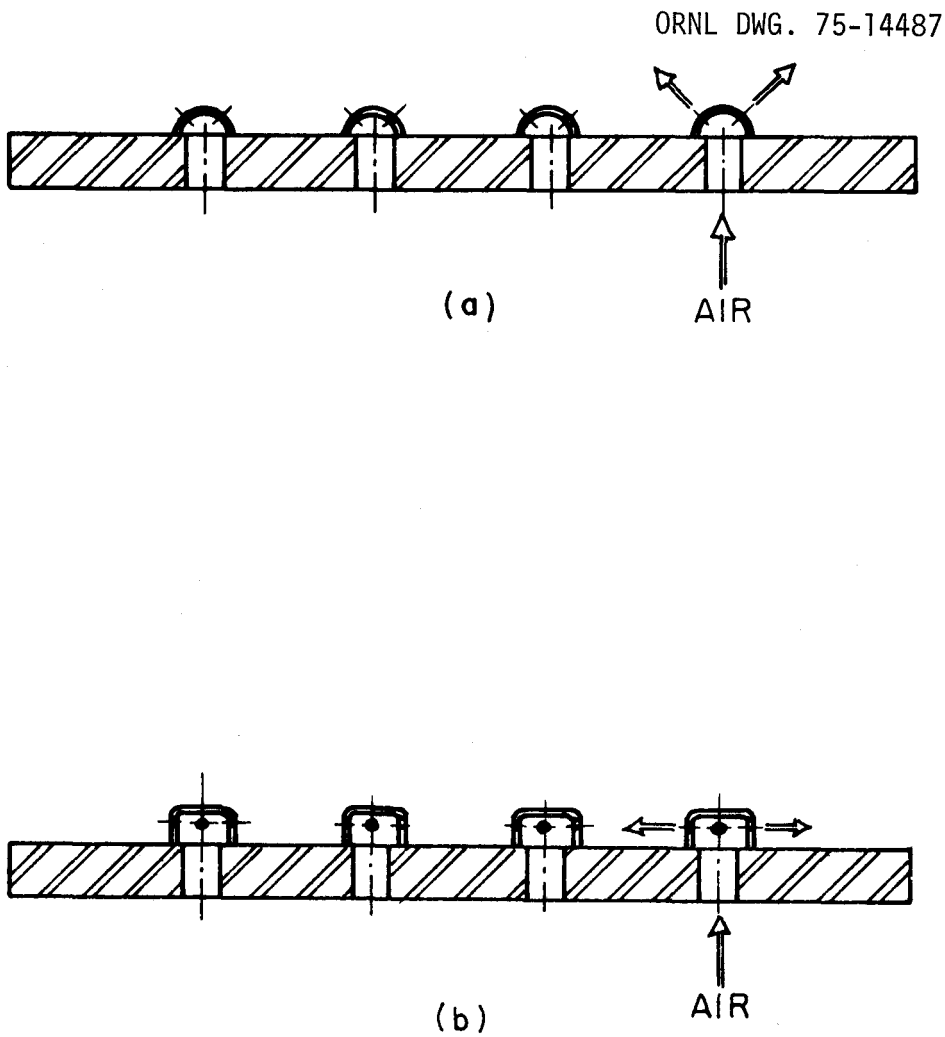

Fig. 6.5. Proposed designs for the air supply ports in the plate supporting the fluidized bed.

can be placed over the air ports to prevent bed material from flowing back down through them under shutdown conditions. The principal problem is to assure adequate air flow passage area so that the pressure drop will not be excessive.

The pressure drop through the bed support grid should be sufficient to provide a good air flow distribution across the bed. Experience with operation of fluidized beds indicates that, for good particle circulation uniformly across the bed, it is desirable to design the grid plate so that the air pressure drop across it will run about half of the pressure drop through the bed itself. This implies that the equivalent air flow passage area in the bed plate should be about 3% of the total area for atmospheric pressure beds.

The temperature of the bed support plate is likely to run substantially above that of the structure for the furnace walls. As a consequence, provision must be made for differential thermal expansion between these two components, and this provision should include measures to minimize air bypass through whatever clearances are provided as well as provisions to prevent flow of bed material back through the clearances under shutdown conditions.

Typical Layouts

Five layouts for the furnace and heater assembly have been chosen from the many layouts that have been prepared to illustrate the principal problems and possibilities. These are presented in this section together with a brief description of the principal features in each case. The first three layouts presented in this section were prepared early in the study and were based on an open cycle system with an economizer and recuperator. The other two layouts presented here were prepared near the end of the conceptual design work and were based on a closed cycle with an economizer, recuperator, and regenerator. In each case the considerations outlined above were the point of departure for the design, and in the latter two cases the design thinking had progressed to the point that the precepts of Table 6.1 could be clearly established.

The first of the five layouts is that shown in Fig. 6.6. Note that in this case the tubes for the east and west banks of the furnace were looped through the fluidized bed with a large vertical gap between the upper and lower legs of the loop. The tubes for the north and south sides of the furnace have a smaller bend radius and would be inserted into the region lying between the upper and lower legs of the tubes for the east and west sides of the furnace. The economizer region in this instance includes a central duct with a bypass valve in it that might be used for controlling the ratio of heat to electricity by allowing a portion of the combustion gases to bypass the economizer. This layout was evolved for a system such as that of Fig. 5.3 that employed a waste heat recovery unit in the stack gas stream. The cross section through the economizer region of this unit is similar to that of Fig. 6.3a.

A second typical layout is that of Fig. 6.7 which makes use of an economizer region similar to that of Fig. 6.3b. It consists of four single rowssets of tubes that are located in the planes of each of the four walls of the fluidized bed. The tubes are mounted so that they are not in contact with the outer wall thereby leaving a flow passage for the flue gas between the outer wall and the tube row. An inner liner defines the flow passage for the flue gas on the bed side of the economizer tubes. This arrangement allows a large fraction of the heat in the flue gas to be transferred to the economizer by radiation from the passage walls. This allows the spacing in the economizer to be increased with a resulting decrease in system pressure losses. The design data for the plant are given in Table 6.2.

The design of this fluidized bed was predicted upon several assumptions that will have to be verified by experimentation. The most important of these is that in the plenum chamber over the fluidized bed the total disengaging height would be only about 2 ft. An adequate disengaging height is necessary so that the flue gas entering the economizer section shown in Fig. 6.7 will not carry an excessive quantity of particulate matter that will have to be separated by the cyclone separator and recirculated to the fluidized bed.

Table 6.2. Data for the Design of Fig. 6.7 for a Coal Burning Total Energy System Incorporating a Fluidized Bed Combustion Chamber, Air Heater, and Recuperator Units and Producing Electric Power with an Air Turbine Driven Generator

Total energy input, Btu/hr	4.2×10^6
Electrical power output, kW(e)	350
Heat output in 250°F/15 psig steam, Btu/hr	1.9×10^6
Thermal efficiency based on electrical output, %	28.3
Thermal efficiency based on total useful output, %	72.4
Compressor pressure ratio	6
Compressor adiabatic efficiency, %	85
Turbine expansion ratio	5.4
Turbine adiabatic efficiency, %	89
Overall mechanical and generator efficiency, %	90
System total pressure loss, %	10
Fluidized bed geometry and flow	
Superficial gas velocity, ft/sec	2.3
Bed width and length, ft	5.1 x 5.2
Tube OD, in	1.0
Tube ID, in	0.83
Tube horizontal centerline spacing, in	3.0
Tube bank vertical centerline spacing, in	2.0
Tube centerline spacing in furnace wall, in	1.5
Total number of tubes	161
Air flow rate through tubes, lb/sec	5.92
Air flow passage area in tube, ft^2	0.605
Air mass flow rate in tubes, lb/sec-ft^2	9.79
Average tube length, ft	9.63
Fluidized bed heat transfer	
Tube-side heat transfer coefficient, Btu/hr-ft^2-°F	32
Combustion gas-side heat transfer coefficient, Btu/hr-ft^2-°F	50
Overall heat transfer coefficient based on tube outside surface area Btu/hr-ft^2-°F	17.2
Total tube surface area, outside, ft	405
Recuperator geometry and flow	
Tube OD, in	1
Tube ID, in	0.83
Total number of U-tubes	164
Effective tube length, ft	33
Tube pitch in a triangular array, in.	1.436
Air flow rate through tubes, lb/sec	5.92
Air flow passage area in tubes, ft^2	0.616
Air mass flow rate in tube, lb/sec-ft^2	9.61
Air flow rate outside tubes, lb/sec	4.92
Air flow passage area outside tubes, ft^2	1.139
Air mass flow rate outside tubes, lb/sec-ft^2	4.32
Recuperator heat transfer	
Tube-side heat transfer coefficient, Btu/hr-ft^2-°F	31.5
Shell-side heat transfer coefficient Btu/hr-ft^2-°F	15.7

Table 6.2 (continued)

Overall heat transfer coefficient based on tube outside surface area, Btu/hr-ft -°F	9.7
Total tube effective surface area, outside, ft	1420
Economizer geometry and flow	
Tube OD, in	1.0
Tube ID, in	0.83
Total number of tubes	161
Effective tube length, ft	14
Tube centerline spacing along furnace wall, in	1.5
Air flow rate through tubes, lb/sec	5.92
Air flow passage area in tubes, ft	0.605
Air mass flow rate in tubes, lb/sec-ft	9.79
Combustion gas flow rate outside tubes, lb/sec	1.1
Combustion gas flow passage area outside tubes, ft	1.26
Combustion gas mass flow rate outside tubes, lb/sec-ft	1.87
Economizer heat transfer	
Tube-side heat transfer coefficient, Btu/hr-ft -°F	31.6
Combustion gas-side heat transfer coefficient Btu/hr-ft -°F	4.4
Average radiant heat flux to heater, Btu/hr-ft	623
Total tube effective surface area, outside, ft	590
Temperature Distribution in heat exchangers	
Compressor air inlet, °F	80
Compressor air outlet, °F	499
High pressure air entering economizer, °F	760
High pressure air leaving economizer, °F	933
High pressure air entering fluidized bed, °F	933
High pressure air leaving fluidized bed, °F	1500
Low pressure air entering regenerator, °F	889
Low pressure air leaving regenerator, °F	578
Combustion gas in fluidized bed, °F	1700
Greatest temperature difference in regenerator, °F	129
Least temperature difference in regenerator, °F	79
LMTD in regenerator, °F	102
Greatest temperature difference in economizer, °F	767
Least temperature difference in economizer, °F	50
LMTD in economizer, °F	263
Greatest temperature difference in fluidized bed, °F	767
Least temperature difference in fluidized bed, °F	200
LMTD in fluidized bed, °F	422

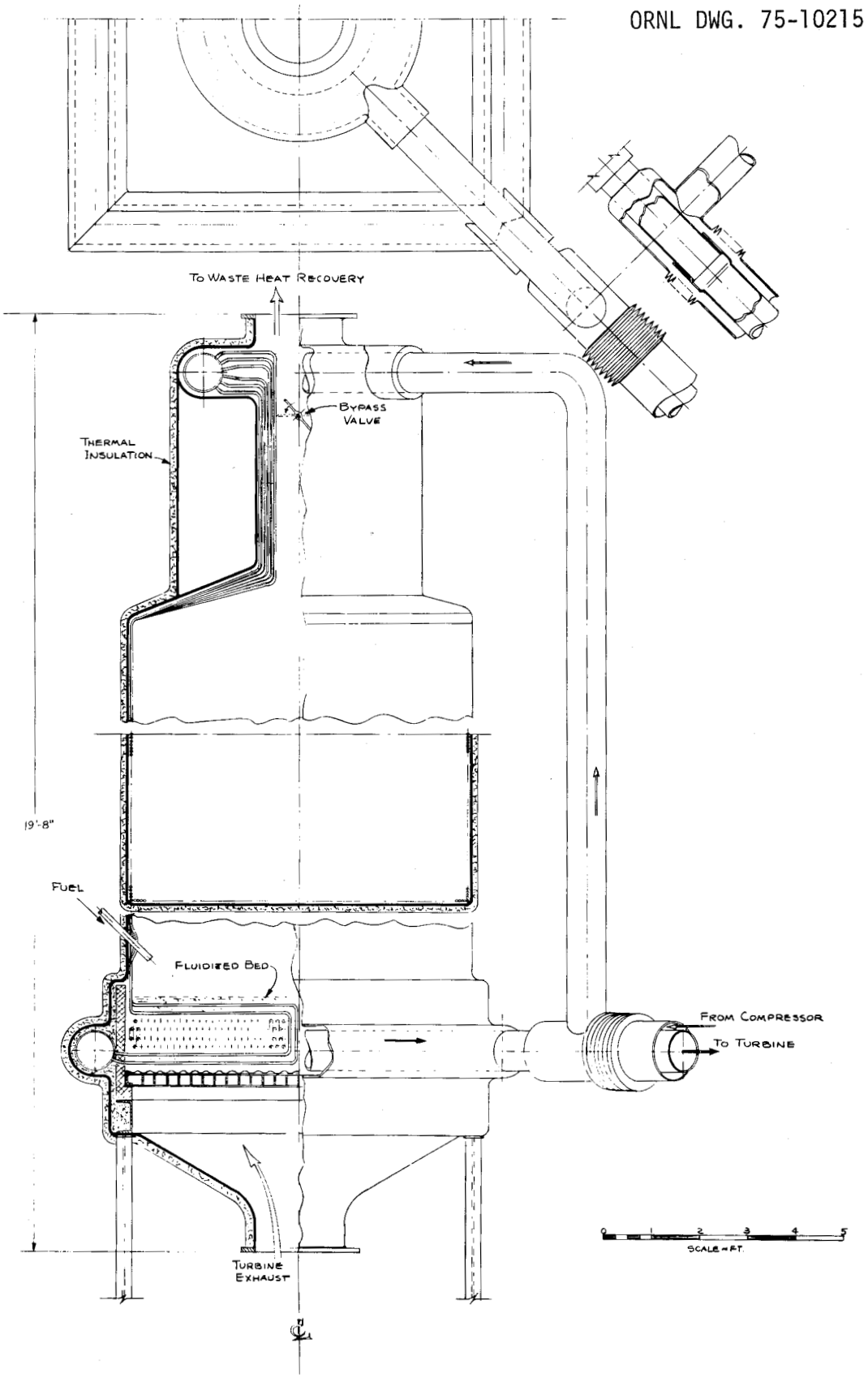

Fig. 6.6. Fluidized bed combustion chamber and air heater unit with an economizer but no integral recuperator.

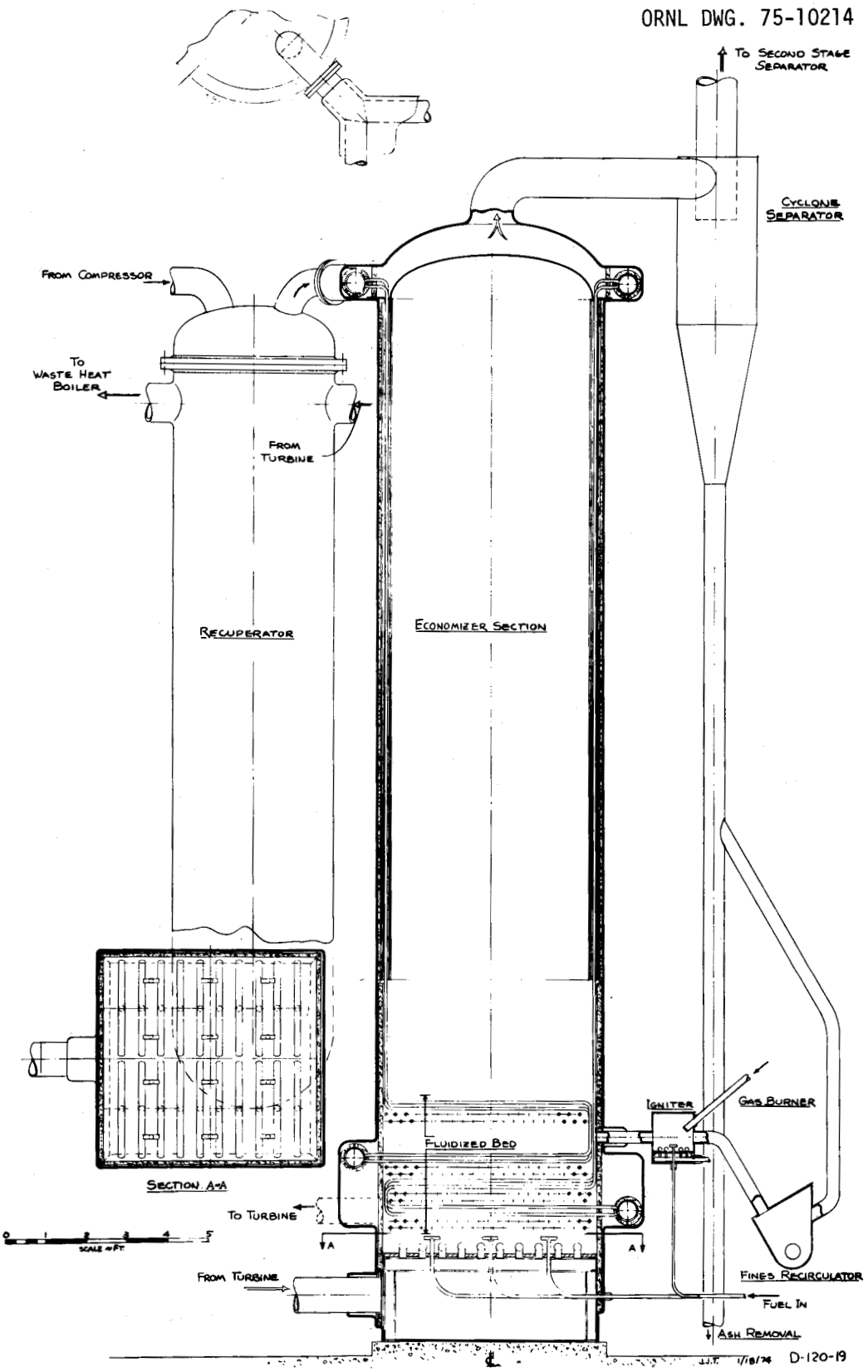

Fig. 6.7. Section through a fluidized bed combustion system with the walls of the plenum above the bed extended vertically upward so that the economizer region is in the form of a hollow square annulus as in Fig. 6.3b.

A second important assumption involves the fuel circulation in the bed. The burning of the fuel was assumed to be uniform in the bed and therefore the fuel must circulate freely in the fluidized bed for this to be accomplished. With the closely spaced heat exchanger tubes in the bed and the low superficial velocity of 2.2 ft/sec it is not certain that adequate circulation of the fuel will be obtained.

The overall layout as shown in Fig. 6.7 offers several advantages. Among these are the inherent simplicity of an open cycle, the ease of fabrication of the economizer since only one tube bend is required in the transition from the fluidized bed exchanger to the gas inlet header, and the overall ease of assembly of the economizer and fluidized bed exchanger.

A design feature of special note is that the tubes were run all the way across the fluidized bed with a manifold for the north and south sides small enough so that they could be pushed between the upper and lower legs of the tubes for the east and west sides in the course of assembly of the furnace. To help provide clearance for this operation, the header sheet would be relatively thick but would represent only about a 60 deg arc of the circular section of the manifold. The welds between this thickened header sheet region and the balance of the manifold would be made after the tube bundles had been assembled to form the furnace. This approach has the advantage that it would be extremely difficult to disassemble the furnace for major repairs if this should prove necessary.

Yet another layout for an open cycle system is shown in Fig. 6.8. In this instance the recuperator was made an integral part of the furnace and economizer so that the tubes carrying the high pressure air from the compressor to the turbine extend continuously from the point where they enter the recuperator all the way through the assembly to the manifold where they leave the fluidized bed. Separation of the combustion gas stream from the air stream through the recuperator would be accomplished by inserting specially shaped strips between the layers of tubes in the return bend region between the economizer and recuperator. Note that the economizer region is similar to that of Fig. 6.2d, i.e., the tubes are arranged in a relatively elongated rectangle. In this instance note that only two layers of tubes are used in a traverse of the bed and hence if they are to be spaced on centerlines 3 diam apart, it is necessary to make

ORNL DWG. 75-10213

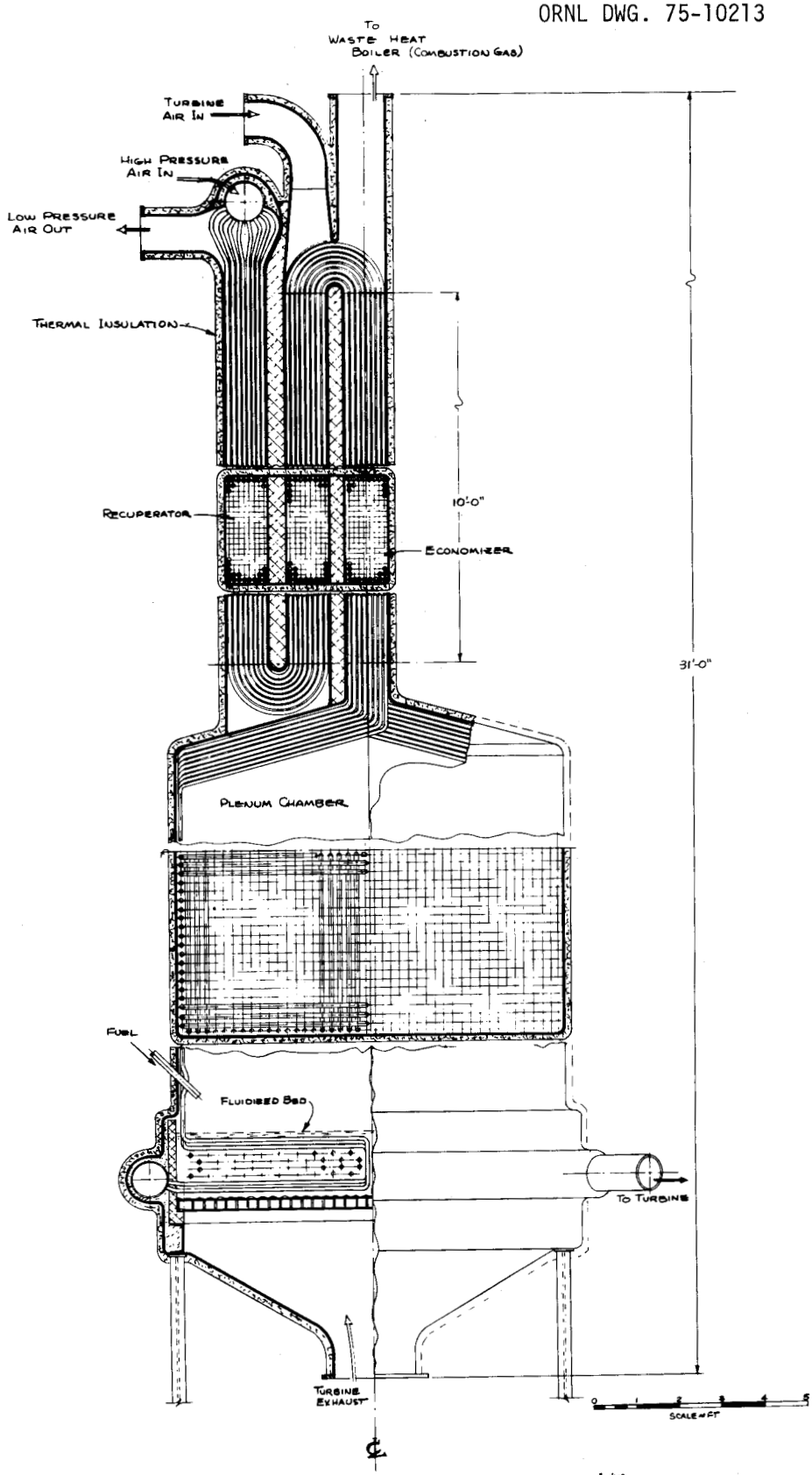

Fig. 6.8. Fluidized bed combustion chamber and air heater unit with an integral economizer and recuperator.

use of a tube centerline spacing in the plenum chamber wall of 1 1/2 tube diam. This effect can be seen in the horizontal cross section of the bed that is shown as a broken out region between the upper and lower portions of the plenum chamber in Fig. 6.8.

The two principal layouts for the fluidized bed-furnace-economizer region that were prepared for the closed cycle system are shown in Figs. 6.9 and 6.10. These layouts are essentially the same except for the method used in handling the problem of carrying the tubes from the hollow square of the plenum chamber into the slab economizer arrangement of Fig. 6.3d. There is little difference in the difficulty of the tube bending operation between these two arrangements. For the layout of Fig. 6.9 the out-of-plane bend lies in the region between the economizer and the high-pressure air inlet manifold just above it whereas in the layout of Fig. 6.10 the out-of-plane bend lies in the region between the plenum chamber and the economizer. The principal advantage of the layout of Fig. 6.10 is that the outer casing is simpler and entails less surface area and hence somewhat lower heat losses to the surroundings.

In reviewing these various layouts it was decided that the layout of Fig. 6.10 would be employed as the reference design for purposes of this report. However, there are many subtle problems involved and it is expected that more detailed studies in the Phase II portion of the effort may lead to substantial changes.

Design data for the reference design of Fig. 6.10 are summarized in Table 6.3.

Heat Exchanger Design Charts for a Coal-Fired Gas Turbine System

The vital questions of overall system design are closely interrelated with the costs of the various heat exchangers employed in the system. The performance and cost of any given heat exchanger in turn involves a host of variables. These variables include the type of heat transfer matrix, the relative mass flow rates on the two sides of the heat exchanger, the passage equivalent diameters and spacing, the heat transfer coefficient for each side, the pressure drop for each side, the temperature rise or temperature drop for each side, and the logarithmic mean temperature difference.

ORNL DWG. 75-14469

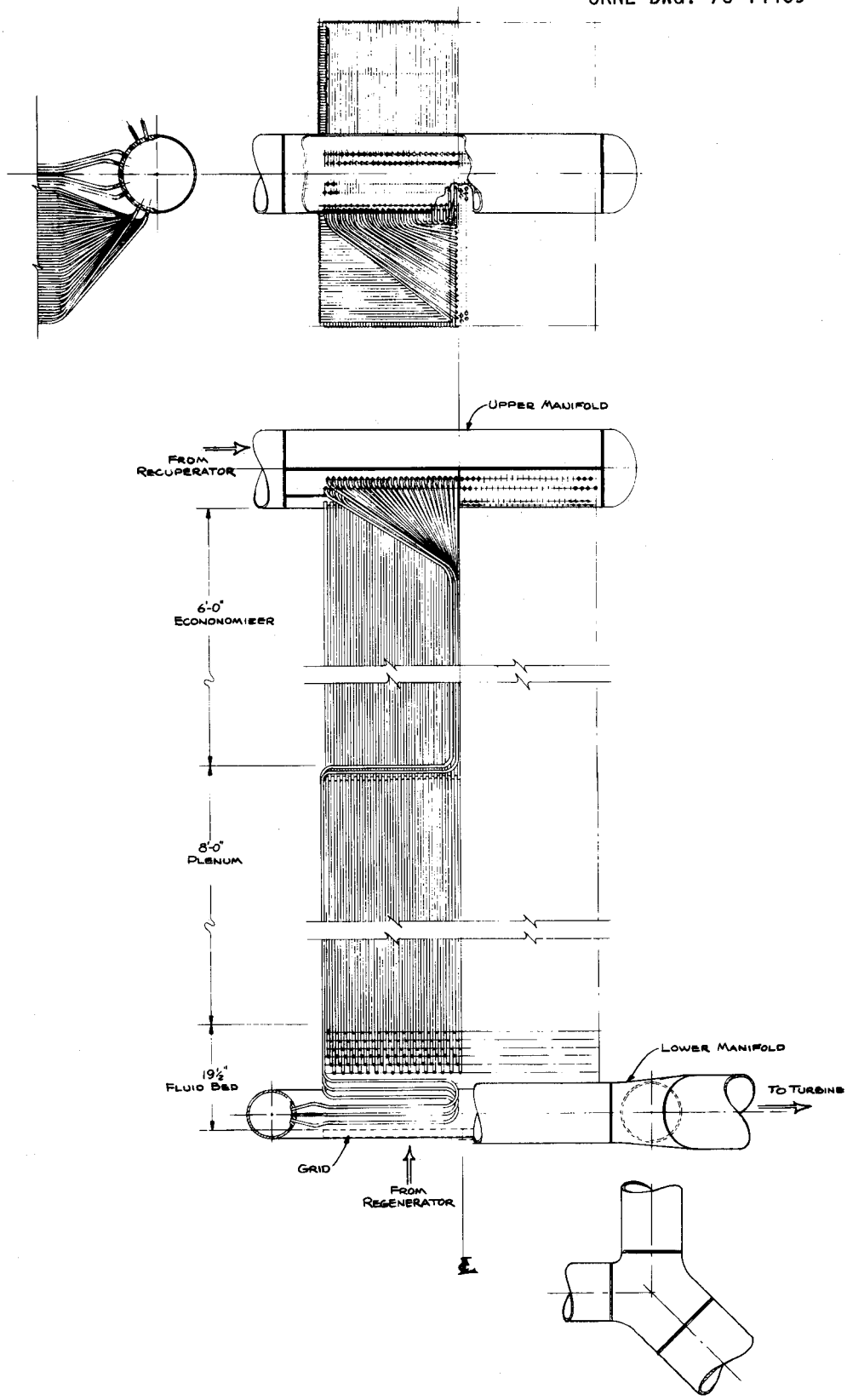

Fig. 6.9. Layout for a fluidized bed combustion system with an economizer region having the cruciform horizontal cross-section shown in Fig. 6.3c.

ORNL DWG. 75-14464

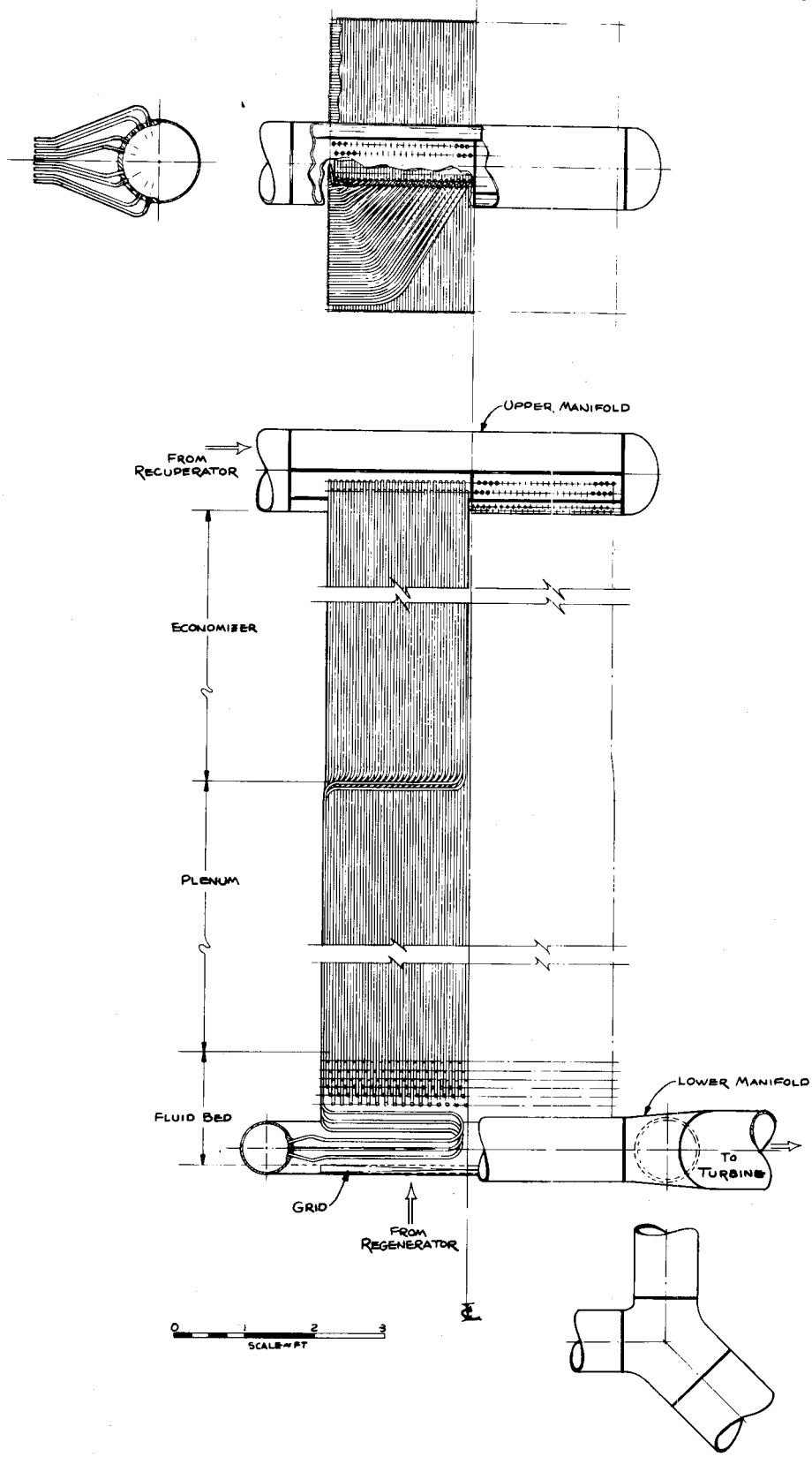

Fig. 6.10. Layout for a fluidized bed combustion system with the economizer region in the form of a flat slab as indicated in Fig. 6.3d. (This layout was chosen as the Reference Design.)

Table 6.3. Principal Parameters for the Reference Design Closed Cycle Gas Turbine with a Fluidized Bed Coal Combustion System

Thermodynamic Cycle	
Net electrical output, kW(e)	673
Gross electrical output, kW(e)	748
Turbine air inlet temperature, ^{o}F	1500
Compressor air inlet temperature, ^{o}F	80
Compressor pressure ratio	3.5
Full load compressor discharge pressure, atm	12
Pressure losses in ducts and heat exchangers, $\Delta P/P$, %	10
Adiabatic efficiency of the turbine, %	87
Adiabatic efficiency of the compressor, %	84
Thermodynamic cycle efficiency, gross, %	31.1
Thermodynamic cycle efficiency, net, %	27.9
Turbine air flow, lb/sec	14.15
Compressor work, Btu/lb air	66.35
Turbine work, Btu/lb air	116.47
Net work from the cycle, Btu/lb air	50.12
Furnace	
Higher heating value of coal, Btu/lb	12,000
Combustion air flow, lb/sec	1.97
Flue gas flow, lb/sec	2.13
Coal flow rate, lb/sec	0.188
Coal flow rate, lb/hr	677
Excess air, %	10
Air temperature into the bed, ^{o}F	997
Fluid bed operating temperature, ^{o}F	1650
Fluid bed operating density, lb/ft^3	55
Superficial gas velocity leaving bed, ft/sec	2.65
Fluid bed cross-sectional area, ft^2	
Fluid bed depth, in.	20
Weight of material in the bed, lb	2300
No. of tubes in the bed	628
Tube OD, in.	0.500
Tube ID, in.	0.444
Tube length in bed, ft	6.5
Air mass flow rate inside tubes, $lb/sec \cdot ft^2$	21.0
Plenum chamber height, ft	8.0
Tube centerline spacing in plenum wall, in.	0.50
Weight of tubing in bed and plenum walls, lb	1460
Total surface area inside tubes, ft^2	1200
Recuperator	
High pressure air inlet temperature, ^{o}F	355
High pressure air outlet temperature, ^{o}F	967
High pressure air mass flow rate, $lb/sec \cdot ft^2$	21.5
Low pressure air mass flow rate, $lb/sec \cdot ft^2$	8.62

Table 6.3 (continued)

Low pressure air inlet temperature, °F	1070
Low pressure air outlet temperature, °F	466
No. of 0.50 in. OD, 0.444 in. ID tubes	611
Tube length, ft	47
High pressure air mean density, lb/ft^3	0.368
Low pressure air mean density, lb/ft^2	0.100
Low pressure air pressure drop, $\Delta P/P$	0.019
High pressure air pressure drop, $\Delta P/P$	0.019
Combined pressure drop, $\Delta P/P$, %	0.038
Total surface area inside tubes, ft^2	
Economizer	
High pressure air inlet temperature, °F	967
High pressure air outlet temperature, °F	1060
High pressure air mass flow rate, $lb/sec\text{-}ft^2$	21.0
Flue gas mass flow rate, $lb/sec\text{-}ft^2$	2.87
Flue gas inlet temperature, °F	1650
Flue gas outlet temperature, °F	1107
Number of 0.50 in. OD, 0.444 in. ID tubes	628
Tube length, ft	4.63
Total surface area inside tubes, ft^2	338
High pressure air mean density, lb/ft^3	0.325
Flue gas air mean density, lb/ft^3	0.0722
High pressure air pressure drop, $\Delta P/P$	0.006
Flue gas air pressure drop, $\Delta P/P$	0.0116
Regenerator	
Heat transfer matrix material	Cercor
Heat transfer matrix dia., in.	30
Heat transfer matrix length, in.	3
Heat transfer matrix face area for flue gas, ft^2	3.27
Heat transfer matrix face area for combustion air, ft^2	1.64
Flue gas inlet temperature, °F	1107
Flue gas outlet temperature, °F	300
Combustion air inlet temperature, °F	80
Combustion outlet temperature, °F	997
Pressure drop, in. H_2O (total for both streams)	10
Heat transfer matrix surface area, ft^2/ft^3	960

Which of these should be specified and which would then be determined depends in part on the judgment of the system designer. Irrespective of how one may approach the system design, however, one finds that a change in a heat exchanger in any one part of the cycle influences conditions, particularly temperatures, in other parts of the cycle so that the system is highly redundant. In principle, it is possible to get solutions by iteration, but if this is done blindly, there are so many combinations and permutations that one is likely to miss the region of best performance without even realizing its existence. Thus, it is extremely helpful to have a set of charts relating the principal performance parameters for each of a set of geometrically similar heat exchangers so that one can see the effects of changes in one or a few heat exchanger design parameters on the others. For these charts to be most useful, the ground rules for drawing up the charts for each particular heat exchanger application, i.e., recuperator, economizer, waste heat boiler, fluidized bed tube matrix, cooler, or regenerator in general must be chosen with care for each particular case.

Basic Relations

A type of chart that has been found extremely useful for the selection of heat transfer matrices for power plant applications is described in Chapter 4 of Ref. 2. The first type of chart makes use of heating effectiveness* as a function of fluid passage length for a series of fluid mass flow rates in the more important of the two fluid streams. As indicated in Ref. 2, for some types of heat exchanger the resulting graph will consist of a fan of straight lines, and charts of this type can be prepared by calculating only a few points and then drawing a fan of straight lines through them. This condition will hold, for example, for the fluidized bed or the waste heat boiler because in both cases the metal surface temperature is kept essentially constant, i.e., at the temperature of the fluidized bed or the temperature of the boiling water for these two cases. That is,

---

*Heating or cooling effectiveness is defined as the ratio of the temperature rise or drop in the fluid stream of prime interest to the difference between the inlet temperatures of the two fluid streams

there will be no change in the temperature on one side of the heat exchanger as the mass flow rate and temperature conditions on the other side of the transfer surface are varied. In the economizer, recuperator, and cooler the situation is rendered more complex because changes in operating conditions on one side of the heat exchanger cause changes in the temperatures on the other side and hence in the log mean temperature difference. These effects lead to a set of curves rather than straight lines on the chart for effectiveness vs flow passage length.

Calculational Procedure and Design Charts for Heat Exchanger Effectiveness

The procedure followed in carrying out the calculations and plotting the design charts for each of the different types of heat exchanger in the system differ in sometimes subtle ways from those followed for the other charts. As a consequence, it seems important to delineate the procedures used in each instance. In all cases in the sections that follow the nomenclature of Table 6.4 has been employed.

Tube Matrix Proportions. In developing a set of reference design charts, it was decided to make use of three representative tube diameters, i.e., 0.5 in., 0.75 in., and 1.0 in. OD tubes. The corresponding tube ID's were taken as 0.444 in., 0.666 in., and 0.888 in. These values together with internal and external surface areas and the internal flow passage areas are listed in Table 6.5. In addition, Table 6.5 includes the centerline spacing, the ratio of tube-side to shell-side flow passage area, the equivalent passage diameter, and the tube surface area per square foot of tube inside flow passage area per foot of length for the configurations considered for both the recuperator and the economizer.

In determining the overall heat transfer coefficient u it is necessary to establish the ratio of the mass flow rates. If the pressure drop ratio $\Delta P/P$ is to be the same for both flows in the recuperator and the pressure ratio across the compressor is about 3.5, the flow passage area on the shell side should be about 2.5 times that on the tube side. This gives a heat transfer coefficient on the shell side that is only 41% of that on the tube side. Allowing for the fact that the weight flow of combustion gas is roughly a sixth of the turbine air weight flow and following a similar rationale the area ratio for the economizer was taken as 0.805 times the tube-side flow passage area.

Table 6.4. Nomenclature

General:

A	Total heat transfer surface area, ft^2
A′	Heat transfer surface area per square foot of tube-side flow passage area per foot of length, ft^2/ft^3
c_p	Specific heat, $Btu/lb \cdot {}^oF$
d_{eq}	Equivalent passage diameter, in
d_o	Tube OD, in.
G′	Mass flow rate, $lb/ft^2 \cdot sec$
h	Heat transfer coefficient, $Btu/hr \cdot ft^2 \cdot {}^oF$
L	Heat transfer matrix length in the air flow direction, ft
P	Absolute pressure, psia
P	Pressure drop, psi
	Ratio of gas density to density of air at standard temperature and pressure
s	Tube spacing, in.
u	Overall heat transfer coefficient, $Btu/hr \cdot ft^2 \cdot {}^oF$
W	Weight flow rate of fluid stream, lb/sec

Temperature Differences:

ITD	Difference between the inlet temperatures of the two fluid streams, ^oF
GTD	Greatest local temperature difference between the two fluid streams, ^oF
LTD	Least local temperature difference between the two fluid streams, ^oF
LMTD	Log arithmic mean temperature difference between two fluid streams, ^oF
t	Temperature rise (or drop) in a fluid stream, ^oF
T	Local temperature difference between two fluid streams, ^oF

Subscripts:

1	Turbine air stream
2	Fluid stream giving up heat to or taking heat from the turbine air stream

Table 6.5. Geometric Data on Reference Design Tube Matrices for the Fluid Bed, Economizer, and Recuperator

Tube OD, in.	0.50	0.75	1.00
Tube ID, in.	0.444	0.666	0.888
Internal flow area, in.^{3}/tube	0.1548	0.3483	0.6192
Inside surface area, ft^2/ft of tube	0.123	0.185	0.246
Cross-sectional area of tube wall, in.^{2}/tube	0.0415	0.0934	0.1660
Mean surface area of matrix, ft^2/ft^3 of internal flow passage	115	172.2	230
Number of tubes for 1 ft^2 of internal flow passage	930	413	232
Recuperator			
Ratio of shell-side to tube-side flow passage areas	2.5	2.5	2.5
Ratio of shell-side volume to total matrix volume	0.6635	0.6635	0.6635
Tube centerline spacing (triangular), in.	0.815	1.222	1.63
Equivalent diameter of shell-side flow passage, in.	1.00	1.50	2.00
Volume of heat transfer matrix, ft^3/ft^3 of tube-side flow passage	3.768	3.768	3.768
Economizer			
Ratio of shell-side to tube-side flow mass flow rates	3.33	3.33	3.33
Ratio of tube-side to shell-side weight flow rates	4.5	4.5	4.5
Ratio of shell-side volume to total matrix volume	0.369	0.369	0.369
Tube centerline spacing (triangular), in.	0.60	0.90	1.20
Equivalent diameter of shell-side flow passage, in.	0.295	0.447	0.590
Volume of heat transfer matrix, ft^3/ft^3 of tube-side flow passage	2.01	2.01	2.01

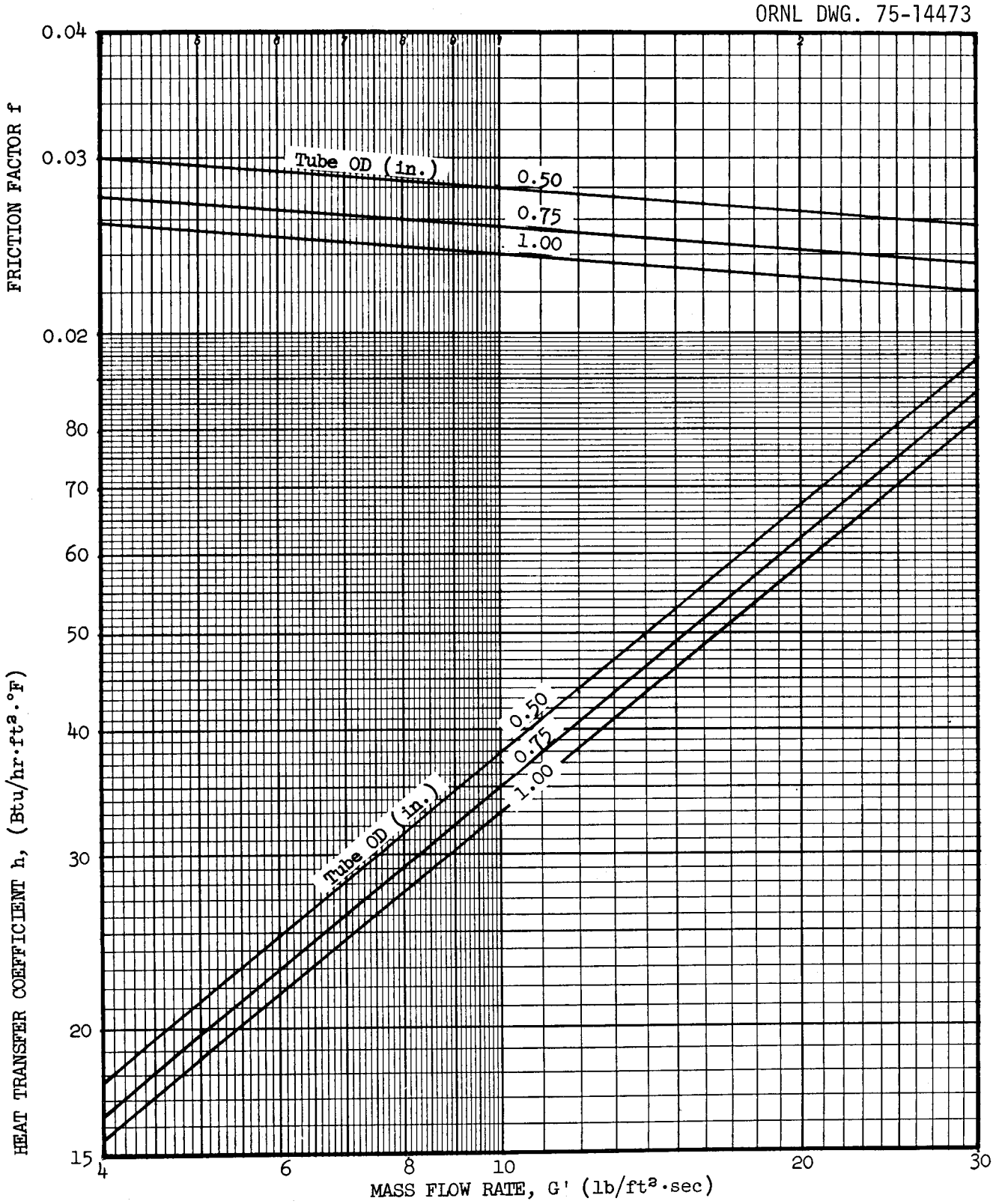

Fig. 6.11. Heat transfer coefficient and friction factor for air flowing through round tubes at 800°F.

Heat Transfer Coefficient. The heat transfer coefficient for flow inside of round tubes is given in Fig. 6.11 as a function of the mass flow rate for the three tube diameters of Table 6.5. These values were estimated from Fig. H5.5, p. 318 of Ref. 2 for a mean temperature of 800°F, the estimated mean temperature in the recuperator. The values were corrected for the somewhat different temperatures in the economizer and fluidized bed by using the curves in Fig. H5.6, p. 319 of Ref. 2. The heat transfer coefficients on the shell side for flow parallel to the tubes in the recuperator and economizer were obtained in a similar fashion using the equivalent diameter on the shell side.

Fluid Bed. The fluidized bed will operate at an essentially constant temperature that will be determined mainly by sulfur removal considerations. This temperature will fall in the range of 1500 to 1700°F. The heat transfer coefficient in the fluidized bed depends primarily on the particle size (see Fig. 6.12) and will be essentially independent of the air flow rate through the bed.[3] For the particle size range of interest in this

ORNL DWG 76-4914

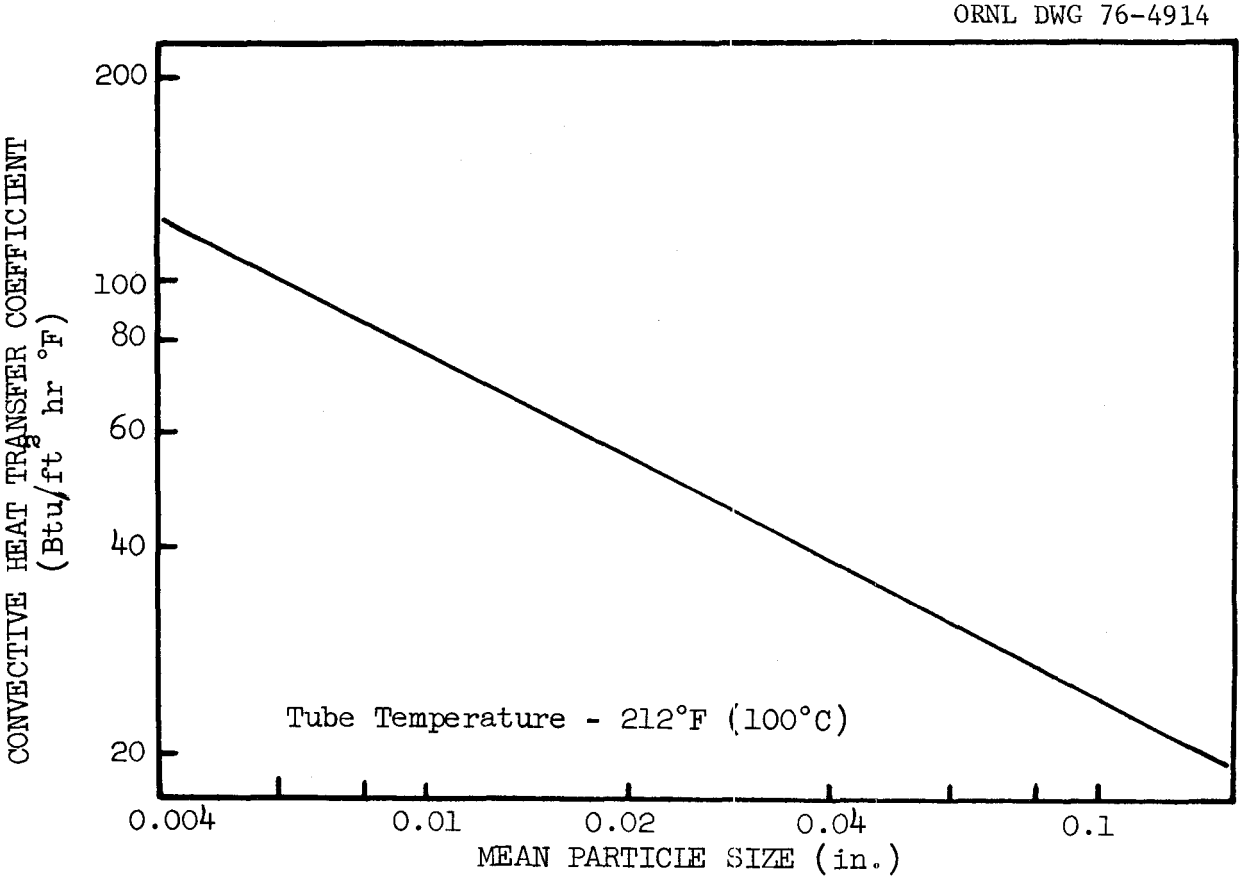

Fig. 6.12. Fluid bed heat transfer coefficients. (Ref. 3).

report, the heat transfer coefficient in the bed will run at least 50 Btu/hr·ft^2·°F. To be conservative, a value of 50 Btu/hr·ft^2·°F will be used here. Under normal operating conditions the air flow and fuel flow rates into the bed will be varied to maintain the bed temperature constant when the rate of heat extraction from the bed is varied. As derived in Ref. 2, page 63-66, for this condition we may write

$$\text{Heating effectiveness} = 1 - e^{-\frac{uA}{W_1 c_p \; 3600}}$$

This can be put in terms of the mass flow rate for the turbine air per square foot of flow passage area. Taking c_p = 0.25 Btu/lb·°F gives

$$\text{Effectiveness} = 1 - e^{-\frac{uA'L}{G_1' 900}}$$

For a typical condition with an air flow rate inside the tubes of 10 lb/ft^2·sec through 1/2 in OD tubes, the heat transfer coefficient inside the tubes as given by Fig. 6.11 will run 38 Btu/hr·ft^2·°F. Thus, the overall heat transfer coefficient u becomes

$$u = \frac{1}{1/50 + 1/38} = 21.59 \text{ Btu/hr·ft}^2\text{·°F}$$

For this condition and the .50 in. OD tubes of Table 6.5 the effectiveness then becomes

$$\text{Effectiveness} = 1 - e^{-\frac{21.59 \times 115 \text{ L}}{10 \times 0.25 \times 3600}} = 1 - e^{-0.2759 \text{ L}}$$

For a typical air flow passage length of 10 ft, the effectiveness becomes 0.937. The effectiveness for other values of the air mass flow rate and tube diameter were calculated and the results are summarized in Table 6.6. A typical chart for the effectiveness as a function of the heated length of tubing is given in Fig. A1 of Appendix A.

Table 6.6. Summary of Calculations for the Heating Effectiveness of the Heater Tubes in the Fluidized Bed (The calculations are for tubes having a 10 ft heated length using the relation:

$$n = 1 - e - \frac{uA}{W_{ep}} = 1 - e \frac{u\ 1150}{G:\ 900\ 2d} = 1 - e - \frac{u\ .6389}{G:\ d}$$

G	8	10	12	14	16	20	25	30
d = 1.0								
h	27.52	32.99	37.96	43.01	48.53	58.33	70.08	81.40
h	50	50	50	50	50	50	50	50
U	17.76	19.88	21.60	23.15	24.63	26.95	29.24	31.06
$e \frac{u\ .8517}{G:}$	.1407	.1733	.2051	.2341	.2590	.3074	.3606	.4060
η@10'	.7579	.7192	.6834	.6523	.6260	.5772	.5263	.4839
d = 3/4								
h	29.15	34.95	40.20	45.55	51.41	61.78	74.23	86.21
h	50	50	50	50	50	50	50	50
U	18.42	20.58	22.32	23.87	25.38	27.70	29.94	31.75
$e \frac{u\ .8517}{G:}$	.1407	.1733	.2051	.2341	.2590	.3074	.3606	.4060
η@10'	.8593	.8267	.7949	.7659	.7410	.6926	.6394	.5940
d = 1/2								
h_1	31.61	37.9	43.6	49.4	55.75	67.0	80.5	93.5
h_2	50	50	50	50	50	50	50	50
U	19.38	2.160	23.31	24.88	26.39	28.65	30.86	32.68
$e \frac{u\ 1.278}{G:}$	.04523	.06327	.08353	.1032	.1215	.1603	.2065	.2486
η@10'	.9548	.9367	.9165	.8968	.8785	.8397	.7935	.7514

Recuperator. For a closed cycle gas turbine, the weight flow of air on the shell-side is equal to that on the tube-side of the heat exchanger. Thus, the temperature rise on the tube-side is equal to the temperature drop on the shell-side, and the temperature difference between the two streams for pure counter flow conditions is constant throughout the length of the heat exchanger. The heat added to either fluid stream may be equated to the heat transferred through the available surface area to give

$$G' c_p \; 3600 \; \delta t = uA'L\Delta T$$

$$\frac{\delta t}{\Delta T} = \frac{u \; A' \; L}{G' c_p \; 3600} = \frac{uA'L}{G'900}$$

where the specific heat of the air is taken as 0.25 Btu/lb·°F. Using the mean surface area value for 0.50 in. OD tubes given in Table 6.5 and $c_p = 0.25$ gives

$$\frac{\delta t}{\Delta T} = \frac{u \; 115L}{G'900} = \frac{0.1275 \; uL}{G'}$$

The effectiveness is given by

$$\text{Effectiveness} = \frac{\delta t}{\Delta T + \delta t} = \frac{1}{\Delta T/\delta t + 1}$$

The overall heat transfer coefficient u can be determined for the heat exchanger proportions of Table 6.5 which give a flow passage area on the shell side 2.5 times that on the tube side. Thus, for 0.50 in. OD tubes, a tube-side mass flow rate of 10 lb/sec·ft^2, and the heat transfer coefficients obtained from Fig. 6.11 gives

$$u = \frac{1}{1/38 + 1/15.6} = \frac{1}{0.0904} = 11.06$$

$$\delta t/\Delta T = \frac{0.1278 \times 11.06}{10} = 0.141 \; L$$

The effectiveness for a tube length of 20 ft becomes

$$\text{Effectiveness} = \frac{1}{1/2.82 + 1} = 0.738$$

The calculations for a typical case the the resulting chart are given in Table 6.7 and Fig. A2 of Appendix A.

Economizer. The heat exchanger between the combustion gases leaving the plenum above the fluidized bed and the air stream flowing from the recuperator to the tube matrix in the furnace presents some difficult problems. In the first place the total weight flow of air in the turbine circuit is roughly 5 times that of the combustion air flow through the furnace, hence the change in the combustion gas stream. Thus, it is more appropriate to design air stream. Note, too, that the log mean temperature difference between the two streams is a complex function of the temperature changes in the streams, i.e., of the mass flow ratios, flow passage length, heat transfer coefficients, etc. In attempting to develop appropriate relations, one can begin by equating the heat added to the turbine air stream to that removed from the combustion gases, i.e.,

$$W_1 c_p \ \delta t_1 = W_2 c_p \ \delta t_2$$

In calculating the log mean temperature difference, one may write from fundamental considerations that

$$ITD = GTD + \delta t_1; \ GTD = ITD - \delta t_1; \ LTD = ITD - \delta t_2$$

$$LMTD = \frac{GTD - LTD}{\ln\left(\frac{LTD}{GTD}\right)} = \frac{ITD - \delta t_1 - ITD + \delta t_2}{\ln\left(\frac{ITD - \delta t_1}{ITD - \delta t_2}\right)} = \frac{\delta t_2 - \delta t_1}{\ln\left(\frac{1 - \delta t_1 / ITD}{1 - \delta t_2 / ITD}\right)}$$

Table 6.7. Summary of Calculations for the Recuperator Heating Effectiveness Chart for 0.50 in. OD Tubes for a Shell-side Flow Passage Area 2.5 Times the Tube-side Flow Passage Area.

G_1', lb/ft²·sec	4.0	6.0	8.0	10.0	12.0	14.0	16.0	20.0	25.0	30.0
G_2', lb/ft²·sec	1.6	2.4	3.2	4.0	4.8	5.6	6.4	8.0	10.0	12.0
h_1, Btu/hr·ft²·°F	17.51	24.86	31.61	37.9	43.6	49.4	55.75	67.0	80.5	93.5
h_2, Btu/hr·ft²·°F	7.45	10.25	13.0	15.6	18.0	20.34	22.7	27.0	32.4	37.4
q_1 @ W=0.0765 lb/ft³	.0224	.0503	.0896	.140	.201	.275				
q_2	.00358	.00807	.0144	.0224	.0323	.044				
$U = 1/(1/h_1 + 1/h_2)$	5.226	7.258	9.212	11.051	12.740	14.408	16.13	19.30	23.06	26.77
f_1	.030	.029	.0285	.028	.0275	.0272	.0270	.0265	.0261	.0258
Tube Length, ft					$\delta t/\Delta t = 0.1275\ U\ L\ /\ G_1'$					
20	3.331	3.084	2.936	2.818	2.707	2.624	2.571	2.461	2.352	2.275
40	6.664	6.169	5.872	5.636	5.415	5.249	5.141	4.922	4.704	4.551
60	9.995	9.254	8.809	8.454	8.122	7.873	7.712	7.382	7.056	6.826
80	13.327	12.338	11.745	11.272	10.829	10.497	10.283	9.843	9.408	9.102
100	16.659	15.423	14.681	14.090	13.537	13.122	12.854	12.304	11.761	11.377
120	19.991	18.507	17.617	16.908	16.244	15.746	15.424	14.765	14.113	13.653
140			20.554	19.727	18.951	18.370	17.995	17.225	16.465	15.928
160							20.566	19.686	18.817	18.204
Tube Length, ft					$\eta = (\delta t/\Delta t)\ /\ (1+\delta t/\Delta t)$					
20	0.769	0.755	0.746	0.738	0.730	0.724	0.720	0.711	0.702	0.695
40	0.870	0.860	0.854	0.849	0.844	0.840	0.837	0.831	0.825	0.820
60	0.909	0.902	0.898	0.894	0.890	0.887	0.885	0.881	0.876	0.872
80	0.930	0.925	0.922	0.919	0.915	0.913	0.911	0.908	0.904	0.901
100	0.943	0.939	0.936	0.934	0.931	0.929	0.928	0.925	0.922	0.919
120	0.952	0.949	0.946	0.944	0.942	0.940	0.939	0.937	0.934	0.932
140			0.953	0.952	0.950	0.948	0.947	0.945	0.943	0.941
160							0.954	0.952	0.950	0.948

$M_1/M_2 = 1.0$; $P_2/P_1 = 4.0$

For a typical case

$$t_2 = 4.5\ \delta t_1\ , \text{ and}$$

$$LMTD = \frac{3.5\ \delta t_1}{\ln\left(\frac{1 - \delta t_1/ITD}{1 - 4.5\delta t_1/ITD}\right)}$$

Equating the heat added to the turbine air to the heat transferred leads to

$$W_1 c_p\ 3600\ \delta t_1 = uALMTD = \frac{3.5\ uA\delta t}{\ln\frac{1 - \delta t_1/ITD}{1 - 4.5\delta t_1/ITD}}$$

Using an air specific heat of 0.25 Btu/lb °F, the turbine air mass flow rate, and the heat transfer surface area per square foot of turbine air flow passage area per foot of tube length yields

$$900G_1' = \frac{3.5\ uA'L}{\ln\frac{1 - \delta t_1/ITD}{1 - 4.5\delta t_1/ITD}}$$

For 0.50 in. OD tubes and the recuperator proportions of Table 6.5 for 0.50 in. diameter tubes gives

$$L = \frac{2.236\ G_1'}{u}\ \ln\left(\frac{1 - \delta t_1/ITD}{1 - 4.5\delta t_1/ITD}\right)$$

This equation can be solved for the tube length by selecting a series of values for the turbine air mass flow rate and the ratio of the turbine air temperature rise to the inlet temperature difference for the assumed ratio of the turbine air temperature rise and combustion air temperature drop. Table 6.8 shows a typical set of calculations, and Fig. A3 the resulting chart which is for the cooling effectiveness, and is based on the temperature drop in the combustion gas.

Table 6.8. Summary of Calculations for the Economizer Cooling Effectiveness Chart for 0.50 in. OD Tubes for a Shell-side Flow Passage Area 3.33 Times the Tube-side Flow Passage Area.

G_1', lb/ft²·sec		4.0	6.0	8.0	10.0	12.0	14.0	16.0	20.0	25.0	30.0
G_2', lb/ft²·sec		1.2	1.8	2.4	3.0	3.6	4.2	4.8	6.0	7.5	9.0
h_1, Btu/hr·ft²·°F		17.51	24.86	31.61	37.9	43.6	49.4	55.75	67.0	80.5	93.5
h_2, Btu/hr·ft²·°F		6.684	9.489	12.066	14.466	16.642	18.856	21.280	25.574	30.727	35.689
$U = 1/(1/h_1 + 1/h_2)$											
$\frac{\delta t_1}{ITD}$	$\eta = \frac{4.5\delta t_1}{ITD}$	Length $= \frac{G'_1 2.236}{U} \ln \frac{1 - \frac{\delta t_1}{ITD}}{1 - \frac{4.5\delta t_1}{ITD}}$									
.15	0.675	1.7774	1.8778	1.9691	2.0529	2.1414	2.2049	2.2329	2.3225	2.4162	2.4963
.16	0.720	2.0313	2.1461	2.2505	2.3462	2.4474	2.5200	2.5520	2.6543	2.7615	2.8530
.17	0.765	2.3331	2.4650	2.5848	2.6948	2.8110	2.8944	2.9311	3.0487	3.1718	3.2769
.18	0.810	2.7037	2.8566	2.9954	3.1228	3.2575	3.3542	3.3967	3.5330	3.6756	3.7975
.19	0.855	3.1808	3.3606	3.5240	3.6738	3.8323	3.9460	3.9961	4.1564	4.3241	4.4675

h_1 = same as for $M_1/M_2 = 1.0$

$h_2 = h_1 \times 0.3817$ (for 0.50 in. tubes)

$M_1/M_2 = 4.5$

If the ratio of the combustion gas temperature drop to the turbine air temperature rise differs substantially from the value of 4.5 chosen for the chart of Fig. A3, that chart can still be used if the length is increased by an appropriate factor, i.e.,

$$\text{Correction factor} = \frac{\ln\left(\dfrac{1 - \delta t_1/\text{ITD}}{1 - \delta t_2/\text{ITD}}\right)}{\ln\left(\dfrac{1 - \delta t_1/\text{ITD}}{1 - 4.5\delta t_1/\text{ITD}}\right)} \left(\frac{3.5}{\delta t_2 - 1}\right)$$

For example, if $\delta t_1/\text{ITD} = 0.15$, increasing the ratio from 4.5 to 5.5 increases the tube length by 28%.

<u>Waste Heat Boiler</u>. The procedure followed in preparing a performance chart for the waste heat boiler was similar to that for the fluidized bed except that the heat transfer matrix was considered to be a bank of finned tubes having the performance characteristics defined for heat transfer matrix A of Fig. 99 in Ref. 4, p. 116, and presented here in Fig. 6.13. Geometric data on this heat transfer matrix are included in Fig. 6.13. The heat transfer coefficient for air at 500°F as evaluated from Fig. 6.13 is plotted in Fig. 6.14. The effectiveness with a uniform temperature of the boiling water on the tube side is given by

$$\text{Effectiveness} = 1 - e^{-\frac{uA'L}{G_1' 900}}$$

For a typical condition in which $G_1' = 10$ lb/sec·ft^2, Re = 9000, Pr = 0.684, $A' = 207.7$ ft^2/ft^2·ft, and L = 1.0 ft, the value of the heat transfer coefficient obtained using Fig. 6.14 is 52.2 Btu/hr·ft^2·°F, and

$$\text{Effectiveness} = 1 - e^{-\frac{52.2 \times 207.7}{9000}} = 0.70$$

The above equation was used to calculate a set of values for constructing a chart for the cooling effectiveness. The calculated values are given in Table 6.9, and a typical chart is shown in Fig. A4 of Appendix A.

Table 6.9. Summary of Calculations for the Heating Effectiveness of the Finned Tube Matrix with the "A" Spacing as Defined by Fig. 6.13 when Operated as a Steam Boiler

Calculated From:

$$N = 1 - e^{-\frac{207.7\ hL}{400\ G'}} = 1 - e^{-\frac{3.0255\ L}{(G')^{0.4}}}$$

G', lb/sec-ft	2	4	6	8	10	12
L, ft	1	1	1	2	2	2
h, Btu/hr-ft -°F	20.1	30.15	38.4	45.6	52.2	58.0
$G'^{0.4}$	1.319	1.741	2.0477	2.297	2.512	2.702
$-3.0255/(G')^{0.4}$						
e	0.10097	0.1759	0.2282	0.0717	0.0899	0.1065
N	0.899	0.824	0.772	0.928	0.900	0.893

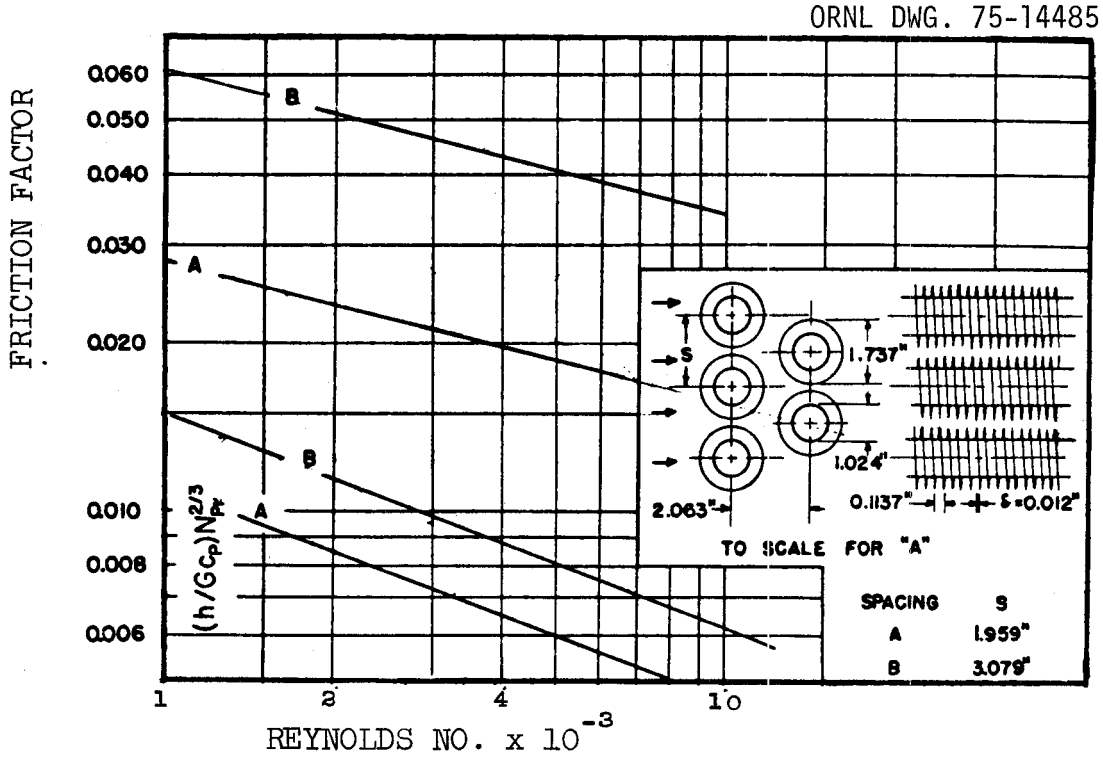

Tube outside diameter - 1.024 in.
Fin pitch - 8.8 per inch
Fin thickness - 0.012 in.
Fin area/total area - 0.825

	A	B	
Flow passage hydraulic dia. - 4 r_h =	0.01927	0.0443	ft
Free-flow/frontal area - σ =	0.439	0.643	
Heat transfer area/total volume - α =	91.2	58.1	ft^2/ft^3

Fig. 6.13. Colburn's j-factor and friction factor for transverse air flow over one-inch finned circular tubes. (Ref. 4).

Cooler. The same basic tube matrix employed for the waste heat boiler was used in the cooler. The situation for the cooler differs from that for the boiler in that there will be a temperature rise in the water so that the log mean temperature difference in the cooler will vary with design conditions. Under most conditions the cooling water into the heat exchanger will run about 60°F and the design outlet temperature will be 150°F so that the water temperature rise will be of the order of 90°F. In carrying out the calculations needed to construct a performance chart for cooling effectiveness as a function of heat transfer matrix length in the cooling air flow direction, one must carry out a derivation similar to that used above for the economizer. Assuming a 90°F temperature rise in the water, the log mean temperature difference becomes

$$\text{LMTD} = \frac{\text{ITD} - 90 - \text{ITD} + \delta t_1}{\ln\left(\dfrac{\text{ITD} - 90}{\text{ITD} - \delta t_1}\right)} = \frac{\delta t_1 - 90}{\ln\left(\dfrac{1 - 90/\text{ITD}}{1 - \delta t_1/\text{ITD}}\right)}$$

The heat transfer coefficient on the water side will be so much higher than that on the air side that it can be neglected and the heat transfer coefficient taken as simply the value defined by Fig. 6.14. The heat loads will be low and hence the fin efficiency high. Equating the heat removed from the air stream to the heat transferred to the tube matrix yields

$$W_1 c_p \; 3600 \; \delta t_1 = uA \; \text{LMTD}$$

Substituting as above to put this in terms of G_1', A', and L and using $c_p = 0.24$ gives

$$864 \; G_1' \; \delta t_1 = uA'L \; (\text{LMTD})$$

Solving this for the length of the heat transfer matrix in the air flow direction yields

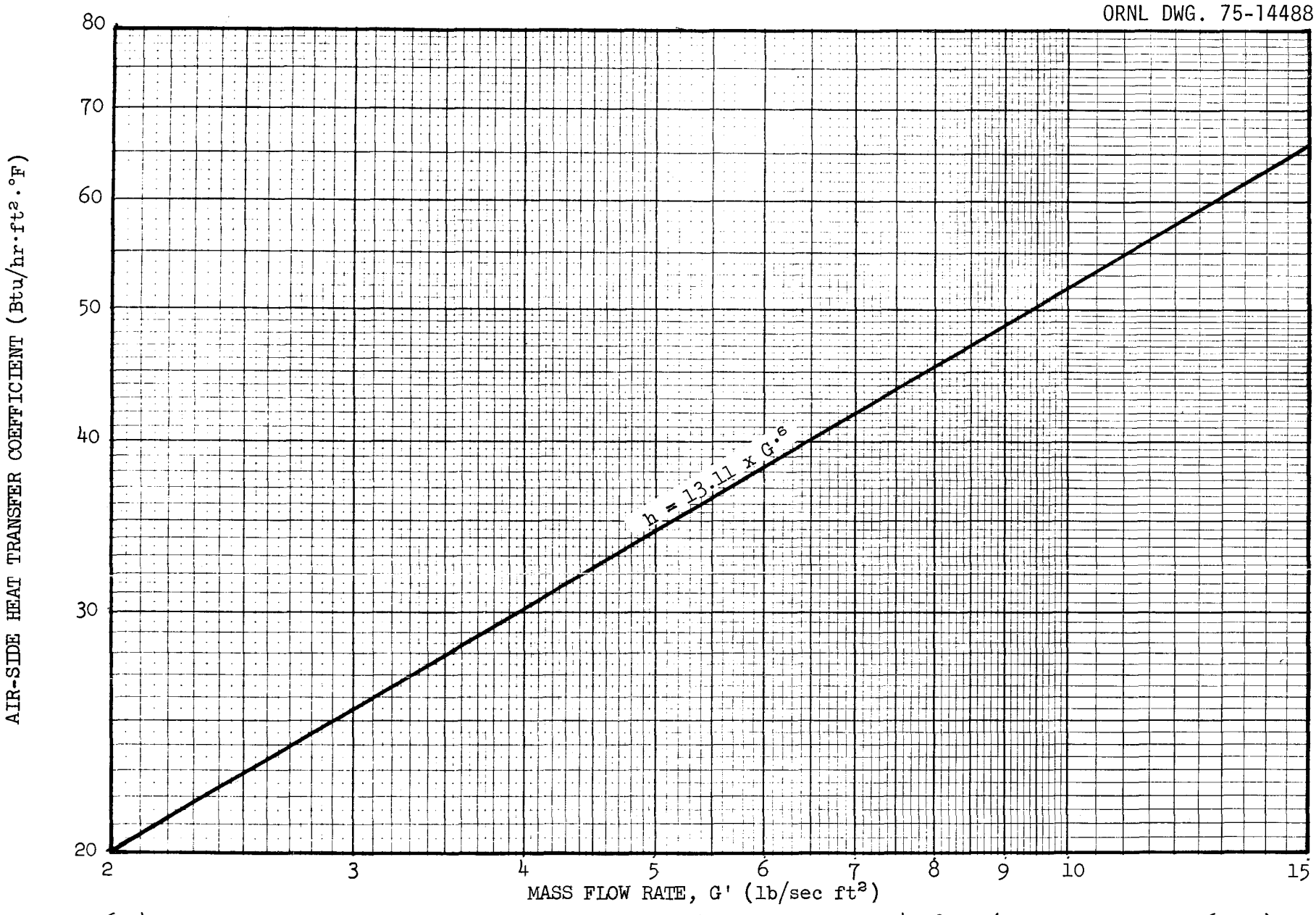

Fig. 6.14. Heat transfer coefficient for air flow over 1" finned tubes at 400°F. (Plotted from Fig. 6.13.)

$$L = \frac{864\ G_1'\ \delta t_1\ \ln\left(\frac{1 - 90/ITD}{1 - \delta t_1/ITD}\right)}{u\ A'\ (\delta t_1 - 90)}$$

Using the above relation the set of values of Table 6.10 were calculated for the construction of a performance chart. The resulting chart is shown in Fig. A5 of Appendix A.

Calculational Procedure for the Construction of Charts for Pressure Drop

The procedure for carrying out calculations on the pressure drop for the various flow passages was considerably simpler than that for the charts for heating or cooling effectiveness. For flow inside of round tubes or for flow outside tubes but parallel to them, the friction factor defined by Fig. H3.4 and the dynamic head given by Fig. H3.3, pages 293 and 294 of Ref. 2 were employed. The Reynolds number for the flow regime of interest was checked in all cases and was found to be comfortably within the turbulent regime (see Fig. H3.1, page 291, Ref. 2) except for the combustion gas flow through the economizer region; this was found to give a Reynolds number around 3000. This would probably require a few turbulators and consequently a small increase in pressure drop, but this increment was neglected at this stage. The pressure drop for a typical condition was computed for a series of air flows for each case, and then a chart was constructed on the premise that the pressure drop would be directly proportional to the air flow passage length. Thus, a set of straight lines was drawn for the series of mass flow rates.

A single chart, that in Fig. A6, can be used for calculating the air pressure drop inside the tubes for the recuperator, economizer, and fluidized bed tube matrices. To allow for differences in air temperature and consequently in air density, the charts were all prepared using the pressure drop parameter $\sigma\Delta P$ where σ is the ratio of the air density to that at standard conditions. Thus the effects of difference in air density are easily handled. In effect, the charts were all drawn for a value of $\sigma = 1.0$. In using the charts the value of σ for the prevailing temperature

Table 6.10. Summary of Calculations for the Heating Effectiveness and Length of the Finned Tube Matrix with the "A" Spacing as Defined by Fig. 6.13 when Operated as a Cooler

G', lb/sec-ft^2		2	4	6	8	10	12
h = u	Btu/hr-ft^2-^{o}F	20.1	30.15	38.4	45.6	52.2	58.0
	LMTD						
δt_1/ITD	$\delta t_2/\delta t_1$ = ab	Length, ft					
.75	.78846	.859	1.134	1.334	1.496	1.636	1.760
.80	.9555	1.041	1.375	1.617	1.814	1.983	2.133
.85	1.18377	1.290	1.703	2.003	2.247	2.457	2.643
.90	1.526	1.700	2.244	2.640	2.961	3.238	3.483
	$\delta t_2/\delta t_1$ = 0.4						
.75	1.92962	.748	.987	1.161	1.303	1.425	1.533
.80	1.22378	.889	1.174	1.380	1.549	1.693	1.822
.85	1.4816	1.077	1.421	1.671	1.875	2.050	2.205
.90	1.8563	1.349	1.780	2.094	2.349	2.569	2.763
	$\delta t_2/\delta t_1$ = 0.8						
.75	.4700	1.025	1.352	1.590	1.784	1.951	2.099
.80	.58779	1.281	1.691	1.989	2.231	2.440	2.625
.85	.75769	1.652	2.180	2.564	2.876	3.145	3.383
.90	1.02962	2.244	2.962	3.484	3.908	4.274	4.598

and pressure conditions in the system can be calculated to establish the pressure drop parameter, $\sigma\Delta P$.

The pressure drops through the recuperator and the economizer for the shell-side flow require separate charts because the mass flow ratios and effective passage diameters are quite different from the values inside the tubes. In addition, there will be some variation in the mass flow ratio in the economizer depending on the choice of design conditions, but if one fixes the ratio of shell-side to tube-side flow passage area, a pressure drop calculated on the basis of the shell-side mass flow rate will be independent of the mass flow ratio through the unit. Typical charts are given in Figs. A7 and A8.

The air pressure drop through the cooler and waste heat boiler can be defined by the same chart. This chart, shown in Fig. A9, was calculated on the basis of the friction factor given in Fig. 6.13.

Heat Exchanger Selection

As indicated previously, the complex interrelationships between the various heat exchanger design parameters determining the size and cost make it very difficult to perceive the effects of changes in heat transfer matrix proportions on pressure drop and effectiveness. The various implicit relations, however, can be made explicit in terms of parameters that are crucial from the standpoint of gas turbine performance by cross-plotting data from the design charts developed above using a reasonable set of design conditions. The most important of these is an assignment of the pressure loss distribution to the various components in the system. The total pressure loss evidences itself in the difference in pressure ratio between the compressor and the turbine, and is commonly expressed as the summation of the ratios of the pressure drop to the absolute pressure for all of the components. That is, the summation of the pressure ratios for the various components will be equal to the difference between the pressure ratios for the compressor and the turbine. On the basis of past experience it is possible to draw up a reasonable distribution of pressure drop between the various components. For purposes of this analysis it was assumed that 30% of the pressure drop in components would occur in the duct work and that 70% would occur in the components themselves.

This is probably an overly generous allowance for duct losses. The distribution of pressure losses chosen for this study is presented in Table 6.11. Note that in each case three parameters are given, i.e., the pressure drop, the parameter $\sigma\Delta P$, and the ratio of the pressure drop to the prevailing absolute pressure, $\Delta P/P$. Using these values it is possible to prepare a cross plot for the mass flow rate as a function of the tube matrix length for each component to give a nearly straight line as in Fig. A10 for a typical overall system pressure loss ratio. The three typical values of Table 6.11 were used; namely, a 5%, 7.5%, and 10% $\Sigma\Delta P/P$ for the system as a whole. Of course, the $\Delta P/P$ for the component in question is the small fraction of the total $\Delta P/P$ defined by Table 6.11.

It is possible to superimpose on the same coordinates a set of lines for typical cooling effectivenesses by cross-plotting data from the appropriate cooling effectiveness chart. The resulting cross plots then yield, in effect, a set of graphical solutions of the diverse complex implicit relations that are involved. For example, with the cross plot of Fig. A10 it is possible to choose a tube matrix length and a turbine air mass flow rate for any desired heating effectiveness and overall system pressure ratio. This enormously simplifies the problem of establishing the proportions for each of the heat exchangers.

Fuel and Limestone Feed System Concepts

The basic concept of the system for feeding crushed coal and limestone into the fluidized bed-gas turbine combustion chamber involves transport and blending of the crushed coal and limestone at a continuous predetermined feed rate that can be controlled by the burn-up parameters of the system.

The main points in the feed system requiring special considerations are at the points of injection of the feed mixture into the fluidized bed, at the point where blending is achieved between the coal and the limestone, and at the exit of the storage or retaining hoppers, where continuous flow rates of solids are supplied to a mechanical and/or pneumatic system for transport to the injection points of the fluidized combustion bed.

Table 6.11. Pressure Distribution in the Various Heat Exchangers of a Closed Cycle System

P_2 = 176.4 psi @ 12 atm

$\sigma_1 \Delta\rho_1 = \frac{\Delta P_1}{P} \frac{12}{100} 14.7\sigma_1$ (High P_1)

$\sigma_1 \Delta\rho_1 = \frac{\Delta P_1}{P} \frac{3}{100} 14.7\sigma_1$ (Low P)

P_2/P_1	3	3.5	4
Compressor efficiency, %	85.8	85	84
Turbine efficiency, %	87.8	87.4	87
System $\Sigma\ \Delta P/P$	5	7.5	10
Recuperator $\frac{\Delta P_1}{P_1}$ %	.75	1.125	1.5
Recuperator σ_1	5.522		
Recuperator $\sigma_1 \Delta p_1$, psi	7.305	10.95	14.61
Bed + Econ. $\frac{\Delta P_1}{P}$, %	1.25	1.875	2.5
Bed + Econ. σ_1	3.692		
Bed + Econ. $\sigma_1 \Delta p_1$, psi	8.14	12.21	16.28
Boiler $\frac{\Delta P_1}{P_1}$, %	.25	.375	.5
Boiler σ_1	1.814		
Boiler $\sigma_1 \Delta p$, psi	.2028	.3042	.4057
Cooler $\Delta P_1/P_1$ %	.25	.375	.5
Cooler σ_1	2.40		
Cooler $\sigma_1 \Delta p_1$,psi	.2646	.3969	.5292

Many years of experience are well documented on fluidized-solids feeding systems.[5,6] However, most of this effort has been directed either to chemical industry processes or boilers in steam-electric generation size plants. Also the fluidized bed coal burning systems under development are much larger scale than will be required for the coal burning MIUS; therefore, obtaining some possibly adaptable types of feeder equipment may be difficult in the size range of interest. This does not mean that completely new development will be required for all components; rather that selection and possible modifications to some of the commerically available equipment may determine the most adaptable concept for this feeder system.

Assuming that the coal and limestone receiving equipment and storage hoppers are commercially available or easily procured and that the crushers (and coal dryer, if required) can maintain a level of crushed solids with a low moisture content of about 4% in one or more hold up bins or pressurized feeder tanks (often referred to as air locks), then the solids can be transported by any one of several means into the fluidized bed.

To simplify the discussion of the basic design concepts required for the feeder system, the vessels ordinarily referred to as hold-up bins, injector storage vessels, or pressurized air locks will be referred to as retention components. Then concepts of solids movement through the retention equipment can be discussed as a feeding process for the coal, the limestone, or a solids mix of the two. Also, this permits discussion of the basic solids flow parameters without consideration of the blending problems or particulate size.

The problem of solids mixing or blending will be discussed separately as well as those points in the feeder system where blending can be achieved satisfactorily.

The basic requirement of the components in a retention system is conversion of the solids mix flow from a batch process (such as dump truck delivery into a storage silo) to a continuous or acceptable semi-continuous flow out of the retention hoppers. Furthermore, some combination of control valves or solids flow control mechanisms, either built into (or between) the retention components and the transport system must consider solids flow limitations as well as meet demands by the fluidized bed combustor. Solids flow limitations are very important where transport is

effected solely by pneumatic methods. A schematic flow sheet for coal and limestone is shown in Fig. 6.15 so that various types of equipment and their advantages can be considered at points along the line of solids flow. A weigh larry is included in this schematic in the event that batch weights are desired during the development of the feeder system, but usually either mechanical or pneumatic feeder systems can be controlled in a manner capable of evaluating solids flow weights from volumetric capacities.

Solids Feed into the Retention Components

Mechanical feeders most commonly used to convey solids from the storage silo to the retention components are screw feeders, belt or bucket type conveyers, or vibratory feeders. If a pressurized retention system or a pneumatic combustor transport system is used, then an open hopper with a rotary outlet or air lock type of valve is usually required in conjunction with mechanical feeders to prevent pressure loss back through the solids in retention. Even when a deep bed of solids is maintained in an open retention bin, gravity induced flow out of the bin into a horizontal transport pipe may be irregular because of particle size variations. Most mechanical feeds tend to cause concentrations of different size particles as they are fed into a retention hopper. Diffusser or spreader devices may be used to minimize segregation or stratification of particle sizes during feed into an open bin.

Use of commercially available mechanical feeders to convey solids directly into the fluidized bed or into pneumatic transport tubes without some type of retention equipment is not likely to provide satisfactory feeding conditions, certainly not without some special adaptations or developments. The Iron Fireman or Canton Vulcan ram type systems are batch feeders that would require special development of all the combustor components that determine primary air flows throughout the fluidized bed.

Pneumatic conveying systems should be readily adaptable for conveying the various sizes of solid particles from either motor transport vehicles or a storage silo to the retention components. Three system arrangements are shown in Fig. 6.16 which has been reproduced from Ref. 7. However,

ORNL DWG. 75-14483

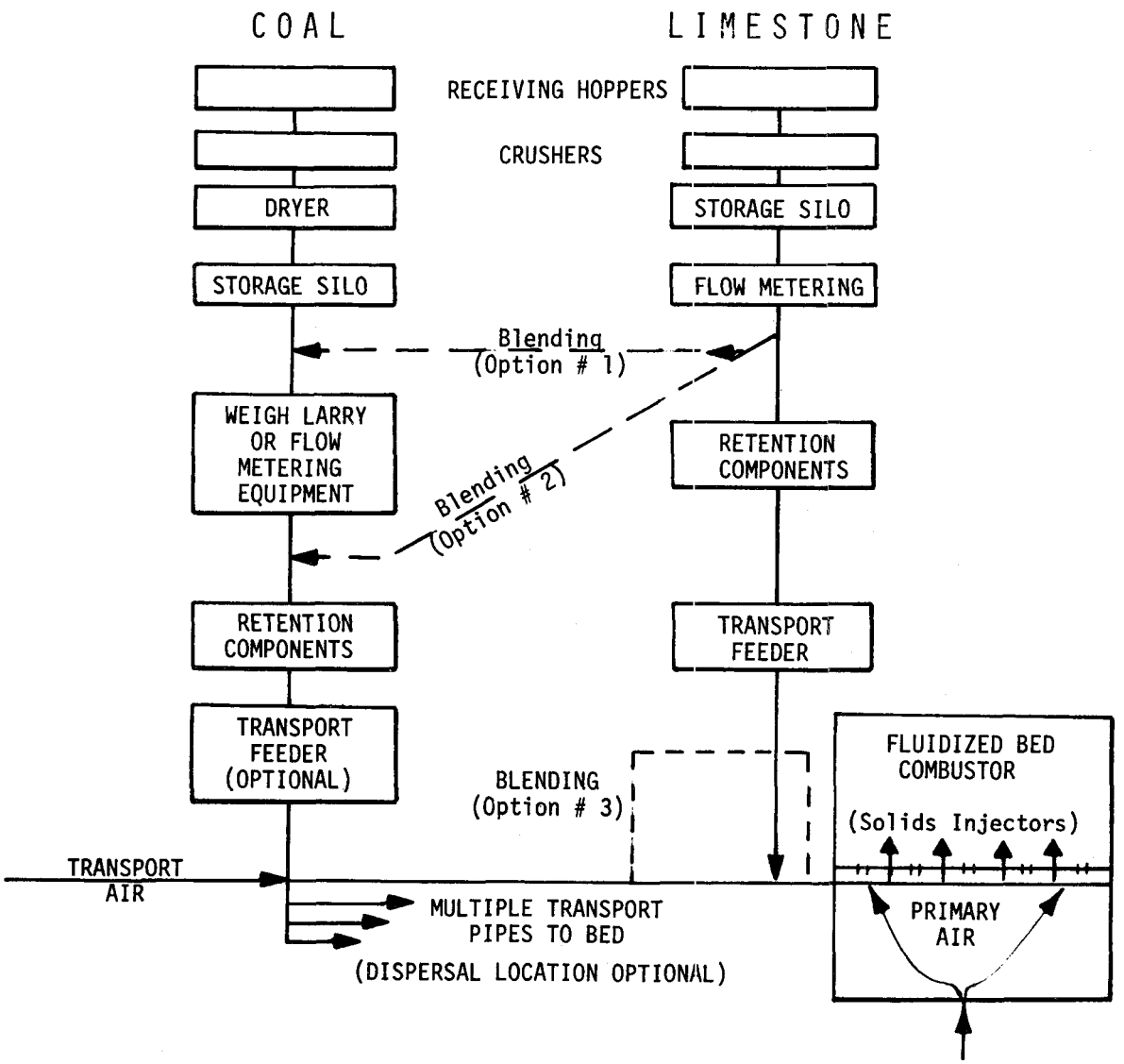

Fig. 6.15. Schematic flowsheet for coal and limestone feed system.

ORNL DWG. 75-14465

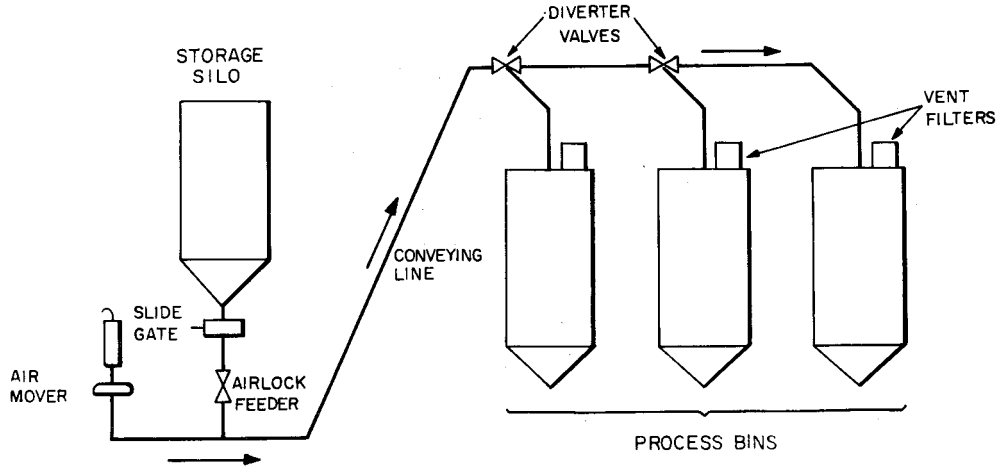

POSITIVE pressure system serving several delivery points with single pipeline

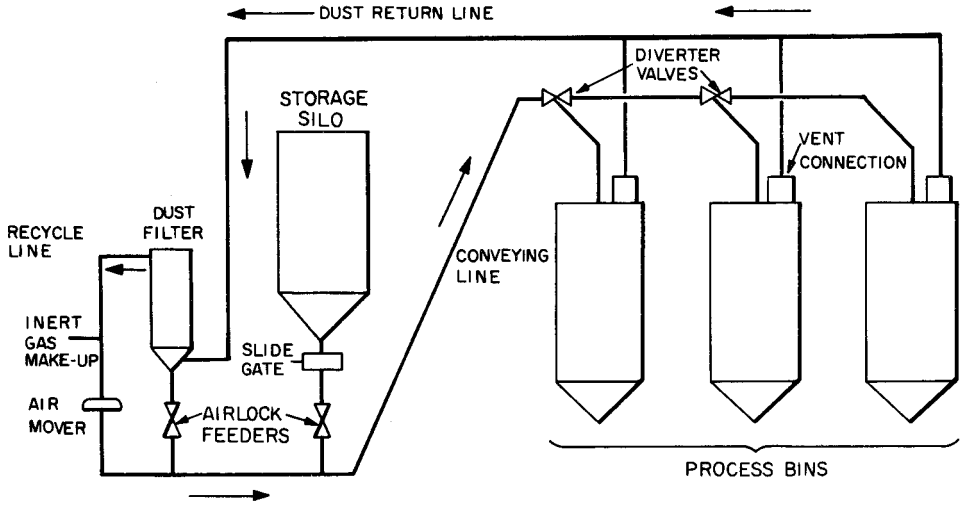

CLOSED LOOP system with positive or negative pressure to prevent contamination

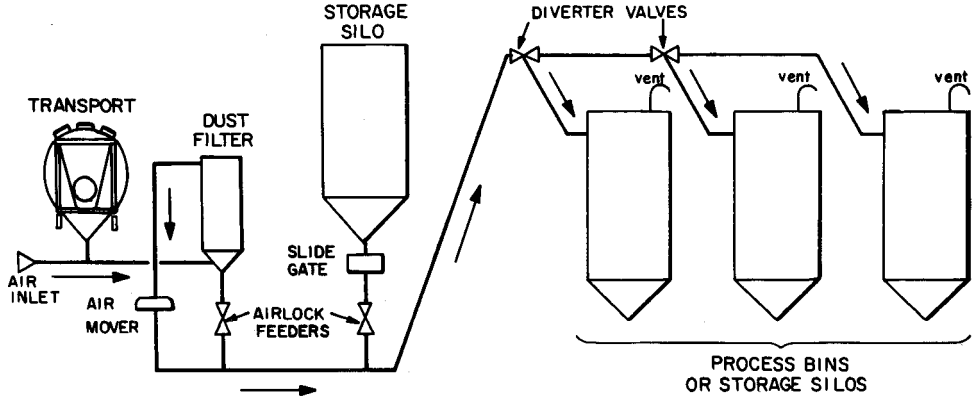

COMBINATION vacuum-pressure system which withdraws by vacuum and delivers material under pressure

Fig. 6.16. Typical pneumatic conveyor arrangements.

these systems may require some type of spreader equipment inside the first retention hopper (shown as process bins) to insure good particle size distribution throughout the depth of the hopper. Stratification or segregation of particle sizes occurs with pneumatic as well as mechanical feeding of variable size particulates into open retention hoppers.

Concepts of Retention Components

A simple cylindrical hopper with a conical bottom can be used for the first retention hopper to receive solids flow from mechanical feeders, and in some cases determination of the conical angle can permit gravity flow out of the hopper without segregation of particle sizes. However, uniform mixing of particle sizes, both into and out of such hoppers, must receive special attention during design. Also, if the first hopper must feed into a second pressurized retention vessel, then a rotary valve or air lock must be used between the two retention hoppers.

A commercially available pressurized system of retention equipment is available from United Conveyors as illustrated in Fig. 6.17 (reproduced from Ref. 8). This combination of components provides a fluidized solids flow system that can feed directly into the horizontal transport tubes to the combustor bed. However, the valving arrangement of this system is such that at least two of each of the components must be used so that one vessel can be filling while the other is being emptied. Also, multiple outlet feeding from pressurized vessels, even with the aid of fluidizing plates, may not be available. Four or more such sets of retention components and flow control equipment to feed separate terminal points in the combustor bed may be rather expensive.

Many types of vibratory feeders, commercially available from manufacturers of materials handling equipment, can be used to insure solids flow out of relatively small outlets of hoppers.

The vibra-flow/volumetric feeder machine shown in Fig. 6.18 is available from Syntron Co. of Homer City, Pennsylvania. Several of the vibratory units made by Syntron have been adapted to special applications at ORNL. Description of one such unit, adapted to flow of pyrolitic carbon-coated microspheres, is included in reports on component development in the TURF program.[9] The type of vibratory feeder in Fig. 6.18 could be

ORNL DWG. 75-14472

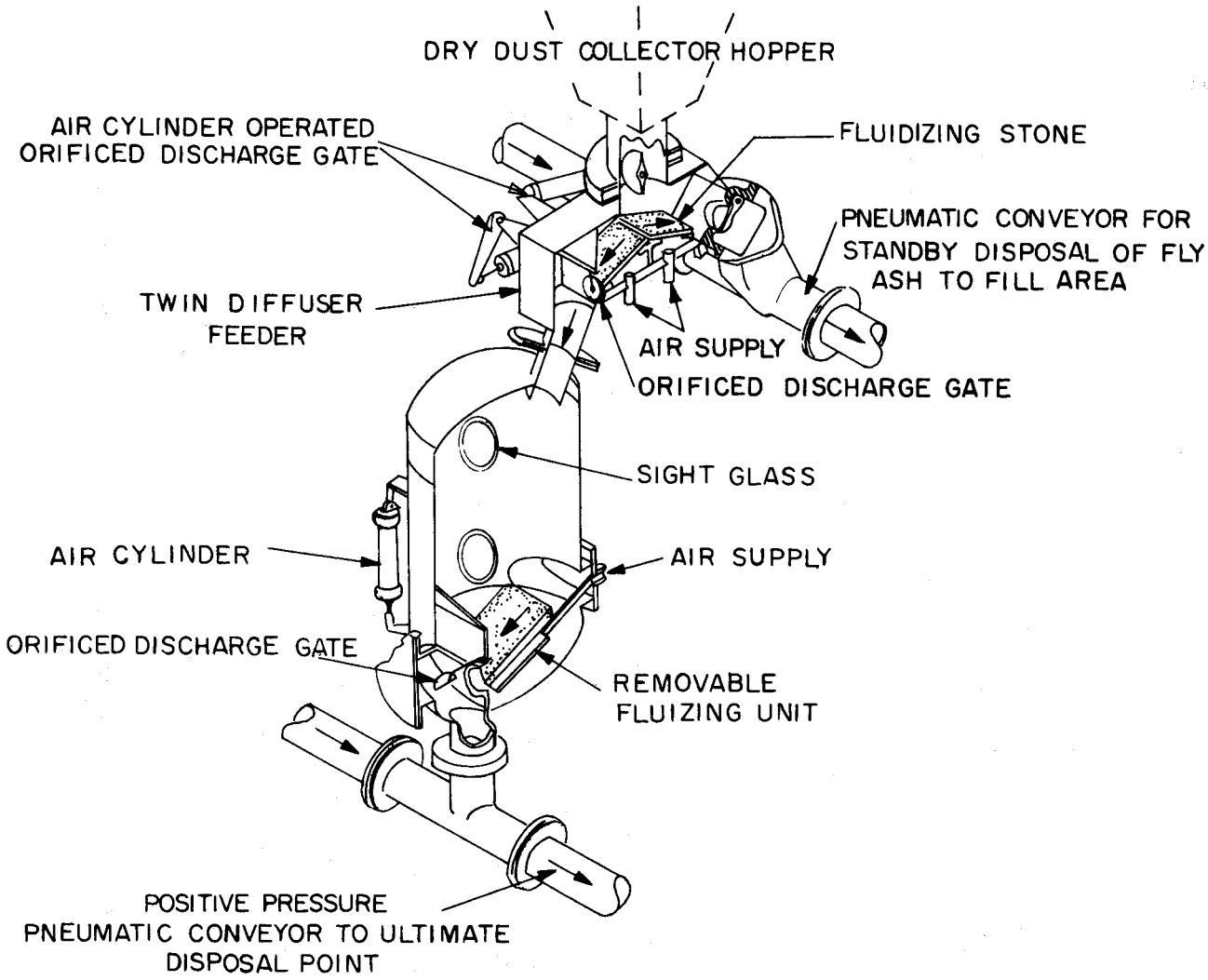

Fig. 6.17. Nuva feeder-positive pressure pneumatic conveyor by United Conveyor Corp.

ORNL DWG 76-2711

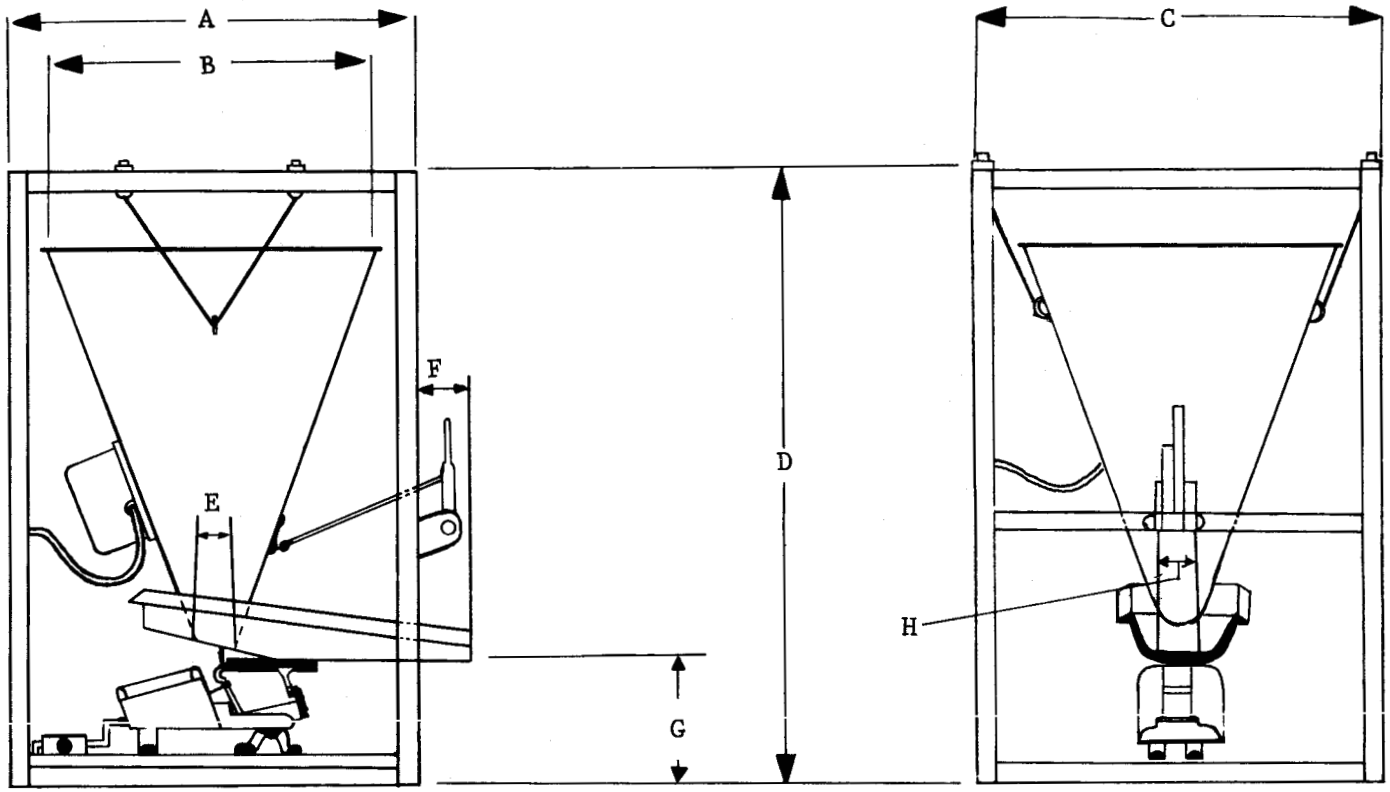

DIMENSIONS:

A	B	C	D	E	F	G	H
31"	24" dia.	31"	48 3/8"	2 1/2" dia.	5"	9 5/8"	4"

Fig. 6.18. Vibrator feeder and conical retention hopper.

modified and possibly made to feed directly into the transport tubes. Several tubes could be built into (or else replace) the tray of the vibratory feeder and, by using flexible metal hose, become a part of the vibrating mass of the unit. With the flexible hoses smaller than the transport tubes and completely filled with solids, electrically controlled feed rates should be possible. Flow-back of the transport air should not be a problem, but, if necessary, two alternately pulsating valves could be located above (or between) retention hoppers.

Transport System

Regardless of the types of feeder equipment used at the exit of the retention hoppers, pneumatic transport is more adaptable than mechanical feeders for uniform delivery and distribution of solids flow into the fluidized bed combustor.

The major concern of the transport system is uniformity of the blended mix of the solids and, therefore, exacting control of the feed rates at point of entry into the transport tube is essential. The various fluid-solids flow characteristics encountered in horizontal transport are represented in Fig. 6.19 as taken from Ref. 7. Some explanation of necessary fluid-solids flow parameters and methods of evaluation are included in Chapters 2 and 10 of Ref. 5. Evaluation of these parameters will be necessary for the coal, the limestone, and the combined solids mix of the two.

Also, the curves in Fig. 6.19 show some basic relationships in fluid-solids flow that can be correlated with the design parameters of primary air flow and solids restoration to maintain the fluidized bed. For instance, to provide continuous solids restoration to the bed the exit velocity of air transporting a predetermined weight (w) of solids may need be kept above saltation velocity (range of dilute flow) for a particular diameter and length of transport tubing. On the other hand, the range of pressure drop as limited by a design of transport tubes that is based on some desired percentage of primary air will limit the transport capability of the solids mixture. A trial and error type of solution may be the best means of covering the range of desired parameters. However, obtaining transport data on crushed coal and limestone should not be too difficult.

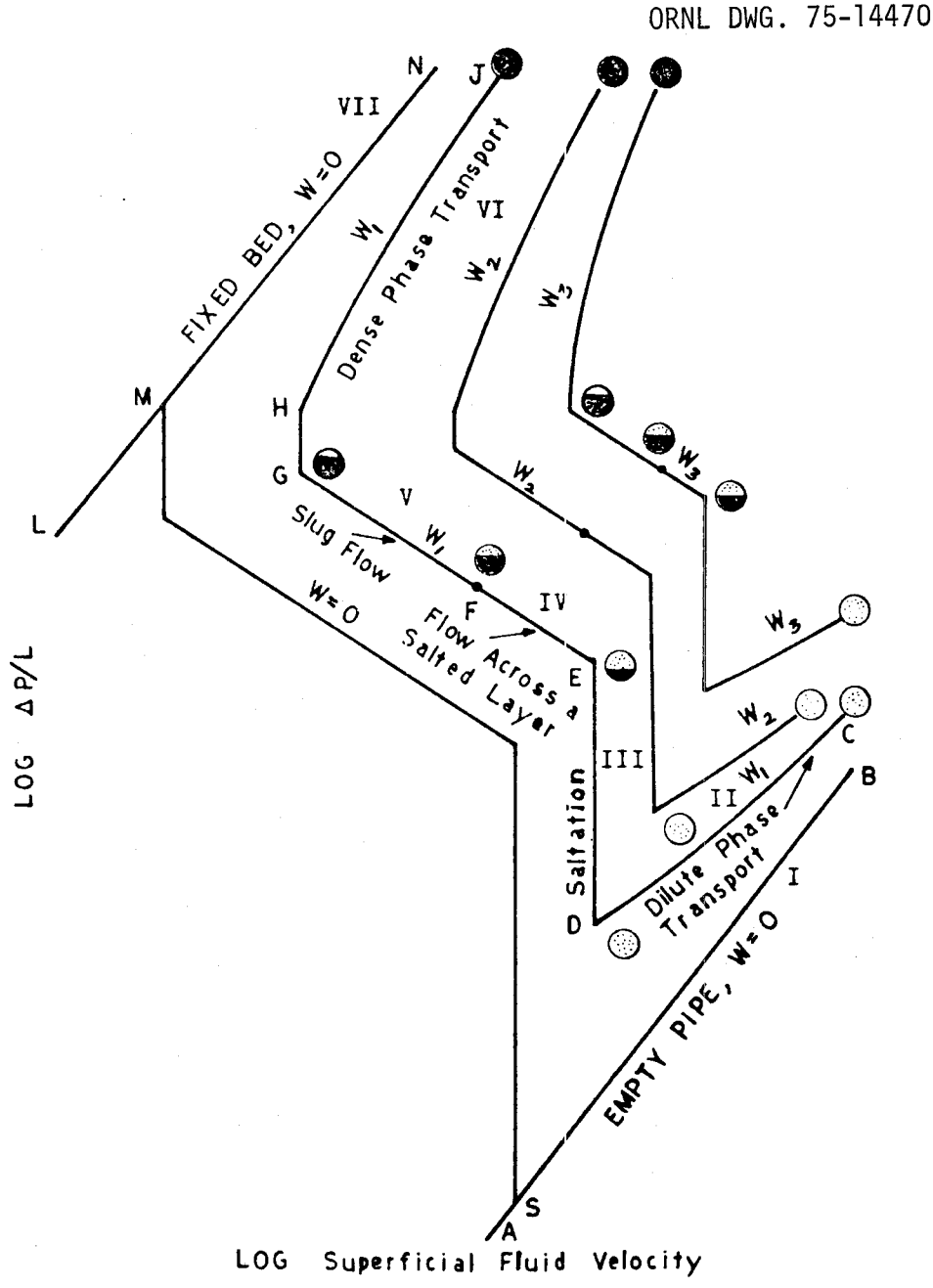

Fig. 6.19. Schematic representation of phase diagram for horizontal fluid-solids flow.

Also note that long tubes and high Δp will permit higher unit weight of solids (w) for the same superficial velocities.

A small solids flow pneumatic transport system and also several components that may be adaptable have been recently developed at ORNL (Ref. 9). Although this development was for much smaller quantities of dense uniform size material, some of the components may be readily adaptable to pneumatic transport of coal and limestone. The pinch valve, shown in Fig. 6.20, can be fairly easily fabricated and could be used with a pulsating type of operation to control flow from a retention hopper. It could also serve as an air lock in conjunction with pressurized vessels.

Another type of hopper outlet and solids flow control arrangement that was used in small scale model studies at ORNL is shown in Fig. 6.21. This bridging of several particle types and sizes was studied with this model. The center rod and gusset type support is simply a means of fabricating a hood or a mushroom-type skirt over the outlet, similar to a hopper that was made by Sanderson and Porter in studies with spheres for the Pebble Bed Reactor. The purpose of the mushroom over the cylindrical outlet or orifice is to take the weight of the bed off of the particulates near the small diameter outlet, and therefore, minimize bridging. With this arrangement, it is possible to raise the cylinder vertically under the mushroom and make the particles bridge and stop particle flow without creating crushing forces that increase abrasion and wear that are often present in valves or gates for stopping solids flow. Also, this type of hopper design is worth consideration as a means of eliminating centralized channelization of solids flow out of hoppers with cones that provide low angles of slope. The development reported in Ref. 10 attempted elimination of all erratic flow patterns. The study was restricted to spheres, but similarities are evident in feeding particulates from storage bins.

Conceptual design of the terminal points of pneumatic transport tubes will depend on the desired method of delivery of solids into the fluidized bed. Determination of the angle of spread and trajectories of the solids delivered must be made adaptable to the combustor tube bundles and the distribution of primary air flow. Even short vertical lengths of transport tubes up through a retaining plate for the bed will affect overall design of the pneumatic transport system. Also the terminal points of

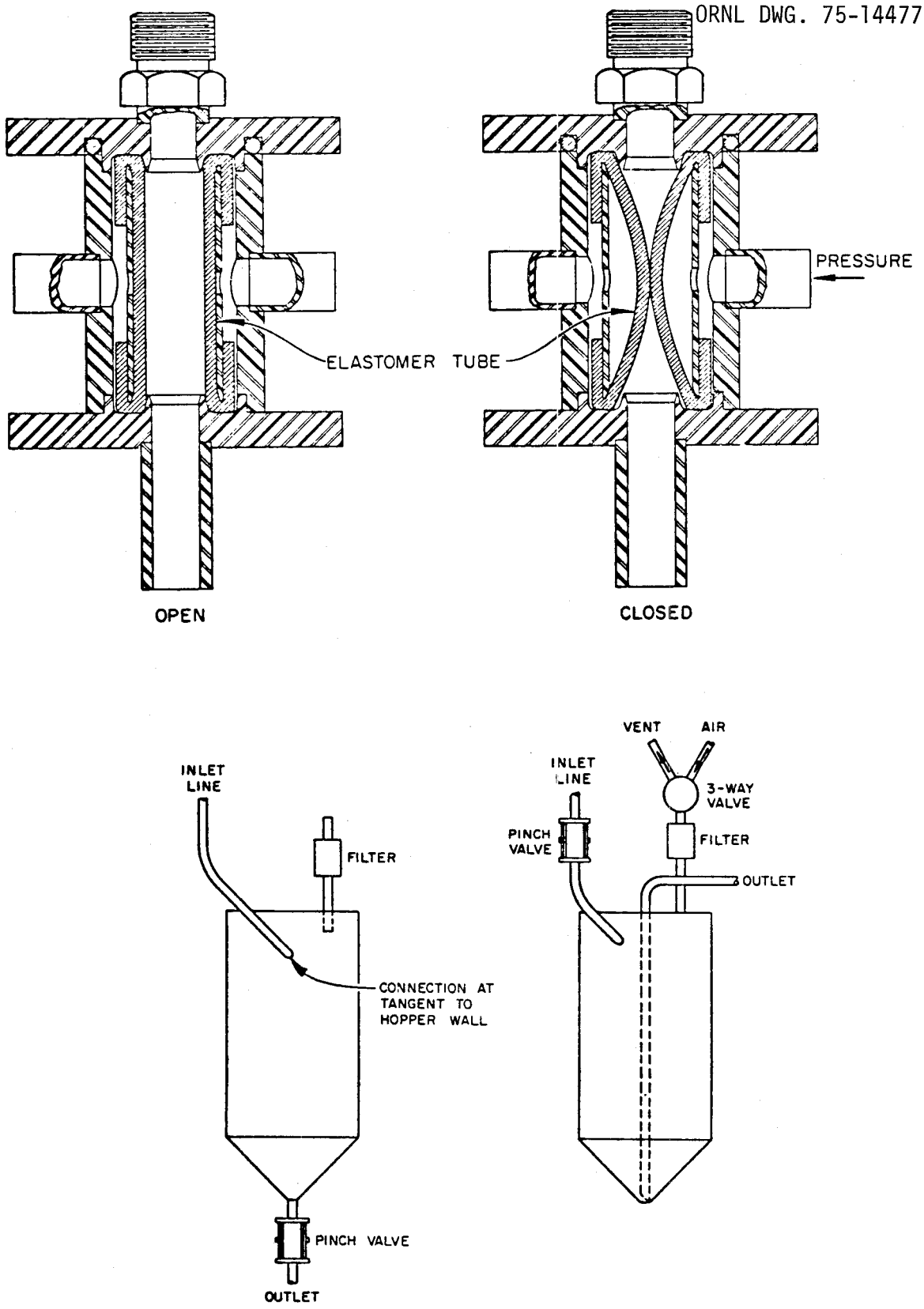

Fig. 6.20. Pinch valve and two applications on hoppers.

ORNL DWG. 75-14467

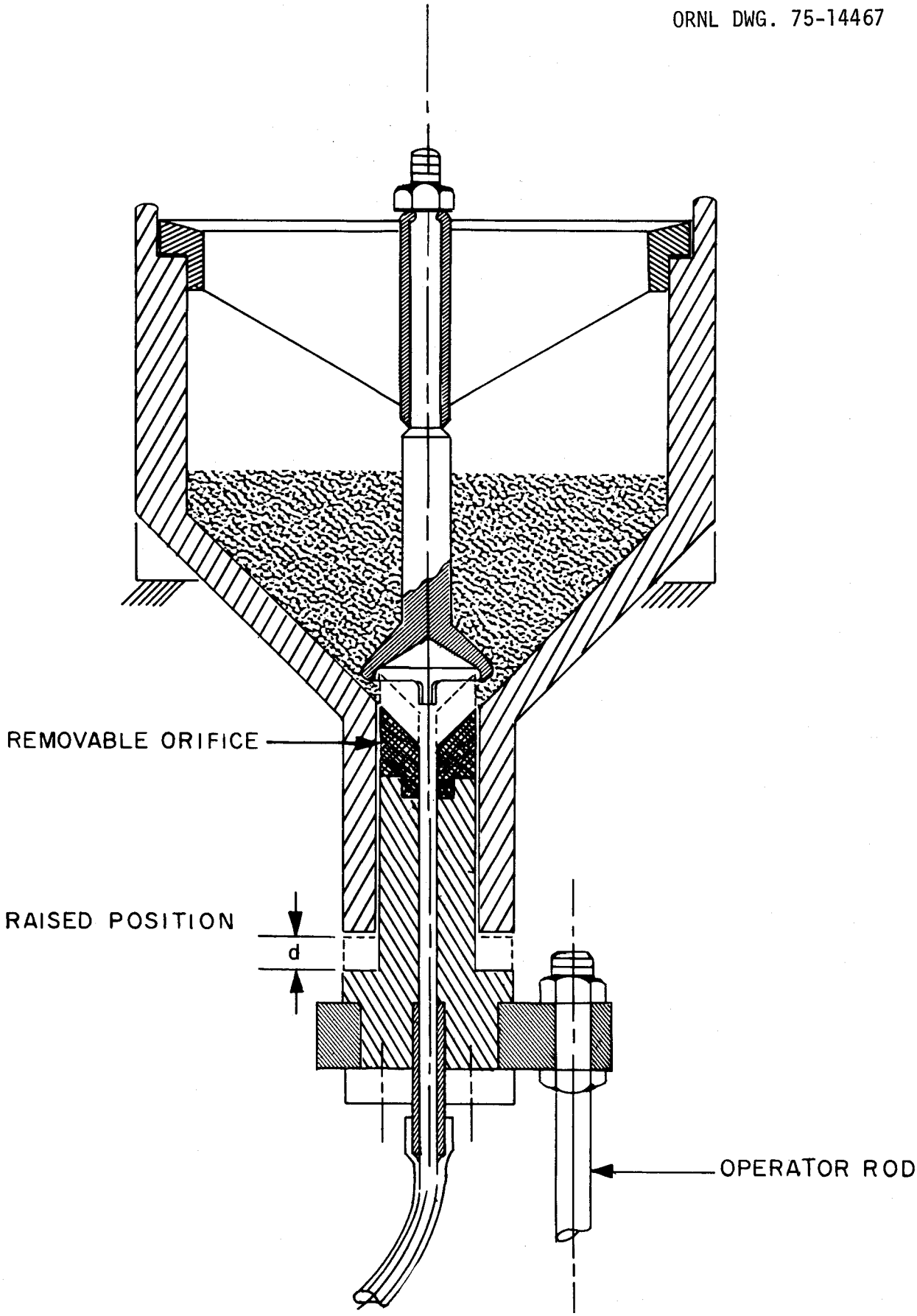

Fig. 6.21. Conical hopper with orificed particle flow.

the vertical tubes should be designed such that the tubes do not fill when the bed of solids rests on the retaining plate. A bubble cap or mushroom on the terminal points may be used, or an arrangement similar to that used by Foster Wheeler Corporation for an atmospheric pressure boiler design may be satisfactory (Ref. 8, Appendix K, Fig. A3-5).

An example of a combined mechanical feed and pneumatic transport system commercially available from Iron Fireman Manufacturing Company is shown in Fig. 6.22. The feed screw in this system feeds from storage (or a retention hopper) and is capable of modulating both air and coal to match the boiler load. Drying and preheating capability can be built into the pneumatic feeder assembly. Design feed rates are several times those needed by the MIUS combustor. Modification of the terminal points of the transport tubes as shown in Fig. 6.22 to a vertical feeding arrangement through a stationary plate under the fluidized bed should not be a major problem, assuming ash goes out the upper end of the combustor. Provision for four or more terminal feed points, on the other hand, may not be possible at the entrance to the transport tubes. If true, then some spreader or diffuser arrangement may be necessary to limit the number of units required. Also, adaptation to components capable of uniform blending of coal and limestone, such as multiple tube vibrators, or dual Nuva pressurized feeders would require special developments.

Blending

Several types of mechanically operated mixing machines or dry-solids blenders are commercially available for various ranges or particle sizes. However, most such mixers are for batch processes with some specified capacity of the resulting solids mix. Basically they all receive two or more materials and repeatedly cut or separate part of the unmixed solids and fold it back into the total volume by a combination of cutting, tumbling or rolling motions. After a predetermined blending time specified for the solids input, the mix can then be transferred into a retention bin or feeder component. Mixing effectiveness or performance of mechanical blenders, such as the rotating drum, V-shaped unit (made of cut

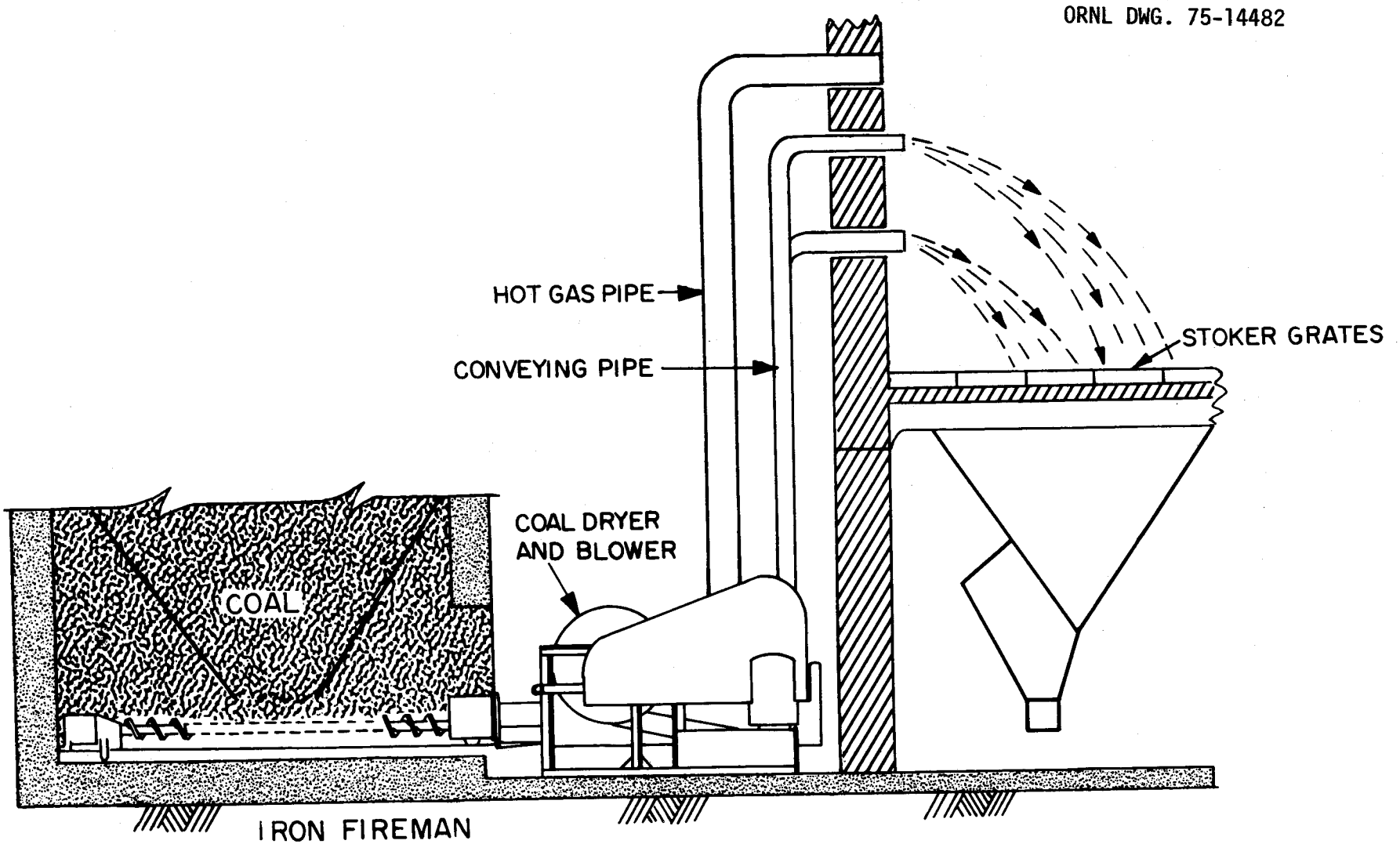

Fig. 6.22. Typical application of Iron Fireman pneumatic spreader stoker.

cylindrical sections), or the double cone type has been evaluated for some particulates of varying size and density.[6]

Referring to Fig. 6.15, the point in the line of coal flow shown as blending option #1 indicates that batch weights of limestone may be desired and can then be mixed with batch weights of coal by any of several means in the retention components. Option #2 indicates that batch weighing of limestone may only be necessary during development or operational shakedown of the feed and mixing components, and that with the limestone flow rates established the weighing larry can be by-passed. However, in either case, spreading or diffusing of alternate batches of coal and limestone feed into an open retention bin will probably result in some stratification of the batches and more than one retention bin might be necessary to provide uniformity of a feeding mixture. Even if a mechanical blender is used as the first component in the retention section gravity transfer of the mixed batches through valves or air locks into the lowest retention vessel must be accomplished in a manner that insures against "unmixing" the blend.[11]

An alternate to option #2 would be to use two weigh larries (or upper retention bins) and provide for simultaneous controlled flows of coal and limestone into a lower retention hopper. Blending the two flows with a mechanical spreader or two diffusers during entry to the lower retention hopper should give acceptable results, even if the solids must pass through individual air lock valves. A fluidized or pressurized feeder, such as the Nuva unit in Fig. 6.17, and air lock valves used between the upper retention bin and the lower hopper may also provide a satisfactory alternate under option #2. However, sampling of mixtures out of the pressurized vessel or before entry into the transport tubes will be required to determine blending mix or limitations of the fluidizing pressure vessel. Also, two pressure vessels will be necessary, if batch feed of the fluidized mix from a single vessel does not adequately meet combustor make-up requirements.

Development of a pneumatic blender as one of the retention components may provide a possible means for continuous feed of fluidized solids mix into the transport tubes. Two types of blenders were developed at ORNL, one for small batches of particles of uniform density and the other for

solids differing in both size and density.[9] These blenders, shown in Figs. 6.23 and 6.24, respectively, suggest a concept of alternate batch feed of coal and limestone into a pneumatic blender, similar to Fig. 6.23, and simultaneous orificed flow of batches from the loader-blender, as in Fig. 6.24. The stepping motors of the loader-blender are for remote adjustment of the variable orifices, and can be replaced by manual adjustment in this application. Very good uniform blending is obtained with particle sizes from about 300 to 800 μm from the loader-blender. The pneumatic batch blender is most effective in elimination of stratified layers formed by batch feed of particulates with the same density. Either of these concepts, or a combination of the two, may be adaptable to blending of non-uniform size coal and limestone particles.

The third option represented in Fig. 6.15 implies that a metered coal flow out of the retention components can be distributed to each of the transport tubes, and that some similar method of metered limestone flow can be phased in with the coal flow to achieve an acceptable blended mix in each of the tubes during pneumatic transport to the combustor. Any one of the solids feed control methods from the retention system, described above for coal flow, could be also used for limestone feed into the transport system. However, a study of the solids transport phase at the intersection of the two flows will be necessary; and a change in diameter of the transport tubes may require study and development.

This option offers some simplification of feeder system concepts that may be worth development. The basic idea of blending the two flowing solids during transport can eliminate problems inherent in the design of the retention components consisting of either pressure vessels or open hoppers. Metered and controllable solids flow rates should provide a means of acceptable blending or mixing ratios, if the pneumatic transport variables can be correlated with design of the retention components of both coal and limestone. This concept could eliminate spreaders, diffusers, or mechanisms that contribute to solids stratification, segregation, or "unmixing" of feed in and out of the retention system. The concept shown in Fig. 6.25 illustrates an outlet under a retention hopper that could be developed to provide a pneumatic control arrangement capable of initiating and maintaining solids flow into the transport tubes. A single tube

ORNL DWG. 75-14486

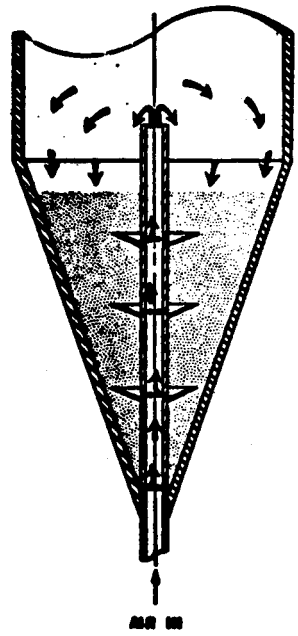

Fig. 6.23. Batch Blender.

ORNL DWG 76-4913

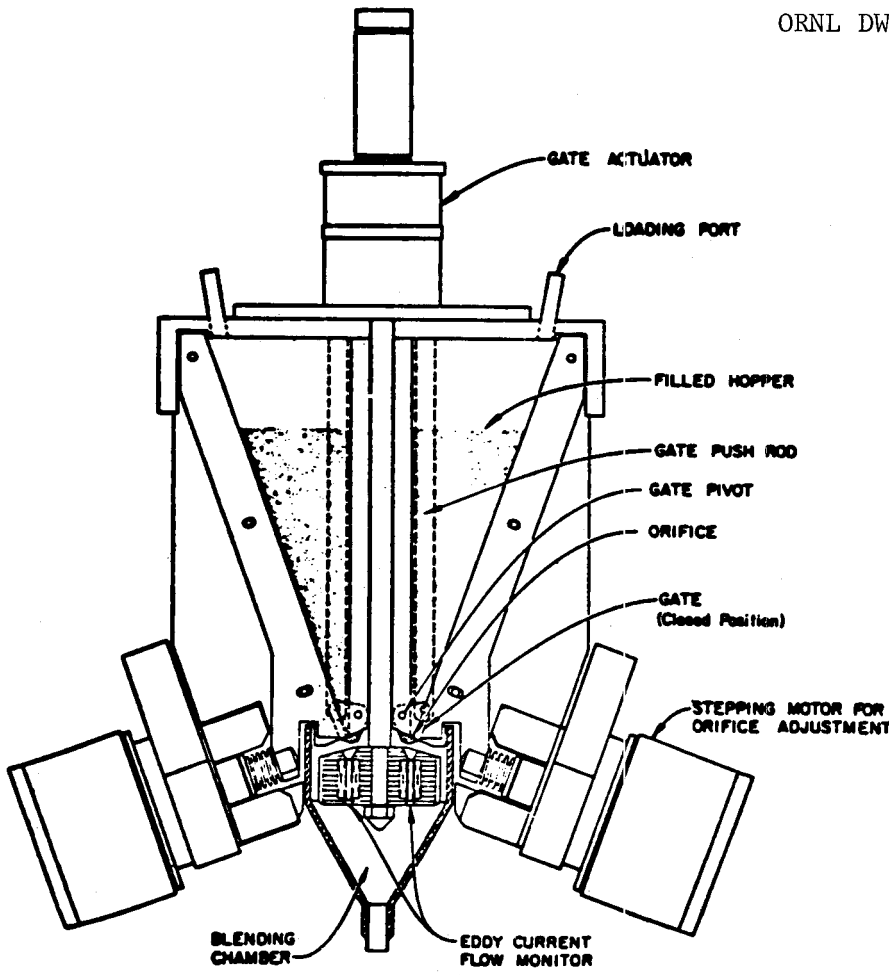

Fig. 6.24. Particle loader-blender.

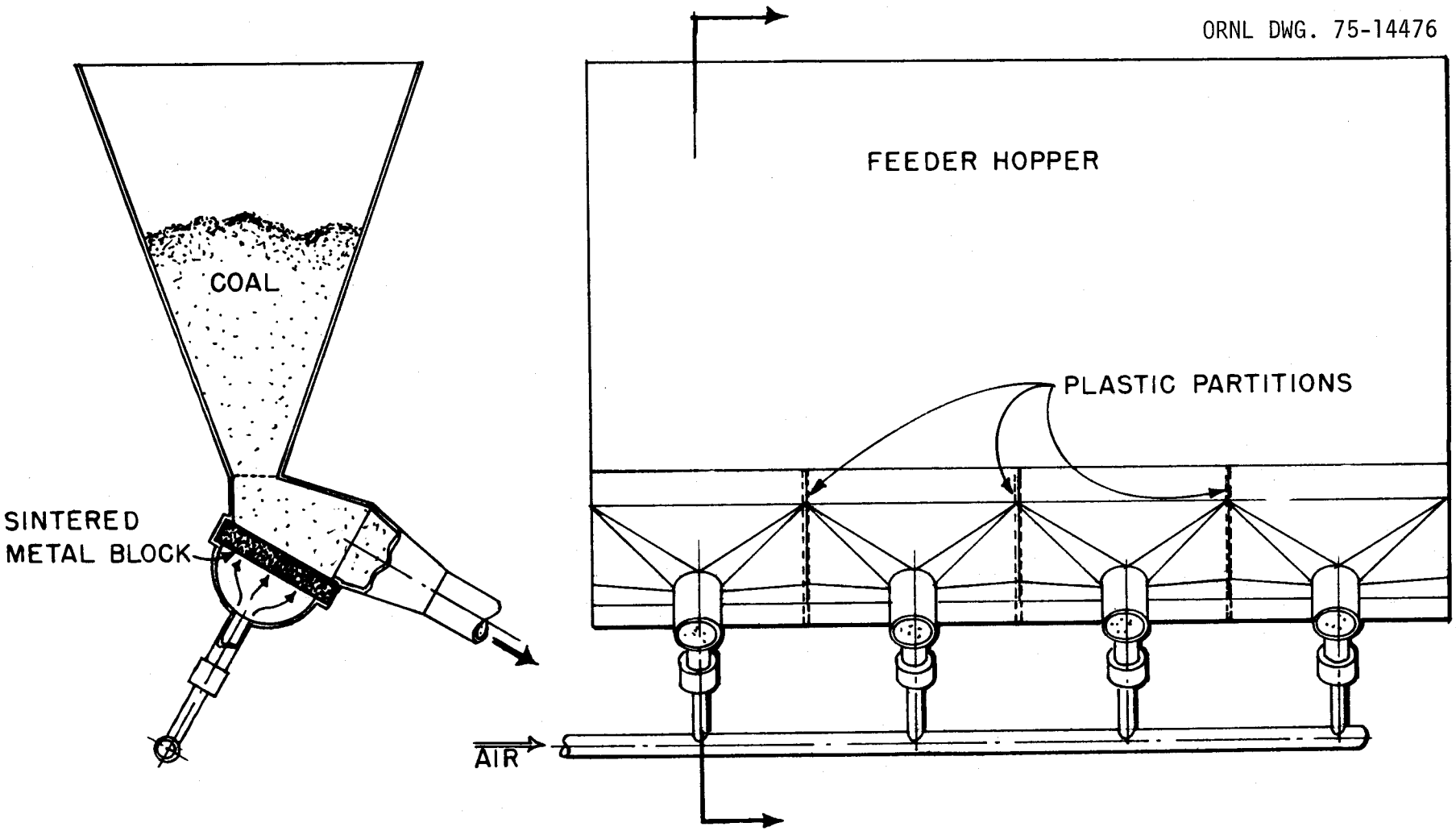

Fig. 6.25. Concept of multiple tube feeder.

preliminary model study would be necessary to determine workable dimensions and feasibility. Also, assuming that air flow is bled from the transport air supply, individual pressure control valve (PCV) settings must be determined for each transport tube. In an actual installation fixed pressure settings should serve to maintain solids flow so long as some minimum solids level is maintained in the hopper. Also solids flow must cease before stoppage of transport air to insure complete solids removal from the tubes when transport is discontinued.

An alternate to this concept is adaptation of vibrator equipment, previously included as part of the retention components. Simple bin-mounted vibrators could be installed to initiate and continue solids feed into the pneumatic transport tubes with a controlled flow rate determined pneumatically. Such hopper outlet-to-transport concepts should be adaptable to both coal and limestone to effect blending by either pneumatic and/or electrical controls during transport.

Adaptation of Commercially Available Systems

The pneumatic spreader-stoker with its built-in dryer and preheater arrangement shown in Fig. 6.22 may be adaptable to feed the fluid bed combustor with minimal development. Modification to vertical transport up through a combustor-retaining plate should pose no major problem, but conversion of the smallest size (750 lb/hr) unit advertised to provide multiple feed points in the fluidized bed will require development. Also, either separate feeder assemblies must be adapted for limestone, or else development of components for controlled blending in either the retention components or the transport tubes must be acceptably proven before a complete system can meet feed requirements.

The pressurized vessel type system with pneumatically operated inlet and outlet valves should be easily adaptable as part of the retention components for the fluidized bed combustor system. It should be able to convert either batch or semicontinuous feed of granular coal or limestone (out of a storage hopper outlet or a mechanical feeder outlet) into an evenly distributed mix of the solids into transport tubes during depressurization of the vessel. Two pressurized vessels with alternate operation of control valves should provide a surging type of solids feed acceptable to the

combustor requirements. However, more detailed information than is included in available pamphlets must be analyzed for such pressurized systems. The primary concerns adaptation of the pressurized system should be available size vessels, operation requirements, adaptability to blending, and relationship of transporting pressure surges to primary air pressure.

Systems Preferred for Development

The pneumatically controllable initiation of solids feed discussed in the concept represented by Fig. 6.25 should prove to be the most acceptable maintenance-free feeder system if it can be developed satisfactorily. The power requirements associated with blending and transport should be lower than any pressurized system. After initiation of solids flow the development should be capable of continuous feed of a uniform mixture of the particulates. Special retention hoppers and design of the outlets for multiple point feed, of course, must also be developed. If, however, the concept proves valid, tie-in to the transport system should be comparatively simple.

Adaptation of a multiple feeder plate on a vibrator that will produce satisfactory amplitudes of the combined vibrating mass can probably be developed more easily in direct consultation with a reputable manufacturer of vibratory equipment. Once the equivalent mass and spring rate are evaluated, and the adjustment of the air gap across the magnet assembly is fixed for a particular vibratory system, the amplitude and solids flow can be controlled by rheostats in the electric circuitry. The vibratory feeder can provide a wide range of feed rates and controlled initiation of solids flow to the pneumatic transport tubes. Maintenance-free operation as dependable as an electric motor is possible for many thousands of hours.

Plant Layouts

A number of plant layouts were prepared to investigate the problems of arranging and coupling the major components required for a complete plant. Provision was made for storing sufficient coal for one month of operation in the winter and for storing the waste ash and spent limestone for a

similar period. In laying out the system an effort was made to give consideration to problems of differential thermal expansion in the duct work, adequate space for maintenance around each component, and provisions for design flexibility so that a range of models of equipment from different vendors might be employed.

Figure 6.26 shows a plan view of a promising conceptual design, and Fig. 6.27 shows a vertical section through this plant. In these layouts it was assumed that the recuperator would be built of 0.50 in. OD tubes, and hence the recuperators shown are large and bulky. As indicated earlier, it is believed that much more compact plate-type recuperators can be obtained commercially within a year, but the data available on these units was not sufficient to make a good system layout at this stage.

Particulate Removal Equipment

The layouts of Figs. 6.26 and 6.27 were made before good data had been assembled on the particulate removal equipment. It now appears that substantially more space must be provided for the components that will be required. Design considerations and the effectiveness of the equipment envisioned are presented at the end of Chapter 3.

Fuel and Limestone Feed Systems

It seems likely that the most difficult problem to be solved in the development of the fluidized bed coal combustor is that involving the preparation, handling, and inspection of the coal and limestone feed materials. For the purposes of this study, it is assumed that the coal and limestone will be crushed to about 8 mesh off-site and will be stored at the site in closed bins or silos in which they will be protected from the weather.

The storage and handling process shown in Fig. 6.28 includes receiving, storage, drying and conveying of the coal and limestone to the fluidized bed combustor. The coal or limestone would arrive at the plant in closed hopper trucks and will be discharged into the storage bins. The storage capacity will be sufficient to supply the fuel and limestone requirements for one month, if deliveries are interrupted. The coal and limestone would be conveyed to weigh tanks which act as buffers between

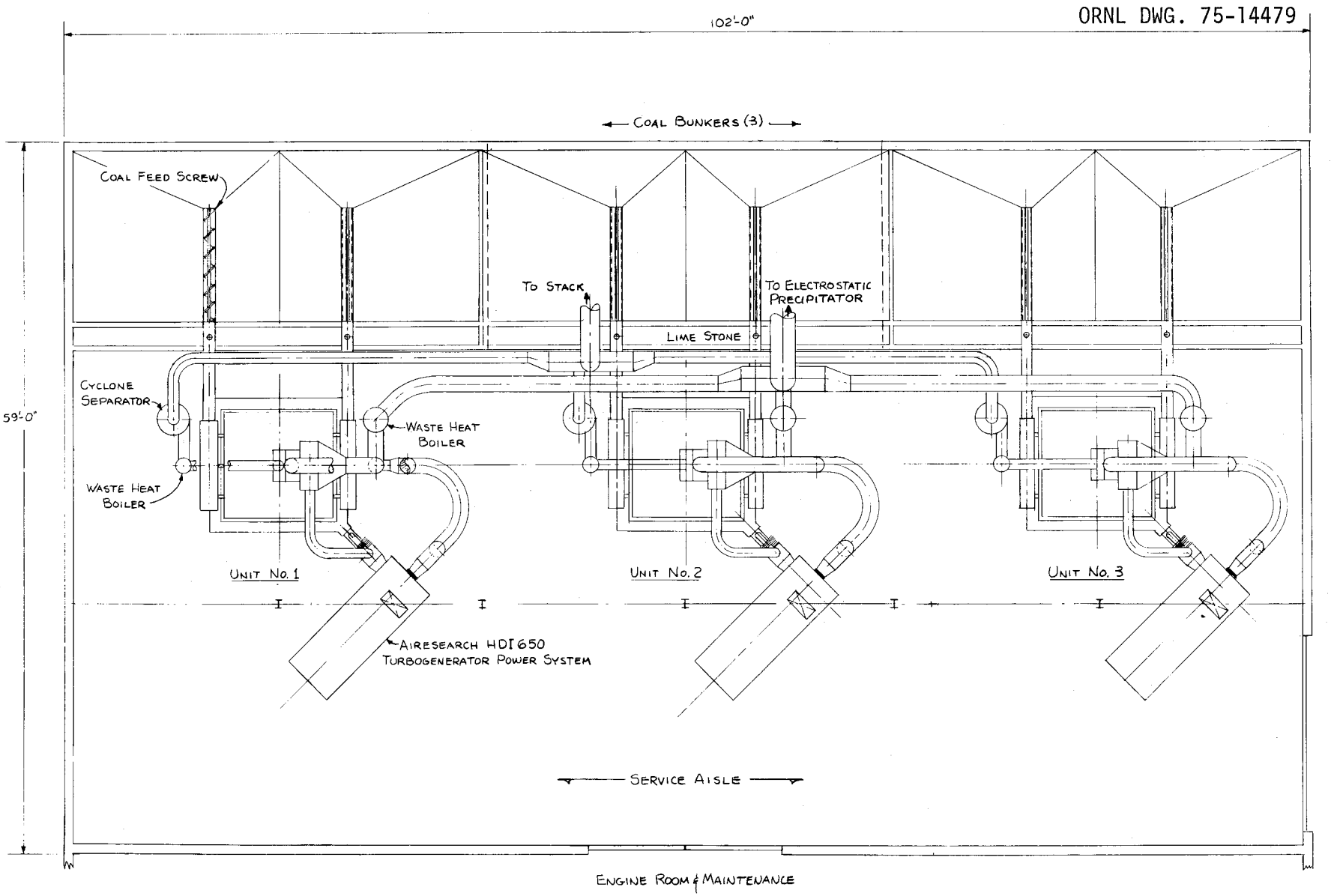

Fig. 6.26. Plan view of a MIUS power plant employing three fluidized bed combustion systems coupled to gas turbines.

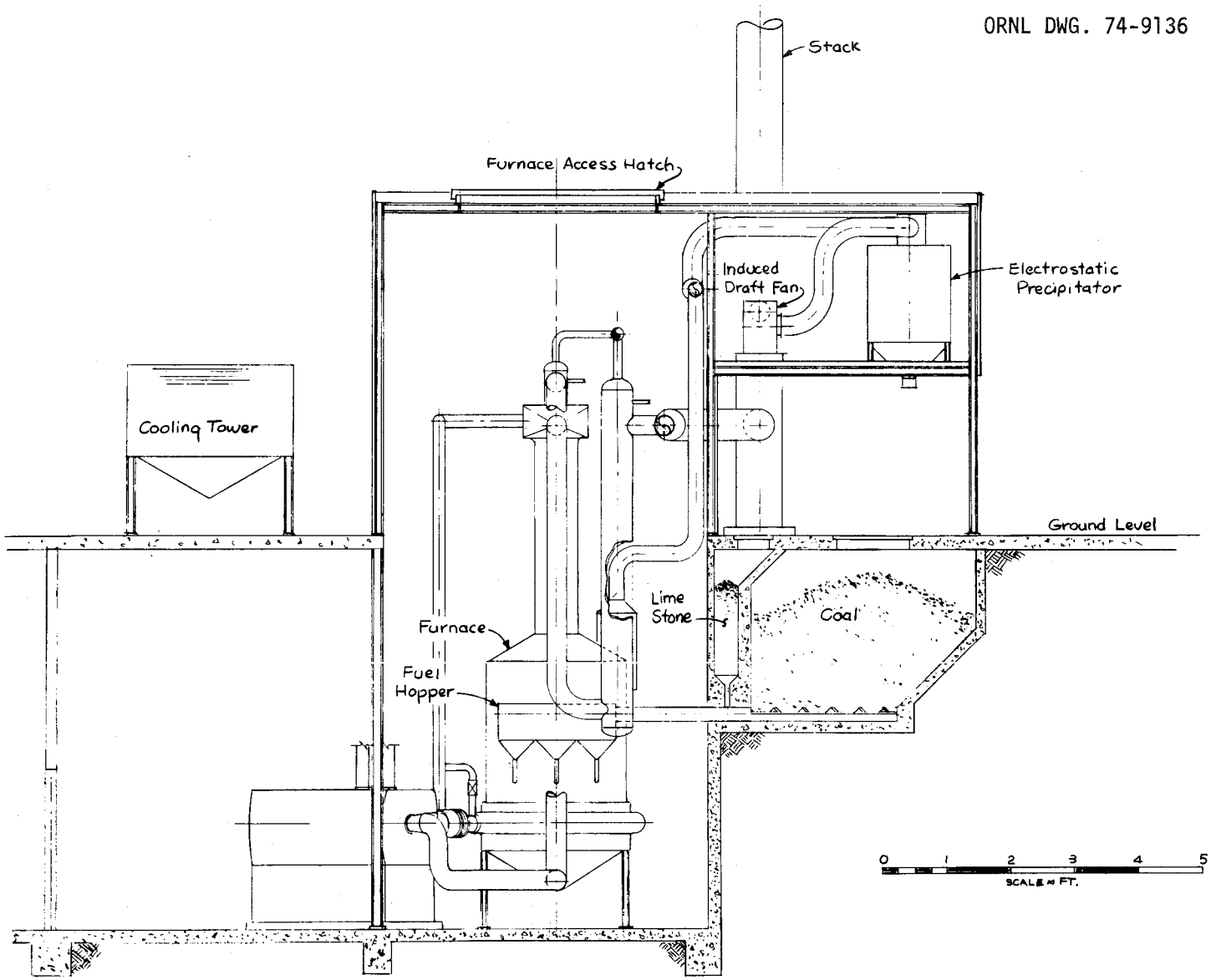

Fig. 6.27. Vertical section through a MIUS plant showing a fluidized bed coal combustion unit coupled to a gas turbine.

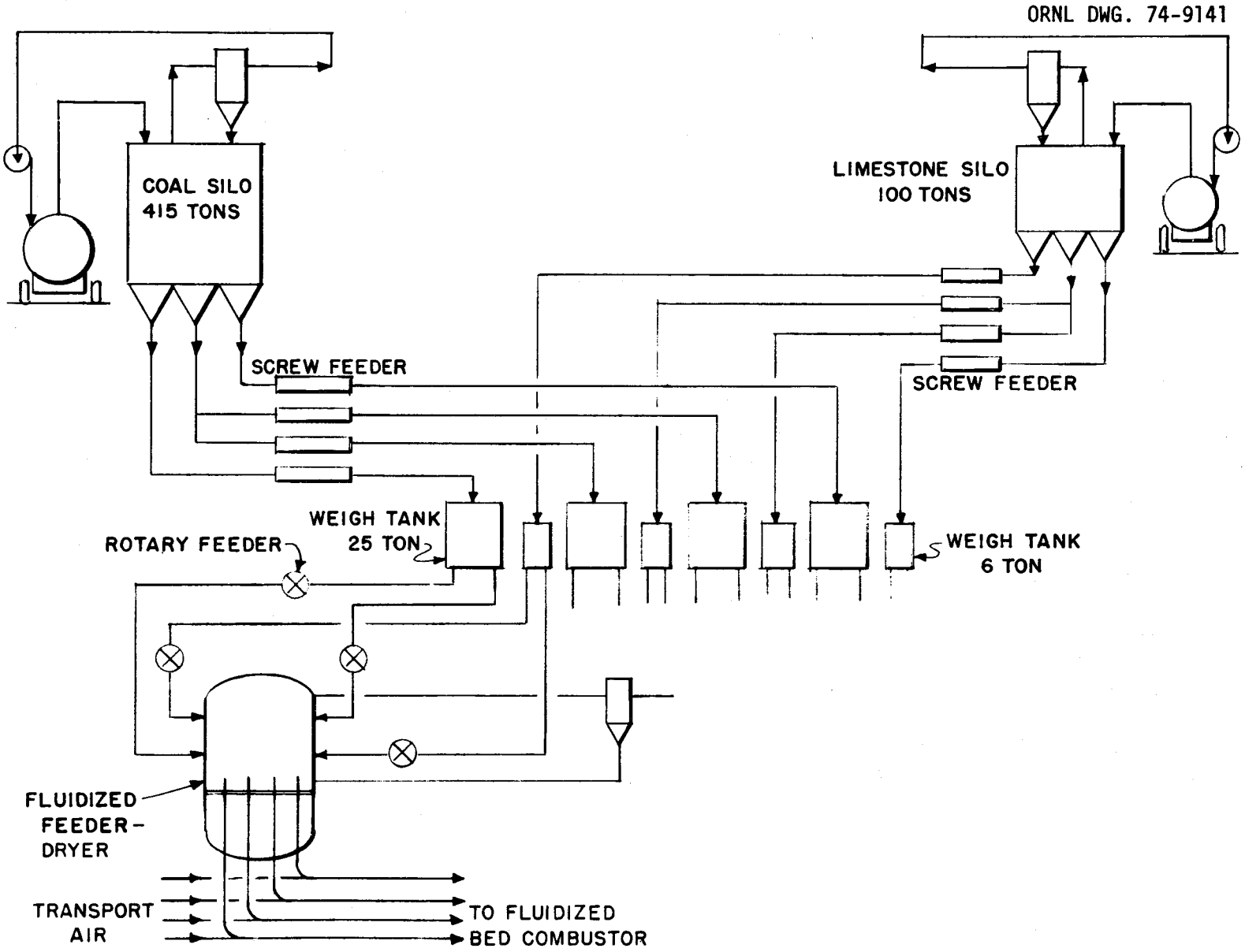

Fig. 6.28. Coal and limestone handling facility.

the batch-type receiving operation and the continuous feeding operation. The weigh tanks are sized to hold a 24 hr reserve in case of feeder malfunctions. The screw feeders are sized to fill the weigh tanks in a one hour period.

The coal and limestone are fed from the weigh tanks through dual rotary feeders to the fluidized feeder-dryer.[8] The coal and limestone are mixed and dried in the fluidized feeder-dryer and fed uniformly to the multiple fuel feed lines required to give even temperatures in the fluidized bed coal-fired combustor.

The fuel injection air system is shown in Fig. 6.29. The system pressure drop is approximately 50 in. of water. The system can be operated under either positive or negative pressure. Feeders in "conventional" coal plants are capable of sealing against pressures of about 60 in. of water gage. The system shown in Fig. 6.29 employs an induced draft fan for the fluidized bed combustor and a booster fan for the fluidized feeder-dryer which allows the continuously operating portion of the fuel feeding system to be operated at negative pressures. Since any system leaks are air into the system and not coal dust out of the system, the negative pressure operation mode (which requires approximately 70% additional pump work as compared to a positive pressure mode of operation) prevents the dispersion of coal dust into the plant ambient atmosphere.

The system described above and shown in Fig. 6.28 and 6.29 is estimated to cost approximately $100,000 or $7.5/kW(e) for a 2000 kW(e) plant capitalized at 15%. This design can probably be greatly simplified by separately feeding the coal and limestone in an "as received" condition directly to the fluidized bed combustor air transport and injection system to give an estimated cost of $5/kW(e). The degree of simplification will depend upon the results of the performance of a demonstration plant designed to investigate the effects of the degree of premixing of the coal and limestone as well as the feed distribution in the fluidized bed combustor, upon the sulfur retention by the limestone, the temperature distribution in the fluidized bed, and the combustion efficiency of the fluidized bed.

The fluidized bed coal-fired combustor firing rate is controlled so as to maintain a constant bed temperature of 1650°F. As shown in

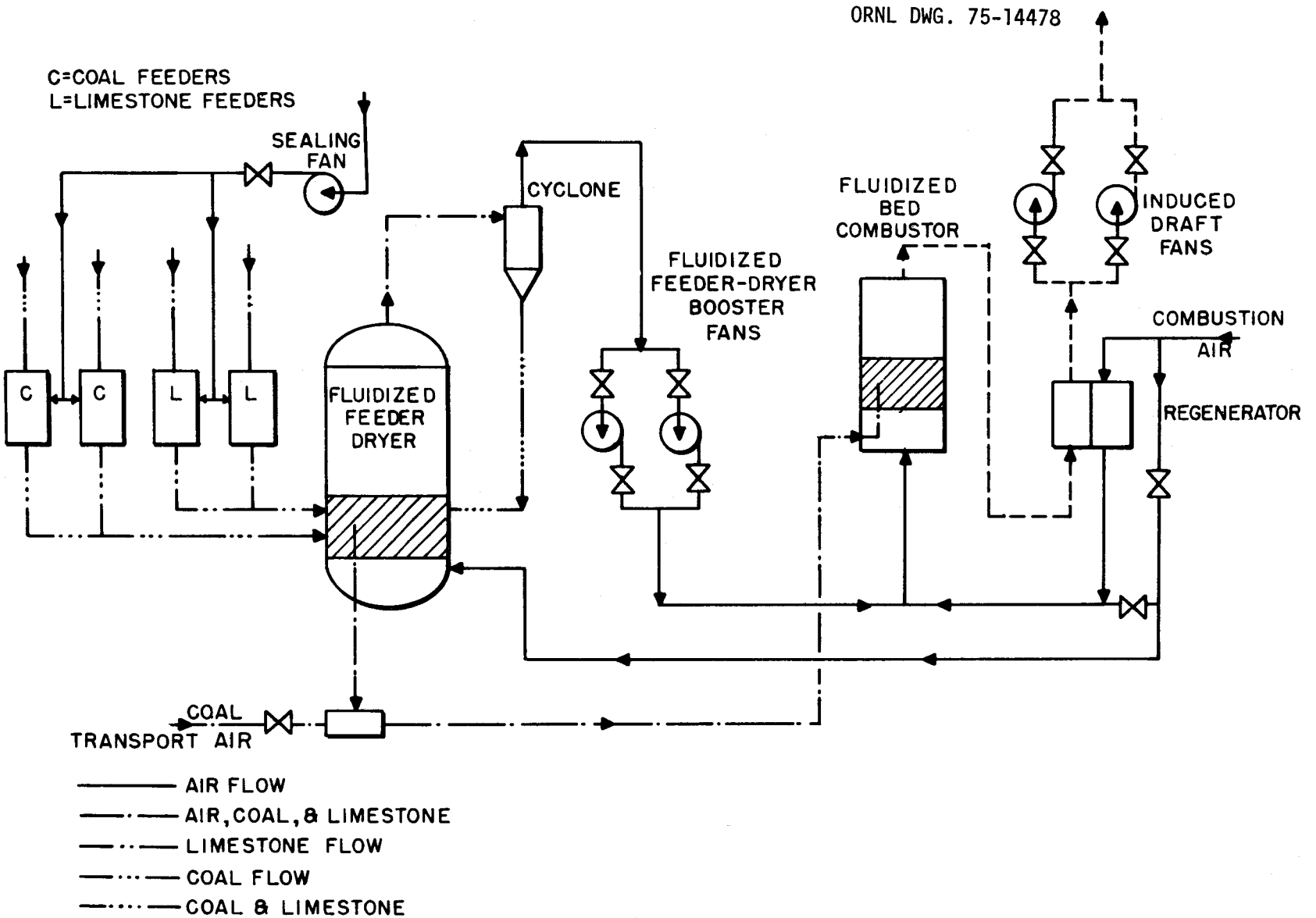

Fig. 6.29. Fuel feed air system.

Fig. 6.30, the coal feed rate is controlled by the flow rate of the modulating air which regulates the flow of the coal and limestone mixture from the fluidized feeder-dryer into the transport air stream. The fluidizing and drying air supplied to the fluidized feeder-dryer is proportioned between the regenerated and unregenerated combustion air so as to maintain an exit air temperature of 250°F from the fluidized feeder-dryer. This will insure that the coal and limestone mixture is sufficiently dry so as not to cause any plugging in the transport lines. The drying air is combined with the regenerated combustion air and fed to the fluidized bed combustor combustion air plenum.

The flow rates of the transport air and the fluidizing and drying air are held constant while the fluidized bed combustor is in operation. The limestone and coal feeds to the fluidized feed-dryer are modulated so as to maintain a constant bed depth in the fluidized feeder-dryer. The required limestone-to-coal ratio as determined by the sulfur content of the coal is maintained by the speed of the respective coal and limestone rotary feeders. The combined combustion air flow rate is controlled by maintaining a constant ratio of the flue gases fed to the induced draft fan to the coal-limestone feed rate.

Capital Cost

It is extremely difficult to estimate the capital costs for a new type of power plant, but a fair insight can be obtained by summing the costs of components. Table 6.12 summarizes the results of an effort to do this for a MIUS installation based on the reference design of Fig. 6.10 and Table 6.3. The costs in Table 6.12 were based on the assumption that these systems would be in production at the modest rate of about a dozen per year so that the design and tooling costs would not be excessive. The major equipment and building items directly related to power production were included, but some other costs--mainly a cooling tower or cooling pond that would be dependent in large measure on the air conditioning system--were not included.

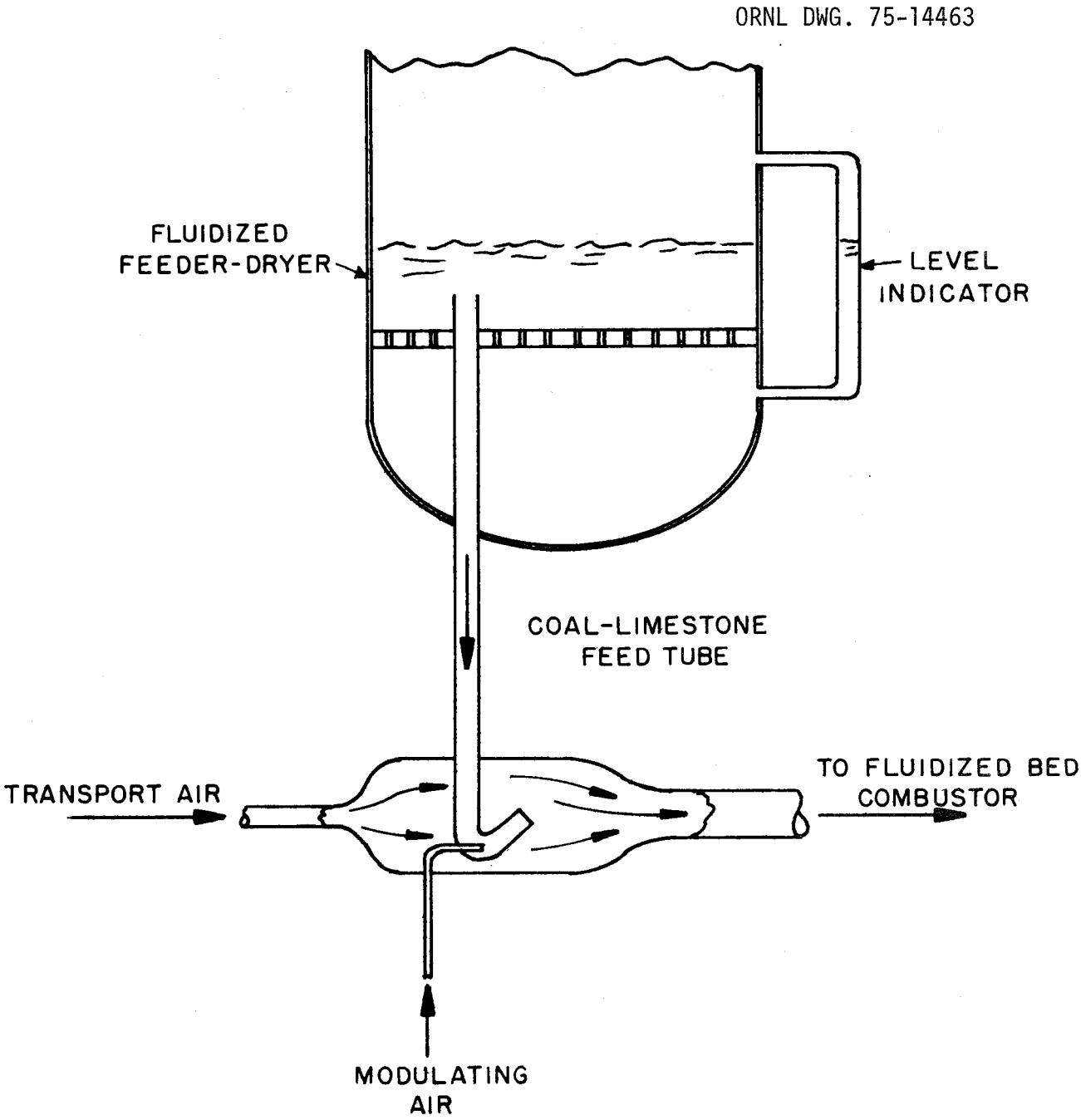

Fig. 6.30. Coal-limestone feed control system.

Table 6.12. Preliminary Estimate of Power Plant Capital Cost per 700 kW(e) Unit

Turbine-generator and controls	$100,000
Fluidized bed-heater-economizer unit	50,000
Recuperator*	25,000
Waste heat recovery unit*	2,000
Cooler*	1,000
Coal and limestone storage, feed, and metering system	35,000
Ash handling and storage system	5,000
Cyclone separators and bag house	20,000
Induced draft fan and stack	10,000
Ducts	10,000
Instrumentation	17,000
Building** (2000 ft^2/unit)	60,000
Design, installation, interest during construction, etc.	110,000
Total	$445,000
Capital cost per Kilowatt***	$635/kW(e)

* Based on $7/ft.

** Based on $30/ft.

*** This includes the equipment for producing domestic hot water and building heat.

The cost of the turbine-generator unit is low in dollars per Kilowatt because it is used in a closed cycle system so that the output of the turbine-compressor unit is increased substantially over the output at atmospheric pressure without an increase in its cost or in the cost of the control system. The cost of the generator and gear box will of course increase with the power output.

The principal uncertainties in the preliminary cost estimates of Table 6.12 lie in the costs of the fluidized bed-heater-economizer unit and its coal and ash handling systems. These uncertainties can be resolved only by building and operating some systems.

References

1. A. M. Squires, Species of Fluidization, Chemical Engineering Progress, Vol. 58, p. 66, April 1962.

2. A. P. Fraas and M. Necati Ozisik, Heat Exchanger Design, John Wiley and Sons, Inc., 1965.

3. H. R. Hoy and J. E. Stanton, Fluidized Combustion Under Pressure, paper presented at the Joint Meeting of the Chemical Institute of Canada and the AIChE, Toronto, May 24, 1970.

4. W. M. Kays and A. L. London, Compact Heat Exchangers, National Press, 1955.

5. Frederick A. Zenz and Donald F. Othmer, Fluidization and Fluid-Particle Systems, Reinhold Publishing Corp., 1960.

6. C yde Orr, Jr., Particulate Technology, MacMillian Company, 1966.

7. M. N. Kraus, Pneumatic Conveyers, Chemical Engineering, Vol. 76, No. 22, p. 61, October 13, 1969.

8. Evaluation of the Fluidized Bed Combustion Process, Vol. III, Appendices, Westinghouse Research Laboratories, Pittsburgh, Pennsylvania, 1972.

9. F. J. Furman, et al., Microsphere Handling Techniques, USAEC Report ORNL-TM-2782, Oak Ridge National Laboratory, March 1970.

10. Design and Feasibility Study of a Pebble Bed Reactor, Sanderson and Porter, New York, N.Y., May 1958.

11. J. R. Johanson, Feeding, Chemical Engineering, Vol. 76, No. 22, pp. 75-83, October 13, 1969.

CHAPTER 7

HOT CORROSION AND STRENGTH OF SUPERALLOYS

Hot corrosion is the term used to describe the degradation of high temperature alloys in combustion product gases. A review of the characteristics of this type of corrosion clearly shows that combustion gases are much more aggressive than air around 900°C. Typically, the reaction rate laws change from a parabolic to linear or accelerated dependence as the environment is changed from air to combustion gases, signifying the conversion of a protective oxide scale to a non-protective one.

A vast amount of work on the hot corrosion problem has been done by the aircraft, petroleum, and electrical power industries. The general observations are that corrosion is highly specific to alloy type and to combustion gas chemistry. Consequently, it is difficult to extrapolate corrosion results from one fuel source and temperature to another. Nonetheless, certain general characteristics emerge as being significant; alloy composition, environment, and the corrosion mechanism.

Effect of Alloy Composition

At 1000°F the ferritic steels based on 12 Cr-1 Mo appear somewhat more resistant than the 300 series alloys to the sulfur compounds in fossil fuels.[1] At high sulfur activities, wall thickness losses average about 2.5×10^{-3} in./1000 hr for the 300 series alloys. Chromium additions to Fe or Co base alloys markedly improve the resistance to sulfidation.[2,3] Aluminum coatings improve the corrosion life of cobalt alloys tenfold in gases contaminated with sulfur and alkali metals at 1600 to 1740°F;[4] however, it has also been reported that alloys that do not form alumina-rich surface scabs are not susceptible to accelerated attack by Na_2SO_4 between 1470 and 1830°F.[5]

Effect of Environment

Oxidation of steel at high temperatures may be greatly accelerated if the oxidizing gas mixture contains sulfur dioxide. The introduction of sulfur dioxide and moisture simultaneously into air greatly increases

the oxidation rate of steel at 900°C, although sulfur dioxide alone appears to have had little effect.[6]

The hot gaseous mixture produced by the burning of fuel often causes rapid oxidation of steel. Naturally, the oxidation rate is greatest if free oxygen is present (i.e., if excess air has been used for the combustion); oxidation may be slow or absent if the gaseous mixture is definitely reducing, although if sulfur compounds are present, hydrogen sulfide in a reducing mixture may then cause serious destruction to some materials — notably alloys rich in nickel.

Nevertheless, serious oxidation is possible even in mixtures containing no free oxygen or sulfur compound. If burned in a deficiency of air, coke or coal will yield a mixture of carbon dioxide and carbon monoxide diluted with much nitrogen; there will be some water vapor, but the amount of water is far greater if the fuel contains largely hydrocarbons and hydrogen.

Measurements[7] of iron-wastage by gas mixtures representing the combustion products of three types of fuel, with and without added sulfur dioxide, are shown in Table 7.1. It will be seen that the scaling rate increases with the amount of water vapor in the mixture, and is further increased by small additions of sulfur dioxide.

Table 7.1. Wastage of Iron by Gas Mixtures

Mixture Representing Products of Combustion from —	Composition of Mixture (Percent by volume)				Scaling Rate at 1000°C. (mg/cm^2 in 1 hour)		
	H_2O	CO_2	N_2	$NaSO_4$	0.05% SO_2	0.10% SO_2	0.20% SO_2
Dry, high-temperature coke	2	18	80	4.4	11.2	14.6	18.6
Coal, oil or producer gas	10	10	80	7.5	17.5	22.5	26.5
Coal gas	20	10	70	12.0	21.5	27.8	32.0

Inconel 713C and Mar-M200 coated with Al and Al-Cr were exposed to JP-5 combustion gases with three levels of sulfur ($<$ .004, .04, and 0.4%) with and without 1 ppm sea salt. The primary cause of corrosion was the sea salt and not the sulfur content of fuel.[8,9] The corrosion of Ni alloys by SO_2 or Na_2SO_4 is enhanced between 800 and 1000°C in the presence of low concentrations of CH_4.[10] The effect is attributed to localized reducing conditions created by the catalytic decomposition of CH_4 to carbon by the alloy surface.

Corrosion Mechanism

The picture which emerges as the mechanism of "hot corrosion" appears to be one in which normally protective oxide scales are destroyed by trace amounts of inorganic solids. The inorganic materials have been identified as alkali metal oxides such as Na_2SO_4, $NaVO_3$, Na_2MoO_3, etc. and oxides of Mo and V. One theory is that the above compounds, which are derived from combustion, rapidly flux the protective oxide and allow the sulfur containing compounds to attack the substrate. A second concept is that these compounds drastically reduce the adhesion of the protective scale. In either case the sulfidation of the substrate means that sulfur in some form is accessible at discontinuities in the normal oxide scale.

Gas-Metal Reactions in Helium

Theoretically, the substitution of helium for air as the coolant should eliminate the oxidation of the alloy tubes; however, in practice, a helium environment has shown evidence of being a more aggressive coolant than air. This characteristic stems from trace levels of active impurity gases in the helium whose concentration is too low, typically 50 to 200 μ/atm, to form a protective oxide film on the alloy surface. As a consequence, the corrosion reactions tend to concentrate below rather than at the gas-metal interface. Obviously, metal consumption at the surfaces will be minimal but the internal reactions which occur between the more reactive alloying elements and the dissolved gases reduce the strength of the alloy.

Corrosion in Fluidized Beds

The relevance of existing data on hot corrosion to the fluidized bed coal burning concept cannot be assessed very well at this stage. Distinguishing features of the fluidized bed are (1) the relatively low temperature of the combustion process (compared to combustion in flames) and (2) the slowly moving bed of ash particles in intimate contact with the metal surfaces. Oxidation of a metal placed in the oxidizing part of a flame introduces factors not operative in oxidation by combustion products in a fluidized bed, because the chemical states of molecules and free radicals at flame temperatures differ markedly from those at lower temperatures. Furthermore, combustion gases emanating from the flame region are not in thermal equilibrium so that there are point-to-point differences in chemical composition.

An example of important differences between flame and bed heating concerns the behavior of sulfate and vanadate compounds. The vapor pressures of these compounds are relatively high at flame temperatures, and they leave the flame region in gaseous form. The compounds condense on cooler surfaces beyond the flame region and thus become intermixed with preexisting oxidation products on these surfaces. In the bed concept, sulfates and vanadates undergo chemical reactions with the coal-ash mixture, and the resultant reaction products will not volatilize significantly as long as the combustion temperature remains below 900°C. Thus, these sulfur-containing compounds can be made relatively nonreactive (depending on the bed composition) before they contact metal surfaces within the bed.

On the other hand, the possible erosion accruing from slowly-moving ash particles is of special concern in the fluidized bed concept. However, the limited materials studies conducted to data have shown no evidence of direct metallic erosion. This observation is not unexpected considering the relatively low fluidizing velocities (2 to 8 ft/sec) associated with the suspended bed. In conventional coal-fired boilers, erosion by particle impaction does not occur at flue gas velocities below approximately 100 ft/sec.

Visual examination of test specimens has also indicated that the scouring action by ash particles is not sufficiently erosive to remove the

protective oxide cover and expose clean metal surfaces to the environment. This is based on specimen weight loss results which show that the rate of corrosion decreases with time, thus indicating the formation of a stable protective oxide layer. Table 7.2 gives the weight loss for several steels (30μ g/cm^2 hr is equivalent to 1.5 x 10^{-6} in./hr). Sulfide penetration of 10 to 20 μm was observed for the austenitic steels in the range 1290 to 1560°F in 100-hr tests and a maximum of 70 μm in the 500-hr tests.

The exposure of X-40,* Nimonic 75,* and EPK-55* to the exhaust atmosphere of a fluidized bed for 200 hr in the range 1565 to 1675°F initiated hot corrosion. Sulfur penetration was most severe in X-40 (approximately 0.009 in.) and least in EPK-55 (0.004 in.).[11]

On the other hand, the presence of the fluidized bed does influence the formation of deposits on the tubes. Tubes situated in the bed exhibit a thin, even, hard and adherent deposit (<0.1 mm thick). The undersides of tubes situated above the bed sometimes are covered with a layer of fine ash, and coarse ash particles formed a layer on the top of these tubes. Both types of layers appear loosely adherent and do not form on the tubes situated in the bed.

High Temperature Strength Considerations

Important considerations for the selection of heat exchanger and ducting materials include creep and stress-rupture strengths, low and hich-cycle fatigue resistance, thermal stability, and the effects of environment on these properties, including gas-metal reactions and erosion.

Effects of a Hot Gas Environment on Mechanical Properties

To date there is not complete agreement as to the effects of combustion gas environments on mechanical properties. If we assume that the disparate data are corect (i.e., do not reflect differences in testing procedures, conditions, etc), we can conclude that the differences accrue from

---

*X-40: 10 Ni—57 Co—25 Cr—0.75 Si—o.4 C

*Nimonic 75: 78.8 Ni—20 Cr—0.2 Ti—0.7 Si—.01 C

*EPK-55: 43.6 Ni—20.0 Co—28.5 Cr—0.75 Cb—2.3 Ti—1.2 Al—0.1 C

Table 7.2. Average Weight Losses of Specimens

Test	Position	Wt. loss in $\mu g/cm^2h$							
		Temp °F	M.C.S.[a]	2¼% Cr	12% Cr	Type 347	Type 316	Esshete[b] 1250	PE 16[c]
Series 1 (Pittsburgh) 100 h duration	In bed	690	91	92	-	-	1	2	-
		940	163	179	-	-	2	3	-
		1100	-	579	-	7	8	9	-
		1320	-	-	-	11	11	21	-
		1560	-	-	-	12	9	20	-
	In freeboard	789	62	74	-	-	1	2	-
		1340	-	-	-	5	4	10	-
		1500	-	-	-	3	2	4	-
Series 2 (Pittsburgh) 500 h duration	In bed	770	48	32	2	-	1	1	-
		920	88	78	6	-	2	1	-
		1090	-	539	5	3	3	4	-
		1310	-	-	3	3	4	6	3
		1560	-	-	308	7	5	7	3
	In freeboard	760	24	25	1	-	<1	<1	-
		1310	-	-	1	1	1	5	1
		1520	-	-	3	-	1	3	2
Series 3 (Pittsburgh + Limestone 18) 465 h duration	In bed	730	41	42	2	-	1	1	-
		930	84	98	6	-	2	2	-
		1100	-	222	3	2	2	3	-
		1320	-	-	7	6	6	13	5
		1560	-	-	475	3	2	3	2
	In freeboard	760	18	18	2	-	<1	<1	-
		1310	-	-	2	2	2	6	2
		1490	-	-	2	2	3	12	2

[a]Medium carbon steel (0.45 C).

[b]15 Cr–10 Ni–0.15 C–6.0 Mn–1 Mo–bal Fe.

[c]17 Cr–43 Ni–0.1 C–3.0 Mo–1.2 Ti–1.2 Al–bal Fe.

environments which are different with respect to impurity concentrations and/or impurity gas ratios. A second factor which may contribute to the apparent conflicts are differences in the thickness of the test section. Because the reactions occur mainly at the metal-gas interface, the extent of a mechanical property change should be dependent on the metal surface-to-volume ratio. Sheet products should be affected more than bar products and thin sections more than thicker sections.

In the absence of more extensive experimental data to resolve these questions, it is not possible to predict the effects of environment on mechanical properties, because in some cases alloys have been observed to be strengthened and in others weakened in gaseous environments. To illustrate the possibilities, we have observed that the creep strength of alloys may be weaker during their interaction with gas constituents than when the alloys were doped with the same constituent prior to creep testing. Alloys exhibiting this characteristic can also undergo accelerated transient creep rates for short periods. In general, such alloys do not form a surface-reaction product. This phenomena is therefore related to the reaction and solution of the impurity gases and the precipitation of a grain-boundary phase at the solubility limit. However, gas-metal reactions resulting in the formation of a surface film are, in general, strengthening provided that the applied stress is lower than that required to crack the film. When this happens, low creep rates may — but not always — be accompanied by low strains at rupture.

Currently accepted practice permits design for long service times to be based on relatively short-term property information (e.g., it permits extrapolation of creep data from less than 50,000-hr tests to several hundred thousand hours). This procedure, considering the "safety margins" incorporated into design and allowable stresses, is acceptable if the materials are metallurgically stable (i.e., do not transform or age to produce a material of different character in terms of strength and/or ductility) under the time-temperature-environment conditions experienced in service. Short-time instabilities are probably sufficiently accounted for in the typical range of data acquisition, but possible longer term changes which might occur from sequential transformations and/or transformations reflecting interaction with the environment are generally poorly known and characterized. Questions of long-time thermal stability and environmental compatibility must be addressed in the selection and qualification of materials for the construction of fluidized bed systems.

Candidate Alloys

The following is a brief survey of the potential of alloy classes or families for heat exchanger service based on design parameters discussed in earlier chapters.

1. Heat exchanger tubes of 1/2-in.-OD x 37.5 to 70-mil wall.
2. Pressure difference of 150 psi (hoop stress of 1000 psi).
3. Service life of 100,000-hr (stress-rupture).
4. Service temperature of 1600°F.
5. Service environment, air/(coal and combustion products).

Carbon and Low-Alloy Steels. This large class of low cost materials is not suitable for use in this application. They have neither the oxidation resistance nor high temperature strength required.

High-Alloy Ferritic Steels. Although chrominum-molybdenum steels of the 12% Cr-1% Mo class offer a significant improvement over the low alloy materials, their service is limited by both oxidation resistance and rupture strength to approximately 1200°F.

Ferritic Stainless Steels. The 440 series of stainless steels (18 to 27 wt % Cr) have the potential for continuous service in air at temperatures up to 1950°F. They are used in applications where resistance to corrosion and scaling is important. Type 446 is also often used in sulfur-bearing atmospheres. Unfortunately, strength considerations would likely limit their service to about 1500°F.

Austenitic Stainless Steels. Three austenitic stainless steels (types 304, 309, and 310) are worthy of consideration for this application. All should meet the strength guideline (i.e., no ruptures in 100,000 hr of 1600°F service), with the latter two meeting it more comfortably. However, type 304 (19% Cr—9% Ni) and 310 (25% Cr—20% Ni) are used in applications requiring high temperature strength and air oxidation and scaling resistance at temperatures up to about 2000°F. Their compatibility with the combustion bed environment needs to be investigated.

Fe-Ni-Base Alloys. Two commonly used alloys of this class are Incoloy 800 (21% Cr—32.5% Ni—0.8% Ti+Al—balance Fe) and A-286 (15% Cr—26% Ni—3.5% Mo+Ti+Al—balance Fe). A-286 is slightly stronger than Incoloy 800 at temperature (both should meet the design guidelines) but is, perhaps, slightly inferior in terms of air oxidation resistance. Both materials need experimental evaluation in terms of their compatibility with the combustion bed (i.e., what corrosion allowance will be necessary and will the interaction of these materials with the environment lead to degradation of rupture life and/or useful service life?). In this regard, it should be noted that an

alloy very slightly modified from the Incoloy 800 composition, Incoloy 802, is used for high temperature sulfidation resistance.

Ni-Base Alloys. A large number of Ni-base superalloys which exceed the strength and air oxidation resistance guidelines are available. These alloys generally have additions of 10 to 25% Cr, up to 10% Co, and lesser amounts of various combinations of W, Cb, Mo, Ti, and Al. These materials may be unattractive from a cost standpoint. Their compatibility with the combustion bed needs evaluation.

Co-Base Alloys. This family of materials also offers high temperature strength and air oxidation resistance. Most of these alloys contain Cr (up to 30%), Ni (about 10%), and lesser additions of Mo, W, and Cb. Their cost is high and their compatibility is unproven.

Conclusions

Regardless of the material or materials chosen for this heat exchanger application, their compatibility with the combustion bed will be a major question. Based on a balance of cost, high temperature strength, and air oxidation resistance, the use of types 309 and 310 stainless steel and Incoloy 800 should be strongly considered.

References

1. W. D. Halstead, J. Inst. of Fuels, 234, (July 1970).

2. T. Narita and K. Nishida, Oxidation of Metals, 6(3) 157-180 (June 1973).

3. C. S. Geggins and F. S. Pettit, Oxide Scale Adherence Mechanisms, PWA-4786 (July 1973).

4. A. Davin and D. Coutsouradis, "Hot Corrosion of Experimental Aluminum-Coated Co-base Alloys," Cobalt 55, 99-100 (June 1972).

5. V. F. Buehring, Recent Development of Ni and Co Alloys, BMI (April 1970).

6. W. H. Hatfield, J. of the Iron St. Inst., p. 115 (1927).

7. H. C. Millett and J. W. Cobb, Trans. Instn, Gas Engrs. 1935-36, 85, 610; 1936-37, 86, 388; also J. W. Cobb, C. B. Marson and H. T. Angus, J. Soc. Chem. Ind. 1927, 46, 61T, 68¢.

8. H. T. Quigg and R. M. Schirimer, Effect of Sulfur in JP-5 Fuel on Hot Corrosion of Coated Superalloys, Report 5058-68R, Phillips Petroleum Co., Bartlesville, Okla. (May 1968).

9. H. J. Wagner and W. F. Simmons, DMIC Rev. of Ni & Co Base Alloys (Nov. 1966).

10. D. W. McKee and G. Romeo, Met Trans. 5 1127 (May 1974).

11. Final Report on Reduction of Atmospheric Pollution, Fluidized Combustion Control Group, National Coal Board, London, England, prepared for the Environmental Protection Agency (September 1971).

CHAPTER 8

INSTRUMENTATION AND CONTROL

Coupling a fluidized bed coal combustion chamber to a gas turbine presents some unusual instrumentation and control problems. In attempting to cope with these problems it seems best to consider first the MIUS requirements, then review the control system employed for a typical coal stoker-steam boiler for an apartment house complex, and then examine the basic control concept envisioned for the fluidized bed coal combustion system coupled to a gas turbine.

MIUS Requirements

Typical yearly requirements for electricity, domestic hot water, space heating, and air conditioning in a housing complex are summarized in Table 4.1 for a set of apartments in Philadelphia. The energy demands at any given time vary widely throughout the course of a day, between weekdays and weekends, and with the weather. Thus, not only does the amount of energy required in any given form vary widely, but also the ratio of electricity to heat varies. These problems are treated in detail in Appendix C, and are summarized briefly below.

In approaching the control problem, it appears best to consider first what might be called the most common set of operating conditions; these entail a power plant output about half the maximum demand. For this condition the electrical power requirements would somewhat exceed the requirements for heat so that some waste heat would be deliberately rejected. The waste heat from the power conversion system can be rejected to the environment by any one of several different routes. Probably the most practical will be either a cooling tower or a cooling pond. The latter appears particularly desirable for MIUS application because it can also be employed as the final step in the cleanup of the effluent from the sewage plant. Thus, for purposes of this discussion, it will be assumed that a cooling pond will be employed for rejection of waste heat from the power conversion system.

Diurnal Variations in Load

Figures 2 to 10 of Appendix C show typical curves for the electrical and heat loads as functions of the time of day for summer, winter, spring, and fall conditions. Note that the requirements for domestic hot water represent about 17% of the requirements for building heating on a typical cold winter day. Note, too, that the maximum rate of change of load is moderate, i.e., about 0.7% per minute. Thus, for normal operation it will not be necessary to employ a control scheme that will accommodate rapid or large step changes in load such as might be encountered for industrial installations.

Although there is no economically attractive system for storing electricity during the hours of low demand so that it can be released during peak demand periods, it is economically attractive to store heat for periods of as much as a few days. Thus the changing ratio of the electrical to the heat load can be accommodated over the course of a day by employing some large hot water storage tanks. So far as diurnal variations in electrical and heat loads are concerned, the control system can be designed so that the power conversion system operates with the appropriate average ratio of electrical output to heat output for the day, and the hot water storage tanks can be used to accommodate the diurnal variations.

Seasonal Variations in Building Heating Loads

The large variations in the ratio of electrical to building heat loads evident in Appendix C, Figs. 2 to 10, in going from either winter or summer to spring or fall imply that the power conversion system should be designed to give the maximum efficiency obtainable to produce electricity from the thermodynamic cycle in order to minimize the amount of waste heat rejected in the spring or fall. It is also important to build the system so that the ratio of heat to electricity can be increased during the peak winter heating months because it is essential that an adequate amount of heat be available on the coldest days in winter. During the peak air conditioning load periods in the summer, the waste heat available from the thermodynamic cycle will not be sufficient to drive an absorption air conditioning system of adequate capacity. For these high air conditioning load periods, electric motor driven Freon compressors can be employed and the air conditioning load

can be divided between the electrically driven compressors and the absorption air conditioning equipment. Thus, during hot weather it is important to operate the thermodynamic cycle in a mode that gives the best possible efficiency for the generation of electricity, and there will be no waste heat rejected from the thermodynamic cycle to the cooling pond.

Control of Conventional Boiler Furnaces with Coal Stokers

Of the various conventional systems in current use in which coal is fired into steam boiler furnaces for apartment house complexes, the system that appears most nearly analogous to the fluidized bed coal combustion system is one in which coal is carried by a screw conveyer from a bin or hopper to a point close to the furnace, dropped into an air stream, and then blown into the furnace, the small particles being suspended in the air stream. The coal and air flow are modulated continuously to provide the required heat input over the entire range from low to high loads. The variation in coal feed rate is obtained by varying the speed of the feed screw employed to deliver coal from the hopper or bin. The air flow is modulated by operating a butterfly valve in the air supply system. About 10% of the full load combustion air flow is used to convey the coal into the furnace; this air is supplied from a blower at a head of 12 to 20 in. of water and the flow is not modulated with load because coal particles would tend to fall out of suspension at low air flow rates. The balance of the combustion air is supplied from a larger blower with a delivery head of three or four in. of water. No induced draft fan is employed.

Control of Fuel-Air Ratio

The fuel-air ratio is ordinarily controlled to give about 25% excess air. Metering of the coal is accomplished by sensing the rotational speed of the feed screw; the coal feed rate is directly proportional to the speed of the feed screw. A linkage is employed on the air supply valve so that the air is kept proportional to the fuel flow.

The pipes carrying the particles suspended in air commonly include horizontal runs of as much as 40 ft and vertical runs of as much as 30 ft, but not both of these maximum distances in series.

Control of Fluidized Bed Coal Combustion Systems Coupled to Steam Boilers

All of the fluidized bed coal combustion system work conducted to date has been carried out with heat removal from the bed via steam boiler tubes, and, as indicated previously, this constrains operation to the vicinity of the design point, i.e., full load operating conditions. Automatic controls have not been employed; manual adjustments of coal feed rates and the air flow have served. Thus, while the experience that has been gained with fluidized bed coal combustion systems is not necessarily applicable to the gas turbine system of interest here, it does provide some important and valuable insights.

The coal feed system used by BCURA is essentially that which they tried initially and found that it worked satisfactorily. They have done little work on improving the system or investigating the effects of variations. The coal is fed to the bed through four 1/2 in. nominal pipes. The pipe runs are straight with T's or crosses at the corners rather than sweeping curves because the latter are subject to erosion. The crosses have the advantage that the pipe plugs can be removed and the pipes can be cleaned if there is any tendency of the coal to form a plug. However, they have never experienced any plugging of their lines. The air flow they employ to carry the coal through the lines is equal to about 8% of the total air flow to the bed. The coal size used in the 1/2 in. pipe lines is 1/8 in. mesh coal with no effort to reduce the fraction of the fines. The pressure drop through about 200 ft of pipe from the hopper to the bed is only about 1 psi. Note that they make use of 200 ft of pipe to build up the pressure drop and thus give them an adequate basis for metering with their existing metering equipment. They agreed that a different set of metering equipment would probably work satisfactorily on a much smaller pressure drop, and that with such a system the long pipe lines that they employ would not be necessary.

In supplying coal to the lines, it is allowed to drop through a pindtle control valve vertically downward into a pipe Tee. The air employed to convey the coal is supplied vertically upward from the bottom leg of the Tee and the coal-air mixture is carried off from the horizontal outlet of the

Tee. They said that in their experience this arrangement worked better than feeding the air horizontally into the Tee with a horizontal air-coal outlet. They make use of a transparent plastic section in their coal feed pipe ahead of the Tee to get a direct visual indication of the coal flow rate.

BCURA experience indicates that the limestone can be mixed with the coal prior to delivering it to the air transport system, and they prefer this mode of operation. Their recent test work indicates that, on a weight basis, limestone is as good as dolomite at least for some bed operating temperature and pressure conditions.

BCURA has not analyzed the problem of rates of change that one might expect to be able to effect, but they have routinely obtained temperature changes in the bed at a rate of 100°C/minute. (ORNL analytical estimates indicate that even faster rates of change are achievable in principle because the mean effective lifetime of a coal particle in the bed is only a matter of a few seconds.)

Basic Concept Envisioned for the Fluidized Bed Coal Burning Gas Turbine

A flow sheet for the system envisioned including the principal components required for control is shown in Fig. 8.1 and design data for the system are given in Table 6.3. The system assumes that the coal will be conveyed from the bin to a point close to the furnace with a comercially available feed screw with a continuously variable speed drive, and that the coal will drop into an air stream representing about 10% of the total combustion air flow and will be conveyed through 1/2 in. (nominal) pipes to tuyeres in the bed support plate.

Control System Design Precepts

After considering a variety of approaches to the control problem, a consistent set of design precepts was evolved that appears to give a reasonably straightforward control system that will meet all of the required boundary conditions. These precepts are as follows:

1. The fluidized bed will be operated at a constant temperature chosen for nearly optimum sulfur removal. To

accomplish this the coal feed flow rate and combustion air flow rate will be slaved to the bed temperature.

2. The gas turbine and generator speed will be held constant to maintain a constant output frequency of 60 Hz. This will be accomplished by varying the pressure in the closed cycle gas turbine system. An air reservoir (see Fig. 8.1) will be provided to facilitate the changes in system pressure level.
3. The rate of heat release in the bed is primarily dependent on the combustion air flow rate, hence the primary control on bed temperature will be on the combustion air flow. The amount of coal in the bed would ordinarily be equivalent to that consumed in about 1 min of operation.
4. The fuel-air ratio would be controlled to provide about 10% excess air.
5. The limestone would be mixed with the coal in the region where the coal is fed into the air stream used to convey it into the furnace. The limestone flow rate would be adjusted to some definite proportion of the coal flow rate depending on the sulfur content of the coal.
6. Emergency control for an abrupt loss in electrical load would be obtained by opening a valve to allow air to bypass the turbine and flow directly from the compressor outlet to the cooler inlet. Only about one-third of the air need be bypassed in order to go from full load to zero load with a gas turbine.
7. The ratio of heat to electrical output can be increased for cold weather conditions by allowing air from the compressor outlet to bypass the recuperator and flow directly to the economizer. This will as much as double the ratio of heat to electrical output.
8. During periods of the day when the electrical load gives a waste heat output from the thermodynamic cycle in excess of the immediate heat load requirements of the housing complex, excess waste heat from the thermodynamic cycle

ORNL DWG. 74-9135

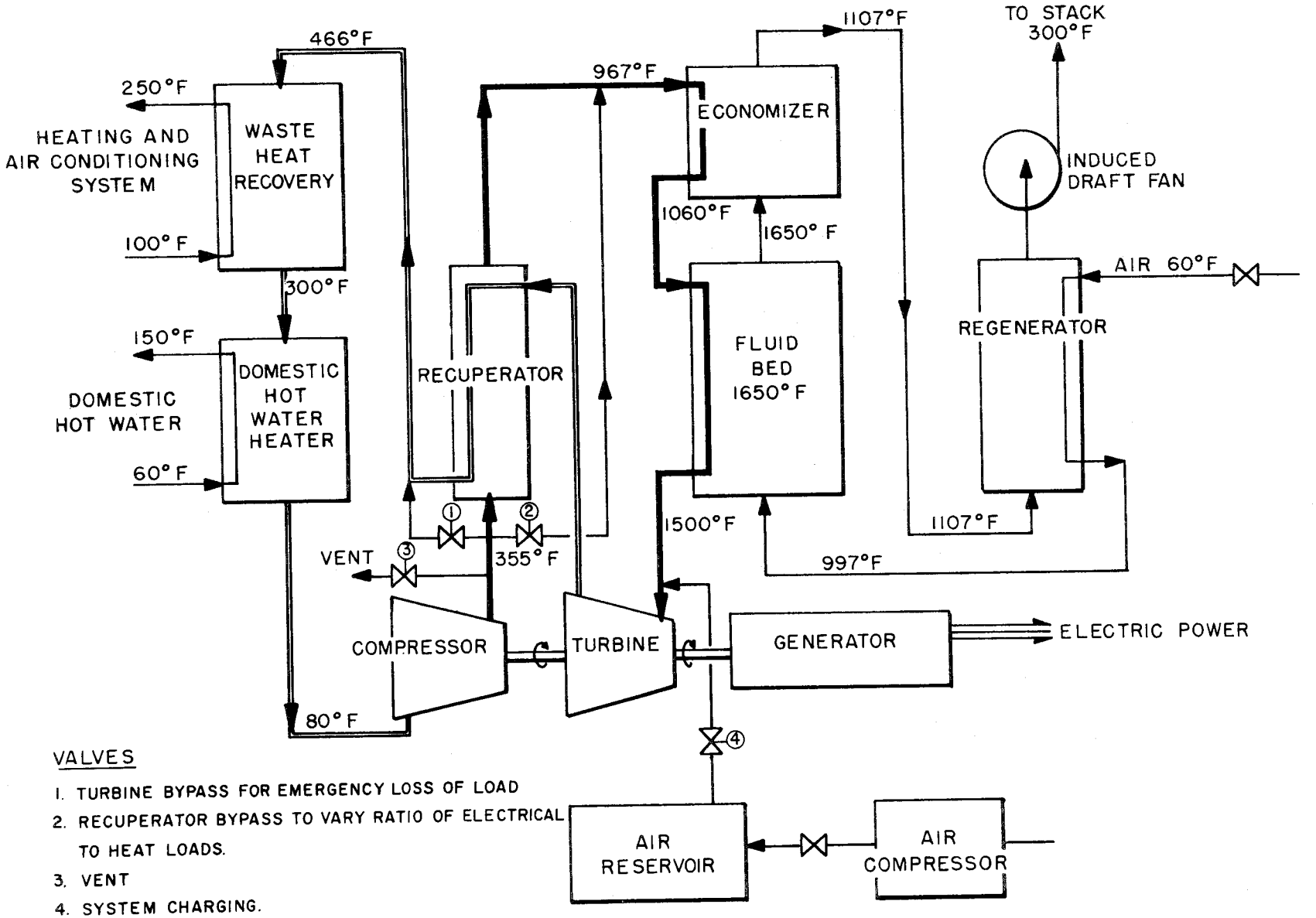

VALVES

1. TURBINE BYPASS FOR EMERGENCY LOSS OF LOAD
2. RECUPERATOR BYPASS TO VARY RATIO OF ELECTRICAL TO HEAT LOADS.
3. VENT
4. SYSTEM CHARGING.

Fig. 8.1. Flow sheet for the reference design closed cycle system.

would be stored in the form of hot water. The heat storage capacity will be reached when the interface between the hot and cold water in the hot water storage tank drops all the way to the bottom of the tank at which point waste heat from the thermodynamic cycle will be dumped to the cooling pond.

9. If the interface between the hot and cold water in the hot water storage tank rises above a point about 25% down from the top, the recuperator bypass will be opened to allow air to bypass directly from the compressor to the economizer, thus degrading the thermodynamic cycle efficiency and increasing the ratio of heat to electrical output. The recuperator bypass valve would be closed when the interface between the hot and cold water dropped below the midpoint of the tank.
10. The air flow rate through the coal feed pipe would be kept constant irrespective of the coal feed rate to avoid settling of coal particles in the feed pipes.
11. The rate at which the electrical load will increase or decrease under normal operating conditions will not exceed about 0.7%/min except in the summer if large Freon compressors are used to supplement the absorption air conditioning system. Starting a large compressor around noon in summer would probably impose a step increase of about 10% in the electrical load, and this would pose a difficult control problem.

The control of closed cycle gas turbines has commonly presented difficulties in that the systems have been relatively sluggish in their response to step changes in the load because they have been designed for high peak pressures, have had large volumes, and/or have tried to make use of the compressor of the gas turbine for charging the high pressure gas reservoid used for control purposes.[1,2,3] Release of gas from the reservoir has commonly been to the compressor inlet, and this had led to a relatively low system response rate to a step increase in load. A much higher response rate can be obtained by using a storage reservoir that represents a large fraction of the gas turbine system, using a separate compressor for charging

the storage reservoir to a pressure well above the maximum system pressure, and allowing the gas added to the system to go through a heat transfer matrix so that it would enter the system just ahead of the turbine inlet temperature. A preliminary analysis indicates that a good way to do this is to place a heat transfer matrix similar to that of the regenerator in the outlet manifold for the tubes in the fluidized bed. This will run at the turbine inlet temperature and will provide sufficient heat capacity so that air from the storage reservoir flowing through this heat transfer matrix will be heated to the turbine inlet temperature. This arrangement should yield a good response characteristic.

The system control problems can be investigated with a digital computer to obtain most of the characteristics of the system. However, extensive tests of the actual system will be required in part because it is extremely difficult to model all of the secondary effects that may prove important and in part because some of the characteristics of the fluidized bed are not well known.

References

1. C. Keller, The Escher Wyss-Ak Closed Cycle Turbine, Its Actual Development and Future Prospects, Trans. ASME, Vol. 67, p. 791, 1946.

2. State-of-the-Art of HTGR Gas Turbine Technology, USAEC Gulf GA-A12098, Gulf General Atomic Company, June 1, 1973.

3. HTGR Gas Turbine Power Plant Control, Safety, and Maintenance Studies, Phase II, Semiannual Progress Report for the Period January 1, 1973 through June 30, 1973, General Atomic Co. Report Gulf GA-A12700, August 15, 1973.

CHAPTER 9

MAJOR PROBLEM AREAS

Coupling a fluidized bed coal combustion chamber to a closed cycle gas turbine presents a substantially different set of problems from those of a steam boiler, particularly from the standpoint of control. Further, the operating temperature, excess air, and nominal air velocity regimes fall in different ranges. Thus the development program must be directed at the solution of quite a number of new or different problems. In the course of the studies and analyses presented in the previous sections special attention was given to major uncertainties and problem areas. These are listed in Table 9.1. They are placed in five major categories on the basis of the approach that it appears will yield the principal information required for their solution. The five types of approach envisioned are detailed design analysis, bench tests of models or components, construction of a demonstration unit, system tests, and basic technology investigations. The first four of these categories fit logically into a main-line program to design, build, and test a fluidized bed coal combustion system coupled to a gas turbine, while the fifth category is more general and involves a range of basic technology work.

Minimal Program to Design, Construct, and Test a Demonstration Unit

The bulk of the questions implicit in Table 9.1 can be answered in large measure by an orderly program to design, construct, and test a demonstration unit. This work will entail extensive liaison with other laboratories and equipment manufacturers to take maximum advantage of their background of experience and capabilities so that costs can be kept to a minimum consistent with the prime objective; namely, demonstrating the feasibility of the concept.

Table 9.1. Summary of Major Problem Areas and Questions

	Design and Analysis	Bench Tests	Detail Design and Construction	System Tests	Basic Technology
Hot manifold and piping design and stress analysis	x				
Economizer design and stress analysis	x				
Tube arrangement in the fluidized bed	x	x			
Detail design of the air ports or tuyeres for the bed	x	x			
Detail design of the ports for the fuel and limestone	x	x			
Effects of fuel form (coal, solid waste, etc.) on choice of fuel feed port design		x			
Detail design of feed ports for starting fuels (gas and/or oil)		x			
Effects of freeboard height in the plenum chamber above the bed on carryover of particulates		x			
Effects on particle carryover of grids of tubes used as baffles in the plenum above the bed		x			
Effectiveness, metering characteristics, and reliability of candidate equipment for the fuel and limestone feed system		x			
Uniformity of fuel distribution to a multiplicity of feed ports operating in parallel		x			
Costs of principal items of equipment			x		
Costs and time required for installing the equipment to give a complete power plant			x		
Stability and control characteristics of the fluidized bed coal combustion system coupled to a closed cycle gas turbine	x			x	
System startup and shutdown characteristics	x			x	
Characteristics of the fluidized bed coal combustion system under hot standby conditions with no heat removal except through heat losses to the surroundings	x			x	
Determine feasibility of on-off control of the combustion air and fuel for operation at loads too low for good fluidization of the bed				x	
Similarities and differences between gas turbine heaters and steam boilers for utilizing fluidized bed combustion systems	x			x	
Effectiveness and reliability of ash removal system				x	
Effects of air temperature entering the bed on both combustion and the behavior of the fuel feed system (e.g., are there coking troubles?)				x	
Effects of bed temperature, inlet air temperature, excess air, load, Ca/S ratio, types of coal and limestone, etc., on emissions of SO_2, NO_x, and particulates as well as on the amount of unburned carbon in the ash				x	
Reliability and maintenance problems of components and the complete system				x	
Feasibility of operating the system unattended				x	
Effects of choice of alloy on corrosion and erosion of the tubes in the bed	x			x	x
Effects of particulate size and character on erosion, corrosion, and deposits in turbine stators and rotors if the hot gases are fed from the fluidized bed without cooling through particulate separators to a gas turbine					x

Analytical Design and Layout Studies

The analytical design and layout studies summarized in Chapter 6 must be extended with particular attention to stress analysis, details of the fluid flow passages, fabrication problems and costs, the performance and cost of commercial components, and system integration problems. The latter include system stability and control from startup through low power to high power and then to shutdown including provisions for all emergency situations that can be envisioned.

Bench Tests

Closely associated with the above design work it will be necessary to carry out a substantial program of bench tests. These will include two major types, the investigation of complex fluid flow problems, and the evaluation of commercial equipment.

A whole series of subtle fluid and fluidized solids flow problems can be investigated nicely with a lucite model of a section of the fluidized bed. This can be built full scale with interchangeable sections as indicated in Fig. 9.1 so that different configurations for the inlet plenum, the tube bank, the air ports, and the fuel supply ports can be tested. Tests of the latter should include operation with various mixtures of coal, limestone, solid wastes, and simulated sewage sludge to determine the extent to which the various port geometries tested will tolerate variations in the particle size and the character of the fuel feed materials. The system would also be used to investigation provisions of port for starting the system with gaseous or liquid fuel, the effectiveness of a tube bank placed as a baffle above the bed to reduce particle carryover, the effects of the height of freeboard in the plenum above the bed, and similar problems. The results of this test work would then be incorporated in the design.

Two or three types of commercial equipment suitable for feeding fuel and limestone to the bed should be selected and purchased to investigate their operation with coal, limestone, and solid wastes. Particular attention should be given to the effects of particle size and character, precision of metering, and tendencies of the mechanisms to jam, clog, or otherwise malfunction. This fuel feed equipment can be coupled to the lucite model of the fluidized bed to investigate the characteristics of

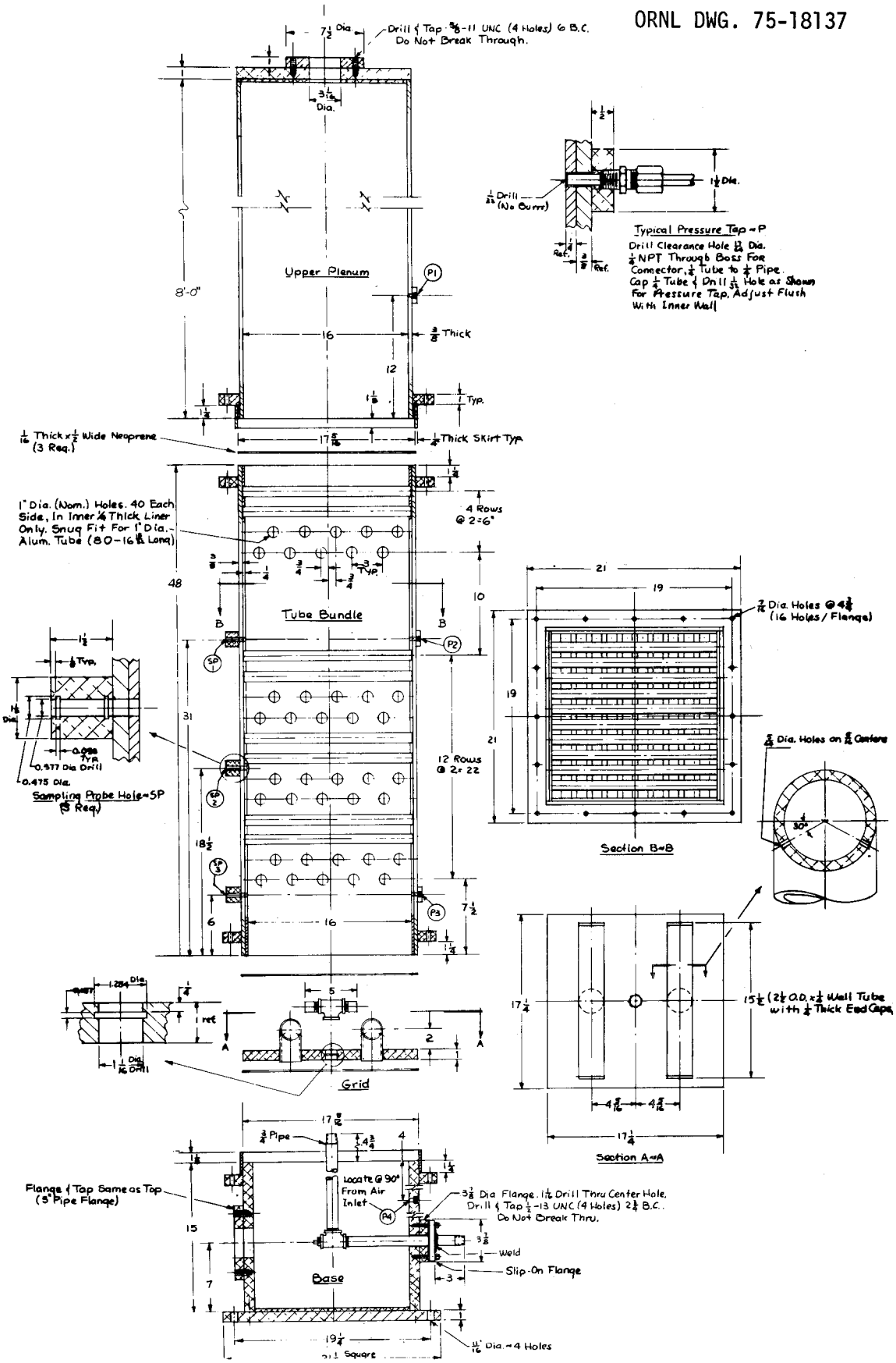

Fig. 9.1. Lucite model of a section of the fluidized bed.

the coupled system. It will also be important to investigate the uniformity of distribution of the fuel flow to a multiplicity of feed points in the bed (probably 9), and the effects of variables such as coal moisture content, degree of drying, etc.

A proposed layout of the bench test facility is shown in Fig. 9.2. The lucite flow model and fuel feeding equipment would be installed on an existing test stand that is equipped with a 6 in. instrument air line. An existing cyclone separator that was used in a previous program would be utilized to remove the larger solid particles carried over by the air that flows through the bed and these particles would be recycled back to the bed by the feed equipment.

Detail Design and Construction

The detail design and construction work should answer in large measure a third set of major questions, principally those concerned with the fabricability, cost, and availability of equipment.

Contracts negotiated with vendors, for example, will provide firm cost data and delivery times for the major components. Similarly, the time required and the costs for installation of the equipment can be determined for a single unit. This will provide a good basis for estimating the costs for production systems.

System Tests

Many of the problems and/or questions in Table 9.1 can be answered only by operation of the complete system. The first and foremost of these is the time required and possible difficulties in startup. Following this it will be important to determine the system stability and control characteristics over the operating range including the system response to small and large step changes in load or an abrupt loss in load, and the possibilities of "banking the fire" and allowing it to stand practically idle but at operating temperature (something out of the question if there are boiler tubes in the bed). The effects of the operating power output on the behavior of both the fluidized bed and the emissions should be determined together with the effects of bed temperature, excess air, combustion air inlet temperature, the Ca/S ratio, methods for segregating the ash from the lime-gypsum mixture, etc.

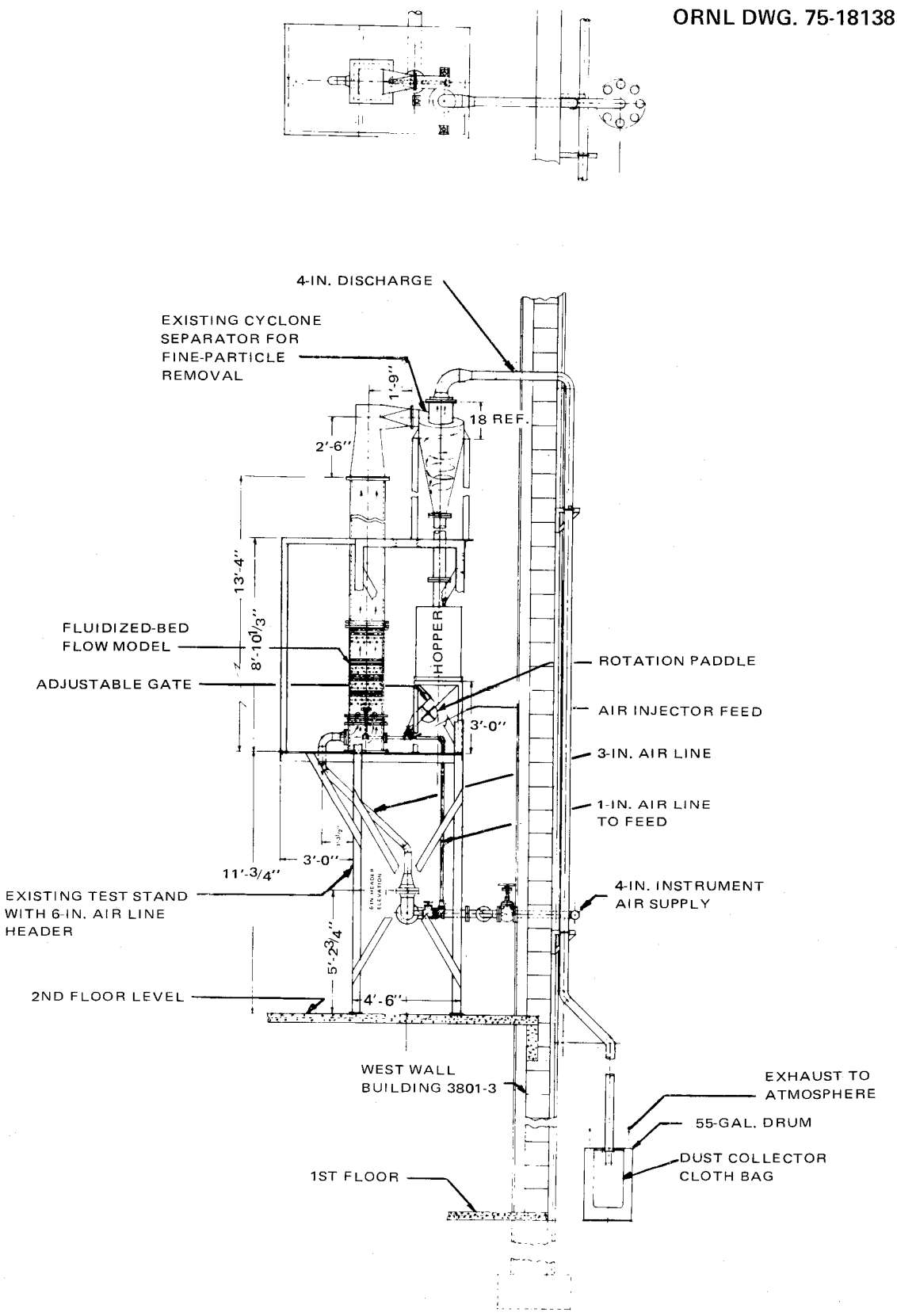

Fig. 9.2. Layout of bench test facility.

Some insight into the reliability of the system components and their maintenance problems will be gained in the course of the above performance tests. A much better insight into these matters can be gained from an endurance test of perhaps 5000 hr. A particularly important set of information from the latter will be the extent to which there is hot gas corrosion of the tubes in the bed. This special set of problems is discussed in the next section.

Basic Technology

At least two of the problem areas in Table 9.1 have broad implications for a variety of advanced energy systems including high temperature gas turbines, potassium vapor topping cycles, and direct combustion MHD systems. These problems and the approaches recommended in connection with the MIUS coal burning gas turbine program are outlined in this section.

Materials Compatibility Studies

The development and selection of heat exchanger and duct materials will require a broad background of mechanical property information and data to gain compliance with ASME licensing rules and codes. Qualification of the materials will require compilation and/or determination of large amounts of information on tensile, creep, and fatigue behavior. In addition, to insure the integrity and continued functioning of structural parts during the desired service life, it will be necessary to account for the effects of chemical and material instabilities (i.e., gas-metal reactions, thermal aging, and possible inter-actions) on mechanical properties and behavior. This requires a dual approach, first to establish the performance limits of prospective materials in fluidized bed environments, and secondly, interact with the system designers to hold the severity of the environment within realistic and predictable limits.

Characterization of Furnace Environment. Although basically an organic material, coal contains a significant burden of inorganic material which varies in concentration and amount depending on the coal source. The major inorganic impurities consist of silicon, aluminum, and iron which are

present as silica, alumino-silicates, and iron pyrite. Other minor impurities include potassium, calcium, magnesium, and sulfur. Although extensive data have been published on the ash content for a wide variety of coals, these data cannot be used directly to predict the environmental conditions for a given fluidized bed system. The chemical reactivity of the combustion gases is strongly process-dependent, and the distribution of inorganic impurities between the limestone and ash is probably strongly dependent on conditions of residence time and temperature peculiar to a particular furnace design. Thus, characterization of the coal combustion products must be approached through studies of an actual fluidized bed in which combustion parameters and bed materials can be varied in accordance with a contrived test envelope. Characterization of the combustion products will be accomplished by removal of ash from preselected positions in the bed at various times in the test program. Flue gases will be chemically analyzed and, if feasible, synthesized gas mixtures will be formulated for more fundamental compatibility studies.

Corrosion of Bed and Duct Materials. A primary goal of our fluidized bed development program will be to study the chemical interaction of limestone-coal-ash mixtures with duct and heat exchanger materials. Of central interest will be the growth and ablation rates of corrosion product scales along exposed metal surfaces, and the mass transport of bed constituents (solids and gases) through these scales. This will include a study of the phase relationships between constituents in the bed and structural metals supporting or contacting the bed. Components will also be examined for evidence of mechanical erosion and, if found, erosion rates will be correlated with aerodynamic conditions in the bed.

Our evaluation of the performance of candidate materials for fluidized beds will entail the inclusion of surveillance specimens at several selected locations within the bed and flue gas regions. Also, the bed itself will be designed to facilitate removal of complete heat exchanger tubes for metallurgical and chemical analyses at various operating times. Surveillance specimens and heat exchanger tubes will be fabricated from a representative grouping or alloy compositions so as to afford back-to-back comparisons of the candidate materials discussed in Chapter 7.

As we gain a better definition of the intrinsic environmental conditions of the fluidized bed concept, additional laboratory tests may be required to establish the detailed kinetics of those corrosion processes which appear important in terms of long-term structural stability.

Our corrosion examinations will make use of a number of new and unique analytical techniques particularly suited to surface reaction studies. These techniques enable the identification of the elemental composition and chemical bonding of compounds on solid surfaces (x-ray photoelectron spectroscopy and Auger spectroscopy), and the identification of the chemical composition of microstructural features (scanning and transmission electron microscope with energy dispersive analysis of x-rays). Use of these techniques will aid our understanding of the chemical processes involved in corrosion and deposition processes in fluidized beds.

We have available within the several research divisions at ORNL an expertise in high-temperature compatibility studies that dates continuously from 1948. These studies have dealt with the effects of both potassium and cesium on metals at temperatures as high as 1300°C. We have conducted extensive studies of the effects of molten salt mixtures, primarily mixed metal fluorides, on ceramic as well as metallic construction materials. Gas-metal reactions involving CO_2, CO, H_2O, H_2, and CH_4 have been investigated at ORNL as part of the gas cooled reactor development program, and currently we are engaged in solid-solid compatibility studies involving the interaction of Cm_2O_3, Al_2O_3, and Eu_2O_3 with various metals and alloys at temperatures ranging to 1800°C. The facilities and experience gained in the above-mentioned programs are directly relevant to the types of compatibility problems that are anticipated for fluidized bed coal combustion systems.

Turbine Bucket Erosion, Corrosion, and Deposits

Erosion, corrosion, and deposits have been major problems in gas turbines and attempts have been made to employ residual fuel oil or coal as the fuel in open cycle systems. If an acceptable solution to these problems could be evolved for a unit suited to MIUS applications, a major saving in capital cost could be effected. The direct combustion system has the

further advantage that the presence of water in the fuel does not degrade the performance because the loss of heat required for vaporization of the water is offset by the increased turbine work stemming from the increased mass flow through the turbine without an increase in the compressor work (except for an almost trivial amount of pump work required for injection of water slurries). This is true even if massive amounts of water are injected as would be the case if slurries of sewage sludge were employed.

G. S. Leighton has suggested that the problems with turbine bucket erosion and deposits are probably dependent on the size and character of the particles suspended in the gas stream, e.g., the smaller the particles the less damaging they probably are, and there may be a size threshold below which no damage would result. The character of the particles may also be an important factor. Not only may there be a substantial variation from one type of coal to another, but, as H. R. Hoy of BCURA has suggested, by carrying out the combustion process in a fluidized bed at temperatures below the fusion point of the ash, the ash particles should not be the usual highly abrasive vitreous cinders characteristic of conventional pulverized coal burners, but rather should be soft, flocculent, snow flake-like particles of mineral matter left by combustion of the carbonaceous matrix in which they occurred. This would, of course, be true of mineral matter present in organic compounds, but Shelton Erlich of Pope, Evans, and Robbins has pointed out that a large fraction of the ash will be present in the coal in the form of slate, and this will simply be roasted in the fluidized bed. In addition to mineral matter present in coal or lignite, if solid wastes are used as fuel, experience at Combustion Power, Inc., indicates that fine particles of glass, bits of aluminum foil, and aluminum oxide formed by partial or complete oxidation of the aluminum foil will also be present in combustible refuse even after a series of processes including magnetic, eddy current, and air flotation separation steps. These particles from solid waste present a still different set of particle types.

In attempting to assess the problem to determine what might be done in this area, it is clear that the first step should be a thorough and critical examination of all of the experience that has been gained in this area. One of the first steps should be a thorough review of the experience with coal-burning gas turbines gained by the Locomotive Development Committee in the

latter 40's and early 50's. This review should include not only an examination of all of the papers and reports that were prepared, but incisive discussions with key personnel in the program should help greatly to turn up both important details and the overall perspective that emerged from that effort. A second major source of empirical information is the experience in burning heavy fuel oils in gas turbines, particularly those that contain substantial amounts of mineral matter. A third major area is the experience that has been gained by Siemens in Germany in operating gas turbines on gas from coal gasification plants. Their experience has led to the specification that the gas going to a gas turbine should not contain more than 1 mg/m^3. It is interesting to note that this goal is difficult to achieve; in the Steinkohlen-Elektrizitat AG in Lünen, Germany they have found 50 mg/m^3 of suspended particles in the gas even after subjecting the gas from their Lurgi coal gasifiers to a cooling and two-stage scrubbing operation. Another major source of information is the group at BCURA where there has been a substantial amount of work on this problem because they believe they can drive a gas turbine with the hot combustion gases after just two stages of cyclone separation of the solid particles lifted from the bed. Their experience gained with cascades of simulated turbine blades operated in the hot gas stream from their fluidized bed should yield some especially important insights, particularly when the results are compared with experience in similar tests with other combustion systems. The experience with combustion products from solid waste gained at Combustion Power, Inc., should provide some further interesting insights.

In addition to the work with gas turbines, the more general area of work concerned with the analysis and classification of particulate matter in combustion products from all types of combustion system should be reviewed to give further perspective. This is such a broad field that it will probably be necessary to be somewhat selective and limit the study to what appears to be a reasonable scope covering representative fuels and combustion systems.

On completing the above survey and analyzing the results it is likely that a number of well-defined problems will emerge, and that some worthwhile experiments to investigate these problems can be suggested. However, it seems unwise to suggest either the character or the scope of such experiments until the above survey of the entire problem area has been completed.

APPENDIX A

Heat Exchanger Design Charts for a Coal-Fired Gas Turbine System

The design charts included here were calculated by the methods presented in Chapter 6.

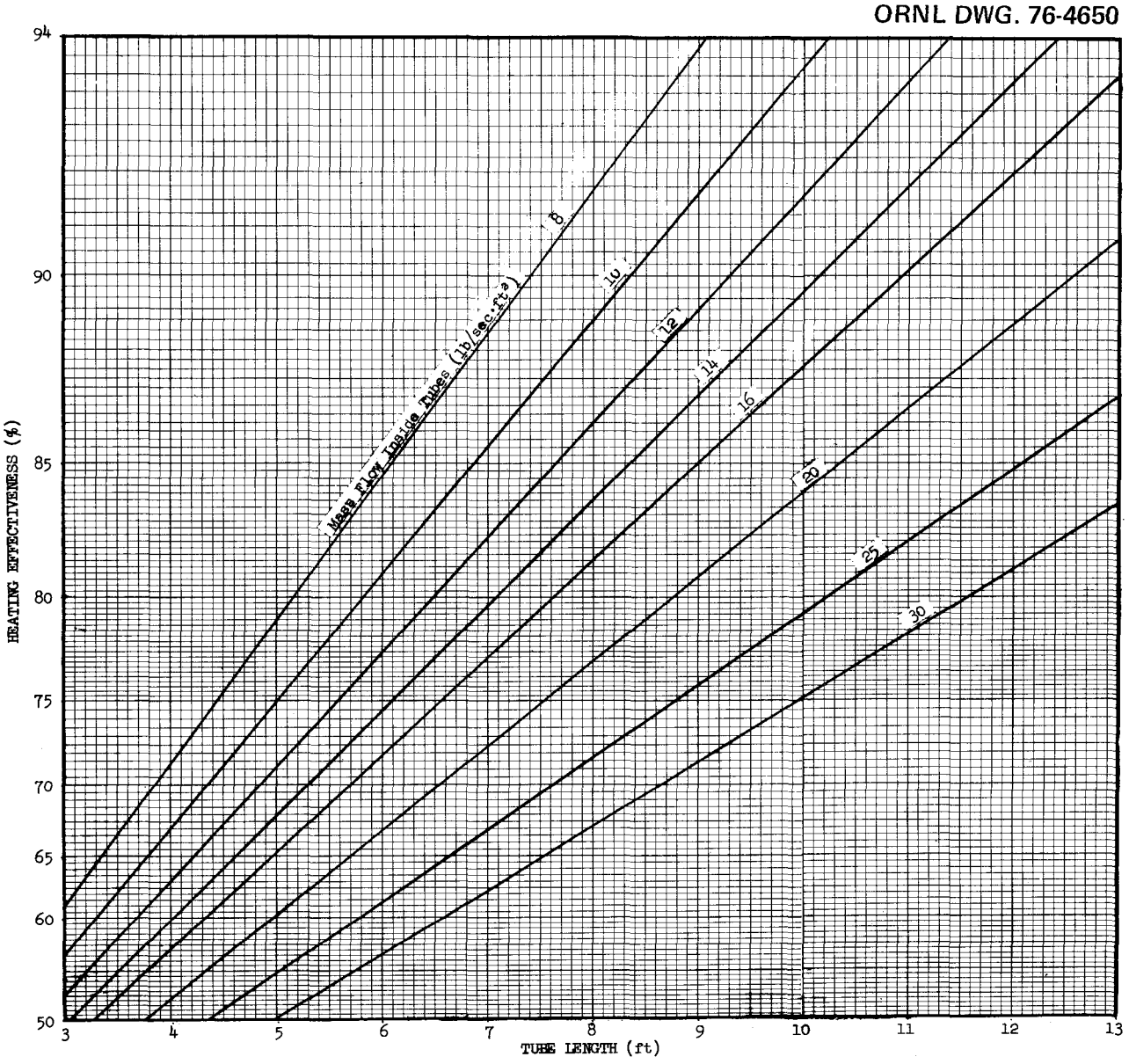

Fig. A.1. Heating effectiveness as a function of tube length in the fluidized bed for 0.50 in. OD and 0.028 in. thick wall tubes.

ORNL DWG. 76-4651

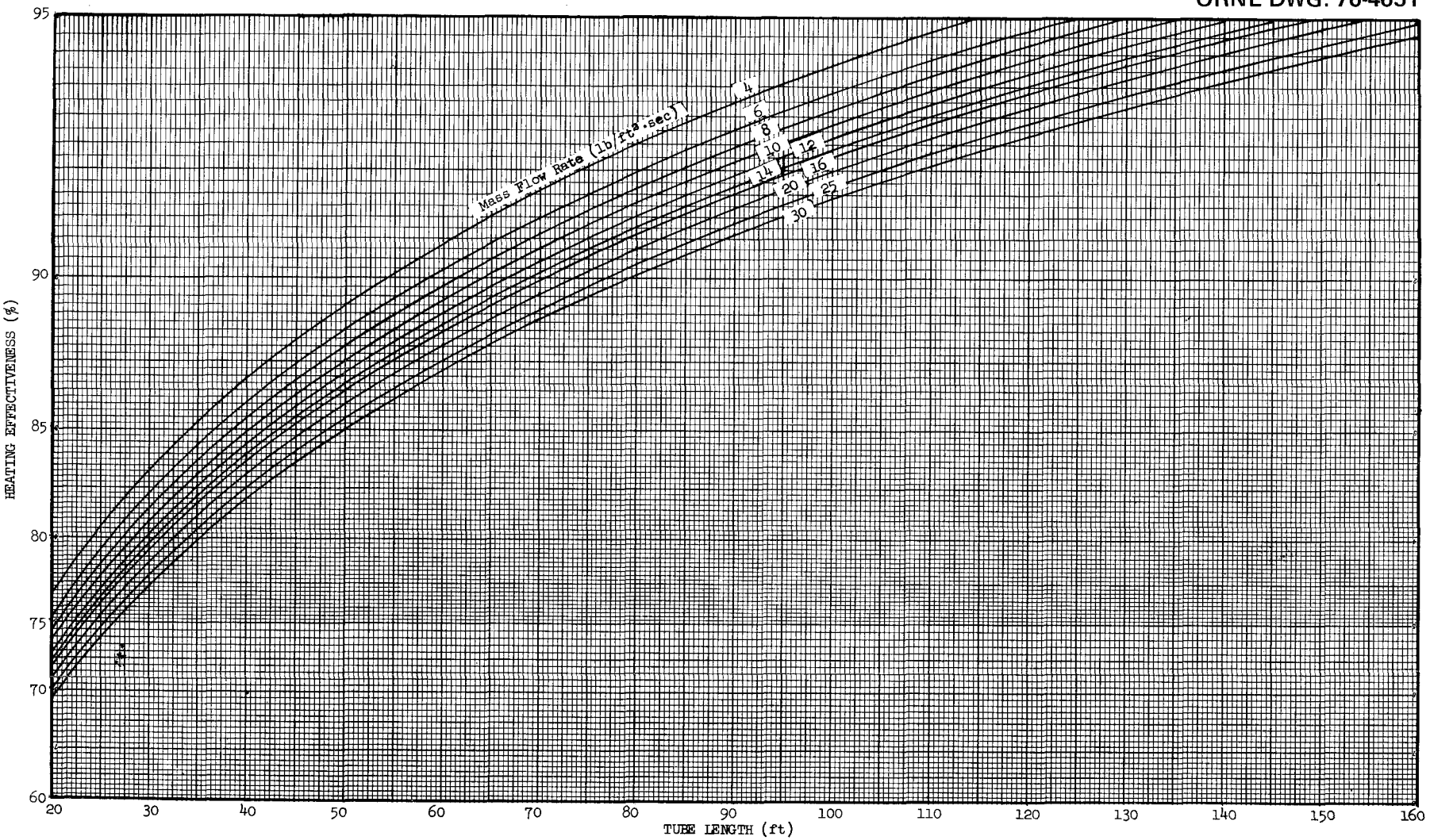

Fig. A.2. Heating effectiveness as a function of tube length in the recuperator for 0.50 in. OD and 0.028 in. thick wall tubes with a shell-side mass flow rate equal to 40% of that inside the tubes.

ORNL DWG. 76-4652

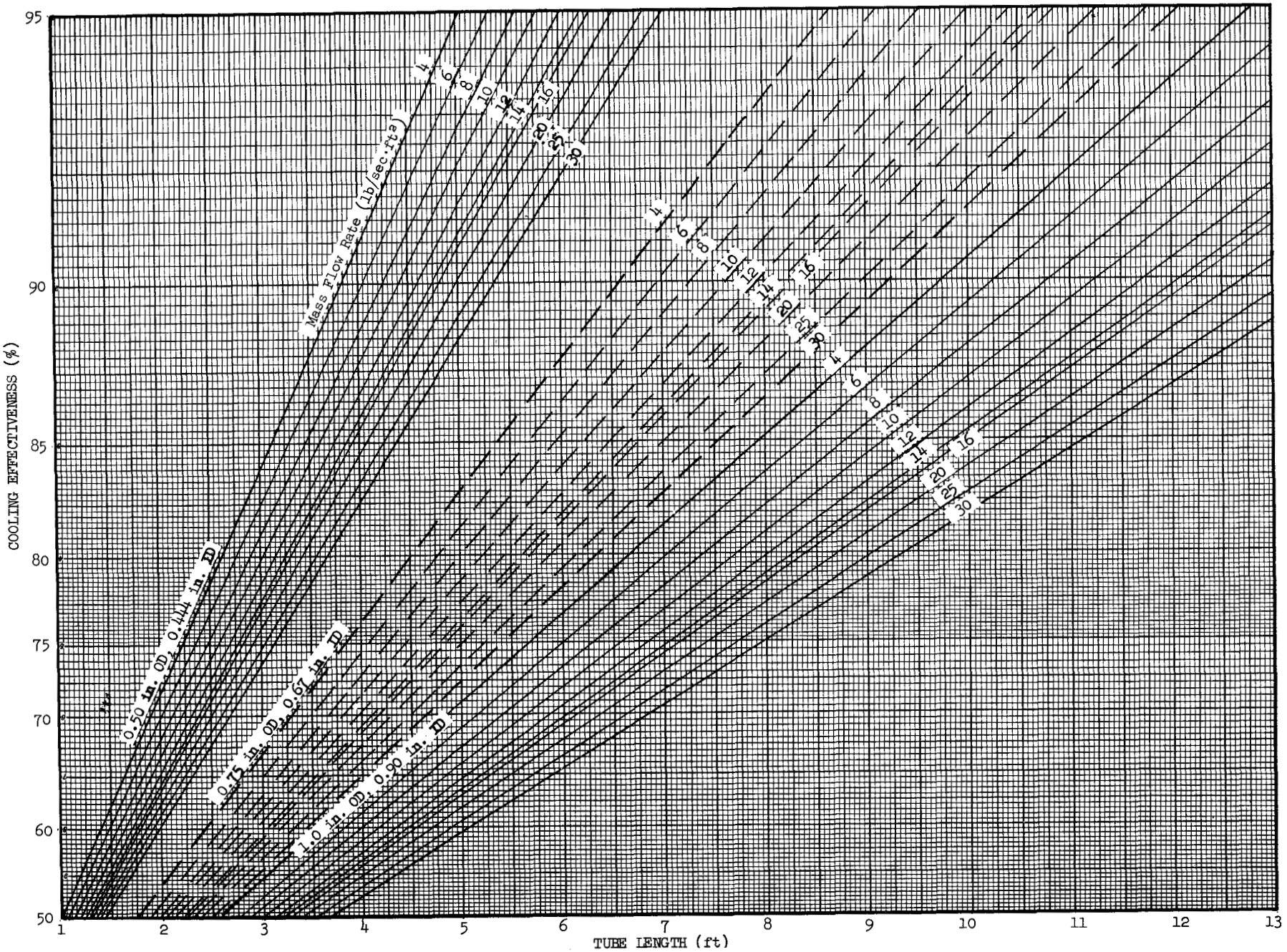

Fig. A.3. Cooling effectiveness for the combustion gases passing through the economizer for a shell-side mass flow rate equal to 30% of the tube-side mass flow rate and the turbine air total weight flow equal to 4.5 times the combustion air weight flow.

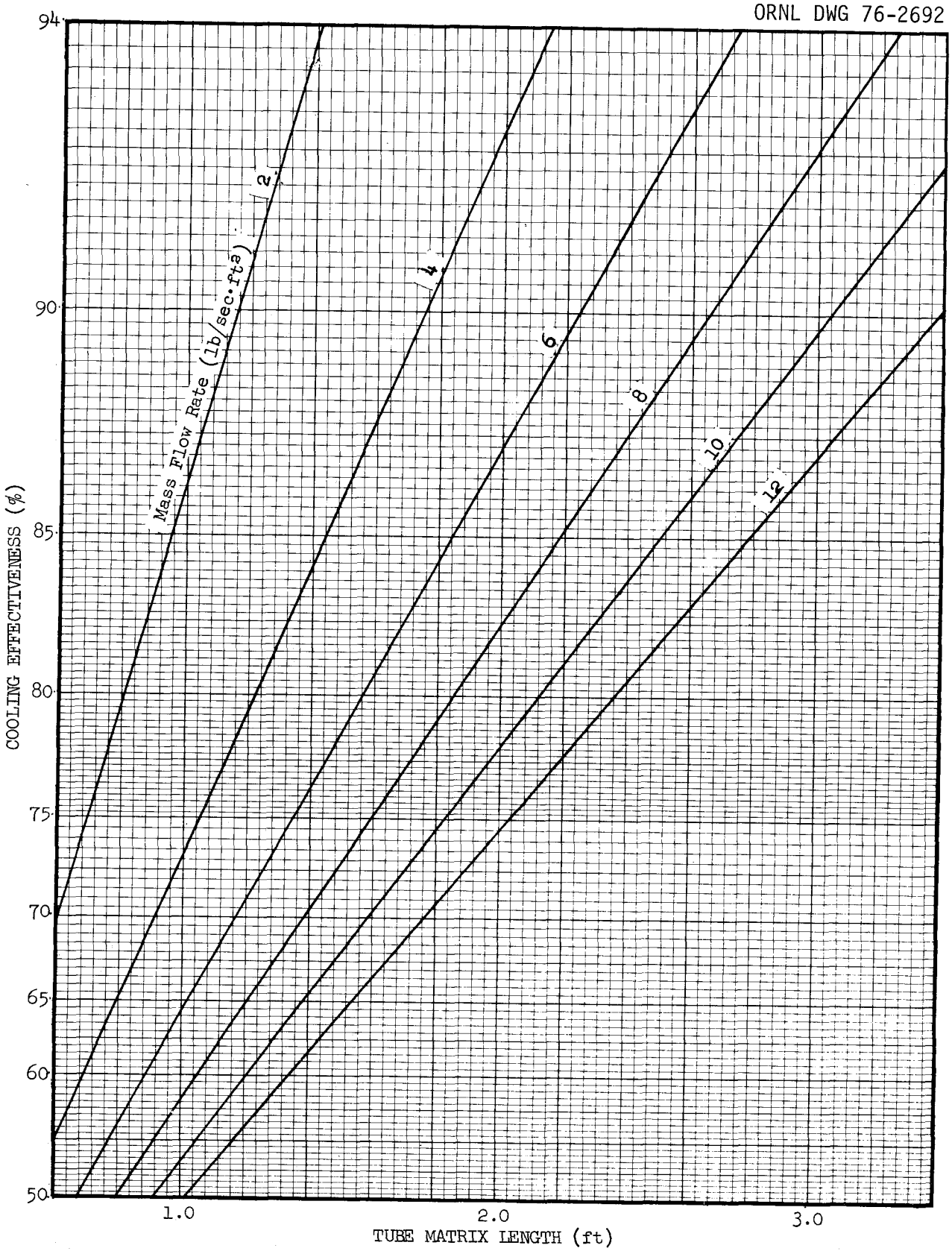

Fig. A.4. Cooling effectiveness as a function of tube matrix length in the air flow direction for the turbine air flow passing over the 1.0 in. OD finned tubes of the waste heat boiler.

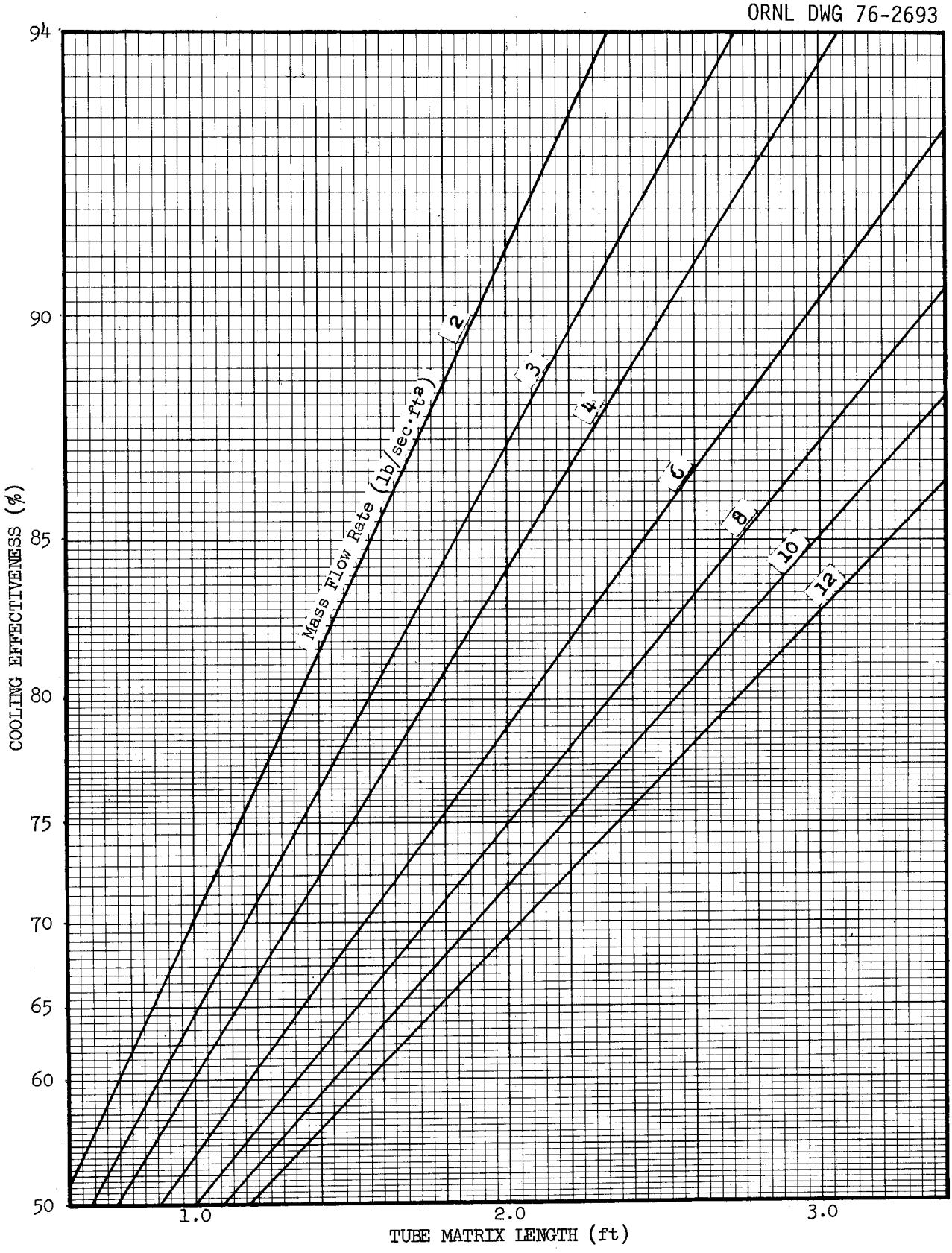

Fig. A.5. Cooling effectiveness as a function of tube matrix length in the air flow direction for the turbine air flow passing over the 1.0 in. OD finned tubes of the turbine air cooler.

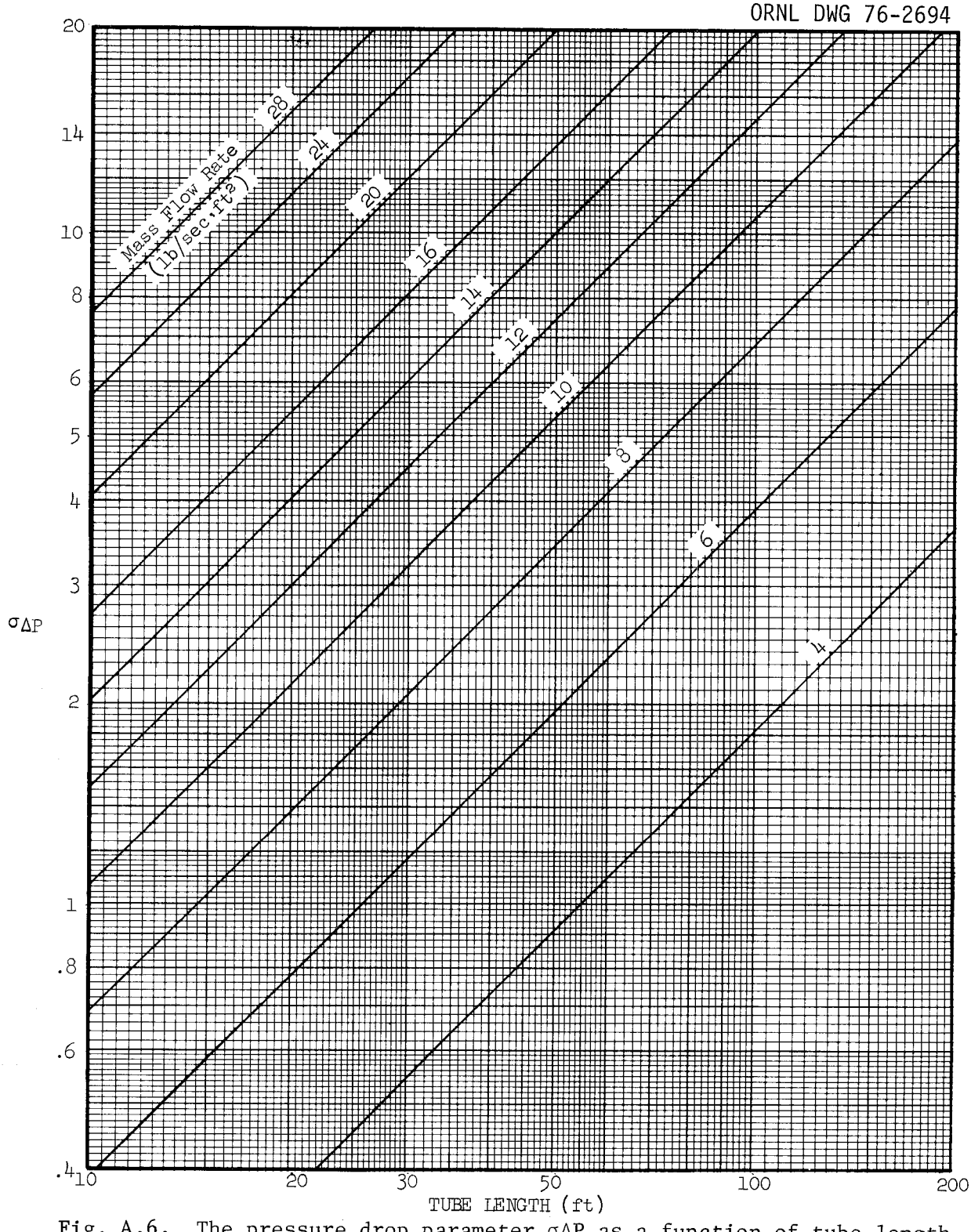

Fig. A.6. The pressure drop parameter σΔP as a function of tube length for the turbine air flow through 0.50 in. OD and 0.028 in. thick wall tubes.

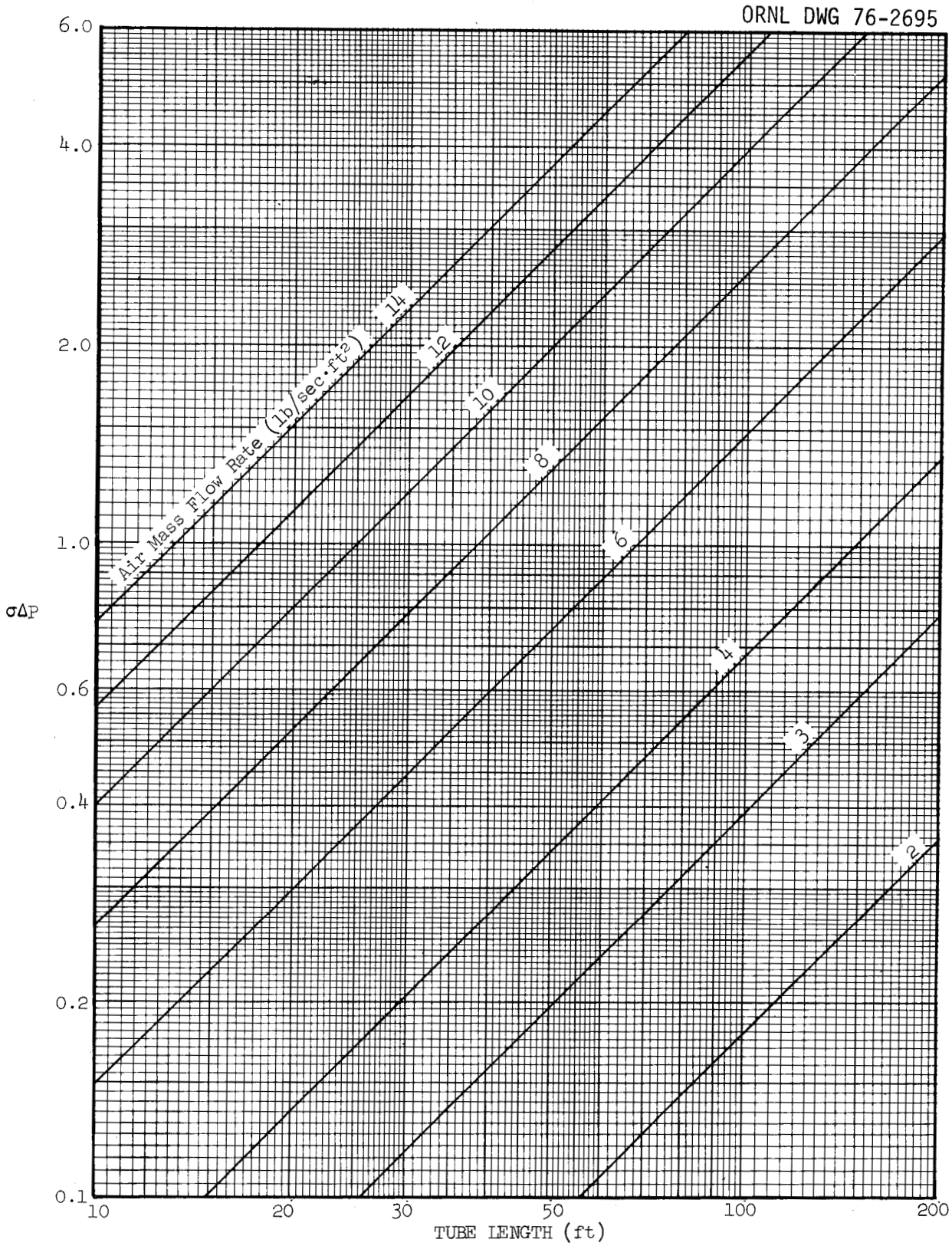

Fig. A.7. The pressure drop parameter σΔP as a function of tube length for the turbine air flow on the shell-side of the recuperator for 0.50 in. OD tubes with the shell-side air mass flow rate equal to 40% of the tube-side mass flow rate.

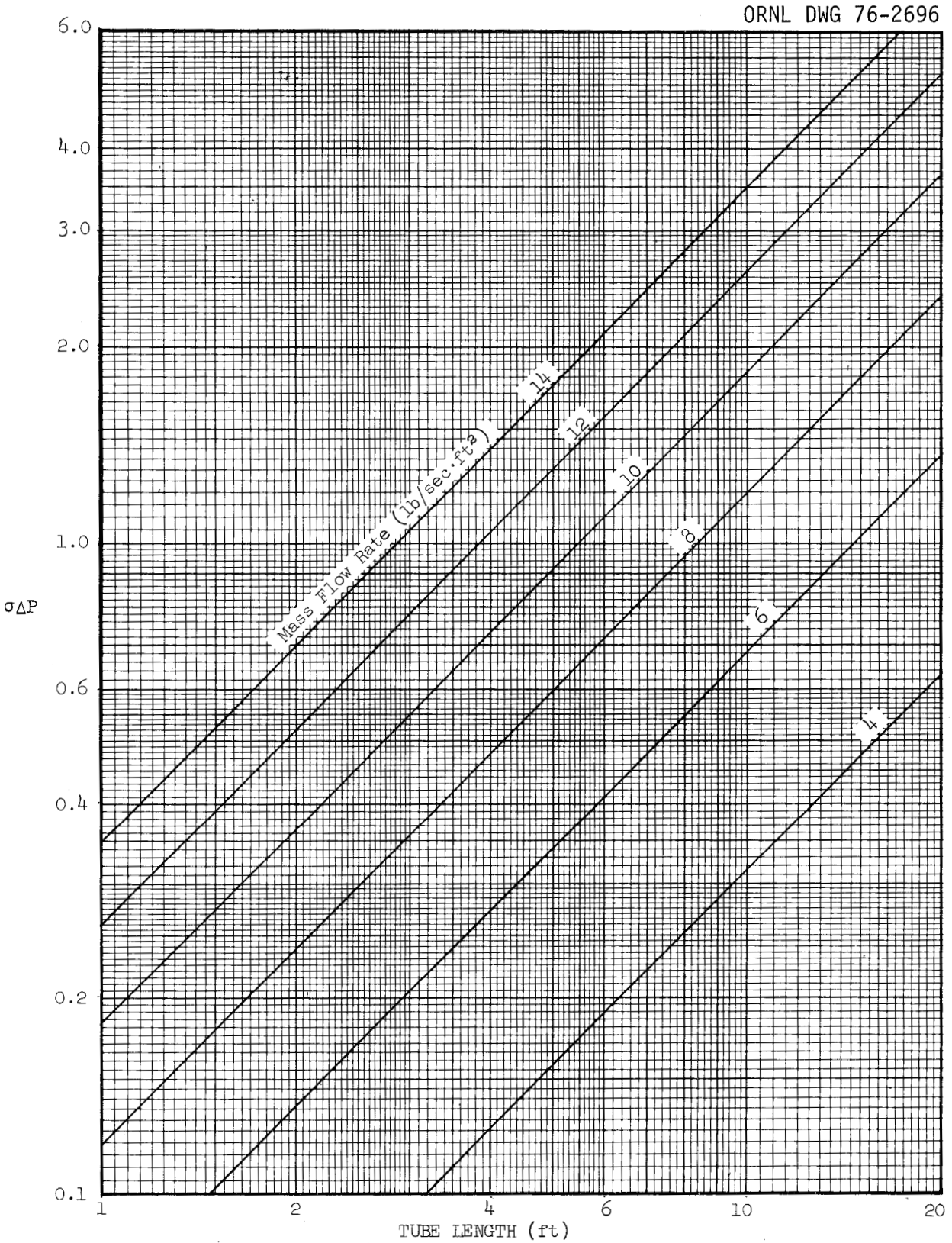

Fig. A.8. The pressure drop parameter σΔP as a function of tube length for the combustion gas flow on the shell-side of the economizer for 0.50 in. OD tubes with the shell-side air mass flow rate equal to 30% of the tube side.

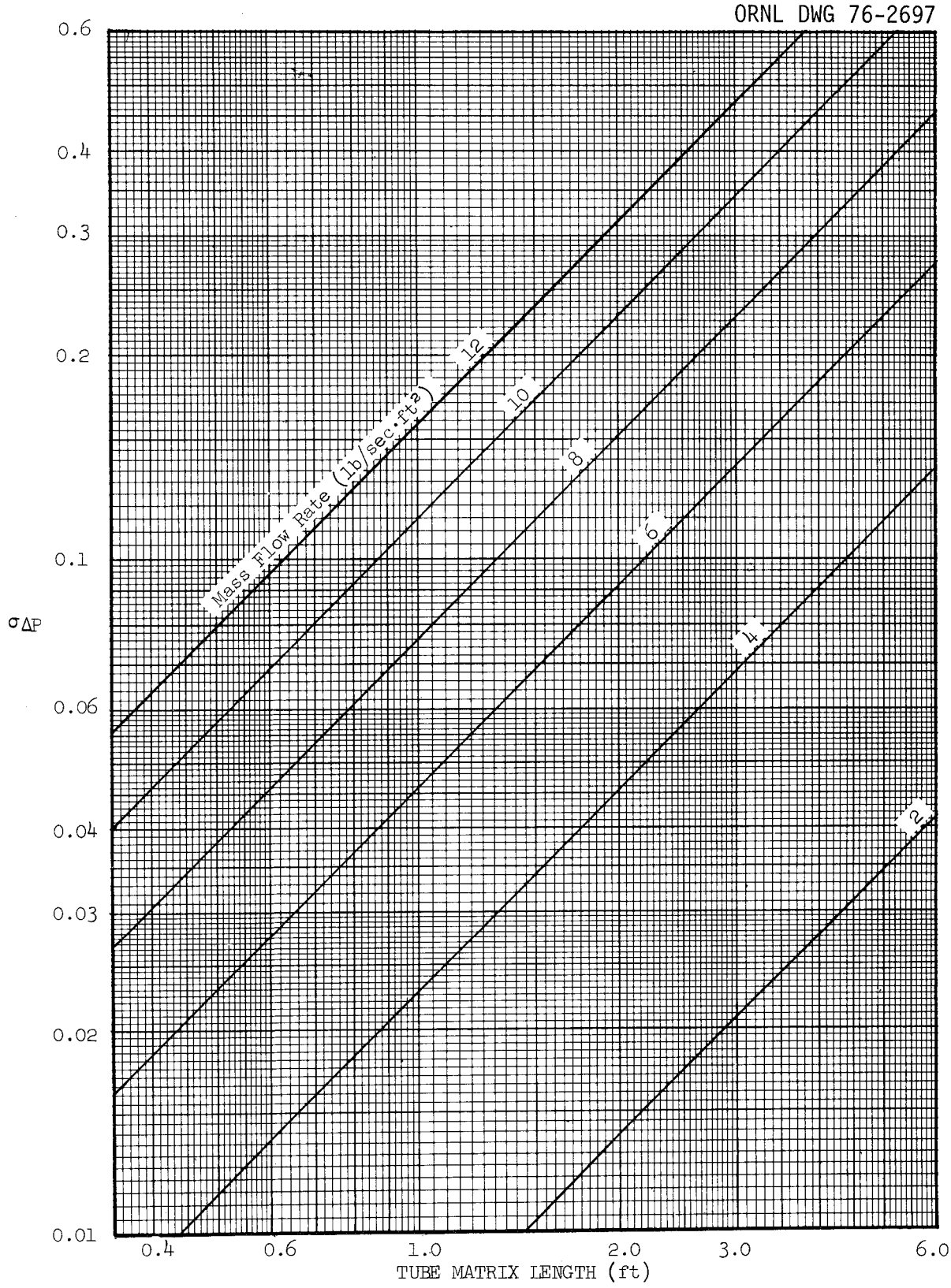

Fig. A.9. The pressure drop parameter $\sigma\Delta P$ as a function of tube matrix length in the direction of air flow for 1.0 in. OD finned tubes in the waste heat boiler and the cooler.

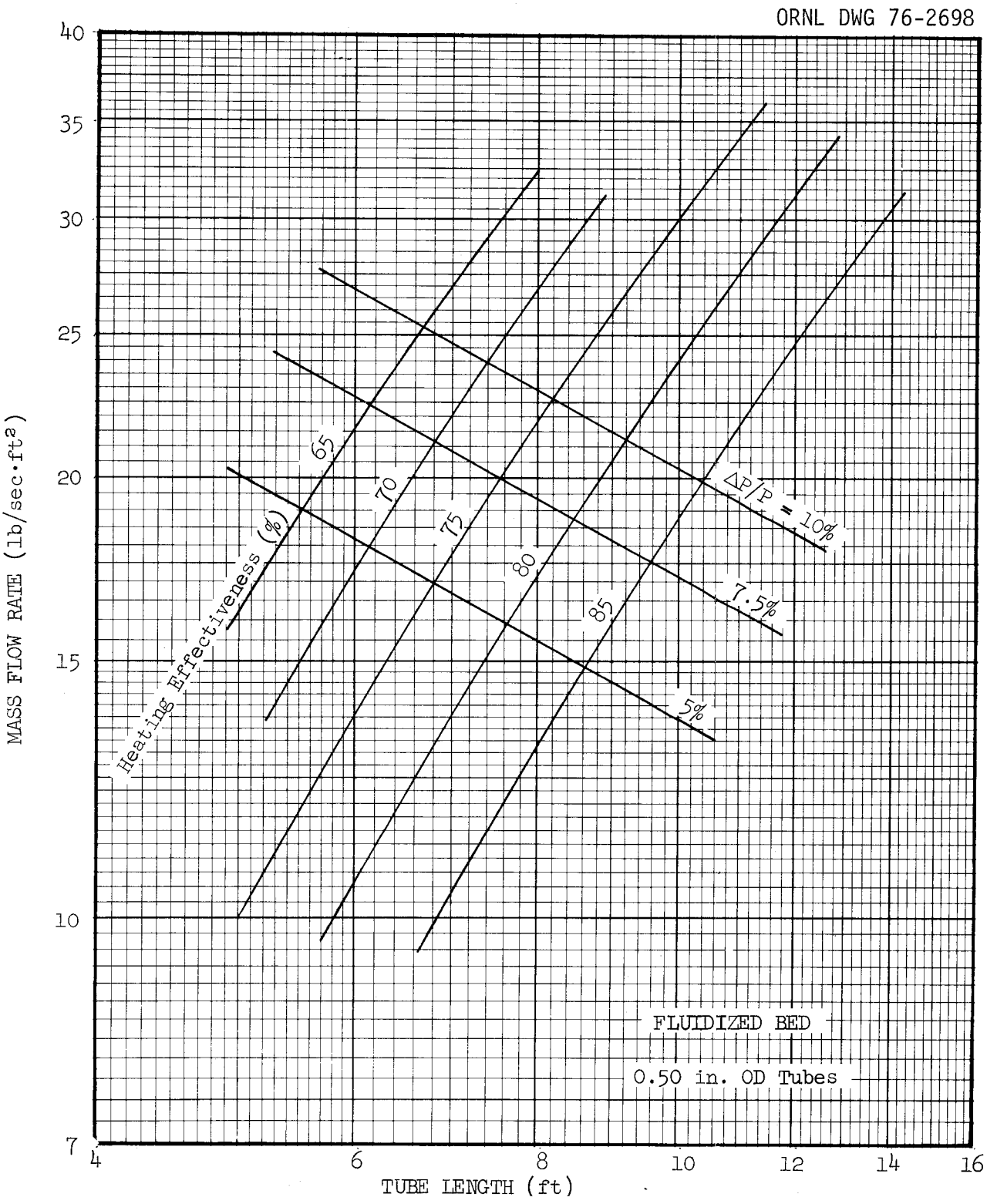

Fig. A.10. Crossplot of data for heating effectiveness and ΔP/P as functions of the air mass flow rate through the tubes and the length of 0.50 in. OD tubes in the fluidized bed.

ORNL DWG 76-2699

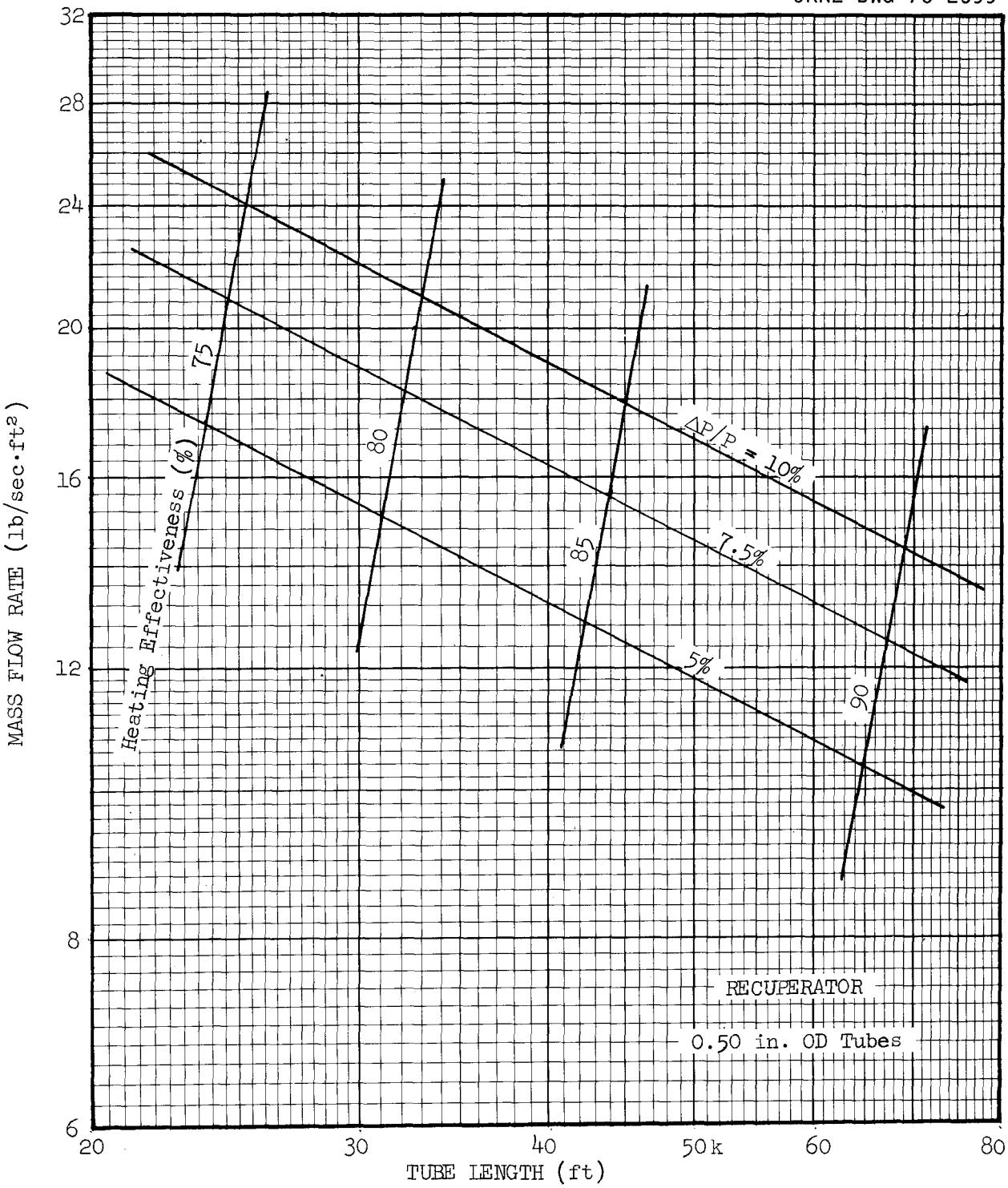

Fig. A.11. Crossplot of data for heating effectiveness and ΔP/P as functions of the air mass flow rate through the tubes and the length of 0.50 in. OD tubes in the recuperator.

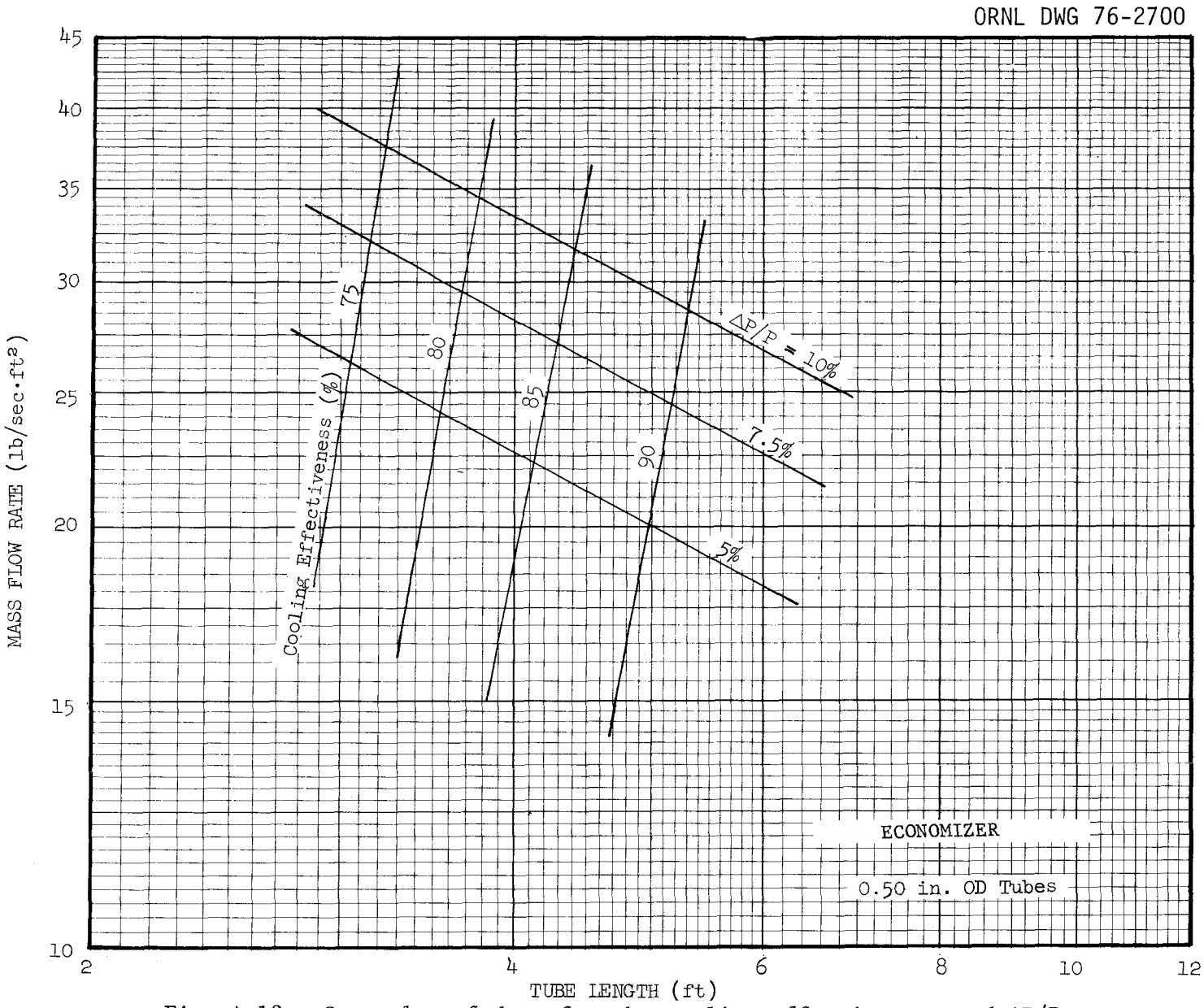

Fig. A.12. Crossplot of data for the cooling effectiveness and ΔP/P as functions of the combustion gas mass flow rate and the length of 0.50 in. OD tubes in the economizer.

ORNL DWG 76-2701

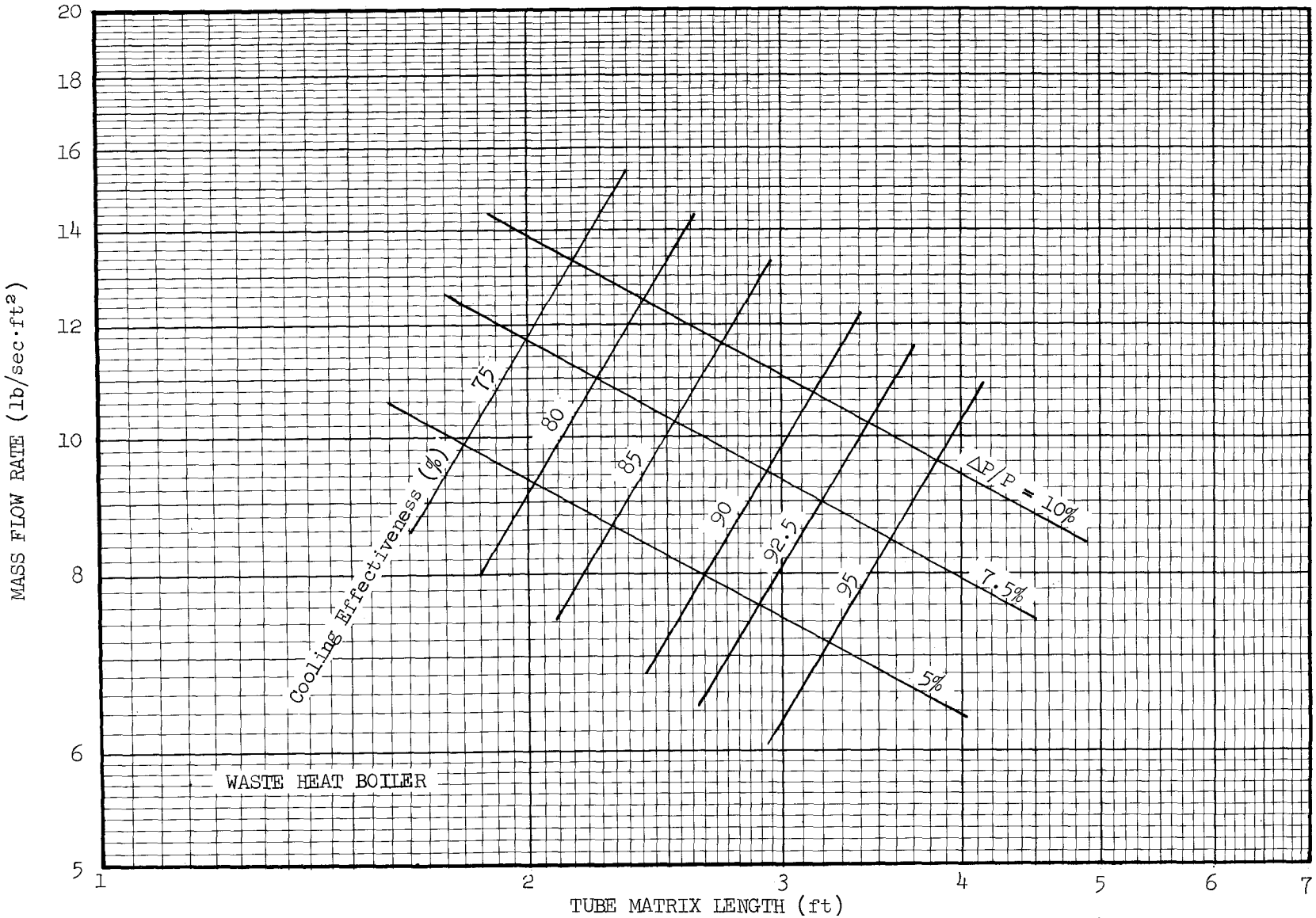

Fig. A.13. Crossplot of data for the cooling effectiveness and ΔP/P for the turbine air as functions of the air mass flow rate and finned tube matrix length in the direction of air flow for the waste heat boiler.

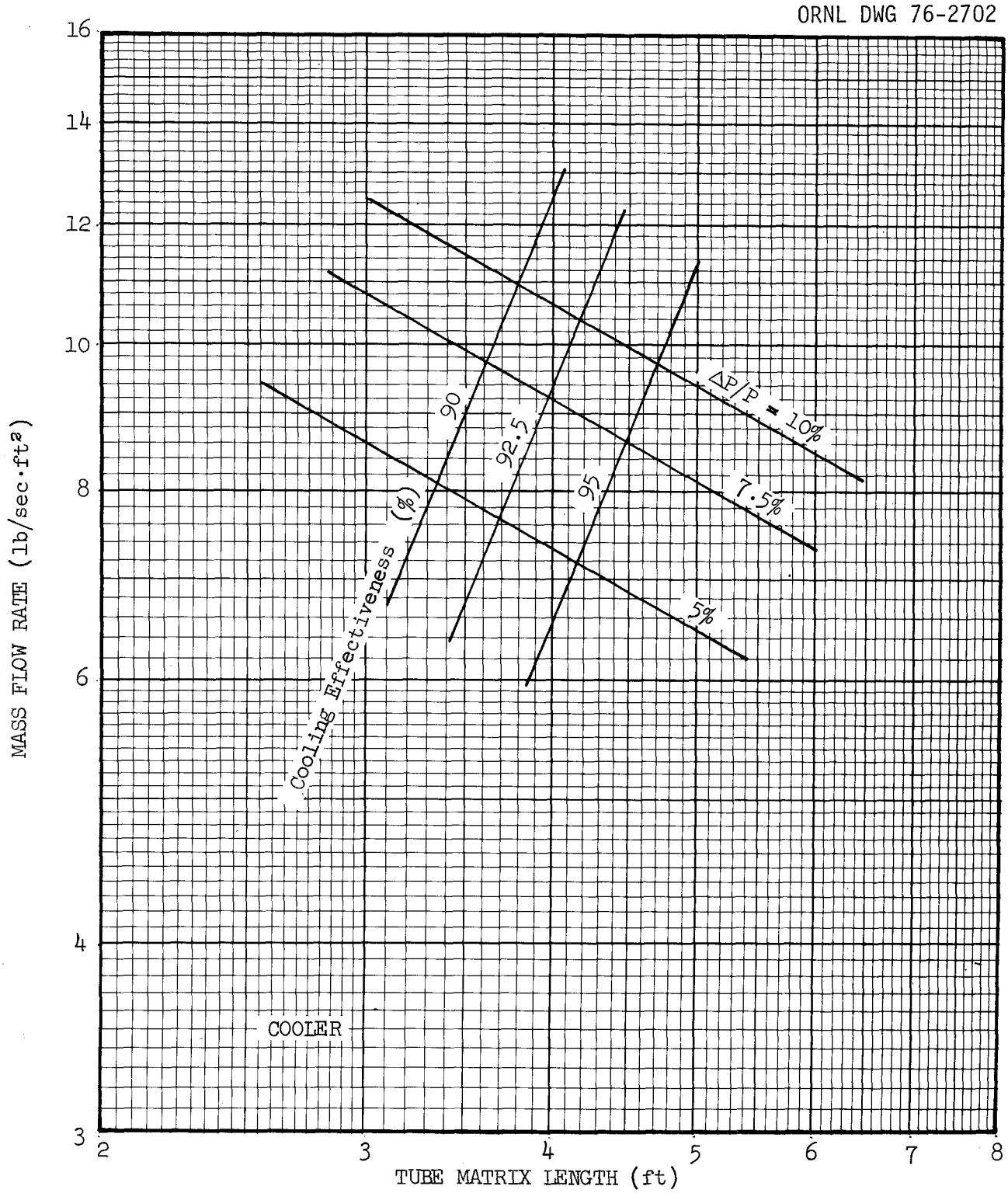

Fig. A.14. Crossplot of data for the cooling effectiveness and ΔP/P as functions of turbine air mass flow rate and finned tube matrix length in the direction of the air flow for the cooler.

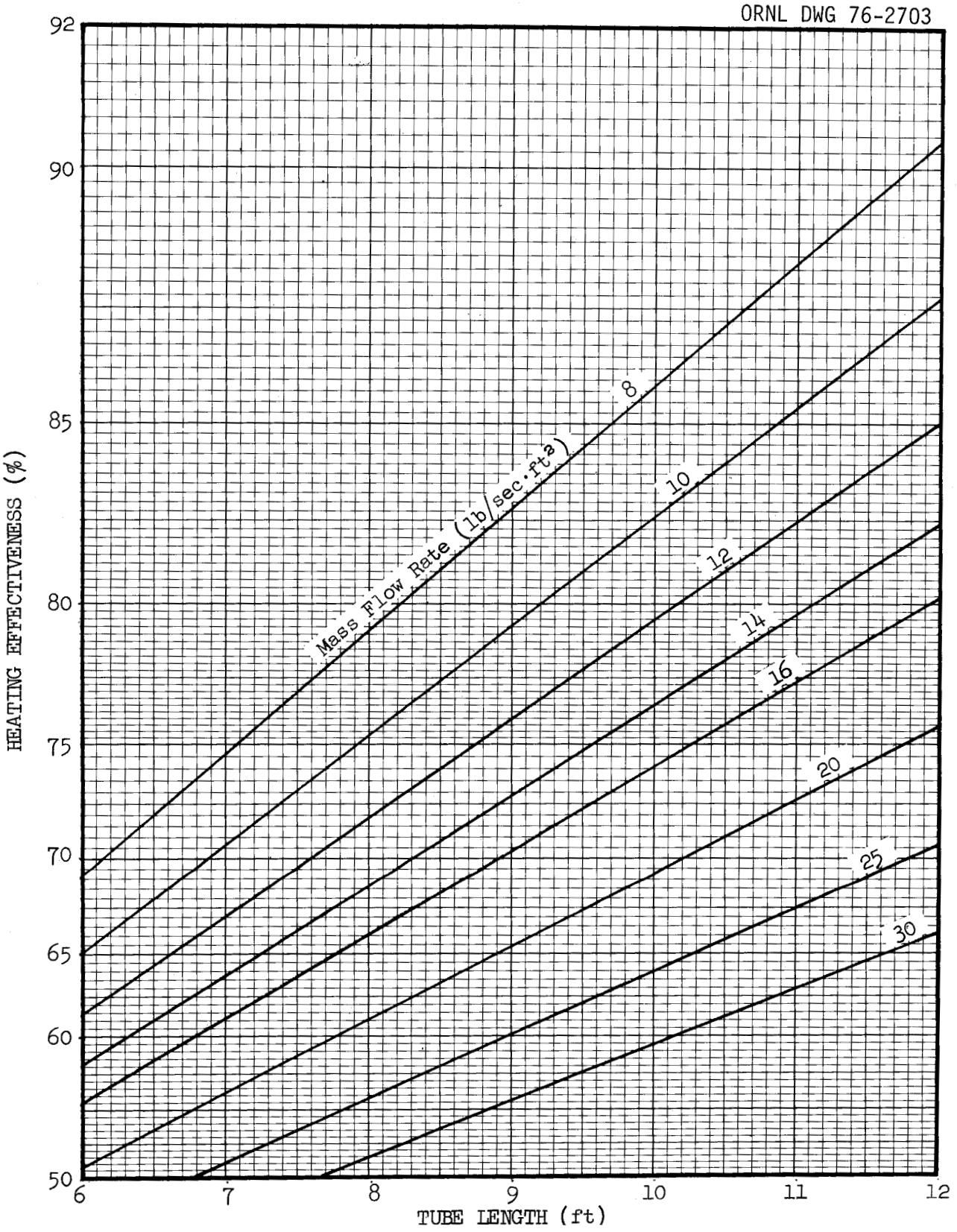

Fig. A.15. Heating effectiveness as a function of tube length in the fluidized bed for 0.75 in. OD and 0.042 in. thick wall tubes.

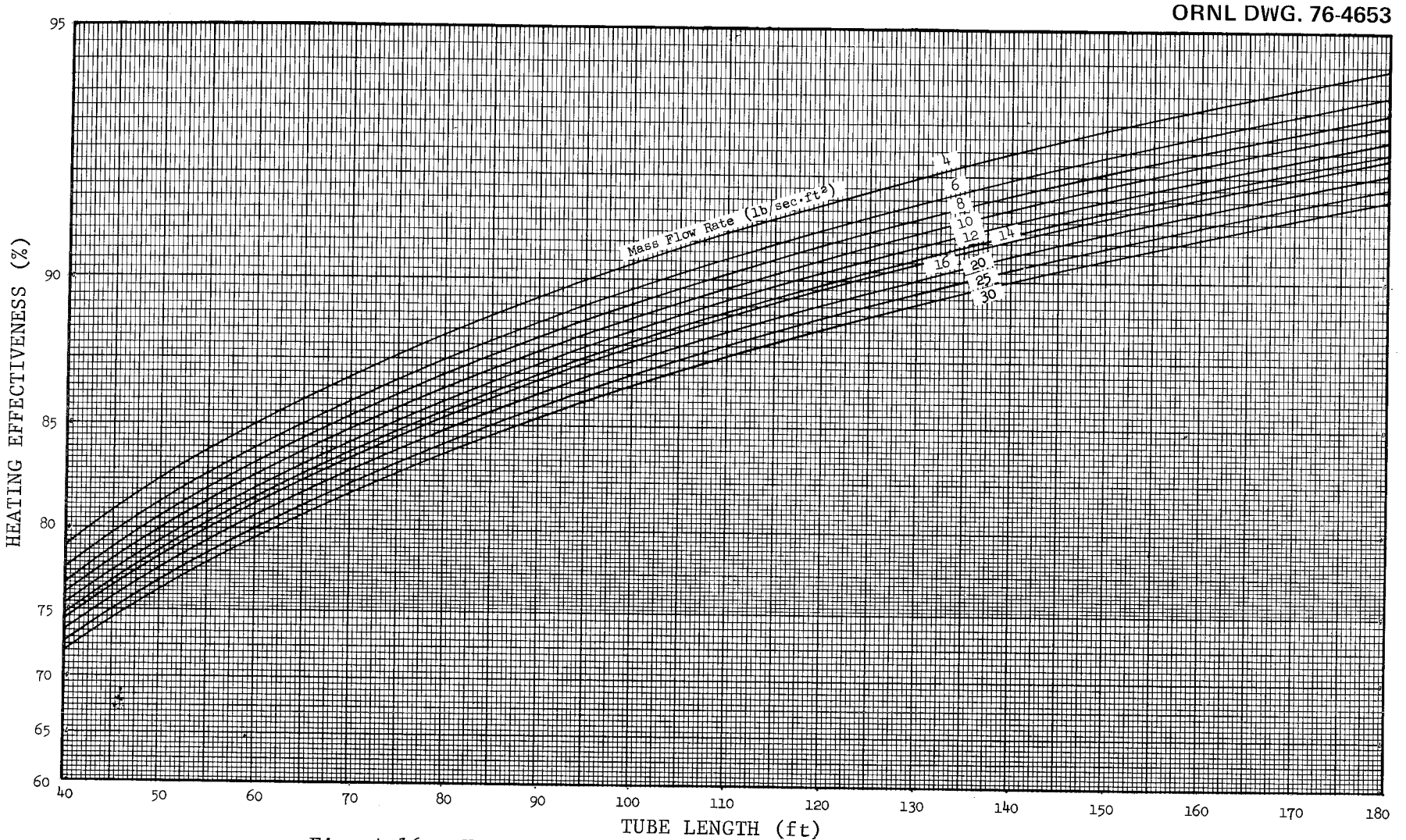

Fig. A.16. Heating effectiveness as a function of tube length in the recuperator for 0.75 in. OD and 0.042 in. thick wall tubes with a shell-side mass flow rate equal to 40% of that inside the tubes.

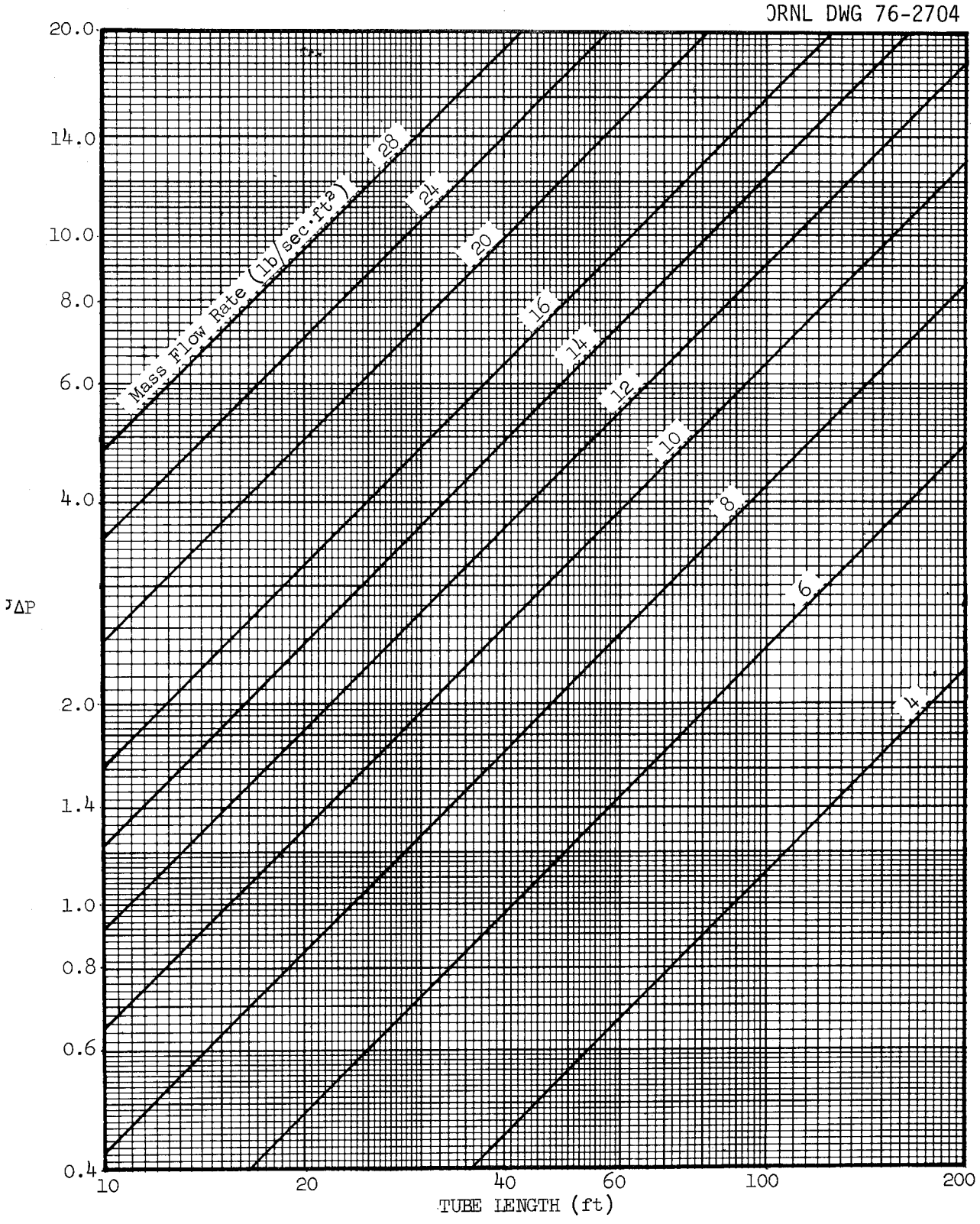

Fig. A.17. The pressure drop parameter $\sigma\Delta P$ as a function of tube length for the turbine air flow through 0.75 in. OD and 0.042 in. thick wall tubes.

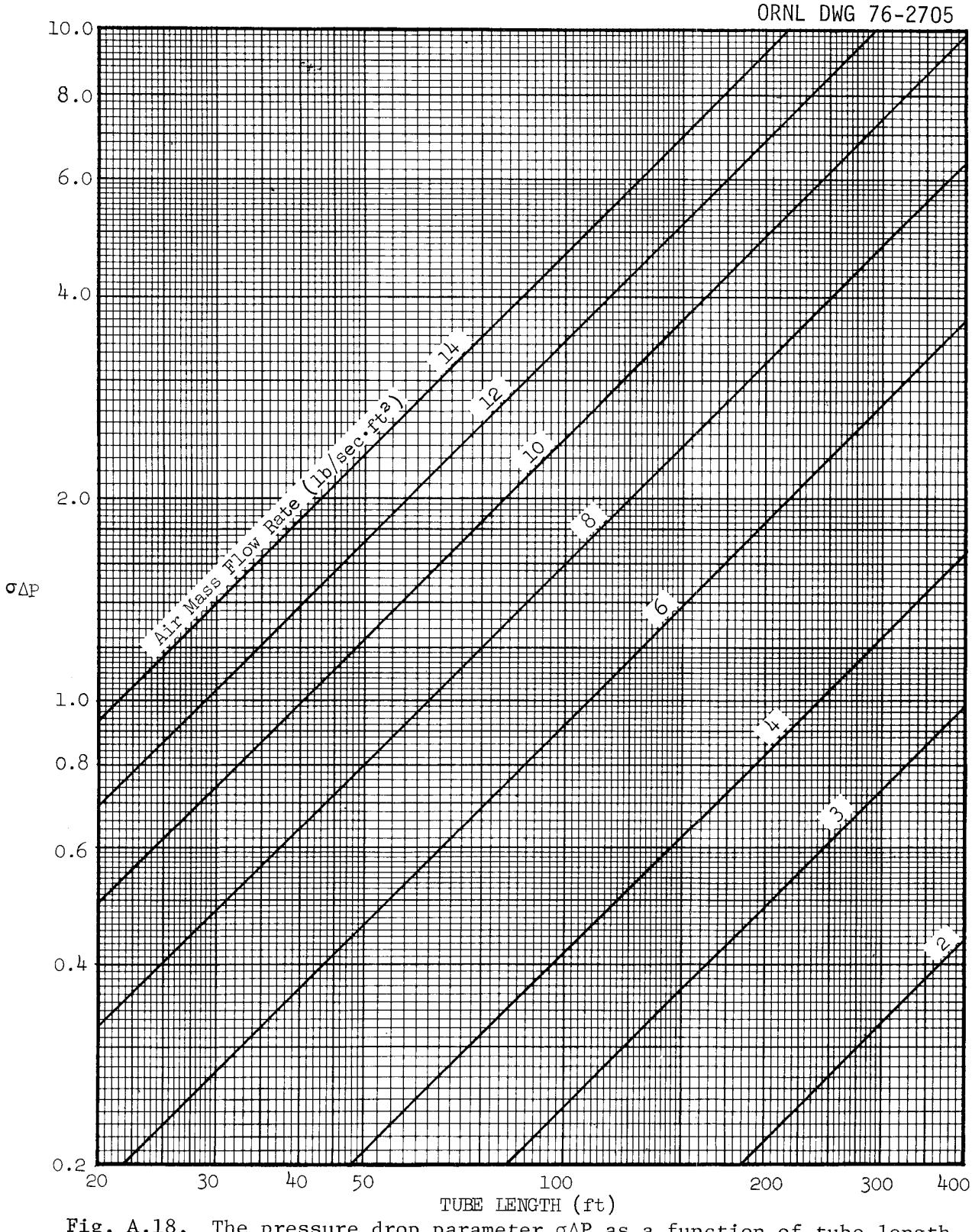

Fig. A.18. The pressure drop parameter $\sigma\Delta P$ as a function of tube length for the turbine air flow on the shell-side of the recuperator for 0.75 in. OD tubes with the shell-side air mass flow rate equal to 40% of the tube-side mass flow rate.

ORNL DWG 76-2706

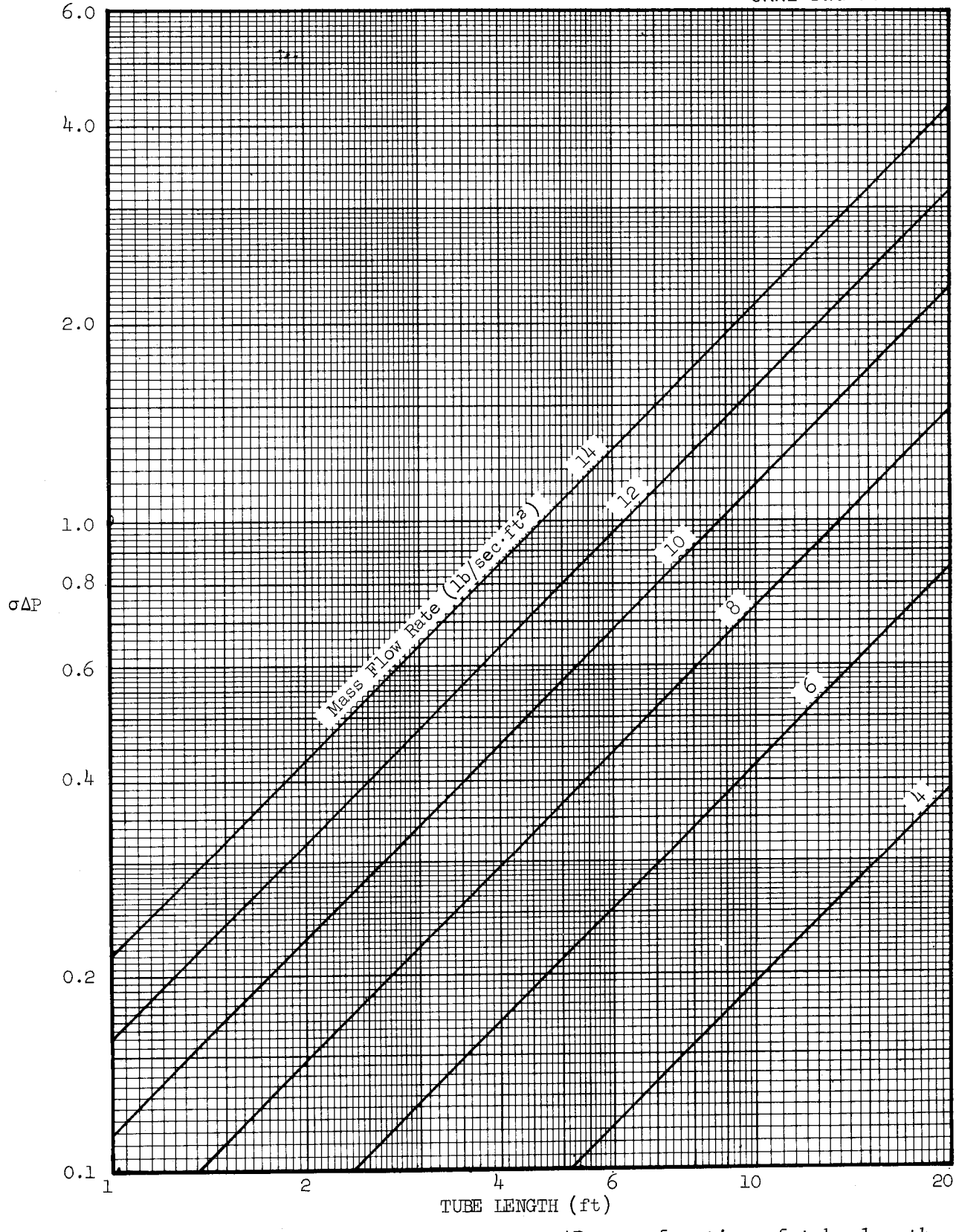

Fig. A.19. The pressure drop parameter σΔP as a function of tube length for the combustion gas flow on the shell-side of the economizer for 0.75 in. OD tubes with the shell-side air mass flow rate equal to 30% of the tube-side mass flow rate.

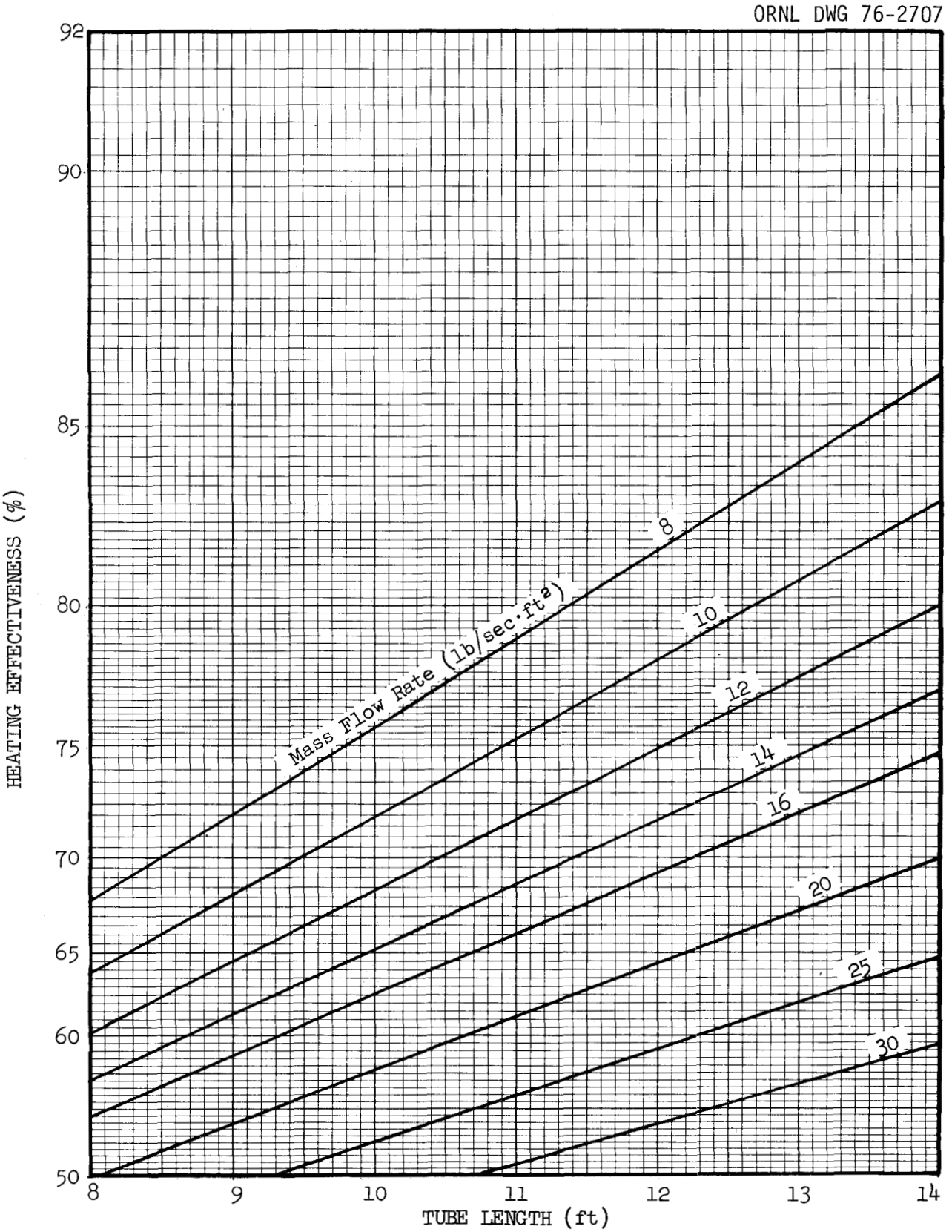

Fig. A.20. Heating effectiveness as a function of tube length in the fluidized bed for 1.0 in. OD and 0.056 in. thick wall tubes.

ORNL DWG 76-4912

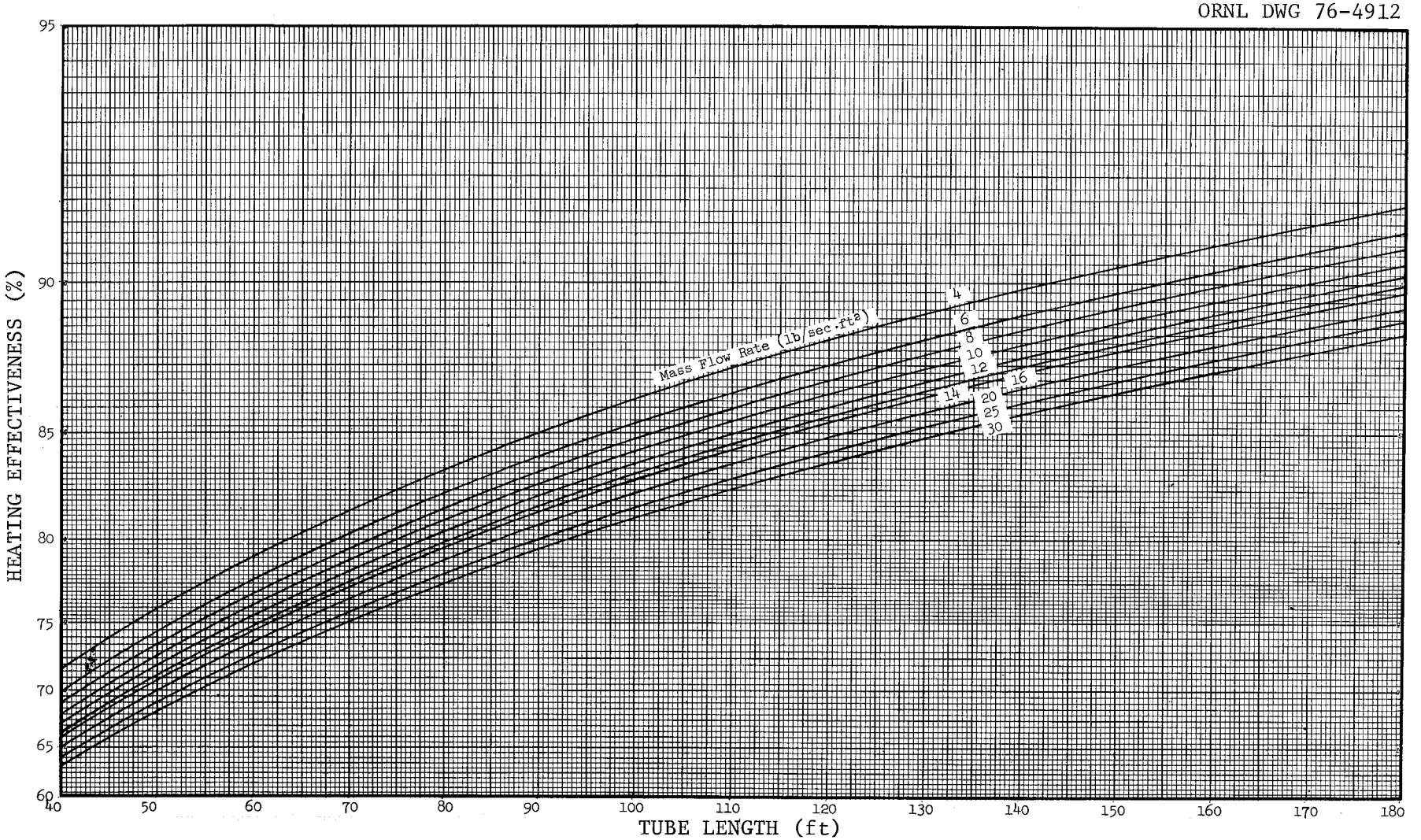

Fig. A.21. Heating effectiveness as a function of tube length in the recuperator for 1.0 in. OD and 0.56 in. thick wall tubes with a shell-side mass flow rate equal to 40% of that inside the tubes.

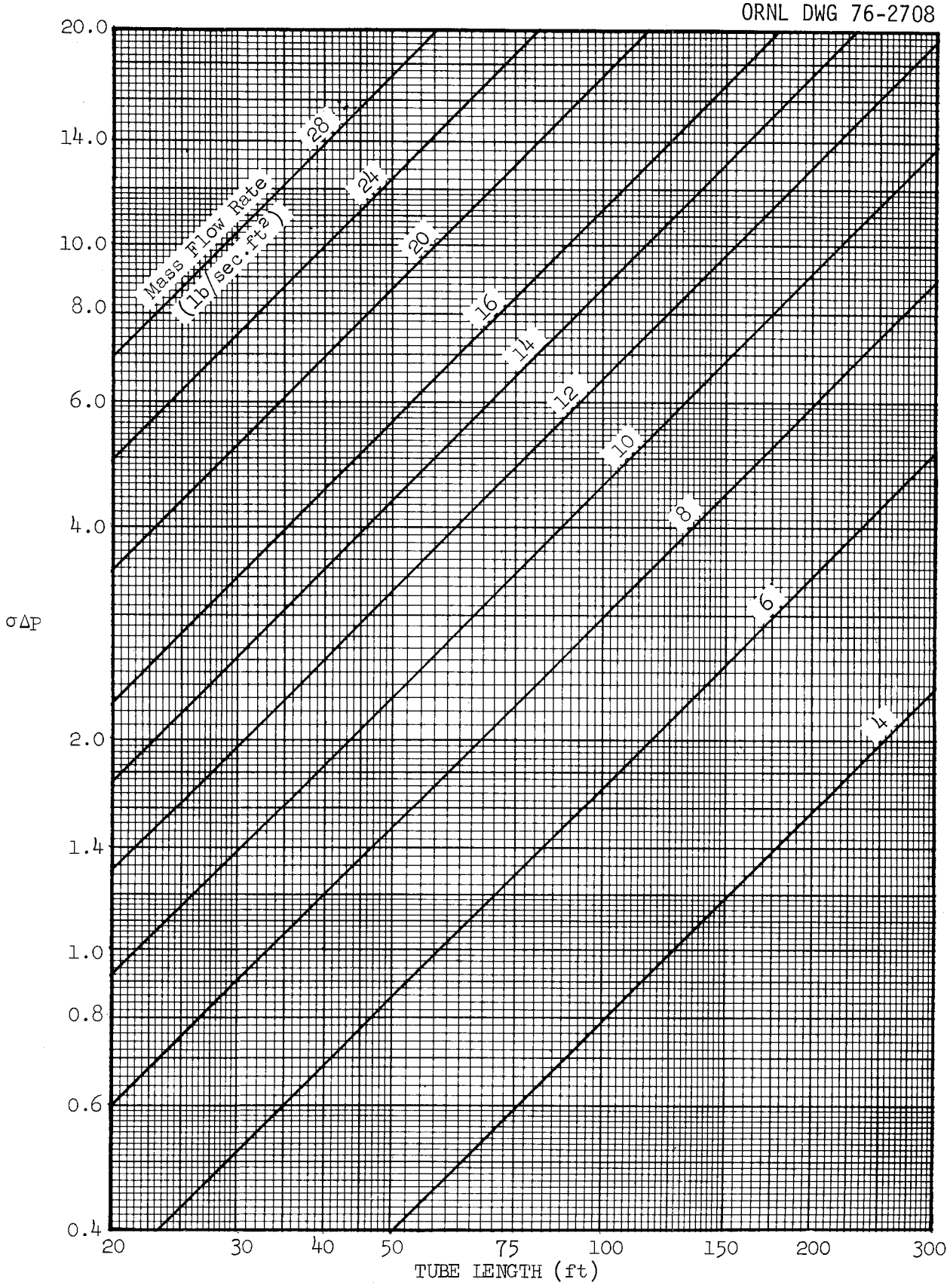

Fig. A.22. The pressure drop parameter σΔP as a function of tube length for the turbine air flow through 1.0 in. OD and 0.056 in. thick wall tubes.

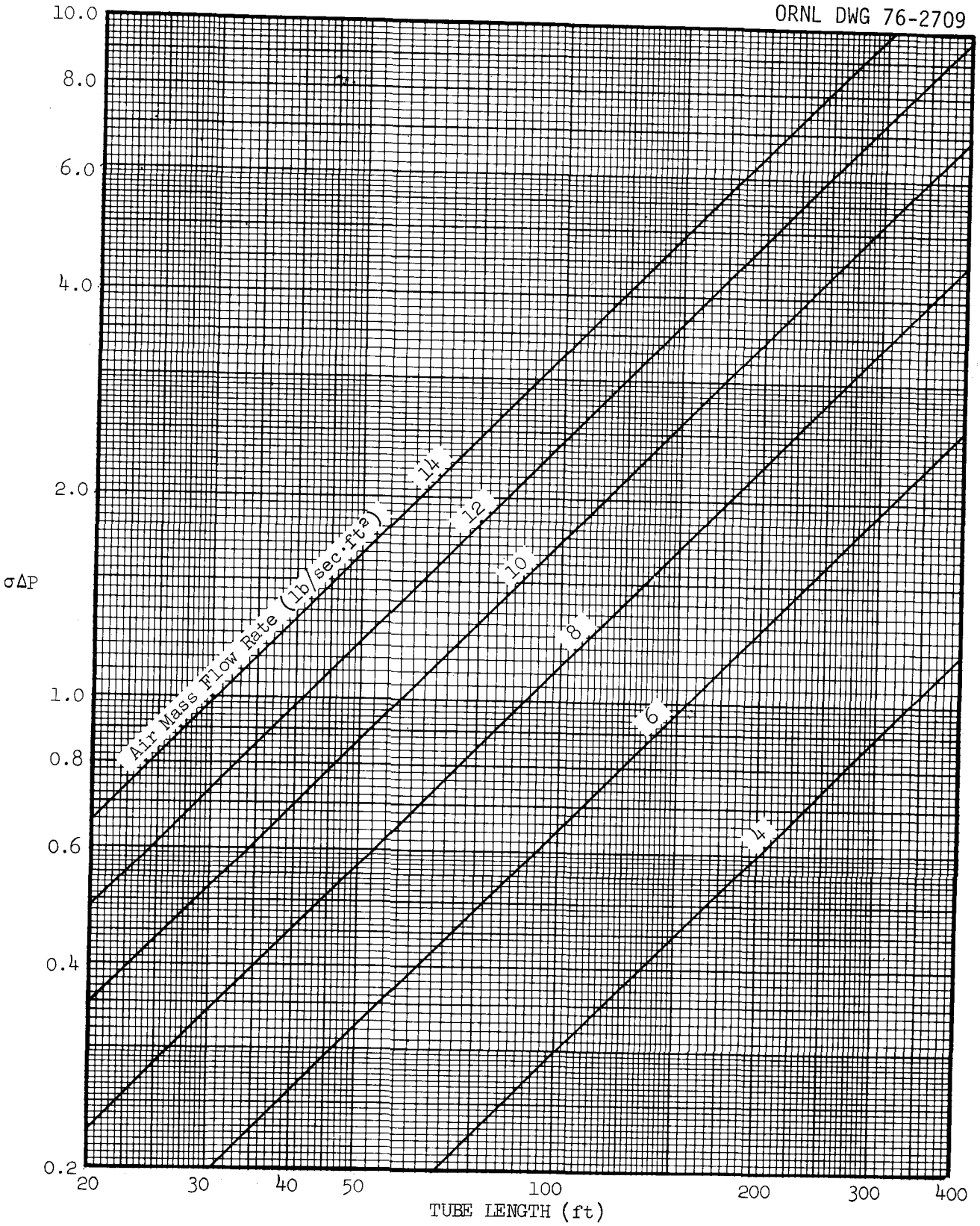

Fig. A.23. The pressure drop parameter σΔP as a function of tube length for the turbine air flow on the shell-side of the recuperator for 1.0 in. OD tubes with the shell-side air mass flow rate equal to 40% of the tube-side mass flow rate.

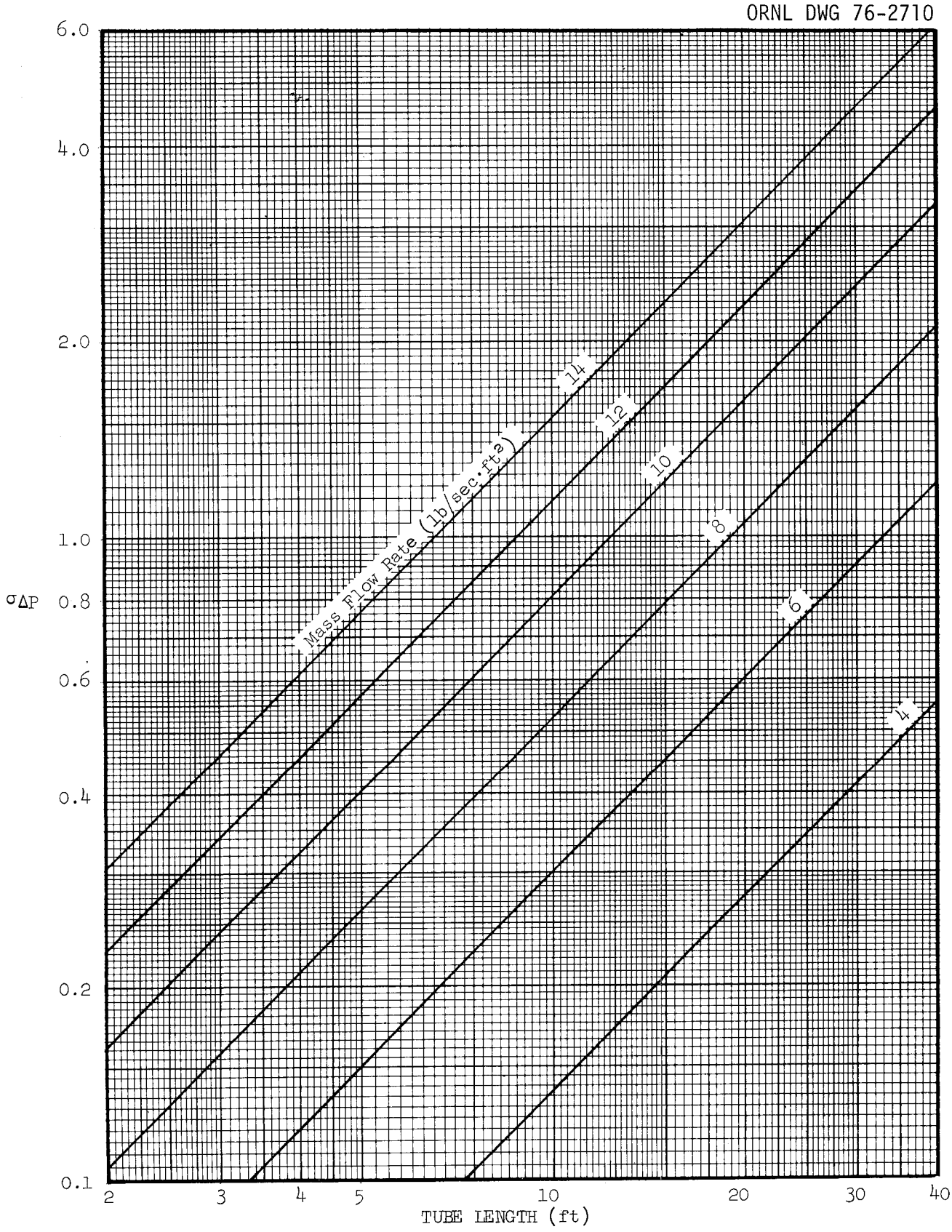

Fig. A.24. The pressure drop parameter σΔP as a function of tube length for the combustion gas flow on the shell-side of the economizer for 1.0 in. OD tubes with the shell-side air mass flow rate equal to 30% of the tube side.

APPENDIX B

Average U.S. Coal Prices by Region and Sulfur Content

The coal prices presented here are those reported by the Federal Power Commission for February 1974.

Reference: Federal Power Commission News, Volume 7, Number 23, pp. 17-19, June 7, 1974.

Table B.1. Average Coal Prices, F.O.B. Plant

GEOGRAPHIC REGION AND STATE	LINE	PURCHASE PRICE BY TYPE OF PURCHASE						PHURCHASE PRICE BY TYPE OF MINING METHOD						LINE
		CONTRACT PURCHASES 1000 TONS	AVG. CONTRACT PRICE		SPOT PURCHASES 1000 TONS	AVG. SPOT PRICE		STRIP AND AUGER			UNDERGROUND			
			¢ PER 10^6 BTU	$ PER TON		¢ PER 10^6 BTU	$ PER TON	QUANTITY 1000 TONS	AVG. PRICE ¢ PER 10^6 BTU	AVG. PRICE $ PER TON	QUANTITY 1000 TONS	AVG. PRICE ¢ PER 10^6 BTU	AVG. PRICE $ PER TON	
NEW ENGLAND														
Connecticut	2	0.0	0.0	0.00	49.0	106.9	26.16	32.8	106.9	26.16	16.2	106.9	26.16	2
Maine	3	0.0	0.0	0.00	0.0	0.0	0.00	0.0	0.0	0.00	0.0	0.0	0.00	3
Massachusetts	4	215.7	136.1	31.87	33.0	123.2	28.26	150.0	149.3	34.35	98.7	112.7	26.90	4
New Hampshire	5	78.4	59.2	16.06	0.0	0.0	0.00	0.0	0.0	0.00	78.4	59.2	16.06	5
Rhode Island	6	12.0	141.5	34.98	0.0	0.0	0.00	0.0	0.0	0.00	12.0	141.5	34.98	6
Vermont	7	0.0	0.0	0.00	0.0	0.0	0.00	0.0	0.0	0.00	0.0	0.0	0.00	7
. . . . . TOTAL	9	306.1	114.4	27.94	82.0	113.2	27.01	182.8	141.3	32.88	205.3	91.9	23.18	9
MIDDLE ATLANTIC														
New Jersey	12	222.4	111.3	27.14	95.9	123.3	30.28	134.1	119.0	28.84	184.1	112.0	27.54	12
New York	13	185.1	61.0	15.44	270.6	87.6	20.63	262.3	79.5	18.43	193.3	72.4	18.65	13
Pennsylvania	14	1,868.0	59.6	14.39	1,011.6	70.1	16.27	1,169.7	66.3	15.67	1,709.9	61.1	14.63	14
. . . . . TOTAL	16	2,275.5	64.8	15.72	1,378.0	77.5	18.10	1,566.1	73.1	17.26	2,087.4	66.8	16.14	16
EAST NORTH CENTRAL														
Illinois	19	2,337.2	48.2	9.92	325.1	49.0	10.87	1,675.6	50.1	10.43	986.7	45.2	9.37	19
Indiana	20	2,044.0	37.4	8.06	271.4	56.1	11.71	2,255.1	39.3	8.44	60.3	47.7	10.16	20
Michigan	21	1,078.2	49.1	11.86	125.4	68.1	16.92	434.3	53.1	12.57	769.3	50.1	12.29	21
Ohio	22	2,024.5	50.3	11.29	1,230.8	88.3	19.59	1,978.1	67.4	14.62	1,277.2	60.5	14.13	22
Wisconsin	23	354.4	51.3	11.56	73.8	67.9	14.68	267.6	56.1	12.39	160.6	50.7	11.60	23
. . . . . TOTAL	25	7,838.3	46.3	10.13	2,026.5	75.8	16.79	6,610.7	52.1	11.22	3,254.2	52.9	12.05	25
WEST NORTH CENTRAL														
Iowa	28	238.9	47.9	9.72	64.4	64.3	14.35	239.0	53.3	11.10	64.3	45.5	9.23	28
Kansas	29	126.2	25.7	4.86	44.5	56.9	12.74	170.6	34.9	6.91	0.0	0.0	0.00	29
Minnesota	30	420.9	38.7	6.55	5.7	69.5	13.84	419.5	38.2	6.44	7.1	76.7	18.71	30
Missouri	31	1,401.6	34.8	7.57	43.0	53.0	10.68	1,178.0	34.3	7.36	266.5	39.6	9.02	31
Nebraska	32	81.7	50.8	10.72	8.8	58.6	12.27	87.7	50.8	10.72	2.8	76.5	15.48	32
North Dakota	33	401.4	16.4	2.20	29.1	23.3	3.15	430.5	16.8	2.26	0.0	0.0	0.00	33
South Dakota	34	12.4	36.0	5.55	0.0	0.0	0.00	12.4	36.0	5.55	0.0	0.0	0.00	34
. . . . . TOTAL	36	2,682.9	34.8	6.76	195.5	55.8	11.40	2,537.7	35.4	6.77	340.7	41.7	9.32	36
SOUTH ATLANTIC														
Delaware	39	0.0	0.0	0.00	47.0	88.1	20.91	41.0	88.3	20.73	6.0	86.3	22.16	39
District of Columbia	40	10.0	89-8	22.65	12.0	127.9	31.46	0.0	0.0	0.00	22.0	110.4	27.46	40
Florida	41	422.5	60.7	13.84	55.3	76.8	18.17	353.3	63.1	14.36	124.5	61.4	14.29	41
Georgia	42	582.0	49.2	11.69	8.0	76.4	19.05	414.2	47.3	11.12	175.8	54.7	13.38	42
Maryland	43	88.9	90.5	23.00	257.0	94.3	21.64	262.9	93.1	21.32	83.0	93.5	24.12	43
North Carolina	44	1,114.7	61.7	15.28	348.3	129.7	30.76	547.5	83.3	20.18	915.5	73.9	18.24	44
South Carolina	45	205.5	82.6	19.61	84.8	110.9	26.18	134.7	95.4	22.67	155.6	86.9	20.55	45
Virginia	46	178.1	66.1	15.74	326.8	130.3	30.99	217.5	123.3	30.09	287.4	96.0	22.98	46
West Virginia	47	1,170.3	47.8	11.40	797.3	114.1	25.96	655.7	99.8	22.26	1,311.9	61.9	14.82	47
. . . . . TOTAL	49	3,771.9	57.5	13.82	1,936.5	115.2	26.77	2,626.8	83.9	19.48	3,081.7	70.8	17.14	49
EAST SOUTH CENTRAL														
Alabama	52	870.2	54.7	12.57	141.1	60.4	14.19	334.4	55.6	12.96	676.9	55.4	12.72	52
Kentucky	53	1,598.7	37.6	8.12	378.8	115.9	25.71	1,373.1	49.4	10.64	604.4	60.8	13.40	53
Mississippi	54	129.4	49.5	11.34	0.0	0.0	0.00	0.0	0.0	0.00	129.4	49.5	11.34	54
Tennessee	55	1,491.8	41.7	9.18	5.8	40.1	8.90	388.5	39.1	8.64	1,109.1	42.6	9.37	55
. . . . . TOTAL	57	4,090.0	43.3	9.56	525.7	99.5	22.44	2,095.9	48.5	10.64	2,519.9	50.8	11.34	57
WEST SOUTH CENTRAL														
Arkansas	60	0.0	0.0	0.00	0.0	0.0	0.00	0.0	0.0	0.00	0.0	0.0	0.00	60
Louisiana	61	0.0	0.0	0.00	0.0	0.0	0.00	0.0	0.0	0.00	0.0	0.0	0.00	61
Oklahoma	62	0.0	0.0	0.00	0.0	0.0	0.00	0.0	0.0	0.00	0.0	0.0	0.00	62
Texas	63	527.0	13.6	1.90	0.0	0.0	0.00	527.0	13.6	1.90	0.0	0.0	0.00	63
. . . . . TOTAL	65	527.0	13.6	1.90	0.0	0.0	0.00	527.0	13.6	1.90	0.0	0.0	0.00	65
MOUNTAIN														
Arizona	68	141.4	17.4	4.11	0.0	0.0	0.00	141.4	17.4	4.11	0.0	0.0	0.00	68
Colorado	69	549.4	34.1	6.77	66.9	53.7	10.78	545.6	35.9	7.11	70.8	38.9	7.92	69
Idaho	70	0.0	0.0	0.00	0.0	0.0	0.00	0.0	0.0	0.00	0.0	0.0	0.00	70
Montana	71	73.0	23.7	3.73	0.0	0.0	0.00	73.0	23.7	3.73	0.0	0.0	0.00	71
Nevada	72	196.1	33.5	7.48	0.0	0.0	0.00	172.0	32.5	7.13	24.1	39.6	9.95	72
New Mexico	73	509.8	18.6	3.36	0.0	0.0	0.00	509.8	18.6	3.36	0.0	0.0	0.00	73
Utah	74	58.0	39.5	9.06	1.0	28.7	6.97	0.0	0.0	0.00	59.0	39.3	9.02	74
Wyoming	75	428.1	19.7	3.30	0.0	0.0	0.00	428.1	19.7	3.30	0.0	0.0	0.00	75
. . . . . TOTAL	77	1,955.8	25.9	4.95	67.9	53.3	10.73	1,869.9	25.6	4.86	153.9	39.2	8.66	77
PACIFIC														
California	80	0.0	0.0	0.00	0.0	0.0	0.00	0.0	0.0	0.00	0.0	0.0	0.00	80
Oregon	81	0.0	0.0	0.00	0.0	0.0	0.00	0.0	0.0	0.00	0.0	0.0	0.00	81
Washington	82	0.0	0.0	0.00	0.0	0.0	0.00	0.0	0.0	0.00	0.0	0.0	0.00	82
. . . . . TOTAL	84	0.0	0.0	0.00	0.0	0.0	0.00	0.0	0.0	0.00	0.0	0.0	0.00	84
UNITED STATES TOTAL	86	23,447.6	47.6	10.40	6,212.2	90.5	20.57	18,016.8	54.5	11.54	11,643.0	60.2	14.05	86

Table B.2. Coal Deliveries and Prices by Sulfur Content

GEOGRAPHIC REGION AND STATE	LINE	0.5% SULFUR OR LESS			0.51% TO 1.0% SULFUR			0.01% TO 1.5% SULFUR			LINE	1.51% TO 2.0% SULFUR			2.01% TO 3.0% SULFUR			3.01% OR MORE SULFUR			AVG. PRICE FOR ALL PURCHASES		LINE	GEOGRAPHIC REGION AND STATE
		QUANTITY 1000 TONS	AVG. PRICE ¢ PER 10^6 BTU	AVG. PRICE $ PER TON	QUANTITY 1000 TONS	AVG. PRICE ¢ PER 10^6 BTU	AVG. PRICE $ PER TON	QUANTITY 1000 TONS	AVG. PRICE ¢ PER 10^6 BTU	AVG. PRICE $ PER TON		QUANTITY 1000 TONS	AVG. PRICE ¢ PER 10^6 BTU	AVG. PRICE $ PER TON	QUANTITY 1000 TONS	AVG. PRICE ¢ PER 10^6 BTU	AVG. PRICE $ PER TON	QUANTITY 1000 TONS	AVG. PRICE ¢ PER 10^6 BTU	AVG. PRICE $ PER TON	¢ PER 10^6 BTU	$ PER TON		
NEW ENGLAND																								NEW ENGLAND
Connecticut	2	0.0	0.0	0.00	0.0	0.0	0.00	0.0	0.0	0.00	2	49.0	106.9	26.16	0.0	0.0	0.00	0.0	0.0	0.00	106.9	26.16	2	Connecticut
Maine	3	0.0	0.0	0.00	0.0	0.0	0.00	0.0	0.0	0.00	3	0.0	0.0	0.00	0.0	0.0	0.00	0.0	0.0	0.00	0.0	0.00	3	Maine
Massachusetts	4	23.0	165.2	36.11	173.7	132.9	31.36	0.0	0.0	0.00	4	19.0	132.3	31.46	33.0	123.2	28.26	0.0	0.0	0.00	134.4	31.39	4	Massachusetts
New Hampshire	5	0.0	0.0	0.00	0.0	0.0	0.00	0.0	0.0	0.00	5	0.0	0.0	0.00	78.4	59.2	16.06	0.0	0.0	0.00	59.2	16.06	5	New Hampshire
Rhode Island	6	0.0	0.0	0.00	12.0	141.5	34.98	0.0	0.0	0.00	6	0.0	0.0	0.00	0.0	0.0	0.00	0.0	0.0	0.00	141.5	34.98	6	Rhode Island
Vermont	7	0.0	0.0	0.00	0.0	0.0	0.00	0.0	0.0	0.00	7	0.0	0.0	0.00	0.0	0.0	0.00	0.0	0.0	0.00	0.0	0.00	7	Vermont
. . . . . TOTAL	9	23.0	165.2	36.11	185.7	133.5	31.59	0.0	0.0	0.00	9	68.0	113.8	27.64	111.4	76.0	19.67	0.0	0.0	0.00	114.2	27.75	9	. . . . . TOTAL
MIDDLE ATLANTIC																								MIDDLE ATLANTIC
New Jersey	12	13.4	132.4	34.62	130.3	124.6	29.77	72.6	96.1	24.56	12	25.0	90.6	22.58	77.0	122.4	29.22	0.0	0.0	0.00	114.9	28.09	12	New Jersey
New York	13	0.7	97.9	19.08	12.9	72.6	15.02	27.3	84.8	19.87	13	155.6	72.3	16.97	169.6	74.0	18.78	89.6	85.5	20.83	76.3	18.52	13	New York
Pennsylvania	14	12.9	41.4	7.00	288.4	79.5	18.81	242.5	68.3	16.49	14	471.7	63.5	15.55	1,494.6	62.3	14.63	369.5	51.4	12.52	63.2	15.05	14	Pennsylvania
. . . . . TOTAL	16	26.9	97.5	21.02	431.6	93.1	22.00	342.4	75.7	18.47	16	652.3	66.6	16.16	1,741.2	66.2	15.68	459.0	58.1	14.14	69.5	16.62	16	. . . . . TOTAL
EAST NORTH CENTRAL																								EAST NORTH CENTRAL
Illinois	19	627.0	70.5	13.75	3.3	114.2	29.92	44.8	54.6	12.86	19	83.5	49.8	11.51	771.4	40.0	8.65	1,132.3	42.0	8.64	48.3	10.03	19	Illinois
Indiana	20	146.0	58.9	11.94	34.7	71.8	12.79	16.6	82.8	17.81	20	4.8	73.8	18.77	816.1	37.8	8.12	1,297.2	37.2	8.06	39.5	8.49	20	Indiana
Michigan	21	1.3	137.8	34.17	84.5	75.6	18.52	0.3	106.8	26.70	21	8.7	68.8	17.39	581.0	47.4	11.58	527.7	50.8	12.16	51.2	12.39	21	Michigan
Ohio	22	0.0	0.0	0.00	290.2	98.7	21.96	206.0	137.2	30.20	22	204.1	70.6	15.22	797.3	63.1	14.55	1,757.7	50.5	11.19	64.6	14.43	22	Ohio
Wisconsin	23	47.9	52.8	11.67	13.6	55.6	11.83	23.9	44.4	10.64	23	88.3	52.0	11.72	109.3	55.1	12.18	145.3	56.5	12.67	54.0	12.10	23	Wisconsin
. . . . . TOTAL	25	822.2	67.3	13.34	426.3	90.8	20.27	291.7	112.7	25.23	25	389.4	61.7	13.72	3.075.1	47.6	10.72	4,860.2	45.3	9.91	52.4	11.50	25	. . . . . TOTAL
WEST NORTH CENTRAL																								WEST NORTH CENTRAL
Iowa	28	90.0	46.0	9.44	36.1	53.9	11.05	0.0	0.0	0.00	28	18.7	62.0	15.01	121.3	52.0	10.70	37.3	55.9	11.25	51.7	10.70	28	Iowa
Kansas	29	22.6	57.9	12.63	2.3	67.2	14.73	0.0	0.0	0.00	29	0.0	0.0	0.00	0.0	0.0	0.00	145.7	30.4	5.90	34.9	6.91	29	Kansas
Minnesota	30	0.0	0.0	0.00	394.8	37.0	6.19	16.9	48.6	7.87	30	2.1	74.4	18.59	7.6	64.5	15.95	5.1	78.6	19.15	39.2	6.64	30	Minnesota
Missouri	31	61.0	45.1	9.55	21.0	52.7	9.18	94.0	49.5	11.69	31	3.8	74.6	18.44	427.0	30.7	6.88	837.8	34.8	7.38	35.3	7.66	31	Missouri
Nebraska	32	0.0	0.0	0.00	90.5	51.5	10.87	0.0	0.0	0.00	32	0.0	0.0	0.00	0.0	0.0	0.00	0.0	0.0	0.00	51.5	10.87	32	Nebraska
North Dakota	33	0.0	0.0	0.00	430.5	16.8	2.26	0.0	0.0	0.00	33	0.0	0.0	0.00	0.0	0.0	0.00	0.0	0.0	0.00	16.8	2.26	33	North Dakota
South Dakota	34	12.4	36.0	5.55	0.0	0.0	0.00	0.0	0.0	0.00	34	0.0	0.0	0.00	0.0	0.0	0.00	0.0	0.0	0.00	36.0	5.55	34	South Dakota
. . . . . TOTAL	36	185.9	46.7	9.60	975.1	32.5	5.15	110.9	49.4	11.11														. . . . . TOTAL
SOUTH ATLANTIC																								SOUTH ATLANTIC
Delaware	39	0.0	0.0	0.00	0.0	0.0	0.00	23.0	86.1	21.02	39	15.0	93.0	20.87	7.0	87.8	21.08	2.0	77.4	19.41	88.1	20.91	39	Delaware
District of Columbia	40	1.0	109.0	27.60	21.0	110.4	27.45	0.0	0.0	0.00	40	0.0	0.0	0.00	0.0	0.0	0.00	0.0	0.0	0.00	110.4	27.46	40	District of Columbia
Florida	41	0.0	0.0	0.00	9.4	130.5	34.09	5.5	69.4	18.62	41	7.9	68.2	16.98	36.7	62.9	14.29	418.3	60.6	13.80	62.6	14.34	41	Florida
Georgia	42	0.0	0.0	0.00	124.0	50.4	12.60	52.0	49.0	11.87	42	27.0	61.4	14.68	159.0	58.7	13.99	228.0	41.1	9.46	49.6	11.79	42	Georgia
Maryland	43	8.0	105.4	22.34	108.9	92.3	23.36	40.0	90.4	19.76	43	120.0	94.4	21.67	69.0	93.1	21.64	0.0	0.0	0.00	93.2	21.99	43	Maryland
North Carolina	44	0.0	0.0	0.00	869.8	78.0	18.91	471.0	67.0	16.90	44	76.7	117.5	27.40	39.2	109.9	26.74	6.3	123.4	29.62	77.4	18.96	44	North Carolina
South Carolina	45	0.0	0.0	0.00	105.4	94.3	22.25	135.7	88.1	20.62	45	20.2	94.1	23.35	29.0	88.5	21.95	0.0	0.0	0.00	90.8	21.53	45	South Carolina
Virginia	44	10.0	107.8	23.84	448.0	106.0	25.18	27.6	127.2	30.55	46	6.7	97.9	25.21	12.4	128.8	32.09	0.2	48.4	10.88	107.7	25.61	46	Virginia
West Virginia	47	52.8	121.4	26.79	674.1	92.1	21.45	294.1	130.5	29.71	47	132.9	106.2	25.86	469.5	49.7	11.48	444.3	33.5	8.06	73.9	17.30	47	West Virginia
. . . . . TOTAL	49	71.8	117.5	25.89	2,360.6	87.6	20.98	948.8	84.3	20.40	49	406.4	99.9	23.68	821.8	61.8	14.43	1,099.0	45.7	10.68	76.7	18.21	49	. . . . . TOTAL
EAST SOUTH CENTRAL																								EAST SOUTH CENTRAL
Alabama	52	0.6	56.5	13.20	265.2	66.9	15.35	119.6	56.9	13.33	52	173.5	54.1	12.91	68.7	57.1	13.88	383.7	47.3	10.62	55.5	12.80	52	Alabama
Kentucky	53	4.4	83.6	18.47	361.3	101.9	23.14	111.1	95.0	21.11	53	168.6	50.6	10.83	116.8	41.4	9.13	1,215.3	34.8	7.44	52.9	11.49	53	Kentucky
Mississippi	54	0.0	0.0	0.00	0.0	0.0	0.00	0.0	0.0	0.00	54	0.0	0.0	0.00	129.4	49.5	11.34	0.0	0.0	0.00	49.5	11.34	54	Mississippi
Tennessee	55	0.0	0.0	0.00	137.2	45.1	10.23	18.1	39.5	9.23	55	8.9	39.0	9.19	138.5	40.7	9.34	1,195.0	41.4	9.04	41.7	9.18	55	Tennessee
. . . . . TOTAL	57	5.0	80.3	17.85	763.6	79.5	18.11	248.8	72.1	16.50	57	351.0	52.1	11.82	453.5	46.0	10.54	2,793.9	39.4	8.56	49.8	11.02	57	. . . . . TOTAL
WEST SOUTH CENTRAL																								WEST SOUTH CENTRAL
Arkansas	60	0.0	0.0	0.00	0.0	0.0	0.00	0.0	0.0	0.00	60	0.0	0.0	0.00	0.0	0.0	0.00	0.0	0.0	0.00	0.0	0.00	60	Arkansas
Louisiana	61	0.0	0.0	0.00	0.0	0.0	0.00	0.0	0.0	0.00	61	0.0	0.0	0.00	0.0	0.0	0.00	0.0	0.0	0.00	0.0	0.00	61	Lousiana
Oklahoma	62	0.0	0.0	0.00	0.0	0.0	0.00	0-0	0.0	0.00	62	0.0	0.0	0.00	0.0	0.0	0.00	0.0	0.0	0.00	0.0	0.00	62	Oklahoma
Texas	63	0.0	0.0	0.00	527.0	13.6	1.90	0.0	0.0	0.00	63	0.0	0.0	0.00	0.0	0.0	0.00	0.0	0.0	0.00	13.6	1.90	63	Texas
. . . . . TOTAL	65	0.0	0.0	0.00	527.0	13.6	1.90	0.0	0.0	0.00	65	0.0	0.0	0.00	0.0	0.0	0.00	0.0	0.0	0.00	13.6	1.90	65	. . . . . TOTAL
MOUNTAIN																								MOUNTAIN
Arizona	68	141.4	17.4	4.11	0.0	0.0	0.00	0.0	0.0	0.00	68	0.0	0.0	0.00	0.0	0.0	0.00	0.0	0.0	0.00	17.4	4.11	68	Arizona
Colorado	69	473.0	36.3	7.06	143.3	35.9	7.70	0.0	0.0	0.00	69	0.0	0.0	0.00	0.0	0.0	0.00	0.0	0.0	0.00	36.2	7.21	69	Colorado
Idaho	70	0.0	0.0	0.00	0.0	0.0	0.00	0.0	0.0	0.00	70	0.0	0.0	0.00	0.0	0.0	0.00	0.0	0.0	0.00	0.0	0.00	70	Idaho
Montana	71	27.0	29.9	3.90	46.0	20.9	3.63	0.0	0.0	0.00	71	0.0	0.0	0.00	0.0	0.0	0.00	0.0	0.0	0.00	23.7	3.73	71	Montana
Nevada	72	196.1	33.5	7.48	0.0	0.0	0.00	0.0	0.0	0.00	72	0.0	0.0	0.00	0.0	0.0	0.00	0.0	0.0	0.00	33.5	7.48	72	Nevada
New Mexico	73	0.0	0.0	0.00	509.8	18.6	3.36	0.0	0.0	0.00	73	0.0	0.0	0.00	0.0	0.0	0.00	0.0	0.0	0.00	18.6	3.36	73	New Mexico
Utah	74	59.0	39.3	9.02	0.0	0.0	0.00	0.0	0.0	0.00	74	0.0	0.0	0.00	0.0	0.0	0.00	0.0	0.0	0.00	39.3	9.02	74	Utah
Wyoming	75	428.1	19.7	3.30	0.0	0.0	0.00	0.0	0.0	0.00	75	0.0	0.0	0.00	0.0	0.0	0.00	0.0	0.0	0.00	19.7	3.30	75	Wyoming
. . . . . TOTAL	77	1,324.6	28.9	5.61	699.1	22.8	4.27	0.0	0.0	0.00	77	0.0	0.0	0.00	0.0	0.0	0.00	0.0	0.0	0.00	26.8	5.15	77	. . . . . TOTAL
PACIFIC																								PACIFIC
California	80	0.0	0.0	0.00	0.0	0.0	0.00	0.0	0.0	0.00	80	0.0	0.0	0.00	0.0	0.0	0.00	0.0	0.0	0.00	0.0	0.00	80	California
Oregon	81	0.0	0.0	0.00	0.0	0.0	0.00	0.0	0.0	0.00	81	0.0	0.0	0.00	0.0	0.0	0.00	0.0	0.0	0.00	0.0	0.00	81	Oregon
Washington	82	0.0	0.0	0.00	0.0	0.0	0.00	0.0	0.0	0.00	82	0.0	0.0	0.00	0.0	0.0	0.00	0.0	0.0	0.00	0.0	0.00	82	Washington
. . . . . TOTAL	84	0.0	0.0	0.00	0.0	0.0	0.00	0.0	0.0	0.00	84	0.0	0.0	0.00	0.0	0.0	0.00	0.0	0.0	0.00	0.0	0.00	84	. . . . . TOTAL
UNITED STATES TOTAL	86	2,459.4	48.4	9.57	6,369.1	72.0	15.13	1,942.5	83.4	19.76	86	1,891.7	72.0	16.88	6,758.0	53.8	12.35	10,238.1	43.4	9.56	56.9	12.53	86	UNITED STATES TOTAL

APPENDIX C

Electrical and Thermal Distribution System Load Profiles for a Total Energy System

Electrical and heat load profiles for typical residential complexes were obtained from other MIUS projects carried out at ORNL for HUD. These are presented here in a form expressly adapted to evaluation of gas turbine performance requirements.

APPENDIX C

Electrical and Thermal Distribution System Load Profiles for a Total Energy System

The electrical and thermal distribution system load profiles for the 720 garden apartment complex described in Ref. 1, shown in the following Fig. 1 through 10, inclusive, were developed from the output data of a computerized analysis of the system. The 1973 ORNL MIUS hourly computer program[2] was used in making the analysis. Accurate development of anticipated electrical and thermal load profiles is considered a basic step in planning a MIUS or total energy system since, as pointed out by Garner in Ref. 3, the design and ultimate economic feasibility of the system depends on the magnitude and character of these loads.

The load profiles for a MIUS or total energy system depend on climatological conditions, structure or building design, occupancy, and modus operandi; lighting, heating and/or cooling, power equipment usage, etc. The profiles will vary from hour-to-hour, day-to-day, and season-to-season.

In the development of load profiles for a MIUS or total energy system for a complex of new structures, three major categories of data are required:

1. Local weather data
2. Building construction and design data
3. Building operating data

A complete climatological history for a given location can be obtained on magnetic tape. The booklet, "Selective Guide to Climatic Data Sources"[4] describes some of the published data and services available from the National Climatic Center. Information required includes mean hourly temperatures throughout the year (both wet-bulk and dry-bulb), extreme temperature variations (high and low) for design purposes, dew-point temperatures, solar radiation factors, wind data, and the like.

Building construction and design data will include fixed, or nonvarying, parameters such as inside design temperatures, structure orientation with respect to the sun, heat-transfer characteristics of the building, and respective areas of all exposed surfaces.

Building operating data includes all parameters that vary with time and contribute to electrical and thermal loads. These include building occupancy (people), illumination level (lighting), power-equipment operations (elevators, office machines, computers, hand-tools, air conditioning and air handling machinery), domestic hot water consumption, process thermal energy consumption, domestic appliances, and building thermal-lag, heat-storage, and air-leakage characteristics.

Accurate determination of the amount of useful exhaust heat available from the prime movers (engines) as a function of the varying electrical load/time profile is a prerequisite to the analysis. At times the recoverable heat may be in excess of that demanded by the thermal-load profile — for example, when the electrical load is high and the thermal load is low. At other times, the thermal load may be high while the electrical load is low, and a deficiency of useful exhaust heat will exist.

A deficiency in useful exhaust heat may be made-up by burning additional fuel in an auxiliary boiler. An excess of exhaust heat results in the waste of useful energy and consequent lowered thermal efficiency and profitability, unless the excess heat can be economically stored for use when there is a deficiency of useful exhaust heat. Fleming[5], in the article "Total Energy Concepts for Refrigeration and Air-Conditioning Engineers" states that heat storage systems are in operation, but, at present time, they are not widely used.

Figure 1 shows a monthly thermal energy load profile for the distribution system. This profile was developed from the computer analysis for year 7 (1963). In Fig. 1, the heat used (required) for space heating and for domestic hot water is shown by the dashed line. The heat available from the engine-generator exhaust is shown by the solid line. During the months of January, February, and December the heat required is greater than the heat available from the engines and the difference is made-up by the auxiliary boilers. During March, it appears that essentially all of the engine available heat is used and only a very small amount must be made-up. However, from April through November, the available heat is greater than that used (for space heating, domestic hot water and/or air conditioning) and a large amount of the available heat is, therefore, unused. The total amount of heat unused during the year is given in Table 1. The total

amount of waste heat available from the engines during the year amounts to about 4.34×10^{10} Btu. Another 9.245×10^{9} Btu of auxiliary boiler makeup heat was required, mainly during the colder winter months of the year, for the space heating and hot water requirements, making the total amount of heat available equal to about 5.27×10^{10} Btu. Of this, a total of 4.208×10^{10} Btu were used during the year for space heating, hot water, and/or air conditioning leaving about 1.059×10^{10} Btu unused during the year. This amount of heat unused amounts to about 24 percent of the available engine-generator exhaust heat. The reason so much heat is unused is shown by the load profiles of Fig. 2 through 10. These profiles graphically illustrate the mismatch that can occur between the heat available from the engines (which closely matches the electrical load curve) and the heat required (or used) which is predominantly a function of climatic conditions. Table 1 shows that the greatest amounts of unused heat occur during the spring months of April and May and the fall months of September, October and November. During these months, the outside temperature can be very close to the equalization temperature (equalization temperature is the outside temperature at which the internal heat offsets the building heat loss) and very little heat would be required (for either space heating or for the absorption chiller). However, even during the other months of the year, there can be several hours during which the outside temperature is within the range of the equalization temperature ($55^{o}F$ to $65^{o}F$ depending on the internal heat gains). Temperature/time frequency data for Philadelphia are shown in Table 2. This table indicates that there are about 1570 hours during the year in the temperature range of $55^{o}F$ to $65^{o}F$, distributed as shown through the year.

Figure 2 shows the outdoor dry-bulb temperature, the coincident total engine-generator load, and the waste heat available during day 34 of year 1 (February of 1955). Figure 3 shows the winter weekday (Day 34, February 1955) system hourly heat requirements and heat available at the central equipment building. During this period, the total heat used (required for domestic hot water and space heating) is in excess of that available and additional makeup heat is required from the auxiliary boiler.

Figures 4, 5, and 6 shows characteristic spring weekday outdoor temperatures, coincident engine-generator electrical loads, heat available (from the engine-generators) and total heat used.

The conditions shown in Fig. 4 are for day 132 in year 7 (May 1963). During this day, the outside temperature varied from a low of 42°F during the early morning hours to a high of about 61°F at 4:00 p.m. When the temperature was between 42°F and 45°F, from 1:00 a.m. to about 7:00 a.m., the heat available was less than the heat used and auxiliary boiler makeup heat was required. However, from 7:00 a.m. on, the heat available exceeded the heat required, consequently, considerable heat was unused. No air-conditioning was required during this period.

Figure 5 shows the conditions that prevailed during another spring day (day 130 of year 7, May 1963) just two days prior to the conditions described in Fig. 4. During this day, the outside temperature varied from about 49°F at midnight to a high of about 87°F at 3:00 p.m. when the temperature abruptly decreased. From 6:00 p.m., when the temperature was about 64°F, to the following morning at 8:00 a.m., the heat available exceeded the heat used resulting in 4.345×10^7 Btu of unused heat. From about 7:00 a.m. to about 6:00 p.m., however, the outside temperature and internal heat gains were such as to require air-conditioning. The total amount of chiller load (absorption plus compression) during this period a amounted to 6.111×10^7 Btu or 5.092×10^3 ton-hours, of which 2.572×10 Btu (2.143×10^3 ton-hrs) were supplied by the absorption chillers and the remainder 3.539×10^7 Btu (2.949×10^3 ton-hours) were supplied from the motor-compressor chillers. In order to supply this portion of A/C load from the absorption chillers an additional amount of heat equal to 5.617×10^7 Btu would be required. About 77 percent (4.345×10^7 Btu) of this amount would be available from heat unused during the 24-hour period if it could be economically stored.

Figure 6 shows the conditions that prevailed during another spring day (day 132 of year 6, May of 1962). The temperature varied from a low of 38°F at 5:00 a.m. to a high of 69°F from 3:00 p.m. to 5:00 p.m. Both space heating and air-conditioning were required, necessitating operation of the auxiliary boiler to supply makeup heat during the early morning hours and operation of the motor-compressor chillers for air-conditioning during the afternoon hours between 2:00 p.m. and 6:00 p.m. since the heat that was available did not match or coincide with the heat that was required.

Figures 7, 8, and 9 illustrate the conditions that could prevail during a characteristic summer day. During this day (day 203 of year 1, July 1955), the outside temperature varied from a low of 74°F at 6:00 a.m. to a high of 100°F at 4:00 p.m. No space heating was required and all of the available engine-generator waste heat not required for domestic hot water was available for use in the absorption chillers as shown in Fig. 8. However, the absorption chillers could not supply all of the required air conditioning load, hence, the remainder of the A/C load was supplied from the motor-compressor units as shown in Fig. 9. The peak air conditioning load of about 980-tons occurred at 6:00 p.m., two hours after the peak temperature of 100°F at 4:00 p.m.

Figure 10 shows the conditions that prevailed during a characteristic fall day (day 287, year 7, October 1963). The outside temperature varied from a low of 34°F at 7:00 a.m. to a high of 71°F at 4:00 p.m. Space heating was required during the early morning hours, necessitating operation of the auxiliary boiler since not enough heat was available from the engine-generator sets. Air conditioning was required in the afternoon, and between the hours of 2:00 p.m. and 5:00 p.m., it was necessary to operate the motor-compressor sets since not enough heat was available to supply the load from the absorption chillers.

Table C.1. System Heat Balance

Month	Heat Available-10^9 Btu			Heat Used - 10^9 Btu				Heat Unused 10^9 Btu
	Eng-Gen	Aux Boil	Total	Sp Heat	Hot Wat	Abs. A/C	Total	
January	3.670	2.749	6.419	4.815	1.549	0.0	6.364	0.055
February	3.409	2.557	5.966	4.471	1.398	0.0	5.869	0.097
March	3.338	0.837	4.175	2.025	1.432	0.0	3.457	0.718
April	3.171	0.122	3.293	0.515	1.188	0.0	1.703	1.590
May	3.401	0.026	3.427	0.161	0.989	1.012	2.162	1.265
June	3.781	0.0	3.781	0.0	0.757	2.059	2.816	0.965
July	4.429	0.0	4.429	0.0	0.662	3.214	3.876	0.553
August	4.073	0.0	4.073	0.0	0.662	2.638	3.300	0.773
September	3.624	0.011	3.635	0.135	0.757	1.168	2.060	1.575
October	3.589	0.061	3.650	0.286	0.989	0.799	2.074	1.576
November	3.356	0.318	3.674	1.140	1.188	0.0	2.328	1.346
December	3.585	2.564	6.149	4.643	1.432	0.0	6.074	0.074
Total	43.426	9.245	52.671	18.191	13.003	10.890	42.084	10.587

Table C.2. Temperature/Time Frequency Data for Philadelphia, Pennsylvania

Degree Days															
Temp. F	Jan hr	Feb hr	Mar hr	Apr hr	May hr	June hr	July hr	Aug hr	Sept hr	Oct hr	Nov hr	Dec hr	%	Total Cum %	hr
100						3	12	5	3				0.8	100.0	23
90					7	80	129	69	27	3			10.3	99.2	314
80				28	71	200	310	276	139	49	3		35.2	88.9	1076
70	6	4	9	77	200	283	261	331	288	145	36	3	53.7	53.7	1643
60	38	26	75	201	319	144	32	63	212	281	118	61	27.4	100.0	1570
50	130	108	184	285	142	10		1	47	203	214	101	24.9	72.6	1425
40	274	301	317	112	5				5	60	245	308	28.4	47.7	1627
30	229	178	140	17						3	101	211	15.4	19.3	879
20	58	53	17									53	3.2	3.9	135
10	9	6	2									7	0.7	0.7	24
0															
-10															
-20															
	744	676	744	720	744	720	744	744	721	744	721	744	100		8766
													Cool	34.9	3056
		Factor $\frac{4523}{4595} = 0.985$											Heat	65.1	5710
City Philadelphia, Pennsylvania														Guide	4523
														This Chart	4595

*R. G. Werden, Weather Data vs. Operating Costs, pp. 60-64, ASHRAE Journal, October 1964.

References

1. A. J. Miller, et al., Initial Comparisons of Modular-Sized Integrated Utility Systems and Conventional Systems, ORNL-HUD-MIUS-6, June 1972.

2. J. V. Wilson, Status of Comparative Analysis (hourly) of Loads and MIUS Energy Requirements, unpublished memorandum, August 1973.

3. Phillip B. Garner, Total Energy, pp. 261-265 in Gas Turbine Engineering Handbook by John W. Sawyer, Gas Turbine Publications, Inc., Stanford, Connecticut, 1966.

4. Staff, National Weather Records Center, Selective Guide to Climatic Data Sources, U.S. Government Printing Office, Washington, D.C., 1969.

5. William S. Fleming, Total Energy Concepts for Refrigeration and Air-Conditioning Engineers, ASHRAE Journal, November 1970.

☆ U.S. GOVERNMENT PRINTING OFFICE: 1976-748-189/315

ORNL/HUD/MIUS-28
(Vol. II of ORNL/HUD/MIUS-27)
UC-90e

INTERNAL DISTRIBUTION

1. T. D. Anderson
2. S. J. Ball
3. S. E. Beall
4. M. Bender
5-69. W. J. Boegly, Jr.
70. R. S. Carlsmith
71. J. E. Christian
72. J. A. Conlin
73. F. L. Culler
74. J. H. DeVan
75. G. G. Fee
76-95. A. P. Fraas
96. W. Fulkerson
97. R. E. Gant
98. M. P. Guthrie
99. R. F. Hibbs
100. R. S. Holcomb
101. H. Inouye
102. J. O. Kolb
103. M. E. Lackey
104. R. N. Lyon
105. J. T. Meador
106-115. W. R. Mixon
116. J. P. Nichols
117. Herman Postma
118. S. A. Reed
119. P. L. Rittenhouse
120. M. W. Rosenthal
121. G. Samuels
122. C. L. Segaser
123. M. J. Skinner
124. I. Spiewak
125. D. A. Sundberg
126. D. B. Trauger
127. J. J. Tudor
128. Biology Library
129-131. Central Research Library
132. Emergency Technology Library
133-135. Laboratory Records Department
136. Laboratory Records, ORNL R.C.
137. MIT Practice School
138. ORNL — Y-12 Technical Library

EXTERNAL DISTRIBUTION

139. R. N. Abrams, Vice President, Gilbert Associates, Inc., P.O. Box 1498, Reading, PA 19603
140. R. E. Balzhiser, Director, Fossil Fuel and Advanced Systems Division, Electric Power Research Institute, P.O. Box 10412, Palo Alto, CA 94304
141-143. J. V. Basilico, Office of Research and Development, Environmental Protection Agency, Air, Land and Water Use, Waste Management Division, Room 3817-A, Washington, D.C. 20460
144. W. C. Best, U.S. Army Facilities Engineering Support Group, Attention: FEFA-RTD, Fort Belvoir, VA 22060
145. T. R. Casberg, Staff Mechanical Engineer, Directorate of Construction Standards and Design, Office of the Deputy Assistant Secretary of Defense (Installations and Housing), The Pentagon, Washington, D.C. 20301
146. Steve Cavros, Office of Conservation, Energy Research and Development Administration, Washington, D.C. 20545
147. A. T. Christensen, Manager — Program Development, General Electric, 777 14th St., N.W., Washington, D.C. 20005
148. E. L. Daman, Vice President, Foster Wheeler Corp., 110 South Orange Avenue, Livingston, NJ 07039

149. J. F. Dinwiddie, FEA/ERDO, Room 206-Old Post Office Bldg., Washington, D.C. 20461
150. L. J. Dugas, Division Vice President, Commonwealth Edison Co., 7601 S. Lawndale Avenue, Chicago, IL 60652
151. Shelton Ehrlich, Director of Combustion Research, Pope, Evans and Robbins, Inc., 320 King St., Alexandria, VA 22314
152. Engineering Library, University of Tennessee, Knoxville, TN 37916
153. S. David Freeman, 7211 Pyle Rd., Bethesda, MD 20034
154. D. A. Furlong, Vice President, Combustion Power Company, Inc., 1346 Willow Road, Menlo Park, CA 94025
155-157. R. J. Gallina, Supervisor Consumer Services, Baltimore Gas and Electric Co., 1508 Woodlawn Drive, Baltimore, MD 21207
158. Martin Gutstein, Special Projects Branch, Lewis Research Center, National Aeronautics and Space Administration, Cleveland, OH 44135
159-164. E. L. Hays, Mail Code EZ, Urban Systems Project Office, Johnson Space Center, National Aeronautics and Space Administration, Houston, TX 77058
165. J. R. Hoffmann, HDQT DAEN-FEP, Washington, D.C. 20314
166. A. A. Jonke, Chemical Engineering Division, Argonne National Laboratory, 9700 South Cass Ave., Argonne, IL 60439
167. D. Kirmse, Reynolds, Smith and Hills, P.O. Box 4850, Jacksonville, FL 32201
168. J. H. Kleinau, Vice President, Copeland Systems, Inc., 2000 Spring Road, Oak Brook, IL 60521
169. H. Landsberg, Director, Division of Energy and Resource Commodities, Resources for the Future, 1755 Massachusetts Avenue, N.W., Washington, D.C. 20036
170. R. I. LaRock, NASA Headquarters, Mail Code NT, 600 Independence Avenue, Washington, D.C. 20546
171-220. T. K. Lau, Office of Fossil Energy, Energy Research and Development Administration, 20 Massachusetts Ave., N.W., Washington, D.C. 20545
221. G. S. Leighton, Office of Conservation, Energy Research and Development Administration, 1016 16th Street, N.W., Washington D.C. 20545
222. G. L. Linsteadt, Head, Technology Utilization Office, Department of the Navy, Naval Weapons Center, China Lake, CA 93555
223-242. G. H. Lovin, Edison Electric Institute, 1015 18th Street, N.W., Washington, D.C. 20036
243-246. H. H. Maschke, Department of Defense, HQDA (DAEN-MCE-U), Washington, D.C. 20314
247. J. L. Mason, Vice President — Engineering, The Garrett Corp., 9851-9951 Sepulveda Boulevard, Los Angeles, CA 90009
248. A. J. Miller, 7102 Cheshire Drive, Knoxville, TN 37919
249-252. M. H. Novinsky, Office of Planning and Development, Dept. of HEW — OFEPM — Room 504, 330 Independence Avenue, S.W., Washington, D.C. 20201
253. Ruth Perks, Library, Energy Research and Development Administration, Washington, D.C. 20545

254-303. C. W. Phillips, National Bureau of Standards, Room A146, Bldg. 225, Washington, D.C. 20234

304-403. J. H. Rothenberg, HUD-MIUS Program Manager, Department of Housing and Urban Development, 451 7th Street, S.W., Room 8158, Washington, D.C. 20410

404. E. G. Sharp, Mitre Corp., 1820 Dolley Madison Blvd., McLean, VA 22101

405. J. Sherman, Department of Housing and Urban Development, 451 7th Street, S.W., Room 8158, Washington, D.C. 20410

406. A. R. Siegel, Director, Division of Community Development Research, Department of Housing and Urban Development, 451 7th Street, S.W., Room 8162, Washington, D.C. 20410

407. L. D. Taylor, Professor of Economics, University of Arizona, Tucson, AZ 85721

408. U.S. Army Engineer Research and Development Laboratories, Library, Fort Belvoir, VA 22060

409. U.S. Naval Civil Engineering Laboratories, Library, Port Hueneme, CA 93041

410. Research and Technical Support Division, Energy Research and Development Administration, Oak Ridge Operations, Oak Ridge, TN 37830

411-587. Given distribution as shown in TID-4500 under Coal Conversion and Utilization — Direct Combustion of Coal category (25 copies — NTIS).